UNIVERSITÀ
DI SIENA
1240

**DIPARTIMENTO DI BIOTECNOLOGIE MEDICHE**

Scuola di Dottorato di Ricerca in Biotecnologie Mediche
Ciclo XXXIV
Coordinatore: Prof. Lorenzo LEONCINI

# *M. tuberculosis* lineages: genetic diversity and its involvement on macrophage infection and on drug tolerance

Relatore:
Prof. Gianni POZZI

Correlatori:
Dott.ssa Daniela M. CIRILLO
Dott. Paolo MIOTTO

Tesi di Dottorato di:
Matteo CHIACCHIARETTA

Anno accademico 2021/2022

PhD thesis

# *M. tuberculosis* lineages: genetic diversity and its involvement on macrophage infection and on drug tolerance

## INDEX

## Summary

A central feature of *Mycobacterium tuberculosis* pathogenesis is the ability to survive within macrophages and colonize hostile environments that are acidic and rich in cholesterol and fatty acids.

The genetic variability among clinical isolates may have dramatic consequences on the outcome of infections. Many in vitro and in vivo studies have demonstrated strain-dependent variation in key aspects of virulence such as stress survival, transmission, pathology, and lethality.

This variability in MTB clinical isolates went neglected for decades; however, recently the scientific community recognized it causes important consequences on the progression of infection. As reduced host response is supposed to be the key to enabling MTB persistence and transmissibility, the immunological state of the host is also important to consider when studying the relative virulence of clinical MTB strains. In this context, the polarization states of macrophages have a huge impact on their function. It affects how macrophages can react to external signals, changing gene expression, membrane composition, receptor exposure, and cytokines production.

In our work, we focused our attention on MTB diversity and its role in pathogenesis and drug resistance acquisition. We proposed a comprehensive approach for better understanding MTB virulence taking into consideration both human (phenotypic) and MTB (genetic) variability.

We selected well-characterized strains belonging to specific MTB lineages and adopt the THP-I-derived macrophage infection model, but considering host variability by deriving M1 or M2 polarized macrophages.

Confocal live microscopy was used to study at a single-cell level different macrophage pathways during the infection. These included phagolysosomal acidification, autophagic flux, and apoptosis. All are mechanisms that MTB hijacks in order to survive within the host. Cytokine profiles were measured in response to the different MTB lineages, along

with the survival of both the macrophages and the bacteria at different time points post-infection.

In M1 macrophages, whereas less virulent/ancient are more efficient in blocking the phagosomal acidification, more virulent/modern strains are likely better at tolerating the acidic environment. However, the number of responsive macrophages remained relatively low. In M2a macrophages, whereas less virulent/ancient strains are less efficient in blocking the phagolysosomal acidification, more virulent/modern strains are blocking phagolysosomal acidification. The number of responsive macrophages was found to vary depending upon the features of the infecting strains, with the most virulent ones inducing the lowest percentages of acidifying cells.

The analysis of the autophagic flux showed less heterogeneity among both the bacterial strains and the macrophage phenotypes considered. Indeed, the induction of autophagy was found negligible in our observations.

In M1 macrophages, bystander non-infected cells of more virulent/ modern showed increased apoptosis (40%). Stratification of the data by mycobacterial burden showed similar apoptotic levels irrespective of the mycobacterial load, despite a trend displaying slightly higher apoptotic levels in bystander non-infected cells or in cells infected with a lower number of mycobacteria could be noted. In contrast, none of the categories induced apoptosis in M2 macrophages at the time point considered.

In M1 cells, the infection with less virulent/ancient lineages reduced the production of pro-inflammatory IL1-β. Likewise, IL-18 levels were lower in M1 cells infected with less virulent/ancient lineages. The chemokine GROα showed a similar pattern between MTB categories considered. In M2 cells we observed the modulation of anti-inflammatory IL-10 when comparing clinical to laboratory strains. Most of the statistically significant differences found were observed within 24h for both polarization types.

Our findings on macrophage survival corroborate the results obtained at the single-cell level, with more virulent/modern lineages causing increased cell death. Interestingly, these data seem to contrast the finding that such

strains showed lower macrophage entry in colony-forming units evaluation studies. Similarly, there was not a direct correlation between pro-inflammatory cytokine production and macrophage killing. Nevertheless, more virulent/modern strains showed increased intramacrophagic replicative capacity compared to less virulent/ancient lineages.

We also studied the genetic variability of the MTB strains during drug resistance acquisition. Among newly investigated mechanisms, the role of smallRNAs in the development of drug resistance has been considered in other bacteria but remains unexplored in MTB. We characterized the smallRNA *ncRv0842c*, cis-encoded to the *Rv0842* gene which codes for a putative efflux pump reported to be involved in rifampicin resistance (RIF-R) development. Accordingly, the present study characterized the role of *ncRv0842c* during RIF challenge and validated the role of a lineage-specific synonymous mutation on the coding region of *Rv0842* affecting the promoter region of the cis-encoded smallRNA.

In order to understand the role of the smallRNA in modulating the efflux pump, we characterized its expression during challenge experiments using sub-inhibitory concentrations of rifampicin. We then generated overexpressing mutants from MTB-selected ancient and modern strains.

qPCR showed basal downregulation of *ncRv0842* in ancient lineages compared to modern lineages. This result confirmed the hypothesis that the synonymous mutation in *Rv0842* (L45L) specific for the ancient lineages, and abrogating the -10 promoter region of the antisense smallRNA is severely affecting the expression of the smallRNA. Under RIF-induced stress, we observed upregulation of *Rv0842*, and downregulation of the smallRNA only in H37Rv (modern lineage) whereas in L5 (ancient lineage) the smallRNA expression was not affected. MABA assay performed on modern lineage mutants overexpressing *ncRv0842c* showed a 1-dilution reduction of the MIC in comparison with their respective control (mock) while the ancient lineage strains did not show any MIC shift despite the overexpression of the smallRNA. Our analysis showed that the unraveling

of smallRNA may provide new insights on MTB lineage-specific adaptation to drug-related stress and uncover the role of silent mutations in determining different phenotypes in MTB.

Our study can contribute to better understanding lineage-specific pathogenicity and highlights the importance of strain- and lineage-specific rational design and development of effective diagnostic tools and vaccines.

# List of abbreviations

- **AM** Alveolar Macrophage
- **AMK** Amikacin
- **BDQ** Bedaquiline
- **CAP** Capreomycin
- **CCL5** CC-chemokine ligand 5
- **CFP** Culture Filtrate Protein
- **CFZ** Clofazimine
- **CXCL** Chemokine CXC ligand
- **DLM** Delamanid
- **EMB** Ethambutol
- **ESAT-6** Early Secretory Antigenic Target 6 (EsxA)
- **ETO** Ethionamide
- **FCR** Fc Receptors
- **FQ** Fluoroquinolone
- **GM-CSF** Granulocyte-Macrophage Colony Stimulating Factor
- **IFN** Interferon
- **IL** Interleukin
- **INH** Isoniazid
- **KAN** Kanamycin
- **LAM** Lipoarabinomannan
- **LEV** Levofloxacin
- **LZN** Linezolid
- **ManLAM** Mannose-capped Lipoarabinomannan
- **M-CSF** Macrophage Colony Stimulating Factor
- **MDR** Multi-drug Resistance
- **MHC** Major Histocompatibility Complex
- **MMP** Matrix Metalloproteinase
- **MOI** Multiplicity of Infection
- **MTBC** Mycobacterium tuberculosis complex

- **NO** Nitric Oxide
- **NOS** Nitrogen Reactive Species
- **ORF** Open Reading Frame
- **OriC** Origin of Replication
- **PAMPS** Pathogen Associated Molecular Patterns
- **PDIM** Phthiocerol dimycocerosate
- **PGL** Phenolic Glycolipid
- **PI3K** Phosphoinositide 3-kinase
- **PIM** Phosphatidylinositol Mannoses
- **PRR** Pattern Recognition Receptors
- **PTKA** Protein Tyrosine Kinase A
- **PZA** Pyrazinamide
- **RIF** Rifampicin
- **RNAP** RNA polymerase
- **ROS** Reactive Oxygen Species
- **SR** Scavenger Receptor
- **STM** Streptomycin
- **TB** Tuberculosis
- **TGF-β** Transforming growth factor beta
- **TH1/2** T helper1/2
- **TLR** Toll Like Receptor
- **TNF** Tumor Necrosis Factor
- **TSS** Transcription Start Site

# *Chapter 1*

# Introduction

## 1.1 Tuberculosis

Tuberculosis (TB) is an airborne infectious disease caused by a group of bacteria belonging to the *Mycobacterium tuberculosis* complex (MTBC) family, of which *M. tuberculosis* (MTB) is the principal etiological agent of the human disease. Recent studies suggest that species belonging to the MTBC were originated in Africa and then diffuse around the globe adapting to the host, in a sort of co-evolutionistic process [1]. This ancient disease has accompanied mankind during its evolution, adapting to the social, demographic changes, and migratory flows that have characterized human history [2]. The history of TB across the centuries is indeed strictly connected with human demographic growth, migrations, and social behaviors, and, in Europe, was considered as a “real plague” during the industrial revolution.
TB in 2021 still represents a global emergency with a high impact on the public health system; furthermore, together with the spread of HIV, the use immunosuppressive therapies, the increasing immigration from high TB endemic countries, and the spread of multidrug-resistant (MDR) strains, TB remains public health concern even in industrialized areas (Fig. 1).


**Fig. 1**: Estimated TB incidence in 2020, for countries with at least 100,000 incident cases [5].

The COVID-19 pandemic has invalidated years of progress we achieved in fighting TB and reducing the TB disease burden. The biggest impact is a large drop in the global number of people newly diagnosed with TB, with a decrease from 7.1 million in 2019 to 5.8 million in 2020 with a substantial fall of 18%, and far short of the approximately 10 million people who developed TB in 2020 [3]. COVID-19 reduced the access to TB diagnosis and treatment, increasing the TB death rate. 2021 WHO report estimates for 2020 1.3 million TB deaths among HIV-negative people and an additional 214000 cases among HIV-positive people [3].

## 1.2 *Mycobacterium tuberculosis*: the etiological agent of TB

Mycobacteria are ubiquitous since they are easily found in water, soil, food and as a pathogen/commensal for animals and humans. The first identification of MTB was attributed to Robert Koch at the end of the XIX century when he demonstrated the correlation and the etiological origin of MTB in TB illness.

Mycobacteria are part of the Mycobacteriaceae family and belong to the Actinobacteria order. The genus *Mycobacterium* includes over 188 species, some of which are pathogenic to humans (MTB*, M. bovis, M. leprae*) some others are specific for animals. The genus *Mycobacterium* is categorized into complexes, which are grouped considering similar phenotypical characteristics as their principal hosts and the type of pathology caused. The MTBC includes: MTB *sensu stricto*, *M. africanum,* and *M. canettii* which are responsible for the majority of human TB cases, plus the animal-adapted species *M. bovis, M. microti, M. caprae, M. pinnipedii* [4]. In addition, *M. canetti,* and other smooth TB bacilli have been added to the complex because of the similarities of the clinical manifestations of the infection, even though their grouping within the complex in terms of phylogenesis is still debated [5].

The observation that the human-adapted MTBC population is phylogeographically organized has led to the hypothesis that the different lineages might be adapted to particular human populations; MTBC strains can be classified into generalists and specialists depending on the host range and the bacterial capacity to survive in a determined population. In particular, generalist strains are more globally spread and do not show a particular prevalence on a specific human population; specialists are predominantly found in restricted areas of the globe with a prevalence on a particular human population [6]. Further details are provided in Section 1.3 “MTB genomic diversity and pathogenicity”. Phylogeny studies suggest the presence of a common ancestor to the MTBC strains. In particular, there is the evidence between a specific absence of a repeated region RD9 and

strains infecting exclusively animals [7]. The high level of conservation in housekeeping genes revealed that between 15000 and 20000 years ago there was a bottleneck event of speciation promoting the selection of mycobacterial species present nowadays [8]. Another bottleneck effect seems to have also occurred for the phylogenetic branch that includes the species *M. africanum, M. microti,* and *M. bovis* [9].

When observed at the microscope, they appear filament-shaped, about 2-4 µm in length and 0.5 µm in width; they are not motile and free of cilia or flagella [10]. The presence of a cell wall rich in mycolic acids gives mycobacteria alcohol-acid-resistance and using Gram staining techniques they are classified as weakly gram-positive. Mycobacteria are non-spore-forming, catalase-positive bacilli with aerobic or microaerophilic metabolism, and they are characterized by a high lipid content. Indeed, lipids in mycobacteria are up to 60% of the dry weight making them the microorganisms with the highest lipid content in the Bacteria kingdom.

Numerous characteristics of mycobacteria (including virulence) have been linked to the uniqueness of their wall, which is characterized by an asymmetrical double layer rich in waxes that acts as a permeability barrier to polar molecules [11]. The cell wall can be divided into two layers: the first one composed of peptidoglycan, arabinogalactan, and a mycolic acid core, and a second one with a layer of amphipathic lipids, non-covalently linked to mycolic acids (Fig. 2). The anchoring proteins, phosphatidylinositol mannoses (PIMs), and lipoarabinomannan (LAM) of the outer parts of the MTB cell wall are responsible, among others, for the development of clinical manifestations and can modulate the immune response of the host. In particular, LAM can inhibit protein kinase C activity and can promote the production of numerous macrophage-associated cytokines such as Tumor Necrosis Factor (TNF)-α, Interleukin (IL)-1, IL-6, and IL-10 [12].

Among cell components, the chordal factor trehalose 6,6-dimycolate is present in virulent *Mycobacterium* species strains. Studies have demonstrated that the chordal factor is a virulence factor, inducing the release of chemokines by macrophages, and granulomatous response [13].

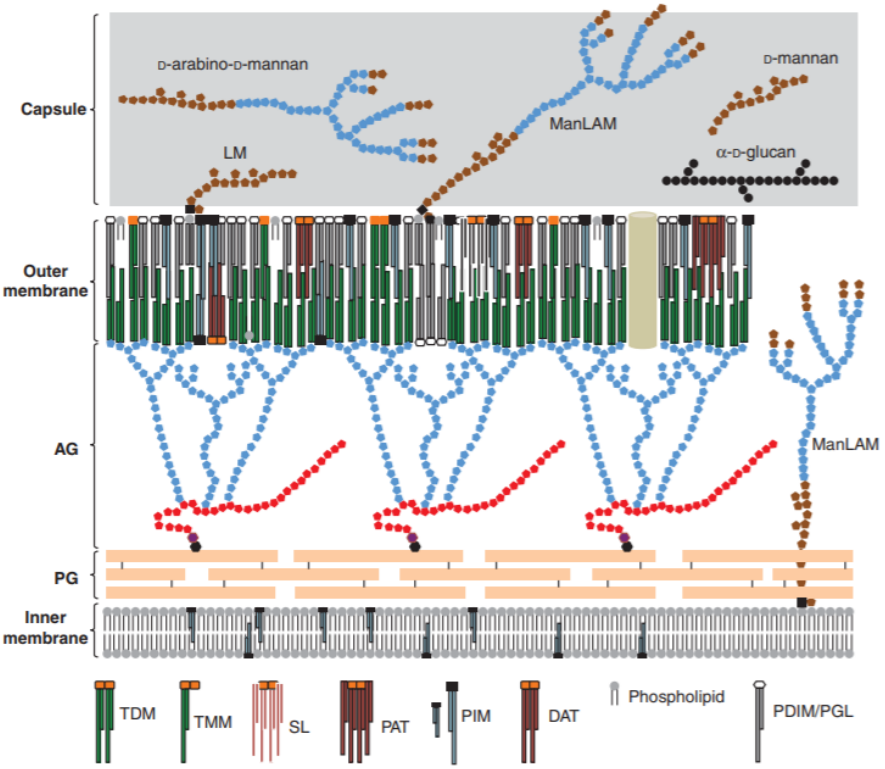


**Fig.2**: Schematic representation of the MTB cell envelope. Light blue symbols represent arabinose residues, red symbols represent galactose residues, brown symbols represent mannose residues, and black circles represent glucose residues. D-arabino D-mannan, D-glucan, and D-mannan are shown in dark green. LM, lipomannan; ManLAM, mannose-capped lipoarabinomannan; AG, arabinogalactan; PG, peptidoglycan [11].

The most widely used MTB reference strain in research laboratories is MTB H37Rv, the genome of which was sequenced in 1998 [14]. MTB H37Rv genome is 4,411,529 base pairs long with high GC content (65.6%). Ribosomal *rrn* RNA gene is present in a single operon, close to the origin of replication site (OriC); this characteristic is common for slow-growing bacteria since having multiple copies of ribosomal operons close to OriC is typical for rapid growing bacteria. Approximately 4000 open reading frames (orf) have been identified by genomic analysis, but recent

proteomic studies revealed the presence of some other possible genes and transcripts not identified before [15].

MTB can synthesize essential amino acids, vitamins, and cofactors, and it is able to metabolize carbohydrates, hydrocarbons, alcohol ketones, and carboxylic acids. MTB is naturally resistant to several antibiotic compounds. Indeed, its strongly hydrophobic cell wall acts as a permeability barrier that prevents antibiotics to enter the cell. In addition, the organism is provided with many potential drug efflux systems including 14 major facilitator superfamily (MFS) members and numerous ABC transporters that further affect drug uptake [14, 16]. Some hydrolytic and modifying enzymes (e.g., β-lactamase and aminoglycoside-acyltransferases) are then encoded in the genome, further reducing the spectrum of antibiotics effective on MTB.

Several virulence factors have been described to be involved in the metabolism of fatty acids, in the synthesis of lipids and mycolic wall acids, in proteins and lipoproteins expressed in the membrane, in enzymes involved in attenuating the oxidative stress in macrophages and secretion systems (Supplementary Table) [16].

In MTB approximately 2000 putative non-coding smallRNAs have been identified by *in silico* prediction and/or RNA sequencing approaches. However, only a few have been confirmed and characterized in details (Table 1).

**Table 1**: MTB smallRNAs with a known mechanism of action

| MTB smallRNA | Classification | Strand | Surrounding genes | Role |
|---|---|---|---|---|
| Mcr7 (MTB000067) | Trans-encoded | + | *aprABC* locus | Mcr7 expression was found to be regulated by the two-component PhoPR system and modulates the translation of tatC gene-regulating its expression and affecting Tat secretory complex [133] |
| MrsI (MTB000142, ncRv11846) | Trans-encoded | + | *blaI -Rv1847* | MrsI was found to respond to several stresses such as lack of iron, oxidative stress, acidic pH, and nutrient deficiency. Deletion of this smallRNA was found to be lethal in an iron-deficient medium [134] |
| B11 (ncRv13660c, MTS2822, 6C) | Trans-encoded | - | *Rv3660c-Rv3661* | B11 secondary structure contains two hairpins, each with 6 consequent cytosine residues in the loop. Its expression is induced by oxidative stress and low pH. Its overexpression is lethal for M. tuberculosis [135] |
| F6 (ncRv10243, MTS194, MTB000051) | Trans-encoded | + | *fadA2-fadE5* | F6 smallRNA expression is upregulated in oxidative stress, hypoxia, low pH, macrophagic infection, and nutrient deficiency [136] |
| Mcr11 (MTS0997, MTB000063) | Trans-encoded | - | *Rv1264-Rv1265* | Mcr11 levels increase upon transition to the stationary growth phase in MTB. Its overexpression causes MTB growth inhibition [137] |
| MTS1338 (DrrS, MTB000077) | Trans-encoded | + | *Rv1733c-Rv1734c* | MTS1338 (DrrS), as for the former smallRNA, is upregulated in the stationary phase of growth and is regulated by the DosR regulon [138] |
| MTS2823 (MTB000078) | Trans-encoded | + | *Rv3661-Rv3662c* | MTS2823 concentration is increased during chronic mice infection. Its overexpression decrease the expression of many genes involved in MTB central metabolism [139] |
| ncRv12659 (MTS2048) | Cis-encoded | + | *Rv2660c* | ncRv12659 is accumulated in mouse infection and during starvation. Its overexpression reduces bacterial growth and changes the transcription of at least 50 MTB gene [140] |

These non-coding RNAs with a length ranging from 50 to 400 nucleotides are able to regulate transcription, translation, stability of mRNAs and proteins. smallRNAs can be encoded in cis or in trans to their target genes, and they can act both as activator and repressor (Fig. 3) [17].

These RNAs can act both regulating virulence-associated processes and drug tolerance mechanisms as reported for many bacteria [18]. For example, as outlined in Fig. 4, in *E. coli* several sRNAs are involved in the regulation of key processes such as cell envelope synthesis, biofilm formation, antibiotic uptake, and efflux. Among other pathogenic bacteria, main studies are focusing on *Staphylococcus aureus*, *Pseudomonas aeruginosa,* and *Salmonella typhimurium* and participate in complex networks which adapt metabolism in response to external stimuli (Table 2). Despite the evidence derived from other bacterial species about the contribution of non-coding RNAs to both drug resistance and pathogenesis, the data

available on MTB remains very limited and scattered throughout a few pioneer studies.

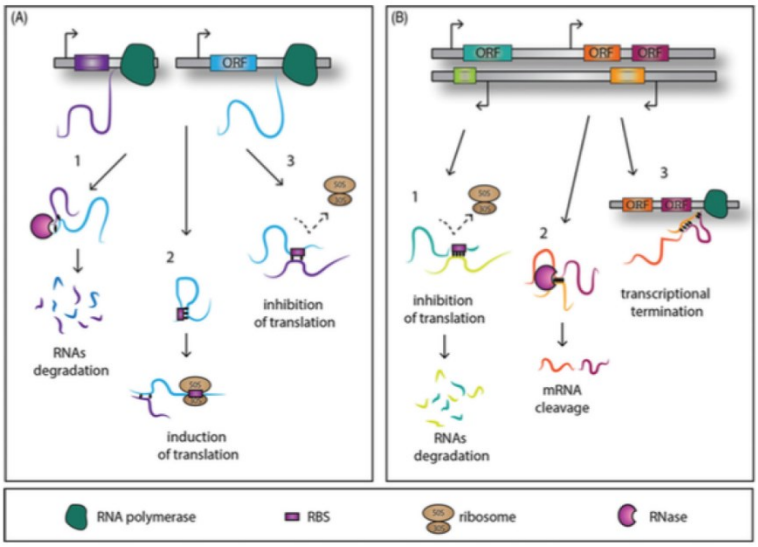


**Fig. 3**: Simplified model of action of trans-encoded (A) and cis-encoded (B) smallRNAs [17]

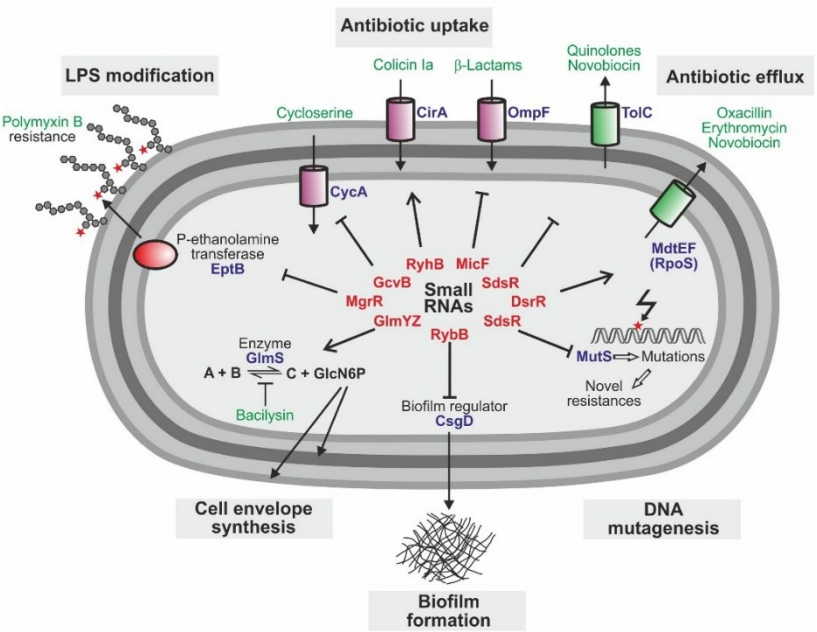


**Fig. 4**: *E. coli* Trans-encoded smallRNAs and their impact on antibiotic resistance and susceptibility. Trans-encoded smallRNA in E. coli are key players in the regulation of antibiotic resistance and are involved in antibiotic uptake, modification of the membrane composition, efflux pump function, production of enzymes, and biofilm formation. SmallRNAs are in red, target proteins in blue, antibiotics in green [19].

**Table 2**: bacterial smallRNA involved in pathogenesis mechanisms [20]

| Bacteria | Diseases | smallRNA (nt) | Target |
|---|---|---|---|
| **Gram -positive bacteria** | | | |
| Staphylococcus aureus | Skin infections, bacteremia, endocarditis, osteomyelitis, toxin-mediated diseases, abscesses, nosocomial infections | RNAIII (514) | hla mRNA<br>spa mRNA<br>rot mRNA<br>SA1000 mRNA |
| Streptococcus pyogenes | Pharyngitis, skin infections, acute rheumatic diseases, scarlet fever, necrotizing fasciitis, glomerulonephritis | FasX (300)<br>Pel (459) | ?<br>? |
| Clostridium perfringens | Food poisoning, wound infections, gas gangrene | VR RNA (400)<br>VirX (400) | ?<br>? |
| **Gram -negative bacteria** | | | |
| Pseudomonas aeruginosa | Burn and wound infections, endocarditis, cystitis, pneumonia in cystic fibrosis patients, septicaemia in immunocompromised patients | RsmY (120)<br>RsmZ (119) | RsmA |
| Vibrio cholerae | Cholera | CsrB (417)<br>CsrC (366)<br>CsrD (351)<br>Qrr1 (96)<br>Qrr2 (108)<br>Qrr3 (107)<br>Qrr4 (107) | CsrA<br><br><br>*hapR* mRNA |
| Salmonella typhimurium | Gastroenteritis, enterocolitis, septicaemia in immunocompromised patients | CsrB (350)<br>tmRNA (363) | CsrA |
| Chlamydia trachomatis | Sexually transmitted genital infections, trachoma | IhtA (120) | *hctA* mRNA |

## 1.3 Pathogenesis of TB

The respiratory tract is the main entry route MTB bacilli. Spread of the infection can occur via droplet secretions, coughing, or sneezing. About 3000 nuclei (5-10 µm in diameter) of infective droplets are emitted coughing and they can remain suspended in the air for several hours. Once inhaled, MTB overcomes the mucociliary barrier and reaches the alveoli. The probability that a healthy person becomes infected by MTB depends mainly on the aerial concentration of these particles, the duration of exposure, and the subject's immune defenses. The factors that can modify the TB illness fate are related both to the bacillus and to the host. Taking into consideration the statistics, about 1-2% of contacts immediately develop active TB while 1 in 3 will develop a latent form of infection. Among those, only 5-10% of latent infected will progress to an active form of TB and become infective, with a high risk in the first two years following the infection [21].

Macrophagic phagocytosis of small bacterial agglomerates (1-3 bacilli) will cause the first contact between MTB and the host innate immune response, and thus activate defense mechanisms. Early phases of the infection are important for the fate of TB when individual differences in the immune response are one of the determining factors in the progression of the disease and in its clinical course.

The interaction between MTB and host cell is highly complex and extremely intimate, and when the infection does not progress to active disease, mycobacteria are cleared or undergo a quiescent phase [22].

As mentioned, macrophages are the first immunological cells responding to MTB. In 90% of the cases, their first contact with MTB activates the immune system and the recruitment of lymphocytes, essential for the formation of a local lesion called granuloma [23]. In immunocompetent people, the infection is controlled by the immune system and the lesions may heal. Primary TB occurs in a person with insufficient immunity to confine and control bacilli in granulomas [22]. When activated, T -cells migrate to the lungs and are involved in the granuloma formation together with activated macrophages, fibroblasts, and dendritic cells. From a histological point of view, MTB is circumscribed within a tissue structure consisting of epithelioid cells of macrophage derivation, monocytes, lymphocytes, and neutrophils (Fig. 5).

Granuloma represents an effective way of containment for the proliferation and spread of the pathogen. Within this hostile ambient, macrophages may kill mycobacteria and produce a necrotic central zone. MTB has adapted to survive and persist in this area. After 2-3 weeks this solid necrotic lesion will become caseous, and it's characterized by low levels of oxygen, low pH, and low nutrients. This will slow MTB metabolisms and activates promoter factors that push MTB to undergo a latency phase [23]. In most cases, the granuloma stops growing and heals, leaving a fibrotic and calcified lesion, within which the mycobacterium can be in a quiescent latent phase. The cell-mediated immune response of $CD4^+$ T lymphocytes keeps infection under control. Whereas the granuloma

represents a containment measure for the host, it can be also beneficial to the pathogen, as exposure to antibiotics and additional immune cells recruitment is also limited.

In immunologically compromised individuals, both primary or a previously established infection can be reactivated and progress into the active form of the disease.

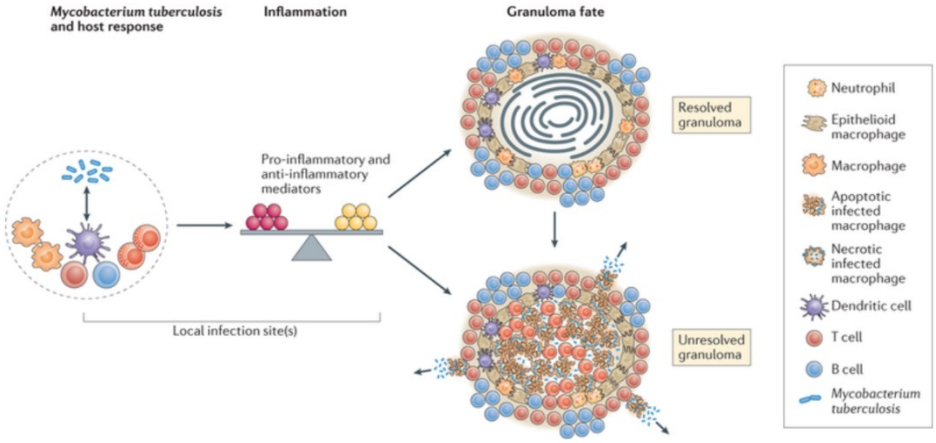


**Fig. 5**: Granuloma fate is influenced by a complex and dynamic exchange of host and bacterial features. This process is highly dynamic and iterative, with multiple components having pleiotropic, knock-on feedback effects on inflammation and the host-pathogen interaction [24].

Cytokines are crucial for immune system activation and TB resolution, but further studies are necessary to completely understand the granuloma formation mechanism and the role of all immune system participant cells (Table 3). TNFα among others plays an important role in granuloma formation and contributes to the recruitment of myeloid cells. It is mainly produced by macrophages, and studies demonstrated that anti-TNF treatment reduces the number of macrophages recruited and thus the granuloma size, impairing the bacilli containment [25]. The balance between IL-12 and IFNγ (Interferon γ) is important for the fate of the illness and for the activation of macrophagic killing functions. IFNγ is mainly produced by $CD4^+$, $CD8^+$, NK when stimulated by dendritic cell's IL-12 and is essential for an efficient establishment of the granuloma, and for controlling bacterial

growth [26]. Human population studies have correlated IL-12 production gene mutations to an improved predisposition to TB infection, and to show a severe form of the disease [27]. During MTB infection the role of Type I IFN can be protective or detrimental for the host. Type I IFN activation during chronic phases of TB causes immunosuppression, inducing IL-10 production and favors bacteria survival [28].

The IL-1 cytokine family is composed of IL-1α, IL-1β, IL-18, and IL-33. IL-1β production after MTB infection is a process that is tightly regulated. Mice model experiments demonstrated the importance of IL-1 signaling in controlling the infection. IL-1α or β knock-out mice show a severe form of TB compared to the control [29].

Macrophage cytokines are crucial for the recruitment of neutrophils and adaptive immunity activation after MTB infection. Among others, macrophages produce pro-inflammatory cytokines such as type I IFN, TNFα, IL-1b IL-2, IL-18, IL-6, and anti-inflammatory cytokines IL-10 and Transforming Growth Factor (TGF)-β. They produce and secern a huge range of chemokines for cells recruitment (CC, CXC, $CX_3C$) and growth factors as M-CSF (Macrophage colony-stimulating factor), GM-CSF (Granulocyte-Macrophage Colony-Stimulating Factor), and Erythropoietin [30]. TNFα membrane expression through ADAM17 complex is essential for granuloma formation and is crucial for TB eradication while the secretion of soluble TNFα is important for catabolism with IL-6 [31, 32].

**Table 3**: Principal cytokines and chemokines and their role in TB [33].

| Cytokine | Receptor/Signal | Role in TB |
|---|---|---|
| TNFα | TNFR1, TNFR2<br>JNK, p38, NFκB | **Positive**: Essential for survival following Mtb infection.<br>Initiation of innate cytokine and chemokine response and phagocyte activation<br>**Negative**: Mediator of tissue damage |
| IFNγ | IFNGR1, IFNGR2<br>JAK/STAT | **Positive**: Essential for survival following Mtb infection.<br>Coordinates and maintains mononuclear inflammation.<br>Expressed by antigen specific T cells<br>**Negative:** Potentially pathogenic |
| IFNα/IFNβ | IFNAR1, IFNAR2<br>JAK,TYK, ISG,ISRE | **Positive**: Required for initial recruitment of phagocytes to the lung<br>**Negative**: Over expression of IFNα/IFNβ results in recruitment of permissive phagocytes and regulation of T cell accumulation and function |
| IL-6 | IL-6R, gp130<br>JAK, STAT3, MAPK | **Positive**: Potentiates early immunity – non essential unless a high dose infection. |
| IL-1α/IL-1β | IL-1R1, IL1RAcP<br>MyD88,IRAK4,NFκB | **Positive**: Essential for survival following Mtb infection.<br>Induction of IL-17. Promotes PGE2 to limit Type I IFN |
| IL-18 | IL-18Rα, IL-18Rβ<br>MyD88,IRAK, NFκB | **Positive**: May augment IFNγ – non-essential. Regulator of neutrophil/monocyte accumulation. of neutrophil and monocyte accumulation, optimal induction of IFNγ by T-cells |
| IL-12<br>p40,p35 | 12Rβ1, IL-12Rβ2<br>JAK2, TYK2, STAT4 | **Positive**: IL-12p40 and IL-12p35 essential for survival following Mtb infection. Mediate early T cell activation, polarization and survival.<br>**Negative**: Over expression of IL-12p70 is toxic during Mtb infection. |
| IL-23<br>p40,p19 | IL-23R, IL-12Rβ1<br>JAK2, TYK2, STAT3 | **Positive**: Required for IL-17 and IL-22 expression during Mtb infection. Non-essential in low dose challenge required for long term control.<br>**Negative:** Mediates increased pathology during chronic challenge |
| IL-27<br>EBI3,p28 | IL-27Rα, gp130<br>JAK1/2,TYK2,STAT1/3 | **Positive**: May control inflammation and reduce pathology<br>**Negative:** Regulates protective immunity to Mtb infection by limiting the migration and survival of T cells at the inflamed site. |
| IL-35<br>p35,EBI3 | IL-12Rβ2,gp130<br>STAT1/4 | **Positive?** Regulate the availability of subunits of IL-12, IL-27<br>**Negative?** Potential immunoregulatory role. |
| IL-17A/F | IL-17RC, IL-17RA | **Positive**: Essential for survival following infection with some strains of Mtb. Induction and maintenance of chemokine gradients for T cell migration.<br>**Negative**: Drives pathology via S100A8/A9 and neutrophils |
| IL-22 | IL-22R1, IL-10R2<br>TYK2,JAK1,STAT3 | **Positive**: Induces antimicrobial peptides and promotes epithelial repair, inhibits intracellular growth of Mtb in macrophages. |

| Chemokine | Receptor | Role in TB |
|---|---|---|
| CCL-3,-4,-5 | CCR1 | **Positive**: Upregulated during infection. Non-essential in mouse model |
| CCL-2,-7,-12 | CCR2 | **Positive**: Maximizes and organizes early macrophage and T cell accumulation in the lung<br>**Negative**: Mediates recruitment of permissive phagocyte accumulation into the lung |
| CCL-17,-22 | CCR4 | **Positive:** Mediates optimal granuloma formation to mycobacterial antigen<br>**Negative**? May limit T cell proliferation via $T_{REG}$ |
| CCL-3,-4,-5 | CCR5 | **Positive**: Regulation of pulmonary infiltrates – non-essential. May mediate early dendritic cell accumulation in the lymph node. May augment macrophage Mtb killing via CCL5? |
| CCL-20 | CCR6 | **Positive**: Expression of CCR6 on T cells specific for Mtb antigens<br>**Negative?** CCL-20 seen at high levels in active TB |
| CCL-19,-21, | CCR7 | **Positive:** Mediates efficient migration of dendritic cells and Mtb-specific T cell activation. |
| CXCL-1,-2,-3,-5,-6,-7,-8 | CXCR1<br>CXCR2 | **Positive:** Expressed on neutrophils mediates accumulation<br>**Negative:** Absence of CXCR2 or CXCL5 results in improved bacterial control and reduced neutrophil accumulation |
| CXCL-9, -10,-11 | CXCR3 | **Positive**: Required for optimal granuloma formation. Expressed on Mtb-specific T cells. Use of CXCL9-11 levels to indicate disease level? Required for early recruitment of T cells to lung |
| CXCL-13 | CXCR5 | **Positive**: Required for correct location of T cells within granulomas. Required for B cell follicle formation in Mtb infected lungs. Required for optimal protection. |

## 1.4 MTB genomic diversity and pathogenicity

The genetic variability of MTB clinical isolates went neglected for decades; however, in the past 10-15 years the scientific community recognized it causes important consequences on the progression of infection. Even though the genomic diversity in MTBC is low compared with other bacteria, at least 44% of non-synonymous SNPs have been predicted to impact gene function, thus altering bacterial phenotype [34]. Drug stress and immune system response cause a selective pressure on the bacteria, which push the fixation of these mutations [35, 36]. Studies based on WGS techniques have recognized 7 main lineages of MTBC that can be classified in clades according to their proximity to their common phylogenetic ancestor. The first (monophyletic) clade, the so-called “modern”, includes MTB lineages 2, 3, and 4 (which includes also the laboratory reference strain H37Rv). Clade 2, the "ancient", includes MTB lineages 1, 7, and *M. africanum* lineages 5, 6 and is paraphyletic not being part of the same phylogenetic group (Fig. 6) [37]. More recently, new strains have been identified and classified as a new Lineage 8 (Table 4).

**Table 4**: MTB lineage classification and spoligotype associated [11]

| Evolutionary age (species) | Lineage name based on LSP/SNP[b] | Lineage and sublineage [RD associated] | | | | Spoligotype family |
|---|---|---|---|---|---|---|
| Ancient lineage (*M. tuberculosis*) | Indo-Oceanic lineage | 1 [RD239] | 1.1 | 1.1.1 | | EAI4 and EAI5 |
| | | | | | 1.1.1.1 | EAI4 |
| | | | | 1.1.2 | | EAI5 and EAI3 |
| | | | | 1.1.3 | | EAI6 |
| | | | 1.2 | 1.2.1 | | EAI2 |
| | | | | 1.2.2 | | EAI1 |
| Modern lineages (*M. tuberculosis*) | East-Asian lineage | 2 | 2.1 (non-Beijing) | | | MANU ancestor and orphan profile |
| | | | 2.2 (Beijing) [RD105, RD207] | 2.2.1 [RD181] | | Beijing |
| | | | | | 2.2.1.1 [RD150] | Beijing |
| | | | | | 2.2.1.2 [RD142] | Beijing |
| | | | | 2.2.2 | | Beijing |
| | East African-Indian lineage | 3 [RD750] | 3.1 | | | CAS except CAS1-Delhi |
| | | | | 3.1.1 | | CAS1-Kili |
| | | | | 3.1.2 | 3.1.2.1 | CAS2 |
| | | | | | 3.1.2.2 | CAS |
| | Euro-American lineage | 4 | 4.1 | 4.1.1 (X-type) | 4.1.1.1 [RD183] | X2 |
| | | | | | 4.1.1.2 | X1 |
| | | | | | 4.1.1.3 [RD193] | X3 and X1 |
| | | | | 4.1.2 | | T1 and H1 |
| | | | | | 4.1.2.1 (Haarlem) [RD182] | T1 and H1 |
| | | | 4.2 | 4.2.1 (Ural) | | H3 and H4 |
| | | | | 4.2.2 | | LAM7-TUR and T1 |
| | | | | | 4.2.2.1 (TUR) [RD182] | LAM7-TUR |
| | | | 4.3 (LAM) | 4.3.1 | | LAM9 |
| | | | | 4.3.2 | | LAM3 |
| | | | | | 4.3.2.1 [RD761] | LAM3 |
| | | | | 4.3.3 [RD115] | | LAM9 and T5 |
| | | | | 4.3.4 [RD174] | 4.3.4.1 | LAM1 |
| | | | | | 4.3.4.2 | LAM11-ZWE, LAM9, LAM1, and LAM4 |
| | | | | | 4.3.4.2.1 | LAM11-ZWE |
| | | | 4.4 | 4.4.1 | 4.4.1.1 (S-type) | S |
| | | | | | 4.4.1.2 | T1 |
| | | | | 4.4.2 | | T1 and T2 |
| | | | 4.5 [RD122] | | | H3, H4, and T1 |
| | | | 4.6 | 4.6.1 (Uganda) [RD724] | 4.6.1.1 | T2-Uganda |
| | | | | | 4.6.1.2 | T2 |
| | | | | 4.6.2 [RD726] | 4.6.2.1 | T3 |
| | | | | | 4.6.2.2 (Cameroon) | LAM10-CAM |
| | | | 4.7 | | | T1 and T5 |
| | | | 4.8 [RD219] | | | T1, T2, T3, T4 and T5 |
| | | | 4.9 (H37Rv-like) | | | T1 |
| Ancient lineages (*M. africanum*) | West-Africa lineage 1 | 5 [RD711] | | | | AFRI_2 and AFRI_3 |
| | West-Africa lineage 2 | 6 [RD702] | | | | AFRI_1 |
| Intermediary lineage (*M. tuberculosis*) | Lineage 7 | 7 | | | | |

[a]Regions of deletion (RD) are given in brackets and appear below the lineage/sublineage in which they are present.
[b]LSP, large sequence polymorphism.

Phenotypic differences found among MTB lineages can be seen both in planktonic growth, gene expression, metabolism, and in *in-vivo*/*in-vitro* macrophagic infection, including in virulence, bacterial-host cell uptake, cytokine induction, and intracellular growth (Fig 6) [38, 39]. Studies also demonstrated that different MTB lineages have different probability rates to develop drug resistance [40, 41].

Despite the progress made in our understanding of the global phylogenetic diversity of MTBC, much remains unknown with respect to both human- and animal-associated MTBC diversity [1]. Despite the number of studies concerning the origin of the MTBC and the proposed African origin, there are little data that explains why modern MTBC lineages are globally

dispersed [42]. There is evidence of a correlation between virulence, transmission, survival to stress and lethality, and the different MTB lineages however, the molecular mechanism that controls this is still poorly understood [43].

Ongoing studies are shedding light on the host-pathogen interactions and demonstrated that the host immune response is differentially induced by different MTB strains [44, 45]. In fact, ancient lineage strains induce a higher macrophagic response compared to the phylogenetic modern ones [45]. Modern lineages delay the immune activation reducing the early inflammatory response, thus providing the bacteria a selective advantage during the early phases of the infection [44]. A reduced host response (associated with high virulence) is supposed to be the key to MTB persistence and transmissibility. Indeed, it has been demonstrated that L2 and L4 lineages are responsible for most TB cases in the world [37].

MTB lineages generally display a strong phylogeographical host adaptation, with lineages associated with geographical regions [46]. Ecologists distinguish between generalists and specialists depending on the size of a species' ecological niche. In infectious diseases, the niche of a pathogen is determined by host availability and the bacteria's capacity to survive (Fig. 6).

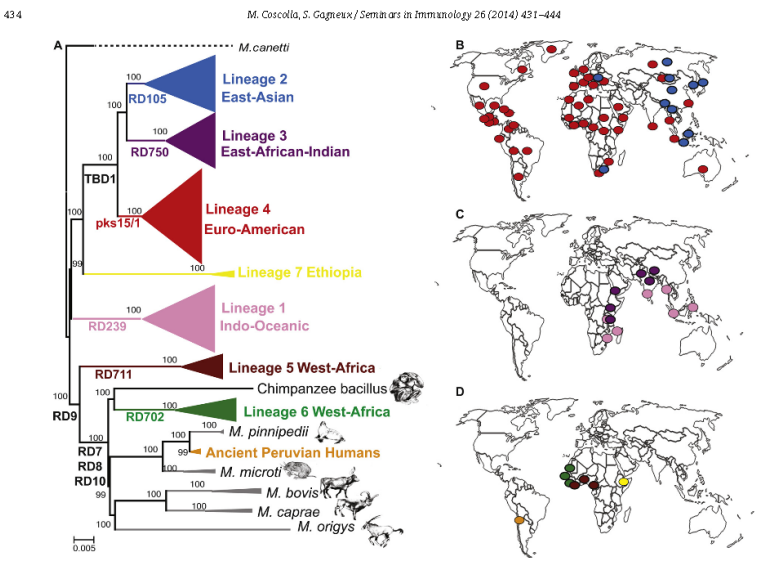


**Fig. 6**: World diffusion of MTBC lineages [37]

Lineage 1 (L1) is predominant in regions of the Indian Ocean, extending from Eastern Africa to Melanesia. Lineage 2 (L2) is mostly distributed, with a predominance in Eastern Eurasia and South East Asia. L3 is similarly distributed to L1 and is frequent among isolates reported from the Indian Ocean and in Northern Africa and across Southern Asia. L4 is well dispersed, with a predominance throughout Africa and Europe and the entire region of the Mediterranean. L5 and L6 are reported at low frequencies in Western and Northern Africa. L7 is limited to Ethiopia. Remarkably, L1–L4 are also reported in Northern Europe, where the majority of TB cases are due to recent immigration [47].

*M. africanum* (L5, L6) was described for the first time in 1968 and it appears very similar to MTB *sensu stricto* [48]. However, *M. africanum* has been associated with a longer latency period and a lower virulence as an adaption to low human population densities. *M. africanum* is almost exclusively found in Africa and represents the etiological agent of almost 40% of TB cases in some West African countries, suggesting a correlation between the pathogen and the host in selected regions [1, 49, 50, 51]. Host-adaptation has been associated, among other hypotheses, with the high-level concentration of vitamin B12 in African population plasma. Vitamin B12 plays an important role in the pathogenesis of TB and mutations in the cobalamin biosynthesis pathway in *M. africanum* could be the reason why *M. africanum* is difficult to find infecting non-African populations [52]. *M. africanum* drug resistance and pathogenesis features are not clear. Its lower frequency of the insurgence of drug resistance, and its reduced virulence are nowadays under debate. At a clinical level, *M. africanum* has been associated with a slower progression to disease compared to MTB (as outlined for other ancient lineages), and it is more commonly found in people living with HIV and the elderly population. Compared to MTB infections, the clinical isolates of *M. africanum* were associated with lower bacterial burdens, lower signs of disease, and tissue pathology, even in hosts lacking IFNγ production [53]. Furthermore, several MTB's key virulence mechanisms have been shown to be affected in *M. africanum*. For

example, the PhoPR two-component system, essential for MTB virulence, for mycolic acid production, and for the secretion of ESAT-6 (Early Secretory Antigenic Target) antigen, shows a SNP (position 71 of PhoR protein) in ancient lineages (*M. africanum*) 5 and 6, and in animal-adapted strains, thus affecting PhoPR regulatory pathway [54]. Of note, a single amino acid change in PhoP protein (position 219) in H37Ra highly attenuates H37Ra strain virulence [55]. The control *of M. africanum* in mice lungs reflects the low immune cells recruitment and low induction of cytokines with low levels of IFNγ, IL-17, and TNFα. DosR expression, the regulon involved in the controls of the adaptation to oxygen limitation and linked to MTB virulence, is significantly lower in *M. africanum* compared to modern strains [56].

Differences are not observed only when comparing relatively (phylogenetically) distant ancient and modern lineages. Indeed, even between the monophyletic modern clade differences have been observed. Lineage 3, when compared to lineage 4, shows a higher anti-inflammatory phenotype, and Beijing strains (L2) commonly induce low levels of TNFα, IL-6, IL-10, and GRO-α compared to the laboratory strain H37Rv (which belongs to L4) [57]. Moreover, L2 strains show a lower uptake and lower cytokine induction when compared to L4 [58, 59]. L2 has been also associated with treatment failure and disease relapse, with high HIV co-infection and it is also found at higher rates in TB meningitis compared with other lineages [60, 61]. The “hypervirulence” of Lineage 2 seems to be related to phenolic glycolipids (PGL) production, which can modulate the immune system by interfering with the effector molecules of the host's innate immune response: in H37Rv the lack of PGL production is due to a deletion of 7pb in the *pks* 15/1 gene which disables the synthesis of these lipids by increasing the immune response. A possible explanation for this correlation could be the presence of mutations in the *mut* gene, which is involved in repairing DNA damage. It is hypothesized that the sequential accumulation of mutations in this gene could cause an increase in the mutation frequency rate in Beijing strains which would confer better adaptability to

stress and the ability to acquire drug resistance, but this hypothesis finds contrasting evidence in the literature [62]. Furthermore, the higher virulence rate is also caused by its ability to grow rapidly in human monocytes and to slow-down host immune response [63] (Fig. 7).

It's also important to underline that there are several important differences between clinical strains and laboratory MTB strains. The canonical most used MTB strains in the laboratory are the so-called H37Rv, H37Ra, Erdman, BCG vaccine strain, CDC1551, and HN878 [64]. These are all modern strains, belonging to lineage 4 (H37Rv, H37Ra, CDC, Erdman) or lineage 2 (HN878). The principal limitation in working with laboratory strain is that the bacilli rapidly adapt to laboratory conditions and lead to genetic modification (such as the loss of PDIM wall component) and thus to potential artifacts. Moreover, even if synonymous mutations are supposed not to affect phenotype and protein activities, a synonymous SNP was found to alter the transcription start site (TSS) position of the *dosR* gene in Lineage 2, generating an increase in its expression [39]. *dosR* gene duplication events have also been observed in L2 strains, causing its upregulation [65]. A completely neglected topic concerns the effect of synonymous mutations on the post-transcriptional regulatory network linked to antisense transcripts, but pioneer studies in *M. bovis* already highlighted implications for how we define so-called "silent" mutations [66].

Deletion events also influence bacteria phenotype. A deletion in the *pks* 15/1 gene in Lineage 4, reduces the phenolic glycolipid production decreasing host immune cell responses [67]. In Lineage 3, deletion in the *Rv1519* gene (annotated as conserved hypothetical protein) causes reduced production of IL-10 by the host [57, 68].

It is difficult to generalize and predict what will be the phenotype of strains, knowing only their lineage. Intra-lineage and sub-lineage differences are present among both modern and ancient strains. Even though phenotypic diversity (and immune specific response) has been associated with the different MTBC lineages, individual strains within these lineages exhibit a huge spectrum of phenotypes, suggesting that sub-

lineage should also be considered when studying host-pathogen interactions [44, 69]. Differences are present also when considering the inflammatory response to “modern” Beijing strains and “ancestral” Beijing strains, with a lower inflammatory response of the former [70].

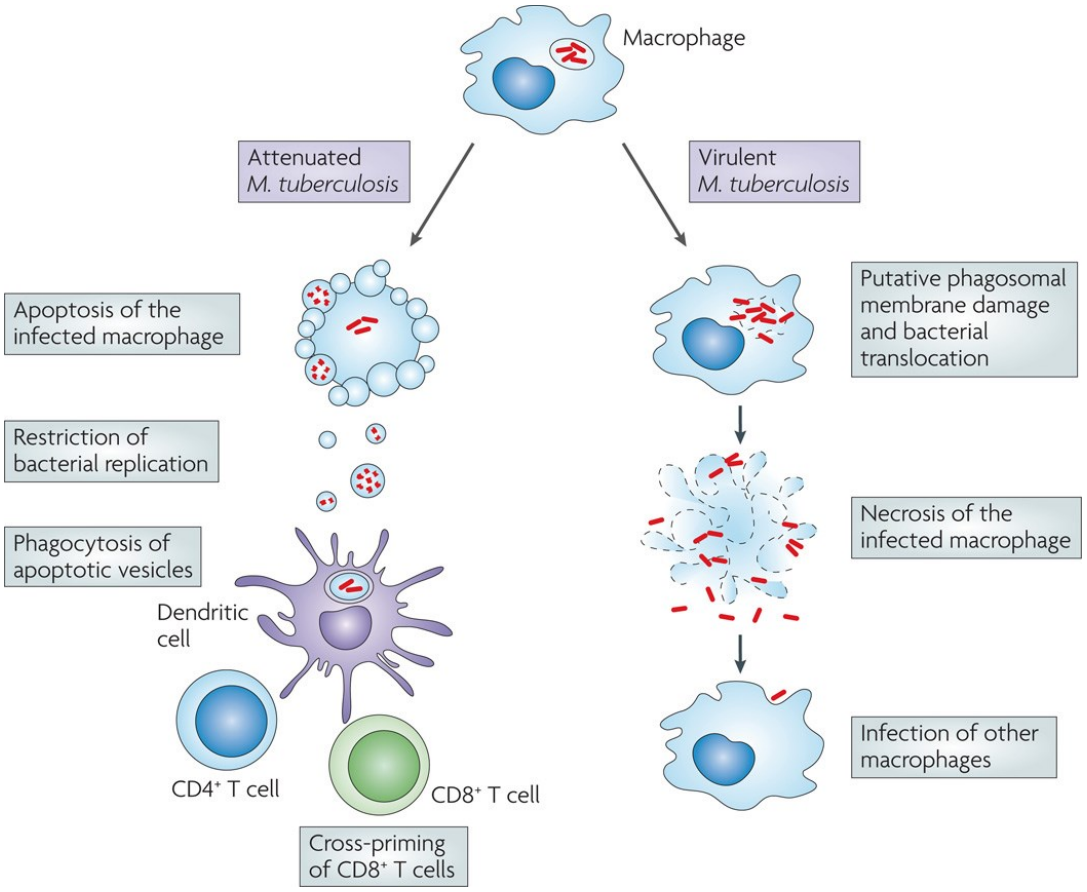


**Fig. 7**: Mycobacterium TB infects macrophages, survives, and replicates in the phagosome. Macrophages infected with attenuated strains of MTB undergo apoptosis. Apoptosis of infected macrophages provides an important link to adaptive immunity, as apoptotic vesicles containing bacterial antigens are taken up by dendritic cells, which presents antigens to naive T cells. By contrast, virulent MTB inhibits apoptosis and, instead, induces necrosis [71].

Studies on L4, investigating the global success of those strains, discovered that it is mainly a consequence of both biological and social phenomena. In a recent study on L4 strains, Stucki et al. discovered the presence of at

least 10 L4 sub-lineages, that can be further divided into specialists and generalists, with some sub-lineages showing an intermediate geographical distribution [6]. In the sub-lineage analyzed in this study, specific T cell epitopes are conserved, but nonsynonymous variation may allow antigens to be differently and selectively recognized by T cell receptors of different human populations [6]. Similarly, in 2021 new evidence allowed to define sub-lineages also in the ancient L5 emphasizing how much this field is evolving with the advent of WGS approaches [72].

It's important to remark that transmission patterns are complicated mechanisms that are not only linked to the intrinsic virulence of individual organisms (Lineages) but depend on several factors, most of them poorly understood, including the role and the variability of the host. For example, as shown in the study of Shanleya et al., despite similar CFU levels seen in the selected MTB isolates, there appeared to be differences in lung pathology in infected guinea pigs [73].

## 1.5 Macrophage phenotypic diversity and mycobacterial infection

Monocytes are important both for the activation of the inflammatory response and for the priming of innate immunity. The monocytes, once generated in the bone marrow, migrate to different tissues where they differentiate into specialized cells following exposure to various microenvironmental factors. Also, macrophages are highly adaptive cells, and their phenotype can change in a plastic way in responding to external stimuli, such as inflammation or pathogen invasion [12].

The activation status of macrophages is called polarization. MØ (naïve, non-polarized) macrophages are activated by the secreted cytokines. According to the signal received, MØ macrophages are driven into a so-called classical M1 pro-inflammatory phenotype, or to a so-called non-classical M2 anti-inflammatory phenotype. The main difference between these cells is that in M2 macrophages the metabolism of arginine is shifted

to ornithine and polyamine, while in M1 cells it is shifted to NO and citrulline. Ornithine produced by M2 can promote cell proliferation and repair through the synthesis of collagen, fibrosis, and other tissue remodeling functions, while the NO produced by class M1 is an important molecular effector with microbicidal activity and inhibition of cell proliferation [74]. The polarization states of macrophages have a huge impact on their function. It affects how macrophages can react to external signals, changing gene expression, membrane composition, receptor exposure, and cytokines production [12] (Fig. 8).

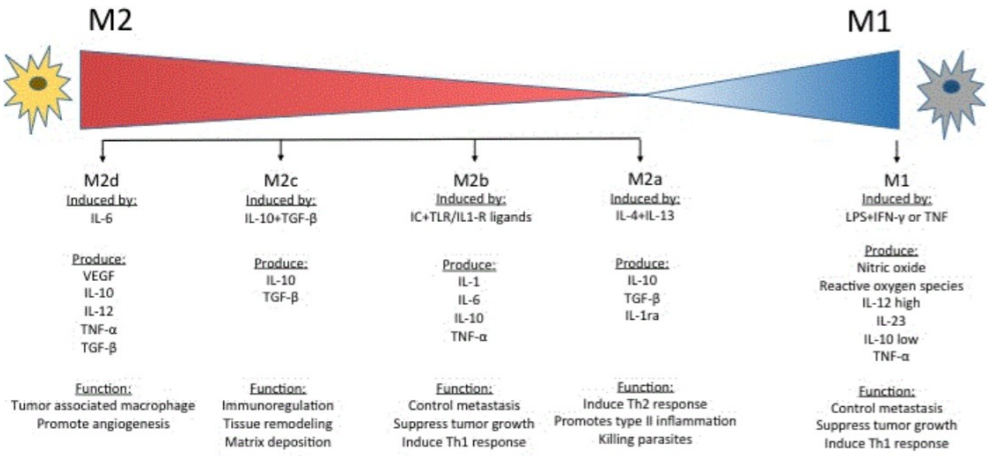


**Fig. 8**: Polarization status of macrophages and principal cytokine that induce the differentiation. The functions of different types of macrophages are highly dependent on the polarization status [74].

$Th_1$ cells signals are the main triggers for the M1 polarization, which enhances the macrophagic antigen presentation, the phagocytosis, the killing capacity, and the capacity to attract other leukocytes [75]. On the other side, molecules produced by $Th_2$ cells are the main drivers for the M2 polarization, thus decreasing phagocytosis, inducing macrophagic fusion, increasing the anti-inflammatory activity and promoting the mannose receptor (CD206) synthesis [76].

In the lung, macrophages constitute a heterogeneous population distributed within two compartments: alveolar macrophages (AM) and interstitial macrophages. The former is mostly represented in the airways (bronchi and alveoli), the latter predominates in the parenchymal tissue. When MTB enters the lungs, AMs are the first line of defense that recruit bloodstream inactive MØ (naïve, non-polarized) macrophages into the alveoli after infection. In this space, recruited MØ macrophages can be polarized toward an M1 or M2 phenotype, depending upon the cytokines at the microenvironment. M2 macrophages are essential to prevent immunopathology, but they are more permissive to MTB infection, whereas M1 macrophages are able to control mycobacterial proliferation, but trigger an increased inflammatory response, increased lung damage, and high IFNγ production [77]. M2 permissiveness is mainly due to the high amount of CD206 that these cells have compared to M1 macrophages. MTB interaction with mannose receptors causes the activation of the phagocytic process and the induction of the production of anti-inflammatory cytokines, the reduction of the oxidative response, and the phagosome maturation [78]. Recent studies showed how M2 permissiveness is also linked to the different metabolic pathways activated. Indeed, M2 metabolism is up-regulated for fatty acid uptake and β-oxidation; intracellular MTB is known to use fatty acids and cholesterol from the host, suggesting that those bacteria in M2 macrophages possess a metabolic advantage (Fig. 9). On the contrary, MTB-infected M1 macrophages show a metabolism with high levels of glycolysis. In addition, M1 activated macrophages are able to produce high levels of ROS, NOS, and NADPH oxidases when compared to non-activated macrophages [79]. These molecules, besides their killing activity on bacteria, are involved in the enhancement of inflammatory activation and tissue damage. MTB has different enzymes involved in oxidative stress escaping such as the superoxide dismutase and KatG protein [80].

Despite MTB macrophage infection have been reported to promote an M1 phenotype with high IFNγ production, the control of the first phases of the

infection is temporary and lasts a maximum of three weeks. Indeed, MTB is able to shift the initial M1 macrophagic polarization status to the more permissive anti-inflammatory M2 phenotype [81, 82]. During this time, MTB produces exosomes rich in MTB lipids that increase the inflammatory response and recruit more neutrophils, dendritic cells, and additional macrophages, that will be also infected by MTB bacilli. MTB ManLAM and secreted ESAT-6 inhibit the interferon T cell pathways, and induce the production of IL-10, allowing the recruiting of anti-inflammatory, more permissive cells, the reduction of NO production, and increasing iron accessibility [83]. This M1/M2 shift occurs in the granuloma when the acute infection progresses into chronic. Recent studies generated a predictive model of TB granuloma progression in time that was dependent on the M1 versus M2 ratio at the site of infection, thus providing further evidence of how critical the balance is between M1 and M2 phenotypes to the containment of the bacteria inside the granuloma, with a delay in M1 polarization that appears to be responsible for increased survival of the bacteria. M1 cells are predominant at early phases of the infection (2 to 4 months post-infection) while at later timepoints they became not protective and may be deleterious due to an excessive inflammation and tissue damage [84].

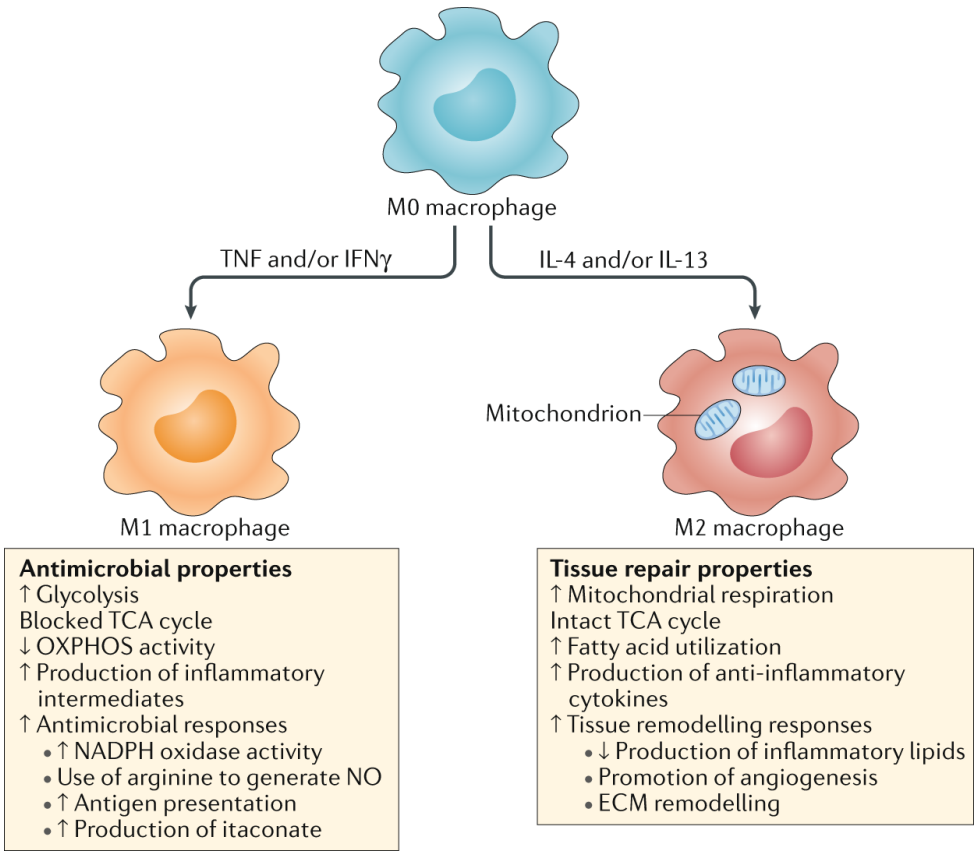


**Fig. 9**: Phenotypic characteristics of the M1-like and M2-like macrophage polarization states.

The M1-like and M2-like macrophage polarization states highlight the pro-inflammatory or anti-inflammatory phenotype of these cells by oversimplifying the extremely heterogeneous nature of macrophages in vivo. M0 macrophages are activated to an M1-like macrophage by exposure to IFNγ and/or tumor necrosis factor (TNF), or LPS. M2-like macrophages are induced through IL-4 and/or IL-13 exposure M1-like macrophages are more glycolytically active and more prone to kill bacteria. By contrast, M2-like macrophages have increased mitochondrial respiration and enhanced fatty acid metabolism. ECM, extracellular matrix; NO, nitric oxide; OXPHOS, oxidative phosphorylation; TCA, tricarboxylic acid cycle [85].

Macrophage polarization status should not be considered an on-off mechanism between pro- and anti-inflammatory phenotypes, but it often shows a spectrum of intermediate states even within the same cell

population [132]. Furthermore, it is not even fixed in time, because the initial polarization status is plastic and tends to shift from a state to another depending upon multiple external stimuli [86]. As a consequence of this operational definition, M1 and M2 phenotypes do not reflect the huge spectrum of the macrophagic population. This seems especially appropriate for the macrophagic populations found in the lungs where AMs have been reported to present a hybrid pattern expressing both M1 and $M2_a$ markers. AM are both crucial for first contact with pathogens and for maintaining homeostasis in the lungs. Given their double role, their activation is tightly regulated and balances both pro- and anti-inflammatory functions. Transcriptomic analysis showed that they express M1 typical proteins such as CD80, CD64, CD86, CD69, TLR2 and 4, CXC-chemokine ligand (CXCL) 9,10 and 11, and CC-chemokine ligand 5 (CCL5), but also typical M2 markers (CD163, CD206, MARCO, matrix metalloproteinase (MMP) 2, 7 and 9, the tyrosine-protein kinase MER, growth arrest-specific proteins, CD163, stabilin, arginase, and the adenosine A3 receptor) [130, 131]. In healthy lungs, this phenotype remains stable even after exposure to environmental stimuli known to alter the alveolar environment, such as the pneumococcal colonization (Fig. 10). AM Pattern Recognition Receptors (PRRs) recognize the Pathogen-Associated

Molecular Patterns (PAMPs) and initiate the inflammatory process producing TNFα, IL-1β, and IFNγ [88]. At the same time, IL-10 and TGFβ and CD206, act as anti-inflammatory signals, reducing the inflammation status of alveoli. The AM peculiar low capacity to act as antigen-presenting cells (APC), to produce low levels of oxidation agents such as ROI and NO, and makes them particularly favorable for MTB dissemination [89, 90]. The presence of CD206 receptors on AMs further facilitates MTB cell enter and the scavenging of the immune response. Thus, the fate of MTB infection strongly depends on how MTB strains interact with AMs and how the resulting macrophagic signals activate or inhibit the recruitment of other immunity participants.

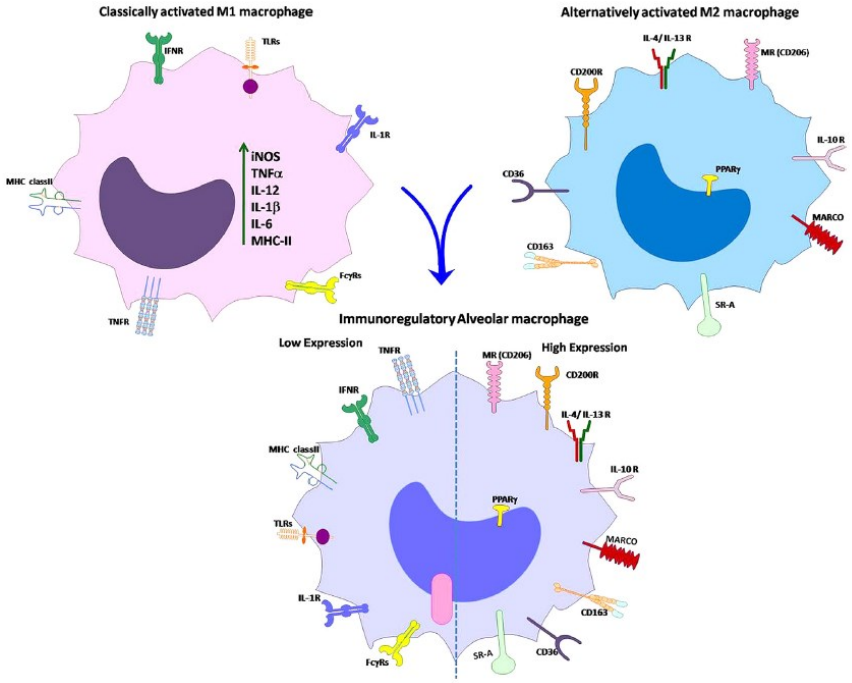


**Fig. 10**: Macrophage phenotypes and external stimuli that drive macrophagic differentiation. The figure reports the mainly expressed receptors found on those macrophage subtypes. AM expresses both M1 and M2 markers [91].

## 1.6 MTB/macrophage interaction

The first interaction between MTB and macrophages mostly occurs when the PRRs of the host cell encounters the recognition of PAMPs on the bacteria's surface. This recognition is driven by a pattern of receptors such as Toll-Like Receptors (TLR), C-type Lectin Receptors, Fc Receptors (FcR), Scavenger Receptors (SR) [9]. Activated PRRs give to the host cells a signal that leads to bacterial phagocytosis, and to the priming of cellular signals such as apoptosis, antigen processing-presentation, inflammasome activation, phagosome maturation, and autophagy [92]. Among other important macrophagic surface proteins, involved in the bacterial recognition/phagocytosis, CLR/CTL (membrane-bound calcium-dependent receptors) play a crucial role: the well-known CD206 recognizes the MTB mannose molecules present in LAM and ManLAM surface glycolipids. Under normal conditions, bacteria are phagocytized by the phagosome, which is then fused with a lysosome to form the phagolysosome. This phagolysosome is acidified to low pH (5.2) and enzymes are activated to degrade bacteria.

When phagocyted into the macrophages, MTB bacilli are exposed to an array of stresses, including oxidative and nitrosative stresses, iron restriction, starvation, and low pH; MTB has evolved several strategies to survive within the macrophages and cope with such unfavorable conditions. Indeed, MTB is able to hijack the macrophagic response and to survive within it by acting at different levels (Table 5).

**Table 5**: Principal MTB escape mechanisms [93]

| | MTB defence mechanisms | Definition |
|---|---|---|
| In the lungs | **Recruitment of permissive monocytes** | Virulent factor PDIM has been associated with the recruitment of low antimicrobial activity monocytes. |
| In the phagosome | **Phagocytosis through specific receptors** | The particular phagocytic receptors MTB engages may influence the ability of macrophage to control the infection (e.g. MR interaction with ManLAM, can impair phagosome maturation) |
| | **Modulation of phagosome maturation** | Prolonged retention of early endosomal markers and blocking of phagosomal maturation (e.g. PIM and ManLAM can impair the acquisition of PI3P and alter RAB protein dynamics. |
| | **Permeabilization of the phagosome** | EsxA and PDIM are among the virulence factor involved in the phagosomal escape mechanisms |
| | **Phagosome perforation** | ESX-I secretes different factors, including EsxA EsxB, involved in the rupture of the phagosome. |
| | **Phagocytosis through specific receptors** | The particular phagocytic receptors MTB engages may influence the ability of macrophage to control the infection (e.g. MR interaction with ManLAM, can impair phagosome maturation) |
| | **Blocking of phagosome maturation** | Interference with RAB, PI3K and the vacuolar H(+)-ATPase. Promotion of phagosome-early endosome fusion. Expression of ROS detoxifying enzymes (e.g. SodA). Blocking of acidification |
| In the cytosol | **Autophagy evasion** | MTB infection reduce the LC3 recruitment. MTB impairs both autophagy initiation and the fusion of autophagosomes with lysosomes at Rab7 level. |
| Other defence mechanisms | **Manipulation of the inflammasome** | Triggering of cGAS-STING patways deactivates the AIM2 inflammasome pathway reducing the production of pro-inflammatory cytokines. |
| | **Apoptosis impairing** | MTB reduces the efferocytosis process, increasing the necrosis levels and impairing apoptosis, by increasing the transcription of MTB anti-apoptotic genes (e.g. PknE, SigH, MPT64 and Rv3654c), thus limiting host ROS and apoptosis triggers factors |

The ability of MTB to block the phagosome maturation and the consequent acidification of the compartment, together with its capacity to survive in low pH environments have been reported to be among the main successful strategies to avoid bacilli eradication. During normal phagocytosis, cell membrane movements phagocyte external debris of bacteria into phagosomes. Macrophages normally recruit RAB5 in early phagosomes, which is replaced with RAB7 in an event called Rab conversion [94] (Fig. 11). At this level, Rab GTPases expressed on the phagosomal surface, attract the v-ATPases that are responsible for a first acidification of this compartment (pH 6). Then the early phagosomes fuse with lysosomes to further lower the internal pH (pH <5,5). This event is altered by MTB infection mainly by the activity of two MTB proteins (Kdk and PtpA) that interfere with its maturation by preventing the phagolysosome fusion event and its consequent acidification [95, 97].

Moreover, the ability to interfere with the phagosome maturation of the MTB ManLAM has been associated with its capacity to block the Phosphatidylinositol 3-phosphate (PI3K)-calmodulin complex, and the further attraction of v-GTPases and V-ATPases, thus stabilizing phagosome internal pH around 6,2. In addition, the interaction between MTB and CD206 causes the induction of anti-inflammatory cytokines and the reduction of the oxidative response [96].

When the phagolysosomal fusion occurs, MTB can survive in low pH environments thanks to its thick, low permeable membrane and securing enzymes, such as proteases MarP and RipA that allow the production of basic components, thus causing the neutralization of phagolysosome pH.

Escaping from phagosomes to the cytosol is the key mechanism that allow MTB to replicate in macrophages. The MTB genome encodes for 5 different ESX systems (ESX-1-ESX-5), a type VII secretion system that allows MTB to secrete soluble virulent factors [98]. *esx-1* is probably the most studied system and it encodes ESAT-6 (EsxA) and the 10 kDa Culture Filtrate Protein (CFP-10; EsxB), considered key virulence determinants of MTB and strong antigens for T-cells [99]. It has been shown that the ESX-1 secretion system together with the MTB membrane component PDIM enables phagolysosomal membrane disruption in macrophages, thus allowing MTB to reach the cytosol [23-100]. Studies on BCG strains (which do not possess the ESX-1 complex) have confirmed the presence of only virulent MTB strains in the cytosol after 4 days from the initial infection in macrophages, as also confirmed by recent FRET-based experiments [101].

Once MTB is in the cytosol, host cells activate cGAS systems to sense bacterial DNA and activate STING signals and Type I IFN production [102]. This leads to the expression of type I IFNs (alpha and β) and the subsequent release of IL-1b and IL-18 after the activation of the inflammasome response [103]. The cytosolic shift of MTB also activates TBK-1, a DNA-responsive kinase, which is involved in the recruitment of LC3-II and the subsequent activation of the autophagic flux. During autophagy, double-membrane autophagosomes phagocyte cytosolic pathogens (xenophagy)

and deliver them to fuse with acidic lysosomes, resulting in the release of lysosomal hydrolases to digest the enclosed contents. During MTB infection, IFNγ increased production, activates macrophages, and induces autophagy for bacterial degradation [189]. MTB has evolved several mechanisms to inhibit the autophagic response. H37Rv has been reported to induce IL-6 production, which selectively inhibits IFNγ induced autophagosome formation [104]. In addition, MTB *eis* gene modulates autophagy in macrophages, by increasing the acetylation of the H3 histones of the IL-10 gene promoter region, thus increasing its expression. Furthermore, MTB inhibits RAB-7, an endosomal marker involved in autophagosome formation [105].

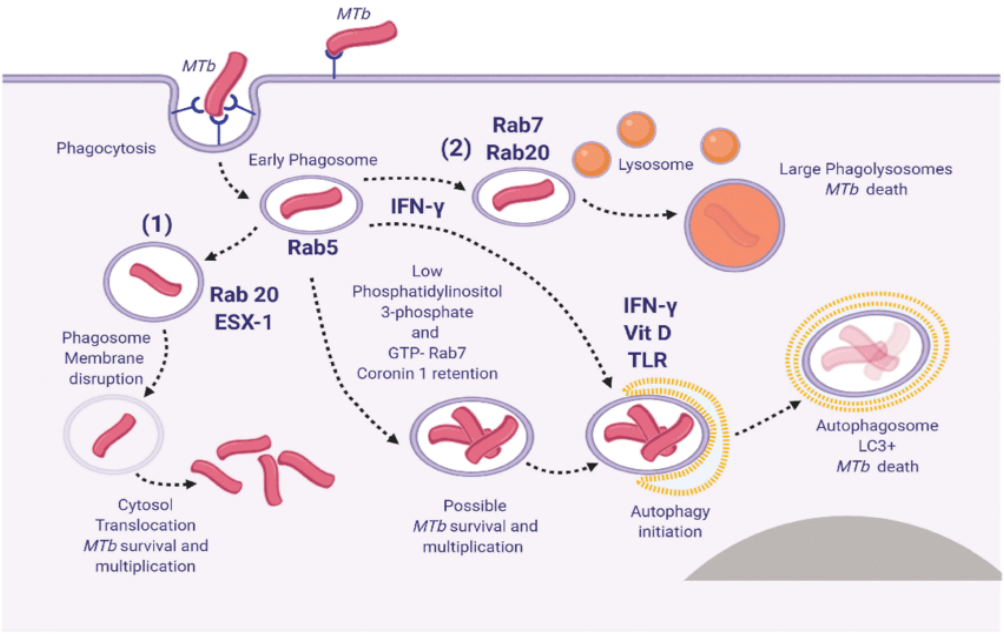


**Fig. 11**: MTB macrophage phagocytosis (1) MTB can prevent early phagosome maturation and by the action of Rab20-trafficking, ESX-1 destabilizes the phagosome membrane allowing bacteria to access the cytosol. (2) Some early phagosomes will undergo normal maturation, will fuse with the lysosomes and MTB will be killed. (3) Blocking of the early phagosome maturation (mainly by inhibiting PI3P generation) followed by MTB replication; (4) Delivery of the early endosomes or early-endosomes-to autolysosomes, where typically the activity of MTB it's controlled [106].

When unable to contain and eradicate MTB infection, engulfed macrophages die. MTB infected macrophages can undergo two forms of cell death (which may lead to drastic differences in the infection outcome): apoptosis or necrosis. Apoptosis is a process mediated by the caspase cascade, which results in the degradation of the cell and the formation of apoptotic vesicles. Apoptosis of MTB-infected cells is generally considered an advantage for the host because it eliminates pathogens, limits tissue inflammation, and promotes T-cell immunity activation [107, 108]. When an apoptotic macrophage dies, MTB is blocked into apoptotic bodies that are engulfed by activated macrophages and dendritic cells in a cascade process called efferocytosis. This facilitates the presentation of antigens to specific T-cells in order to activate the adaptative immunity. Necrotic death, on the other hand, is associated with the release of viable MTB bacilli for subsequent reinfection [107]. MTB generally kills infected cells via necrosis, which is characterized by the loss of macrophagic membrane integrity, and the release of cellular components in the extracellular space [109]. The role of MTB in cellular apoptosis is not clear. Several studies highlight that virulent MTB strains evolved several mechanisms to suppress host cell apoptosis and promote necrosis in order to replicate in the macrophages, and this effect is depending on both the virulence of the strains and on the multiplicity of the infection (MOI). MTB possesses several genes known to be involved in the apoptosis inhibition process (e.g., *nuoG* and *secA2*) [146]. Protein Phosphatase Mg2+/Mn2+-dependent 1A (PPM1A), has been identified as a key regulator of the innate antibacterial and antiviral response in macrophages and is targeted by MTB to prevent host macrophage apoptosis [107]. It is important to consider that the fate of an infected cell depends on many external factors and bacterial virulence only cannot explain the entire process. In general, virulent strains are associated with high levels of necrosis and apoptosis inhibition, however, there are studies that contradict this model, showing how even high virulent strains can induce a high level of apoptosis, even at low MOI; in fact, the *esxA*

gene, secreted by the ESX-1 system and encoding for the membranolytic protein EsxA, is considered pro-apoptotic [110].

## 1.7 Resistance to antimicrobials

Despite the introduction of an effective drug regimen (INH, RIF, PZA, and EMB), TB remains a major cause of morbidity and mortality globally. Drug resistance is due to genetic mutations (SNPs, deletions, and insertions), whereas drug tolerance is caused by epigenetic changes in gene expression and post-translational changes in drug-associated proteins.
WHO uses five categories to classify cases of drug-resistant TB: INH (INH)-resistant TB, RR-TB, MDR-TB, pre-XDR-TB, and XDR-TB (Table 6) [111].

**Table 6**: WHO drug resistance definitions [111]

| Drug resistance | Definition |
|---|---|
| **Isoniazid-resistant-TB** | Resistance to isoniazid |
| **RR-TB** | Resistance to rifampicin |
| **MDR-TB** | Resistance to both isoniazid and rifampicin |
| **Pre-XDR-TB** | TB caused by MTB strains that fulfil the definition of multidrug resistant and rifampicin-resistant TB (MDR/RR-TB) and which are also resistant to any fluoroquinolone. |
| **XDR-TB** | TB caused by MTB strains that fulfil the definition of MDR/RR-TB and which are also resistant to any fluoroquinolon and at least one addictional Group A drug. |

Anti-TB drugs are classified into three main categories. The first-line drugs are rifampicin (RIF / R), INH (INH / H), pyrazinamide (PZA / Z), ethambutol (EMB / E) (Table 7). They show a great activity against tuberculous bacilli and/or fewer side effects; they are the most used drugs and for this reason, the majority of resistance occurs against them.

**Table 7**: First line antitubercular drugs and their effects

| Anti TB Drugs (First Line) | Isoniazid | Rifampicin | Ethambutol | Pyrazinamide |
|---|---|---|---|---|
| **Main mechanism** | Mycolic acid syntesis inhibition | RNA polymerase inhibition | Mycolic acid-Arabinosyltransferase inhinibition | Mycolic acid inhibition |
| **Effect** | Bactericidal | Bactericidal | Bacteriostatic | Bactericidal |

Drugs used for the treatment of MDR- can be divided into three groups [114]: (Table 8)

- Group A: fluoroquinolones (FQ, levofloxacin and moxifloxacin), BDQ and linezolid (LZD)
- Group B: clofazimine (CFZ) and cycloserine or terizidone
- Group C: included all other medicines that can be used when a regimen cannot be composed with Group A and B agents.

**Table 8**: Grouping of medicines recommended for use in longer MDR-TB regimens [114]

| Groups and steps | Medicine | Abbreviation |
|---|---|---|
| Group A: Include all three medicines | Levofloxacin *or* moxifloxacin | Lfx Mfx |
| | Bedaquiline[b,c] | Bdq |
| | Linezolid[d] | Lzd |
| Group B: Add one or both medicines | Clofazimine | Cfz |
| | Cycloserine *or* terizidone | Cs Trd |
| Group C: Add to complete the regimen and when medicines from Groups A and B cannot be used | Ethambutol | E |
| | Delamanid[e] | Dlm |
| | Pyrazinamide[f] | Z |
| | Imipenem–cilastatin *or* meropenem[g] | Ipm–Cln Mpm |
| | Amikacin (*or* streptomycin)[h] | Am (S) |
| | Ethionamide *or* prothionamide[i] | Eto Pto |
| | *P*-aminosalicylic acid[i] | PAS |

The standard drug treatment regimen currently recommended by WHO, for drug-sensitive TB, consists of a 2-month intensive phase with RIF, INH, PZA, and EMB, followed by a 4-month phase with INH and RIF only. New regimens are now on use for MDR TB, in order to improve effectiveness and treatment adherence. In patients with confirmed RIF-susceptible, Isoniazid (INH)-resistant TB, treatment with RIF, EMB, PZA, and LEV is recommended for 6 months. A shorter BDQ-containing regimen of 9–12 months is recommended in patients with multidrug- or RIF-resistant TB. In multidrug TB all three Group A drugs and at least one Group B drug should be included to ensure the treatment to be effective. If only one or two Group A agents are used, both Group B agents are to be included. If the regimen cannot be composed with agents from Groups A and B alone, Group C agents are added (Table 8).

Genetic resistance to anti-tuberculous drugs develops thanks to spontaneous mutations at a variable frequency ($10^{-6}$ to $10^{-8}$) for the different genes involved (Table 9)[112]. Once resistance mutation has occurred, the consequent selection is caused by selective pressure linked to an inappropriate regimen. An increased treatment failure and death is associated with the most resistant forms of TB [113].

**Table 9**: List of genes reported to be associated with phenotypical resistance to the listed TB-drugs [115]

| Drug | Tier 1 | Tier 2 |
|---|---|---|
| INH | *ahpC, inhA, katG* | *mshA, ndh, Rv1258c, Rv2752c* |
| RIF | *rpoB* | *rpoA, rpoC, Rv2752c* |
| EMB | *embA, embB, embC* | *embR, ubiA* |
| PZA | *pncA, clpC1, panD* | *Rv1258c, PPE35, Rv3236c* |
| FQ | *gyrA, gyrB* | None |
| BDQ | *pepQ, Rv0678, mmpL5, mmpS5, atpE* | *Rv1979c* |
| LZD | *rplC, rrl* | None |
| CFZ | *pepQ, Rv0678, mmpL5, mmpS5* | *Rv1979c* |
| DLM | *fgd1, ddn, fbiA, fbiB, fbiC, Rv2983* | None |
| AMK | *rrs, eis, whiB7* | *whiB6, ccsA, fprA, aftB* |
| STM | *rrs, rpsL, gid, whiB7, Rv1258c* | *whiB6* |
| ETO | *inhA, ethA* | *ethR, mshA, Rv3083, ndh* |
| KAN | *rrs, eis, whiB7* | None |
| CAP | *rrs, tlyA* | *whiB6, ccsA, fprA, aftB* |

Tier 1: gene considered most probably to contain resistance mutations.

Tier 2: genes with a reasonable pre-test probability of containing resistance

INH: Isoniazid; RIF: Rifampicin; EMB: Etambutol; PZA: Pyrazinamide; FQ: Fluoroquinolon; BDQ: Bedaquilin; LZD: Linezolid; CFZ: Clofazimin; DLM: Delamanid; AMK: Amikacin; STM: Streptomicin; ETO: Ethionamide; KAN: Kanamicin; CAP: Capreomicin

RIF is a drug discovered in 1967 that has become the key drug for TB treatment due to its high activity against MTB. RIF is active both on replicating and dormant mycobacteria. RIF potent antibiotic activity is due to its ability to inhibit bacterial RNA polymerase (RNAP) and thus cause cell death. Bacterial RNAP is an essential holoenzyme, structurally very similar to the homologous enzyme in Eukaryotes and Archaea despite the low sequence identity. Over 95% of the mutations conferring RIF resistance are grouped into three main sites: RIF clusters I, II, and III, but most are found in an 81bp region of cluster I called RRDR (RIF resistance determining region) [116]. The most frequent replacements are Ser450Leu, His445Tyr, as the cytosine to thymine transitions are very common and are particularly favored in MTB because of its high G/C content and due to exposure to ROS (Reactive Oxygen Species), produced by the host's immune system during infection [117]. Mutations in essential genes cause a decrease in

cellular fitness, resulting in a slower rate of growth and lower virulence. In RIF-resistant strains of MTB, it has been found that compensatory mutations in *rpoA* and *rpoC* (coding for the α and β 'subunits of RNA polymerase) may be present which do not cause drug resistance but restore the original fitness by compensating the *rpoB* mutation [118].

INH is a prodrug capable of interfering with the biosynthesis of MTB bacterial cell wall by altering the synthesis of mycolic acids. It is active only on growing bacteria and, once it has entered the cell, it needs to be activated to its anionic form by a catalase-peroxidase KatG encoded by the *katG* (*Rv1908c*) gene. The active form reacts with NAD+ to form an INH-NAD adduct capable of binding the active site of the NADH-dependent enoyl-ACP reductase (InhA), a type II fatty acid synthetase enzyme (FAS II) that reduces the monounsaturated acyl ACP to acyl ACP [119]. Resistance to INH is associated with mutations in *katG* (50-95% of which 94% is Ser315Thr) and *inhA* (8-43%). Mutations in *ndh* gene, encoding for an NADH dehydrogenase, are associated with resistance to both INH and ethionamide. mutations in ndh gene cause defects in the oxidation of NADH to NAD thus accumulating NADH in the bacteria. High levels of NADH inhibits the binding of the INH-NAD adduct to InhA enzyme, impairing its activity [19].

EMB is a bacteriostatic drug that inhibits the proliferation of actively replicating bacteria and is used in combination with INH and RIF for standard TB treatments. It interferes with the transfer of arabinogalactan in the synthesis of the bacterial wall. The genes involved in drug resistance to EMB are part of the *emb* gene cluster, which includes 3 contiguous genes, *embA*, *embB* and *embC*. The first two encode for an arabinosyl transferase involved in the arabinosilation of arabinogalactans, while *embC* is involved in the arabinosylation of lipoarabinomannans. Most resistance-conferring mutations fall into a hot spot region called the ERDR (Ethambutol Resistance Determining Region) of *embB*, of which the most frequent is at codon 306 [120].

Unlike any other anti-TB antibiotics, PZA does not exhibit activity against growing bacteria at physiological pH; however, it is an indispensable drug both for sensitive strains and for the treatment of MDR cases [121]. It can act on latent state bacteria and only in acid pH environments, typically found within granulomas. PZA is an analog of nicotinic acid, it is a prodrug that needs activation in its active form (POA, pyrazinoic acid) by a pyrazinamidase encoded by the *pncA* gene [122]. PZA passively enters the cell and is converted into POA which is secreted by a weak efflux pump. Here, in an acidic environment, it can re-enter and accumulate in the cell, where it destroys the membrane energy potential by interfering with the production of energy. PZA acts only in acidic compartments such as phagolysosomes, or in low pH environments that are formed in some areas of the lungs during the early stages of infection [123]. The mutations that confer resistance can be found throughout the *pncA* gene and in the 82 base pairs upstream of the 5' region of the gene. Mutations associated with resistance to PZA have also been recently described in the *rpsA* and *panD* genes, but their contribution to PZA resistance is poorly known [124].

FQs inhibit type II topoisomerase (DNA gyrase) by binding to the enzyme and inhibiting DNA supercoiling. MTB has only topoisomerase II, unlike other bacteria that have topoisomerase II and IV. Resistance to FQs has been associated with the presence of mutations in a QRDR (Quinolone Resistance Determining Region) hot spot region in the *gyrA* gene and with mutations in the *gyrB* gene [125].

Delamanid (DLM) is a nitro-dihydro-imidazo-oxazole derivative that inhibits mycolic acid synthesis. Its antibacterial activity is specific for mycobacteria, inhibiting methoxy- and keto-mycolic acid synthesis through the F420 coenzyme and generating nitrous oxide. Mycobacterial resistance to DLM may develop due to a mutation in one of the five coenzyme F420 genes necessary for the activation of DLM. Mutations in the genes of the F420 signaling pathway of the MTBC (*dnn*, *fgd1*, *fbiA*, *fbiB*, *fbiC*, and *fbiD*), can lead to DLM resistance [126].

Bedaquiline (BDQ) is the first new antitubercular agent approved by the U.S. Food and Drug Administration (FDA) since 1970's. It possesses a potent bactericidal activity as an inhibitor of the ATP synthase proton pump. The main mutations that give resistance to BDQ are on the C subunit of ATP synthase encoded by the *atpE* (*Rv1305*) gene. In addition, mutations in the transcriptional regulator *Rv0687* gene were frequently associated with an increase of the BDQ MIC (Minimal Inhibitory Concentration) due to an upregulation of the MmpL5/MmpS5 efflux pump expression, which also leads to cross-resistance to CFZ [127].

The mechanism of antimicrobial action of CFZ is not entirely clear. In *Mycobacterium* TB, CFZ appears to act as a prodrug, which is reduced by the NADH complex causing the reduction of the available cellular ATP. CFZ is thought to compete with menaquinone (MK-4), a factor involved in the electron transfer chain [128].

LZD is an antibiotic in the oxazolidinone class. It inhibits protein synthesis by binding the bacterial 23S ribosomal RNA subunit and preventing the formation of the 70S ribosomal unit. Drug resistance for LZD usually occurs by SNPs in *rrl* and *rplC* genes. Mutations in *rplC* are associated with high LZD MIC values, while *rrl* mutations correlate with lower LZD MICs [129].

## Aim of the PhD project: role of the genetic diversity of MTB and its involvement on macrophage infection and on drug tolerance

Tuberculosis (TB) remains a major cause of morbidity and mortality worldwide and new vaccines candidates have not shown advantages compared to the Bacillus Calmette-Guerin (BCG) vaccine. *Mycobacterium tuberculosis* (MTB) evolved several strategies to survive within host cells and the metabolism of the bacterium is closely joined with the intraphagosomal milieu and to the immunological state of the host [141]. In addition, the genetic variability of MTB clinical isolates, and drug resistance development, have important consequences on the outcome of infections and on diagnostic approaches [43, 142]. In fact, as outlined strain-dependent variations (MTB lineages) have been associated with key pathogenic aspects [143, 144], thus contributing to the wide spectrum of TB clinical presentations [23, 145].

So far, the research in the field focused on either the host variability or pathogen variability in a mutual and exclusive way, and anyhow these topics remain in their infancy in TB. In this PhD project, we aimed at better understanding the role of the genetic diversity of MTB in the pathogenesis and in drug tolerance. In particular, for the pathogenesis, we hypothesized to design an experimental plan which brought together macrophage phenotypic plasticity and MTB genetic variability to advance our knowledge in the host-pathogen interactions. We analyzed the acidification of the phagosomes, the autophagic flux, the induction of apoptosis, and cytokine production in classically (M1) and alternatively (M2) activated THP-1 macrophage-like cells challenged with different MTB clinical isolates representative of ancient and modern phylogenetic lineages.

For a better understanding of the role of the genetic diversity of MTB in drug resistance mechanisms, we decided to focus our attention on the neglected topic of smallRNAs. In our laboratory, we consolidated the evidence available on the smallRNA candidates. This was the starting point for addressing the role of lineage-specific mutations mapping in smallRNAs

in this project. The analysis identified a mutation-specific for ancient lineages and mapping in the promoter region of the sRNA *ncRv0842c*, cis-encoded to the *Rv0842* gene, coding for a putative efflux pump reported to be involved in RIF resistance development. Accordingly, we characterized the role of *ncRv0842c* during RIF challenge to provide insights on the different mechanisms of drug tolerance among phylogenetically different strains of MTB.

## Bibliography


**1.** Gagneux S. Host-pathogen coevolution in human tuberculosis. *Philos Trans R Soc Lond B Biol Sci*. 2012;367(1590):850-859. doi:10.1098/rstb.2011.0316

**2.** Bates JH, Stead WW. The history of tuberculosis as a global epidemic. Med Clin North Am. 1993;77(6):1205-1217. doi:10.1016/s0025-7125(16)30188-2

**3.** Global tuberculosis control: WHO report 2011

**4.** Palomino et al., Tuberculosis 2007.

**5.** Canetti G. Infection caused by atypical mycobacteria and antituberculous immunity. Lille Med. 1970; 15:280–282. [PubMed: 5446090]

**6.** Stucki D, Brites D, Jeljeli L, et al. Mycobacterium tuberculosis lineage 4 comprises globally distributed and geographically restricted sublineages. Nat Genet. 2016;48(12):1535-1543. doi:10.1038/ng.3704

**7.** Smith NH, Hewinson RG, Kremer K, Brosch R, Gordon SV. Myths and misconceptions: the origin and evolution of Mycobacterium tuberculosis. Nat Rev Microbiol. 2009;7(7):537-544. doi:10.1038/nrmicro2165

**8.** Sreevatsan S, Pan X, Stockbauer KE, et al. Restricted structural gene polymorphism in the Mycobacterium tuberculosis complex indicates evolutionarily recent global dissemination. Proc Natl Acad Sci U S A. 1997;94(18):9869-9874. doi:10.1073/pnas.94.18.9869

**9.** Brosch R, Gordon SV, Marmiesse M, et al. A new evolutionary scenario for the Mycobacterium tuberculosis complex. Proc Natl Acad Sci U S A. 2002;99(6):3684-3689. doi:10.1073/pnas.052548299

**10.** Gupta RS, Lo B, Son J. Phylogenomics and Comparative Genomic Studies Robustly Support Division of the Genus *Mycobacterium* into an Emended Genus *Mycobacterium* and Four Novel Genera [published correction appears in Front Microbiol. 2019 Apr 09;10:714]. *Front Microbiol*. 2018;9:67. Published 2018 Feb 13. doi:10.3389/fmicb.2018.00067

**11.** Natarajan A, Beena PM, Devnikar AV, Mali S. A systemic review on tuberculosis. Indian J Tuberc. 2020;67(3):295-311. doi:10.1016/j.ijtb.2020.02.005

**12.** Khan A, Singh VK, Hunter RL, Jagannath C. Macrophage heterogeneity and plasticity in tuberculosis. J Leukoc Biol. 2019;106(2):275-282. doi:10.1002/JLB.MR0318-095RR

**13.** Volkman HE, Clay H, Beery D, Chang JC, Sherman DR, Ramakrishnan L. Tuberculous granuloma formation is enhanced by a mycobacterium virulence determinant. PLoS Biol. 2004;2(11):e367. doi:10.1371/journal.pbio.0020367

**14.** Cole ST, Brosch R, Parkhill J, et al. Deciphering the biology of Mycobacterium tuberculosis from the complete genome sequence [published correction appears in Nature 1998 Nov 12;396(6707):190]. Nature. 1998;393(6685):537-544. doi:10.1038/31159

**15.** Jungblut PR, Müller EC, Mattow J, Kaufmann SH. Proteomics reveals open reading frames in Mycobacterium tuberculosis H37Rv not predicted by genomics. Infect Immun. 2001;69(9):5905-5907. doi:10.1128/IAI.69.9.5905-5907.2001

**16.** Forrellad MA, Klepp LI, Gioffré A, et al. Virulence factors of the Mycobacterium tuberculosis complex. Virulence. 2013;4(1):3-66. doi:10.4161/viru.22329

**17.** Oliva G, Sahr T, Buchrieser C. Small RNAs, 5' UTR elements and RNA-binding proteins in intracellular bacteria: impact on metabolism and virulence. FEMS Microbiol Rev. 2015;39(3):331-349. doi:10.1093/femsre/fuv022

**18.** Heroven AK, Nuss AM, Dersch P. RNA-based mechanisms of virulence control in Enterobacteriaceae. RNA Biol. 2017;14(5):471-487. doi:10.1080/15476286.2016.1201617

**19.** Dersch P, Khan MA, Mühlen S, Görke B. Roles of Regulatory RNAs for Antibiotic Resistance in Bacteria and Their Potential Value as Novel Drug Targets. Front Microbiol. 2017;8:803. Published 2017 May 5. doi:10.3389/fmicb.2017.00803

**20.** Toledo-Arana A, Repoila F, Cossart P. Small noncoding RNAs controlling pathogenesis. Curr Opin Microbiol. 2007;10(2):182-188. doi:10.1016/j.mib.2007.03.004

**21.** WHO and Stop TB partnership, The Stop Tb Strategy, Building on and enhancing DOTS to meet the TB-related Millennium Development Goals, 2006.

**22.** Hunter RL. The Pathogenesis of Tuberculosis: The Early Infiltrate of Post-primary (Adult Pulmonary) Tuberculosis: A Distinct Disease Entity. Front Immunol. 2018;9:2108. Published 2018 Sep 19. doi:10.3389/fimmu.2018.02108

**23.** Malik AN, Godfrey-Faussett P. Effects of genetic variability of Mycobacterium tuberculosis strains on the presentation of disease. Lancet Infect Dis. 2005;5(3):174-183. doi:10.1016/S1473-3099(05)01310-1

**24.** Cadena AM, Fortune SM, Flynn JL. Heterogeneity in tuberculosis. Nat Rev Immunol. 2017;17(11):691-702. doi:10.1038/nri.2017.69

**25.** Egen JG, Rothfuchs AG, Feng CG, Winter N, Sher A, Germain RN. Macrophage and T cell dynamics during the development and disintegration of mycobacterial granulomas. Immunity. 2008;28(2):271-284. doi:10.1016/j.immuni.2007.12.010

**26.** Cooper AM, Mayer-Barber KD, Sher A. Role of innate cytokines in mycobacterial infection. Mucosal Immunol. 2011;4(3):252-260. doi:10.1038/mi.2011.13

**27.** Boisson-Dupuis S, El Baghdadi J, Parvaneh N, et al. IL-12Rβ1 deficiency in two of fifty children with severe tuberculosis from Iran, Morocco, and Turkey. PLoS One. 2011;6(4):e18524. Published 2011 Apr 13. doi:10.1371/journal.pone.0018524

**28.** McNab FW, Ewbank J, Howes A, et al. Type I IFN induces IL-10 production in an IL-27-independent manner and blocks responsiveness to IFN-γ for production of IL-12 and bacterial killing in Mycobacterium tuberculosis-infected macrophages. J Immunol. 2014;193(7):3600-3612. doi:10.4049/jimmunol.1401088

**29.** Yamada H, Mizumo S, Horai R, Iwakura Y, Sugawara I. Protective role of interleukin-1 in mycobacterial infection in IL-1 alpha/beta double-knockout mice. Lab Invest. 2000;80(5):759-767. doi:10.1038/labinvest.3780079

**30.** Marakalala MJ, Martinez FO, Plüddemann A, Gordon S. Macrophage Heterogeneity in the Immunopathogenesis of Tuberculosis. Front Microbiol. 2018;9:1028. Published 2018 May 23. doi:10.3389/fmicb.2018.01028

**31.** Fremond C, Allie N, Dambuza I, Grivennikov S, Yeremeev V, Quesniaux V, et al. 2005. Membrane TNF confers protection to acute mycobacterial infection. Respir Res 6 136, doi:10.1186/1465-9921-6-136

**32.** Mahamed D, Boulle M, Ganga Y, et al. Intracellular growth of Mycobacterium tuberculosis after macrophage cell death leads to serial killing of host cells [published correction appears in Elife. 2017 May 05;6:]. Elife. 2017;6:e22028. Published 2017 Jan 28. doi:10.7554/eLife.22028

**33.** Domingo-Gonzalez R, Prince O, Cooper A, Khader SA. Cytokines and Chemokines in Mycobacterium tuberculosis Infection. Microbiol Spectr. 2016;4(5):10.1128/microbiolspec.TBTB2-0018-2016. doi:10.1128/microbiolspec.TBTB2-0018-2016

**34.** Achtman M. Evolution, population structure, and phylogeography of genetically monomorphic bacterial pathogens. Annu Rev Microbiol. 2008;62:53-70. doi:10.1146/annurev.micro.62.081307.162832

**35.** Farhat MR, Shapiro BJ, Kieser KJ, et al. Genomic analysis identifies targets of convergent positive selection in drug-resistant Mycobacterium tuberculosis. Nat Genet. 2013;45(10):1183-1189. doi:10.1038/ng.2747

**36.** Osório NS, Rodrigues F, Gagneux S, et al. Evidence for diversifying selection in a set of Mycobacterium tuberculosis genes in response to antibiotic- and nonantibiotic-related pressure. Mol Biol Evol. 2013;30(6):1326-1336. doi:10.1093/molbev/mst038

**37.** Coscolla M, Gagneux S. Consequences of genomic diversity in Mycobacterium tuberculosis. Semin Immunol. 2014;26(6):431-444. doi:10.1016/j.smim.2014.09.012

**38.** Gehre F, Otu J, DeRiemer K, et al. Deciphering the growth behaviour of Mycobacterium africanum [published correction appears in PLoS Negl Trop Dis. 2013 Jun;7(6). doi:10.1371/annotation/fb002e1b-e345-4832-a793-d2f4988de308.]. PLoS Negl Trop Dis. 2013;7(5):e2220. Published 2013 May 16. doi:10.1371/journal.pntd.0002220

**39.** Rose G, Cortes T, Comas I, Coscolla M, Gagneux S, Young DB. Mapping of genotype-phenotype diversity among clinical isolates of mycobacterium tuberculosis by sequence-based transcriptional profiling. Genome Biol Evol. 2013;5(10):1849-1862. doi:10.1093/gbe/evt138

**40.** Ford CB, Shah RR, Maeda MK, et al. Mycobacterium tuberculosis mutation rate estimates from different lineages predict substantial differences in the emergence of drug-resistant tuberculosis. Nat Genet. 2013;45(7):784-790. doi:10.1038/ng.2656

**41.** McGrath M, Gey van Pittius NC, van Helden PD, Warren RM, Warner DF. Mutation rate and the emergence of drug resistance in Mycobacterium tuberculosis. J Antimicrob Chemother. 2014;69(2):292-302. doi:10.1093/jac/dkt364

**42.** Hershberg R, Lipatov M, Small PM, et al. High functional diversity in Mycobacterium tuberculosis driven by genetic drift and human demography. PLoS Biol. 2008;6(12):e311. doi:10.1371/journal.pbio.0060311

**43.** Homolka S, Niemann S, Russell DG, Rohde KH. Functional genetic diversity among Mycobacterium tuberculosis complex clinical isolates: delineation of conserved core and lineage-specific transcriptomes during intracellular survival. PLoS Pathog. 2010;6(7):e1000988. Published 2010 Jul 8. doi:10.1371/journal.ppat.1000988

**44.** Portevin D, Gagneux S, Comas I, Young D. Human macrophage responses to clinical isolates from the Mycobacterium tuberculosis complex discriminate between ancient and modern lineages. PLoS Pathog. 2011;7(3):e1001307. doi:10.1371/journal.ppat.1001307

**45.** Sarkar R, Lenders L, Wilkinson KA, Wilkinson RJ, Nicol MP. Modern lineages of Mycobacterium tuberculosis exhibit lineage-specific patterns of growth and cytokine induction in human monocyte-derived macrophages. PLoS One. 2012;7(8):e43170. doi:10.1371/journal.pone.0043170

**46.** Hirsh AE, Tsolaki AG, DeRiemer K, Feldman MW, Small PM. Stable association between strains of Mycobacterium tuberculosis and their human host populations. Proc Natl Acad Sci U S A. 2004;101(14):4871-4876. doi:10.1073/pnas.0305627101

**47.** O'Neill MB, Shockey A, Zarley A, et al. Lineage specific histories of Mycobacterium tuberculosis dispersal in Africa and Eurasia. Mol Ecol. 2019;28(13):3241-3256. doi:10.1111/mec.15120

**48.** Castets M, Boisvert H, Grumbach F, Brunel M, Rist N. Tuberculosis bacilli of the African type: preliminary note, Rev Tuberc Pneumol (Paris). 1968 Mar;32(2):179-84.

**49.** de Jong BC, Hill PC, Aiken A, et al. Progression to active tuberculosis, but not transmission, varies by Mycobacterium tuberculosis lineage in The Gambia. J Infect Dis. 2008;198(7):1037-1043. doi:10.1086/591504

**50.** Gagneux S, DeRiemer K, Van T, et al. Variable host-pathogen compatibility in Mycobacterium tuberculosis. Proc Natl Acad Sci U S A. 2006;103(8):2869-2873. doi:10.1073/pnas.0511240103

**51.** de Jong BC, Antonio M, Gagneux S. Mycobacterium africanum--review of an important cause of human tuberculosis in West Africa. PLoS Negl Trop Dis. 2010;4(9):e744. Published 2010 Sep 28. doi:10.1371/journal.pntd.0000744

**52.** Winglee K, Manson McGuire A, Maiga M, et al. Whole Genome Sequencing of Mycobacterium africanum Strains from Mali Provides Insights into the Mechanisms of Geographic Restriction. PLoS Negl Trop Dis. 2016;10(1):e0004332. Published 2016 Jan 11. doi:10.1371/journal.pntd.0004332

**53.** Cá B, Fonseca KL, Sousa J, et al. Experimental Evidence for Limited in vivo Virulence of Mycobacterium africanum. Front Microbiol. 2019;10:2102. Published 2019 Sep 10. doi:10.3389/fmicb.2019.02102

**54.** Gonzalo-Asensio J, Malaga W, Pawlik A, et al. Evolutionary history of tuberculosis shaped by conserved mutations in the PhoPR virulence regulator. Proc Natl Acad Sci U S A. 2014;111(31):11491-11496. doi:10.1073/pnas.1406693111

**55.** Chesne-Seck ML, Barilone N, Boudou F, Asensio JG, Kolattukudy PE, Martin C, et al. A Point Mutation in the Two-Component Regulator PhoP-PhoR Accounts for the Absence of Polyketide-Derived Acyltrehaloses but Not That of Phthiocerol Dimycocerosates in *Mycobacterium tuberculosis* H37Ra. J Bacteriol. 2008; 190:1329–1334.

**56.** Ofori-Anyinam B, Dolganov G, Van T, et al. Significant under expression of the DosR regulon in M. tuberculosis complex lineage 6 in sputum. Tuberculosis (Edinb). 2017;104:58-64. doi:10.1016/j.tube.2017.03.001

**57.** Newton SM, Smith RJ, Wilkinson KA, Nicol MP, Garton NJ, Staples KJ, et al. A deletion defining a common Asian lineage of Mycobacterium tuberculosis associates with immune subversion. Proc Natl Acad Sci USA. 2006; 103:15594–15598.

**58.** Wang C, Peyron P, Mestre O, et al. Innate immune response to Mycobacterium tuberculosis Beijing and other genotypes. PLoS One. 2010;5(10):e13594. Published 2010 Oct 25. doi:10.1371/journal.pone.0013594

**59.** Reiling N, Homolka S, Walter K, et al. Clade-specific virulence patterns of Mycobacterium tuberculosis complex strains in human primary macrophages and aerogenically infected mice. mBio. 2013;4(4):e00250-13. Published 2013 Jul 30. doi:10.1128/mBio.00250-13

**60.** Caws M, Thwaites G, Dunstan S, et al. The influence of host and bacterial genotype on the development of disseminated disease with Mycobacterium tuberculosis. PLoS Pathog. 2008;4(3):e1000034. Published 2008 Mar 28. doi:10.1371/journal.ppat.1000034

**61.** Lan NT, Lien HT, Tung le B, Borgdorff MW, Kremer K, van Soolingen D. Mycobacterium tuberculosis Beijing genotype and risk for treatment failure and relapse, Vietnam. Emerg Infect Dis. 2003;9(12):1633-1635. doi:10.3201/eid0912.030169

**62.** Cohen T, Sommers B, Murray M. The effect of drug resistance on the fitness of Mycobacterium tuberculosis. Lancet Infect Dis. 2003;3(1):13-21. doi:10.1016/s1473-3099(03)00483-3

**63.** Ebrahimi-Rad M, Bifani P, Martin C, et al. Mutations in putative mutator genes of Mycobacterium tuberculosis strains of the W-Beijing family. Emerg Infect Dis. 2003;9(7):838-845. doi:10.3201/eid0907.020803

**64.** Casali N, Nikolayevskyy V, Balabanova Y, et al. Evolution and transmission of drug-resistant tuberculosis in a Russian population. Nat Genet. 2014;46(3):279-286. doi:10.1038/ng.2878

**65.** Domenech P, Kolly GS, Leon-Solis L, Fallow A, Reed MB. Massive gene duplication event among clinical isolates of the Mycobacterium tuberculosis W/Beijing family. J Bacteriol. 2010;192(18):4562-4570. doi:10.1128/JB.00536-10

**66.** Golby P, Nunez J, Witney A, et al. Genome-level analyses of Mycobacterium bovis lineages reveal the role of SNPs and antisense transcription in differential gene expression. BMC Genomics. 2013;14:710. Published 2013 Oct 17. doi:10.1186/1471-2164-14-710

**67.** Constant P, Perez E, Malaga W, et al. Role of the pks15/1 gene in the biosynthesis of phenolglycolipids in the Mycobacterium tuberculosis complex. Evidence that all strains synthesize glycosylated p-hydroxybenzoic methyl esters and that strains devoid of phenolglycolipids harbor a frameshift mutation in the pks15/1 gene. J Biol Chem. 2002;277(41):38148-38158. doi:10.1074/jbc.M206538200

**68.** Sinsimer D, Huet G, Manca C, et al. The phenolic glycolipid of Mycobacterium tuberculosis differentially modulates the early host cytokine response but does not in itself confer hypervirulence. Infect Immun. 2008;76(7):3027-3036. doi:10.1128/IAI.01663-07

**69.** Schürch AC, van Soolingen D. DNA fingerprinting of Mycobacterium tuberculosis: from phage typing to whole-genome sequencing. Infect Genet Evol. 2012;12(4):602-609. doi:10.1016/j.meegid.2011.08.032

**70.** Chen YY, Chang JR, Huang WF, et al. The pattern of cytokine production in vitro induced by ancient and modern Beijing Mycobacterium tuberculosis strains. PLoS One. 2014;9(4):e94296. Published 2014 Apr 11. doi:10.1371/journal.pone.0094296

**71.** Behar SM, Divangahi M, Remold HG. Evasion of innate immunity by Mycobacterium tuberculosis: is death an exit strategy?. Nat Rev Microbiol. 2010;8(9):668-674. doi:10.1038/nrmicro2387

**72.** Sanoussi CN, Coscolla M, Ofori-Anyinam B, et al. Mycobacterium tuberculosis complex lineage 5 exhibits high levels of within-lineage genomic diversity and differing gene content compared to the type strain H37Rv. Microb Genom. 2021;7(7):000437. doi:10.1099/mgen.0.000437

**73.** Shanley CA, Henao-Tamayo MI, Bipin C, et al. Biology of clinical strains of Mycobacterium tuberculosis with varying levels of transmission. Tuberculosis (Edinb). 2018;109:123-133. doi:10.1016/j.tube.2018.02.003

**74.** Weagel E. et al., Macrophage Polarization and Its Role in Cancer, J Clin Cell Immunol 2015, 6:4 DOI: 10.4172/2155-9899.1000338

**75.** Martinez FO, Gordon S. The M1 and M2 paradigm of macrophage activation: time for reassessment. F1000Prime Rep. 2014;6:13. Published 2014 Mar 3. doi:10.12703/P6-13

**76.** Stein M, Keshav S, Harris N, Gordon S. Interleukin 4 potently enhances murine macrophage mannose receptor activity: a marker of alternative immunologic macrophage activation. J Exp Med. 1992;176(1):287-292. doi:10.1084/jem.176.1.287

**77.** Huang L, Nazarova EV, Tan S, Liu Y, Russell DG. Growth of Mycobacterium tuberculosis in vivo segregates with host macrophage metabolism and ontogeny. J Exp Med. 2018;215(4):1135-1152. doi:10.1084/jem.20172020

**78.** Kang PB, Azad AK, Torrelles JB, et al. The human macrophage mannose receptor directs Mycobacterium tuberculosis lipoarabinomannan-mediated phagosome biogenesis. J Exp Med. 2005;202(7):987-999. doi:10.1084/jem.20051239

**79.** Bogdan C, Röllinghoff M, Diefenbach A. Reactive oxygen and reactive nitrogen intermediates in innate and specific immunity. Curr Opin Immunol. 2000;12(1):64-76. doi:10.1016/s0952-7915(99)00052-7

**80.** Olive AJ, Sassetti CM. Tolerating the Unwelcome Guest; How the Host Withstands Persistent Mycobacterium tuberculosis. Front Immunol. 2018;9:2094. Published 2018 Sep 12. doi:10.3389/fimmu.2018.02094

**81.** Martin CJ, Carey AF, Fortune SM. A bug's life in the granuloma. Semin Immunopathol. 2016;38(2):213-220. doi:10.1007/s00281-015-0533-1

**82.** Lugo-Villarino G, Vérollet C, Maridonneau-Parini I, Neyrolles O. Macrophage polarization: convergence point targeted by mycobacterium tuberculosis and HIV. Front Immunol. 2011;2:43. Published 2011 Sep 15. doi:10.3389/fimmu.2011.00043

**83.** Schreiber T, Ehlers S, Heitmann L, et al. Autocrine IL-10 induces hallmarks of alternative activation in macrophages and suppresses antituberculosis effector mechanisms without compromising T cell immunity. J Immunol. 2009;183(2):1301-1312. doi:10.4049/jimmunol.0803567

**84.** Marino S, Cilfone NA, Mattila JT, Linderman JJ, Flynn JL, Kirschner DE. Macrophage polarization drives granuloma outcome during Mycobacterium tuberculosis infection. Infect Immun. 2015;83(1):324-338. doi:10.1128/IAI.02494-14

**85.** Russell DG, Huang L, VanderVen BC. Immunometabolism at the interface between macrophages and pathogens. Nat Rev Immunol. 2019;19(5):291-304. doi:10.1038/s41577-019-0124-9

**86.** Arora S, Olszewski MA, Tsang TM, McDonald RA, Toews GB, Huffnagle GB. Effect of cytokine interplay on macrophage polarization during chronic pulmonary infection with Cryptococcus neoformans. Infect Immun. 2011;79(5):1915-1926. doi:10.1128/IAI.01270-10

**87.** Mitsi E, Kamng'ona R, Rylance J, et al. Human alveolar macrophages predominately express combined classical M1 and M2 surface markers in steady state. Respir Res. 2018;19(1):66. Published 2018 Apr 18. doi:10.1186/s12931-018-0777-0

**88.** Hussell T, Bell TJ. Alveolar macrophages: plasticity in a tissue-specific context. Nat Rev Immunol. 2014;14(2):81-93. doi:10.1038/nri3600

**89.** MacMicking JD, North RJ, LaCourse R, Mudgett JS, Shah SK, Nathan CF. Identification of nitric oxide synthase as a protective locus against tuberculosis. Proc Natl Acad Sci U S A. 1997;94(10):5243-5248. doi:10.1073/pnas.94.10.5243

**90.** Fels AO, Cohn ZA. The alveolar macrophage. J Appl Physiol (1985). 1986;60(2):353-369. doi:10.1152/jappl.1986.60.2.353

**91.** Rajaram MV, Ni B, Dodd CE, Schlesinger LS. Macrophage immunoregulatory pathways in tuberculosis. Semin Immunol. 2014;26(6):471-485. doi:10.1016/j.smim.2014.09.010

**92.** Mortaz E, Adcock IM, Tabarsi P, et al. Interaction of Pattern Recognition Receptors with Mycobacterium Tuberculosis. J Clin Immunol. 2015;35(1):1-10. doi:10.1007/s10875-014-0103-7

**93.** Upadhyay S, Mittal E, Philips JA. Tuberculosis and the art of macrophage manipulation. Pathog Dis. 2018;76(4):fty037. doi:10.1093/femspd/fty037

**94.** Rink J, Ghigo E, Kalaidzidis Y, Zerial M. Rab conversion as a mechanism of progression from early to late endosomes. Cell. 2005;122(5):735-749. doi:10.1016/j.cell.2005.06.043

**95.** Upadhyay S, Mittal E, Philips JA. Tuberculosis and the art of macrophage manipulation. Pathog Dis. 2018;76(4):fty037. doi:10.1093/femspd/fty037

**96.** Vergne I, Fratti RA, Hill PJ, Chua J, Belisle J, Deretic V. Mycobacterium tuberculosis phagosome maturation arrest: mycobacterial phosphatidylinositol analog phosphatidylinositol mannoside stimulates early endosomal fusion. Mol Biol Cell. 2004;15(2):751-760. doi:10.1091/mbc.e03-05-0307

**97.** Wong D, Li W, Chao JD, et al. Protein tyrosine kinase, PtkA, is required for Mycobacterium tuberculosis growth in macrophages. Sci Rep. 2018;8(1):155. Published 2018 Jan 9. doi:10.1038/s41598-017-18547-9

**98.** Abdallah AM, Gey van Pittius NC, Champion PA, et al. Type VII secretion--mycobacteria show the way. Nat Rev Microbiol. 2007;5(11):883-891. doi:10.1038/nrmicro1773

**99.** Gröschel MI, Sayes F, Simeone R, Majlessi L, Brosch R. ESX secretion systems: mycobacterial evolution to counter host immunity. Nat Rev Microbiol. 2016;14(11):677-691. doi:10.1038/nrmicro.2016.131

**100.** Augenstreich J, Arbues A, Simeone R, et al. ESX-1 and phthiocerol dimycocerosates of Mycobacterium tuberculosis act in concert to cause phagosomal rupture and host cell apoptosis. Cell Microbiol. 2017;19(7):10.1111/cmi.12726. doi:10.1111/cmi.12726

**101.** van der Wel N, Hava D, Houben D, et al. M. tuberculosis and M. leprae translocate from the phagolysosome to the cytosol in myeloid cells. Cell. 2007;129(7):1287-1298. doi:10.1016/j.cell.2007.05.059

**102.** Collins AC, Cai H, Li T, et al. Cyclic GMP-AMP Synthase Is an Innate Immune DNA Sensor for Mycobacterium tuberculosis. Cell Host Microbe. 2015;17(6):820-828. doi:10.1016/j.chom.2015.05.005

**103.** Kupz A, Zedler U, Stäber M, Perdomo C, Dorhoi A, Brosch R, Kaufmann SH. 2016. ESAT-6-dependent cytosolic pattern recognition drives noncognate tuberculosis control in vivo. J Clin Invest 126:2109–2122. doi:10.1172/JCI84978

**104.** Nagabhushanam V, Solache A, Ting LM, Escaron CJ, Zhang JY, Ernst JD. Innate inhibition of adaptive immunity: Mycobacterium tuberculosis-induced IL-6 inhibits macrophage responses to IFN-gamma. J Immunol 171: 4750–4757, 2003. doi:10.4049/jimmunol.171.9.4750.

**105.** Lam A, Prabhu R, Gross CM, Riesenberg LA, Singh V, Aggarwal S. Role of apoptosis and autophagy in tuberculosis. Am J Physiol Lung Cell Mol Physiol. 2017;313(2):L218-L229. doi:10.1152/ajplung.00162.2017

**106.** Tăbăran AF, Matea CT, Mocan T, et al. Silver Nanoparticles for the Therapy of Tuberculosis. Int J Nanomedicine. 2020;15:2231-2258. Published 2020 Mar 31. doi:10.2147/IJN.S241183

**107.** Schaaf K, Smith SR, Duverger A, et al. Mycobacterium tuberculosis exploits the PPM1A signaling pathway to block host macrophage apoptosis. Sci Rep. 2017;7:42101. Published 2017 Feb 8. doi:10.1038/srep42101

**108.** Aberdein, J. D., Cole, J., Bewley, M. A., Marriott, H. M. & Dockrell, D. H. Alveolar macrophages in pulmonary host defence the unrecognized role of apoptosis as a mechanism of intracellular bacterial killing. Clin Exp Immunol 174, 193–202, doi: 10.1111/cei.12170 (2013).

**109.** Aguilo JI, Alonso H, Uranga S, et al. ESX-1-induced apoptosis is involved in cell-to-cell spread of Mycobacterium tuberculosis. Cell Microbiol. 2013;15(12):1994-2005. doi:10.1111/cmi.12169

**110.** Behar SM, Martin CJ, Booty MG, et al. Apoptosis is an innate defense function of macrophages against Mycobacterium tuberculosis. Mucosal Immunol. 2011;4(3):279-287. doi:10.1038/mi.2011.3

**111.** WHO announces updated definitions of extensively drug-resistant tuberculosis27 January 2021

**112.** Zhang Y, Yew WW. Mechanisms of drug resistance in Mycobacterium tuberculosis: update 2015. Int J Tuberc Lung Dis. 2015;19(11):1276-1289. doi:10.5588/ijtld.15.0389

**113.** Gandhi NR, Moll A, Sturm AW, et al. Extensively drug-resistant tuberculosis as a cause of death in patients co-infected with tuberculosis and HIV in a rural area of South Africa. Lancet. 2006;368(9547):1575-1580. doi:10.1016/S0140-6736(06)69573-1

**114.** WHO consolidated guidelines on tuberculosis Module 4: TreatmentDrug-resistant tuberculosis

**115.** WHO Catalogue of mutations in Mycobacterium tuberculosis complex and their association with drug resistance 2021

**116.** Koch A, Mizrahi V, Warner DF. The impact of drug resistance on Mycobacterium tuberculosis physiology: what can we learn from rifampicin?. Emerg Microbes Infect. 2014;3(3):e17. doi:10.1038/emi.2014.17

**117.** Warner DF. The role of DNA repair in M. tuberculosis pathogenesis. Drug Discov Today 2010; 7: e5–e11.

**118.** Comas I, Borrell S, Roetzer A, et al. Whole-genome sequencing of rifampicin-resistant Mycobacterium tuberculosis strains identifies compensatory mutations in RNA polymerase genes. Nat Genet. 2011;44(1):106-110. Published 2011 Dec 18. doi:10.1038/ng.1038

**119.** Rozwarski DA, Grant GA, Barton DH, Jacobs WR Jr, Sacchettini JC. Modification of the NADH of the isoniazid target (InhA) from Mycobacterium tuberculosis. Science. 1998;279(5347):98-102. doi:10.1126/science.279.5347.98

**120.** Zhang N, Torrelles JB, McNeil MR, et al. The Emb proteins of mycobacteria direct arabinosylation of lipoarabinomannan and arabinogalactan via an N-terminal recognition region and a C-terminal synthetic region. Mol Microbiol. 2003;50(1):69-76. doi:10.1046/j.1365-2958.2003.03681.x

**121.** Njire M, Tan Y, Mugweru J, et al. Pyrazinamide resistance in Mycobacterium tuberculosis: Review and update. Adv Med Sci. 2016;61(1):63-71. doi:10.1016/j.advms.2015.09.007

**122.** Scorpio A, Zhang Y. Mutations in pncA, a gene encoding pyrazinamidase/nicotinamidase, cause resistance to the antituberculous drug pyrazinamide in tubercle bacillus. Nat Med. 1996;2(6):662-667. doi:10.1038/nm0696-662

**123.** Zhang Y, Wade MM, Scorpio A, Zhang H, Sun Z. Mode of action of pyrazinamide: disruption of Mycobacterium tuberculosis membrane transport and energetics by pyrazinoic acid. J Antimicrob Chemother. 2003;52(5):790-795. doi:10.1093/jac/dkg446

**124.** Shi W, Zhang X, Jiang X, et al. Pyrazinamide inhibits trans-translation in Mycobacterium tuberculosis. Science. 2011;333(6049):1630-1632. doi:10.1126/science.1208813

**125.** Ramaswamy S, Musser JM. Molecular genetic basis of antimicrobial agent resistance in Mycobacterium tuberculosis: 1998 update. Tuber Lung Dis. 1998;79(1):3-29. doi:10.1054/tuld.1998.0002

**126.** Khoshnood S, Taki E, Sadeghifard N, et al. Mechanism of Action, Resistance, Synergism, and Clinical Implications of Delamanid Against Multidrug-Resistant Mycobacterium tuberculosis. Front Microbiol. 2021;12:717045. Published 2021 Oct 7. doi:10.3389/fmicb.2021.717045

**127.** Battaglia S, Spitaleri A, Cabibbe AM, et al. Characterization of Genomic Variants Associated with Resistance to Bedaquiline and Delamanid in Naive Mycobacterium tuberculosis Clinical Strains. J Clin Microbiol. 2020;58(11):e01304-20. Published 2020 Oct 21. doi:10.1128/JCM.01304-20

**128.** Mirnejad R, Asadi A, Khoshnood S, et al. Clofazimine: A useful antibiotic for drug-resistant tuberculosis. Biomed Pharmacother. 2018;105:1353-1359. doi:10.1016/j.biopha.2018.06.023

**129.** Bharadwaj R. Linezolid-resistant Mycobacterium tuberculosis: Will it impact the tuberculosis elimination programme?. Indian J Med Res. 2021;154(1):16-18. doi:10.4103/ijmr.IJMR_3537_20

**130.** Lim JJ, Grinstein S, Roth Z. Diversity and Versatility of Phagocytosis: Roles in Innate Immunity, Tissue Remodeling, and Homeostasis. Front Cell Infect Microbiol. 2017;7:191. Published 2017 May 23. doi:10.3389/fcimb.2017.00191

**131.** Shaykhiev R, Krause A, Salit J, et al. Smoking-dependent reprogramming of alveolar macrophage polarization: implication for pathogenesis of chronic obstructive pulmonary disease. J Immunol. 2009;183(4):2867-2883. doi:10.4049/jimmunol.0900473

**132.** Pena OM, Afacan N, Pistolic J, et al. Synthetic cationic peptide IDR-1018 modulates human macrophage differentiation. PLoS One. 2013;8(1):e52449. doi:10.1371/journal.pone.0052449

**133.** Solans L, Gonzalo-Asensio J, Sala C, et al. The PhoP-dependent ncRNA Mcr7 modulates the TAT secretion system in Mycobacterium tuberculosis. PLoS Pathog. 2014;10(5):e1004183. Published 2014 May 29. doi:10.1371/journal.ppat.1004183

**134.** Gerrick ER, Barbier T, Chase MR, et al. Small RNA profiling in Mycobacterium tuberculosis identifies MrsI as necessary for an anticipatory iron sparing response. Proc Natl Acad Sci U S A. 2018;115(25):6464-6469. doi:10.1073/pnas.1718003115

**135.** Arnvig KB, Young DB. Identification of small RNAs in Mycobacterium tuberculosis. Mol Microbiol. 2009;73(3):397-408. doi:10.1111/j.1365-2958.2009.06777.x

**136.** Houghton J, Rodgers A, Rose G, et al. The Mycobacterium tuberculosis sRNA F6 Modifies Expression of Essential Chaperonins, GroEL2 and GroES. Microbiol Spectr. 2021;9(2):e0109521. doi:10.1128/Spectrum.01095-21

**137.** Girardin RC, McDonough KA. Small RNA Mcr11 requires the transcription factor AbmR for stable expression and regulates genes involved in the central metabolism of Mycobacterium tuberculosis. Mol Microbiol. 2020;113(2):504-520. doi:10.1111/mmi.14436

**138.** Salina EG, Grigorov A, Skvortsova Y, et al. MTS1338, A Small Mycobacterium tuberculosis RNA, Regulates Transcriptional Shifts Consistent With Bacterial Adaptation for Entering Into Dormancy and Survival Within Host Macrophages. Front Cell Infect Microbiol. 2019;9:405. Published 2019 Nov 26. doi:10.3389/fcimb.2019.00405

**139.** Ami VKG, Balasubramanian R, Hegde SR. Genome-wide identification of the context-dependent sRNA expression in Mycobacterium tuberculosis. BMC Genomics. 2020;21(1):167. Published 2020 Feb 18. doi:10.1186/s12864-020-6573-5

**140.** Wright JR. Immunomodulatory functions of surfactant. Physiol Rev. 1997;77(4):931-962. doi:10.1152/physrev.1997.77.4.931

**141.** Russell DG. Mycobacterium tuberculosis and the intimate discourse of a chronic infection. Immunol Rev. 2011;240(1):252-268. doi:10.1111/j.1600-065X.2010.00984.x

**142.** Miotto P, Cabibbe AM, Mantegani P, et al. GenoType MTBDRsl performance on clinical samples with diverse genetic background. *Eur Respir J*. 2012;40(3):690-698. doi:10.1183/09031936.00164111

**143.** Rao Muvva J, Ahmed S, Rekha RS, et al. Immunomodulatory Agents Combat Multidrug-Resistant Tuberculosis by Improving Antimicrobial Immunity. *J Infect Dis*. 2021;224(2):332-344. doi:10.1093/infdis/jiab100

**144.** Kato-Maeda M, Metcalfe JZ, Flores L. Genotyping of Mycobacterium tuberculosis: application in epidemiologic studies. *Future Microbiol*. 2011;6(2):203-216. doi:10.2217/fmb.10.165

**145.** Scott C, Cavanaugh JS, Silk BJ, et al. Comparison of Sputum-Culture Conversion for Mycobacterium bovis and M. tuberculosis. *Emerg Infect Dis*. 2017;23(3):456-462. doi:10.3201/eid2303.161916

**146.** Butler RE, Brodin P, Jang J, et al. The balance of apoptotic and necrotic cell death in Mycobacterium tuberculosis infected macrophages is not dependent on bacterial virulence. PLoS One. 2012;7(10):e47573. doi:10.1371/journal.pone.0047573

## *Chapter 2*

# Interplay between macrophage heterogeneity and Mycobacterium tuberculosis complex phylogenetic lineages during infection


## Abstract

Host heterogeneity and bacterial genotypic background are key players in determining the outcome of infection, but their interplay remains largely uncharacterized. To reduce this knowledge gap, we considered cytokines production, phagolysosomal acidification, and mycobacterial survival during infection with either modern or ancient MTB lineages in classically and alternatively activated macrophages.

THP-1-derived macrophages either polarized toward M1 or M2 subtypes were infected with: H37Rv, H37Ra, Beijing (lineage L2) *M. africanum* (lineage L6). Infection was carried out at MOI 10:1. Live single-cell confocal microscopy was used to analyze phagolysosomal acidification at 6h and 24h post-infection (p.i.), autophagy and apoptosis at 24h p.i. Supernatants were collected at 4, 24, and 48h p.i. for measuring 20 cytokines/chemokines levels by Bio-Plex Multiplex-Immunoassay. After 48h p.i. cells were lysed for CFU count on 7H10 agar plates.

M2 infected cells induce the production of M1 specific marker, indicating an M1 shift at early phases. Variability among cytokine and chemokine pattern production appears to be higher in M1 cells, where the different MTB categories induce different host responses. In general, ancient/specialist strains induce a lower production of pro-inflammatory cytokine compared to modern/generalist strains.

Confocal microscopy showed that in M1 cells acidification is delayed by modern strains, whereas at earlier time points ancient virulent strains are not blocking acidification. At 24h p.i. none of the strains is blocking phagosomal acidification, but ancient strains displayed lower levels of acidification compared to modern strains. In M2 cells at 24h p.i. modern strains blocked acidification, whereas ancient strains were less efficient in

blocking the acidification of phagosomes. CFU data show a faster reduction of the bacterial load in L6 when compared to the modern ones. H37Ra CFUs are lower than H37Rv strains in both M1 and M2 cell types.

Our data highlight the role played in the infection by both the macrophage's activation status and the pathogen's features.

## Introduction

Despite our increasing understanding of the pathogenesis of tuberculosis (TB), several gaps remain to meet the challenge of eradicating the disease. *Mycobacterium tuberculosis* (MTB) survives in macrophages that are crucial immune system components for the formation of the granuloma, but also provide a survival niche from which the bacteria may disseminate. While in the macrophages, MTB is exposed to an array of stresses, including oxidative and nitrosative stresses, iron restriction, starvation, and low pH. MTB can block the phagosome maturation and the consequent acidification of the compartments, it can modulate the apoptosis and it's able to inhibit ROS production [1].

MTB has been considered a unique clone and the laboratory strain H37Rv has been largely used as a reference strain for research studies. However, the MTB phylogeny is composed of at least 7 different lineages and H37Rv is not representative of the genetic heterogeneity of this pathogen. This genotypic variation is associated with variation in transmission capacity and in the propensity to acquire drug resistance. This means that regional variation in the prevalence of specific lineages or sub-lineages can have consequences for the observed epidemiology of TB [2]. More broadly, the different distribution of the lineages also reflects the heterogeneity in the host-pathogen co-evolution and adaptation. Within the MTB complex (MTBC) it is possible to distinguish phylogenetically modern lineages (L2, L3, L4), that are considered to be more virulent, generalist (e.g. capable of causing disease in many different human populations), most geographically widespread, and ancient lineages (L1, L5, L6, L7), which are less virulent and that are more prone to infect populations in restricted geographical areas of the globe. Modern lineages 2 (Beijing), 3 (CAS/Delhi) and 4 (Haarlem, H37Rv) possess a large deletion known as TbD1 and are associated with major TB epidemics, and high transmission rate compared to Lineage 1 (Indo-oceanic), 5 and 6 (*M. africanum*). Modern MTB strains,

in general, induce low early inflammatory response than ancient lineages [3, 4].

Despite this microbe-centric classification, evaluating the virulent features of a microorganism is strongly related and dependent on the host system [5]. In this context, human heterogeneity at various levels should be taken into consideration. Besides genetic variability among individuals, human alveolar macrophages have been reported to show a mixed, plastic M1/M2 macrophagic phenotype [6, 7]. However, only a few studies kept into account the polarization status of the host's macrophages in *in vitro/ex vivo* infection models [8].

In this work, we studied early host-pathogen interaction between MTB and human macrophages, taking into consideration both host macrophage phenotypic variability (resembling alveolar macrophages plasticity) and MTB genetic diversity considering major phylogenetical differences. In particular, we focused our attention on phagolysosomal acidification, autophagy (self-degradative process), apoptosis (programmed cell death), and necrosis (cell injury) in classically (M1) or alternatively (M2) activated THP-1-derived macrophage-like cells. A single-cell approach was considered to better appreciate the heterogeneity of the fate of the host-pathogen interaction. Cytokines induction, macrophagic and bacterial survival were also considered to investigate the virulence features of the MTB lineages considered.

## Materials and Methods

- ***M. tuberculosis* strains selection and classification**

Clinical isolates representative of main ancient (L1, L6) and modern lineages (L2, L4) and previously characterized were kindly provided by Prof. Stefan Niemann (Research Center Borstel, Borstel, Germany) [9]. *M. tuberculosis* H37Rv NCTC 7416, *M. tuberculosis* H37Ra NCTC 7417, and *M. bovis* BCG NCTC 5692 were also included (Table 1).

Strain lineages were then classified and grouped according to seven categories considering the capacity to cause outbreaks and to develop drug resistance and/or association with worse clinical outcomes based on literature data (Table 1) [10-21]:

- ✓ **Basic**: grouping is simplified by considering ancient lineages less virulent, and modern lineages more virulent
- ✓ **Disease**: grouping is based on the ability of the strain to cause disease in an immunocompetent host
- ✓ **Phylogenesis**: grouping is defined according to the phylogeny of the lineages
- ✓ **Virulence, absolute**: grouping is based on virulence features
- ✓ **Virulence, relative**: grouping is based on virulence features in comparison with the H37Rv reference strain
- ✓ **Geographical distribution** and **host adaptation**: grouping is based on the definitions provided in Stucki et al related to the niche width of MTB strains [16].
- ✓ **Laboratory adaptation**: grouping is based on the laboratory selection of the strain [22]

- **Sequencing**

Whole-genome sequencing was performed by Illumina technology. Briefly, DNA libraries were generated using Nextera XT Library Prep kit (Illumina, San Diego, USA) according to the manufacturer's protocol, and libraries

were run on MiniSeq or NextSeq devices (Illumina, San Diego, USA). Variant calling for genetic analysis of the strains was performed according to the MTBseq pipeline (reference genome: *M. tuberculosis* H37Rv Genbank NC_000962.3) [23].

- **Electroporation**

All mycobacterial strains were engineered with the pSMT3::mCherry plasmid (Ex/Em 587-610 nm). The pSMT3::mCherry plasmid was a kind gift from Prof. Giovanni Delogu (Università Cattolica del Sacro Cuore, Rome, Italy). Briefly, bacteria were cultured in liquid 7H9 medium + Albumin Dextrose Catalase Oleic Acid (OADC) supplement (Becton Dickinson New Jersey, USA), 0.05% Tween® 80 (Sigma Aldrich, St. Luis, MO, USA) until $OD_{600}$ 0.4-0.6. Bacteria were centrifuged and washed twice with 10% glycerol, to eliminate salt and contaminants, in order to achieve the electro-competence, and resuspended in 10% glycerol for frozen stockage. Competent cells were electroporated (2500V, 25µF, 200 ohms) with 2µg of salt-free plasmid and selected on 50 µg/mL Hygromycin (Roche, Basel, Switzerland) 7H10 agar plates (Becton Dickinson, New Jersey, USA) [24].

For macrophage infection, the strains were thawed on selective Middlebrook 7H10 agar medium supplemented with 10% OADC supplement, 0.05% Tween® 80. and 50µg/mL Hygromycin. A single colony was picked up and used for inoculating Middlebrook 7H9 liquid medium supplemented with 10% Middlebrook OADC supplement, 0.05% Tween® 80. and 50µg/mL hygromycin and incubated at 37 °C until $OD_{600}$ ~0.3. Bacterial suspensions were centrifuged at 17000 g for 5 minutes, washed with sterile PBS, and resuspended in complete RPMI (cRPMI) medium w/o antibiotics, de-clumped by 10 passages through a 21-gauge needle, and diluted in cRPMI immediately before the infection.

**Table 1**: MTB strains considered in this study and classification used for the analysis of the results. Assay performed: y (yes) n (no)

| Strain | Alias | Lineage Nomenclature | Lineage type | Grouping | | | | | | | Assay performed | | | | | |
|---|---|---|---|---|---|---|---|---|---|---|---|---|---|---|---|---|
| | | | | Basic | Disease | Phylogenesis | Virulence_abs | Virulence_ref | Geo_host_adaptation | Lab adaptation | Phagosomal acidification | Autophagy | Apoptosis | Cytokine producion | CFU | Cell Survival |
| *M. africanum* 5684/02 | Afri 1 | 6 | ancient | Less/ancient | Causing | Ancient | Less | Less | Specialist | Clinical | y | y | y | y | y | y |
| *M. africanum* 10514/01 | Afri 2 | 6 | ancient | Less/ancient | Causing | Ancient | Less | Less | Specialist | Clinical | y | y | y | y | y | y |
| *M. bovis* BCG NCTC 5692 | BCG | bovis | animal | BCG | Non-causing | Animal | Less | Less | Other | Laboratory | y | y | n | n | n | y |
| *M. tuberculosis* 12594/02 | Beijing 1 | 2 | modern | More/modern | Causing | Modern | More | More | Generalist | Clinical | y | y | y | y | y | y |
| *M. tuberculosis* 1934/03 | Beijing 2 | 2 | modern | More/modern | Causing | Modern | More | More | Generalist | Clinical | y | y | y | y | y | y |
| *M. tuberculosis* CDC1551 | CDC | 4 | modern | More/modern | Causing | Modern | More | More | Intermediate | Clinical | y | n | n | n | n | y |
| *M. tuberculosis* 1797/03 | EAI 1 | 1 | ancient | Less/ancient | Causing | Ancient | Less | Less | Specialist | Clinical | y | n | n | n | n | n |
| *M. tuberculosis* 4850/03 | EAI 2 | 1 | ancient | Less/ancient | Causing | Ancient | Less | Less | Specialist | Clinical | y | n | n | n | n | n |
| *M. tuberculosis* H37Ra NCTC 7417 | H37Ra | 4 | modern | H37Ra | Non-causing | Modern | Less | Less | Other | Laboratory | y | y | n | y | y | y |
| *M. tuberculosis* H37Rv NTCT 7416 | H37Rv | 4 | modern | H37Rv | Causing | Modern | More | H37Rv | Generalist | Laboratory | y | y | y | y | y | y |

- **Cells preparation and infection for confocal microscopy** [25]

THP-1 (ATCC® TIB-202™) cells were differentiated in cRPMI (with L-glutamine 2mM, Hepes 10mM, Non-essential amino acids 100nM, Sodium Pyruvate 1mM, Sigma Aldrich, Missouri, USA) supplemented with 10% FBS (Fetal Bovin Serum, Euroclone, Italy), antibiotics (penicillin G 100 U/ml and streptomycin sulfate 100 U/ml, Sigma Aldrich Missouri, USA), and 100 nM of phorbol 12-myristate 13-acetate (PMA, Sigma Aldrich Missouri, USA) for 3 days in Eppendorf Cell Imaging 96-wells plates (55000 cells/well) bottom glass 170µm thick (Eppendorf, Germany) [26]. Type I collagen (Sigma Aldrich, Missouri, USA) was used for cell adhesion. Given the lack of standard protocols for recapitulating the alveolar macrophage *in vitro* cell lines, we opted to consider the two extremes of the dynamic state of activation of the macrophage. Three days after removal of the PMA, macrophage-like cells were polarized in cRPMI medium without antibiotics for 16 h with either lipopolysaccharide (50ng/mL, Sigma Aldrich Missouri, USA) to induce an M1-like phenotype or human IL-4 (20 ng/mL, E. coli-derived human IL-4 protein (R&Dsystems, Minnesota, USA) to induce an M2a-like phenotype prior to the infection (from here on "M2") [27]. Effective polarization of cells was evaluated by checking the expression of specific markers for M1 (TNFα, IL-1β, CD80. IL-6), and M2 (CD206, IL-10) (data not shown). THP-1 derived macrophages were infected with mycobacteria at a theoretical multiplicity of infection (MOI) 10:1. Infection was carried out by centrifugation (300 g x 5 min, room temperature) followed by two hours of incubation at 37 °C $CO_2$ 5.0%. Macrophage-like cells were then washed twice and supplemented with cRPMI without antibiotics. cRPMI without phenol red in case the infection was set up for imaging readouts.

- **Live imaging microscopy**

Phagolysosomal acidification: macrophages were stained with Hoechst 33342 NucBlue™ Live ReadyProbes™ Reagent (Ex/Em 360-460 nm, ThermoFisher, Massachusset, USA) for nuclei, and with LysoSensor™ Green DND-189 (Ex/Em 443-505 nm, $pK_a$ 5.2, ThermoFisher) for monitoring

phagolysosome acidification according to manufacturer's instructions. Indeed, the LysoSensor dye is an acidotropic probe that accumulates in acidic organelles as the result of protonation. This protonation also relieves the fluorescence quenching of the dye by its weakly basic side chain, resulting in an increase in fluorescence intensity. Thus, the LysoSensor Green exhibits a pH-dependent increase in fluorescence intensity upon acidification only, with very low background in the cytosol as it is almost nonfluorescent except when inside acidic compartments. All images have been acquired and analyzed using the same settings for allowing quantitative comparison of LysoSensor intensities (Supplementary Phagolysosomal acidification). Imaging experiments were performed at 6- and 24-hours post-infection (p.i.). For each strain, 6 images (2 positions for each well out of 3 wells per strain) were acquired as *z*-stacks (0.89 µm x 7 stacks) in at least two independent experiments.

Induction of autophagosomes: macrophages were stained with Hoechst 33342 for nuclei (Ex/Em 450-461 nm), and with CYTO-ID® Green (Ex/Em 499-548 nm) from the CYTO-ID® autophagy detection kit 2.0 (Enzo Biochem, Farmingdale, NYS, USA) according to manufacturer's instructions for monitoring induction of autophagosomes. The dye exhibits bright fluorescence upon incorporation into pre-autophagosomes, autophagosomes, and auto-phagolysosomes, whereas it shows limited staining of lysosomes [28]. Imaging experiments were performed at 24 h p.i. As control of autophagy induction, macrophages were treated with 500nM of rapamycin and 50µM of chloroquine overnight. For each strain, 8 images (2 positions for each well out of 4 wells per strain) were acquired as *z*-stacks (1.48 µm x 4 stacks) in at least two independent experiments.

Induction of apoptosis and necrosis: macrophages were stained with CytoCalcein Violet for cytosol (Ex/Em 405-450 nm, a marker for living cells cytoplasm), with Apopxin Green (Ex/Em 490-525 nm, apoptotic marker), and 7-AAD (Ex/Em 546/657, necrotic marker) according to the

Apoptosis/Necrosis assay kit (Abcam, Cambridge, UK) for monitoring apoptosis/necrosis at 24 h p.i. Apopxin targets the hallmark of apoptosis-exposed phosphatidylserine. Loss of plasma membrane integrity represents a straightforward approach to demonstrate late-stage apoptosis and necrosis, and it is detected by the ability of the membrane-impermeable 7-AAD to label the nucleus. As control of apoptosis, macrophages were treated with 5 μg/mL cyclohexamide and 2ng/mL TNFα overnight. For each strain, 4 images (2 positions for each well out of 2 wells per strain) were acquired as *z*-stacks (1.48 μm x 4 stacks) in at least two independent experiments.

All experiments were carried out using a Leica TCS SP5 confocal microscope equipped with an incubator chamber allowing to stably maintain cells at 37 °C in 5% $CO_2$. Unless otherwise specified, images were acquired as 16-bit, 1024×1024 resolution, TIFF files using a 63x, 1.40 NA immersion oil objective. A 405 nm UV diode laser was used for Hoechst 33342, a 458 nm Argon laser was used for LysoSensor, a 488 nm laser was used for CYTO-ID and Apopxin, a 561 nm laser was used for dsRed and 7-AAD.

- Immunofluorescence

THP-1 PMA derived macrophages were plated on 96well plates as described above and infected with MTB strains at MOI 10:1. After 24h post-infection cells were stained with LysoSensor Green and Hoechst in order to measure lysosomal acidification. After the image acquisition, well positions were saved for the subsequent immunofluorescence analysis on the same selected cells. Cells were fixed with 3,7% Paraformaldehyde for 10 minutes, permeabilized with an Hepes-Triton-X-100 buffer (Sigma Aldrich, Missouri, USA), and stained with antibodies. Targeted human protein: IFNγ, TNFα, MIP-1β, and MCP-1. Primary and secondary antibodies have been used at a final concentration of 1 μg/ml (Table 2).

For IFNγ and TNFα cells were analyzed at confocal microscopy using the pre-saved positions in order to compare acidification and cytokine production within the same cells.

**Table 2**: Primary and secondary antibodies for ImmunoFluorescence assay

| Protein target (human) | Primary antibody | | | Secondary antibody | | | |
|---|---|---|---|---|---|---|---|
| IFN-gamma | IFN gamma Monoclonal Antibody (25718) | Mouse/IgG2a | Unconjugated | Donkey anti-Mouse IgG (H+L) Highly Cross-Adsorbed Secondary Antibody | Donkey/IgG | Alexa Fluor Plus 647 | # A32787 |
| CCL4 (MIP-1 beta) | CCL4 Polyclonal Antibody | Rabbit/IgG | Unconjugated | Goat anti-Rabbit IgG (H+L) Highly Cross-Adsorbed Secondary Antibody | Goat/IgG | Alexa Fluor Plus 488 | # A32731 |
| TNF-alpha | TNF alpha Monoclonal Antibody (28401) | Mouse/IgG1 | Unconjugated | Donkey anti-Mouse IgG (H+L) Highly Cross-Adsorbed Secondary Antibody | Donkey/IgG | Alexa Fluor Plus 647 | # A32787 |
| MCP-1 | MCP-1 Polyclonal Antibody | Rabbit/IgG | Unconjugated | Goat anti-Rabbit IgG (H+L) Highly Cross-Adsorbed Secondary Antibody | Goat/IgG | Alexa Fluor Plus 488 | # A32731 |

- **Images and data analysis**

Images were processed for single-cell analysis with Fiji software [29]. Stacks have been analyzed by applying the maximum intensity projection method. As a general rule, at least 5 infected plus 5 non-infected cells (unless not available) were considered for each acquisition. Effective cell infection was visually inspected by the use of orthogonal views.

Phagolysosomal acidification: Single-cells were manually segmented. Acidified phagolysosomes and mycobacteria were selected by thresholding the 458 nm and the 561 nm channels, respectively. LysoSensor signal was acquired as mean signal intensity in cells region of interest (ROI). Acidified phagolysosomes and mycobacteria counts were also acquired for each single cell ROI. To analyze the spatial relationship between bacteria and lysosomes (colocalization) we wrote a custom pipeline in Matlab. Briefly, the confocal stacks are maximal projected and the individual cells are segmented manually. Next, the cell nuclei and the bacteria are automatically segmented, and the average LysoSensor intensity around the segmented bacteria L_bac is calculated (in a region of 1 pixel in width). Such intensity is compared to the average LysoSensor intensity in the cell $\langle L \rangle$, to provide an inclusion index $I_i=( L_{bac}-\langle L \rangle)/\langle L \rangle$ . Such index would be higher than zero when bacteria are located inside lysosomes and lower than zero when bacteria are excluded from lysosomal compartments. Random positioning of bacteria would provide $I_i=0$. All images have been acquired and analyzed using the settings as reported in Supplementary Phagolysosomal acidification.

Induction of autophagosomes: Single-cells were manually segmented. Autophagosomes and mycobacteria were selected by thresholding the 488 nm and the 561 nm channel, respectively. CYTO-ID signal was acquired as mean signal intensity in cells region of interest (ROI). mCherry mean signal across the cells ROI has been used as a proxy for mycobacterial burden. The autophagic pathway was analyzed by considering both the number and the size of autophagosomes [30]. The number of autophagosomes per cell was calculated using MatLab. All images have been acquired and analyzed using the settings as reported in Supplementary Autophagy.

Induction of apoptosis and necrosis: Single cells were manually segmented. CytoCalcein Violet, and Apopxin Green were acquired as mean signal intensity in cells region of interest (ROI). Signal from 7-AAD in the nuclei was never observed at the timepoints considered, thus analysis on the necrosis was not performed. Apoptotic cells have been identified using FlowClust (ver. 3.9), a Bioconductor R package implementing a robust model-based clustering approach based on multivariate t mixture models with the Box-Cox transformation for gating cell populations (rule of identifying outliers: 83% quantile) [31]. All images have been acquired and analyzed using the settings as reported in Supplementary Apoptosis. High mycobacterial burden was considered when dsRed signal was found to be equal or above the central value of the distribution of all dsRed signals in infected cells. Signals below this value were defined as low mycobacterial burden.

Statistical analysis: Linear mixed-effects (LME) models were employed to evaluate differences among strains in the three main fields of investigation (phagolysosomal acidification, autophagic pathway, and apoptosis) [32, 33]. Uninfected control THP-1 macrophages (M1 or M2) were used for normalization. The logarithmic transformation or the Ordered Quantile normalization transformation of the outcome were considered to satisfy underlying model assumptions. Zero-inflated Mixed-effects Poisson

models were applied to properly analyze count data with excess zeros [34]. These procedures were employed to properly account for the dependence structure among observations, by including nested random-effect terms, thus considering in the model unobservable sources of heterogeneity among experimental units. Post-hoc analysis was performed considering all the pairwise comparisons. Linear mixed-effects models were also applied to properly evaluate the relationship between two numeric variables. Analyses were performed using R statistical software [35].

- **Cells preparation and infection for CFUs and cytokine immunoassay** [36]

For CFU and cytokine analyses we used the same infection protocol as described for confocal microscopy, except for the fact that infections were carried out in 6well (Nunc™ Cell-Cultured Treated 1,25 x $10^6$ cells/well) instead of 96well plates. Bacteria used for these experiments are indicated in Table 1, and included modern strains H37Rv NCTC 7416, H37Ra NCTC 7417, 2x L2, 2x L6. Macrophage-like cells were then washed twice and supplemented with cRPMI without antibiotics. Supernatants were collected at 4, 24 and 48 hours post-infection and analyzed with Bio-Plex Pro™ Human Cytokine 20-plex Assay (Bio-Rad, California, USA) according to the manufacturer's instructions. Cytokines and chemokines included in the customized panel were selected in order to cover the entire spectrum of most commonly activated macrophagic molecules in responding to MTB infection. Pro-inflammatory cytokines: IL-1β, IL-6, TNFα, IL-15; IFNγ; IL-18; Anti-inflammatory cytokines: IL-1ra, IL-10; Chemokines: IP-10 (cxcl10-Interferon gamma-induced protein 10), MIP-1β (CCL4-Macrophage Inflammatory Protein), IL-8 (CXCL8), MCP-1 (CCL2-monocyte chemoattractant protein-1), RANTES (CCL5), SDF-1α (CXCL12), GRO-α (CXCL1), MIP-1α (CCL3-Macrophage Inflammatory Protein); Growth factors: VEGF (Vascular endothelial growth factor), PDGF-bb (Platelet-derived growth-stimulating factor), G-CSF (Granulocyte colony-stimulating factor), FGF basic.

Four independent experimental replicates were considered. Linear mixed-effects (LME) models were employed to evaluate differences among strains. Logarithmic and Ordered Quantile normalization transformations of the outcome were considered to satisfy underlying model assumptions. These procedures were employed to properly account for the dependence structure among observations, by including nested random-effect terms, thus considering in the model unobservable sources of heterogeneity among experimental units [32, 33]. Post-hoc analysis after LME was performed considering all the pairwise comparisons. Analyses were performed using R statistical software.

For mycobacterial survival, cells were lysed with sterile water. Supernatants and cell lysate were serially diluted and plated on 7H10 agar plate in order to count MTB CFUs at 4h, 24h, and 48h post-infection.

- **Macrophage survival**

THP-1 were plated and differentiated in 96well plates as described above (M1 or M2) and infected with MTB strains at MOI 5:1. MTB strains used for this experiment include the laboratory strains H37Rv, H37Ra, *M. bovis* BCG NCTC 5692, CDC 1551 and clinical strains 2x L2, 2x L6. After 48h and 5 days post-infection, cells viability was assessed by the use of the crystal violet assay as previously described [37]. Briefly, cells were fixed with cold (-20°C) methanol (Sigma Aldrich, Missouri, USA) and stained with crystal violet. This experiment relies on the detachment of adherent cells from cell culture plates during cell death where only live, adherent cells are fixed and stained with Crystal violet. After a wash step, the Crystal violet dye is solubilized with lysis buffer (0.1M sodium citrate, 50% Ethanol, pH 4,2) and measured by absorbance at 570 nm using the BioTek™ Gen5™ software (Agilent). The percentage of cell death compared to the uninfected control was considered.

## Results

We report here main findings using the grouping geographical-host (geo-host), as it somehow encompasses different features (phylogeny, distribution, host adaptation); however, it should be kept in mind that this grouping would lose to pick-up relevant differences between laboratory and clinical isolates and would not allow gaining details in terms of direct comparison with H37Rv, for example. For this reason, the same analyses described here for the group geo-host adaptation have been performed for all the grouping proposed in Table 1 and reported as Supplementary.

- **Phagolysosomal acidification**

The LysoSensor Green has been used to evaluate the level of acidification of phagolysosomes of THP-1 M1 and M2 macrophages infected with H37Rv, H37Ra, BCG, CDC, Afri, EAI and Beijing at 6 and 24 h p.i. (Fig. 1). A total of 7384 single cells (4098 at 6 h p.i.; 3286 at 24 h p.i.) were considered for the analysis (on average, for each strain tested, M1: 176 not infected cells + 172 infected cells; M2: 180 not infected cells + 174 infected cells) (Supplementary Phagolysosomal acidification). Data were normalized on THP-1 macrophages not infected control and strains were grouped as previously reported in Table 1.

At 6 h p.i. in M1 macrophages, only categories intermediate and other displayed blocking of phagolysosomal acidification, and specialist strains showed the highest number of acidified macrophages (50% vs <25% of all the other categories). A bystander effect in non-infected M1 macrophages was observed for specialist strains at 6 h p.i, despite it was not found statistically significant (Fig. 2). At 24 h p.i. none of the categories is blocking the acidification of the phagolysosomes. However, despite an increase in the acidification of the phagolysosomes was observed, the number of macrophages displaying such acidification was found generally low (<25%) (Fig. 3).

**Phagolysosomal acidification**

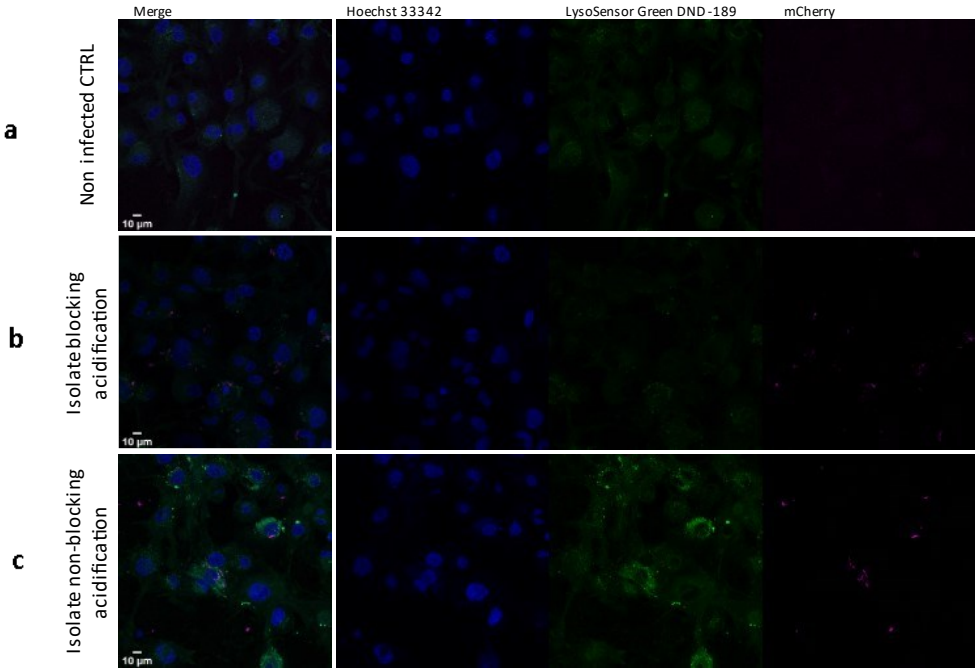


**Fig. 1**: THP-1 cells non-infected (a); infected with acidification-blocking bacteria (b); infected with non-acidification-blocking bacteria (c). The fluorescence images were acquired after staining with Lysosensor (Green) and Hoechst (Blue). Bacteria are reported in red. The reported images are illustrative of the pipeline adopted

**M1 – 6 h p.i.**

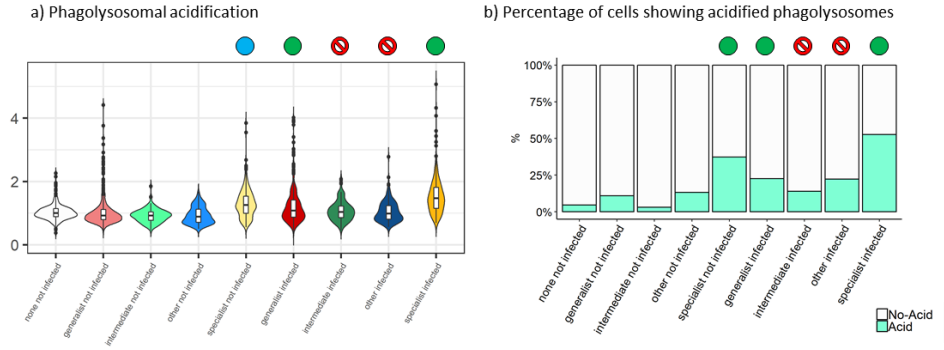


| Par | Value | Std.Error | p.value |
|---|---|---|---|
| (Intercept) | 0.0034 | 0.0759 | 0.9648 |
| groupgeneralist not infected | 0.0463 | 0.0553 | 0.4025 |
| groupintermediate not infected | -0.0365 | 0.0769 | 0.6354 |
| groupother not infected | -0.1016 | 0.0654 | 0.1208 |
| groupspecialist not infected | 0.1075 | 0.057 | 0.0597 |
| groupgeneralist infected | 0.1539 | 0.0553 | 0.0055 |
| groupintermediate infected | 0.1132 | 0.0771 | 0.142 |
| groupother infected | -0.0272 | 0.0656 | 0.6783 |
| groupspecialist infected | 0.2576 | 0.0572 | 0 |

| Contrast | estimate | SE | p.value |
|---|---|---|---|
| none not infected-generalist not infected | -0.0463 | 0.0553 | 0.483 |
| none not infected-intermediate not infected | 0.0365 | 0.0769 | 0.663 |
| none not infected-other not infected | 0.1016 | 0.0654 | 0.1812 |
| none not infected-specialist not infected | -0.1075 | 0.057 | 0.1303 |
| none not infected-generalist infected | -0.1539 | 0.0553 | 0.0164 |
| none not infected-intermediate infected | -0.1132 | 0.0771 | 0.2005 |
| none not infected-other infected | 0.0272 | 0.0656 | 0.6783 |
| none not infected-specialist infected | -0.2576 | 0.0572 | 0 |
| generalist not infected-intermediate not infected | 0.0827 | 0.0749 | 0.3597 |
| generalist not infected-other not infected | 0.1478 | 0.0673 | 0.0675 |
| generalist not infected-specialist not infected | -0.0612 | 0.0586 | 0.3748 |
| intermediate not infected-other not infected | 0.0651 | 0.0872 | 0.52 |
| intermediate not infected-specialist not infected | -0.1439 | 0.0798 | 0.1317 |
| other not infected-specialist not infected | -0.2091 | 0.0674 | 0.0067 |
| generalist infected-intermediate infected | 0.0407 | 0.0751 | 0.6414 |
| generalist infected-other infected | 0.1811 | 0.0675 | 0.0196 |
| generalist infected-specialist infected | -0.1037 | 0.0588 | 0.1337 |
| intermediate infected-other infected | 0.1404 | 0.0874 | 0.1734 |
| intermediate infected-specialist infected | -0.1445 | 0.0801 | 0.1317 |
| other infected-specialist infected | -0.2849 | 0.0676 | 1e-04 |
| generalist not infected-generalist infected | -0.1077 | 0.0141 | 0 |
| intermediate not infected-intermediate infected | -0.1497 | 0.022 | 0 |
| other not infected-other infected | -0.0744 | 0.0177 | 1e-04 |
| specialist not infected-specialist infected | -0.1502 | 0.0143 | 0 |

| Par | Estimate | se | OR | pvalue |
|---|---|---|---|---|
| (Intercept) | -3.5823 | 0.8396 | 0.0278 | 0 |
| groupgeneralist not infected | 0.6037 | 0.6792 | 1.8289 | 0.3741 |
| groupintermediate not infected | 0.0514 | 0.9665 | 1.0527 | 0.9576 |
| groupother not infected | 0.3002 | 0.735 | 1.3502 | 0.6829 |
| groupspecialist not infected | 1.5245 | 0.6226 | 4.5927 | 0.0143 |
| groupgeneralist infected | 2.1602 | 0.6538 | 8.6725 | 0.001 |
| groupintermediate infected | 1.826 | 0.862 | 6.2087 | 0.0341 |
| groupother infected | 0.9688 | 0.7215 | 2.6349 | 0.1793 |
| groupspecialist infected | 2.675 | 0.6242 | 14.513 | 0 |

| Contrast | estimate | SE | p.value |
|---|---|---|---|
| none not infected-generalist not infected | -0.6037 | 0.6792 | 0.4988 |
| none not infected-intermediate not infected | -0.0514 | 0.9665 | 0.9576 |
| none not infected-other not infected | -0.3002 | 0.735 | 0.745 |
| none not infected-specialist not infected | -1.5245 | 0.6226 | 0.0492 |
| none not infected-generalist infected | -2.1602 | 0.6538 | 0.0057 |
| none not infected-intermediate infected | -1.826 | 0.862 | 0.1024 |
| none not infected-other infected | -0.9688 | 0.7215 | 0.3074 |
| none not infected-specialist infected | -2.675 | 0.6242 | 1e-04 |
| generalist not infected-intermediate not infected | 0.5523 | 0.9195 | 0.6923 |
| generalist not infected-other not infected | 0.3035 | 0.7255 | 0.745 |
| generalist not infected-specialist not infected | -0.9208 | 0.5871 | 0.2157 |
| intermediate not infected-other not infected | -0.2489 | 1.0007 | 0.8385 |
| intermediate not infected-specialist not infected | -1.4731 | 0.9031 | 0.2057 |
| other not infected-specialist not infected | -1.2242 | 0.6569 | 0.1497 |
| generalist infected-intermediate infected | 0.3342 | 0.7838 | 0.745 |
| generalist infected-other infected | 1.1913 | 0.6837 | 0.1777 |
| generalist infected-specialist infected | -0.5149 | 0.5613 | 0.4988 |
| intermediate infected-other infected | 0.8571 | 0.887 | 0.4988 |
| intermediate infected-specialist infected | -0.8491 | 0.7907 | 0.4527 |
| other infected-specialist infected | -1.7062 | 0.6456 | 0.0329 |
| generalist not infected-generalist infected | -1.5565 | 0.339 | 1e-04 |
| intermediate not infected-intermediate infected | -1.7746 | 0.5888 | 0.0124 |
| other not infected-other infected | -0.6686 | 0.3247 | 0.1052 |
| specialist not infected-specialist infected | -1.1506 | 0.2256 | 0 |

**Fig. 2** : Phagosomal acidification at 6h p.i. in M1 cells with statistical reports

**M1 – 24 h p.i.**

a) Phagolysosomal acidification

b) Percentage of cells showing acidified phagolysosomes

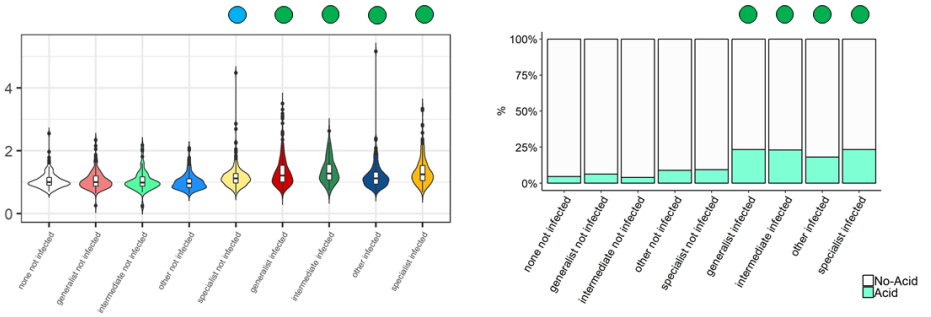


| Par | Value | Std.Error | p.value |
|---|---|---|---|
| (Intercept) | 0.0091 | 0.0429 | 0.8315 |
| groupgeneralist not infected | 0.0412 | 0.0323 | 0.2028 |
| groupintermediate not infected | 0.0206 | 0.0444 | 0.643 |
| groupother not infected | -0.0215 | 0.0381 | 0.5724 |
| groupspecialist not infected | 0.0263 | 0.0323 | 0.416 |
| groupgeneralist infected | 0.1879 | 0.0318 | 0 |
| groupintermediate infected | 0.2727 | 0.0435 | 0 |
| groupother infected | 0.1259 | 0.0367 | 6e-04 |
| groupspecialist infected | 0.1353 | 0.0324 | 0 |

| Contrast | estimate | SE | p.value |
|---|---|---|---|
| none not infected-generalist not infected | -0.0412 | 0.0323 | 0.3042 |
| none not infected-intermediate not infected | -0.0206 | 0.0444 | 0.7014 |
| none not infected-other not infected | 0.0215 | 0.0381 | 0.7014 |
| none not infected-specialist not infected | -0.0263 | 0.0323 | 0.5547 |
| none not infected-generalist infected | -0.1879 | 0.0318 | 0 |
| none not infected-intermediate infected | -0.2727 | 0.0435 | 0 |
| none not infected-other infected | -0.1259 | 0.0367 | 0.0019 |
| none not infected-specialist infected | -0.1353 | 0.0324 | 1e-04 |
| generalist not infected-intermediate not infected | 0.0206 | 0.0426 | 0.7014 |
| generalist not infected-other not infected | 0.0627 | 0.0377 | 0.1653 |
| generalist not infected-specialist not infected | 0.0149 | 0.0321 | 0.7014 |
| intermediate not infected-other not infected | 0.0421 | 0.0492 | 0.5538 |
| intermediate not infected-specialist not infected | -0.0057 | 0.0446 | 0.8977 |
| other not infected-specialist not infected | -0.0478 | 0.0372 | 0.3042 |
| generalist infected-intermediate infected | -0.0848 | 0.0412 | 0.0864 |
| generalist infected-other infected | 0.062 | 0.0358 | 0.1653 |
| generalist infected-specialist infected | 0.0526 | 0.0316 | 0.1653 |
| intermediate infected-other infected | 0.1468 | 0.0473 | 0.0047 |
| intermediate infected-specialist infected | 0.1374 | 0.0438 | 0.0047 |
| other infected-specialist infected | -0.0093 | 0.036 | 0.8296 |
| generalist not infected-generalist infected | -0.1467 | 0.0191 | 0 |
| intermediate not infected-intermediate infected | -0.2521 | 0.0325 | 0 |
| other not infected-other infected | -0.1475 | 0.0236 | 0 |
| specialist not infected-specialist infected | -0.109 | 0.0181 | 0 |

| Par | Estimate | se | OR | pvalue |
|---|---|---|---|---|
| (Intercept) | -3.1976 | 0.4593 | 0.0409 | 0 |
| groupgeneralist not infected | 0.3895 | 0.5143 | 1.4763 | 0.4488 |
| groupintermediate not infected | 0.1034 | 0.7496 | 1.109 | 0.8902 |
| groupother not infected | 0.9072 | 0.5479 | 2.4774 | 0.0977 |
| groupspecialist not infected | 0.5002 | 0.4771 | 1.649 | 0.2945 |
| groupgeneralist infected | 1.9578 | 0.4494 | 7.0841 | 0 |
| groupintermediate infected | 2.0397 | 0.5309 | 7.6883 | 1e-04 |
| groupother infected | 1.7688 | 0.4842 | 5.8637 | 3e-04 |
| groupspecialist infected | 1.6527 | 0.4506 | 5.2213 | 2e-04 |

| Contrast | estimate | SE | p.value |
|---|---|---|---|
| none not infected-generalist not infected | -0.3895 | 0.5143 | 0.6732 |
| none not infected-intermediate not infected | -0.1034 | 0.7496 | 0.8902 |
| none not infected-other not infected | -0.9072 | 0.5479 | 0.2607 |
| none not infected-specialist not infected | -0.5002 | 0.4771 | 0.5468 |
| none not infected-generalist infected | -1.9578 | 0.4494 | 1e-04 |
| none not infected-intermediate infected | -2.0397 | 0.5309 | 7e-04 |
| none not infected-other infected | -1.7688 | 0.4842 | 0.001 |
| none not infected-specialist infected | -1.6527 | 0.4506 | 0.001 |
| generalist not infected-intermediate not infected | 0.2861 | 0.6951 | 0.8168 |
| generalist not infected-other not infected | -0.5177 | 0.4955 | 0.5468 |
| generalist not infected-specialist not infected | -0.1106 | 0.4089 | 0.8583 |
| intermediate not infected-other not infected | -0.8038 | 0.7382 | 0.5468 |
| intermediate not infected-specialist not infected | -0.3967 | 0.6866 | 0.728 |
| other not infected-specialist not infected | 0.407 | 0.4483 | 0.5822 |
| generalist infected-intermediate infected | -0.0818 | 0.3691 | 0.8604 |
| generalist infected-other infected | 0.1891 | 0.3384 | 0.728 |
| generalist infected-specialist infected | 0.3051 | 0.2853 | 0.5468 |
| intermediate infected-other infected | 0.2709 | 0.4453 | 0.728 |
| intermediate infected-specialist infected | 0.387 | 0.4073 | 0.5822 |
| other infected-specialist infected | 0.116 | 0.3328 | 0.8313 |
| generalist not infected-generalist infected | -1.5683 | 0.3303 | 0 |
| intermediate not infected-intermediate infected | -1.9363 | 0.646 | 0.0093 |
| other not infected-other infected | -0.8616 | 0.3756 | 0.0655 |
| specialist not infected-specialist infected | -1.1526 | 0.2684 | 1e-04 |

**Fig. 3** : Phagosomal acidification at 24h p.i. in M1 cells with statistical reports

In M2 macrophages, none of the category is blocking the acidification of the phagolysosomes at 6 h p.i. and between 25% (other) and 50% (specialist and generalist) of macrophages showed acidification. A bystander effect in non-infected M2 macrophages was observed for specialist strains at 6 h p.i, with approx. 40% of bystander cells showed acidification (Fig. 4). As the time of infection progresses, generalist and intermediate categories are blocking the acidification of the phagolysosomes. The number of acidified macrophages also decreased below 25% except for the category other (50%). A bystander effect in non-infected M2 macrophages was observed for specialist strains at 24 h p.i, despite it was not found statistically significant (Fig. 5).

**M2 – 6 h p.i.**

a) Phagolysosomal acidification

b) Percentage of cells showing acidified phagolysosomes

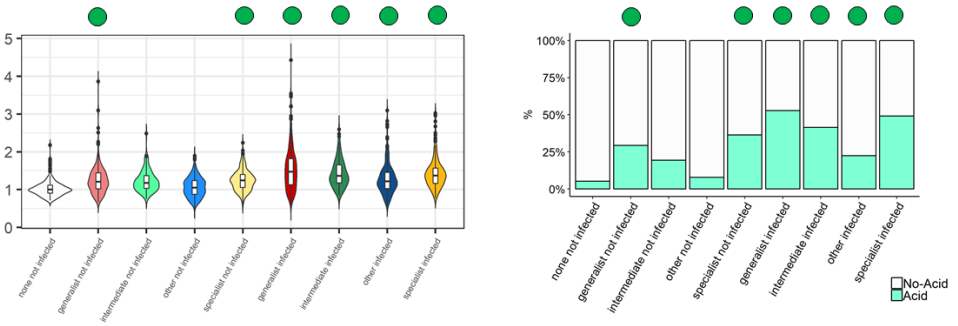


| Par | Value | Std.Error | p.value |
|---|---|---|---|
| (Intercept) | -0.0103 | 0.0505 | 0.8387 |
| groupgeneralist not infected | 0.1843 | 0.0441 | 0 |
| groupintermediate not infected | 0.1018 | 0.0612 | 0.0966 |
| groupother not infected | 0.0694 | 0.0518 | 0.1809 |
| groupspecialist not infected | 0.1644 | 0.0458 | 8e-04 |
| groupgeneralist infected | 0.3254 | 0.044 | 0 |
| groupintermediate infected | 0.2311 | 0.0615 | 2e-04 |
| groupother infected | 0.2086 | 0.052 | 1e-04 |
| groupspecialist infected | 0.2734 | 0.0459 | 0 |

| Par | Estimate | se | OR | pvalue |
|---|---|---|---|---|
| (Intercept) | -3.2009 | 0.6363 | 0.0407 | 0 |
| groupgeneralist not infected | 1.6574 | 0.5541 | 5.2456 | 0.0028 |
| groupintermediate not infected | 0.8911 | 0.7029 | 2.4377 | 0.2049 |
| groupother not infected | 1.2315 | 0.6648 | 3.4263 | 0.064 |
| groupspecialist not infected | 2.0146 | 0.5667 | 7.498 | 4e-04 |
| groupgeneralist infected | 3.1396 | 0.5477 | 23.0938 | 0 |
| groupintermediate infected | 2.4219 | 0.6849 | 11.2672 | 4e-04 |
| groupother infected | 2.6032 | 0.6298 | 13.5067 | 0 |
| groupspecialist infected | 2.8956 | 0.5666 | 18.0946 | 0 |

| Contrast | estimate | SE | p.value |
|---|---|---|---|
| none not infected-generalist not infected | -0.1843 | 0.0441 | 1e-04 |
| none not infected-intermediate not infected | -0.1018 | 0.0612 | 0.1656 |
| none not infected-other not infected | -0.0694 | 0.0518 | 0.2553 |
| none not infected-specialist not infected | -0.1644 | 0.0458 | 8e-04 |
| none not infected-generalist infected | -0.3254 | 0.044 | 0 |
| none not infected-intermediate infected | -0.2311 | 0.0615 | 5e-04 |
| none not infected-other infected | -0.2086 | 0.052 | 2e-04 |
| none not infected-specialist infected | -0.2734 | 0.0459 | 0 |
| generalist not infected-intermediate not infected | 0.0825 | 0.0598 | 0.251 |
| generalist not infected-other not infected | 0.1149 | 0.0535 | 0.064 |
| generalist not infected-specialist not infected | 0.0199 | 0.0468 | 0.6993 |
| intermediate not infected-other not infected | 0.0324 | 0.0691 | 0.6973 |
| intermediate not infected-specialist not infected | -0.0626 | 0.0634 | 0.3883 |
| other not infected-specialist not infected | -0.095 | 0.0535 | 0.1403 |
| generalist infected-intermediate infected | 0.0943 | 0.06 | 0.1855 |
| generalist infected-other infected | 0.1168 | 0.0537 | 0.064 |
| generalist infected-specialist infected | 0.052 | 0.0468 | 0.337 |
| intermediate infected-other infected | 0.0225 | 0.0694 | 0.7457 |
| intermediate infected-specialist infected | -0.0423 | 0.0637 | 0.5796 |
| other infected-specialist infected | -0.0648 | 0.0537 | 0.3039 |
| generalist not infected-generalist infected | -0.1411 | 0.0135 | 0 |
| intermediate not infected-intermediate infected | -0.1294 | 0.0207 | 0 |
| other not infected-other infected | -0.1393 | 0.0168 | 0 |
| specialist not infected-specialist infected | -0.109 | 0.0139 | 0 |

| Contrast | estimate | SE | p.value |
|---|---|---|---|
| none not infected-generalist not infected | -1.6574 | 0.5541 | 0.0067 |
| none not infected-intermediate not infected | -0.8911 | 0.7029 | 0.3383 |
| none not infected-other not infected | -1.2315 | 0.6648 | 0.1396 |
| none not infected-specialist not infected | -2.0146 | 0.5667 | 0.0011 |
| none not infected-generalist infected | -3.1396 | 0.5477 | 0 |
| none not infected-intermediate infected | -2.4219 | 0.6849 | 0.0011 |
| none not infected-other infected | -2.6032 | 0.6298 | 1e-04 |
| none not infected-specialist infected | -2.8956 | 0.5666 | 0 |
| generalist not infected-intermediate not infected | 0.7663 | 0.6158 | 0.3383 |
| generalist not infected-other not infected | 0.4259 | 0.5959 | 0.5697 |
| generalist not infected-specialist not infected | -0.3572 | 0.4812 | 0.5697 |
| intermediate not infected-other not infected | -0.3404 | 0.748 | 0.6773 |
| intermediate not infected-specialist not infected | -1.1236 | 0.6569 | 0.1744 |
| other not infected-specialist not infected | -0.7832 | 0.5857 | 0.3345 |
| generalist infected-intermediate infected | 0.7177 | 0.5921 | 0.3383 |
| generalist infected-other infected | 0.5364 | 0.5454 | 0.4593 |
| generalist infected-specialist infected | 0.244 | 0.474 | 0.6619 |
| intermediate infected-other infected | -0.1813 | 0.6974 | 0.7949 |
| intermediate infected-specialist infected | -0.4737 | 0.6363 | 0.5697 |
| other infected-specialist infected | -0.2924 | 0.5424 | 0.6619 |
| generalist not infected-generalist infected | -1.4822 | 0.2261 | 0 |
| intermediate not infected-intermediate infected | -1.5308 | 0.3463 | 1e-04 |
| other not infected-other infected | -1.3717 | 0.326 | 1e-04 |
| specialist not infected-specialist infected | -0.881 | 0.2259 | 3e-04 |

**Fig. 4** : Phagosomal acidification at 6h p.i. in M2 cells with statistical reports

**M2 – 24 h p.i.**

a) Phagolysosomal acidification

b) Percentage of cells showing acidified phagolysosomes

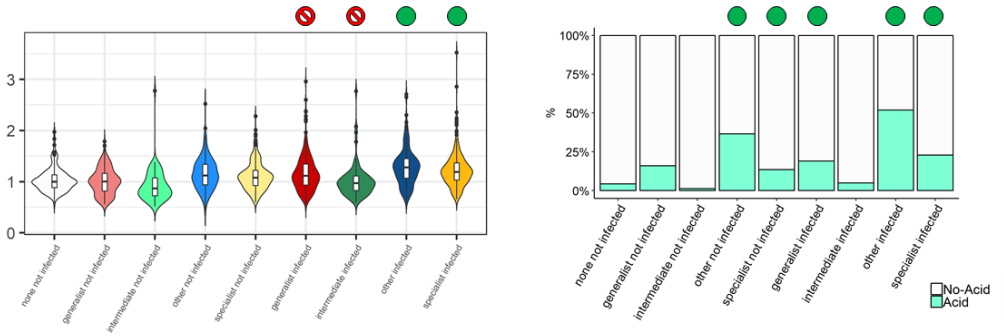


| Par | Value | Std.Error | p.value |
|---|---|---|---|
| (Intercept) | 0.0089 | 0.0545 | 0.87 |
| groupgeneralist not infected | -0.0689 | 0.0316 | 0.0292 |
| groupintermediate not infected | -0.0716 | 0.0421 | 0.0894 |
| groupother not infected | 0.0026 | 0.0364 | 0.9437 |
| groupspecialist not infected | 0.0109 | 0.0315 | 0.7289 |
| groupgeneralist infected | 0.0347 | 0.031 | 0.2632 |
| groupintermediate infected | -0.0083 | 0.0426 | 0.8447 |
| groupother infected | 0.1243 | 0.0356 | 5e-04 |
| groupspecialist infected | 0.1061 | 0.0316 | 8e-04 |

| Par | Estimate | se | OR | pvalue |
|---|---|---|---|---|
| (Intercept) | -3.574 | 0.6275 | 0.028 | 0 |
| groupgeneralist not infected | 1.1131 | 0.5049 | 3.0436 | 0.0275 |
| groupintermediate not infected | -0.0353 | 1.1207 | 0.9653 | 0.9749 |
| groupother not infected | 1.5681 | 0.4806 | 4.7973 | 0.0011 |
| groupspecialist not infected | 1.1996 | 0.4875 | 3.3188 | 0.0139 |
| groupgeneralist infected | 1.6838 | 0.4892 | 5.3859 | 6e-04 |
| groupintermediate infected | 1.4906 | 0.7107 | 4.4397 | 0.036 |
| groupother infected | 2.5577 | 0.4779 | 12.906 | 0 |
| groupspecialist infected | 1.9581 | 0.4754 | 7.0859 | 0 |

| Contrast | estimate | SE | p.value |
|---|---|---|---|
| none not infected-generalist not infected | 0.0689 | 0.0316 | 0.0585 |
| none not infected-intermediate not infected | 0.0716 | 0.0421 | 0.1431 |
| none not infected-other not infected | -0.0026 | 0.0364 | 0.9471 |
| none not infected-specialist not infected | -0.0109 | 0.0315 | 0.8747 |
| none not infected-generalist infected | -0.0347 | 0.031 | 0.3716 |
| none not infected-intermediate infected | 0.0083 | 0.0426 | 0.9215 |
| none not infected-other infected | -0.1243 | 0.0356 | 0.008 |
| none not infected-specialist infected | -0.1061 | 0.0316 | 0.0038 |
| generalist not infected-intermediate not infected | 0.0027 | 0.0403 | 0.9471 |
| generalist not infected-other not infected | -0.0715 | 0.0362 | 0.0882 |
| generalist not infected-specialist not infected | -0.0799 | 0.0314 | 0.0294 |
| intermediate not infected-other not infected | -0.0742 | 0.0465 | 0.1664 |
| intermediate not infected-specialist not infected | -0.0825 | 0.0423 | 0.0882 |
| other not infected-specialist not infected | -0.0084 | 0.0356 | 0.9215 |
| generalist infected-intermediate infected | 0.0431 | 0.0404 | 0.3812 |
| generalist infected-other infected | -0.0805 | 0.0351 | 0.0294 |
| generalist infected-specialist infected | -0.0714 | 0.0309 | 0.0507 |
| intermediate infected-other infected | -0.1328 | 0.0463 | 0.017 |
| intermediate infected-specialist infected | -0.1145 | 0.0429 | 0.0264 |
| other infected-specialist infected | 0.0182 | 0.035 | 0.7625 |
| generalist not infected-generalist infected | -0.1037 | 0.0171 | 0 |
| intermediate not infected-intermediate infected | -0.0683 | 0.0281 | 0.0529 |
| other not infected-other infected | -0.1217 | 0.0195 | 0 |
| specialist not infected-specialist infected | -0.0952 | 0.0158 | 0 |

| Contrast | estimate | SE | p.value |
|---|---|---|---|
| none not infected-generalist not infected | -1.1131 | 0.5049 | 0.066 |
| none not infected-intermediate not infected | 0.0353 | 1.1207 | 0.9749 |
| none not infected-other not infected | -1.5681 | 0.4806 | 0.0053 |
| none not infected-specialist not infected | -1.1996 | 0.4875 | 0.0416 |
| none not infected-generalist infected | -1.6838 | 0.4892 | 0.0035 |
| none not infected-intermediate infected | -1.4906 | 0.7107 | 0.0784 |
| none not infected-other infected | -2.5577 | 0.4779 | 0 |
| none not infected-specialist infected | -1.9581 | 0.4754 | 5e-04 |
| generalist not infected-intermediate not infected | 1.1483 | 1.0546 | 0.3489 |
| generalist not infected-other not infected | -0.455 | 0.3167 | 0.2412 |
| generalist not infected-specialist not infected | -0.0865 | 0.3425 | 0.8353 |
| intermediate not infected-other not infected | -1.6033 | 1.0551 | 0.2205 |
| intermediate not infected-specialist not infected | -1.2349 | 1.0548 | 0.3223 |
| other not infected-specialist not infected | 0.3685 | 0.2927 | 0.2939 |
| generalist infected-intermediate infected | 0.1932 | 0.5786 | 0.8056 |
| generalist infected-other infected | -0.8739 | 0.2967 | 0.011 |
| generalist infected-specialist infected | -0.2743 | 0.2897 | 0.4125 |
| intermediate infected-other infected | -1.0671 | 0.5957 | 0.1352 |
| intermediate infected-specialist infected | -0.4675 | 0.5895 | 0.4889 |
| other infected-specialist infected | 0.5996 | 0.2669 | 0.0659 |
| generalist not infected-generalist infected | -0.5707 | 0.2952 | 0.1064 |
| intermediate not infected-intermediate infected | -1.5259 | 1.1313 | 0.2661 |
| other not infected-other infected | -0.9896 | 0.2527 | 7e-04 |
| specialist not infected-specialist infected | -0.7585 | 0.2485 | 0.0091 |

**Fig. 5** : Phagosomal acidification at 24h p.i. in M2 cells with statistical reports

In terms of the number of mycobacteria per cell (MOI), in M1 macrophages no statistically relevant differences in effective MOI were observed at 6 h p.i. Colocalization with acidified compartments was similar among all the groups (Fig. 6). At 24h p.i. specialist strains showed lower MOI values compared to the other groups. Colocalization with acidified compartments was found lower for specialist and intermediate strains (Fig. 7).

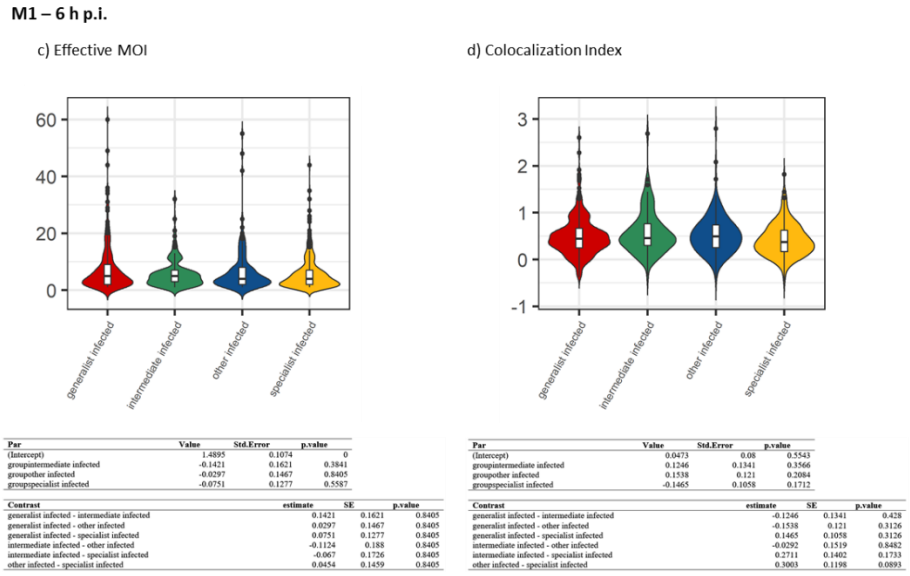


| Par | Value | Std.Error | p.value |
|---|---|---|---|
| (Intercept) | 1.4895 | 0.1074 | 0 |
| groupintermediate infected | -0.1421 | 0.1621 | 0.3841 |
| groupother infected | -0.0297 | 0.1467 | 0.8405 |
| groupspecialist infected | -0.0751 | 0.1277 | 0.5587 |

| Contrast | estimate | SE | p.value |
|---|---|---|---|
| generalist infected - intermediate infected | 0.1421 | 0.1621 | 0.8405 |
| generalist infected - other infected | 0.0297 | 0.1467 | 0.8405 |
| generalist infected - specialist infected | 0.0751 | 0.1277 | 0.8405 |
| intermediate infected - other infected | -0.1124 | 0.188 | 0.8405 |
| intermediate infected - specialist infected | -0.067 | 0.1726 | 0.8405 |
| other infected - specialist infected | 0.0454 | 0.1459 | 0.8405 |

| Par | Value | Std.Error | p.value |
|---|---|---|---|
| (Intercept) | 0.0473 | 0.08 | 0.5543 |
| groupintermediate infected | 0.1246 | 0.1341 | 0.3566 |
| groupother infected | 0.1538 | 0.121 | 0.2084 |
| groupspecialist infected | -0.1465 | 0.1058 | 0.1712 |

| Contrast | estimate | SE | p.value |
|---|---|---|---|
| generalist infected - intermediate infected | -0.1246 | 0.1341 | 0.428 |
| generalist infected - other infected | -0.1538 | 0.121 | 0.3126 |
| generalist infected - specialist infected | 0.1465 | 0.1058 | 0.3126 |
| intermediate infected - other infected | -0.0292 | 0.1519 | 0.8482 |
| intermediate infected - specialist infected | 0.2711 | 0.1402 | 0.1733 |
| other infected - specialist infected | 0.3003 | 0.1198 | 0.0893 |

**Fig. 6**: MTB colocalization with acidified compartments at 6h p.i in M1 cells and statistical reports

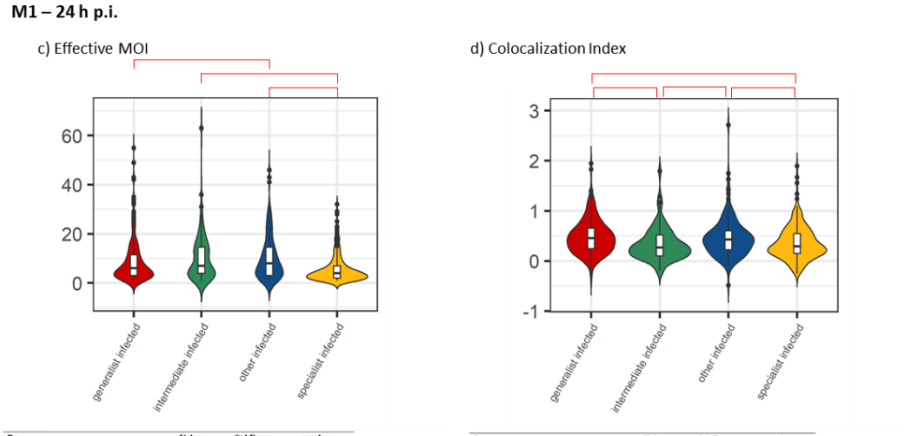


| Par | Value | Std.Error | p.value |
|---|---|---|---|
| (Intercept) | 1.6426 | 0.1203 | 0 |
| groupintermediate infected | 0.1433 | 0.1195 | 0.2348 |
| groupother infected | 0.4187 | 0.105 | 2e-04 |
| groupspecialist infected | -0.1752 | 0.0937 | 0.0664 |

| Contrast | estimate | SE | p.value |
|---|---|---|---|
| generalist infected - intermediate infected | -0.1433 | 0.1195 | 0.2348 |
| generalist infected - other infected | -0.4187 | 0.105 | 5e-04 |
| generalist infected - specialist infected | 0.1752 | 0.0937 | 0.0796 |
| intermediate infected - other infected | -0.2753 | 0.1417 | 0.0796 |
| intermediate infected - specialist infected | 0.3185 | 0.1325 | 0.0385 |
| other infected - specialist infected | 0.5938 | 0.1065 | 0 |

| Par | Value | Std.Error | p.value |
|---|---|---|---|
| (Intercept) | 0.1697 | 0.0802 | 0.0347 |
| groupintermediate infected | -0.535 | 0.1412 | 4e-04 |
| groupother infected | -0.0769 | 0.1162 | 0.5107 |
| groupspecialist infected | -0.3273 | 0.103 | 0.0023 |

| Contrast | estimate | SE | p.value |
|---|---|---|---|
| generalist infected - intermediate infected | 0.535 | 0.1412 | 0.0021 |
| generalist infected - other infected | 0.0769 | 0.1162 | 0.5107 |
| generalist infected - specialist infected | 0.3273 | 0.103 | 0.007 |
| intermediate infected - other infected | -0.4581 | 0.1592 | 0.0111 |
| intermediate infected - specialist infected | -0.2077 | 0.1496 | 0.2043 |
| other infected - specialist infected | 0.2504 | 0.1166 | 0.0537 |

**Fig. 7**: MTB colocalization with acidified compartments at 24h p.i in M1 cells and statistical reports

In M2 macrophages, specialist strains showed lower MOI values compared to the other groups at 6 h p.i.. Colocalization with acidified compartments was found lower for specialist and intermediate strains (Fig. 8). No statistically relevant differences in effective MOI at 24 h p.i. were observed, even though generalist strains displayed a higher distribution of MOI values. Colocalization with acidified compartments was similar among all the groups (Fig. 9).

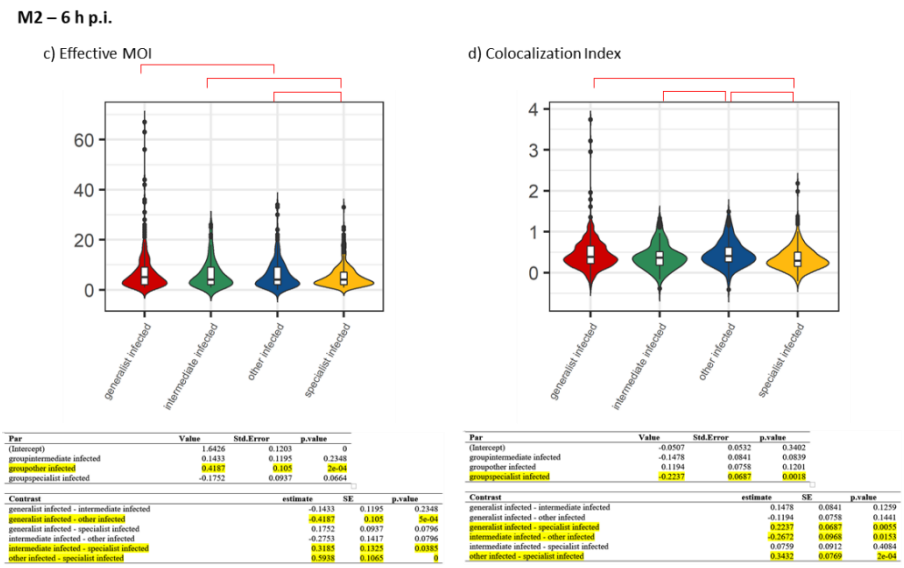


**Fig. 8**: MTB colocalization with acidified compartments at 6h p.i in M2 cells and statistical reports

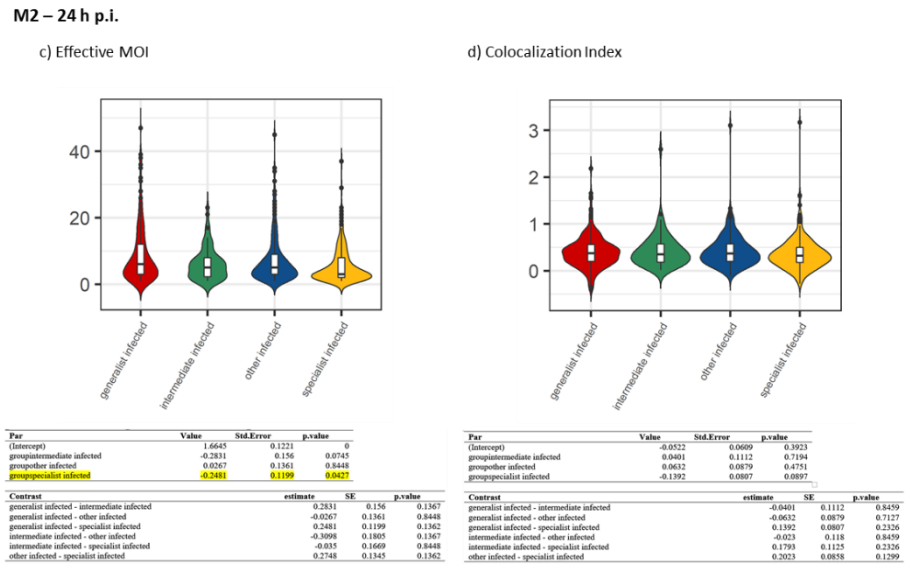


**Fig. 9**: MTB colocalization with acidified compartments at 24h p.i in M2 cells and statistical reports

No correlation between MOI and the colocalization index was found (Supplementary Phagolysosomal acidification).

- **Autophagic flux**

We evaluated the autophagic flux in THP-1 M1 and M2 macrophages infected with H37Rv, H37Ra, L6, and L2 at 24 h p.i. by the use of the CYTO-ID kit (Fig. 10). A total of 1960 single cells were considered for the analysis (on average, for each strain tested, M1: 64 not infected cells + 67 infected cells; M2: 60 not infected cells + 63 infected cells) (Supplementary Autophagy). The size and the number of autophagosomes were considered, and strains were grouped as previously reported in Table 1.

In M1 macrophages, only the group "other" showed some degree of autophagy; indeed, whereas also generalist and specialist groups are showing an increase in the number of autophagosomes, their size does not show statistically increased size, thus suggesting poor maturation and progression in the autophagic flux (Fig. 11).

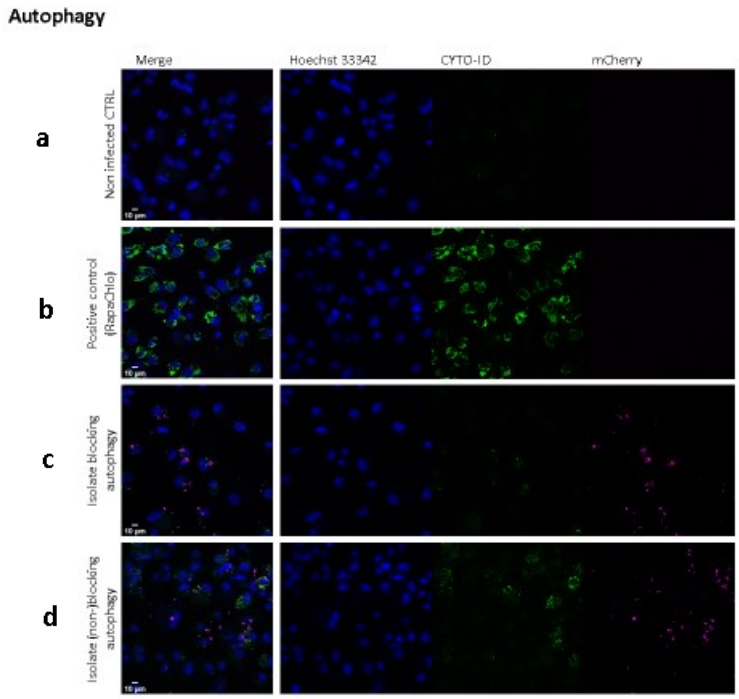


**Fig. 10**: THP-1 cells non-infected (a); treated with autophagy inducer (b); infected with autophagy-blocking bacteria (c); infected with autophagy non-blocking bacteria (d). The fluorescence images were acquired after staining with CYTO-ID (Green) and Hoechst (Blue). Bacteria are reported in red. The reported images are illustrative of the pipeline adopted

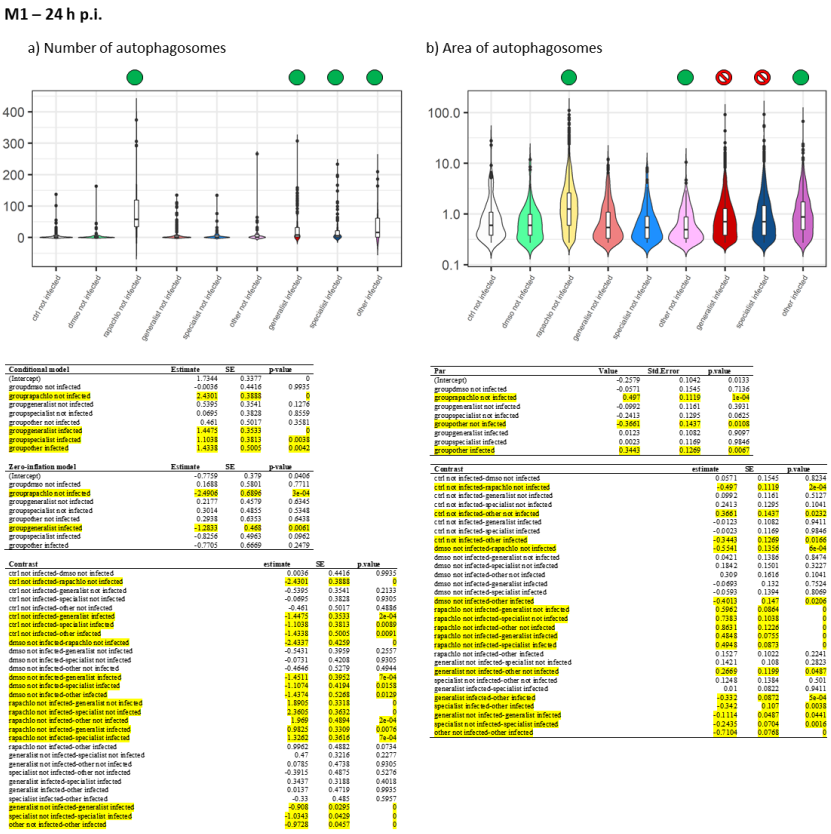


| Conditional model | Estimate | SE | p-value |
|---|---|---|---|
| (Intercept) | 1.7344 | 0.3377 | 0 |
| groupdmso not infected | -0.0036 | 0.4416 | 0.9935 |
| grouprapachlo not infected | 2.4301 | 0.3888 | 0 |
| groupgeneralist not infected | 0.5395 | 0.3541 | 0.1276 |
| groupspecialist not infected | 0.0695 | 0.3828 | 0.8559 |
| groupother not infected | 0.461 | 0.5017 | 0.3581 |
| groupgeneralist infected | 1.4475 | 0.3333 | 0 |
| groupspecialist infected | 1.1038 | 0.3813 | 0.0038 |
| groupother infected | 1.4338 | 0.5005 | 0.0042 |

| Zero-inflation model | Estimate | SE | p-value |
|---|---|---|---|
| (Intercept) | -0.7759 | 0.379 | 0.0406 |
| groupdmso not infected | 0.1688 | 0.5801 | 0.7711 |
| grouprapachlo not infected | 2.4908 | 0.6896 | 3e-04 |
| groupgeneralist not infected | 0.2177 | 0.4579 | 0.6345 |
| groupspecialist not infected | 0.3014 | 0.4855 | 0.5348 |
| groupother not infected | 0.2958 | 0.6533 | 0.6438 |
| groupgeneralist infected | -1.2833 | 0.488 | 0.0061 |
| groupspecialist infected | -0.8256 | 0.4983 | 0.0962 |
| groupother infected | -0.7705 | 0.6669 | 0.2479 |

| Contrast | estimate | SE | p.value |
|---|---|---|---|
| ctrl not infected-dmso not infected | 0.0036 | 0.4416 | 0.9935 |
| ctrl not infected-rapachlo not infected | -2.4301 | 0.3888 | 0 |
| ctrl not infected-generalist not infected | -0.5395 | 0.3541 | 0.2133 |
| ctrl not infected-specialist not infected | -0.0695 | 0.3828 | 0.9305 |
| ctrl not infected-other not infected | -0.461 | 0.5017 | 0.4886 |
| ctrl not infected-generalist infected | -1.4475 | 0.3333 | 2e-04 |
| ctrl not infected-specialist infected | -1.1038 | 0.3813 | 0.0039 |
| ctrl not infected-other infected | -1.4338 | 0.5005 | 0.0091 |
| dmso not infected-rapachlo not infected | -2.4337 | 0.4259 | 0 |
| dmso not infected-generalist not infected | -0.5431 | 0.3959 | 0.2557 |
| dmso not infected-specialist not infected | -0.0731 | 0.4208 | 0.9305 |
| dmso not infected-other not infected | -0.4646 | 0.5279 | 0.4944 |
| dmso not infected-generalist infected | -1.4511 | 0.3692 | 7e-04 |
| dmso not infected-specialist infected | -1.1074 | 0.4194 | 0.0158 |
| dmso not infected-other infected | -1.4374 | 0.5268 | 0.0129 |
| rapachlo not infected-generalist not infected | 1.8905 | 0.3318 | 0 |
| rapachlo not infected-specialist not infected | 2.3605 | 0.3832 | 0 |
| rapachlo not infected-other not infected | 1.969 | 0.4894 | 2e-04 |
| rapachlo not infected-generalist infected | 0.9422 | 0.3369 | 0.0076 |
| rapachlo not infected-specialist infected | 1.3262 | 0.3816 | 7e-04 |
| rapachlo not infected-other infected | 0.9962 | 0.4882 | 0.0734 |
| generalist not infected-specialist not infected | 0.47 | 0.3216 | 0.2277 |
| generalist not infected-other not infected | 0.0785 | 0.4738 | 0.9305 |
| specialist not infected-other not infected | -0.3915 | 0.4875 | 0.5276 |
| generalist infected-specialist infected | 0.3437 | 0.3188 | 0.4018 |
| generalist infected-other infected | 0.0137 | 0.4719 | 0.9935 |
| specialist infected-other infected | -0.33 | 0.485 | 0.5957 |
| generalist not infected-generalist infected | -0.908 | 0.0295 | 0 |
| specialist not infected-specialist infected | -1.0343 | 0.0429 | 0 |
| other not infected-other infected | -0.9728 | 0.0457 | 0 |

| Par | Value | Std.Error | p.value |
|---|---|---|---|
| (Intercept) | -0.2579 | 0.1042 | 0.0133 |
| groupdmso not infected | -0.0571 | 0.1545 | 0.7136 |
| grouprapachlo not infected | 0.497 | 0.1119 | 1e-04 |
| groupgeneralist not infected | -0.0992 | 0.1161 | 0.3931 |
| groupspecialist not infected | -0.2413 | 0.1295 | 0.0625 |
| groupother not infected | -0.3681 | 0.1437 | 0.0108 |
| groupgeneralist infected | 0.0123 | 0.1082 | 0.9097 |
| groupspecialist infected | 0.0023 | 0.1169 | 0.9846 |
| groupother infected | 0.3443 | 0.1289 | 0.0087 |

| Contrast | estimate | SE | p.value |
|---|---|---|---|
| ctrl not infected-dmso not infected | 0.0571 | 0.1545 | 0.8234 |
| ctrl not infected-rapachlo not infected | -0.497 | 0.1119 | 2e-04 |
| ctrl not infected-generalist not infected | 0.0992 | 0.1161 | 0.5127 |
| ctrl not infected-specialist not infected | 0.2413 | 0.1295 | 0.1041 |
| ctrl not infected-other not infected | 0.3681 | 0.1437 | 0.0232 |
| ctrl not infected-generalist infected | -0.0123 | 0.1082 | 0.9411 |
| ctrl not infected-specialist infected | -0.0023 | 0.1169 | 0.9846 |
| ctrl not infected-other infected | -0.3443 | 0.1289 | 0.0166 |
| dmso not infected-rapachlo not infected | -0.5541 | 0.1356 | 8e-04 |
| dmso not infected-generalist not infected | 0.0421 | 0.1386 | 0.8474 |
| dmso not infected-specialist not infected | 0.1842 | 0.1501 | 0.2227 |
| dmso not infected-other not infected | 0.309 | 0.1616 | 0.1041 |
| dmso not infected-generalist infected | -0.0693 | 0.132 | 0.7524 |
| dmso not infected-specialist infected | -0.0593 | 0.1394 | 0.8069 |
| dmso not infected-other infected | -0.4013 | 0.147 | 0.0206 |
| rapachlo not infected-generalist not infected | 0.5962 | 0.0864 | 0 |
| rapachlo not infected-specialist not infected | 0.7383 | 0.1038 | 0 |
| rapachlo not infected-other not infected | 0.8631 | 0.1226 | 0 |
| rapachlo not infected-generalist infected | 0.4848 | 0.0755 | 0 |
| rapachlo not infected-specialist infected | 0.4948 | 0.0873 | 0 |
| rapachlo not infected-other infected | 0.1527 | 0.1022 | 0.2341 |
| generalist not infected-specialist not infected | 0.1421 | 0.108 | 0.2823 |
| generalist not infected-other not infected | 0.2669 | 0.1199 | 0.0487 |
| specialist not infected-other not infected | 0.1248 | 0.1384 | 0.301 |
| generalist infected-specialist infected | 0.01 | 0.0822 | 0.9411 |
| generalist infected-other infected | -0.332 | 0.0872 | 5e-04 |
| specialist infected-other infected | -0.342 | 0.107 | 0.0038 |
| generalist not infected-generalist infected | -0.1114 | 0.0487 | 0.0441 |
| specialist not infected-specialist infected | -0.2435 | 0.0704 | 0.0016 |
| other not infected-other infected | -0.7104 | 0.0768 | 0 |

**Fig. 11**: Autophagic flux at 24h p.i. in M1 cells with statistical reports

In M2 macrophages, despite a certain increase in the number of autophagosomes, their size does not show statistically increased size, thus suggesting poor maturation and progression in the autophagic flux. None of the group is inducing autophagy (Fig. 12). No correlation between MOI and autophagy was found (Supplementary Autophagy).

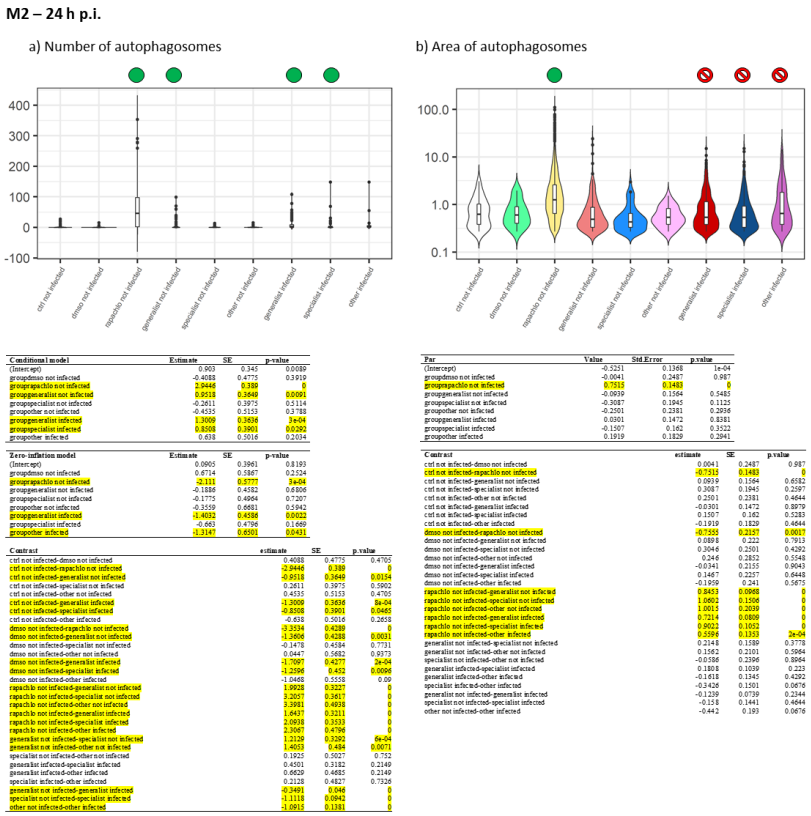


**Fig. 12**: Autophagic flux at 24h p.i. in M2 cells with statistical reports

- **Apoptosis and necrosis**

We evaluated the induction of apoptosis and necrosis THP-1 M1 and M2 macrophages infected with H37Rv, H37Ra, L6, and L2 at 24 h p.i. (Fig 13). A total of 2470 single cells were considered for the analysis (on average, for each strain tested, M1: 98 not infected cells + 75 infected cells; M2: 104 not infected cells + 79 infected cells) (Supplementary Apoptosis). Despite the marker for necrosis 7-AAD had a spectrum overlapping to one of mCherry mycobacteria (7-AAD Ex/Em 546/657; mCherry Ex/Em 587-610 nm) and both have been imaged using the 561 laser, the morphology of the bacteria and of the necrotic cells was completely different and easily distinguishable (Supplementary Apoptosis). However, in our testing conditions (24 h p.i.) necrosis was never observed, thus necrosis was not further considered.

In M1 macrophages, bystander non-infected cells of generalist and other strains showed increased apoptosis (40%). Despite not statistically

significant, also macrophages infected with generalist strains showed a similar increase in the percentage of apoptosis. Stratification of the data by mycobacterial burden showed higher apoptotic levels in bystander non-infected cells or in cells infected with lower mycobacterial load (Fig. 14).

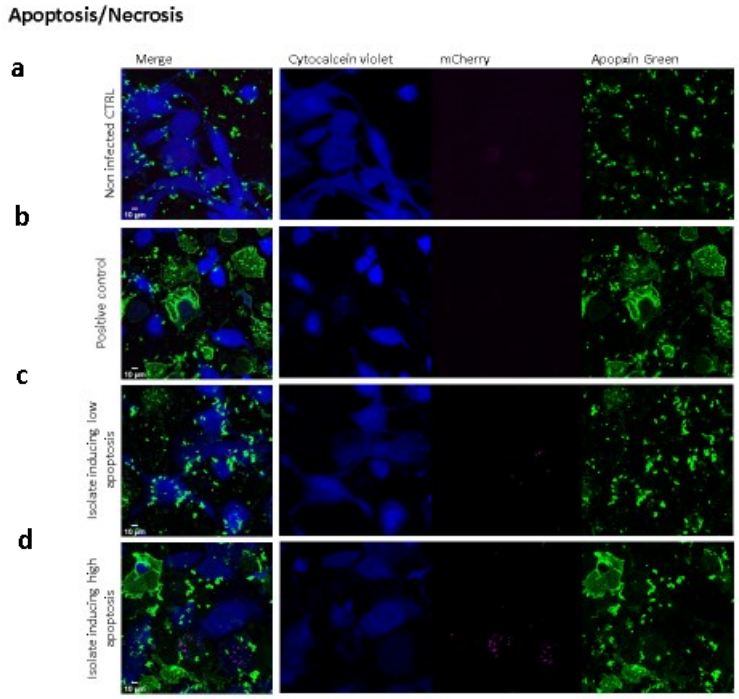


**Fig. 13**: THP-1 cells non-infected (a); treated with apoptosis inducer (b); infected with apoptosis-blocking bacteria (c); infected with apoptosis non-blocking bacteria (d). The fluorescence images were acquired after staining with CytoCalcein (Green) and Hoechst (Blue). Bacteria are reported in red. The reported images are illustrative of the pipeline adopted

**M1 – 24 h p.i.**

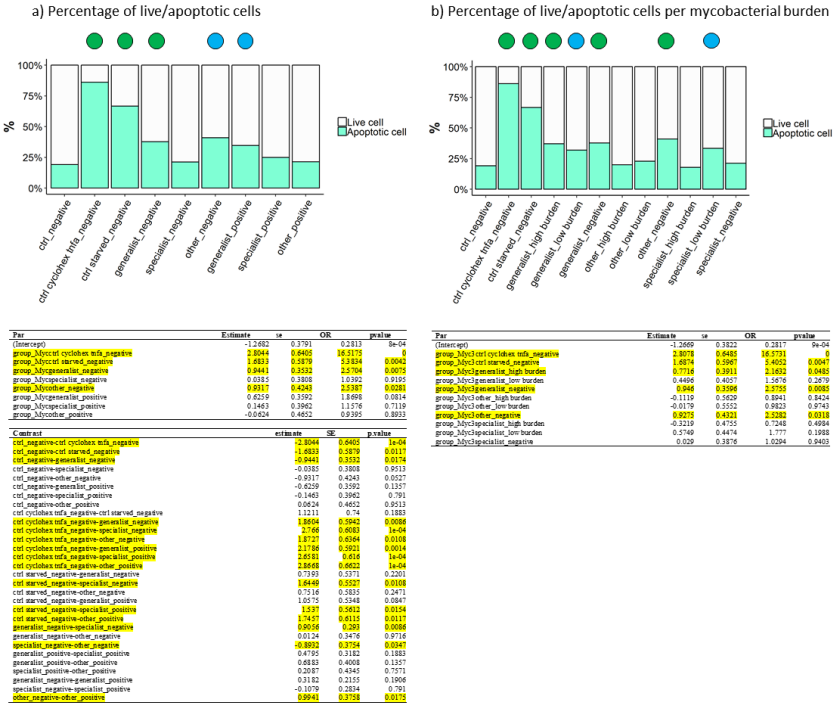


| Par | Estimate | se | OR | pvalue |
|---|---|---|---|---|
| (Intercept) | -1.2682 | 0.3791 | 0.2813 | 8e-04 |
| group_Mycctrl cyclohex tnfa_negative | 2.8044 | 0.6405 | 16.5175 | 0 |
| group_Mycctrl starved_negative | 1.6833 | 0.5879 | 5.3834 | 0.0042 |
| group_Mycgeneralist_negative | 0.9441 | 0.3532 | 2.5704 | 0.0075 |
| group_Mycspecialist_negative | 0.0385 | 0.3808 | 1.0392 | 0.9195 |
| group_Mycother_negative | 0.9317 | 0.4243 | 2.5387 | 0.0281 |
| group_Mycgeneralist_positive | 0.6259 | 0.3592 | 1.8698 | 0.0814 |
| group_Mycspecialist_positive | 0.1463 | 0.3962 | 1.1576 | 0.7119 |
| group_Mycother_positive | -0.0624 | 0.4652 | 0.9395 | 0.8933 |

| Contrast | estimate | SE | p.value |
|---|---|---|---|
| ctrl_negative-ctrl cyclohex tnfa_negative | -2.8044 | 0.6405 | 1e-04 |
| ctrl_negative-ctrl starved_negative | -1.6833 | 0.5879 | 0.0117 |
| ctrl_negative-generalist_negative | -0.9441 | 0.3532 | 0.0174 |
| ctrl_negative-specialist_negative | -0.0385 | 0.3808 | 0.9513 |
| ctrl_negative-other_negative | -0.9317 | 0.4243 | 0.0527 |
| ctrl_negative-generalist_positive | -0.6259 | 0.3592 | 0.1357 |
| ctrl_negative-specialist_positive | -0.1463 | 0.3962 | 0.791 |
| ctrl_negative-other_positive | 0.0624 | 0.4652 | 0.9513 |
| ctrl cyclohex tnfa_negative-ctrl starved_negative | 1.1211 | 0.74 | 0.1883 |
| ctrl cyclohex tnfa_negative-generalist_negative | 1.8604 | 0.5942 | 0.0086 |
| ctrl cyclohex tnfa_negative-specialist_negative | 2.766 | 0.6083 | 1e-04 |
| ctrl cyclohex tnfa_negative-other_negative | 1.8727 | 0.6364 | 0.0108 |
| ctrl cyclohex tnfa_negative-generalist_positive | 2.1786 | 0.5921 | 0.0014 |
| ctrl cyclohex tnfa_negative-specialist_positive | 2.6581 | 0.616 | 1e-04 |
| ctrl cyclohex tnfa_negative-other_positive | 2.8668 | 0.6622 | 1e-04 |
| ctrl starved_negative-generalist_negative | 0.7393 | 0.5371 | 0.2201 |
| ctrl starved_negative-specialist_negative | 1.6449 | 0.5527 | 0.0108 |
| ctrl starved_negative-other_negative | 0.7516 | 0.5835 | 0.2471 |
| ctrl starved_negative-generalist_positive | 1.0575 | 0.5348 | 0.0847 |
| ctrl starved_negative-specialist_positive | 1.537 | 0.5612 | 0.0154 |
| ctrl starved_negative-other_positive | 1.7457 | 0.6115 | 0.0117 |
| generalist_negative-specialist_negative | 0.9056 | 0.293 | 0.0086 |
| generalist_negative-other_negative | 0.0124 | 0.3476 | 0.9716 |
| specialist_negative-other_negative | -0.8933 | 0.3754 | 0.0347 |
| generalist_positive-specialist_positive | 0.4795 | 0.3182 | 0.1883 |
| generalist_positive-other_positive | 0.6883 | 0.4008 | 0.1357 |
| specialist_positive-other_positive | 0.2087 | 0.4345 | 0.7571 |
| generalist_negative-generalist_positive | 0.3182 | 0.2155 | 0.1906 |
| specialist_negative-specialist_positive | -0.1079 | 0.2834 | 0.791 |
| other_negative-other_positive | 0.9941 | 0.3758 | 0.0175 |

| Par | Estimate | se | OR | pvalue |
|---|---|---|---|---|
| (Intercept) | -1.2669 | 0.3822 | 0.2817 | 9e-04 |
| group_Myc3 ctrl cyclohex tnfa_negative | 2.8078 | 0.6485 | 16.5731 | 0 |
| group_Myc3 ctrl starved_negative | 1.6874 | 0.5967 | 5.4052 | 0.0047 |
| group_Myc3generalist_high burden | 0.7716 | 0.3911 | 2.1632 | 0.0485 |
| group_Myc3generalist_low burden | 0.4496 | 0.4057 | 1.5676 | 0.2679 |
| group_Myc3generalist_negative | 0.946 | 0.3598 | 2.5755 | 0.0095 |
| group_Myc3other_high burden | -0.1119 | 0.5629 | 0.8941 | 0.8424 |
| group_Myc3other_low burden | -0.0179 | 0.5552 | 0.9823 | 0.9743 |
| group_Myc3other_negative | 0.9275 | 0.4321 | 2.5282 | 0.0318 |
| group_Myc3specialist_high burden | -0.3219 | 0.4755 | 0.7248 | 0.4984 |
| group_Myc3specialist_low burden | 0.5749 | 0.4474 | 1.777 | 0.1988 |
| group_Myc3specialist_negative | 0.029 | 0.3878 | 1.0294 | 0.9403 |

**Fig. 14**: Apoptosis levels at 24h p.i. in M1 cells with statistical reports

In M2 macrophages, only bystander non-infected cells of other strains showed a slight, statistically not significant increase in apoptosis (30%) (Fig. 15).

**M2 – 24 h p.i.**

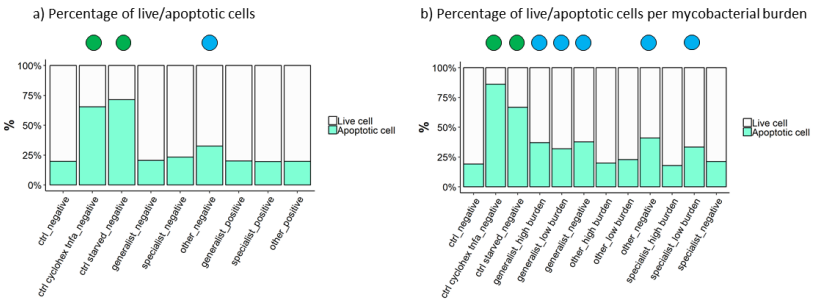


| Par | Estimate | se | OR | pvalue |
|---|---|---|---|---|
| (Intercept) | -1.4453 | 0.4587 | 0.2357 | 0.0016 |
| group_Mycctrl cyclohex tnfa_negative | 1.6424 | 0.6211 | 5.1677 | 0.0082 |
| group_Mycctrl starved_negative | 1.9314 | 0.6735 | 6.8991 | 0.0041 |
| group_Mycgeneralist_negative | 0.1847 | 0.376 | 1.2029 | 0.6233 |
| group_Mycspecialist_negative | 0.3807 | 0.403 | 1.4624 | 0.3448 |
| group_Mycother_negative | 0.7893 | 0.4487 | 2.2018 | 0.0786 |
| group_Mycgeneralist_positive | 0.0858 | 0.38 | 1.0896 | 0.8213 |
| group_Mycspecialist_positive | -0.0294 | 0.4383 | 0.971 | 0.9465 |
| group_Mycother_positive | 0.077 | 0.4908 | 1.08 | 0.8754 |

| Contrast | estimate | SE | p.value |
|---|---|---|---|
| ctrl_negative-ctrl cyclohex tnfa_negative | -1.6424 | 0.6211 | 0.0314 |
| ctrl_negative-ctrl starved_negative | -1.9314 | 0.6735 | 0.0314 |
| ctrl_negative-generalist_negative | -0.1847 | 0.376 | 0.8499 |
| ctrl_negative-specialist_negative | -0.3807 | 0.403 | 0.5172 |
| ctrl_negative-other_negative | -0.7893 | 0.4487 | 0.1684 |
| ctrl_negative-generalist_positive | -0.0858 | 0.38 | 0.9177 |
| ctrl_negative-specialist_positive | 0.0294 | 0.4383 | 0.9792 |
| ctrl_negative-other_positive | -0.077 | 0.4908 | 0.9379 |
| ctrl cyclohex tnfa_negative-ctrl starved_negative | -0.289 | 0.7839 | 0.8905 |
| ctrl cyclohex tnfa_negative-generalist_negative | 1.4577 | 0.5727 | 0.0364 |
| ctrl cyclohex tnfa_negative-specialist_negative | 1.2617 | 0.5907 | 0.0817 |
| ctrl cyclohex tnfa_negative-other_negative | 0.8531 | 0.6223 | 0.3007 |
| ctrl cyclohex tnfa_negative-generalist_positive | 1.5566 | 0.5733 | 0.0314 |
| ctrl cyclohex tnfa_negative-specialist_positive | 1.6718 | 0.6127 | 0.0314 |
| ctrl cyclohex tnfa_negative-other_positive | 1.5654 | 0.6533 | 0.0452 |
| ctrl starved_negative-generalist_negative | 1.7467 | 0.6291 | 0.0314 |
| ctrl starved_negative-specialist_negative | 1.5507 | 0.6455 | 0.0452 |
| ctrl starved_negative-other_negative | 1.1421 | 0.6746 | 0.1809 |
| ctrl starved_negative-generalist_positive | 1.8456 | 0.6314 | 0.0314 |
| ctrl starved_negative-specialist_positive | 1.9608 | 0.6657 | 0.0314 |
| ctrl starved_negative-other_positive | 1.8544 | 0.7092 | 0.0314 |
| generalist_negative-specialist_negative | -0.196 | 0.3238 | 0.7784 |
| generalist_negative-other_negative | -0.6046 | 0.3792 | 0.2078 |
| specialist_negative-other_negative | -0.4086 | 0.4059 | 0.4961 |
| generalist_positive-specialist_positive | 0.1152 | 0.3707 | 0.9071 |
| generalist_positive-other_positive | 0.0089 | 0.4316 | 0.9836 |
| specialist_positive-other_positive | -0.1064 | 0.4836 | 0.9177 |
| generalist_negative-generalist_positive | 0.0989 | 0.2299 | 0.8702 |
| specialist_negative-specialist_positive | 0.4101 | 0.322 | 0.338 |
| other_negative-other_positive | 0.7123 | 0.3748 | 0.1325 |

| Par | Estimate | se | OR | pvalue |
|---|---|---|---|---|
| (Intercept) | -1.4519 | 0.4671 | 0.2341 | 0.0019 |
| group_Myc3 ctrl cyclohex tnfa_negative | 1.6417 | 0.6211 | 5.1743 | 0.0093 |
| group_Myc3 ctrl starved_negative | 1.9332 | 0.6838 | 6.9113 | 0.0047 |
| group_Myc3generalist_high burden | 0.2176 | 0.4263 | 1.2431 | 0.6097 |
| group_Myc3generalist_low burden | -0.0153 | 0.4183 | 0.9849 | 0.9709 |
| group_Myc3generalist_negative | 0.1931 | 0.384 | 1.213 | 0.6152 |
| group_Myc3other_high burden | -0.0368 | 0.6144 | 0.9639 | 0.9233 |
| group_Myc3other_low burden | 0.17 | 0.5606 | 1.1853 | 0.7617 |
| group_Myc3other_negative | 0.7962 | 0.4586 | 2.2171 | 0.0825 |
| group_Myc3specialist_high burden | -0.3125 | 0.5468 | 0.599 | 0.5487 |
| group_Myc3specialist_low burden | 0.3892 | 0.4961 | 1.4757 | 0.4328 |
| group_Myc3specialist_negative | 0.389 | 0.4118 | 1.4755 | 0.3448 |

**Fig. 15** Apoptosis levels at 24h p.i. in M2 cells with statistical reports

- **Cytokine production**

Cytokines induction analysis was performed on macrophages infected with H37Rv, H37Ra, L2, or L6 MTB strains. Uninfected controls were used as calibrators for analysis. For consistency with the previous analyses, strains grouped according to seven categories above-mentioned (Table 1), even though given the reduced number of strains tested some categories are in this case redundant. The first important result we obtained is about the M1/M2 cytokine-chemokine pattern production. In general, in M2 cells the infection with different MTB categories produces a more homogeneous cytokine pattern compared to infected M1 cells, where the differences among strains are more pronounced. Among the analytes considered, we found IL-1β, IL-6, TNFα, IL-15 pro-inflammatory cytokines to be the most modulated by MTB infection, when compared to the uninfected control cells. In fact, with few exceptions (IL-1β, IL-18) in M2 cells, different MTB categories do not show statistical differences. In M1 cells most of the differences between generalist and specialist strains, are found both in pro-inflammatory cytokines (IL-1β, IL-15, IL-18), in anti-inflammatory cytokines (IL-1ra), and in growth factors (FGF, G-CSF). In general, laboratory strains were found to induce higher levels of pro-inflammatory cytokines compared to clinical isolates. Detailed statistical analysis is reported in Supplementary Cytokines.

Pro-inflammatory cytokines: in both M1 and M2 macrophages, specialist strains induced a significantly lower level of IL-1β compared to generalist strains at all time points considered. Expression patterns of this cytokine are similar between M1 and M2 infected macrophages (Fig. 16). Main differences in IL-1β production were found when comparing L6 and L2 infected cells at 4h p.i. (in M2 cells) and at 24h p.i. (M1 cells), where induction levels of L6 strains are similar to the non-infected control. In general, specialists induce a minor production of this cytokine in both cell types considered. IL-18 production is low, with similar production in M1 and M2 cells. Specialist strains induce a lower production of this cytokine

compared to generalist ones. IL-15 induction is statistically higher in M1 cells when infected with generalist strains.

No statistical differences were found comparing IL-6 production in specialists vs generalists strains, but IL-6 levels observed in M2 macrophages are lower than M1.

As for IL-6, TNFα shows no statistical differences comparing specialists vs generalists strains, and is mostly induced in laboratory strains in M2 cells.

IL-15, IFNγ, IL-18 are poorly released in response to MTB infection in both M1 and in M2 cells at the time points considered. IFNγ production is negligible at the time points considered with low production both in M1 and M2 infected cells. Immunofluorescence and single-cell analysis on TNFα and IFNγ showed similar findings (Supplementary Cytokine). We performed a correlation analysis between these cytokines levels and (i) bacillary load or (ii) phagolysosomal acidification; despite a few correlations could be found, they were most likely strain-specific rather than providing evidence for more general assumptions (Supplementary Cytokine). In all cytokine considered, both in M1 and M2 cells, laboratory strains induce a higher production of pro-inflammatory cytokine, compared to clinical ones.

Anti-inflammatory cytokines: most of the differences among MTB categories are found in M1 infected cells. IL-1ra is highly induced compared to the control, especially in generalist strains, which are statistically different compared to specialists in M1 cells at all time points considered (Fig. 16). In M2 cells, laboratory strains induce a high level of this cytokine at 24h p.i. IL-10 is slightly induced by MTB infection; Specialists vs Generalists show no differences in their expression pattern. Contrarily from pro-inflammatory cytokines, anti-inflammatory production, in laboratory strains infected cells is similar to the clinical ones. Statistical differences are found only in the IL-1ra secretion, in M2 cells at 24h p.i., and in the IL-10 production at 4h p.i. in M1 cells and at 24h p.i.in M2 cells.

Chemokines: lower differences are found in the chemokine measurements, with M1 and M2 infected cells that show similar production patterns (Fig. 17). No statistical differences are found in the induction of IL-8, MCP-1 and RANTES.

MIP-1β production confirms what we observed in the immunofluorescence assay, where the level in M1 cells infected with generalist strains is statistically higher than specialist strains at 24h p.i.

Same confirm for MCP-1 production, who despite the high induction compared to the non infected control, show no statistical differences among categories considered.

Considering the differences among clinical and laboratory infected cells, once again laboratory strains induce a higher production of the selected chemokine (MIP-1α/β, SDF-1α, GROα). Immunofluorescence and single-cell analysis on MCP-1 and MIP-1β showed similar findings (Supplementary Cytokine).

Growth factors: similar results are found considering growth factor production. In general, specialist strains induce a lower secretion of those molecules, especially in M1 cells (Fig. 18). Major differences are found in the G-CSF and in the FGF basic production (M1 at 4 and 24h p.i, - M2 at 48h p.i.). Laboratory strains induce a higher induction of growth factors FGF basic, G-CSF, and PDGF-bb compared to clinical strains.

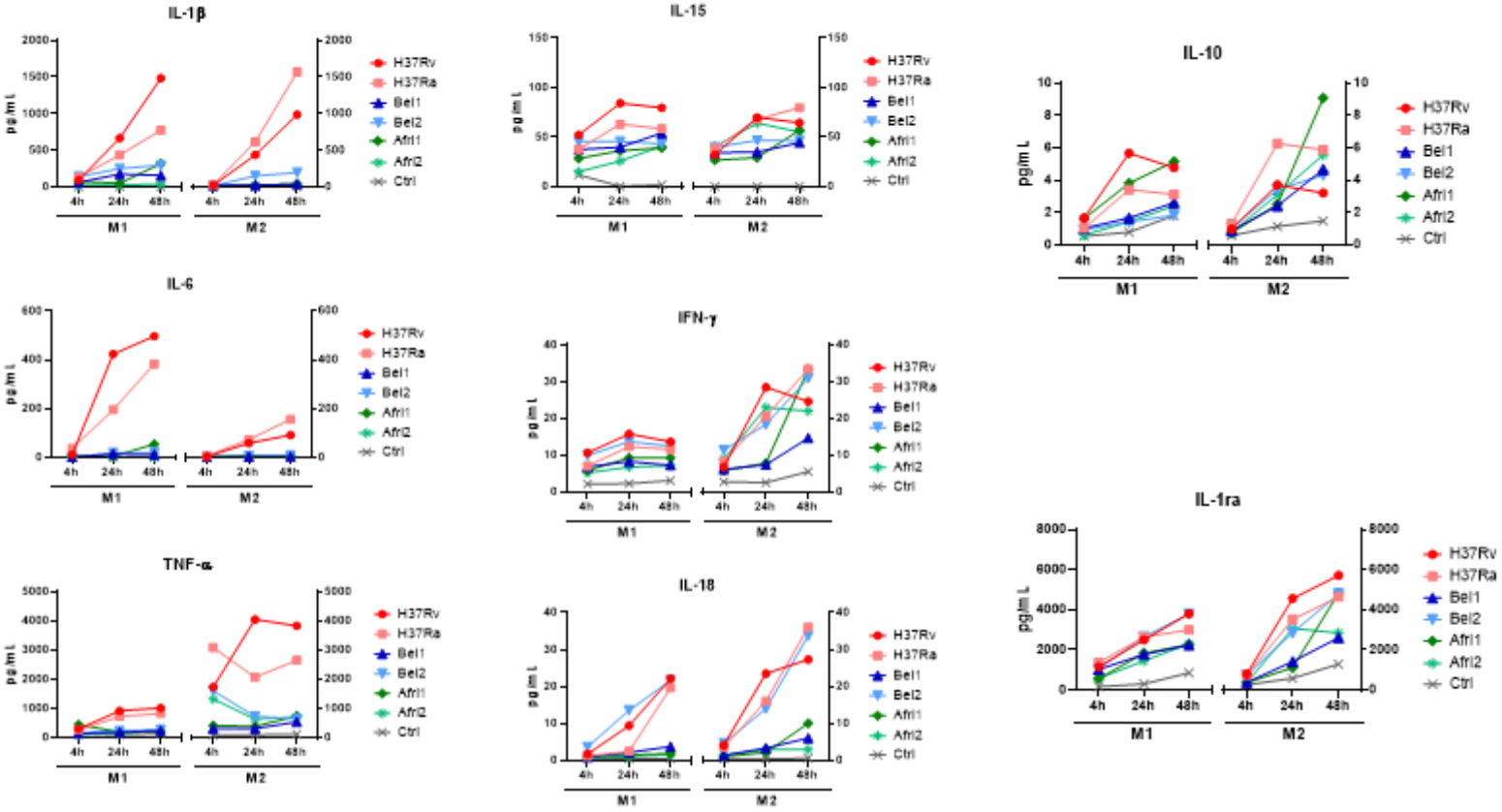


**Fig. 16**: Pro and anti-inflammatory cytokine results. MTB strains used: H37Rv, H37Ra, L2 (Bei1, Bei2), L6 (Afri1, Afri2)

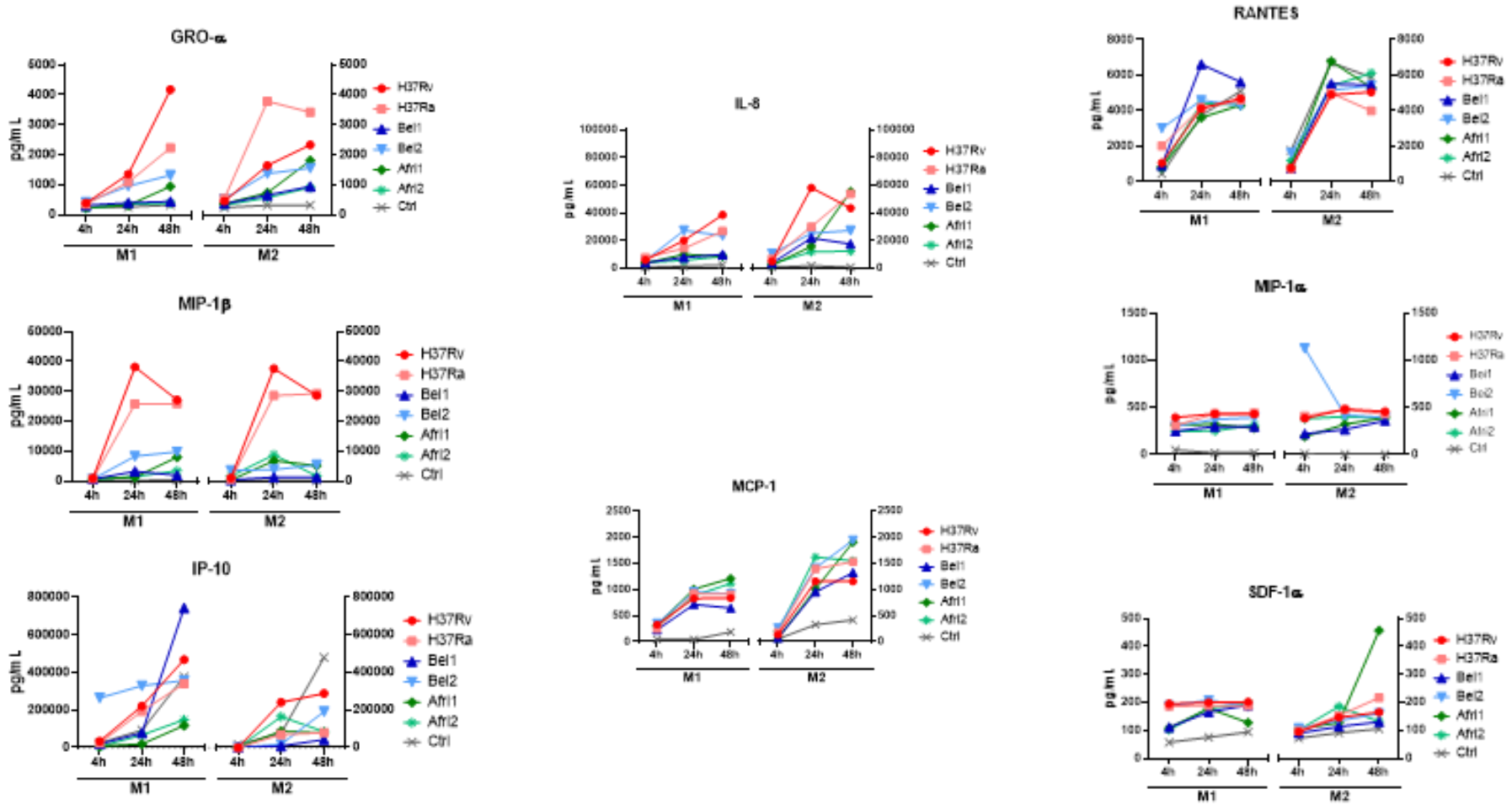


**Fig. 17**: Chemokine results. MTB strains used: H37Rv, H37Ra, L2 (Bei1, Bei2), L6 (Afri1, Afri2)

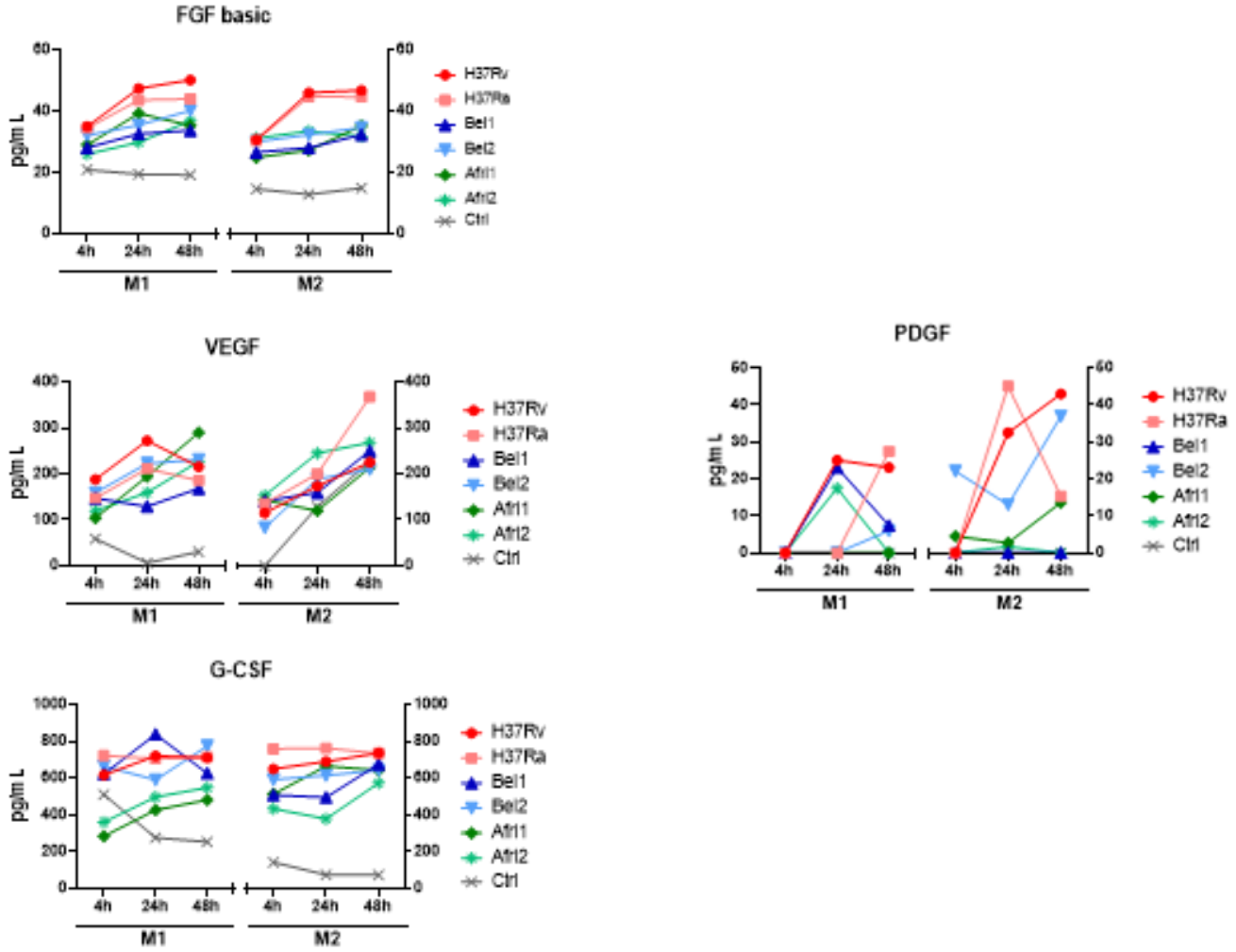


**Fig. 18**: Growth factors results. MTB strains used: H37Rv, H37Ra, L2 (Bei1, Bei2), L6 (Afri1, Afri2)

- **Cell survival**

We first evaluated the amount of healthy cells after the cytokine polarization of THP-1 (T0), before MTB infection. Results show how cytokine M1 induction with LPS causes a loss of about 20% of the THP-1 derived macrophages, while treatment with IL-4 (M2 polarization) causes the loss of about 11% of the cells. Whereas different MTB strains are associated with different levels of M1 macrophages death, M2 macrophages display less heterogeneity in survival after MTB challenge.

In M1 macrophages, at 48 h p.i. more virulent strains induce a reduction of live cells of about 50% compared to the 20% induced less virulent strains. As the infection progresses, at 5 days p.i. we could no longer appreciate differences among the categories considered.

In M2 macrophages, at 48h p.i. the level of cell death (about 20%) is lower compared to M1 cells, with no statistical differences among categories. This result is in line with apoptosis levels found for those categories. At 5 days p.i. MTB infection causes an increased M2 cell death (about 60%), compared to M1(about 40%). More virulent/generalist strains induce higher cell loss compared to less virulent/specialist ones (Fig. 19).

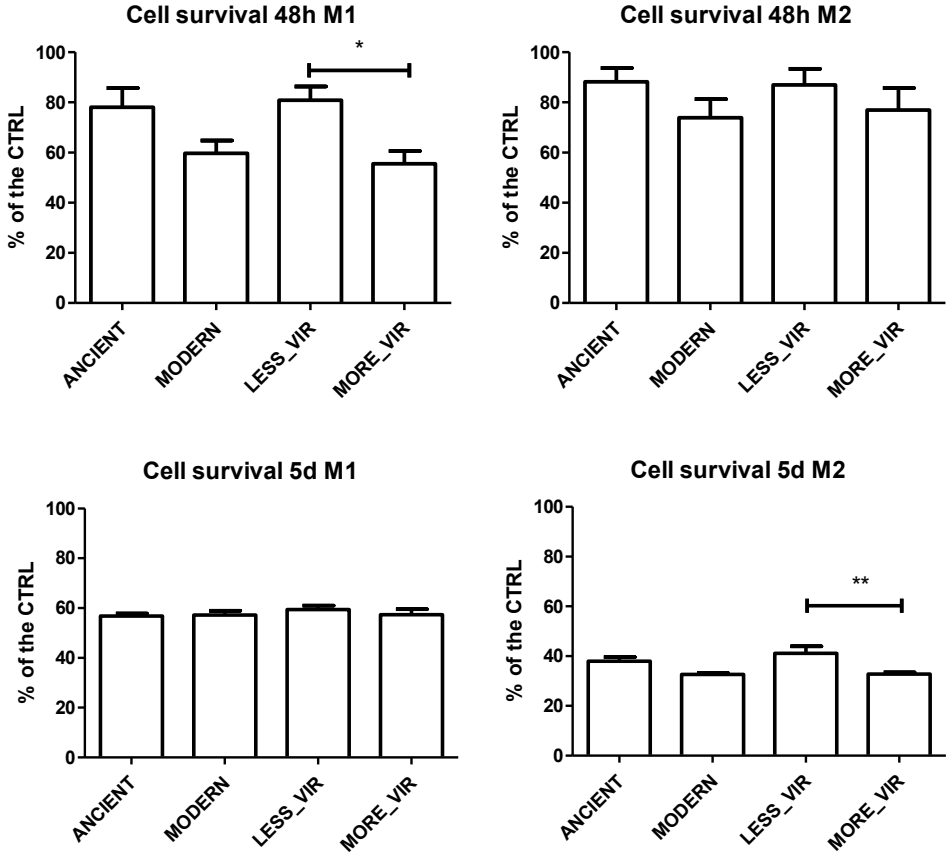


**Fig. 19**: Cell survival at 48h and 5days post-infection.

- **CFU**

CFU counts were performed on the selected MTB strains to study both the macrophagic entry (CFU at 4h p.i.) and the survival capacity (CFU at 48h p.i.). At 4h p.i. data were normalized on the CFU of the inoculum. The number of bacteria that effectively are phagocytized by the macrophages is below 10% of the inoculum in all the MTB strains selected. Differences are present considering M1/M2 cell phenotype: entry of bacteria is increased in M2 cells in all MTB strains selected. Higher CFU levels are found in H37Ra infected cells, while H37Rv and L6 show a similar CFU level. L2 uptake resulted to be very low compared to all other strains, with CFU values close to 1% of the inoculum in M1 cells and to 3% in M2 cells. At 48h p.i. CFU were normalized on the CFU at 4h p.i. (representing the number of bacteria actually internalized by the macrophages). H37Rv and H37Ra show

similar CFU counts, while clinical strains appear to grow more in infected macrophages. L2 strains show a higher number of CFU, despite the initial lower uptake, with larger growth in M1 cells (Fig. 20).

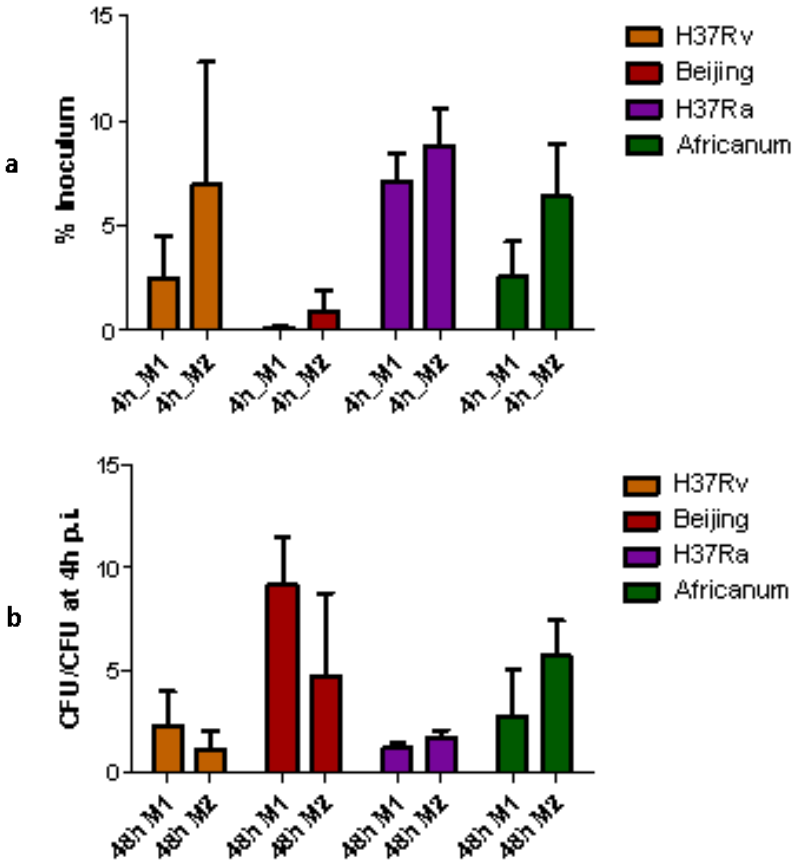


**Fig. 20**: a) CFU results at 4h p.i. (% of the inoculum) and b) at 48h p.i. (normalized on CFU at 4h) Beijing: Generalist; Africanum: Specialist

# Discussion

How MTB survives within the macrophages is a key point in the pathogenesis and virulence of MTB. Early views of pathogenicity and virulence were pathogen-centered and were based on the assumption that these characteristics were intrinsic properties of bacteria, focusing mainly on the capacity of some microbes to cause disease in healthy hosts [38]. The definition of bacterial virulence has changed over time, and it's now considered as a relative capacity to cause damage, both at cellular or at organ/tissue level. In this view, virulence is a property of the pathogen, but it is modulated by host susceptibility and resistance [39, 40].

Despite their central role in MTBC infection, the phenotype of the macrophages is an underestimated component of *in vitro/ex vivo* infection models. Alveolar macrophages have specifically evolved for the alveolar environment where they exert their role against invasive organisms but also prevent inflammation and tissue damage. Alveolar macrophages exhibit an intermediate phenotype between pro-inflammatory, classically activated (M1), and anti-inflammatory, alternatively activated (M2) macrophages, and express both M1 and M2 markers [41]. As a point of note, despite the presence of both M1/M2 marker sets, they are skewed in favor of the M2 phenotype, with high CD206 and low toll-like receptors [42]. Alveolar macrophages generate a non-canonical NRF2-driven transcriptional response to Mycobacterium TB, which was recently demonstrated in an *in-vivo* mouse model. NRF-2 has been associated with anti-inflammatory responses, and it may create an M2-like phenotype that inhibits IL-1 and IL-6 production [43].

On the other end, the genetic diversity of MTBC has been increasingly recognized as another important player in determining the fate of the host-pathogen interaction [44]. The interaction between immune cells and pathogens is complex, and at the single-cell level, their dynamics culminate in heterogeneous outcomes of infection.

In this work, we studied early host-pathogen interaction between MTB and human macrophages, taking into consideration both host macrophage phenotypic variability (resembling alveolar macrophages plasticity) and MTB genetic diversity considering major phylogenetical differences. In particular, we focused our attention on phagolysosomal acidification, autophagy, apoptosis. Cytokines induction, macrophage and bacterial survival were also considered. In terms of differentiation, functions, and reactions to external stimuli, THP-1 generated macrophages have been described to behave similarly to human macrophages [45]. The adoption of a single-cell analytical approach allowed to better appreciate the heterogeneity of the host-pathogen interaction for some of the above-mentioned analyses.

Despite previous studies, focusing mainly on the laboratory strain *M. tuberculosis* H37Rv, reported that mycobacteria arrest the maturation of their phagosomes and avoid further acidification of the bactericidal compartment, there is evidence that MTB can reside in acidic phagosomes (thus surviving low pH stress) [46]. The biogenesis of mycobacterial phagosomes is a complex and dynamic process. As a result, various features such as vacuolar proton-ATPase exclusion, synthesis of antacid compounds, selective prevention of fusion with active lysosomes, interference with phagosome integrity and repair, and acidic resistance all contribute to the MTB escape from the immune system mechanisms [47 – 49]. Concerning phagosomal acidification, in M1 macrophages acidification is delayed by more virulent, modern, generalist isolates, whereas at earlier time points less virulent, ancient, specialist strains are not blocking acidification. At later time points, none of the strains is blocking phagosomal acidification, but less virulent, ancient, specialist strains displayed lower levels of acidification compared to more virulent, modern, generalist/intermediate strains. In addition, more virulent, modern, generalist/intermediate isolates displayed higher colocalization with

LysoSensor positive regions, thus suggesting higher colocalization with regions at lower pH.

Macrophages classically activated prior to ingestion of mycobacteria are able to acidify the phagosomal compartments [50, 51]. The higher level of acidification together with the higher colocalization of more virulent, modern, generalist isolates with acidified compartments suggest they are better at tolerating the acidic environment. In support of this view, L2 strains constitutively overexpress the DosR regulon, a regulon playing a pivotal role in protecting mycobacteria from acidification during intramacrophagic infection [52 - 54]. Similarly, L2 strains harbor a lineage-specific mutation in KefB (*Rv3236c* gene), a potassium/proton antiporter relevant for arresting phagosomal acidification [54, 55]. Diversely, isolates belonging L5 and L6 (*M. africanum*) harbor mutations negatively affecting the two-component virulence regulatory system PhoP/PhoR, a regulon involved in the adaptive response to acidic pH [57]. Recently, evidences correlate the levels of sulfolipid-1 (SL-1) and lysosomal delivery: strains showing lower SL-1 production display a reduction in the delivery to lysosomes [58]. Interestingly, L5 and L6 lineages have been reported an impaired SL-1 production likely due to the mutations affecting the PhoP/PhoR regulatory system whereas L1 possesses a lineage-specific mutation Ala43pro in the *papA2* gene abrogating cell wall SL-1 [59, 60]. Despite recent findings that found no statistically significant differences in survival of modern and L1 isolates in acidic pH in vitro, the transcriptional regulatory network of ancient and modern lineages is obviously distinct, with crucial implications for stress response [61].

The picture observed in alternatively activated macrophages (M2) was different. Acidification is observed at early time points with clinical isolates, but not with laboratory strains. However, at 24 h p.i. more virulent, modern, generalist/intermediate strains blocked acidification, whereas less virulent, ancient, specialist strains were less efficient in blocking the acidification of phagolysosomes. Contrary to what observed in M1 macrophages, in alternatively activated macrophages no differences in

terms of colocalization of mycobacteria within acidified compartments were observed. The acidification level and the number of acidified organelles were generally lower compared to classically activated macrophages. Similarly, the Colocalization Index was also generally lower in M2 macrophages.

These macrophages are able to mount a weak response barely able to counteract less virulent, ancient, specialist strains at the time points considered, while more virulent, modern, generalist/intermediate strains quickly hijack macrophage antimicrobial defenses. The acidification of phagosomes depends on the organism phagocytosed and the specific receptor starting the signaling pathway. The mechanisms besides this sharper difference in coping with phagosomal acidification observed only in M2 macrophages require further elucidation; however, we noticed that ancient, animal, specialist strains harbor a mutation (Thr171Ala) in the phosphatidylinositol 3-phosphate phosphatase SapM (*Rv3310* gene), an enzyme playing a crucial role in blocking phagosome maturation in M2 and unpolarized macrophages only [62]. It's possible that this mutation, in combination with the genetic background, explains why ancient isolates are less effective at preventing phagosome acidification in alternatively activated macrophages.

The differences in response timing between M1 and M2 macrophages are consistent with prior findings. Indeed, when phagosomes from activated or M1 macrophages were compared to those from resting or M2 macrophages, they displayed a delayed acidification kinetics [63- 65].

To be noted that laboratory strains showed higher capacity to block phagolysosomal acidification compared to clinical isolates. This highlights the fact that infection models based only on reference laboratory strains are not always able to completely recapitulate the pathogenesis of tuberculosis. Irrespectively from the macrophagic phenotype, ancient, specialist isolates showed lower bacillary load compared to modern, generalist isolates. At early time points p.i. there was an increase in the number of M1 macrophages showing phagosomal acidification in presence

of less virulent, ancient, specialist strains; however, after this initial response, the number of such cells was reduced. More virulent, modern, generalist isolates did not caused an increase in the number of responsive cells. Overall, at 24 h p.i. only a relatively small amount of M1 macrophages challenged with mycobacteria (15-25%) displayed phagosomal acidification. Limited bystander effect in non-infected macrophages was observed. Similarly to classically activated macrophages, at early time points p.i. there was an increase in the number of M2 macrophages showing phagosomal acidification, but after 24 h only animal lineages and laboratory/non-causing strains maintained a high percentage of "acidified" cells, whereas either less virulent, ancient, specialist and more virulent, modern, generalist isolates displayed low or very low number of responsive cells (<10%). In M2 macrophages a consistent bystander effect in non-infected cells was observed.

The use of a single-cell analytical approach highlighted the heterogeneity of the macrophagic response to *M. tuberculosis* infection. Whereas a general increase in the phagosomal acidification could be observed, our data suggest this increment is mainly due to a relatively small proportion of cells rather than being a population-average response (at least when considering macrophages infected with either less virulent, ancient, specialist and more virulent, modern, generalist isolates). Furthermore, the differences in acidification time could be also due to fluctuations in the levels of *M. tuberculosis* damaging (virulence) factors as already hypothesized [66].

A bystander effect on non-infected macrophages was previously observed mainly during studies on apoptosis, and this was found to be induced by less virulent strains [67 – 70]. For the first time, we report a similar effect in terms of acidification. Mycobacterial protein and lipid antigens or exosomes derived from infected cells can reach non-infected bystander cells, a phenomenon modulating the response of immune cells and reported to affect subsequent IFNγ activation of macrophages [71]. Notably, the bystander increase of acidification was found in M2 macrophages and

was mainly driven by less virulent, ancient, specialist strains MTB is able to evade macrophagic clearance due to autophagy [72]. Our data did not show relevant differences among less virulent, ancient, specialist, and more virulent, modern, generalist strains as either the categories were able to block the formation of autophagosomes. Previous findings showed similar results, despite highlighting a difference in the mechanism used by different genotypes to hinder autophagy [72, 73].

Other parameters we evaluated were induction of apoptosis and necrosis. At the time point considered (24 h p.i.) we could not observe necrosis, thus we limited our analysis to apoptosis. Apoptosis has been considered to have a debatable role with groups supporting a protective effect for the host and contributing to infection control, whereas others suggest a detrimental effect increasing mycobacterial dissemination [74 -77]. Apoptosis was observed only in bystander non-infected cells of more virulent, modern and generalist isolates. Induction of apoptosis by virulent strains seems contradictory to its protective role against MTB. However, previous findings highlighted that apoptosis signals at day 1 p.i. progressed to necrosis at later timepoints; furthermore, exposure of phosphatidylserine is observed in different forms of programmed cell death (namely apoptosis, necroptosis and ferroptosis) [78]. Apoptosis data are in line with what we observed with the cell survival assay, where in M1 macrophages, more virulent strains induce a major cells death rate compared to less virulent strains, while in M2 cells we found lower induction of apoptosis, with no statistical differences among MTB categories.

Data on human and mice models show how the principal protection against TB depends on the activation of the Th1 response, and the subsequent production of pro-inflammatory cytokines such as IFNy and TNFα, which are involved in the granuloma formation. The role of macrophages in phagocyting bacteria and presenting antigens is crucial for the T cell priming and in controlling MTB infection. Because their

expression often links with efficient immune responses, type-1 inflammatory cytokines are critical in the protection against MTB, and genetic deficiencies of these factors lead to improved TB susceptibility. MTB infection can drive macrophages toward M1 in the early phase, and shift their status into M2 phenotypes in intermediate and late phases. This strategy is thought to be put in place for an attempt by the host to halter the pathophysiology caused by MTB or a bacterial strategy to shield from immune attack [79 - 81].

In our study we decided to focus our attention on the cytokine/chemokine production at the early phases of the interaction between MTB different strains and human macrophages.

Cytokine, chemokine and growth factors selected in this study are the main produced elements involved in the macrophagic early response to MTB infection. In general, MTB appears to strongly modulate the production of pro-inflammatory cytokines and to induce an M1 shift in the pre-activated M2 cells, increasing pro-inflammatory production. The interleukin 1 and type 1 interferon (type 1 IFN) signaling pathways are well studied in mice but poorly understood in human models. They have been shown to play opposing roles in tuberculosis. Type-1 IFNs contribute to pathogenesis through weakening of host resistance to MTB while IL-1β is required for host control of infection. We found IL-1β production highly increased in time, especially in the laboratory strains H37Rv and H37Ra [82]. Differences are also found between L2 and L6 strains, with the latter that induce the lowest IL-1β production. Those results are in line with the results coming from the single cell level experiment, where virulent strains induce a higher delay in the acidification of M1 cells at earl timepoints, while in M2 we saw a blocking of the acidification at later timepoints (unlike less virulent strains). Of notice, the induction of TNFα and IFNγ appears to be higher in M2 cells, showing a more rapid shift to M1 polarization, particularly in the laboratory strains. It important to remark that in literature it is reported that cell death caused by MTB strains, is non-directly correlated with IL-1β secretion [83].

IL-6 has been associated to host protection by the expression of early immune response, and low levels of IL-6 are associated with lung lesions and cavitary TB. Our data show that M2 cells are less capable of expressing IL-6 following MTB infection in all strains considered, thus suggesting a lower capacity to inhibit damages caused by MTB. In M1 cells, clinical strains are able to retard IL-6 production, thus increasing cellular damage, compared to the laboratory strains [84]. IL-18 is a potent immunoregulatory cytokine with different immunological properties. It regulates the mechanisms of both innate and adaptive immunity and plays a key role in host defense, mostly regulating IFNγ release. In our study, we observed poor secretion of this cytokine, indicating immune suppression of the infected cells from MTB strains. Once again, higher levels are found in laboratory strains and in one of the two L6 strains selected. IL-15 secretion is slowed by MTB infection since the amount measured in both M1 and M2 cells is low. IL-15 participate to the activation and proliferation of T and natural killer (NK) cells. High concentrations of this cytokine favor TNFα, IL-1, and IL-6 production, whereas very low concentrations favor IL-10 production, thus increasing MTB survival. All strains considered inhibit the IL-15 production, with statistical differences among the categories selected at early timepoints.

Concerning anti-inflammatory cytokines, IL-10 production is suppressed by MTB infection, even in the M2 cells, confirming an M1 shift, while the IL-1ra, antagonist of IL-1β, is highly produced. The induction of IL-1ra is reported to play an important role in the establishment of the infection. Low levels of this cytokine are correlated with better survival in MTB-infected mice.

The expression of chemokine and growth factors in MTB infection plays important role in the recruitment of other immunity cells, implicated in the formation of granuloma and the containment of TB. Expression of those factors has been seen after 12 days post-infection in mice and is not modulated after the first contact with the pathogen [85]. In our study, most of the chemokines selected are not modulated by MTB at the time point

considered and show low differences among MTB categories selected, while growth factors (VEGF, G-CSF, FGF) resulted to show differences in M1 cells.

Another expected, but important result we obtained, is about the differences we found in the cytokine production of cells infected with clinical or laboratory strains. Those strains appear to increase pro-inflammatory cytokines, far more than clinical strains, which seem to delay the immune system reducing the inflammatory response.

Finally, we also considered the strains' capacity to replicate in the host and kill macrophages as an extreme measure of virulence (intended as "capacity to cause damage" as previously defined). Our data show how there is not a direct correlation between cytokine induction and the killing capacity of MTB strains. Indeed, despite low differences in pro-inflammatory signalling secretion between ancient/specialist/less virulent and modern/generalist/more virulent strains, the latter are more able to induce cell death and to replicate within macrophages. L2 strains showed a lower macrophagic uptake, but an increased capacity to replicate in macrophages and to kill the host [86]. These findings are confirmed by literature data. Our single-cell based study further contribute to show how important are both the intrinsic virulence capacity of MTB strains and the activation status of the receiving host. In M1 macrophages, higher phagolysosomal acidification and colocalization of modern/generalist/more virulent strains would be expected to correlate with improved infection control, whereas the outcome is, as mentioned, lower macrophagic survival. The strategy adopted by MTB in M2 macrophages is somehow completely different, with modern/generalist/more virulent strains escaping acidified compartments.

Our study further contribute to better understand the role of the genetic diversity of MTBC strains in the pathogenesis of TB and in relationship with defined host conditions. Future studies should be directed toward the identification of individual factors responsible for lineage-specific behaviours.

## References


1. Huang L, Nazarova EV, Russell DG. Mycobacterium tuberculosis: Bacterial Fitness within the Host Macrophage. Microbiol Spectr. 2019;7(2):10.1128/microbiolspec.BAI-0001-2019. doi:10.1128/microbiolspec.BAI-0001-2019
2. Barbier M, Wirth T. The Evolutionary History, Demography, and Spread of the Mycobacterium tuberculosis Complex. Microbiol Spectr. 2016;4(4):10.1128/microbiolspec.TBTB2-0008-2016. doi:10.1128/microbiolspec.TBTB2-0008-2016
3. Bottai D, Frigui W, Sayes F, et al. TbD1 deletion as a driver of the evolutionary success of modern epidemic Mycobacterium tuberculosis lineages. Nat Commun. 2020;11(1):684. Published 2020 Feb 4. doi:10.1038/s41467-020-14508-5
4. Portevin D, Gagneux S, Comas I, Young D. Human macrophage responses to clinical isolates from the Mycobacterium tuberculosis complex discriminate between ancient and modern lineages. PLoS Pathog. 2011;7(3):e1001307. doi:10.1371/journal.ppat.1001307
5. Casadevall A. The Pathogenic Potential of a Microbe. mSphere. 2017;2(1):e00015-17. Published 2017 Feb 22. doi:10.1128/mSphere.00015-17
6. Möller M, Kinnear CJ, Orlova M, et al. Genetic Resistance to Mycobacterium tuberculosis Infection and Disease. Front Immunol. 2018;9:2219. Published 2018 Sep 27. doi:10.3389/fimmu.2018.02219
7. Rosain J, et al. Mendelian susceptibility to mycobacterial disease: 2014-2018 update. Immunol Cell Biol. 2019 Apr;97(4):360-367. doi: 10.1111/imcb.12210. Epub 2018 Oct 25. PMID: 30264912.
8. Khan A, Singh VK, Hunter RL, Jagannath C. Macrophage heterogeneity and plasticity in tuberculosis. J Leukoc Biol. 2019;106(2):275-282. doi:10.1002/JLB.MR0318-095RR
9. Homolka S, Niemann S, Russell DG, Rohde KH. Functional genetic diversity among Mycobacterium tuberculosis complex clinical isolates: delineation of conserved core and lineage-specific transcriptomes during intracellular survival. PLoS Pathog. 2010;6(7):e1000988. Published 2010 Jul 8. doi:10.1371/journal.ppat.1000988
10. Cá B, Fonseca KL, Sousa J, et al. Experimental Evidence for Limited in vivo Virulence of Mycobacterium africanum. Front Microbiol. 2019;10:2102. Published 2019 Sep 10. doi:10.3389/fmicb.2019.02102
11. Shanley CA, Henao-Tamayo MI, Bipin C, et al. Biology of clinical strains of Mycobacterium tuberculosis with varying levels of transmission. Tuberculosis (Edinb). 2018;109:123-133. doi:10.1016/j.tube.2018.02.003
12. Wiens KE, Woyczynski LP, Ledesma JR, et al. Global variation in bacterial strains that cause tuberculosis disease: a systematic review and meta-analysis. BMC Med. 2018;16(1):196. Published 2018 Oct 30. doi:10.1186/s12916-018-1180-x

**13.** Reiling N, Homolka S, Kohl TA, et al. Shaping the niche in macrophages: Genetic diversity of the M. tuberculosis complex and its consequences for the infected host. Int J Med Microbiol. 2018;308(1):118-128. doi:10.1016/j.ijmm.2017.09.009

**14.** Tientcheu LD, Koch A, Ndengane M, Andoseh G, Kampmann B, Wilkinson RJ. Immunological consequences of strain variation within the Mycobacterium tuberculosis complex. Eur J Immunol. 2017;47(3):432-445. doi:10.1002/eji.201646562

**15.** Winglee K, Manson McGuire A, Maiga M, et al. Whole Genome Sequencing of Mycobacterium africanum Strains from Mali Provides Insights into the Mechanisms of Geographic Restriction. PLoS Negl Trop Dis. 2016;10(1):e0004332. Published 2016 Jan 11. doi:10.1371/journal.pntd.0004332

**16.** Stucki D, Brites D, Jeljeli L, et al. Mycobacterium tuberculosis lineage 4 comprises globally distributed and geographically restricted sublineages. Nat Genet. 2016;48(12):1535-1543. doi:10.1038/ng.3704

**17.** Coscolla M, Gagneux S. Consequences of genomic diversity in Mycobacterium tuberculosis. Semin Immunol. 2014;26(6):431-444. doi:10.1016/j.smim.2014.09.012

**18.** Coscolla M, Gagneux S. Does M. tuberculosis genomic diversity explain disease diversity?. Drug Discov Today Dis Mech. 2010;7(1):e43-e59. doi:10.1016/j.ddmec.2010.09.004

**19.** Gagneux S, DeRiemer K, Van T, et al. Variable host-pathogen compatibility in Mycobacterium tuberculosis. Proc Natl Acad Sci U S A. 2006;103(8):2869-2873. doi:10.1073/pnas.0511240103

**20.** Gagneux S. Ecology and evolution of Mycobacterium tuberculosis. Nat Rev Microbiol. 2018;16(4):202-213. doi:10.1038/nrmicro.2018.8

**21.** O'Neill MB, Shockey A, Zarley A, et al. Lineage specific histories of Mycobacterium tuberculosis dispersal in Africa and Eurasia. Mol Ecol. 2019;28(13):3241-3256. doi:10.1111/mec.15120

**22.** Borrell S, Trauner A, Brites D, et al. Reference set of Mycobacterium tuberculosis clinical strains: A tool for research and product development. PLoS One. 2019;14(3):e0214088. Published 2019 Mar 25. doi:10.1371/journal.pone.0214088

**23.** Kohl TA, Utpatel C, Schleusener V, et al. MTBseq: a comprehensive pipeline for whole genome sequence analysis of Mycobacterium tuberculosis complex isolates. PeerJ. 2018;6:e5895. Published 2018 Nov 13. doi:10.7717/peerj.5895

**24.** Maciag A, Dainese E, Rodriguez GM, et al. Global analysis of the Mycobacterium tuberculosis Zur (FurB) regulon [published correction appears in J Bacteriol. 2007 Jul;189(13):4974]. J Bacteriol. 2007;189(3):730-740. doi:10.1128/JB.01190-06 PMID: 17098899

**25.** Genin M, Clement F, Fattaccioli A, Raes M, Michiels C. M1 and M2 macrophages derived from THP-1 cells differentially modulate the response of cancer cells to etoposide. BMC Cancer. 2015;15:577. Published 2015 Aug 8. PMID: 26253167

**26.** Genin M, Clement F, Fattaccioli A, Raes M, Michiels C. M1 and M2 macrophages derived from THP-1 cells differentially modulate the response of cancer cells to etoposide. BMC Cancer. 2015;15:577. Published 2015 Aug 8. doi:10.1186/s12885-015-1546-9

**27.** Mantovani A, Sica A, Sozzani S, Allavena P, Vecchi A, Locati M. The chemokine system in diverse forms of macrophage activation and polarization. Trends Immunol. 2004;25(12):677–86.

**28.** Oeste CL, Seco E, Patton WF, Boya P, Pérez-Sala D. Interactions between autophagic and endo-lysosomal markers in endothelial cells. Histochem Cell Biol. 2013;139(5):659-670. doi:10.1007/s00418-012-1057-6. PMID: 23203316

**29.** 28. doi:10.1038/nmeth.2019

**30.** Klionsky DJ, Abdelmohsen K, Abe A, et al. Guidelines for the use and interpretation of assays for monitoring autophagy (3rd edition) [published correction appears in Autophagy. 2016;12(2):443. Selliez, Iban [corrected to Seiliez, Iban]]. Autophagy. 2016;12(1):1-222. PMID: 26799652

**31.** Lo K, Hahne F, Brinkman RR, Gottardo R. flowClust: a Bioconductor package for automated gating of flow cytometry data. BMC Bioinformatics. 2009;10:145. Published 2009 May 14. doi:10.1186/1471-2105-10-145. PMID: 19442304

**32.** Laird, N.M., and Ware, J. H. (1982). Random-effects models for longitudinal data. Biometrics 38, 963–974. doi: 10.2307/2529876

**33.** Pinheiro, J. C., and Bates, D. M. (2000). Mixed-Effects Models in s and S-Plus. New York, NY: Springer.

**34.** Brooks, Mollie E., et al. "glmmTMB balances speed and flexibility among packages for zero-inflated generalized linear mixed modeling." The R journal 9.2 (2017): 378-400.

**35.** R Core Team (2013). R: A language and environment for statistical computing. R Foundation for Statistical Computing, Vienna, Austria. URL http://www.R-project.org/

**36.** Genin M, Clement F, Fattaccioli A, Raes M, Michiels C. M1 and M2 macrophages derived from THP-1 cells differentially modulate the response of cancer cells to etoposide. BMC Cancer. 2015;15:577. Published 2015 Aug 8. PMID: 26253167

**37.** Feoktistova M, Geserick P, Leverkus M. Crystal Violet Assay for Determining Viability of Cultured Cells. Cold Spring Harb Protoc. 2016;2016(4):pdb.prot087379. Published 2016 Apr 1. doi:10.1101/pdb.prot087379

**38.** Casadevall A, Pirofski LA. Host-pathogen interactions: redefining the basic concepts of virulence and pathogenicity. Infect Immun. 1999;67(8):3703-3713. doi:10.1128/IAI.67.8.3703-3713.1999

**39.** Casadevall A. The Pathogenic Potential of a Microbe. mSphere. 2017;2(1):e00015-17. Published 2017 Feb 22. doi:10.1128/mSphere.00015-17

**40.** Casadevall A, Pirofski LA. Microbial virulence results from the interaction between host and microorganism. Trends Microbiol. 2003;11(4):157-159. doi:10.1016/s0966-842x(03)00008-8

**41.** Rajaram MV, Ni B, Dodd CE, Schlesinger LS. Macrophage immunoregulatory pathways in tuberculosis. Semin Immunol. 2014;26(6):471-485. doi:10.1016/j.smim.2014.09.010

**42.** Lim JJ, Grinstein S, Roth Z. Diversity and Versatility of Phagocytosis: Roles in Innate Immunity, Tissue Remodeling, and Homeostasis. Front Cell Infect Microbiol. 2017;7:191. Published 2017 May 23. doi:10.3389/fcimb.2017.00191

**43.** Rothchild AC, Olson GS, Nemeth J, et al. Alveolar macrophages generate a noncanonical NRF2-driven transcriptional response to Mycobacterium tuberculosis in vivo. Sci Immunol. 2019;4(37):eaaw6693. doi:10.1126/sciimmunol.aaw6693

**44.** Gagneux, S. Strain variation in the Mycobacterium tuberculosis complex: its role in biology, epidemiology and control. Advances in Experimental Medicine and Biology 1019. Springer International Publishing AG 2017. Cham, Switzerland. ISBN 978-3-319-64369-4. DOI 10.1007/978-3-319-64371-7

**45.** Madhvi A, Mishra H, Leisching GR, Mahlobo PZ, Baker B. Comparison of human monocyte derived macrophages and THP1-like macrophages as in vitro models for M. tuberculosis infection. Comp Immunol Microbiol Infect Dis. 2019;67:101355. PMID: 31586851

**46.** Vandal OH, Nathan CF, Ehrt S. Acid resistance in Mycobacterium tuberculosis. J Bacteriol. 2009;191(15):4714-4721. doi:10.1128/JB.00305-09. PMID: 19465648

**47.** Seto S, Matsumoto S, Tsujimura K, Koide Y. Differential recruitment of CD63 and Rab7-interacting-lysosomal-protein to phagosomes containing Mycobacterium tuberculosis in macrophages. Microbiol Immunol. 2010;54(3):170-174. PMID: 20236428

**48.** Schnettger L, Rodgers A, Repnik U, et al. A Rab20-Dependent Membrane Trafficking Pathway Controls M. tuberculosis Replication by Regulating Phagosome Spaciousness and Integrity. Cell Host Microbe. 2017;21(5):619-628.e5. PMID: 28494243

**49.** Buter J, Cheng TY, Ghanem M, et al. Mycobacterium tuberculosis releases an antacid that remodels phagosomes. Nat Chem Biol. 2019;15(9):889-899. PMID: 31427817

**50.** Schaible UE, Sturgill-Koszycki S, Schlesinger PH, Russell DG. Cytokine activation leads to acidification and increases maturation of Mycobacterium avium-containing phagosomes in murine macrophages. J Immunol. 1998;160(3):1290-1296. PMID: 9570546

**51.** Via LE, Fratti RA, McFalone M, Pagan-Ramos E, Deretic D, Deretic V. Effects of cytokines on mycobacterial phagosome maturation. J Cell Sci. 1998;111 ( Pt 7):897-905. PMID: 9490634

**52.** Domenech P, Zou J, Averback A, et al. Unique Regulation of the DosR Regulon in the Beijing Lineage of Mycobacterium tuberculosis. J Bacteriol. 2016;199(2):e00696-16. Published 2016 Dec 28. PMID: 27799329

**53.** Network analysis identifies regulators of lineage-specific phenotypes in Mycobacterium tuberculosis Amir Banaei-Esfahani, Andrej Trauner, Sonia Borrell, Sebastian M. Gygli, Tige R. Rustad, Julia Feldmann, Ludovic C. Gillet, Olga T. Schubert, David R. Sherman, Christian Beisel, Sebastien Gagneux, Ruedi Aebersold, Ben C. Collins bioRxiv 2020.02.14.943365; doi: https://doi.org/10.1101/2020.02.14.943365

**54.** Reichlen MJ, Leistikow RL, Scobey MS, Born SEM, Voskuil MI. Anaerobic Mycobacterium tuberculosis Cell Death Stems from Intracellular Acidification Mitigated by the DosR Regulon. J Bacteriol. 2017;199(23):e00320-17. Published 2017 Oct 31. PMID: 28874407

**55.** Butler RE, Cihlarova V, Stewart GR. Effective generation of reactive oxygen species in the mycobacterial phagosome requires K+ efflux from the bacterium. Cell Microbiol. 2010;12(8):1186-1193. PMID: 20331644

**56.** Khare G, Reddy PV, Sidhwani P, Tyagi AK. KefB inhibits phagosomal acidification but its role is unrelated to M. tuberculosis survival in host. Sci Rep. 2013;3:3527. Published 2013 Dec 18. PMID: 24346161

**57.** Gonzalo-Asensio J, Malaga W, Pawlik A, et al. Evolutionary history of tuberculosis shaped by conserved mutations in the PhoPR virulence regulator. Proc Natl Acad Sci U S A. 2014;111(31):11491-11496. PMID: 25049399

**58.** Sachdeva K, Goel M, Sudhakar M, et al. Mycobacterium tuberculosis (Mtb) lipid mediated lysosomal rewiring in infected macrophages modulates intracellular Mtb trafficking and survival. J Biol Chem. 2020;295(27):9192-9210. PMID: 32424041

**59.** Malone K.M., Gordon S.V. (2017) Mycobacterium tuberculosis Complex Members Adapted to Wild and Domestic Animals. In: Gagneux S. (eds) Strain Variation in the Mycobacterium tuberculosis Complex: Its Role in Biology, Epidemiology and Control. Advances in Experimental Medicine and Biology, vol 1019. Springer, Cham. https://doi.org/10.1007/978-3-319-64371-7_7

**60.** Panchal V, Jatana N, Malik A, et al. A novel mutation alters the stability of PapA2 resulting in the complete abrogation of sulfolipids in clinical mycobacterial strains. FASEB Bioadv. 2019;1(5):306-319. Published 2019 Apr 10. PMID: 32123834

**61.** Network analysis identifies regulators of lineage-specific phenotypes in Mycobacterium tuberculosis Amir Banaei-Esfahani, Andrej Trauner, Sonia Borrell, Sebastian M. Gygli, Tige R. Rustad, Julia Feldmann, Ludovic C. Gillet, Olga T. Schubert, David R. Sherman, Christian Beisel, Sebastien Gagneux, Ruedi Aebersold, Ben C. Collins bioRxiv 2020.02.14.943365; doi: https://doi.org/10.1101/2020.02.14.943365

**62.** Canton J. Phagosome maturation in polarized macrophages. J Leukoc Biol. 2014;96(5):729-738. doi:10.1189/jlb.1MR0114-021R. PMID: 24868088

**63.** Canton J, Khezri R, Glogauer M, Grinstein S. Contrasting phagosome pH regulation and maturation in human M1 and M2 macrophages. Mol Biol Cell. 2014;25(21):3330-3341. PMID: 25165138

**64.** Pauwels AM, Trost M, Beyaert R, Hoffmann E. Patterns, Receptors, and Signals: Regulation of Phagosome Maturation. Trends Immunol. 2017;38(6):407-422. PMID: 28416446

**65.** Podinovskaia M, Lee W, Caldwell S, Russell DG. Infection of macrophages with Mycobacterium tuberculosis induces global modifications to phagosomal function. Cell Microbiol. 2013;15(6):843-859. PMID: 23253353

**66.** Bussi C, Gutierrez MG. Mycobacterium tuberculosis infection of host cells in space and time. FEMS Microbiol Rev. 2019;43(4):341-361. doi:10.1093/femsre/fuz006

**67.** Russell DG. Who puts the tubercle in tuberculosis?. Nat Rev Microbiol. 2007;5(1):39-47. PMID: 17160001

**68.** Kelly DM, ten Bokum AM, O'Leary SM, O'Sullivan MP, Keane J. Bystander macrophage apoptosis after Mycobacterium tuberculosis H37Ra infection. Infect Immun. 2008;76(1):351-360. PMID: 17954721

**69.** Wojtas B, Fijalkowska B, Wlodarczyk A, et al. Mannosylated lipoarabinomannan balances apoptosis and inflammatory state in mycobacteria-infected and uninfected bystander macrophages. Microb Pathog. 2011;51(1-2):9-21. PMID: 21440050

**70.** Gupta S, Rodriguez GM. Mycobacterial extracellular vesicles and host pathogen interactions. Pathog Dis. 2018;76(4):fty031. PMID: 29722822

**71.** Singh PP, LeMaire C, Tan JC, Zeng E, Schorey JS. Exosomes released from M. tuberculosis infected cells can suppress IFN-γ mediated activation of naïve macrophages. PLoS One. 2011;6(4):e18564. Published 2011 Apr 14. PMID: 21533172

**72.** Haque MF, Boonhok R, Prammananan T, et al. Resistance to cellular autophagy by Mycobacterium tuberculosis Beijing strains. Innate Immun. 2015;21(7):746-758. PMID: 26160686

**73.** Romagnoli A, Petruccioli E, Palucci I, et al. Clinical isolates of the modern Mycobacterium tuberculosis lineage 4 evade host defense in human macrophages through eluding IL-1β-induced autophagy. Cell Death Dis. 2018;9(6):624. Published 2018 May 24. PMID: 29795378

**74.** Porcelli SA, Jacobs WR Jr. Tuberculosis: unsealing the apoptotic envelope. Nat Immunol. 2008;9(10):1101-1102. PMID: 18800161

**75.** Davis JM, Ramakrishnan L. The role of the granuloma in expansion and dissemination of early tuberculous infection. Cell. 2009;136(1):37-49. PMID: 19135887

**76.** Aguiló N, Marinova D, Martín C, Pardo J. ESX-1-induced apoptosis during mycobacterial infection: to be or not to be, that is the question. Front Cell Infect Microbiol. 2013;3:88. Published 2013 Dec 4. PMID: 24364000

**77.** Behar SM, Briken V. Apoptosis inhibition by intracellular bacteria and its consequence on host immunity. Curr Opin Immunol. 2019;60:103-110. PMID: 31228759

**78.** Amaral EP, Costa DL, Namasivayam S, et al. A major role for ferroptosis in Mycobacterium tuberculosis-induced cell death and tissue necrosis. J Exp Med. 2019;216(3):556-570. PMID: 30787033

**79.** mmunology in natura: clinical, epidemiological and evolutionary genetics of infectious diseases.Quintana-Murci L, Alcaïs A, Abel L, Casanova JLNat Immunol. 2007 Nov; 8(11):1165-71.

**80.** Lugo-Villarino G, Vérollet C, Maridonneau-Parini I, Neyrolles O. Macrophage polarization: convergence point targeted by mycobacterium tuberculosis and HIV. Front Immunol. 2011;2:43. Published 2011 Sep 15. doi:10.3389/fimmu.2011.00043

**81.** Deretic V, Vergne I, Chua J, et al. Endosomal membrane traffic: convergence point targeted by Mycobacterium tuberculosis and HIV. Cell Microbiol. 2004;6(11):999-1009. doi:10.1111/j.1462-5822.2004.00449.x

**82.** Thobakgale C, Naidoo K, McKinnon LR, et al. Interleukin 1-Beta (IL-1β) Production by Innate Cells Following TLR Stimulation Correlates With TB Recurrence in ART-Treated HIV-Infected Patients. J Acquir Immune Defic Syndr. 2017;74(2):213-220. doi:10.1097/QAI.0000000000001181

**83.** Krishnan N, Robertson BD, Thwaites G. Pathways of IL-1β secretion by macrophages infected with clinical Mycobacterium tuberculosis strains. Tuberculosis (Edinb). 2013;93(5):538-547. doi:10.1016/j.tube.2013.05.002

# *Chapter 3*

## *ncRv0842c*, a smallRNA regulating the efflux pump *Rv0842* involved in rifampicin tolerance in *Mycobacterium tuberculosis*


### Abstract

Regulatory pathways mediated by smallRNAs (sRNAs) in *Mycobacterium tuberculosis* (MTB) and their role in stress response are still poorly understood. We identified the smallRNA *ncRv0842c* cis-encoded to the *Rv0842* gene, a putative efflux pump putatively involved in response to rifampicin (RIF). The aim of our study was to characterize the role of *ncRv0842c* during RIF challenge in different MTB lineages.

First, we looked at lineage-specific mutations mapping in smallRNAs. We then selected *ncRv0842c* for further characterization. qPCR was performed on different MTB strains belonging to ancient (L1, L5) and modern (L2, L4) lineages to assess the expression of *ncRv0842c* and *Rv0842* in both basal and RIF-induced stress. H37Rv strain was used as a reference. Overexpression of *ncRv0842c* was achieved by the use of the pMV261 plasmid as a vector. RIF Minimum Inhibitory Concentration (MIC) was determined by microplate AlamarBlue assay (MABA). The effect of *ncRv0842c* overexpression was compared to the one obtained by the use of carbonyl cyanide 3-chlorophenylhydrazone (CCCP).

WGS analysis revealed a synonymous mutation in *Rv0842* (L45L) specific for ancient lineages abrogating the -10 promoter region of the cis-encoded smallRNA *ncRv0842c*. Basal expression analysis showed a strong down-regulation of the smallRNA *ncRv0842* in L5 compared to H37Rv. During RIF challenge, the efflux pump was up-regulated whereas the sRNA was down-regulated in H37Rv, while the smallRNA expression was consistently not affected by RIF stress in L5. MABA assay performed on the *ncRv0842c* overexpressing mutant in H37Rv and L4 clinical isolates showed a 1-dilution reduction of the RIF MIC in comparison with their own control strain

(empty pMV261). Similarly, a 1-dilution reduction of the MIC was observed when control strains were treated with CCCP. The mutant strains belonging to L1 and L5 did not show MIC changes for RIF despite the overexpression of the smallRNA.

*ncRv0842c* is a negative regulator of the efflux pump *Rv0842* and is downregulated during RIF stress. Our data showed that synonymous mutations may have an important effect on regulatory pathways. In addition, the characterization of lineage-specific mutations involving the smallRNA post-transcriptional regulatory network would provide a better understanding of stress response in MTB.

# Introduction

Tuberculosis, caused by *M. tuberculosis* (MTB) complex species, globally is the top infectious cause of death after COVID-19; an estimated 9.9 million people developed and 1.5 million died from the disease in 2020. Drug resistance poses a serious threat to ongoing efforts in controlling the epidemic.

The World Health Organization (WHO) framework for ending the global TB epidemic relies in part on the early identification of drug-resistant cases in order to implement timely and appropriate treatment and infection control strategies. Global progress has been made in the rapid detection of drug resistance as a result of improvement of genotype-phenotype association studies and broad implementation of WHO-endorsed assays [1]. However, despite the identification of genetic markers with high predictive values for the detection of drug resistance, our capacity to diagnose resistant cases for many drugs is below the target-product-profiles described by the WHO to support the End TB Strategy [2]. One underlining concept behind this diagnostic gap is likely the fact that whereas the main drivers of resistance are often only a few key mutations, a larger proportion of mutations contribute to resistance by their cumulative (especially when non-essential genes are involved in the mechanisms of drug resistance) and or regulatory effects.

Another relevant topic drawing attention in the field is related to better understanding the role of genetic diversity within the MTB complex in both intrinsic and acquired drug resistance. This complexity has not always been considered in the past.

Like other pathogenic bacteria, MTB has to adapt to rapidly changing conditions and thus has evolved a plethora of sensory systems that activate or repress the expression of genes in response to shifting environmental and host signals [3]. In particular, small regulatory RNAs (smallRNAs) have recently emerged as major regulators of adaptive responses and regulate essential pathways in bacteria to respond quickly to their environment [4].

Despite an increasing number of smallRNAs have been identified in MTB, their potential role in drug resistance has not been explored, and much more attention has been paid to their potential role in virulence and stress response [5].

We propose an improved approach to achieve a better understanding of MTB drug resistance focusing on smallRNAs and keeping into account the genetic background of the strains.

# Methods:

- **MTB strains**

For initial assessment 20 modern MTB (eight L4 strains, nine L2, four L3) and two ancient MTB strains (L5) were selected in order to study the baseline expression of the candidate_1080 (renamed *ncRv0842c*) smallRNA both in exponential and stationary growth phases. Strains selected included MDR, non-MDR, clade-related and sporadic isolates.

For further characterization of *ncRv0842c* nine phylogenetically modern clinical strains (L3 and L4) were selected from our laboratory collection, according to the RIF (RIF) DST results (four RIF-sensible strains and five with Increased MIC - iM strains, with RIF-MIC close to the RIF breakpoint). As control, the laboratory strain H37Rv (NTCC7416) and two ancient MTB lineage-reference RIF -sensible strains (L1 and L5), selected from ITM (Anversa) collection, were included in the study (Table 1) [6]. In addition, strains were checked for kanamycin susceptibility to allow the overexpression of the smallRNA *ncRv0842c* by the use of the pMV261 plasmid harboring a kanamycin resistance cassette.

**Table 1**: MTB strain selected for this study, and their RIF MIC (µg/mL)

| Strain (rpoB mutation) | Lineage | MABA MIC | RIF DST |
|---|---|---|---|
| *BG 3009* | L4 | 0.03 µg/mL | S |
| *CCM123* | L4 | 0.06 µg/mL | S |
| *CCM321* | L4 | 0.06 µg/mL | S |
| *CCM190* | L4 | 0.06 µg/mL | S |
| *R246 (Asp453Tyr; Thr444Ser)* | L4 | 0.5 µg/mL | iM |
| *R399 (Leu430Pro)* | L3 | 0.25 µg/mL | iM |
| *R453 (Leu452Pro)* | L3 | 0.125 µg/mL | iM |
| *R749 (Leu452Pro)* | L3 | 0.25 µg/mL | iM |
| *R743 (Leu450Pro)* | L3 | 0.25 µg/mL | iM |
| *L1-082* | L1 | 0.03 µg/mL | S |
| *L5-097* | L5 | 0.015 µg/mL | S |

For mutant strains overexpressing the smallRNA, competent cells were prepared by washing three times a well-growth bacterial suspension in sterilized ice-cold PBS with 10% glycerol. When required, 40 µl of competent cells were incubated in ice with 2.5 µg of pMV261 (MOCK control) or pMV*ncRv0842c* for 1 minute; then, the suspension was moved into a 0.2 cm electroporation cuvette and electroporated with the MicroPulser (Bio-Rad, California, USA) apparatus at 2.5 kV, 25 uF, and 200 Ω. Electroporated bacteria were collected from the cuvette, diluted with 1 ml of new complete 7H9 media without antibiotics and let recovered for 24 h before being plated on 7H10 agar plates complemented with kanamycin (50 µg/ml) to obtain transformed colonies. After 21 days, at least 3 colonies for each plate were selected, checked for the presence of the plasmids by performing end-point PCR. Transformed colonies were grown in the presence of kanamycin to allow plasmid retention.

- **Plasmids**

  pMV*nc0842c* for constitutive overexpression of the smallRNA was prepared by cloning the smallRNA *ncRv0842c in-frame* with $P_{hsp60}$ promoter in the plasmid backbone pMV261 (low copy, KAN-R). To avoid the addition of unrequired nucleotides to the 5'region of the smallRNA, the UTR region of the promoter was truncated, and the smallRNA was cloned directly after the Transcription Start Site of the promoter (TSS). An artificial terminator was added to the 3' region of the smallRNA as previously described [7].

- **Culture media and bacterial culture**

  Complete Middlebrook 7H9 (Becton, Dickinson, Franklin Lakes California USA) liquid culture medium was prepared accordingly to manufacturer instruction, and enriched with 10% of OADC (Oleic Albumin Dextrose Catalase, BBL™ Middlebrook) supplement and 0.05% Tween80 (Sigma-Aldrich, Missouri, USA).

  Middlebrook 7H10 plates (Becton, Dickinson, Franklin Lakes California USA) were prepared accordingly to manufacturer instruction, enriched with 10% of OADC, and poured in sterile 10 cm non-treated culture plate (20 ml per plate).

  The MTB laboratory reference strain H37Rv (NTCC7416) and the clinical isolates selected for the study were grown in 7H9 at 37 °C using vented flasks (Corning®, Sigma Aldrich, Missouri, USA). Experiments were performed with bacteria in log-Phase ($OD_{600}$ 0.2 to 0.5). Selective 7H9 media for plasmid selection were added with 50µg/mL of kanamycin (Sigma Aldrich, Missouri, USA), and/or RIF (Sigma Aldrich, Missouri, USA) at sub-inhibitory concentrations.

- **Whole genome sequencing**

  Genomic DNA of the selected strains was extracted as described in and sequenced for Whole Genome Sequencing (WGS) analysis using Illumina technology as previously described [8]. Briefly, the library was constructed

using a Nextera XT Library Preparation Kit (Illumina, California, USA) and was sequenced on Illumina HiSeq 2500 platform. FASTQ data obtained were analyzed on the MTBseq bioinformatic tool specific for MTB [9].

- **Genetic variability in MTB smallRNAs**

  Previous work in our laboratory described nearly 2000 smallRNA candidates [14]. Further studies based on RNAseq and literature evidence allowed to identify 756 "likely true" smallRNAs (data not shown) [15]. WGS data from 1811 isolates were collected for variants identification. Strains were divided into ancient lineages and modern lineages. Regions belonging to smallRNA candidates were selected for further analysis. SNPs presence was compared between ancient and modern lineages, selecting mutations present in one of the two categories in at least 95% of the isolates.

- **Northern blot**

  The existence of the predicted smallRNA *ncRv0842c* was confirmed by Northern Blot on exponential and stationary phase H37Rv RNA. Northern blot analysis was conducted using $^{32}P$ labeled, customized RNA probes, complementary to the smallRNA sequence. RNA probes were obtained transcribing the DNA oligo RNA polymerase T7. X-ray film was developed with a Phosporimager (Typhoon Amersham Biosciences Corp, California USA).

- **Sub inhibitory RIF stress**

  RIF-induced stress was assessed at sub-inhibitory concentrations (25%, 50%, 90% RIF-MIC) on H37Rv and on L5 strains. Bacterial total RNA was extracted after 30m, 6h, and 24h post-treatment using the mirVana™ miRNA Isolation Kit (ThermoFisher, Massachusetts, USA) according to manufacturer instructions. Non-treated bacteria were used as a control. Briefly, the MTB cultures were grown in 30mL in complete 7H9 with RIF. To obtain the complete lysis of the wax and lipid-rich MTB membrane, the samples were homogenated in a TissueLyser (Qiagen, Hilden, Germany)

with zirconia beads (Zirconia/Silica Bead, 0.1 mm Diameter, BioSpec Oklahoma, USA). An Acid-Phenol:Chloroform ectraction was performed following the mirVana kit protocol. This assay is specific for the extraction of total bacterial RNA, and has a high yield on preserving smallRNA.

The *TURBO* DNA-*free* Kit (Invitrogen, Massachusetts, USA) was used to remove DNA carry-over from RNA samples. Briefly, 5 µl of 10x DNAse buffer and 1 µl of DNAse were added to 44 µl of RNA and incubated 25 minutes at 37 °C in a water bath. Then, to block the DNAse reaction, the solution was moved in ice and added with 50 µl of Acid-Phenol: Chloroform, vortex, and centrifuge at 13000 rpm for 5'. 40 µl of the aqueous solution was supplemented with 0.1 Vol of 3M Sodium acetate and 3 Vol ice-cold 100% Ethanol and precipitated overnight at -20°C. The day after, the solutions were centrifuged at 13000 rpm, 4° C for 15'; the pellets were washed with 1 V of ice-cold 75% Ethanol, resuspended in Nuclease free water, and quantified by Bioanalyzer 2100 RNA 6000 nanochip (Agilent, California, USA).

- **Real-Time PCR**

Extracted RNA (2 ng) was retrotranscribed with the High-Capacity cDNA Reverse Transcription (RT) Kit (Applied Biosystems, Massachusetts, USA) following the manufacturer's instruction.

Quantitative Real-Time (qRT-PCR) was carried out in an Applied Biosystems™ 7500 Real-Time PCR System (ThermoFisher, Massachusetts, USA) using a SYBR® Green-based chemistry. Briefly, experiments were performed in 96-well plates (ThermoFisher, Massachusetts, USA), the reaction mix was composed of 12.5 µL of 2X Universal SYBR™ Green PCR Master Mix (Applied technology), 100 nM of both forward and reverse primers (10 µM mother solution), 5 µL of first-strand cDNA and nuclease-free water to the final volume of 25 µL. The thermocycler was set with the following parameters: 95 °C for 5 min followed by 40 cycles of denaturation (95° for 30 s), annealing (58° for 30 s) and elongation (72° for 30 s). To

ensure the reaction specificity, the melting curves were assessed for each primer setup experiment.

The ΔCT value was calculated using the SigA gene as endogenous control. H37Rv was used as calibrator for the experiments.

- **MGIT TPP**

The BACTEC MGIT 960 (Becton Dickinson, New Jersey, USA), culture system was used to calculate the Time To Positivity (TTP) of H37Rv strain carrying the overexpressing plasmid pMV*ncRv0842c*. The mock H37Rv strain was used as a control. Briefly, 800 µl of OADC, 200 µl of bacterial suspension ($OD_{600}$ 0.01) and 8 µl or 16 µl of 0.562 mg/ml RIF (respectively 90% and 2x 90% RIF-MIC) were added to a 7 ml 7H9 MGIT tube. The difference between the TTP from the mock strain and the overexpressing strain was calculated to obtain the ΔTTP (in hours, h).

- **Minimum inhibitory concentration (MIC)**

Microplate Alamar Blue assay (MABA) was used to determine the MIC of RIF and/or Carbonyl cyanide m-chlorophenyl-hydrazone (CCCP) for the selected strains. The drug concentrations tested ranged from 4 µg/mL to 0.0007 µg/mL for RIF and from 10 µg/mL to 0.02 µg/mL for CCCP. For each experiment, the selected drug was pre-diluted at 4x higher concentration in 7H9 enriched with OADC and KAN w/o Tween80 (7H9_MABA), and subsequentially, 9 two-fold serial dilutions were performed in 7H9_MABA directly in the 96-well round-bottom tissue culture plates with a low evaporation lid (Becton Dickinson, New Jersey, USA).

Bacteria growth at Log phase were diluted in 7H9_MABA at $OD_{600}$ 0.011 and inoculated on the previously prepared plates and incubated for 1 week at 37 °C.

To determine the MIC, the cell viability reagent AlamarBlue (Sigma-Aldrich, Missouri, USA) was added to each well; AlamarBlue is a stabilized solution containing the cell-permeable blue dye known as resazurin. Viable cells

(cells with active metabolism) are able to reduce the resazurin to resorufin, a pink dye; this colorimetric change can be easily detected.

The MIC is defined as the lower drug concentration able to sufficiently decrease the cell viability to prevent the colorimetric switch [10].

- **Drugs Combination Assay**

The combination assay between RIF and CCCP was performed with a constant concentration of CCCP (90% MIC determined as previously described). For each experiment, RIF was pre-diluted at 4x higher concentration in 7H9_MABA enriched with 2x 90% MIC of CCCP (7H9_MABA_CCCP); 9 twofold serial dilutions were carried out in 7H9_MABA_CCCP directly in the 96-well round-bottom tissue culture plates with a low evaporation lid (Becton Dickinson, New Jersey, USA). Bacteria growth at Log phase were diluted in 7H9_MABA at $OD_{600}$ 0.011 and inoculated on the previously prepared plates and incubated for 1 week at 37 °C.

The experiments were carried out as previously described only on the Mock control strains and the obtained MICs were compared with the MIC obtained for the corresponding *ncRv0842c* overexpressing strains in absence of CCCP.

# Results

**Sequencing analysis**

To characterize the strains selected for smallRNA expression, whole-genome sequencing (WGS) was performed using Illumina technology. Sequencing produced results with a mean coverage >30 and the genomes were analyzed using the MTBseq software. Variant calls were mapped on genomic regions matching with smallRNA candidates, including 3' and 5' flanking regions (+/- 100 nucleotides) to avoid the omission of mutations in UTRs. The comparison between 85 ancient and 1726 modern lineages produced a list of 64 unique SNPs on 64 different smallRNA candidates: 22 SNPs were present only in ancient lineages while 42 in modern lineages. Among the ancient specific lineages, only 7 candidates harbor a SNP involving the coding region of the AS gene, while the remaining candidates involved UTRs or intergenic regions (Table 2). Interestingly, among the SNPs affecting AS smallRNAs we found two unique mutations, specific for ancient lineages and found to be synonymous on the CDS strand (Candidate_1221 and Candidate_1080). We decided to further investigate the role of the synonymous mutation of Candidate_1080.

This synonymous mutation falls in the *Rv0842* efflux pump gene at position 45 (ctA→ctG Leu45Leu), and coincides with a Tag→Cag mutation on the opposite (candidate_1080, renamed as *ncRv0842c*) strand, affecting its -10 promoter region (Fig. 3). Ancient-lineage specificity for this SNP was confirmed by cross-checking WGS data at the Leibniz-Zentrum database (Borstel, Germany).

**Table 2**: smallRNA candidates specific for ancient MTB strains from the WGS analysis. Among smallRNA considered, the candidate_1080 (renamed *ncRv0842c* according to the proposed standard nomenclature) was selected for this study [11]. *ncRv0842c* has an ancient specific SNP affecting its -10 promoter region. AS: antisense; UTR: Untranslated region; IG: Intergenic; CDS: Coding Sequence.

| Variant (coordinates) | Candidate smallRNA (Strand) | smallRNA type | SNP location | Codon change (on the AS gene) |
|---|---|---|---|---|
| 1639643t>c | candidate_1221 (-) | AS | CDS *Rv1453* | cgt-cgc / Arg-Arg |
| 1639643t>c | candidate_2064 (+) | AS | 3' UTR *Rv1454c* | / |
| 1906336a>g | candidate_2074 (+) | Whitin UTRs | 3' UTR *Rv1681* / 5' UTR *Rv1682* | / |
| 1931470c>t | candidate_2075 (+) | AS | 5' UTR *Rv1704c* | / |
| 2039884t>g | candidate_1296 (-) | AS | CDS *Rv1800* | tgt-tgg / Cys-Trp |
| 2052687g>c | candidate_1298 (-) | AS | 3' UTR *Rv1809* | / |
| 2447539t>c | candidate_1366 (-) | Whitin UTRs | 5' UTR *Rv2185c* / 3' UTR *Rv2186c* | / |
| 3007238t>c | candidate_1863 (-) | Whitin UTRs | 5' UTR *Rv2689c* / 3' UTR *Rv2689c* | / |
| 3027606c>g | candidate_1461 (-) | AS | CDS *Rv2714* | ctg-ctc / Leu-Leu |
| 3369869c>a | candidate_2123 (+) | AS | 5' UTR *Rv3010c* / 3' UTR *Rv3011c* | / |
| 3415332a>g | candidate_1507 (-) | AS | 3' UTR *Rv3053c* | / |
| 4200220t>c | candidate_886 (+) | AS | 5' UTR *Rv3753c* | / |
| 2097144g>c | candidate_1310 (-) | AS | CDS *Rv1847* | gtg-ctg / Val-Leu |
| 2097144g>c | candidate_2081 (+) | AS | 5' UTR *Rv1846c* | / |
| 2019236t>g | candidate_1282 (-) | AS | CDS *Rv1782* | gtc-ctt / Val-Pro |
| 1496964g>t | candidate_2059 (+) | AS | 3' UTR *Rv1329c* | / |
| 1203824t>c | candidate_1129 (-) | AS | CDS *Rv1078* | cag-tag / Gln-Stop |
| 1040706t>g | candidate_135 (+) | AS | CDS *Rv0932c* | tcg-gcg / Ser-Ala |
| 938246a>g | candidate_1080 (-) | AS | CDS *Rv0842* | cta-ctg / Leu-Leu |
| 1287112t>c | candidate_161 (+) | IG | IG | / |
| 139756t>c | candidate_668 (+) | IG | IG | / |
| 3302683c>t | candidate_442 (+) | IG | IG | / |

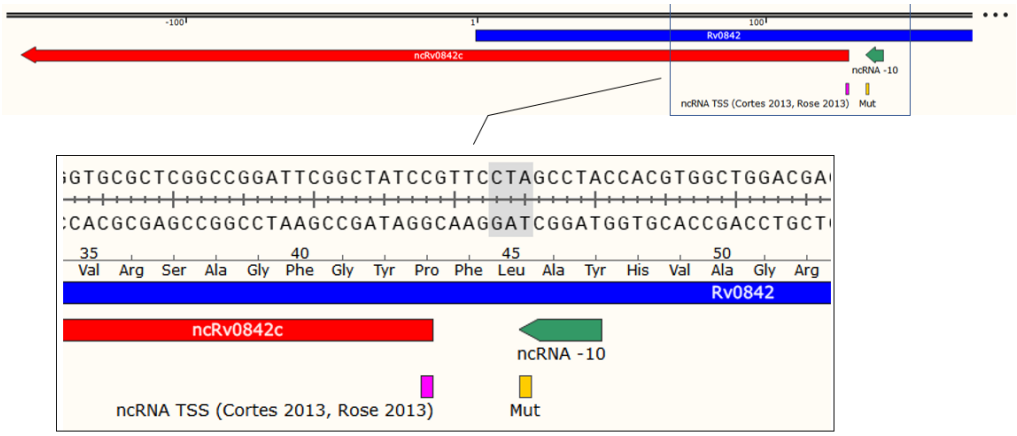


**Fig. 3**: WGS analysis show a synonymous mutation in *Rv0842* (L45L) specific for the ancient lineages (L1, L5, L6) abrogating the -10 promoter region of the cis-encoded smallRNA *ncRv0842c*

**Northern blot**

Northern blot was performed to confirm the existence of the predicted smallRNA *ncRv0842c*. The predicted size of the smallRNA candidate *ncRv0842c* is 283bp; according to its coordinates, 937956 – 938239 (*strand* -), it resulted to overlap for 127bp the gene *Rv0842*, coding for an efflux pump member of the major facilitator superfamily (MFS).

The 127 bp overlap entails that the TSS and the promoter region of the smallRNA candidates are antisense to the coding region of the gene.

To avoid unreliable results, RNA was extracted from a planktonic culture in both exponential and stationary growth phases and the Northern blot revealed a defined band, raging around 250bp, in both tested conditions even if the band obtained for the Log-phase extract shows a higher intensity.

The other bands shown in the image (Fig. 4) have lower signal intensity, thus indicating that they are either products of RNA maturation or degradation of the *ncRv0842c*.

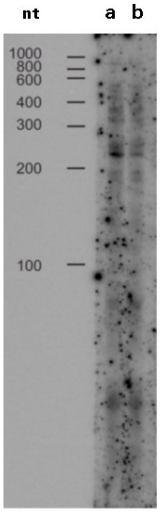


**Fig. 4**: Northern blot analysis revealed the presence of a specific band at the expected length (about 250) at exponential (a) and at stationary (b) growth phase. Multiple bands indicate putative maturation fragments of the smallRNA.

**qRT-PCR**

The expression of the smallRNA *ncRv0842c* was measured using a q-RT PCR and the *sigA* gene was used as an endogenous control to normalize the results obtained.

The pilot experiments were run on RNA extracted from a planktonic culture in both exponential and stationary growth phases and in the strains belonging to the different lineages of MTB and in *M. africanum*. Results were normalized on the laboratory strain H37Rv. qRT-PCR showed that the basal expression of *ncRv0842c* in the *M. africanum* strains considered is greatly lower in comparison with H37Rv, in both exponential (-16 fold change; *P-value* 0.046) and stationary phase (-32 fold change; *P-value* 0.013) (Fig. 5). Drug resistance background nor epidemiological features (sporadic vs clade-related isolates) did not show to affect the baseline expression of the smallRNA (data not shown).

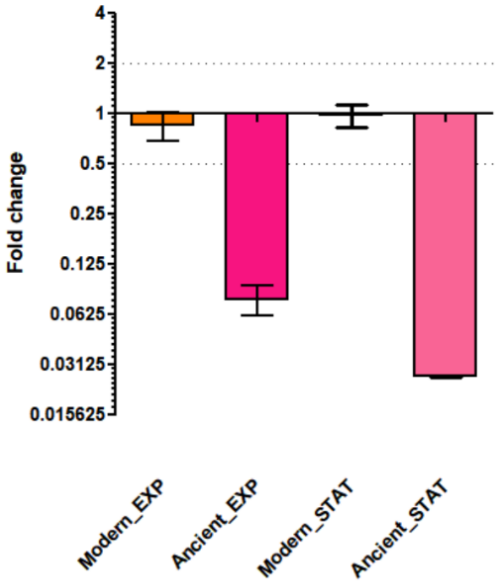


**Fig. 5**: qPCR of *ncRV0842c* smallRNA in modern and ancient MTB strains (normalized on H37Rv values). Result show that *ncRv0842c* is strongly downregulated in ancient lineages both in exponential and stationary planktonic growth phases

To better characterize the function of *ncRv0842c* we constructed an over-expressing plasmid using the vector pMV261 and cloning the smallRNA at

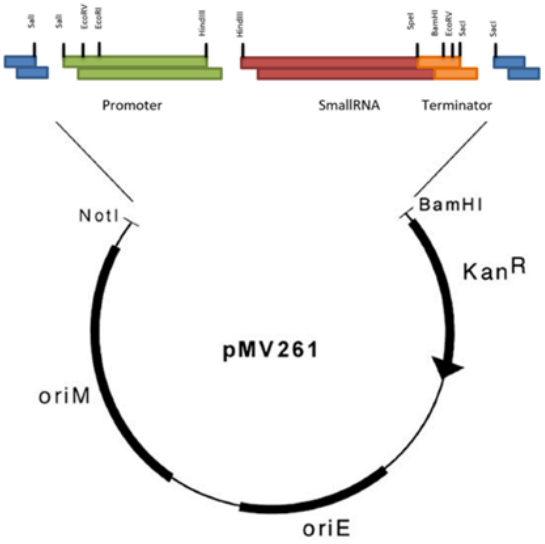


the restriction sites NotI and BamHI (Fig. 6).

**Fig.6**: pMV261 overexpressing the smallRNA *ncRv0842c*. OriE: E. coli Origin of Replication; $Kan^R$: kanamycin resistance cassette, OriM: MTB Origin of Replication.

Our previous work based on RNAseq, highlighted the up-regulation of *Rv0842* and the simultaneous down-regulation of *ncRv0842c* during RIF stress (data not shown). Literature data showed that the *Rv0842* efflux pump was induced during several antibiotic-based stresses, including RIF [12]. In particular, clinical isolates monoresistant to RIF showed over-expression of the efflux pump [13]. Accordingly, the subsequent experiments aimed to characterize the smallRNA function in H37Rv and *M. africanum* in response to the sub-inhibitory concentration of RIF (RIF-challenge).

Before proceeding with the RIF-challenge, the MIC for RIF was assessed on the strains considered and resulted 0.0625 µg/mL for H37Rv and the 2 *M. africanum* isolates; therefore, for the subsequent experiments, RIF concentrations equal to 0.0156 µg/L (25%), 0.0312 µg/mL (50%) and 0.0562 µg/mL (90%) were used. For this study, early (30 minutes), middle (6 hours) and late (24h) time points were selected.

The use of RIF at 25% MIC was not showing significant changes (data not shown). *ncRv0842c* was found down-regulated (-4 fold changes) in H37Rv treated with 50% of the MIC (p-value 0.0059). Despite the amplitude of the regulation decreased (-2 fold changes), a similar trend was observed at 90% of the MIC. The efflux pump *Rv0842* resulted significantly up-regulated (2 fold change), in comparison with the untreated control with 90% of the MIC (*P-value* 0.0089), whereas lower RIF concentrations (50% MIC) induced slight changes in the expression of the pump (Fig. 7 A).

Regarding the *M. africanum* strains, the expression of *Rv0842* resulted slightly induced under treatment with 90% of the MIC, however, the difference with the control was not found statistically significant (*P-value* 0.05). On the contrary, the smallRNA expression levels were mostly unaffected and strongly downregulated (-128 fold changes) compared to H37Rv (*P-value* <0.001) (Fig. 7 B), thus aligned with the baseline expression profiling showed above (Fig. 5).

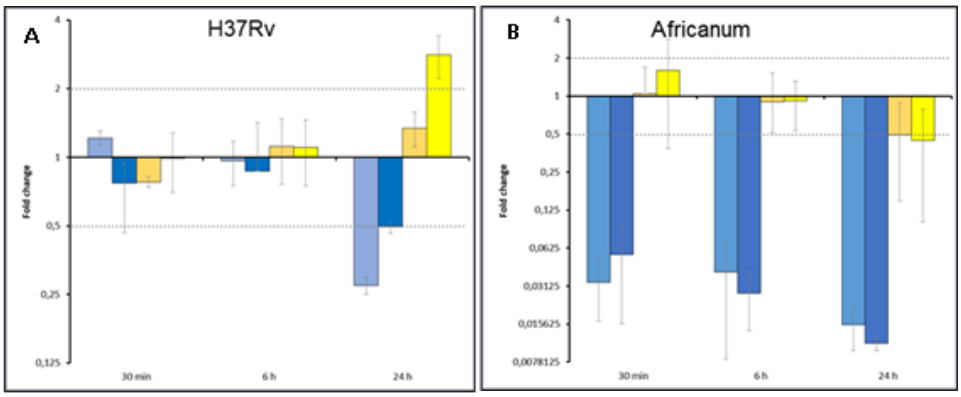


**Fig. 7**: qPCR expression data of the smallRNA *ncRv0842c* (blue) and the AS efflux pump *Rv0842* (yellow). A) H37Rv. B) *M. africanum* strains expression values normalized on H37Rv.

**MGIT TTP**

To ensure that the over-expression of *ncRv0842c* does not affect the *in vitro* growth of the mutant strains, thus introducing a bias in the phenotypical evaluation discussed in the next paragraphs, the "time to

positivity" (TTP) of H37Rv strain carrying the overexpressing plasmid pMV*ncRv0842c* and of the H37Rv strain containing the empty plasmid was assessed by the BACTEC MGIT 960. Experiments were performed in basal conditions (no RIF), during the RIF-challenge (90% RIF MIC) and in extreme conditions (2x 90% RIF MIC).

In basal conditions, the growth rate resulted unaffected by the overexpression of the smallRNA. On the contrary, in both RIF-induced stress conditions, the constitutive overexpression of *ncRv0842c* causes growth delays during RIF challenge in MGIT TTP assay (ΔTTP>100 hr). (Fig. 8). Similar findings were confirmed by testing a RIF-S, modern lineage clinical isolate (data not shown).

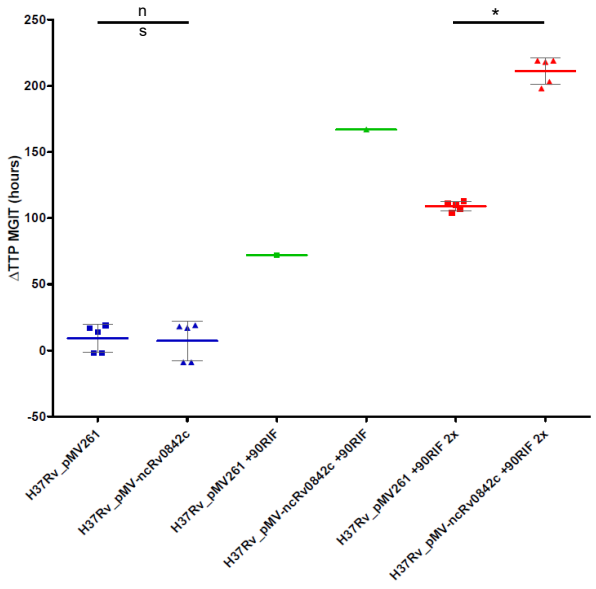


**Fig. 8**: TPP in MGIT of H37Rv under RIF stress. Blue) H37Rv with the empty control vector pMV261 and the *ncRv0842c* overexpressing plasmid w/o RIF-stress. Green) H37Rv with the empty control vector pMV261 and the *ncRv0842c* overexpressing plasmid with 90% of RIF-MIC. Red) H37Rv with the empty control vector pMV261 and the *ncRv0842c* overexpressing plasmid with 2x 90%RIF-MIC.

## Minimum inhibitory concentration (MIC)

To evaluate the functional role of the smallRNA *ncRv0842c,* the minimum inhibitory concentrations (MICs), defined as the lower drug concentration

required to inhibit visible growth as detected by resazurin reduction, were assessed for six “S” (RIF-sensible) and five “iM” (increased RIF MIC) strains overexpressing *ncRv0842c* and on their respective controls (mock, pMV261 empty plasmid). As shown in the graph below, RIF MIC is reproducibly and consistently reduced by ≥1 MIC dilution when the smallRNA is over-expressed in all the modern strains selected, thus halving the concentration of RIF required to inhibit the bacterial growth (Fig. 9). This phenotype cannot be reproduced on strains carrying the L45L mutation on *Rv0842* gene (ancient lineages) in which the basal expression of the smallRNA is almost completely switched off.

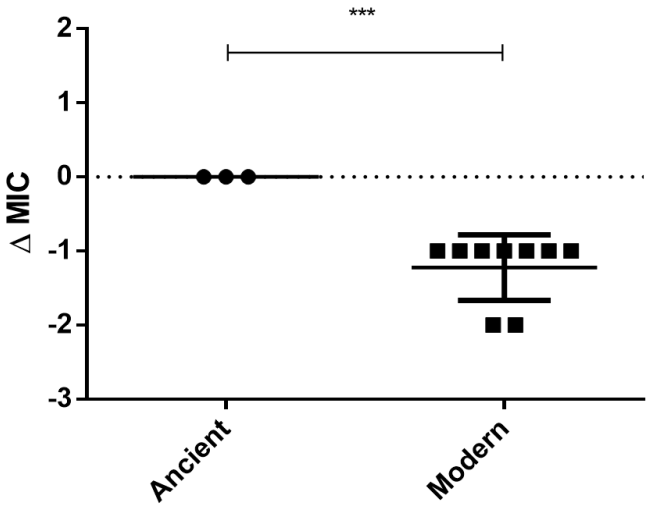


**Fig. 9**: MABA delta MIC variation of modern and ancient MTB strain carrying the smallRNA overexpressing plasmid. Modern strains’ RIF sensitivity is increased by about 1 MIC dilution. Each point represents the average delta MIC value of a strain. Experiments were performed at least 2 times, with 3 technical replicates each.

To confirm that the observed ΔMIC can be attributed to the downregulation of an efflux pump, we tested the effect of the well-characterized efflux pump inhibitor CCCP on mock control strains. The phenotypic effect of CCCP was assessed by calculating the RIF-MIC of the mock control strains undergoing sub-inhibitory (90% MIC) CCCP stress.

As a control, we tested the contribution of CCCP, randomly in three of the selected strains. The graphic below demonstrated that the sub-inhibitory administration (90% MIC) of CCCP has a phenotypic effect comparable to the overexpression of *ncRv0842c* (Fig. 10), thus supporting the hypothesis that the smallRNA is acting as a negative regulator of the efflux pump *Rv0842*.

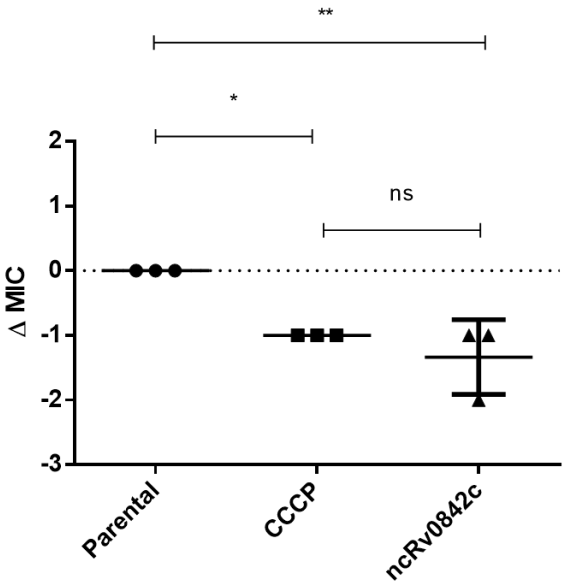


**Fig. 10**: Delta MIC variation. MABA assay demonstrated that the sub-inhibitory administration (90% MIC) of CCCP has a phenotypical effect comparable to the overexpression of *ncRv0842c*. Each point represents the average delta MIC value of a strain. Experiments were performed at least 2 times, with 3 technical replicates each.

# Discussion

The DNA mutations, discovered and categorized thanks to extensively genomic studies conducted over the last three decades, failed to fully explains all the resistance found among the different strains; thus, suggesting that other, epigenetic, mechanisms are involved in the drug resistance or drug-tolerance development.

MTB smallRNAs have only recently become a topic of study; despite it being predicted that H37Rv genome encodes for at least 92 noncoding RNAs and a few additional hundreds have been predicted, just a few of them have been studied and characterized; therefore, their mechanisms of action and their functions within the cell are still mostly unidentified [14]. The mode of action of these regulatory molecules is very different from protein regulators, for which the waiting time is determined primarily by the turn-over rate of the protein[15].

Unraveling the biological functions and the mechanism of action of smallRNA may lead to the development of new therapeutic strategies to counteract the resistance development of MTB.

In the present study, we investigated whether MTB lineage-specific SNPs could map in smallRNA coding regions. The comparison between ancient and modern lineages identified a list of 65 lineage-specific SNPs involving smallRNA regions.

Interestingly, a synonymous mutation on the gene encoding for *Rv0842* (ctA→ctG) at codon 45 was found specific for the ancient lineages (L1, L5, L6) and mapped in the promoter region of *ncRv0842c.* We characterized the role of the smallRNA *ncRv0842c cis-encoded* to the *Rv0842* gene (a putative major facilitator superfamily (MFS) efflux pump) in different MTB lineages exposed to RIF stress.

The smallRNA was found to be strongly downregulated in ancient strains when compared to H37Rv and other modern strains, both in the exponential and in the stationary phase. This finding confirmed that the

synonymous mutation, L45L, abrogates the -10 promoter region of *ncRv0842c* consequently affecting the expression of this *cis*-econded regulator without affecting the amino acidic sequence of the efflux pump.
To study the mechanism of action of the smallRNA and to evaluate its capability to regulate the antisense gene, the expression levels of both the efflux pump and its smallRNA were analyzed under treatment with different RIF sub-inhibitory concentrations. In H37Rv (representative of modern lineages), RIF challenge induced the down-regulation of the smallRNA and the over-expression of the efflux pump. These findings suggest that the smallRNA acts as a negative post-transcriptional regulator by mediating or contributing to the degradation of *Rv0842* mRNA.

Concerning the ancient lineage strains, both the smallRNA and the efflux pump expression resulted unaffected by RIF-stress. On one side, these results confirm that the synonymous mutation impairs the expression of the smallRNA in ancient lineages; on the other side, it seems the efflux pump is unresponsive to RIF challenge, thus suggesting that additional stress response networks are missing. Future studies will help to shed light in the explanation of the efflux pump involvement in ancient MTB strains.

To characterize further the role of the smallRNA, we generated overexpressing mutants where the *ncRv0842c* is expressed by means of a constitutive promoter. Mutants were generated in clinical isolates belonging to both ancient and modern lineages. To evaluate the metabolic burden of the plasmid we considered the TTP in MGIT. Accordingly, we could not find any difference in TPP between mock strains harboring the empty vector (pMV261) and mutant strains overexpressing the smallRNA (pMVn*cRv0842c*) in a standard culture medium. However, a growth delay (approx. 3 days) was observed when RIF was added to the tube containing the mutant strains pMV*ncRv0842c*, whereas RIF was not affecting TTP in mock strains. These findings further support the hypothesis that the smallRNA and its cis-encoded target CDS are involved in RIF transportation.
H37Rv pMV261*ncRv0842c* over-expressing mutant showed a 1-dilution RIF MIC reduction in several rounds of independent experiments. To validate

our findings, we selected 9 phylogenetically modern clinical strains showing different RIF MIC to be transformed with pMV261*ncRv0842c* over-expressing plasmid and evaluated if the overexpression of the smallRNA affected the strain-specific MIC for RIF. MABA assay showed that RIF MIC is reduced at least by 1-dilution when the smallRNA is overexpressed in all the strains selected. This effect on MIC cannot be reproduced in ancient strains pMV261*ncRv0842c* over-expressing mutant, at least, not with a low-copy plasmid. Also, the MIC reduction was not observed in RIF resistant clinical strains harboring mutations in the RRDR (the region of interaction between RIF and its target RNA polymerase) and engineered by pMV261*ncRv0842c* (data not shown).

To further elucidate the mechanism of action of *ncRv0842c*, we used the CCCP efflux pump inhibitor. CCCP has been reported to act on the *Rv0842* efflux pump, reducing its activity [13]. Mock strains (pMV261) treated with sub-inhibitory concentrations of CCCP recapitulate the phenotypic 1-dilution reduction on the MIC RIF, thus confirming that *ncRv0842c* is one of the regulators of *Rv0842*.

Despite our experimental does not permit a fine understanding of the dose-response profile, our results suggest that the down-regulation of *ncRv0842c* happens at lower RIF concentrations (50% MIC) compared to the up-regulation of the *Rv0842* pump (90%), thus pointing out for a possible mechanism of drug tolerance, rather than resistance. Further studies better focusing on the dose-response analysis are needed to further elucidate this aspect.

Besides characterizing for the first time the role of *ncRv0842c* in response to RIF, our study provides a few additional cues. First, the definition of synonymous mutation could be obsolete when cis-encoded post-transcriptional regulators are involved. Second, lineage-specific mutations can have relevant effects without directly affecting protein functions, thus suggesting that complex post-transcriptional regulatory networks are involved in determining lineage-specific features. These

findings provide the baseline for further studies in this underestimated area in TB.

## References


1. WHO consolidated guidelines on tuberculosis. Module 3: Diagnosis - Rapid diagnostics for tuberculosis detection 2021 update Catalogue of mutations in Mycobacterium tuberculosis complex and their association with drug resistance. Geneva: World Health Organization; 2021.
2. Target product profile for next-generation drug-susceptibility testing at peripheral centres. Geneva: World Health Organization; 2021.
3. Forrellad MA, Klepp LI, Gioffré A, et al. Virulence factors of the Mycobacterium tuberculosis complex. Virulence. 2013;4(1):3-66. doi:10.4161/viru.22329
4. Heroven AK, Nuss AM, Dersch P. RNA-based mechanisms of virulence control in Enterobacteriaceae. RNA Biol. 2017;14(5):471-487. doi:10.1080/15476286.2016.1201617
5. Ami VKG, Balasubramanian R, Hegde SR. Genome-wide identification of the context-dependent sRNA expression in Mycobacterium tuberculosis. BMC Genomics. 2020;21(1):167. Published 2020 Feb 18. doi:10.1186/s12864-020-6573-5
6. Borrell S, Trauner A, Brites D, et al. Reference set of Mycobacterium tuberculosis clinical strains: A tool for research and product development. PLoS One. 2019;14(3):e0214088. Published 2019 Mar 25. doi:10.1371/journal.pone.0214088
7. Arnvig KB, Young DB. Identification of small RNAs in Mycobacterium tuberculosis. Mol Microbiol. 2009;73(3):397-408. doi:10.1111/j.1365-2958.2009.06777.x
8. Cabibbe AM, Trovato A, De Filippo MR, et al. Countrywide implementation of whole genome sequencing: an opportunity to improve tuberculosis management, surveillance and contact tracing in low incidence countries. Eur Respir J. 2018;51(6):1800387. Published 2018 Jun 28. doi:10.1183/13993003.00387-2018
9. Kohl TA, Utpatel C, Schleusener V, et al. MTBseq: a comprehensive pipeline for whole genome sequence analysis of Mycobacterium tuberculosis

complex isolates. PeerJ. 2018;6:e5895. Published 2018 Nov 13. doi:10.7717/peerj.5895

**10.** Franzblau SG, Witzig RS, McLaughlin JC, et al. Rapid, low-technology MIC determination with clinical Mycobacterium tuberculosis isolates by using the microplate Alamar Blue assay. J Clin Microbiol. 1998;36(2):362-366. doi:10.1128/JCM.36.2.362-366.1998

**11.** Lamichhane G, Arnvig KB, McDonough KA. Definition and annotation of (myco)bacterial non-coding RNA. Tuberculosis (Edinb). 2013;93(1):26-29. doi:10.1016/j.tube.2012.11.010

**12.** Li P, Gu Y, Li J, Xie L, Li X, Xie J. Mycobacterium tuberculosis Major Facilitator Superfamily Transporters. J Membr Biol. 2017;250(6):573-585. doi:10.1007/s00232-017-9982-x

**13.** Li G, Zhang J, Guo Q, et al. Study of efflux pump gene expression in rifampicin-monoresistant Mycobacterium tuberculosis clinical isolates. J Antibiot (Tokyo). 2015;68(7):431-435. doi:10.1038/ja.2015.9

**14.** Pellin D, Miotto P, Ambrosi A, Cirillo DM, Di Serio C. A genome-wide identification analysis of small regulatory RNAs in Mycobacterium tuberculosis by RNA-Seq and conservation analysis. PLoS One. 2012;7(3):e32723. doi:10.1371/journal.pone.0032723

**15.** Miotto P, Merker M, Tizzano B, Merella S, Bucci G, Lazarevic D, Cittaro D, Niemann S, Cirillo DM. The role of smallRNAs during stress response in Mycobacterium tuberculosis. (25-28 April 2015 – 25th European Congress of Clinical Microbiology and Infectious Diseases (ECCMID)", Copenhagen, DK)

# *Chapter 4*

## Conclusions

The genetic variability among MTB clinical isolates may have dramatic consequences on the outcome of infection. Many in vitro and in vivo studies have demonstrated strain-dependent variation in key aspects of virulence such as stress survival, transmission, pathology, drug resistance and lethality [1]. On the other hand, the immunological state of the host is also important and is becoming increasingly relevant over the years. Indeed, the polarization states of macrophages have a huge impact on their functions and early phases of infection are crucial for the immune response activation and for the eradication of the infection [2].

In order to keep into account both the host and the pathogen sides, we adopted an experimental plan specifically suited for considering as relevant variables the phenotypic diversity of macrophages and the genetic variability of MTB. The fate of TB infection highly depends on the activation status of the host immunity, and the early phases of the infection are crucial for immunity priming and for the development of a granuloma [3]. The use of THP-1 cells allowed us to use a reproducible standardized model of host-pathogen interaction, which has been reported to act similar to human monocyte-derived macrophages [4]. However, despite this model based on the THP-1 cell line being recognized in the field, the phenotypic status of the macrophage is often neglected when focusing on mycobacterial virulence. Similarly, only in recent years, researchers begun considering strains different from Herdman, H37Rv, H37Ra or CDC1551. Thus, our approach combining both human and MTB variability, despite its simplicity, represents the most comprehensive concept for unravelling MTB virulence. Indeed, virulence features of a given pathogen cannot be unlinked from the susceptibility (and resistance) features of the host.

We decided to focus our attention on the early phases of the MTB-macrophage interaction because of high importance in mounting an effective immune response, thus influencing the outcome of infection. In

addition, the laboratory is particularly interested in smallRNAs. As mentioned, these key regulatory molecules are among the most rapid, cost-effective and efficient modulators of gene expression in organisms. They act at the post-transcriptional level and are reported to be the earlier players in broad stress response with implications also for drug resistance and virulence for many bacteria. In this view, we found it more relevant to focus on the earlier phases of the host-pathogen interaction as this study will represent the baseline for further characterizing the role of smallRNAs in the very first stages of infection.

The use of M1 and M2 polarized THP-1-derived macrophages recapitulate the two extreme phenotypes found in the alveolar macrophages. This, combined with the different MTB lineages considered, provided a broader view of the diverse fates of the MTB-macrophage interaction.

In this project, we investigated the outcome of this interaction keeping into account different aspects and experimental strategies considering host response, bacterial escape, survival mechanisms. First, the host-pathogen interaction has been analyzed at a single-cell level by live-imaging confocal microscopy, giving us a large amount of information about how both host and MTB diversity could influence the infection, but also providing valuable details about the heterogeneity found even within the same infected macrophages. The analysis on the acidification of the phagolysosomes provided relevant hints on how much the genetic diversity of MTB affect this process, and highlighted those previous findings based on the laboratory strains are not always recapitulating the behaviour of clinical isolates. Furthermore, our approach based on earlier time points showed a clear discrepancy between the time of response in M1 and M2 macrophages. We could also show data about the percentage of macrophages effectively bringing the mycobacteria to an acidified compartment, and to shed light on the microenvironment of infection with an outlook on bystander cells. Similar conclusions can be drawn for the evaluation of apoptosis. The lack of induction of autophagy was probably the most common feature observed in all the settings. Several studies

highlighted a central role for autophagy in mycobacterial clearance; however, despite blocking autophagy seems a common strategy across MTB lineages, literature evidence suggests that different mechanisms to achieve this scope evolved [5].

In general, this project contributed to expanding our knowledge on the implications of MTB genetic diversity. Even though we cannot foresee a direct impact in the clinical management of TB, our study poses relevant bases for further dissection of the cellular and molecular mechanisms behind these observations. In the long term, this could further contribute in building evidence for translational applications related to the use of genotypic approaches for developing better diagnostic and treatment strategies tailored keeping into account the genetic background of MTB.

The reasons for selecting earlier time points in our study design have been outlined above. This brings together some limitations in the study as medium-long term effects of the host-pathogen interaction are lost. In particular, this could have hindered relevant findings related to autophagy and apoptosis/necrosis, both expected to happen later. Furthermore, whereas our single-cell approach tracked relevant mechanisms in the macrophages, we could only follow the processes in their entirety without dissecting specific molecular pathways. Both the use of additional time points and more specific molecular markers for sub-processes could represent further improvements to our approach.

In our second work, we decided to study the impact of genetic variability of the MTB strains directly on the smallRNAs. SmallRNAs are recently emerged as key factors in the regulation of critical bacterial features (as observed for microRNAs in humans), but MTB smallRNAs are poorly characterized [6]. The advent of next-generation sequencing enabled access to WGS and this technology renewed the interest in identifying new markers of drug resistance in MTB. Indeed, molecular DST seems the most obvious and achievable approach to support the WHO End TB Strategy in providing universal DST access. In 2021, the WHO published the first

catalogue of mutations associated with drug resistance in MTB [7]. Interestingly, despite the genotype-phenotype associations derived in the catalogue were considering data from nearly 40,000 clinical isolates, this could not help in identifying new genetic markers to fill the gaps in sensitivity for the detection of resistance. Indeed, the sensitivity of the genetic markers reported for rifampicin is still between 90-95%, whereas for isoniazid the catalogue is reporting a sensitivity close to 90%. The primary aim of this exercise was to provide confidence around the interpretation of mutations, rather than discover new markers; however, the fact that the analysis of so many isolates did not allow to go further close to 100% in sensitivity clearly suggests that new approaches and targets need to be considered.

For the first time, we identified and characterized a smallRNA (*ncRv0842c*) involved in the detoxification of antibiotic stress. Interestingly, we found a lineage-specific synonymous mutation abrogating the expression of the smallRNA, highlighting the existence of main differences in antibiotic tolerance between ancient and modern lineage, but also providing evidence on the need to redefine the concept of silent mutation that keeps into account the network of antisense regulators.

Among the limitations of this study, there is the lack of a specific inhibitory compound for the efflux pump (*Rv0842*) regulated by the smallRNA that prompted us to use a broad efflux pump inhibitor such as the CCCP. Also, it would be useful to achieve smallRNA silencing in modern strains and analyze how this affects rifampicin MIC. Given the fact that the efflux pump is an MSF, the inclusion of additional drugs could provide further data.

As a future perspective, we aim to increase the number of smallRNAs characterized for their role in both virulence and drug resistance. The availability of data for lineage-specific smallRNA variants will be an additional aid to the selection and analysis of the candidates.

In conclusion, this project contributed new relevant insights on the role of MTB genetic diversity in delineating pathogenic features, and on how it could affect yet unexplored smallRNA-based regulatory pathways.

# References

**1.** Homolka S, Niemann S, Russell DG, Rohde KH. Functional genetic diversity among Mycobacterium tuberculosis complex clinical isolates: delineation of conserved core and lineage-specific transcriptomes during intracellular survival. PLoS Pathog. 2010;6(7):e1000988. Published 2010 Jul 8. doi:10.1371/journal.ppat.1000988

**2.** Lugo-Villarino G, Vérollet C, Maridonneau-Parini I, Neyrolles O. Macrophage polarization: convergence point targeted by mycobacterium tuberculosis and HIV. Front Immunol. 2011;2:43. Published 2011 Sep 15. doi:10.3389/fimmu.2011.00043

**3.** Hunter RL. The Pathogenesis of Tuberculosis: The Early Infiltrate of Post-primary (Adult Pulmonary) Tuberculosis: A Distinct Disease Entity. Front Immunol. 2018;9:2108. Published 2018 Sep 19. doi:10.3389/fimmu.2018.02108

**4.** Madhvi A, Mishra H, Leisching GR, Mahlobo PZ, Baker B. Comparison of human monocyte derived macrophages and THP1-like macrophages as in vitro models for M. tuberculosis infection. Comp Immunol Microbiol Infect Dis. 2019;67:101355. PMID: 31586851

**5.** Strong EJ, Lee S. Targeting Autophagy as a Strategy for Developing New Vaccines and Host-Directed Therapeutics Against Mycobacteria. Front Microbiol. 2021;11:614313. Published 2021 Jan 14. doi:10.3389/fmicb.2020.614313

**6.** Gerrick ER, Barbier T, Chase MR, et al. Small RNA profiling in Mycobacterium tuberculosis identifies MrsI as necessary for an anticipatory iron sparing response. Proc Natl Acad Sci U S A. 2018;115(25):6464-6469. doi:10.1073/pnas.1718003115

**7.** WHO Catalogue of mutations in Mycobacterium tuberculosis complex and their association with drug resistance 2021

# ANNEX

## Characterization of *Mycobacterium tuberculosis* smallRNA *ncRv0757c*

### Introduction

Small non-coding RNAs (smallRNAs) have been identified as crucial elements that regulate gene expression in bacterial stress responses and virulence [1]. In this perspective, the investigation of smallRNAs in different lineages of MTB will provide further information about the regulation of the stress response in this pathogen.

We are investigating the role of *Mycobacterium tuberculosis* (MTB) smallRNAs during macrophage infection by means of in vitro and ex vivo infection models with the goal of determining whether these regulatory molecules are involved in the survival and in the virulence of the tubercle bacilli and if differences among lineages exist. Interestingly, several genes involved in the pathogenesis of tuberculosis and playing a relevant role in MTB survival during macrophages infection have been shown to be under the putative regulation of cis-encoded smallRNAs [2]. Whereas current research is starting to delineate the role of genetic diversity in determining the spectrum of virulence features across the 7 main MTB phylogenetic lineages described, no data are available on how this heterogeneity affects smallRNA expression and function. Moreover, since virulence is a relative capacity of a microbe to cause damage in a susceptible organism, the complex heterogeneity of the human immune system cannot be ignored [3].

In particular, the phenotypic diversity and plasticity of human macrophages (first line of defense against MTB) is an underestimated variable in experimental designs aiming at dissecting the pathogenesis of MTB strains.

PhoP (response regulator of a two-component system in which *phoR* is the response regulator) is a key regulator of pathogenesis in MTB: it is a transcriptional regulator that controls at least 2% of the genome of *M. tuberculosis* and among the genes under its regulation, there are relevant virulence factors and key players in acidic pH stress response, with the latter considered one of the crucial features enabling intramacrophagic survival to MTB [4].

Despite the central role of PhoP in virulence, surprisingly its mechanism of action differs between modern and ancient strains [5]. *phoP* mutants have been considered for the development of new vaccine candidates because the deletion of this gene in SO2 mutant causes an attenuation of the virulence [6]. Even though, the precise mechanism by which PhoP is involved in pH response remains poorly clear. The study of the mechanism of regulation of *phop*, including smallRNAs, is crucial to fully understand the complexity of the regulon and to develop an attenuated strain in order to test new vaccine candidates for TB. In this study, we decided to focus our attention on the smallRNA *ncRv0757c* which is antisense (AS) to the 5' region (promoter) of the gene *phoP*. In our laboratory, we previously confirmed the existence of this RNA by northern blot (data not shown).

## Methods

To study the role of the smallRNA taking consideration of both human and bacteria variability, we decided to use a model of in vitro infection using THP-1 derived macrophages polarized toward M1-like (LPS) or M2-like (IL-4) macrophages. THP-1 (ATCC® TIB-202™) cells were differentiated in complete RPMI (with L-glutamine 2mM, Hepes 10mM, Non-essential amino acids 100nM, Sodium Pyruvate 1mM, Sigma Aldrich, Missouri, USA) supplemented with 10% FBS (Fetal Bovin Serum, Euroclone), antibiotics (penicillin G 100 U/ml and streptomycin sulfate 100 U/ml, Sigma Aldrich Missouri, USA), and 100 nM of phorbol 12-myristate 13-acetate (PMA,

Sigma-Aldrich Missouri, USA) for 3 days in Nunc™ 12 wells plates (500000 cells/well) (Thermo Fisher, Massachusset, USA) [7]. Type I collagen (Sigma Aldrich, Missouri, USA) was used for cell adhesion. Three days after removal of the PMA, macrophage-like cells were polarized in cRPMI medium without antibiotics for 16 h with either lipopolysaccharide (50ng/mL, Sigma-Aldrich Missouri, USA) to induce an M1-like phenotype or human IL-4 (20 ng/mL, *E. coli*-derived human IL-4 protein, R&Dsystems) to induce an M2-like phenotype prior to the infection [7,8]. We tested the intramacrophagic expression of both *phoPR* regulon and the *ncRv0757c* smallRNA of different MTB lineages, including laboratory strains (H37Rv, H37Ra), and 13 clinical strains belonging to modern (more virulent) and ancient (less virulent) strains (Table 1). Intramacrophagic expression was evaluated by means of qPCR based on TaqMan chemistry. Ribosomal RNA 16S was used as endogenous control.

**Table 1**: Strains selected for this study

| Strain | *Lineage* | | | Characteristics |
|---|---|---|---|---|
| | Name | N | Phylogenetic Origin | |
| *M. africanum* | West African | 6 | Ancient | Less virulent, clinical isolate |
| *M. tuberculosis* | EAI | 1 | Ancient | Less virulent, clinical isolate |
| *M. tuberculosis* | Beijing | 2 | Modern | More virulent, clinical isolate |
| *M. tuberculosis* | CDC1551 | 4 | Modern | More virulent, clinical isolate |
| *M. tuberculosis* | H37Ra | 4 | Modern | Less virulent, laboratory strain |
| *M. tuberculosis* | Haarlem | 4 | Modern | Virulent, clinical isolate |
| *M. tuberculosis* | H37Rv | 4 | Modern | Virulent, reference strain |
| *M. bovis* | Bovis | n.a. | Intermediate | Intermediate phenotype |
| *M. bovis* BCG | Bovis | n.a. | Intermediate | Vaccine strain |

## Results and discussion

We measured the smallRNA baseline expression in exponential and in stationary phases in modern and ancient strains and we found no statistical difference between the strain tested in planktonic growth (Fig. 1).

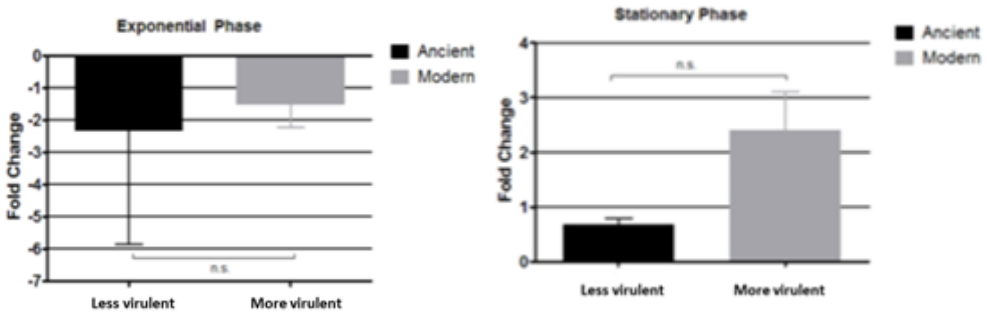


**Fig. 1**: ncRv0757c smallRNA expression in less virulent and more virulent MTB strains (normalized of H37Rv) in exponential and stationary growth phases.

We infected polarized macrophages at a MOI 10:1 and we measured the intramacrophagic expression of the smallRNA in the same MTB strains. In M1 macrophages the smallRNA *ncRv0757c* is highly upregulated in more virulent strains at 4h p.i. (compared to H37Rv) and its upregulation is manteined up to 48h, while the smallRNA is highly downregulated in less virulent strains (compared to H37Rv). We also observed a decreasing trend of the smallRNA upregulation during time, suggesting that the smallRNA is accomplish its function at early timepoints after infection but it is slowly disabled when infection time progresses (Fig. 2). In M2 macrophages the expression of the small-RNA does not change during time in both virulent and less virulent categories (Fig. 2).

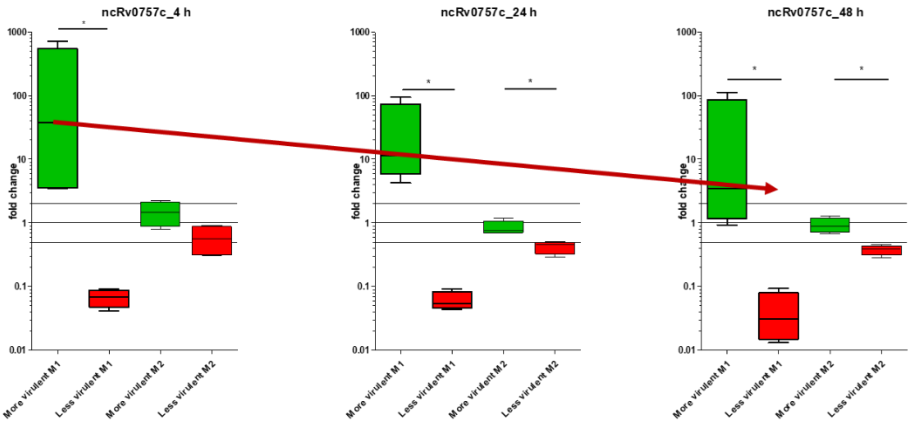


**Fig. 2**: MTB *ncRv0757c* expression in M1 and M2 THP-1 derived macrophages, at 4, 24 and 28h post-infection. Green: More virulent strains; Red: less virulent strains.

Concerning the expression of the response regulator *phoP*, we saw that in M1 macrophages its expression is slightly upregulated at 4h p.i. only in virulent strains while it remains invariable in less virulent strains. No changes in the expression of *phoP* were observed in M2 macrophages (Fig. 3).

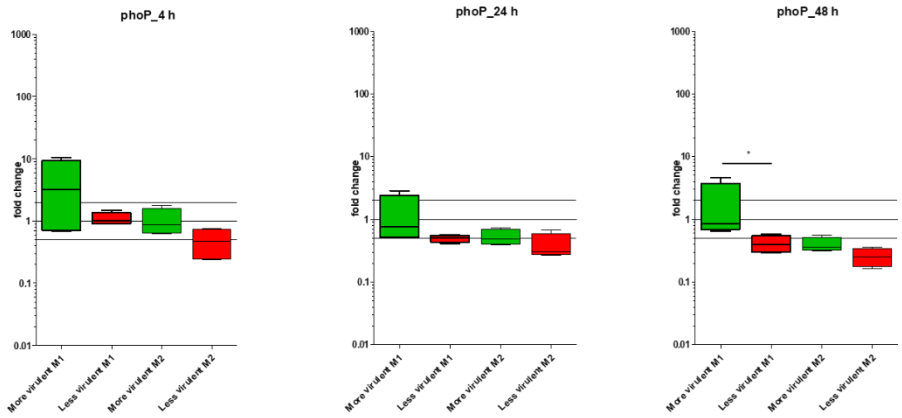


**Fig. 3**: MTB *phoP* expression in M1 and M2 THP-1 derived macrophages, at 4, 24 and 28h post-infection. Green: More virulent strains; Red: less virulent strains.

In order to better understand the mechanism of action of this smallRNA we decided to engineer over-expressing plasmids, taking into consideration

the work published by K. Arnvig et al. in which the target smallRNA is under the control of *M. smegmatis rrnB* promoter [9]. An artificial terminator to the smallRNA sequence is also included [9]. First attempts in obtaining detectable over-expression of *ncRv0757c* in MTB were unsuccessful. We decided to switch to the use of the low copy plasmid pMV261 in order to overexpress *ncRv0757c* under the control of a strong constitutive MTB promoter ($P_{hsp60}$). Our preliminary data show a colony phenotype similar to the SO2 *phoP* mutant vaccine candidate, with smaller colonies and with lower growth rate (Fig. 4). However, the phenotype obtained was found to be unstable.

We are now evaluating the use alternative over-expressing strategies. In particular, we working in collaboration with the University of Padua at the following constructs:

- Integrative plasmid pYUB413 with $P_{rrnB}$ promoter
- Replicative inducible plasmid pFRA71 with $P_{ptr}$ (pristinamycin inducible) promoter.

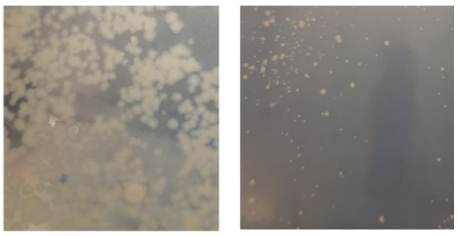


**Fig. 4**: preliminary phenotypical results of H37Rv overexpressing the smallRNA *ncRv0757c* with the replicative vector pMV261

In addition, recent findings showed that even few nucleotides (<5) modifying the 5' of the smallRNA can lead to severe and faster degradation of the regulator [10]. Given that two different 5' ends at a few nucleotides of

distance have been described for *ncRv0757c*, we are also evaluating how this can affect the overexpression strategy. This is particularly relevant for the inducible approach as it requires the inclusion of a nucleotidic stretch at the 5' end of the target smallRNA for pristinamycin binding [10].

Our hypothesis is that this smallRNA could act inhibiting *phoP* at a transcriptional or post-transcriptional level. The smallRNA exerts its effect at an early timepoint in more virulent strains but so far we don't have enough data to confirm that our proposed mechanism is correct. This is particularly complex because the smallRNA is part of a complicated (and yet not fully decoded in MTB) regulatory network tightly tuning *phoP* response to stresses (Fig 5).

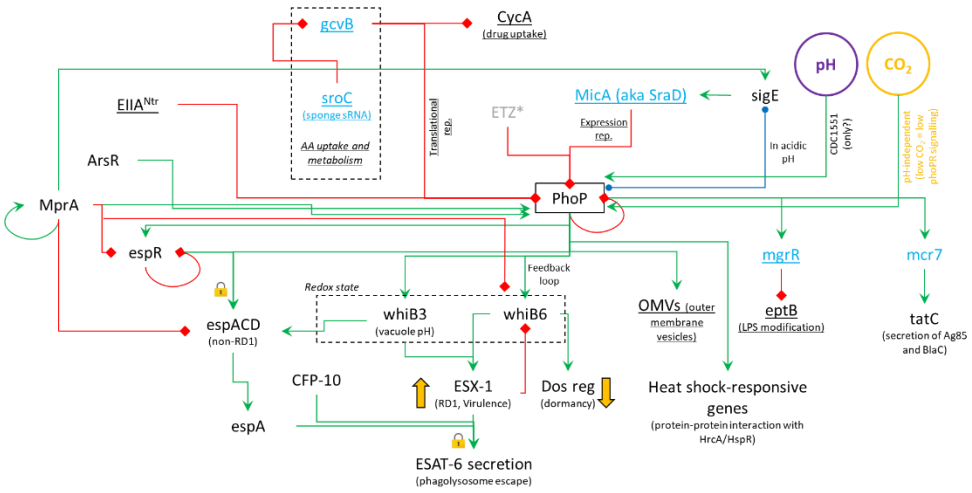


**Fig. 5**: MTB PhoP regulation network [11-28]
Red lines with square ends: inhibition/repression
Blue lines with circle ends: interaction
Green lines with arrow ends: activation/induction
Underlined text: observed in bacteria other then mycobacteria
Blue text: smallRNAs
Grey text: chemical compounds
*The ethoxzolemide (ETZ) inhibits the phoPR operon (not *phoP* directly); observed in CDC1551 (not in other strains)
Lock: co-requirement of elements

The early induction of *Rv0757c* reduced *phoP* mediated virulence in "more virulent" strains at early timepoint after phagocytosis, contributing to hiding the bacteria to the immune system, while in less virulent strains this

pathway seems less relevant at the time point considered. This hypothesis seems aligned with our findings on phagolysosomal acidification, where the modern/more virulent strains were found to delay M1 macrophagic response (further information on Chapter 2).

As a next step, the use of *ncRv0757c* overexpressing mutant strains will allow to further elucidate the mechanism of action of the smallRNA and its effects on the *phoPR* operon, including broader influence on cytokines secretion, phagolysosomal acidification, apoptosis, and autophagy. The mutants will be analyzed for their ability to survive inside the macrophages and to kill macrophages.

# References


**1.** Oliva G, Sahr T, Buchrieser C. Small RNAs, 5' UTR elements and RNA-binding proteins in intracellular bacteria: impact on metabolism and virulence. FEMS Microbiol Rev. 2015;39(3):331-349. doi:10.1093/femsre/fuv022

**2.** Coskun FS, Płociński P, van Oers NSC. Small RNAs Asserting Big Roles in Mycobacteria. Noncoding RNA. 2021;7(4):69. Published 2021 Oct 29. doi:10.3390/ncrna7040069

**3.** Casadevall A, Pirofski LA. Microbial virulence results from the interaction between host and microorganism. Trends Microbiol. 2003;11(4):157-159. doi:10.1016/s0966-842x(03)00008-8

**4.** Gonzalo-Asensio J, Mostowy S, Harders-Westerveen J, et al. PhoP: a missing piece in the intricate puzzle of Mycobacterium tuberculosis virulence. PLoS One. 2008;3(10):e3496. doi:10.1371/journal.pone.0003496

**5.** Cá B, Fonseca KL, Sousa J, et al. Experimental Evidence for Limited in vivo Virulence of Mycobacterium africanum. Front Microbiol. 2019;10:2102. Published 2019 Sep 10. doi:10.3389/fmicb.2019.02102

**6.** Aporta A, Arbues A, Aguilo JI, et al. Attenuated Mycobacterium tuberculosis SO2 vaccine candidate is unable to induce cell death. PLoS One. 2012;7(9):e45213. doi:10.1371/journal.pone.0045213

**7.** Genin M, Clement F, Fattaccioli A, Raes M, Michiels C. M1 and M2 macrophages derived from THP-1 cells differentially modulate the response of cancer cells to etoposide. BMC Cancer. 2015;15:577. Published 2015 Aug 8. doi:10.1186/s12885-015-1546-9

**8.** Weagel E. et al., Macrophage Polarization and Its Role in Cancer, J Clin Cell Immunol 2015, 6:4 DOI: 10.4172/2155-9899.1000338

**9.** Arnvig KB, Young DB. Identification of small RNAs in Mycobacterium tuberculosis. Mol Microbiol. 2009;73(3):397-408. doi:10.1111/j.1365-2958.2009.06777.x

**10.** Moores A, Riesco AB, Schwenk S, Arnvig KB. Expression, maturation and turnover of DrrS, an unusually stable, DosR regulated small RNA in Mycobacterium tuberculosis. PLoS One. 2017;12(3):e0174079. Published 2017 Mar 21. doi:10.1371/journal.pone.0174079

**11.** Felden B, Cattoir V. Bacterial Adaptation to Antibiotics through Regulatory RNAs. Antimicrob Agents Chemother. 2018;62(5):e02503-17. Published 2018 Apr 26. doi:10.1128/AAC.02503-17

**12.** Solans L, Gonzalo-Asensio J, Sala C, et al. The PhoP-dependent ncRNA Mcr7 modulates the TAT secretion system in Mycobacterium tuberculosis. PLoS Pathog. 2014;10(5):e1004183. Published 2014 May 29. doi:10.1371/journal.ppat.1004183

**13.** Chen Z, Hu Y, Cumming BM, et al. Mycobacterial WhiB6 Differentially Regulates ESX-1 and the Dos Regulon to Modulate Granuloma Formation and Virulence in Zebrafish. Cell Rep. 2016;16(9):2512-2524. doi:10.1016/j.celrep.2016.07.080

**14.** Solans L, Aguiló N, Samper S, et al. A specific polymorphism in Mycobacterium tuberculosis H37Rv causes differential ESAT-6 expression and identifies WhiB6 as a novel ESX-1 component. Infect Immun. 2014;82(8):3446-3456. doi:10.1128/IAI.01824-14

**15.** Rodríguez-Castillo JG, Pino C, Niño LF, et al. Comparative genomic analysis of Mycobacterium tuberculosis Beijing-like strains revealed specific genetic variations associated with virulence and drug resistance. Infect Genet Evol. 2017;54:314-323. doi:10.1016/j.meegid.2017.07.022

**16.** Pang X, Samten B, Cao G, et al. MprAB regulates the espA operon in Mycobacterium tuberculosis and modulates ESX-1 function and host cytokine response. J Bacteriol. 2013;195(1):66-75. doi:10.1128/JB.01067-12

**17.** Bosserman RE, Nguyen TT, Sanchez KG, et al. WhiB6 regulation of ESX-1 gene expression is controlled by a negative feedback loop in Mycobacterium marinum. Proc Natl Acad Sci U S A. 2017;114(50):E10772-E10781. doi:10.1073/pnas.1710167114

**18.** Refai A, Gritli S, Barbouche MR, Essafi M. Mycobacterium tuberculosis Virulent Factor ESAT-6 Drives Macrophage Differentiation Toward the Pro-inflammatory M1 Phenotype and Subsequently Switches It to the Anti-inflammatory M2 Phenotype. Front Cell Infect Microbiol. 2018;8:327. Published 2018 Sep 18. doi:10.3389/fcimb.2018.00327

**19.** Zhuge X, Sun Y, Xue F, et al. A Novel PhoP/PhoQ Regulation Pathway Modulates the Survival of Extraintestinal Pathogenic Escherichia coli in Macrophages. Front Immunol. 2018;9:788. Published 2018 Apr 17. doi:10.3389/fimmu.2018.00788

**20.** Johnson BK, Colvin CJ, Needle DB, Mba Medie F, Champion PA, Abramovitch RB. The Carbonic Anhydrase Inhibitor Ethoxzolamide Inhibits the Mycobacterium tuberculosis PhoPR Regulon and Esx-1 Secretion and Attenuates Virulence. Antimicrob Agents Chemother. 2015;59(8):4436-4445. doi:10.1128/AAC.00719-15

**21.** Anil Kumar V, Goyal R, Bansal R, et al. EspR-dependent ESAT-6 Protein Secretion of Mycobacterium tuberculosis Requires the Presence of Virulence Regulator PhoP. J Biol Chem. 2016;291(36):19018-19030. doi:10.1074/jbc.M116.746289

**22.** Cumming BM, Rahman MA, Lamprecht DA, et al. Mycobacterium tuberculosis arrests host cycle at the G1/S transition to establish long term infection [published correction appears in PLoS Pathog. 2017 Jul 14;13(7):e1006490]. PLoS Pathog. 2017;13(5):e1006389. Published 2017 May 22. doi:10.1371/journal.ppat.1006389

**23.** Zhang P, Fu J, Zong G, Liu M, Pang X, Cao G. Novel MprA binding motifs in the phoP regulatory region in Mycobacterium tuberculosis. Tuberculosis (Edinb). 2018;112:62-68. doi:10.1016/j.tube.2018.08.002

**24.** Pang X, Vu P, Byrd TF, et al. Evidence for complex interactions of stress-associated regulons in an mprAB deletion mutant of Mycobacterium tuberculosis. Microbiology (Reading). 2007;153(Pt 4):1229-1242. doi:10.1099/mic.0.29281-0

**25.** Gao CH, Yang M, He ZG. An ArsR-like transcriptional factor recognizes a conserved sequence motif and positively regulates the expression of phoP in mycobacteria. Biochem Biophys Res Commun. 2011;411(4):726-731. doi:10.1016/j.bbrc.2011.07.014

**26.** Choi J, Kim H, Chang Y, Yoo W, Kim D, Ryu S. Programmed Delay of a Virulence Circuit Promotes Salmonella Pathogenicity. mBio. 2019;10(2):e00291-19. Published 2019 Apr 9. doi:10.1128/mBio.00291-19

**27.** Sevalkar RR, Arora D, Singh PR, et al. Functioning of Mycobacterial Heat Shock Repressors Requires the Master Virulence Regulator PhoP. J Bacteriol. 2019;201(12):e00013-19. Published 2019 May 22. doi:10.1128/JB.00013-19

**28.** Stewart GR, Snewin VA, Walzl G, et al. Overexpression of heat-shock proteins reduces survival of Mycobacterium tuberculosis in the chronic phase of infection. Nat Med. 2001;7(6):732-737. doi:10.1038/89113

## Supplementary Table

| Category | Gen Name | Rv number | Description | Attenuation evidences | |
|---|---|---|---|---|---|
| | | | | Model | Result |
| **Lipids and Fatty Acid Metabolism** | *kasB* | Rv2246 | 3-oxoacyl-[acyl-carrier protein] synthase 2 kasb | C57BL/6 mice (lda) | Reduced CFUs in organs and lung pathology<br>Increased animal survival |
| **Mycolic acid synthesis** | *mmaA4* | Rv0642c | Methoxy mycolic acid synthase 4 | C57BL/6 mice (lda/iv) | Reduced CFUs in organs |
| | *pcaA* | Rv0470c | Mycolic acid synthase (cyclopropane synthase) | C57BL/6 mice (iv)[†] | Failed to persist in the spleens |
| | | | | C57BL/6 mice (iv) | Failed to persist in organs<br>Increased animal survival |
| | | | | C57BL/6 mice (lda) | Reduced CFUs in lung |
| | *mymA* operon | Rv3083 to Rv3089 | Propable Monooxygenase (Hydroxylase) | Activated J774 macrophages and guinea pigs (sc) | Reduced CFUs |
| | - | Rv2869c | Membrane bound metalloprotease | C57BL/6 mice (lda) | Reduced CFUs in lung |
| | *treS* | Rv0126 | Trehalose synthase | C57BL/6 mice (iv) | Reduced CFUs in lung<br>Increased animal survival |
| **Synthesis of complex lipids** | *pks15*<br>*pks1* | Rv2946c<br>Rv2947c | Probable polyketide synthases | C57BL/6J mice (in) and MAM MH-S | Reduced CFUs |
| **PDIM** | | | | B6D2 F1 mice (lda) | Increased animal survival |
| | | | | Rabbits (intracisternally) | Reduced CFUs in cerebrospinal fluid and organs |
| | *pks10* | Rv1660 | Possible chalcone synthase | C57BL/6J mice (in) and MAM MH-S | Reduced CFUs |
| | *pks12* | Rv2048c | Probable polyketide synthase | C57BL/6J mice (in) and MAM MH-S | Reduced CFUs |
| | *fadD26* | Rv2930 | Fatty-acid-Coa synthase | C57BL/6 mice (iv) | Reduced CFUs in lung |
| | | | | BALB/c mice (iv) | Reduced CFUs in lung |
| | | | | BALB/c mice (in) | Reduced CFUs in organs |
| | *fadD28* | Rv2941 | Fatty-acid-Coa synthase | C57BL/6 mice (iv) | Reduced CFUs in lung |
| | *mmpL7* | Rv294 | Conserved transmembrane transport protein | C57BL/6 mice (iv) | Reduced CFUs in lung |
| | *drrC* | Rv2938 | Probable daunorubicin-dim-integral membrane ABC-transporter | BALB/c mice (iv) | Reduced CFUs in lung |
| | | | | C57BL/6 mice (lda.) | Reduced CFUs in organs.<br>Increased animal survival |
| | *pks5* | Rv1527c | Probable polyketide synthase | BALB/c mice (lda) | Reduced CFUs in organs |
| | *pks7* | Rv1661 | Probable polyketide synthase | BALB/c mice (lda) | Reduced CFUs in organs |

| Category | Gen Name | Rv number | Description | Attenuation evidences | |
|---|---|---|---|---|---|
| | | | | Model | Result |
| **SL** | *mmpL8* | Rv3823c | Probable conserved integral membrane transport protein | C57BL/6 mice (iv) | Reduced CFUs in organs |
| **Others genes related in lipid synthesis** | *fadD33* | Rv1345 | Possible polyketide synthase | C57BL/6 and B6D2/F1 mice (lda) | Increased animal survival |
| | | | | BALB/c mice (iv) | Reduced CFUs in liver |
| | *icl1* | Rv0467 | Isocitrate lyases | C57BL/6 and BALB/c mice (iv). Activated MBMDM | Failed to persist. Increased animal survival Reduced lung pathology |
| | *icl1* and *icl2* | Rv0467 and Rv1915-Rv1916 | Isocitrate lyases | C57BL/6; IFN-$\gamma^{-/-}$ and TNF-R1$^{-/-}$ mice (iv). Non-activated and activated BMDM and HBMDM | Reduced CFUs, increased animal survival reduced lung pathology |
| | *plcA*<br>*plcB*<br>*plcC*<br>*plcD* | Rv2351c<br>Rv2350c<br>Rv2349c<br>Rv1755c | Probable phospholipase C | BALB/c mice (lda) | Reduced CFUs in organs |
| **Catabolism of cholesterol** | *choD* | Rv3409c | Putative cholesterol oxidase | C57BL/6 (iv) and mouse peritoneal macrophages | Reduced CFUs |
| | *hsaC* | *Rv3568c* | 3,4-DHSA dioxygenase | SCID mice (iv) | Increase survival |
| | | | | Guinea pig (a) | Modestly reduced CFUs and granulome formation in lungs. |
| | *igr* operon: *cyp125* | Rv3545c | Putative cytochrome P450 | C57BL/6 mice (a) | Reduced CFUs |
| | *fadE28/29* | Rv3544c-Rv3543c | Acyl coenzyme A dehydrogenases | | |
| | - | Rv3542c-Rv3541c | CHPs | | |
| | *ltp2* | Rv3540c | Probable lipid carrier protein | | |
| **Cell Envelope Proteins** | *erp* | Rv3810 | Exported repetitive protein | MBMDM and BALB/c mice (iv)[‡] | Reduced CFUs in macrophages and organs |
| **Cell wall proteins** | *fbpA* | Rv3804 | Fibronectin binding protein, mycoly-ltransferese | BALB/c mice (ip)* | Reduced CFUs in organs. |
| | | | | THP-1 and J774 macrophages | Reduced CFUs. |
| | *mce1* | Rv0166 to Rv0174 | Mammalian cell entry proteins. Possible lipids ABC-transporters. | BALB/c mice (it) (*mce1, 2* and *3* mutants) | Reduced CFUs in organs, reduced tissue pathology and increased animal survival |
| | *mce2* | Rv0586-0594 | | C57BL/6 mice (lda) | Reduced CFUs and gross lesion in lung. Increased animal survival |
| | *mce3* | Rv1964 to Rv1971 | Mammalian cell entry proteins. Possible lipids ABC-transporters. | C57BL/6 mice (lda) (*mce3, 4* mutants) | Reduced CFUs in organs and less tissue pathology in lung. Increased survival |
| | *mce4* | Rv3501c to Rv3494c | Cholesterol transporter | | |

| Category | Gen Name | Rv number | Description | Attenuation evidences | |
|---|---|---|---|---|---|
| | | | | Model | Result |
| | *ompATb* | Rv0899 | Pore-forming protein | THP1 and MBMDM<br>BALB/c mice (lda) | Reduced CFUs in macrophagues and organs |
| | *hbhA* | Rv0475 | Heparin binding hemaglutinin protein (Adhesine) | A549 pneumocytes.<br>BALB/c mice (lda)‡ | Reduced adhesion and CFUs in pneumocytes and reduced CFUs in spleen |
| | *pstA1* | Rv0930 | Inorganic phosphate-ABC transporter | Resting and activated MBMDM | Reduced CFUs |
| | *phoT* | Rv0820 | | Resting and activated MBMDM and C57BL/6J mice (iv) | Reduced CFUs in macrophages and lung |
| | *caeA* | Rv2224c | Carboxylesterase for esters of 3 to 7 carbon atoms | BALB/c mice (lda) | Reduced CFUs and gross pathology in organs |
| | | | | BALB/c mice (iv) | Increased survival and weight |
| | | | | C57BL/6 mice (lda) | Moderated reduction in CFUs |
| | *kefB* | Rv3236c | $K^+/H^+$ antiporter, affecting ROS production | J774 macrophages† | Reduced phagosome ROS production |
| | *oppABCD* | Rv3666c to Rv3663c | Oligopeptide ABC-transporter | BALB/c mice (lda) | Reduced CFUs in organs in the chronic infection. Increased survival |
| | *ctaC* | Rv2200c | Citocrome C oxidase unit II | MBMDM | Reduced CFUs |
| **Lipoproteins** | *lppX* | Rv2945c | Carrier of DIM and antigen | BALB/c mice (lda) | Reduced CFUs in lung |
| | *lpqH* | Rv3763 | Antigen<br>Apoptogenic | C57BL/6 mice (lda) | Reduced CFUs in lung |
| | *lprG* | Rv1411c | Cell wall assembly<br>TLR2 agonist | BALB/c mice (ip)* | Reduced bacterial load in spleens |
| | | | | BALB/c mice (it)* | Reduced CFUs in lung |
| | *lprG-p55* | Rv1411c-Rv1410c | Antibiotic efflux pump (P55) | J774macrophages* | Reduced CFUs |
| | *pstS-1* | Rv0934 | Inorganic phosphate transport. Antigen and apoptogenic | BALB/c and C57BL/6 mice (iv) | Reduced CFUs in organs |
| | | | | Mouse peritoneal macrophages | Reduced multiplication |
| | *lpqY* | Rv1235 | ABC-transporter (Recycling system of threalose) | SCID mice (BALB/c mice background) (lda) | Increased survival |
| | | | | C57BL/6 mice (lda) | Reduced UFCs in organs. |
| | *modA* | Rv1857 | Molybdenum ABC transporter | CBA/J mice (lda) | Reduced CFUs in ungsand slight increased |
| | | | | BALB/c mice (iv) | Reduced CFUs in lung |
| **Secretion system** | *esxA* | Rv3875 | Esx-1 component or substrate (C or S) | Guinea pigs (sc)* | Reduced CFUs in spleen |
| | RD1 | Rv3868 to Rv3875 and Rv3877 | Esx-1 C or S | THP-1 macrophage | Reduced CFUs |
| | | | | C57BL/6 mice (a) | Reduced CFUs in organs<br>Total survival |

| Category | Gen Name | Rv number | Description | Attenuation evidences | |
|---|---|---|---|---|---|
| | | | | Model | Result |
| | *esxB* | Rv3874 | Esx-1 C or S | THP-1 macrophage | Reduced CFUs |
| | *espH* | Rv3867 | Esx-1 C or S | BMDM | Reduced CFUs |
| | | | | C57BL/6 mice (lda) | Reduced CFUs in organs |
| | *espG1* | Rv3865 | Esx-1 C or S | BMDM | Reduced CFUs |
| | | | | C57BL/6 mice (lda) | Reduced CFUs in organs<br>Total survival |
| | *espA* | Rv3614 | Esx-1 C or S | C57BL/6 mice (iv) | Reduced CFUs in organs<br>Increased animal survival |
| | *espC* | Rv3615 | Esx-1 C or S | BMDM | Reduced CFUs |
| | *eccCd* | Rv3877 | Esx-1 C or S | BMDM | Reduced CFUs |
| | *espR* | Rv3849 | Esx-1 C or S | C57BL/6 mice (iv) | Reduced CFUs in lung |
| | *mycP1* | Rv3883 | Esx-5 C or S | MBMDM | Reduced CFUs |
| | | | | BALB/c mice (lda) | Reduced CFUs in lung |
| | *eccD5* | Rv1795 | Esx-5 C or S | MBMDM | Reduced CFUs |
| | *ppe25 to pe19* | Rv1787 to Rv1791 | Signal peptidase for lipoproteins | MBMDM | Reduced CFUs |
| | *lspA* | Rv1539 | Preprotein translocase ATPase | J774 macrophages | Reduced CFUs |
| | | | | CBA/J mice | Reduced CFUs in lung |
| | *secA2* | Rv1821 | Accesory SecA protein | C57BL/6 mice (iv) | Reduced CFUs in organs<br>Increased animal survival |
| | | | | C57BL/6 -SCID mice (iv) | Increased animal survival |
| | | | | C57BL/6 mice (lda) | Increased animal survival<br>Reduced CFUs in organs |
| | *secA2* | Rv1821 | Accesory SecA protein | BMDM from C57BL/6 mice, $NOS2^{-/-}$ and $pho^{-/-}$ mice (lda) | Reduced CFUs |
| **Proteins Inhibiting Antimicrobial Effectors of the Macrophage** | *acr1 (hspX)* | Rv2031c | Dormancy-associated protein | MBMDM /THP-1 macrophages | Reduced CFUs |
| | *acr2* | Rv0251c | Alpha-crystallin (Acr) family of molecular chaperones | C57BL/6 mice (iv) | Reduced weight loss |
| **Oxidative and nitrosative stresses** | - | Rv2136c | Likely involved in the synthesis of peptidoglycan | C57BL/6 mice (lda) | Reduced CFUs in organs and reduced gross pathology in lung |

| Category | Gen Name | Rv number | Description | Attenuation evidences | |
|---|---|---|---|---|---|
| | | | | Model | Result |
| | *ponA2* | Rv3682 | Probable transglycosylase and transpeptidase | C57BL/6 mice (lda) | Moderated reduction in CFUs |
| | *ahpC* | Rv2428 | Alkyl ydroperoxide reductase c | Guinea pigs (sc) (Antisense)* | Reduced tissue pathology and CFUs |
| | | | | J774 macrophages | Reduced CFUs |
| | *sodC* | Rv0432 | Superoxide dismutase (SOD) protein | Activated murine peritoneal C57BL/6 mice and iNOS$^{-/-}$ macrophages | Reduced CFUs |
| | *mel2* | Rv1936 to Rv1941 | Bioluminescence-related proteins | Activated J774, MBMDM from infected mice and human PBMC-derived macrophages | Reduced CFUs |
| | | | | C57BL/6 and Phox$^{-/-}$ and iNOS$^{-/-}$ mice (lda) | Moderated reduction of CFUs in organs |
| | | | | BALB/c mice (iv) | Reduced CFUs and increased survival |
| | | | | Guinea pigs (im) | Reduced CFUs in spleen and reduced number of lesion in tissues |
| | *katG* | Rv1908c | Catalase-peroxidase enzyme | C57BL/6 mice (iv) | Reduced CFUs |
| | | | | NOS2$^{-/-}$ mice (iv) | Reduced CFUs |
| | | | | BMDM from C57BL/6 and NOS2$^{-/-}$ mice | Reduced CFUs |
| | | | | Activated BMDM NOS2$^{-/-}$ | Reduced CFUs |
| | | | | Guinea pigs* | Moderated reduction in CFUs |
| | | | | BALB/c mice and MHC class II-knockout mice (ip) | Reduced baterial load in organs |
| **Phagosome arresting** | *tpX* | Rv1932 | Thiol peroxidase | Resting and activated BMDM from BALB/c and C57BL/6 mice | Reduced CFUs |
| | | | | BALB/c mice (iv) | Reduced CFUs and increased animal survival |
| | *ndk* | Rv2445c | Nucleoside diphosphate kinase | RAW 264.7 macrophages (Antisense)† | Reduced CFUs |
| | *ptpA* | Rv2234 | Low-molecular weight tyrosine phosphatase | THP-1 macrophage | Reduced CFUs |
| | *pe_pgrs30* | Rv1651c | Member of the PE family | BALB/c mice (lda) | Reduced CFUs |
| | | | | BALB/c mice (lda) | Reduced tissue damage |
| | | | | J774.1 and THP-1 macrophages | Reduced CFUs |

| Category | Gen Name | Rv number | Description | Attenuation evidences | |
|---|---|---|---|---|---|
| | | | | Model | Result |
| **Inhibition of apoptosis** | *nuoG* | Rv3151 | Subunit of the type I NADH dehydrogenase, NADH-1 | BALB/c mice (iv) | Increased animal survival and reduced CFUs in organs |
| | | | | SCID mice (iv) | Increased animal survival |
| | *pknE* | Rv1743 | Serine/threonine kinase E | THP-1 macrophages | Reduced bacterial survival |
| | - | Rv3654c-Rv3655c | CHP | U937 apoptotic macrophages | Reduced CFUs |
| **Protein Kinases** | *pknD* | Rv0931c | Protein kinase D | Brain microvascular endothelial cells (HBMEC) | Impaired invasion |
| | | | | BALB/c mice (iv) | Reduced CFUs in brain |
| | | | | BALB/c mice (iv) | Increased animal survival |
| | *pknG* | Rv0410c | Protein kinase G | BALB/c mice (iv) | Reduced CFUs in organs |
| | | | | SCID mice (iv) | Increased animal survival |
| **Proteases** | *mycP1* | Rv3883c | Subtilisin-like serine protease. | MBMDM /BALB/c (ld a) | Reduced CFUs in organs |
| **Serine proteases** | *htrA2 (pepD)* | Rv0983 | HtrA-like serine protease and chaperone. | BALB/c, SCID and C57BL/6 mice(iv) | Increased animal survival and less tissue pathology |
| | - | Rv3671c | Serine protease | C57BL/6 mice (lda) | Reduced CFUs in organs and reduced gross pathology in lung |
| **ATP-dependent proteases** | *clgR* | Rv2745c | Transcriptional regulator | MBMDM | Reduced CFUs in organs |
| **Metallo-proteases** | *zmp1* | Rv0198c | $Zn^{2+}$ Metallo-protease | J774and RAW264.7 macrophages BALB/c mice (lda) | Reduced CFUs in organs |
| | | | | THP1 macrophage | No differences in CFU's |
| | | | | SCID mice (iv) | Reduced survival |
| | | | | C57BL/6 mice (lda) | Increased CFU's in organs |
| | *rip1* | Rv2869c | S2P class of metallo-proteases | C57BL/6 mice (a) | Reduced CFUs in organ and reduced tissue pathology |
| **Proteasome-associated proteins** | *pafA* | Rv2097c | Mycobacterial proteasomal ATPase | C57BL/6 and iNOS$^{-/-}$ mice Resting BMDM from both | Reduced CFUs in organs and pathology |
| | *mpa* | Rv2115c | Mycobacterial proteasomal ATPase | MBMDM BALB/c mice (lda) | Reduced CFUs in organs and less tissue pathology. Increased animal survival |
| **Metals-Transporter Proteins** | *mbtB* | Rv2383c | Iron ABC Transporter | Macrophage-like cell line THP-1. | Reduced CFUs and retarded for ability to grow in this cell line. |

| Category | Gen Name | Rv number | Description | Attenuation evidences | |
|---|---|---|---|---|---|
| | | | | Model | Result |
| **Metal importers** | *irtAB* | Rv1348-Rv1349 | Iron-dependent regulatory protein. Repressor of *mtb* and *mtb-2* loci. | THP-1 macrophages. C57B/6 mice (lda) | Reduced CFUs in macrophages and lung |
| | *ideR* | Rv2711 | | - | Essential |
| | *mgtC* | Rv1811 | $Mg^{2+}$ transport P-type ATPase. $Mg^{2+}$ uptake | HBMDM. BALB/c mice (iv) | Reduced CFUs in macrophages and organs |
| **Metal exporters** | *ctpC* | Rv3270 | $Zn^{2+}$ efflux transporter P-type ATPase | Human macrophages | Reduced CFUs |
| | *ctpV* | Rv0969 | $Cu^{2+}$ efflux transporter P-type ATPase | BALB/c mice (lda) | Increased survival and lower tissue damage in lung |
| | | | | Guinea pigs (lda) | Reduced CFUs and lower tissue damage in lung |
| **Gene Expression Regulators** | *phoPR* | Rv0757 to Rv0758 | TCS | THP1 macrophages | Reduced CFUs |
| | | | | C57BL/6 MICE (lda) | Reduced CFUs in lung |
| **Two component system (TCS)** | *phoP* | Rv0757 | Transcriptional regulator | MBMDM | Reduced CFUs |
| | | | | BALB/c mice (iv) | Reduced CFUs |
| | | | | SCID mice (lda/iv) | Improved survival |
| | *aprABC* | Rv2396abc | Expressed in acidic medium dependent on PhoP | Resting and activated C57BL/6 BMDM | Defects in intracellular replication |
| | *senX3-regX3* | Rv0490-Rv0491 | TCS | THP-1 macrophages | Reduced CFUs |
| | | | | DBA mice | Moderate reduced CFUs in lung |
| | *senX3* | Rv0490 | Sensor | BALB/c mice (iv) | Reduced CFUs in lung |
| | *regX3* | Rv0491 | Transcriptional Regulator | BALB/c mice (iv) | Reduced CFUs in lung |
| | *dosRS dosT* | Rv3133c-Rv3132c Rv2027c | TCS | C57BL/6 MICE (lda) | Reduced lung pathology. Increased CFUs |
| | *dosR (devR)* | Rv3133c | Transcriptional Regulator | C57BL/6 mice (lda) | Moderate reduction CFUs in lung |
| | | | | Guinea pigs (lda) | Reduction CFUs in lung |
| | | | | Rabbit (lda) | Moderate reduction CFUs in lung |
| | | | | Guinea pigs (sc) | Reduced lung pathology |
| | *mprAB* | Rv0981-Rv0982 | TCS | BALB/c mice (iv) | Reduced CFUs in lung latent stage |

| Category | Gen Name | Rv number | Description | Attenuation evidences | |
|---|---|---|---|---|---|
| | | | | Model | Result |
| Sigma factors | *sigA* | Rv2703 | Sigma factor A | C57BL/6 mice (lda) (Antisense) | Reduced CFUs in lung |
| | | | | MonoMac6 cells (Antisense) | Reduced CFUs |
| | *sigC* | Rv2069 | Sigma factor C | DBA/2 mice (lda) | Modest reduction of CFUs in lung, increased animal survival and reduced lung pathology |
| | | | | SCID mice (lda) | Modest reduction of CFUs in lung and increased animal survival |
| | | | | Guinea pigs (lda) | Reduced lung pathology |
| | | | | DBA/2 mice (lda/iv) | Increased survival and reduced lung pathology |
| | | | | Guines pigs (ida) | Reduced lung and spleen pathology |
| | *sigD* | Rv3414c | Sigma factor D | C3H mice (iv) | Increased animal survival |
| | | | | BALB/c mice (iv) | Increased animal survival |
| | *sigE* | Rv1221 | Sigma factor E | SCID mice | Increased animal survival |
| | | | | BALB/c mice (iv) | Reduced CFUs in organs |
| | | | | C3H/HeJ mice (a) | Increased animal survival |
| | | | | Unactivated THP-1 and J774 or activated J774 macrophages | Reduced CFUs |
| | *sigF* | Rv3286c | Sigma factor F | BALB/c mice (iv) | Increased animal survival |
| | | | | BALB/c mice (iv) | Reduced CFUs and pathology in tissues |
| | | | | Guinea pigs (ida) | Moderated reduction in organ pathology |
| | *sigG* | Rv0182c | Sigma factor G | J774macrophages | Moderated reduction in CFUs |
| | *sigH* | Rv3223c | Sigma factor H | C3H and C57BL/6 mice | Reduced pathology in tissues |
| | | | | C3H:He mice | Increased animal survival |
| | | | | BMDM from rhesus monkey | Reduced CFUs at late time post infection |
| | *sigL* | Rv0735 | Sigma factor L | BALB/c mice (iv) | Increased animal survival |

| Category | Gen Name | Rv number | Description | Attenuation evidences | |
|---|---|---|---|---|---|
| | | | | Model | Result |
| Other transcriptional regulators | - | Rv0485 | Member of the nagc/xylr repressor family | BALB/c mice (iv) | Reduced lung pathology |
| | | | | BALB/c mice (iv) | Modestly increased survival |
| | | | | SCID (iv) | Modestly increased survival |
| | - | Rv1931c | AraC transcriptional regulator | BALB/c mice (iv) and BMDM from BALB/c mice | Reduced CFUs |
| | *hspR* | Rv0353 | Transcriptional repressor | C57BL/6 mice (iv) | Reduced CFUs in organs |
| | *whiB3* | Rv3416 | Whib-like regulator family | C57BL/6 mice (iv)* | Increased animal survival |
| | *mosR* | Rv0348 | Mycobacterial operons of survival regulator | BALB/c mice (lda) | Reduced CFUs |
| | *virS* | Rv3082c | AraC family of transcriptional regulator | BALB/c mice (lda) | Increased animal survival |
| | *phoY2* | Rv0821c | Probable phosphate-transport system transcriptional regulator | Activated J774 macrophage. Guinea pig (sc) | Reduced CFUs |
| **Proteins of Unknown Function** | *pe_pgrs33* | Rv1818c | PE_PGRS family protein | BALB/c mice (iv) | Reduced CFUs |
| **The PE/PPE families** | *pe_pgrs51* | Rv3367 | PE_PGRS family | J774 and BMDM macrophages† | Reduced CFUs |
| | *ppe46* | Rv3018 | PPE family | BALB/c mice (iv) | Moderate reduced CFUs in lung |
| | - | Rv1099c | CHP | C57BL/6J mice (iv) | Reduced CFUs in organs |
| **Others proteins with unknown function** | - | Rv0573c | CHP | C57BL/6J mice (iv) | Reduced CFUs in organs |
| | - | Rv0204c | Integral membrane protein | BALB/c mice (iv) | Moderate reduced CFUs in lung |
| | - | Rv2452c | Hypothetical proteins | BALB/c mice (iv) | Moderate reduced CFUs in lung |
| | - | Rv1290c | CHP | CB-17/Icr SCID mice (iv) | Markedly increased surival |
| | - | Rv1891 | CHP | CB-17/Icr SCID mice (iv) | Moderate increased survival |
| | - | Rv3404c | CHP | CB-17/Icr SCID mice (iv) | Moderate increased survival |
| | - | Rv1503c to Rv1507c | CHP | BALB/c mice (lda) | Markely reduced CFUs in organs |
| | - | Rv0199 | Conserved membrane protein | MBMDM | Reduced CFUs |
| | *mmpl4* | Rv0450c | Conserved membrane transport protein | C57BL/6 and (C57BL/6 x DBA2) F1 mice (a) | Reduced CFUs in organs and increased life survival |
| | - | Rv2136c | Conserved transmembrane protein | C57BL/6 mice (lda) | Markedly reduced CFUs in organs. Decreased gross pathology in lung |

| Category | Gen Name | Rv number | Description | Attenuation evidences | |
|---|---|---|---|---|---|
| | | | | Model | Result |
| Other Virulence Factors | *RD2* | Rv1979c to Rv1982 | Region of Difference | C57BL/6 mice (lda) | Reduced CFUs in lung and tissue pathology |
| | | | | RAW macrophages | Reduced CFUs at late times |
| | *acg* | Rv2032 | Uncertain | BALB/c mice (iv) | Reduced CFUs |
| | | | | SCID mice (iv) | Increased animal survival |
| | | | | BMDM from BALB/c mice | Reduced CFUs |
| | *pckA* | Rv0211 | Phosphoenolpyruvate carboxykinase | BMDM from BALB/c mice† | Reduced CFUs |
| | | | | BALB/c mice (iv)† | Reduced CFUs in spleen |
| | *ptpB* | Rv0153c | Tyrosine phosphatase | Guinea pigs | Reduced CFUs in spleen |
| | | | | Activated J774macrophages | Reduced CFUs |
| | *hsp22.5* | Rv0990c | Novel heat shock protein | BALB/c mice (a) | Reduced CFUs in organs and increased animal survival |

**Supplementary Table**: Principal MTB virulence factors [12]

# RELAZIONE SULL'ATTIVITÀ SVOLTA DA MATTEO CHIACCHIARETTA

Il dottorando Matteo Chiacchiaretta, iscritto al Dottorato in Biotecnologie Mediche dell'Università di Siena, ciclo XXXIV, ha svolto durante il corso di dottorato le seguenti attività:

## ATTIVITÀ DI RICERCA

L'attività di ricerca del Dr. Matteo Chiacchiaretta si è fondamentalmente orientata allo studio di caratterizzazione della variabilità genetica di *M. tuberculosis* e del suo coinvolgimento nelle infezioni e nei meccanismi di tolleranza ai farmaci antitubercolari

Gli argomenti trattati sono stati:

- *Host-pathogen interaction* tra ceppi dell' MTB complex e macrofagi pro ed anti-infiammatori
- Caratterizzazione dello smallRNA *ncRv0842c* di MTB coinvolto nella risposta alla rifampicina, e il suo ruolo in diversi ceppi dell'MTB complex
- Dati preliminari sullo smallRNA *nc0757c* coinvolto nella regolazione del gene *phoP* in diversi lineage dell' MTB complex

## TESI DI DOTTORATO

*Titolo*: M. tuberculosis lineages: genetic diversity and its involvement on macrophage infection and on drug tolarance

*Tutore: Daniela Maria Cirillo*
*Co-tutore: Paolo Miotto*

*Descrizione delle tematiche e dei principali risultati*

Lo studio ha permesso di indagare la variabilità genetica dei ceppi clinici dell'MTB complex e di correlarla ai meccanismi di patogenesi e di *drug-resistance acquisition.* I risultati hanno mostrato come sia per quanto riguarda la virulenza, sia per quanto riguarda la regolazione di geni importanti per la tolleranza ai farmaci, esista una variabilità non trascurabile tra i ceppi di MTB, che va ad influenzare drasticamente l'esito dell'infezione. Lo studio ha permesso di indagare con diverse strategie in contemporanea (*single-cell level*, produzione di citochine, sopravvivenza) le differenze che esistono tra i ceppi selezionati, tenendo anche in considerazione lo stato immunologico dell'ospite. Per la prima volta, è stato studiato uno smallRNA coinvolto nella regolazione di un gene importante per i meccanismi di tolleranza ai farmaci. Lo studio ha dimostrato l'importanza di mutazioni sinonime nell'espressione degli smallRNA e la differenza che esiste tra i ceppi dell'MTB complex.

**PARTECIPAZIONE A CONGRESSI, SCUOLE E CORSI**

· Matteo Chiacchiaretta, Rita Sorrentino, Federica Cugnata, Alessandra Aiello, Assunta Navarra, Valentina Vanini, Daniela M. Cirillo, Delia Goletti, Paolo Miotto. Interplay between macrophage heterogeneity and Mycobacterium tuberculosis complex phylogenetic lineages during in vitro infection 23-26 April 2022 (accepted abstract) – "32st European Congress of Clinical Microbiology and Infectious Diseases (ECCMID)"

· Russo G, Di Marco F, Chiacchiaretta M, Spitaleri A, Ambrosi A, Goletti D, Codecasa LR, Miotto P*, Cirillo DM. Serum human microRNAs in the differential diagnosis between active tuberculosis and tuberculosis infection. (19-22 October 2021 – "52nd Union World Conference on Lung Health – Lung Health for All, Solutions for a New Era. Joint meeting with TBScience 2021", virtual event)

· Chiacchiaretta M, Sorrentino R*, Spitaleri A, Cirillo DM, Miotto P. ncRv0842c, a smallRNA regulating the efflux pump Rv0842 involved in rifampicin tolerance in Mycobacterium tuberculosis. (9-12 July 2021 – "31st European Congress of Clinical Microbiology and Infectious Diseases (ECCMID)", virtual event)

· Cabibbe AM, Vanoni C, Chiacchiaretta M, Battaglia S, Spitaleri A, Cugnata F, Miotto P*, Cirillo DM. Epidemiological dynamics and characterization of a successful pre-XDR Mycobacterium tuberculosis clone actively transmitted in Italy. (9-12 July 2021 – "31st European Congress of Clinical Microbiology and Infectious Diseases (ECCMID)", virtual event)

· Chiacchiaretta M, Sorrentino R, Audisio A, Goletti D, Vanini V, Aiello A, Cirillo DM, Miotto P. Interplay between macrophage polarization and M. tuberculosis lineages. (28-29 June 2021 – "41st Annual Congress of the European Society of Mycobacteriology", virtual event)

· Battaglia S, Chiacchiaretta M, Gabro VS, Robinson E, Cirillo DM, Köser CU, Schön T, Miotto P. Lineage 1 has elevated pyrazinamide minimum inhibitory concentrations compared with other lineages of Mycobacterium tuberculosis complex. (28-29 June 2021 – "41st Annual Congress of the European Society of Mycobacteriology", virtual event)

· Cabibbe AM*, Vanoni C, Chiacchiaretta M, Battaglia S, Spitaleri A, Cugnata F, Miotto P, Cirillo DM. In vitro characterization of a successful multidrug-resistant Mycobacterium tuberculosis clone actively transmitted in Italy. (28-29 June 2021 – "41st Annual Congress of the European Society of Mycobacteriology", virtual event)

· Chiacchiaretta M, Bresciani N, Agresti A, Zambrano S, Mazza D, Cugnata F, Tassan Din C, Cirillo DM, Miotto P*. Classically (M1) and alternatively (M2) activated macrophages infected with generalists and specialists Mycobacterium tuberculosis complex isolates display differential phagosomal acidification patterns. (2-4 December 2020 – "Keystone eSymposium "Tuberculosis: science aimed at ending the epidemic", virtual event)

· Chiacchiaretta M, Spitaleri A, Cirillo DM, Miotto P. ncRv0842c, a smallRNA regulating the efflux pump Rv0842 involved in rifampicin tolerance in Mycobacterium tuberculosis. (20-24 October 2020 – "51st Union World Conference on Lung Health – TBScience 2020", virtual event)

· Chiacchiaretta M, Bresciani N, Russo G, Cirillo DM*, Miotto P. Characterization of the intramacrophagic expression profile of the smallRNA ncRv0757c in different Mycobacterium tuberculosis lineages. (29-30 October 2019 – "2nd TBScience meeting – The 50th Union World Conference on Lung Health", Hyderabad, IND)

· Chiacchiaretta M*, Bresciani N, Russo G, Tassan Din C, Cirillo DM, Miotto P. Characterization of the intramacrophagic expression profile of the smallRNA ncRv0757c in different Mycobacterium tuberculosis lineages (30 June - 3 July 2019 – "40th Annual Congress of the European Society of Mycobacteriology", Valencia, E)

· Chiacchiaretta M, Bresciani N, Agresti A, Zambrano S, Mazza D, Cugnata F, Tassan Din C, Cirillo DM, Miotto P*. The role of Mycobacterium tuberculosis complex genetic variation and of macrophage phenotype during early stages of infection (30 June - 3 July 2019 – "40th Annual Congress of the European Society of Mycobacteriology", Valencia, E)

· Chiacchiaretta M*, Bresciani N, Agresti A, Zambrano S, Mazza D, Cugnata F, Tassan Din C, Cirillo DM, Miotto P. Mycobacterium tuberculosis complex genetic variation and macrophage polarization

status influence phagolysosomal acidification during infection (5-7 June 2019 – "11th Italian Conference on AIDS and Antiviral Research", Milano, I)

· Chiacchiaretta M*, Bresciani N, Russo G, Tassan Din C, Cirillo DM, Miotto P. Characterization of the intramacrophagic expression profile of the smallRNA ncRv0757c in different Mycobacterium tuberculosis lineages. (16-18 March 2019 – "San Raffaele Scientific Retreat", Baveno, I)

· Tassan Din C, Chiacchiaretta M, Bresciani N, Agresti A, Zambrano S, Mazza D, Cugnata F, Cirillo DM, Miotto P*. The role of Mycobacterium tuberculosis complex genetic variation during macrophage infection. (14-16 March 2019 – "San Raffaele Scientific Retreat", Baveno, I)

· Chiacchiaretta M, Bresciani N, Agresti A, Zambrano S, Mazza D, Cugnata F, Tassan Din C, Cirillo DM, Miotto P*. Lysosomal acidification induced by different Mycobacterium tuberculosis complex lineages during human macrophage infection. (17-21 January 2019 – "Keystone Symposium on tuberculosis: Tuberculosis: Mechanisms, Pathogenesis and Treatment", Banff – AB, CDN)

Chiacchiaretta M, Bresciani N, Agresti A, Zambrano S, Tassan Din C, Cirillo DM, Miotto P. Single-cell live confocal microscopy for monitoring lysosomal acidification induced by different M. tuberculosis complex lineages during macrophage infection. (1-4 July 2018 – "39th Annual Congress of the European Society of Mycobacteriology", Dresden, D)

**PUBBLICAZIONI**

Durante il periodo del Dottorato il Dr Matteo Chiacchiaretta ha prodotto 2 pubblicazioni accettate e 3 manuscript in submission.

Articoli pubblicati:

· Gona F, Bongiorno D, Aprile A, et al. Emergence of two novel sequence types (3366 and 3367) NDM-1- and OXA-48-co-producing K. pneumoniae in Italy. Eur J Clin Microbiol Infect Dis. 2019;38(9):1687-1691. doi:10.1007/s10096-019-03597-w

· Fowler PW, Gibertoni Cruz AL, Hoosdally SJ, et al. Corrigendum: Automated detection of bacterial growth on 96-well plates for high-throughput drug susceptibility testing of Mycobacterium tuberculosis. Microbiology (Reading). 2019;165(5):585. doi:10.1099/mic.0.000795

In particolare sulle tematiche connesse alla ricerca svolta nell'ambito del dottorato ha pubblicato i seguenti articoli:
Manuscripts under submission:

· Chiacchiaretta M, Sorrentino R, Bresciani N, Agresti A, Zambrano S, Mazza D, Tassan Din C, Cugnata F, Aiello A, Navarra A, Goletti D, Cirillo DM, Miotto P. Classically (M1) and alternatively (M2) activated macrophages infected with generalists and specialists Mycobacterium tuberculosis complex isolates display differential phagosomal acidification patterns

· Chiacchiaretta M, Sorrentino R, Di Marco F, Spitaleri A, Cirillo DM, Miotto P *ncRv0842c*, a smallRNA regulating the efflux pump Rv0842 involved in rifampicin tolerance in Mycobacterium tuberculosis

· Lineage 1 has elevated pyrazinamide minimum inhibitory concentrations compared with other lineages of Mycobacterium tuberculosis complex

Data 28/01/2022

Firma del dottorando

Visto
(Il Tutore)

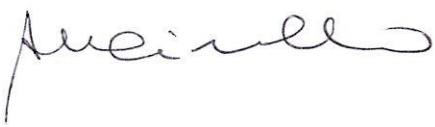

# Phagolysosomal acidification

| | LysoSensor |
|---|---|
| **Wells/sample** | 3 |
| **Acquisition positions/well** | 2 |
| **Channels** | Hoechst, LysoSensor, dsRed |
| **Z-stacks** | 0.89 µm x7 |

6 h p.i.

| | | NOT infected | | Infected | | TOT | |
|---|---|---|---|---|---|---|---|
| | | N of cells | Replicates | N of cells | Replicates | Not inf | Inf |
| M1 | CTRL | 197 | 8 | *na* | *na* | *1141* | *909* |
| | H37Rv | 130 | 3 | 116 | 3 | | |
| | H37Ra | 119 | 3 | 105 | 3 | | |
| | BCG | 78 | 2 | 84 | 2 | | |
| | CDC1551 | 129 | 3 | 122 | 3 | | |
| | Beijing | 182 | 5 | 199 | 5 | | |
| | EAI | 146 | 4 | 137 | 4 | | |
| | Afri | 160 | 4 | 146 | 4 | | |
| M2 | CTRL | 190 | 8 | *na* | *na* | *1116* | *932* |
| | H37Rv | 111 | 3 | 113 | 3 | | |
| | BCG | 73 | 2 | 84 | 2 | | |
| | H37Ra | 131 | 3 | 121 | 3 | | |
| | CDC1551 | 134 | 3 | 123 | 3 | | |
| | Beijing | 186 | 5 | 218 | 5 | | |
| | EAI | 142 | 4 | 134 | 4 | | |
| | Afri | 149 | 4 | 139 | 4 | | |
| TOT | | *2257* | | *1841* | | | |
| | | 4098 | | | | | |

24 h p.i.

| | | NOT infected | | Infected | | TOT | |
|---|---|---|---|---|---|---|---|
| | | N of cells | Replicates | N of cells | Replicates | Not inf | Inf |
| M1 | CTRL | 152 | 8 | *na* | *na* | *813* | *806* |
| | H37Rv | 77 | 3 | 110 | 3 | | |
| | H37Ra | 73 | 3 | 111 | 3 | | |
| | BCG | 51 | 2 | 76 | 2 | | |
| | CDC1551 | 75 | 3 | 91 | 3 | | |
| | Beijing | 129 | 5 | 169 | 5 | | |
| | EAI | 136 | 4 | 127 | 4 | | |
| | Afri | 120 | 4 | 122 | 4 | | |
| M2 | CTRL | 138 | 8 | *na* | *na* | *859* | *808* |
| | H37Rv | 87 | 3 | 105 | 3 | | |
| | BCG | 70 | 2 | 80 | 2 | | |
| | H37Ra | 94 | 3 | 109 | 3 | | |
| | CDC1551 | 84 | 3 | 82 | 3 | | |
| | Beijing | 126 | 5 | 162 | 5 | | |
| | EAI | 141 | 4 | 141 | 4 | | |
| | Afri | 119 | 4 | 129 | 4 | | |
| TOT | | *1672* | | *1614* | | | |
| | | 3286 | | | | | |

Total

| | | NOT infected | | Infected | | TOT | |
|---|---|---|---|---|---|---|---|
| | | N of cells | Replicates | N of cells | Replicates | Not inf | Inf |
| M1 | CTRL | 349 | 8 | *na* | *na* | *1954* | *1715* |
| | H37Rv | 207 | 3 | 226 | 3 | | |
| | H37Ra | 192 | 3 | 216 | 3 | | |
| | BCG | 129 | 2 | 160 | 2 | | |
| | CDC1551 | 204 | 3 | 213 | 3 | | |
| | Beijing | 311 | 5 | 368 | 5 | | |
| | EAI | 282 | 4 | 264 | 4 | | |
| | Afri | 280 | 4 | 268 | 4 | | |
| M2 | CTRL | 328 | 8 | *na* | *na* | *1975* | *1740* |
| | H37Rv | 198 | 3 | 218 | 3 | | |
| | BCG | 143 | 2 | 164 | 2 | | |
| | H37Ra | 225 | 3 | 230 | 3 | | |
| | CDC1551 | 218 | 3 | 205 | 3 | | |
| | Beijing | 312 | 5 | 380 | 5 | | |
| | EAI | 283 | 4 | 275 | 4 | | |
| | Afri | 268 | 4 | 268 | 4 | | |
| TOT | | *3929* | | *3455* | | | |
| | | 7384 | | | | | |

*Acquisition:*

obj. **63x, oil NA 1.40**
**z-stacks: 0.89 µm x 7 stacks**
Res. **16-bit** format: **1024x1024**
Laser 405 (for Hoechst) = **6%**; gain: 898.9, offset: 0%
Laser 458 (for LysoSensor) = **10% (Argon power: 30%); gain: 724.8**, offset: 0%
Laser 453 (for dsRed) = **15%; gain: 844.9**, offset: 0%
Confocal: AP **24** FD **6 O** INT **0** FIM **100%**

*Analysis:*

4 h p.i. and 24 h p.i.; (N of phagolysosomes), phago**lysosomes intensity and % of active cells, MOI, colocalization myc/acidic compartments**

**Hoechst (Ex/Em 350/461)**

threshold (Huang, Red; no flags on Dark background and Stack histogram) = approx. 215
size = 40-inf µm$^2$ circularity = 0-1 (Show: outlines; flag only Add to Manager)

**LysoSensor (Ex/Em 443/505)**

**threshold (Huang, Red; no flags on Dark background and Stack histogram) = 155**
**size = 0.5-1.8 µm$^2$ circularity = 0-1 (Show: overlay mask; NO flag on Add to Manager)**

**dsRed (Ex/Em 584-557)**

**threshold (Huang, Red; no flags on Dark background and Stack histogram) = 215**
**size = 2-100 µm$^2$ circularity = 0-0.9 (Show: overlay mask; NO flag on Add to Manager)**

**Grouping: Geo-host adaptation**

**M1 – 6 h p.i.**

a) Phagolysosomal acidification

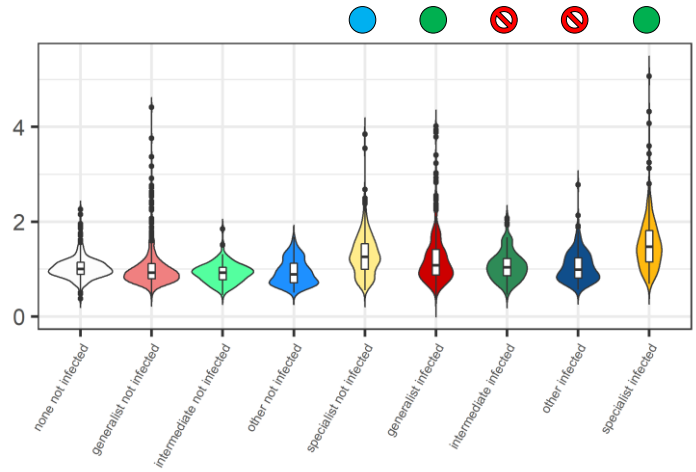


b) Percentage of cells showing acidified phagolysosomes

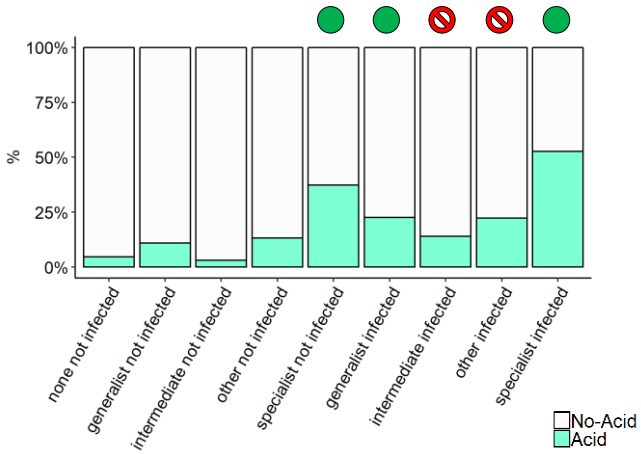


| Par | Value | Std.Error | p.value |
|---|---|---|---|
| (Intercept) | 0.0034 | 0.0759 | 0.9648 |
| groupgeneralist not infected | 0.0463 | 0.0553 | 0.4025 |
| groupintermediate not infected | -0.0365 | 0.0769 | 0.6354 |
| groupother not infected | -0.1016 | 0.0654 | 0.1208 |
| groupspecialist not infected | 0.1075 | 0.057 | 0.0597 |
| groupgeneralist infected | 0.1539 | 0.0553 | 0.0055 |
| groupintermediate infected | 0.1132 | 0.0771 | 0.142 |
| groupother infected | -0.0272 | 0.0656 | 0.6783 |
| groupspecialist infected | 0.2576 | 0.0572 | 0 |

| Contrast | estimate | SE | p.value |
|---|---|---|---|
| none not infected-generalist not infected | -0.0463 | 0.0553 | 0.483 |
| none not infected-intermediate not infected | 0.0365 | 0.0769 | 0.663 |
| none not infected-other not infected | 0.1016 | 0.0654 | 0.1812 |
| none not infected-specialist not infected | -0.1075 | 0.057 | 0.1303 |
| none not infected-generalist infected | -0.1539 | 0.0553 | 0.0164 |
| none not infected-intermediate infected | -0.1132 | 0.0771 | 0.2005 |
| none not infected-other infected | 0.0272 | 0.0656 | 0.6783 |
| none not infected-specialist infected | -0.2576 | 0.0572 | 0 |
| generalist not infected-intermediate not infected | 0.0827 | 0.0749 | 0.3597 |
| generalist not infected-other not infected | 0.1478 | 0.0673 | 0.0675 |
| generalist not infected-specialist not infected | -0.0612 | 0.0586 | 0.3748 |
| intermediate not infected-other not infected | 0.0651 | 0.0872 | 0.52 |
| intermediate not infected-specialist not infected | -0.1439 | 0.0798 | 0.1317 |
| other not infected-specialist not infected | -0.2091 | 0.0674 | 0.0067 |
| generalist infected-intermediate infected | 0.0407 | 0.0751 | 0.6414 |
| generalist infected-other infected | 0.1811 | 0.0675 | 0.0196 |
| generalist infected-specialist infected | -0.1037 | 0.0588 | 0.1337 |
| intermediate infected-other infected | 0.1404 | 0.0874 | 0.1734 |
| intermediate infected-specialist infected | -0.1445 | 0.0801 | 0.1317 |
| other infected-specialist infected | -0.2849 | 0.0676 | 1e-04 |
| generalist not infected-generalist infected | -0.1077 | 0.0141 | 0 |
| intermediate not infected-intermediate infected | -0.1497 | 0.022 | 0 |
| other not infected-other infected | -0.0744 | 0.0177 | 1e-04 |
| specialist not infected-specialist infected | -0.1502 | 0.0143 | 0 |

| Par | Estimate | se | OR | pvalue |
|---|---|---|---|---|
| (Intercept) | -3.5823 | 0.8396 | 0.0278 | 0 |
| groupgeneralist not infected | 0.6037 | 0.6792 | 1.8289 | 0.3741 |
| groupintermediate not infected | 0.0514 | 0.9665 | 1.0527 | 0.9576 |
| groupother not infected | 0.3002 | 0.735 | 1.3502 | 0.6829 |
| groupspecialist not infected | 1.5245 | 0.6226 | 4.5927 | 0.0143 |
| groupgeneralist infected | 2.1602 | 0.6538 | 8.6725 | 0.001 |
| groupintermediate infected | 1.826 | 0.862 | 6.2087 | 0.0341 |
| groupother infected | 0.9688 | 0.7215 | 2.6349 | 0.1793 |
| groupspecialist infected | 2.675 | 0.6242 | 14.513 | 0 |

| Contrast | estimate | SE | p.value |
|---|---|---|---|
| none not infected-generalist not infected | -0.6037 | 0.6792 | 0.4988 |
| none not infected-intermediate not infected | -0.0514 | 0.9665 | 0.9576 |
| none not infected-other not infected | -0.3002 | 0.735 | 0.745 |
| none not infected-specialist not infected | -1.5245 | 0.6226 | 0.0492 |
| none not infected-generalist infected | -2.1602 | 0.6538 | 0.0057 |
| none not infected-intermediate infected | -1.826 | 0.862 | 0.1024 |
| none not infected-other infected | -0.9688 | 0.7215 | 0.3074 |
| none not infected-specialist infected | -2.675 | 0.6242 | 1e-04 |
| generalist not infected-intermediate not infected | 0.5523 | 0.9195 | 0.6923 |
| generalist not infected-other not infected | 0.3035 | 0.7255 | 0.745 |
| generalist not infected-specialist not infected | -0.9208 | 0.5871 | 0.2157 |
| intermediate not infected-other not infected | -0.2489 | 1.0007 | 0.8385 |
| intermediate not infected-specialist not infected | -1.4731 | 0.9031 | 0.2057 |
| other not infected-specialist not infected | -1.2242 | 0.6569 | 0.1497 |
| generalist infected-intermediate infected | 0.3342 | 0.7838 | 0.745 |
| generalist infected-other infected | 1.1913 | 0.6837 | 0.1777 |
| generalist infected-specialist infected | -0.5149 | 0.5613 | 0.4988 |
| intermediate infected-other infected | 0.8571 | 0.887 | 0.4988 |
| intermediate infected-specialist infected | -0.8491 | 0.7907 | 0.4527 |
| other infected-specialist infected | -1.7062 | 0.6456 | 0.0329 |
| generalist not infected-generalist infected | -1.5565 | 0.339 | 1e-04 |
| intermediate not infected-intermediate infected | -1.7746 | 0.5888 | 0.0124 |
| other not infected-other infected | -0.6686 | 0.3247 | 0.1052 |
| specialist not infected-specialist infected | -1.1506 | 0.2256 | 0 |

OBSERVATIONS

In M1 macrophages, only categories intermediate and other displayed blocking of phagolysosomal acidification at 6 h p.i., and specialist strains showed the highest number of acidified macrophages (50% vs <25% of all the other categories). A bystander effect in non-infected M1 macrophages was observed for specialist strains at 6 h p.i, despite it was not found statistically significant.

- Acidification of phagolysosomes observed
- Acidification of phagolysosomes not observed (blocked)
- Acidification trend observed, stastically not significant

**Grouping: Geo-host adaptation**

**M1 – 6 h p.i.**

c) Effective MOI

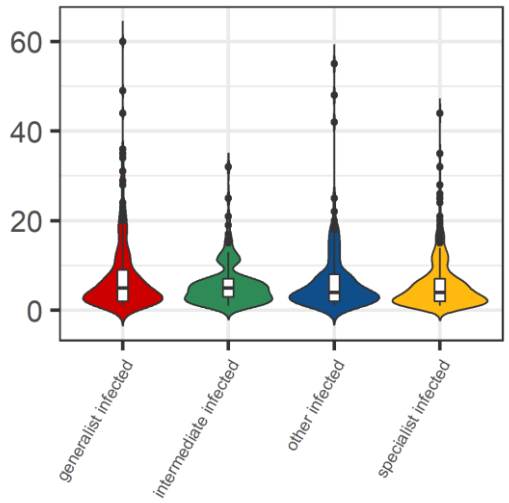


| Par | Value | Std.Error | p.value |
|---|---|---|---|
| (Intercept) | 1.4895 | 0.1074 | 0 |
| groupintermediate infected | -0.1421 | 0.1621 | 0.3841 |
| groupother infected | -0.0297 | 0.1467 | 0.8405 |
| groupspecialist infected | -0.0751 | 0.1277 | 0.5587 |

| Contrast | estimate | SE | p.value |
|---|---|---|---|
| generalist infected - intermediate infected | 0.1421 | 0.1621 | 0.8405 |
| generalist infected - other infected | 0.0297 | 0.1467 | 0.8405 |
| generalist infected - specialist infected | 0.0751 | 0.1277 | 0.8405 |
| intermediate infected - other infected | -0.1124 | 0.188 | 0.8405 |
| intermediate infected - specialist infected | -0.067 | 0.1726 | 0.8405 |
| other infected - specialist infected | 0.0454 | 0.1459 | 0.8405 |

d) Colocalization Index

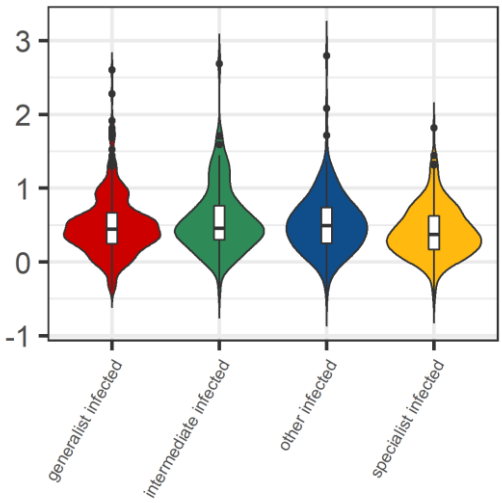


| Par | Value | Std.Error | p.value |
|---|---|---|---|
| (Intercept) | 0.0473 | 0.08 | 0.5543 |
| groupintermediate infected | 0.1246 | 0.1341 | 0.3566 |
| groupother infected | 0.1538 | 0.121 | 0.2084 |
| groupspecialist infected | -0.1465 | 0.1058 | 0.1712 |

| Contrast | estimate | SE | p.value |
|---|---|---|---|
| generalist infected - intermediate infected | -0.1246 | 0.1341 | 0.428 |
| generalist infected - other infected | -0.1538 | 0.121 | 0.3126 |
| generalist infected - specialist infected | 0.1465 | 0.1058 | 0.3126 |
| intermediate infected - other infected | -0.0292 | 0.1519 | 0.8482 |
| intermediate infected - specialist infected | 0.2711 | 0.1402 | 0.1733 |
| other infected - specialist infected | 0.3003 | 0.1198 | 0.0893 |

OBSERVATIONS

In M1 macrophages, no statistically relevant differences in effective MOI were observed. Colocalization with acidified compartments was similar among all the groups.

**Grouping: Geo-host adaptation**

**M1 – 24 h p.i.**

a) Phagolysosomal acidification

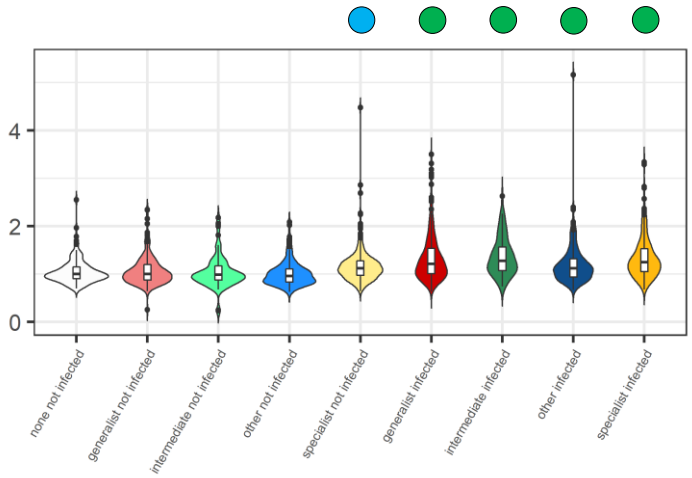


b) Percentage of cells showing acidified phagolysosomes

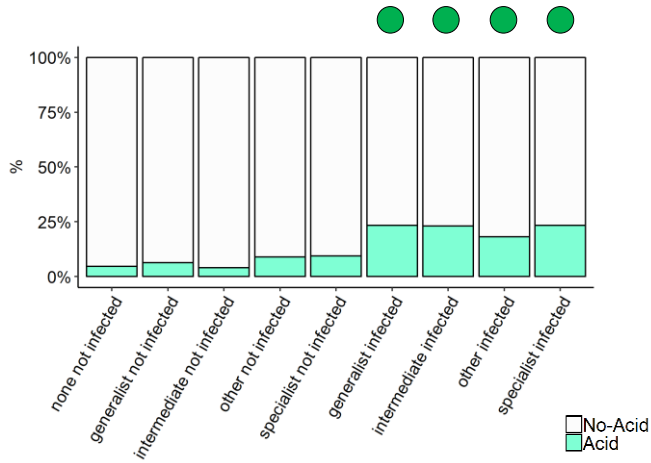


| Par | Value | Std.Error | p.value |
|---|---|---|---|
| (Intercept) | 0.0091 | 0.0429 | 0.8315 |
| groupgeneralist not infected | 0.0412 | 0.0323 | 0.2028 |
| groupintermediate not infected | 0.0206 | 0.0444 | 0.643 |
| groupother not infected | -0.0215 | 0.0381 | 0.5724 |
| groupspecialist not infected | 0.0263 | 0.0323 | 0.416 |
| groupgeneralist infected | 0.1879 | 0.0318 | 0 |
| groupintermediate infected | 0.2727 | 0.0435 | 0 |
| groupother infected | 0.1259 | 0.0367 | 6e-04 |
| groupspecialist infected | 0.1353 | 0.0324 | 0 |

| Contrast | estimate | SE | p.value |
|---|---|---|---|
| none not infected-generalist not infected | -0.0412 | 0.0323 | 0.3042 |
| none not infected-intermediate not infected | -0.0206 | 0.0444 | 0.7014 |
| none not infected-other not infected | 0.0215 | 0.0381 | 0.7014 |
| none not infected-specialist not infected | -0.0263 | 0.0323 | 0.5547 |
| none not infected-generalist infected | -0.1879 | 0.0318 | 0 |
| none not infected-intermediate infected | -0.2727 | 0.0435 | 0 |
| none not infected-other infected | -0.1259 | 0.0367 | 0.0019 |
| none not infected-specialist infected | -0.1353 | 0.0324 | 1e-04 |
| generalist not infected-intermediate not infected | 0.0206 | 0.0426 | 0.7014 |
| generalist not infected-other not infected | 0.0627 | 0.0377 | 0.1653 |
| generalist not infected-specialist not infected | 0.0149 | 0.0321 | 0.7014 |
| intermediate not infected-other not infected | 0.0421 | 0.0492 | 0.5538 |
| intermediate not infected-specialist not infected | -0.0057 | 0.0446 | 0.8977 |
| other not infected-specialist not infected | -0.0478 | 0.0372 | 0.3042 |
| generalist infected-intermediate infected | -0.0848 | 0.0412 | 0.0864 |
| generalist infected-other infected | 0.062 | 0.0358 | 0.1653 |
| generalist infected-specialist infected | 0.0526 | 0.0316 | 0.1653 |
| intermediate infected-other infected | 0.1468 | 0.0473 | 0.0047 |
| intermediate infected-specialist infected | 0.1374 | 0.0438 | 0.0047 |
| other infected-specialist infected | -0.0093 | 0.036 | 0.8296 |
| generalist not infected-generalist infected | -0.1467 | 0.0191 | 0 |
| intermediate not infected-intermediate infected | -0.2521 | 0.0325 | 0 |
| other not infected-other infected | -0.1475 | 0.0236 | 0 |
| specialist not infected-specialist infected | -0.109 | 0.0181 | 0 |

| Par | Estimate | se | OR | pvalue |
|---|---|---|---|---|
| (Intercept) | -3.1976 | 0.4593 | 0.0409 | 0 |
| groupgeneralist not infected | 0.3895 | 0.5143 | 1.4763 | 0.4488 |
| groupintermediate not infected | 0.1034 | 0.7496 | 1.109 | 0.8902 |
| groupother not infected | 0.9072 | 0.5479 | 2.4774 | 0.0977 |
| groupspecialist not infected | 0.5002 | 0.4771 | 1.649 | 0.2945 |
| groupgeneralist infected | 1.9578 | 0.4494 | 7.0841 | 0 |
| groupintermediate infected | 2.0397 | 0.5309 | 7.6883 | 1e-04 |
| groupother infected | 1.7688 | 0.4842 | 5.8637 | 3e-04 |
| groupspecialist infected | 1.6527 | 0.4506 | 5.2213 | 2e-04 |

| Contrast | estimate | SE | p.value |
|---|---|---|---|
| none not infected-generalist not infected | -0.3895 | 0.5143 | 0.6732 |
| none not infected-intermediate not infected | -0.1034 | 0.7496 | 0.8902 |
| none not infected-other not infected | -0.9072 | 0.5479 | 0.2607 |
| none not infected-specialist not infected | -0.5002 | 0.4771 | 0.5468 |
| none not infected-generalist infected | -1.9578 | 0.4494 | 1e-04 |
| none not infected-intermediate infected | -2.0397 | 0.5309 | 7e-04 |
| none not infected-other infected | -1.7688 | 0.4842 | 0.001 |
| none not infected-specialist infected | -1.6527 | 0.4506 | 0.001 |
| generalist not infected-intermediate not infected | 0.2861 | 0.6951 | 0.8168 |
| generalist not infected-other not infected | -0.5177 | 0.4955 | 0.5468 |
| generalist not infected-specialist not infected | -0.1106 | 0.4089 | 0.8583 |
| intermediate not infected-other not infected | -0.8038 | 0.7382 | 0.5468 |
| intermediate not infected-specialist not infected | -0.3967 | 0.6866 | 0.728 |
| other not infected-specialist not infected | 0.407 | 0.4483 | 0.5822 |
| generalist infected-intermediate infected | -0.0818 | 0.3691 | 0.8604 |
| generalist infected-other infected | 0.1891 | 0.3384 | 0.728 |
| generalist infected-specialist infected | 0.3051 | 0.2853 | 0.5468 |
| intermediate infected-other infected | 0.2709 | 0.4453 | 0.728 |
| intermediate infected-specialist infected | 0.387 | 0.4073 | 0.5822 |
| other infected-specialist infected | 0.116 | 0.3328 | 0.8313 |
| generalist not infected-generalist infected | -1.5683 | 0.3303 | 0 |
| intermediate not infected-intermediate infected | -1.9363 | 0.646 | 0.0093 |
| other not infected-other infected | -0.8616 | 0.3756 | 0.0655 |
| specialist not infected-specialist infected | -1.1526 | 0.2684 | 1e-04 |

OBSERVATIONS

At 24 h p.i. none of the category is blocking the acidification of the phagolysosomes. However, despite an increase in the acidification of the phagolysosomes was observed, the number of macrophages displaying such acidification was found generally low (<25%).

- Acidification of phagolysosomes observed
- Acidification of phagolysosomes not observed (blocked)
- Acidification trend observed, stastically not significant

**Grouping: Geo-host adaptation**

**M1 – 24 h p.i.**

c) Effective MOI

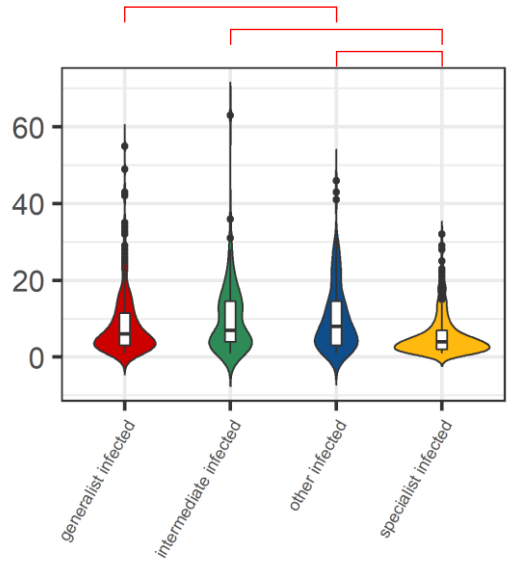


| Par | Value | Std.Error | p.value |
|---|---|---|---|
| (Intercept) | 1.6426 | 0.1203 | 0 |
| groupintermediate infected | 0.1433 | 0.1195 | 0.2348 |
| groupother infected | 0.4187 | 0.105 | 2e-04 |
| groupspecialist infected | -0.1752 | 0.0937 | 0.0664 |

| Contrast | estimate | SE | p.value |
|---|---|---|---|
| generalist infected - intermediate infected | -0.1433 | 0.1195 | 0.2348 |
| generalist infected - other infected | -0.4187 | 0.105 | 5e-04 |
| generalist infected - specialist infected | 0.1752 | 0.0937 | 0.0796 |
| intermediate infected - other infected | -0.2753 | 0.1417 | 0.0796 |
| intermediate infected - specialist infected | 0.3185 | 0.1325 | 0.0385 |
| other infected - specialist infected | 0.5938 | 0.1065 | 0 |

d) Colocalization Index

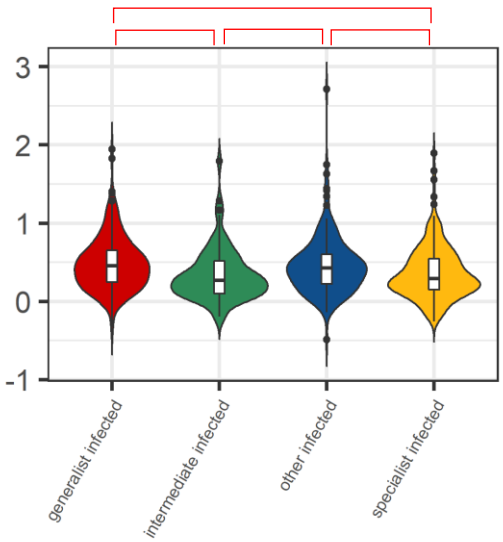


| Par | Value | Std.Error | p.value |
|---|---|---|---|
| (Intercept) | 0.1697 | 0.0802 | 0.0347 |
| groupintermediate infected | -0.535 | 0.1412 | 4e-04 |
| groupother infected | -0.0769 | 0.1162 | 0.5107 |
| groupspecialist infected | -0.3273 | 0.103 | 0.0023 |

| Contrast | estimate | SE | p.value |
|---|---|---|---|
| generalist infected - intermediate infected | 0.535 | 0.1412 | 0.0021 |
| generalist infected - other infected | 0.0769 | 0.1162 | 0.5107 |
| generalist infected - specialist infected | 0.3273 | 0.103 | 0.007 |
| intermediate infected - other infected | -0.4581 | 0.1592 | 0.0111 |
| intermediate infected - specialist infected | -0.2077 | 0.1496 | 0.2043 |
| other infected - specialist infected | 0.2504 | 0.1166 | 0.0537 |

OBSERVATIONS

Specialist strains showed lower MOI values compared to the other groups. Colocalization with acidified compartments was found lower for specialist and intermediate strains.

**Grouping: Geo-host adaptation**

**M2 – 6 h p.i.**

a) Phagolysosomal acidification

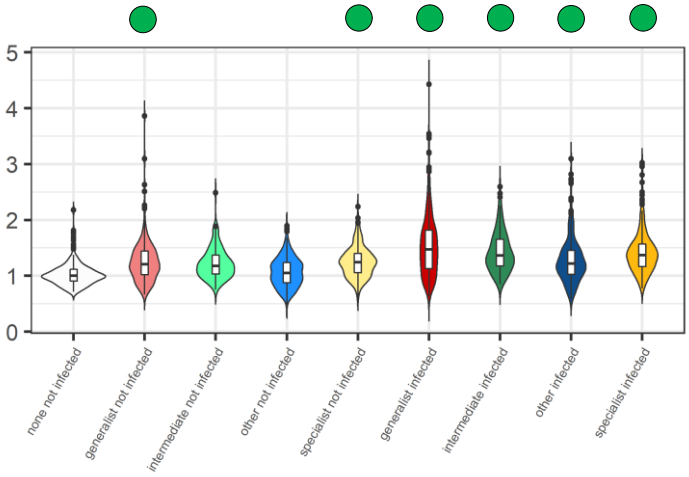


b) Percentage of cells showing acidified phagolysosomes

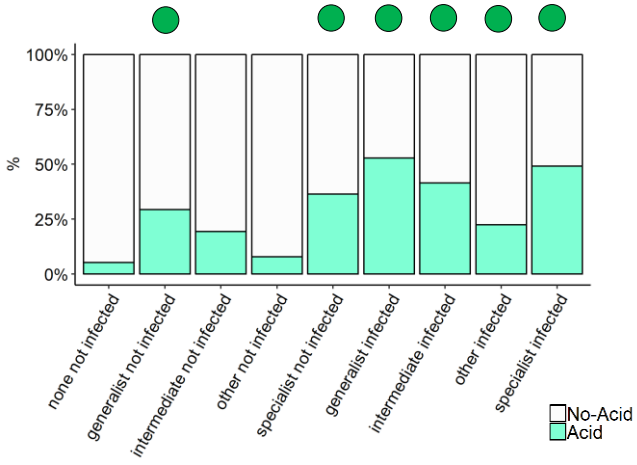


| Par | Value | Std.Error | p.value |
|---|---|---|---|
| (Intercept) | -0.0103 | 0.0505 | 0.8387 |
| groupgeneralist not infected | 0.1843 | 0.0441 | 0 |
| groupintermediate not infected | 0.1018 | 0.0612 | 0.0966 |
| groupother not infected | 0.0694 | 0.0518 | 0.1809 |
| groupspecialist not infected | 0.1644 | 0.0458 | 3e-04 |
| groupgeneralist infected | 0.3254 | 0.044 | 0 |
| groupintermediate infected | 0.2311 | 0.0615 | 2e-04 |
| groupother infected | 0.2086 | 0.052 | 1e-04 |
| groupspecialist infected | 0.2734 | 0.0459 | 0 |

| Contrast | estimate | SE | p.value |
|---|---|---|---|
| none not infected-generalist not infected | -0.1843 | 0.0441 | 1e-04 |
| none not infected-intermediate not infected | -0.1018 | 0.0612 | 0.1656 |
| none not infected-other not infected | -0.0694 | 0.0518 | 0.2553 |
| none not infected-specialist not infected | -0.1644 | 0.0458 | 8e-04 |
| none not infected-generalist infected | -0.3254 | 0.044 | 0 |
| none not infected-intermediate infected | -0.2311 | 0.0615 | 5e-04 |
| none not infected-other infected | -0.2086 | 0.052 | 2e-04 |
| none not infected-specialist infected | -0.2734 | 0.0459 | 0 |
| generalist not infected-intermediate not infected | 0.0825 | 0.0598 | 0.251 |
| generalist not infected-other not infected | 0.1149 | 0.0535 | 0.064 |
| generalist not infected-specialist not infected | 0.0199 | 0.0468 | 0.6993 |
| intermediate not infected-other not infected | 0.0324 | 0.0691 | 0.6973 |
| intermediate not infected-specialist not infected | -0.0626 | 0.0634 | 0.3883 |
| other not infected-specialist not infected | -0.095 | 0.0535 | 0.1403 |
| generalist infected-intermediate infected | 0.0943 | 0.06 | 0.1855 |
| generalist infected-other infected | 0.1168 | 0.0537 | 0.064 |
| generalist infected-specialist infected | 0.052 | 0.0468 | 0.337 |
| intermediate infected-other infected | 0.0225 | 0.0694 | 0.7457 |
| intermediate infected-specialist infected | -0.0423 | 0.0637 | 0.5796 |
| other infected-specialist infected | -0.0648 | 0.0537 | 0.3039 |
| generalist not infected-generalist infected | -0.1411 | 0.0135 | 0 |
| intermediate not infected-intermediate infected | -0.1294 | 0.0207 | 0 |
| other not infected-other infected | -0.1393 | 0.0168 | 0 |
| specialist not infected-specialist infected | -0.109 | 0.0139 | 0 |

| Par | Estimate | se | OR | pvalue |
|---|---|---|---|---|
| (Intercept) | -3.2009 | 0.6363 | 0.0407 | 0 |
| groupgeneralist not infected | 1.6574 | 0.5541 | 5.2456 | 0.0028 |
| groupintermediate not infected | 0.8911 | 0.7029 | 2.4377 | 0.2049 |
| groupother not infected | 1.2315 | 0.6648 | 3.4263 | 0.064 |
| groupspecialist not infected | 2.0146 | 0.5667 | 7.498 | 4e-04 |
| groupgeneralist infected | 3.1396 | 0.5477 | 23.0938 | 0 |
| groupintermediate infected | 2.4219 | 0.6849 | 11.2672 | 4e-04 |
| groupother infected | 2.6032 | 0.6298 | 13.5067 | 0 |
| groupspecialist infected | 2.8956 | 0.5666 | 18.0946 | 0 |

| Contrast | estimate | SE | p.value |
|---|---|---|---|
| none not infected-generalist not infected | -1.6574 | 0.5541 | 0.0067 |
| none not infected-intermediate not infected | -0.8911 | 0.7029 | 0.3383 |
| none not infected-other not infected | -1.2315 | 0.6648 | 0.1396 |
| none not infected-specialist not infected | -2.0146 | 0.5667 | 0.0011 |
| none not infected-generalist infected | -3.1396 | 0.5477 | 0 |
| none not infected-intermediate infected | -2.4219 | 0.6849 | 0.0011 |
| none not infected-other infected | -2.6032 | 0.6298 | 1e-04 |
| none not infected-specialist infected | -2.8956 | 0.5666 | 0 |
| generalist not infected-intermediate not infected | 0.7663 | 0.6158 | 0.3383 |
| generalist not infected-other not infected | 0.4259 | 0.5959 | 0.5697 |
| generalist not infected-specialist not infected | -0.3572 | 0.4812 | 0.5697 |
| intermediate not infected-other not infected | -0.3404 | 0.748 | 0.6773 |
| intermediate not infected-specialist not infected | -1.1236 | 0.6569 | 0.1744 |
| other not infected-specialist not infected | -0.7832 | 0.5857 | 0.3345 |
| generalist infected-intermediate infected | 0.7177 | 0.5921 | 0.3383 |
| generalist infected-other infected | 0.5364 | 0.5454 | 0.4593 |
| generalist infected-specialist infected | 0.244 | 0.474 | 0.6619 |
| intermediate infected-other infected | -0.1813 | 0.6974 | 0.7949 |
| intermediate infected-specialist infected | -0.4737 | 0.6363 | 0.5697 |
| other infected-specialist infected | -0.2924 | 0.5424 | 0.6619 |
| generalist not infected-generalist infected | -1.4822 | 0.2261 | 0 |
| intermediate not infected-intermediate infected | -1.5308 | 0.3463 | 1e-04 |
| other not infected-other infected | -1.3717 | 0.326 | 1e-04 |
| specialist not infected-specialist infected | -0.881 | 0.2259 | 3e-04 |

OBSERVATIONS

In M2 macrophages, none of the category is blocking the acidification of the phagolysosomes at 6 h p.i. and between 25% (other) and 50% (specialist and generalist) of macrophages showed acidification. A bystander effect in non-infected M2a macrophages was observed for specialist strains at 6 h p.i, with approx. 40% of bystander cells showing acidification.

- Acidification of phagolysosomes observed
- Acidification of phagolysosomes not observed (blocked)
- Acidification trend observed, stastically not significant

**Grouping: Geo-host adaptation**

**M2 – 6 h p.i.**

c) Effective MOI

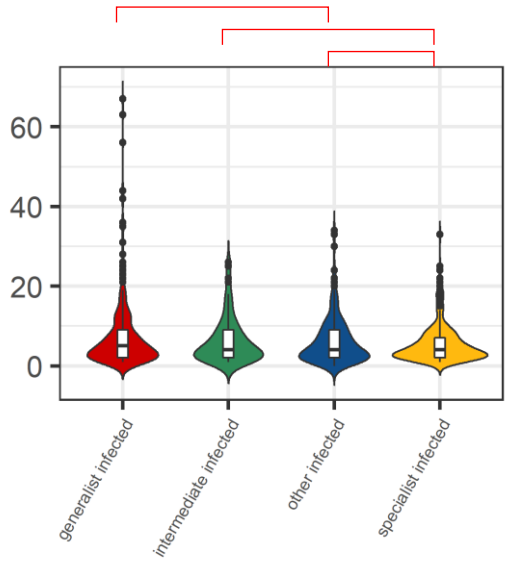


| Par | Value | Std.Error | p.value |
|---|---|---|---|
| (Intercept) | 1.6426 | 0.1203 | 0 |
| groupintermediate infected | 0.1433 | 0.1195 | 0.2348 |
| groupother infected | 0.4187 | 0.105 | 2e-04 |
| groupspecialist infected | -0.1752 | 0.0937 | 0.0664 |

| Contrast | estimate | SE | p.value |
|---|---|---|---|
| generalist infected - intermediate infected | -0.1433 | 0.1195 | 0.2348 |
| generalist infected - other infected | -0.4187 | 0.105 | 5e-04 |
| generalist infected - specialist infected | 0.1752 | 0.0937 | 0.0796 |
| intermediate infected - other infected | -0.2753 | 0.1417 | 0.0796 |
| intermediate infected - specialist infected | 0.3185 | 0.1325 | 0.0385 |
| other infected - specialist infected | 0.5938 | 0.1065 | 0 |

d) Colocalization Index

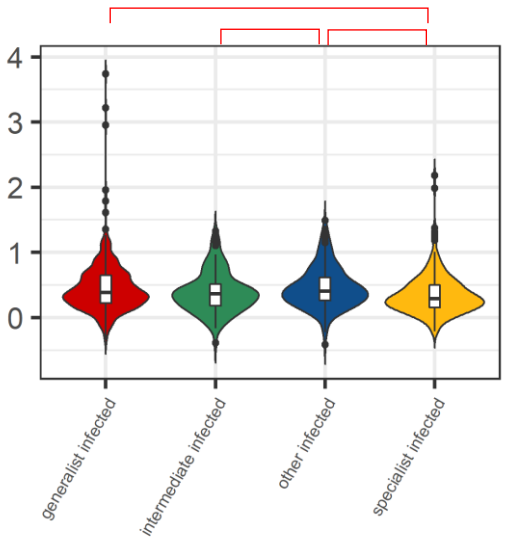


| Par | Value | Std.Error | p.value |
|---|---|---|---|
| (Intercept) | -0.0507 | 0.0532 | 0.3402 |
| groupintermediate infected | -0.1478 | 0.0841 | 0.0839 |
| groupother infected | 0.1194 | 0.0758 | 0.1201 |
| groupspecialist infected | -0.2237 | 0.0687 | 0.0018 |

| Contrast | estimate | SE | p.value |
|---|---|---|---|
| generalist infected - intermediate infected | 0.1478 | 0.0841 | 0.1259 |
| generalist infected - other infected | -0.1194 | 0.0758 | 0.1441 |
| generalist infected - specialist infected | 0.2237 | 0.0687 | 0.0055 |
| intermediate infected - other infected | -0.2672 | 0.0968 | 0.0153 |
| intermediate infected - specialist infected | 0.0759 | 0.0912 | 0.4084 |
| other infected - specialist infected | 0.3432 | 0.0769 | 2e-04 |

OBSERVATIONS

Specialist strains showed lower MOI values compared to the other groups. Colocalization with acidified compartments was found lower for specialist and intermediate strains.

**Grouping: Geo-host adaptation**

**M2 – 24 h p.i.**

a) Phagolysosomal acidification

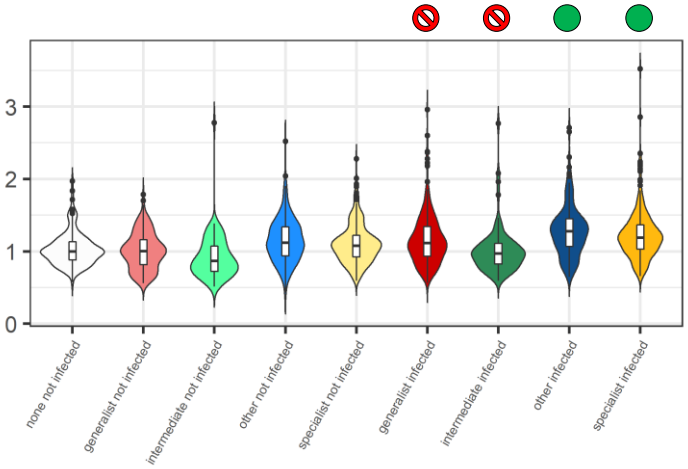


b) Percentage of cells showing acidified phagolysosomes

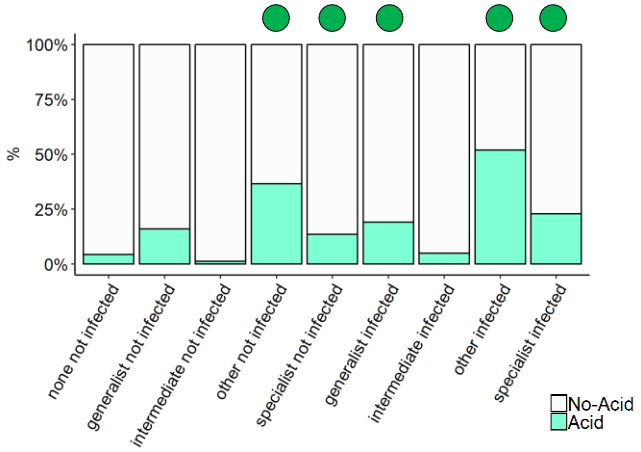


| Par | Value | Std.Error | p.value |
|---|---|---|---|
| (Intercept) | 0.0089 | 0.0545 | 0.87 |
| groupgeneralist not infected | -0.0689 | 0.0316 | 0.0292 |
| groupintermediate not infected | -0.0716 | 0.0421 | 0.0894 |
| groupother not infected | 0.0026 | 0.0364 | 0.9437 |
| groupspecialist not infected | 0.0109 | 0.0315 | 0.7289 |
| groupgeneralist infected | 0.0347 | 0.031 | 0.2632 |
| groupintermediate infected | -0.0083 | 0.0426 | 0.8447 |
| groupother infected | 0.1243 | 0.0356 | 5e-04 |
| groupspecialist infected | 0.1061 | 0.0316 | 8e-04 |

| Contrast | estimate | SE | p.value |
|---|---|---|---|
| none not infected-generalist not infected | 0.0689 | 0.0316 | 0.0585 |
| none not infected-intermediate not infected | 0.0716 | 0.0421 | 0.1431 |
| none not infected-other not infected | -0.0026 | 0.0364 | 0.9471 |
| none not infected-specialist not infected | -0.0109 | 0.0315 | 0.8747 |
| none not infected-generalist infected | -0.0347 | 0.031 | 0.3716 |
| none not infected-intermediate infected | 0.0083 | 0.0426 | 0.9215 |
| none not infected-other infected | -0.1243 | 0.0356 | 0.003 |
| none not infected-specialist infected | -0.1061 | 0.0316 | 0.0038 |
| generalist not infected-intermediate not infected | 0.0027 | 0.0403 | 0.9471 |
| generalist not infected-other not infected | -0.0715 | 0.0362 | 0.0882 |
| generalist not infected-specialist not infected | -0.0799 | 0.0314 | 0.0294 |
| intermediate not infected-other not infected | -0.0742 | 0.0465 | 0.1664 |
| intermediate not infected-specialist not infected | -0.0825 | 0.0423 | 0.0882 |
| other not infected-specialist not infected | -0.0084 | 0.0356 | 0.9215 |
| generalist infected-intermediate infected | 0.0431 | 0.0404 | 0.3812 |
| generalist infected-other infected | -0.0895 | 0.0351 | 0.0294 |
| generalist infected-specialist infected | -0.0714 | 0.0309 | 0.0507 |
| intermediate infected-other infected | -0.1326 | 0.0463 | 0.017 |
| intermediate infected-specialist infected | -0.1145 | 0.0429 | 0.0264 |
| other infected-specialist infected | 0.0182 | 0.035 | 0.7625 |
| generalist not infected-generalist infected | -0.1037 | 0.0171 | 0 |
| intermediate not infected-intermediate infected | -0.0633 | 0.0281 | 0.0529 |
| other not infected-other infected | -0.1217 | 0.0195 | 0 |
| specialist not infected-specialist infected | -0.0952 | 0.0158 | 0 |

| Par | Estimate | se | OR | pvalue |
|---|---|---|---|---|
| (Intercept) | -3.574 | 0.6275 | 0.028 | 0 |
| groupgeneralist not infected | 1.1131 | 0.5049 | 3.0436 | 0.0275 |
| groupintermediate not infected | -0.0353 | 1.1207 | 0.9653 | 0.9749 |
| groupother not infected | 1.5681 | 0.4806 | 4.7973 | 0.0011 |
| groupspecialist not infected | 1.1996 | 0.4875 | 3.3188 | 0.0139 |
| groupgeneralist infected | 1.6838 | 0.4892 | 5.3859 | 6e-04 |
| groupintermediate infected | 1.4906 | 0.7107 | 4.4397 | 0.036 |
| groupother infected | 2.5577 | 0.4779 | 12.906 | 0 |
| groupspecialist infected | 1.9581 | 0.4754 | 7.0859 | 0 |

| Contrast | estimate | SE | p.value |
|---|---|---|---|
| none not infected-generalist not infected | -1.1131 | 0.5049 | 0.066 |
| none not infected-intermediate not infected | 0.0353 | 1.1207 | 0.9749 |
| none not infected-other not infected | -1.5681 | 0.4806 | 0.0053 |
| none not infected-specialist not infected | -1.1996 | 0.4875 | 0.0416 |
| none not infected-generalist infected | -1.6838 | 0.4892 | 0.0035 |
| none not infected-intermediate infected | -1.4906 | 0.7107 | 0.0784 |
| none not infected-other infected | -2.5577 | 0.4779 | 0 |
| none not infected-specialist infected | -1.9581 | 0.4754 | 5e-04 |
| generalist not infected-intermediate not infected | 1.1483 | 1.0546 | 0.3489 |
| generalist not infected-other not infected | -0.455 | 0.3167 | 0.2412 |
| generalist not infected-specialist not infected | -0.0865 | 0.3425 | 0.8353 |
| intermediate not infected-other not infected | -1.6033 | 1.0551 | 0.2205 |
| intermediate not infected-specialist not infected | -1.2349 | 1.0548 | 0.3223 |
| other not infected-specialist not infected | 0.3685 | 0.2927 | 0.2939 |
| generalist infected-intermediate infected | 0.1932 | 0.5786 | 0.8056 |
| generalist infected-other infected | -0.8739 | 0.2967 | 0.011 |
| generalist infected-specialist infected | -0.2743 | 0.2897 | 0.4125 |
| intermediate infected-other infected | -1.0671 | 0.5957 | 0.1352 |
| intermediate infected-specialist infected | -0.4675 | 0.5895 | 0.4889 |
| other infected-specialist infected | 0.5996 | 0.2669 | 0.0659 |
| generalist not infected-generalist infected | -0.5707 | 0.2952 | 0.1064 |
| intermediate not infected-intermediate infected | -1.5259 | 1.1313 | 0.2661 |
| other not infected-other infected | -0.9896 | 0.2527 | 7e-04 |
| specialist not infected-specialist infected | -0.7585 | 0.2485 | 0.0091 |

OBSERVATIONS

As the infection progresses, generalist and intermediate categories are blocking the acidification of the phagolysosomes. The number of acidified macrophages also decreased below 25% except for the category other (50%). A bystander effect in non-infected M2a macrophages was observed for specialist strains at 24 h p.i, despite it was not found statistically significant.

- Acidification of phagolysosomes observed
- Acidification of phagolysosomes not observed (blocked)
- Acidification trend observed, stastically not significant

**Grouping: Geo-host adaptation**

**M2 – 24 h p.i.**

c) Effective MOI

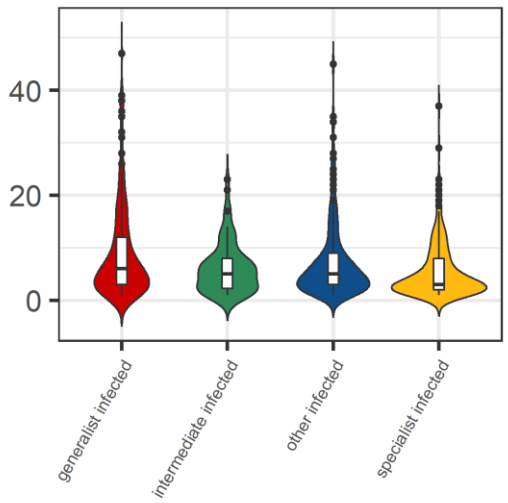


| Par | Value | Std.Error | p.value |
|---|---|---|---|
| (Intercept) | 1.6645 | 0.1221 | 0 |
| groupintermediate infected | -0.2831 | 0.156 | 0.0745 |
| groupother infected | 0.0267 | 0.1361 | 0.8448 |
| groupspecialist infected | -0.2481 | 0.1199 | 0.0427 |

| Contrast | estimate | SE | p.value |
|---|---|---|---|
| generalist infected - intermediate infected | 0.2831 | 0.156 | 0.1367 |
| generalist infected - other infected | -0.0267 | 0.1361 | 0.8448 |
| generalist infected - specialist infected | 0.2481 | 0.1199 | 0.1362 |
| intermediate infected - other infected | -0.3098 | 0.1805 | 0.1367 |
| intermediate infected - specialist infected | -0.035 | 0.1669 | 0.8448 |
| other infected - specialist infected | 0.2748 | 0.1345 | 0.1362 |

d) Colocalization Index

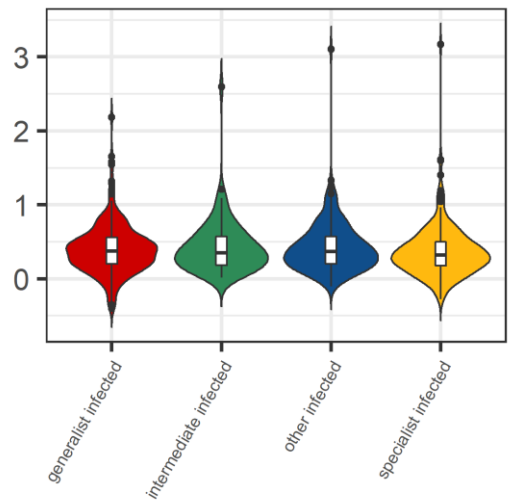


| Par | Value | Std.Error | p.value |
|---|---|---|---|
| (Intercept) | -0.0522 | 0.0609 | 0.3923 |
| groupintermediate infected | 0.0401 | 0.1112 | 0.7194 |
| groupother infected | 0.0632 | 0.0879 | 0.4751 |
| groupspecialist infected | -0.1392 | 0.0807 | 0.0897 |

| Contrast | estimate | SE | p.value |
|---|---|---|---|
| generalist infected - intermediate infected | -0.0401 | 0.1112 | 0.8459 |
| generalist infected - other infected | -0.0632 | 0.0879 | 0.7127 |
| generalist infected - specialist infected | 0.1392 | 0.0807 | 0.2326 |
| intermediate infected - other infected | -0.023 | 0.118 | 0.8459 |
| intermediate infected - specialist infected | 0.1793 | 0.1125 | 0.2326 |
| other infected - specialist infected | 0.2023 | 0.0858 | 0.1299 |

OBSERVATIONS

No statistically relevant differences in effective MOI at 24 h p.i., even though generalist strains displayed an higher distribution of MOI values. Colocalization with acidified compartments was similar among all the groups.

**Grouping: Basic**

**M1 – 6 h p.i.**

a) Phagolysosomal acidification

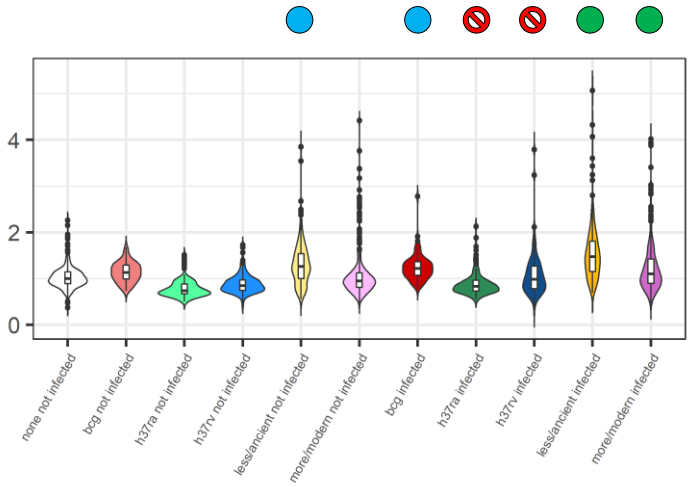


b) Percentage of cells showing acidified phagolysosomes

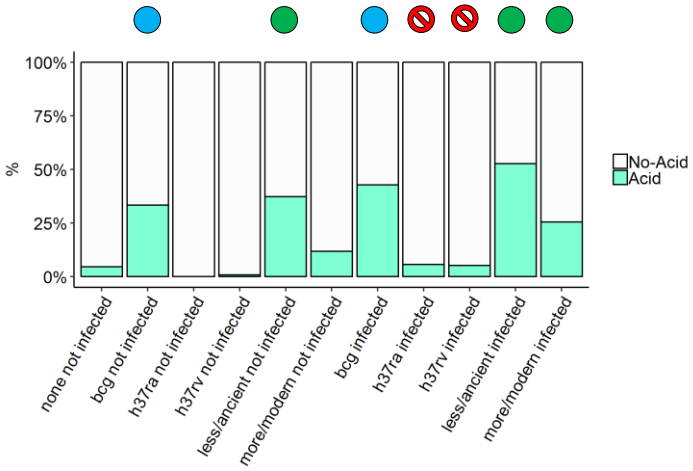


| Par | Value | Std.Error | p.value |
|---|---|---|---|
| (Intercept) | 0.0057 | 0.0692 | 0.9345 |
| groupbcg not infected | 0.0151 | 0.1015 | 0.882 |
| grouph37ra not infected | -0.1856 | 0.0793 | 0.0193 |
| grouph37rv not infected | -0.0647 | 0.0798 | 0.4178 |
| groupless/ancient not infected | 0.1341 | 0.058 | 0.0208 |
| groupmore/modern not infected | 0.0508 | 0.057 | 0.3733 |
| groupbcg infected | 0.0803 | 0.1013 | 0.4281 |
| grouph37ra infected | -0.1042 | 0.0796 | 0.1907 |
| grouph37rv infected | 0.0489 | 0.0803 | 0.5429 |
| groupless/ancient infected | 0.2842 | 0.0581 | 0 |
| groupmore/modern infected | 0.1729 | 0.057 | 0.0025 |

| Par | Estimate | se | OR | pvalue |
|---|---|---|---|---|
| (Intercept) | -3.5104 | 0.7705 | 0.0299 | 0 |
| groupbcg not infected | 0.8759 | 0.942 | 2.401 | 0.3525 |
| grouph37ra not infected | -14.8252 | 582.0863 | 0 | 0.9797 |
| grouph37rv not infected | -1.2669 | 1.3848 | 0.2817 | 0.3603 |
| groupless/ancient not infected | 1.7648 | 0.6365 | 5.8405 | 0.0056 |
| groupmore/modern not infected | 0.8433 | 0.6914 | 2.324 | 0.2226 |
| groupbcg infected | 1.2845 | 0.9366 | 3.6128 | 0.1702 |
| grouph37ra infected | 0.8777 | 0.9127 | 2.4054 | 0.3362 |
| grouph37rv infected | 0.7321 | 1.0357 | 2.0794 | 0.4797 |
| groupless/ancient infected | 2.9099 | 0.6374 | 18.3541 | 0 |
| groupmore/modern infected | 2.4233 | 0.6719 | 11.2825 | 3e-04 |

| Contrast | estimate | SE | p.value |
|---|---|---|---|
| none not infected-bcg not infected | -0.0151 | 0.1015 | 0.882 |
| none not infected-h37ra not infected | 0.1856 | 0.0793 | 0.052 |
| none not infected-h37rv not infected | 0.0647 | 0.0798 | 0.4995 |
| none not infected-less/ancient not infected | -0.1341 | 0.058 | 0.052 |
| none not infected-more/modern not infected | -0.0508 | 0.057 | 0.4791 |
| none not infected-bcg infected | -0.0803 | 0.1013 | 0.4995 |
| none not infected-h37ra infected | 0.1042 | 0.0796 | 0.267 |
| none not infected-h37rv infected | -0.0489 | 0.0803 | 0.5939 |
| none not infected-less/ancient infected | -0.2842 | 0.0581 | 0 |
| none not infected-more/modern infected | -0.1729 | 0.057 | 0.0095 |
| bcg not infected-h37ra not infected | 0.2006 | 0.1223 | 0.186 |
| bcg not infected-h37rv not infected | 0.0798 | 0.1234 | 0.5848 |
| bcg not infected-less/ancient not infected | -0.1191 | 0.0966 | 0.2933 |
| bcg not infected-more/modern not infected | -0.0357 | 0.1063 | 0.7816 |
| h37ra not infected-h37rv not infected | -0.1209 | 0.0895 | 0.258 |
| h37ra not infected-less/ancient not infected | -0.3197 | 0.087 | 0.0014 |
| h37ra not infected-more/modern not infected | -0.2363 | 0.0834 | 0.0163 |
| h37rv not infected-less/ancient not infected | -0.1988 | 0.0892 | 0.0605 |
| h37rv not infected-more/modern not infected | -0.1155 | 0.0836 | 0.2549 |
| less/ancient not infected-more/modern not infected | 0.0833 | 0.0589 | 0.2504 |
| bcg infected-h37ra infected | 0.1845 | 0.1224 | 0.2306 |
| bcg infected-h37rv infected | 0.0314 | 0.1236 | 0.8228 |
| bcg infected-less/ancient infected | -0.2039 | 0.0966 | 0.0762 |
| bcg infected-more/modern infected | -0.0926 | 0.1062 | 0.4791 |
| h37ra infected-h37rv infected | -0.1531 | 0.0903 | 0.1753 |
| h37ra infected-less/ancient infected | -0.3885 | 0.0874 | 1e-04 |
| h37ra infected-more/modern infected | -0.2771 | 0.0837 | 0.0041 |
| h37rv infected-less/ancient infected | -0.2354 | 0.0897 | 0.0279 |
| h37rv infected-more/modern infected | -0.124 | 0.084 | 0.2335 |
| less/ancient infected-more/modern infected | 0.1113 | 0.0591 | 0.1227 |
| bcg not infected-bcg infected | -0.0653 | 0.0265 | 0.0407 |
| h37ra not infected-h37ra infected | -0.0814 | 0.0237 | 0.003 |
| h37rv not infected-h37rv infected | -0.1136 | 0.0231 | 0 |
| less/ancient not infected-less/ancient infected | -0.1501 | 0.0143 | 0 |
| more/modern not infected-more/modern infected | -0.1222 | 0.0138 | 0 |

| Contrast | estimate | SE | p.value |
|---|---|---|---|
| none not infected-bcg not infected | -0.8759 | 0.942 | 0.5483 |
| none not infected-h37ra not infected | 14.8252 | 582.0863 | 0.9814 |
| none not infected-h37rv not infected | 1.2669 | 1.3848 | 0.5483 |
| none not infected-less/ancient not infected | -1.7648 | 0.6365 | 0.0389 |
| none not infected-more/modern not infected | -0.8433 | 0.6914 | 0.4411 |
| none not infected-bcg infected | -1.2845 | 0.9366 | 0.3911 |
| none not infected-h37ra infected | -0.8777 | 0.9127 | 0.5483 |
| none not infected-h37rv infected | -0.7321 | 1.0357 | 0.6715 |
| none not infected-less/ancient infected | -2.9099 | 0.6374 | 1e-04 |
| none not infected-more/modern infected | -2.4233 | 0.6719 | 0.0027 |
| bcg not infected-h37ra not infected | 15.701 | 582.0868 | 0.9814 |
| bcg not infected-h37rv not infected | 2.1427 | 1.5937 | 0.3911 |
| bcg not infected-less/ancient not infected | -0.889 | 0.8381 | 0.5055 |
| bcg not infected-more/modern not infected | 0.0326 | 0.9672 | 0.9814 |
| h37ra not infected-h37rv not infected | -13.5583 | 582.0872 | 0.9814 |
| h37ra not infected-less/ancient not infected | -16.59 | 582.0863 | 0.9814 |
| h37ra not infected-more/modern not infected | -15.6685 | 582.0863 | 0.9814 |
| h37rv not infected-less/ancient not infected | -3.0317 | 1.4184 | 0.1628 |
| h37rv not infected-more/modern not infected | -2.1101 | 1.422 | 0.3445 |
| less/ancient not infected-more/modern not infected | 0.9215 | 0.5751 | 0.3053 |
| bcg infected-h37ra infected | 0.4068 | 1.183 | 0.9475 |
| bcg infected-h37rv infected | 0.5524 | 1.2976 | 0.9023 |
| bcg infected-less/ancient infected | -1.6254 | 0.839 | 0.205 |
| bcg infected-more/modern infected | -1.1388 | 0.949 | 0.4411 |
| h37ra infected-h37rv infected | 0.1456 | 1.0474 | 0.9814 |
| h37ra infected-less/ancient infected | -2.0321 | 0.9258 | 0.1628 |
| h37ra infected-more/modern infected | -1.5455 | 0.9097 | 0.2843 |
| h37rv infected-less/ancient infected | -2.1778 | 1.0791 | 0.1906 |
| h37rv infected-more/modern infected | -1.6912 | 1.0683 | 0.3053 |
| less/ancient infected-more/modern infected | 0.4866 | 0.5523 | 0.5516 |
| bcg not infected-bcg infected | -0.4086 | 0.3474 | 0.4411 |
| h37ra not infected-h37ra infected | -15.7029 | 582.0859 | 0.9814 |
| h37rv not infected-h37rv infected | -1.9989 | 1.1041 | 0.2458 |
| less/ancient not infected-less/ancient infected | -1.145 | 0.2251 | 0 |
| more/modern not infected-more/modern infected | -1.58 | 0.3054 | 0 |

OBSERVATIONS

BCG, H37Rv, and H37Ra were found to block acidification of the phagolysosomes in M1 macrophages at 6 h p.i. Less/ancient strains also induced acidification in a higher percentage (50%) of cells compared to the other groups.

- Acidification of phagolysosomes observed
- Acidification of phagolysosomes not observed (blocked)
- Acidification trend observed, stastically not significant

**Grouping: Basic**

**M1 – 6 h p.i.**

c) Effective MOI

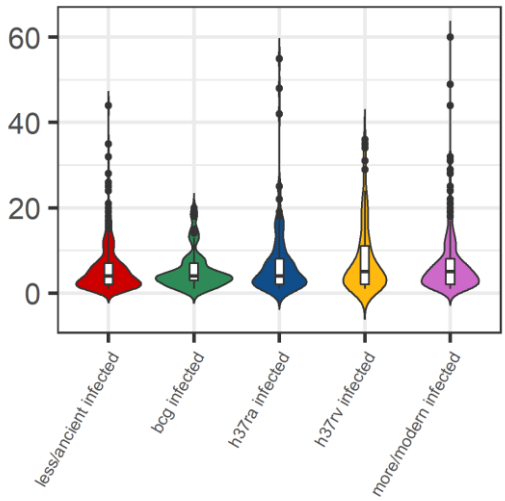


| Par | Value | Std.Error | p.value |
|---|---|---|---|
| (Intercept) | 1.3998 | 0.1168 | 0 |
| groupbcg infected | -0.0196 | 0.2119 | 0.9268 |
| grouph37ra infected | 0.1092 | 0.1902 | 0.5682 |
| grouph37rv infected | 0.1091 | 0.1949 | 0.5779 |
| groupmore/modern infected | 0.0388 | 0.1302 | 0.767 |

| Contrast | estimate | SE | p.value |
|---|---|---|---|
| less/ancient infected - bcg infected | 0.0196 | 0.2119 | 0.9996 |
| less/ancient infected - h37ra infected | -0.1092 | 0.1902 | 0.9996 |
| less/ancient infected - h37rv infected | -0.1091 | 0.1949 | 0.9996 |
| less/ancient infected - more/modern infected | -0.0388 | 0.1302 | 0.9996 |
| bcg infected - h37ra infected | -0.1287 | 0.2669 | 0.9996 |
| bcg infected - h37rv infected | -0.1286 | 0.2689 | 0.9996 |
| bcg infected - more/modern infected | -0.0583 | 0.2326 | 0.9996 |
| h37ra infected - h37rv infected | 1e-04 | 0.2007 | 0.9996 |
| h37ra infected - more/modern infected | 0.0704 | 0.1824 | 0.9996 |
| h37rv infected - more/modern infected | 0.0703 | 0.1825 | 0.9996 |

d) Colocalization Index

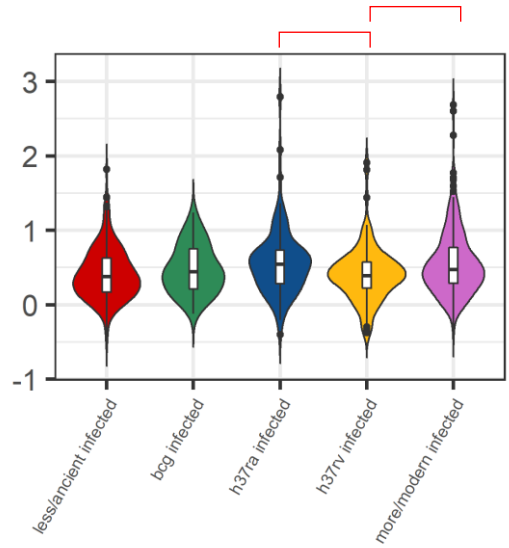


| Par | Value | Std.Error | p.value |
|---|---|---|---|
| (Intercept) | -0.0522 | 0.0991 | 0.5983 |
| groupbcg infected | 0.1116 | 0.1679 | 0.5087 |
| grouph37ra infected | 0.2712 | 0.1543 | 0.0839 |
| grouph37rv infected | -0.1589 | 0.1582 | 0.3193 |
| groupmore/modern infected | 0.2451 | 0.1047 | 0.0226 |

| Contrast | estimate | SE | p.value |
|---|---|---|---|
| less/ancient infected - bcg infected | -0.1116 | 0.1679 | 0.5653 |
| less/ancient infected - h37ra infected | -0.2712 | 0.1543 | 0.2097 |
| less/ancient infected - h37rv infected | 0.1589 | 0.1582 | 0.5321 |
| less/ancient infected - more/modern infected | -0.2451 | 0.1047 | 0.0753 |
| bcg infected - h37ra infected | -0.1596 | 0.2157 | 0.5653 |
| bcg infected - h37rv infected | 0.2705 | 0.2173 | 0.4363 |
| bcg infected - more/modern infected | -0.1335 | 0.1868 | 0.5653 |
| h37ra infected - h37rv infected | 0.4301 | 0.16 | 0.0464 |
| h37ra infected - more/modern infected | 0.0261 | 0.1468 | 0.8594 |
| h37rv infected - more/modern infected | -0.4039 | 0.1456 | 0.0464 |

OBSERVATIONS

H37Rv showed lower colocalization with acidified compartments. No statistically relevant differences in effective MOI were observed among the categories in M1 macrophages, irrespectively from the time point considered.

**Grouping: Basic**

**M1 – 24 h p.i.**

a) Phagolysosomal acidification

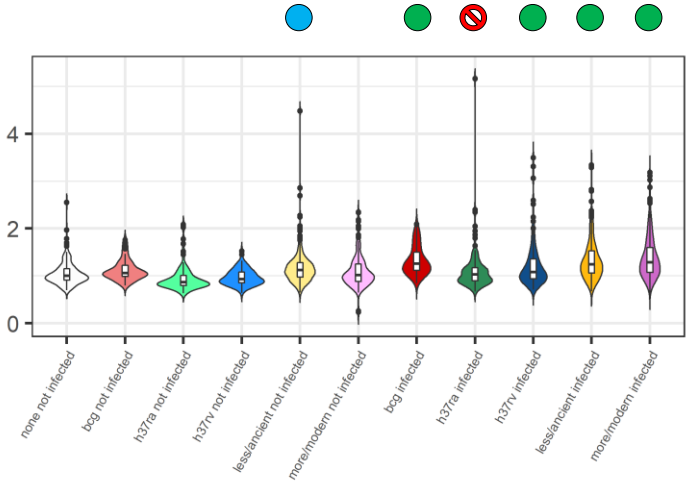


b) Percentage of cells showing acidified phagolysosomes

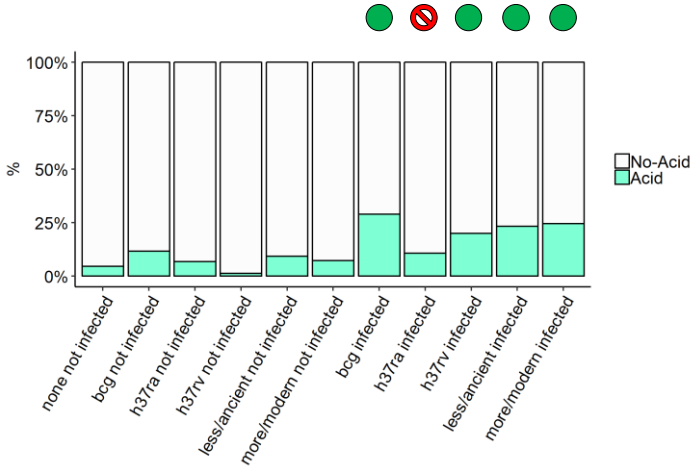


| Par | Value | Std.Error | p.value |
|---|---|---|---|
| (Intercept) | 0.0174 | 0.0363 | 0.6328 |
| groupbcg not infected | 0.0522 | 0.0553 | 0.3454 |
| grouph37ra not infected | -0.0886 | 0.0465 | 0.0567 |
| grouph37rv not infected | -0.0205 | 0.0461 | 0.6568 |
| groupless/ancient not infected | 0.044 | 0.0325 | 0.1757 |
| groupmore/modern not infected | 0.0294 | 0.033 | 0.3727 |
| groupbcg infected | 0.2095 | 0.0529 | 1e-04 |
| grouph37ra infected | 0.0464 | 0.0447 | 0.2994 |
| grouph37rv infected | 0.1162 | 0.0449 | 0.0097 |
| groupless/ancient infected | 0.1544 | 0.0326 | 0 |
| groupmore/modern infected | 0.2248 | 0.0323 | 0 |

| Par | Estimate | se | OR | pvalue |
|---|---|---|---|---|
| (Intercept) | -3.1636 | 0.4495 | 0.0423 | 0 |
| groupbcg not infected | 0.844 | 0.6733 | 2.3256 | 0.21 |
| grouph37ra not infected | 0.9602 | 0.6738 | 2.6121 | 0.1542 |
| grouph37rv not infected | -1.0824 | 1.1144 | 0.3388 | 0.3314 |
| groupless/ancient not infected | 0.5498 | 0.4805 | 1.7329 | 0.2526 |
| groupmore/modern not infected | 0.528 | 0.5087 | 1.6956 | 0.2993 |
| groupbcg infected | 1.9837 | 0.5712 | 7.2697 | 5e-04 |
| grouph37ra infected | 1.4416 | 0.5806 | 4.2274 | 0.013 |
| grouph37rv infected | 1.8728 | 0.5358 | 6.5068 | 5e-04 |
| groupless/ancient infected | 1.6986 | 0.454 | 5.4662 | 2e-04 |
| groupmore/modern infected | 1.9572 | 0.4554 | 7.0796 | 0 |

| Contrast | estimate | SE | p.value |
|---|---|---|---|
| none not infected-bcg not infected | -0.0522 | 0.0553 | 0.4318 |
| none not infected-h37ra not infected | 0.0886 | 0.0465 | 0.1103 |
| none not infected-h37rv not infected | 0.0205 | 0.0461 | 0.7183 |
| none not infected-less/ancient not infected | -0.044 | 0.0325 | 0.2863 |
| none not infected-more/modern not infected | -0.0294 | 0.033 | 0.4499 |
| none not infected-bcg infected | -0.2095 | 0.0529 | 3e-04 |
| none not infected-h37ra infected | -0.0464 | 0.0447 | 0.3881 |
| none not infected-h37rv infected | -0.1162 | 0.0449 | 0.0308 |
| none not infected-less/ancient infected | -0.1544 | 0.0326 | 0 |
| none not infected-more/modern infected | -0.2248 | 0.0323 | 0 |
| bcg not infected-h37ra not infected | 0.1408 | 0.0672 | 0.0747 |
| bcg not infected-h37rv not infected | 0.0727 | 0.0674 | 0.3876 |
| bcg not infected-less/ancient not infected | 0.0082 | 0.0522 | 0.8752 |
| bcg not infected-more/modern not infected | 0.0228 | 0.0575 | 0.7329 |
| h37ra not infected-h37rv not infected | -0.0681 | 0.0508 | 0.2863 |
| h37ra not infected-less/ancient not infected | -0.1326 | 0.0486 | 0.0225 |
| h37ra not infected-more/modern not infected | -0.118 | 0.0471 | 0.0335 |
| h37rv not infected-less/ancient not infected | -0.0645 | 0.0492 | 0.2889 |
| h37rv not infected-more/modern not infected | -0.0499 | 0.0469 | 0.3876 |
| less/ancient not infected-more/modern not infected | 0.0146 | 0.0323 | 0.7183 |
| bcg infected-h37ra infected | 0.1631 | 0.064 | 0.032 |
| bcg infected-h37rv infected | 0.0933 | 0.0646 | 0.2607 |
| bcg infected-less/ancient infected | 0.0551 | 0.0498 | 0.3876 |
| bcg infected-more/modern infected | -0.0152 | 0.0548 | 0.8038 |
| h37ra infected-h37rv infected | -0.0699 | 0.0478 | 0.2607 |
| h37ra infected-less/ancient infected | -0.108 | 0.047 | 0.0506 |
| h37ra infected-more/modern infected | -0.1784 | 0.045 | 3e-04 |
| h37rv infected-less/ancient infected | -0.0382 | 0.0481 | 0.4983 |
| h37rv infected-more/modern infected | -0.1085 | 0.045 | 0.0399 |
| less/ancient infected-more/modern infected | -0.0703 | 0.0318 | 0.059 |
| bcg not infected-bcg infected | -0.1573 | 0.0359 | 1e-04 |
| h37ra not infected-h37ra infected | -0.135 | 0.0309 | 1e-04 |
| h37rv not infected-h37rv infected | -0.1367 | 0.03 | 0 |
| less/ancient not infected-less/ancient infected | -0.1104 | 0.018 | 0 |
| more/modern not infected-more/modern infected | -0.1954 | 0.0197 | 0 |

| Contrast | estimate | SE | p.value |
|---|---|---|---|
| none not infected-bcg not infected | -0.844 | 0.6733 | 0.4901 |
| none not infected-h37ra not infected | -0.9602 | 0.6738 | 0.3855 |
| none not infected-h37rv not infected | 1.0824 | 1.1144 | 0.5927 |
| none not infected-less/ancient not infected | -0.5498 | 0.4805 | 0.5525 |
| none not infected-more/modern not infected | -0.528 | 0.5087 | 0.5819 |
| none not infected-bcg infected | -1.9837 | 0.5712 | 0.003 |
| none not infected-h37ra infected | -1.4416 | 0.5806 | 0.057 |
| none not infected-h37rv infected | -1.8728 | 0.5358 | 0.003 |
| none not infected-less/ancient infected | -1.6986 | 0.454 | 0.0016 |
| none not infected-more/modern infected | -1.9572 | 0.4554 | 2e-04 |
| bcg not infected-h37ra not infected | -0.1162 | 0.7856 | 0.9359 |
| bcg not infected-h37rv not infected | 1.9263 | 1.1877 | 0.3336 |
| bcg not infected-less/ancient not infected | 0.2942 | 0.5809 | 0.7503 |
| bcg not infected-more/modern not infected | 0.316 | 0.6403 | 0.7503 |
| h37ra not infected-h37rv not infected | 2.0425 | 1.1462 | 0.2617 |
| h37ra not infected-less/ancient not infected | 0.4104 | 0.6159 | 0.6846 |
| h37ra not infected-more/modern not infected | 0.4321 | 0.6217 | 0.6846 |
| h37rv not infected-less/ancient not infected | -1.6322 | 1.083 | 0.3679 |
| h37rv not infected-more/modern not infected | -1.6104 | 1.082 | 0.3679 |
| less/ancient not infected-more/modern not infected | 0.0218 | 0.4011 | 0.9567 |
| bcg infected-h37ra infected | 0.5421 | 0.6118 | 0.5927 |
| bcg infected-h37rv infected | 0.1109 | 0.5731 | 0.926 |
| bcg infected-less/ancient infected | 0.2851 | 0.4313 | 0.6846 |
| bcg infected-more/modern infected | 0.0265 | 0.4825 | 0.9567 |
| h37ra infected-h37rv infected | -0.4313 | 0.4824 | 0.5927 |
| h37ra infected-less/ancient infected | -0.257 | 0.4874 | 0.7503 |
| h37ra infected-more/modern infected | -0.5156 | 0.466 | 0.5528 |
| h37rv infected-less/ancient infected | 0.1743 | 0.4381 | 0.8059 |
| h37rv infected-more/modern infected | -0.0844 | 0.3987 | 0.926 |
| less/ancient infected-more/modern infected | -0.2586 | 0.2933 | 0.5927 |
| bcg not infected-bcg infected | -1.1397 | 0.5064 | 0.0949 |
| h37ra not infected-h37ra infected | -0.4814 | 0.5595 | 0.5927 |
| h37rv not infected-h37rv infected | -2.9552 | 1.0384 | 0.0221 |
| less/ancient not infected-less/ancient infected | -1.1488 | 0.2682 | 2e-04 |
| more/modern not infected-more/modern infected | -1.4292 | 0.3142 | 2e-04 |

OBSERVATIONS

At 24 h p.i., only H37Ra was retaining the blocking of the acidification of the phagolysosomes. However, despite an increase in the acidification of the phagolysosomes was observed, the number of macrophages displaying such acidification was found generally low (25%).

- Acidification of phagolysosomes observed
- Acidification of phagolysosomes not observed (blocked)
- Acidification trend observed, stastically not significant

**Grouping: Basic**

**M1 – 24 h p.i.**

c) Effective MOI

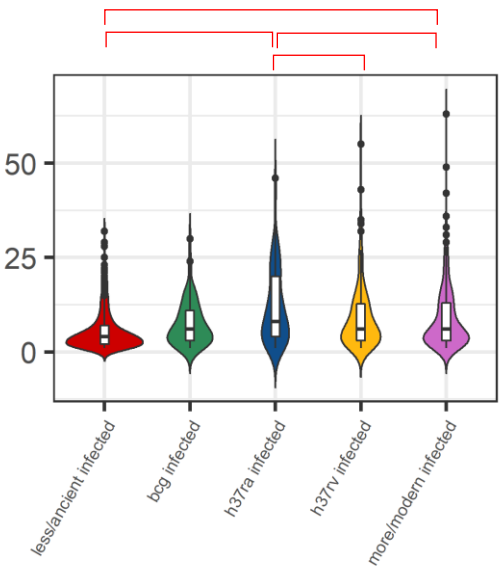


| Par | Value | Std.Error | p.value |
|---|---|---|---|
| (Intercept) | 1.4775 | 0.134 | 0 |
| groupbcg infected | 0.4793 | 0.1543 | 0.0029 |
| grouph37ra infected | 0.6163 | 0.1567 | 2e-04 |
| grouph37rv infected | 0.0909 | 0.1604 | 0.5728 |
| groupmore/modern infected | 0.2335 | 0.0988 | 0.0214 |

| Contrast | estimate | SE | p.value |
|---|---|---|---|
| less/ancient infected - bcg infected | -0.4793 | 0.1543 | 0.0096 |
| less/ancient infected - h37ra infected | -0.6163 | 0.1567 | 0.0014 |
| less/ancient infected - h37rv infected | -0.0909 | 0.1604 | 0.5728 |
| less/ancient infected - more/modern infected | -0.2335 | 0.0988 | 0.0428 |
| bcg infected - h37ra infected | -0.137 | 0.2153 | 0.5728 |
| bcg infected - h37rv infected | 0.3884 | 0.2177 | 0.1325 |
| bcg infected - more/modern infected | 0.2458 | 0.1797 | 0.2521 |
| h37ra infected - h37rv infected | 0.5254 | 0.1358 | 0.0014 |
| h37ra infected - more/modern infected | 0.3828 | 0.143 | 0.0239 |
| h37rv infected - more/modern infected | -0.1426 | 0.142 | 0.3992 |

d) Colocalization Index

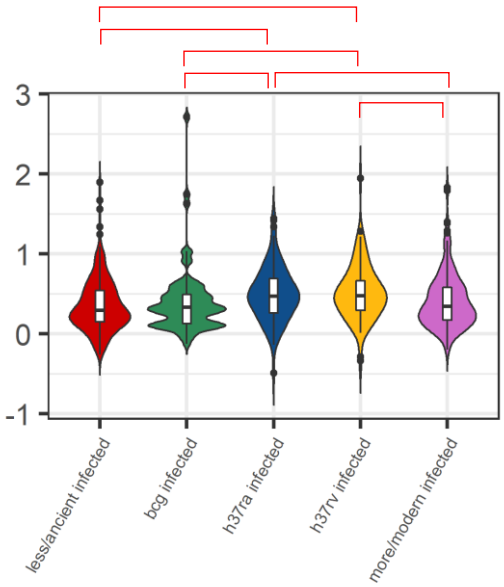


| Par | Value | Std.Error | p.value |
|---|---|---|---|
| (Intercept) | -0.2816 | 0.1095 | 0.0104 |
| groupbcg infected | 0.0636 | 0.16 | 0.6924 |
| grouph37ra infected | 0.7087 | 0.1571 | 0 |
| grouph37rv infected | 0.7889 | 0.1571 | 0 |
| groupmore/modern infected | 0.135 | 0.1031 | 0.1956 |

| Contrast | estimate | SE | p.value |
|---|---|---|---|
| less/ancient infected - bcg infected | -0.0636 | 0.16 | 0.6976 |
| less/ancient infected - h37ra infected | -0.7087 | 0.1571 | 1e-04 |
| less/ancient infected - h37rv infected | -0.7889 | 0.1571 | 1e-04 |
| less/ancient infected - more/modern infected | -0.135 | 0.1031 | 0.2794 |
| bcg infected - h37ra infected | -0.6451 | 0.215 | 0.0066 |
| bcg infected - h37rv infected | -0.7253 | 0.2145 | 0.0026 |
| bcg infected - more/modern infected | -0.0714 | 0.1829 | 0.6976 |
| h37ra infected - h37rv infected | -0.0802 | 0.1438 | 0.6976 |
| h37ra infected - more/modern infected | 0.5737 | 0.1479 | 7e-04 |
| h37rv infected - more/modern infected | 0.6538 | 0.1423 | 1e-04 |

OBSERVATIONS

H37Rv and H37Ra showed higher colocalization with acidified compartments. No statistically relevant differences in effective MOI were observed among the categories in M1 macrophages, irrespectively from the time point considered.

**Grouping: Basic**

**M2 – 6 h p.i.**

a) Phagolysosomal acidification

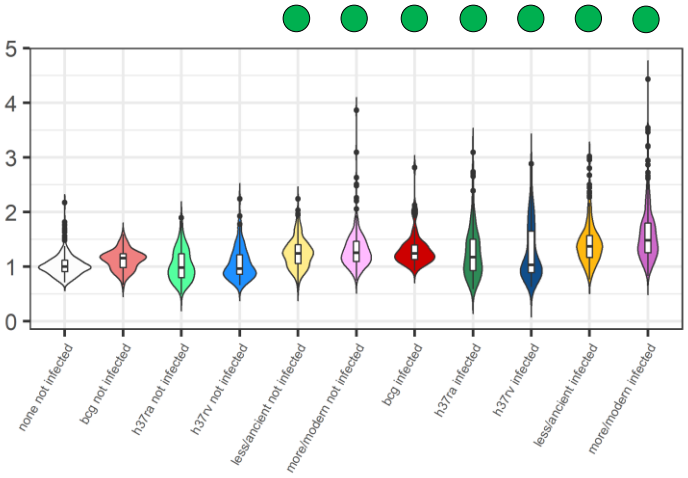


b) Percentage of cells showing acidified phagolysosomes

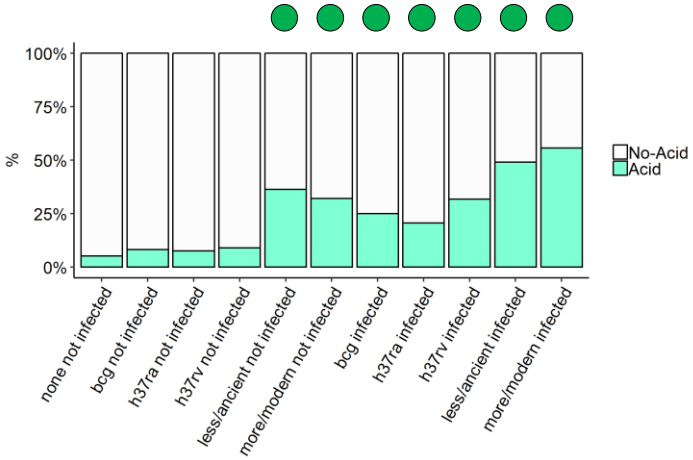


| Par | Value | Std.Error | p.value |
|---|---|---|---|
| (Intercept) | -0.0077 | 0.042 | 0.8545 |
| groupbcg not infected | 0.123 | 0.0795 | 0.1222 |
| grouph37ra not infected | 0.0073 | 0.0617 | 0.9055 |
| grouph37rv not infected | 0.0416 | 0.0623 | 0.5042 |
| groupless/ancient not infected | 0.1856 | 0.0462 | 1e-04 |
| groupmore/modern not infected | 0.2127 | 0.0456 | 0 |
| groupbcg infected | 0.2296 | 0.0794 | 0.0039 |
| grouph37ra infected | 0.1687 | 0.0621 | 0.0067 |
| grouph37rv infected | 0.1675 | 0.0624 | 0.0074 |
| groupless/ancient infected | 0.2946 | 0.0464 | 0 |
| groupmore/modern infected | 0.3585 | 0.0455 | 0 |

| Par | Estimate | se | OR | pvalue |
|---|---|---|---|---|
| (Intercept) | -3.172 | 0.602 | 0.0419 | 0 |
| groupbcg not infected | 0.755 | 0.9531 | 2.1276 | 0.4283 |
| grouph37ra not infected | 1.2814 | 0.7846 | 3.6017 | 0.1024 |
| grouph37rv not infected | -0.0263 | 0.821 | 0.974 | 0.9744 |
| groupless/ancient not infected | 2.078 | 0.5798 | 7.9888 | 3e-04 |
| groupmore/modern not infected | 1.8699 | 0.5617 | 6.4876 | 9e-04 |
| groupbcg infected | 2.1862 | 0.8833 | 8.9015 | 0.0133 |
| grouph37ra infected | 2.6218 | 0.7381 | 13.7602 | 4e-04 |
| grouph37rv infected | 2.3266 | 0.7461 | 10.2435 | 0.0018 |
| groupless/ancient infected | 2.9587 | 0.5796 | 19.2736 | 0 |
| groupmore/modern infected | 3.2052 | 0.5582 | 24.6607 | 0 |

| Contrast | estimate | SE | p.value |
|---|---|---|---|
| none not infected-bcg not infected | -0.123 | 0.0795 | 0.1944 |
| none not infected-h37ra not infected | -0.0073 | 0.0617 | 0.9321 |
| none not infected-h37rv not infected | -0.0416 | 0.0623 | 0.5847 |
| none not infected-less/ancient not infected | -0.1856 | 0.0462 | 3e-04 |
| none not infected-more/modern not infected | -0.2127 | 0.0456 | 0 |
| none not infected-bcg infected | -0.2296 | 0.0794 | 0.0104 |
| none not infected-h37ra infected | -0.1687 | 0.0621 | 0.0167 |
| none not infected-h37rv infected | -0.1675 | 0.0624 | 0.0167 |
| none not infected-less/ancient infected | -0.2946 | 0.0464 | 0 |
| none not infected-more/modern infected | -0.3585 | 0.0455 | 0 |
| bcg not infected-h37ra not infected | 0.1157 | 0.0941 | 0.3196 |
| bcg not infected-h37rv not infected | 0.0814 | 0.0949 | 0.5102 |
| bcg not infected-less/ancient not infected | -0.0626 | 0.0763 | 0.5148 |
| bcg not infected-more/modern not infected | -0.0897 | 0.0827 | 0.3894 |
| h37ra not infected-h37rv not infected | -0.0343 | 0.0718 | 0.6713 |
| h37ra not infected-less/ancient not infected | -0.1783 | 0.0667 | 0.0167 |
| h37ra not infected-more/modern not infected | -0.2053 | 0.0646 | 0.0053 |
| h37rv not infected-less/ancient not infected | -0.144 | 0.0685 | 0.0692 |
| h37rv not infected-more/modern not infected | -0.1711 | 0.0651 | 0.0178 |
| less/ancient not infected-more/modern not infected | -0.0271 | 0.0467 | 0.6145 |
| bcg infected-h37ra infected | 0.0609 | 0.0942 | 0.5847 |
| bcg infected-h37rv infected | 0.0621 | 0.0948 | 0.5847 |
| bcg infected-less/ancient infected | -0.065 | 0.0762 | 0.5102 |
| bcg infected-more/modern infected | -0.1289 | 0.0825 | 0.1944 |
| h37ra infected-h37rv infected | 0.0012 | 0.0723 | 0.9866 |
| h37ra infected-less/ancient infected | -0.1259 | 0.0672 | 0.1125 |
| h37ra infected-more/modern infected | -0.1898 | 0.0649 | 0.0102 |
| h37rv infected-less/ancient infected | -0.1271 | 0.0687 | 0.1125 |
| h37rv infected-more/modern infected | -0.191 | 0.0651 | 0.0102 |
| less/ancient infected-more/modern infected | -0.0639 | 0.0467 | 0.2611 |
| bcg not infected-bcg infected | -0.1066 | 0.0266 | 3e-04 |
| h37ra not infected-h37ra infected | -0.1614 | 0.0219 | 0 |
| h37rv not infected-h37rv infected | -0.1258 | 0.0223 | 0 |
| less/ancient not infected-less/ancient infected | -0.109 | 0.014 | 0 |
| more/modern not infected-more/modern infected | -0.1458 | 0.0132 | 0 |

| Contrast | estimate | SE | p.value |
|---|---|---|---|
| none not infected-bcg not infected | -0.755 | 0.9531 | 0.5774 |
| none not infected-h37ra not infected | -1.2814 | 0.7846 | 0.239 |
| none not infected-h37rv not infected | 0.0263 | 0.821 | 0.9744 |
| none not infected-less/ancient not infected | -2.078 | 0.5798 | 0.0019 |
| none not infected-more/modern not infected | -1.8699 | 0.5617 | 0.0038 |
| none not infected-bcg infected | -2.1862 | 0.8833 | 0.0359 |
| none not infected-h37ra infected | -2.6218 | 0.7381 | 0.0019 |
| none not infected-h37rv infected | -2.3266 | 0.7461 | 0.0064 |
| none not infected-less/ancient infected | -2.9587 | 0.5796 | 0 |
| none not infected-more/modern infected | -3.2052 | 0.5582 | 0 |
| bcg not infected-h37ra not infected | -0.5264 | 1.0983 | 0.7311 |
| bcg not infected-h37rv not infected | 0.7813 | 1.1336 | 0.6361 |
| bcg not infected-less/ancient not infected | -1.323 | 0.8506 | 0.2622 |
| bcg not infected-more/modern not infected | -1.1149 | 0.929 | 0.4084 |
| h37ra not infected-h37rv not infected | 1.3077 | 0.8827 | 0.2851 |
| h37ra not infected-less/ancient not infected | -0.7966 | 0.7783 | 0.5023 |
| h37ra not infected-more/modern not infected | -0.5885 | 0.744 | 0.5774 |
| h37rv not infected-less/ancient not infected | -2.1044 | 0.8302 | 0.0328 |
| h37rv not infected-more/modern not infected | -1.8962 | 0.7762 | 0.0364 |
| less/ancient not infected-more/modern not infected | 0.2082 | 0.4859 | 0.7311 |
| bcg infected-h37ra infected | -0.4356 | 1.0034 | 0.7311 |
| bcg infected-h37rv infected | -0.1404 | 1.0198 | 0.9167 |
| bcg infected-less/ancient infected | -0.7725 | 0.77 | 0.5023 |
| bcg infected-more/modern infected | -1.019 | 0.8551 | 0.4084 |
| h37ra infected-h37rv infected | 0.2951 | 0.7547 | 0.7379 |
| h37ra infected-less/ancient infected | -0.337 | 0.7293 | 0.7311 |
| h37ra infected-more/modern infected | -0.5834 | 0.6888 | 0.5774 |
| h37rv infected-less/ancient infected | -0.6321 | 0.7565 | 0.5774 |
| h37rv infected-more/modern infected | -0.8786 | 0.699 | 0.406 |
| less/ancient infected-more/modern infected | -0.2465 | 0.4817 | 0.7311 |
| bcg not infected-bcg infected | -1.4312 | 0.5083 | 0.0155 |
| h37ra not infected-h37ra infected | -1.3404 | 0.4263 | 0.0064 |
| h37rv not infected-h37rv infected | -2.353 | 0.5066 | 0 |
| less/ancient not infected-less/ancient infected | -0.8807 | 0.2259 | 7e-04 |
| more/modern not infected-more/modern infected | -1.3353 | 0.2061 | 0 |

OBSERVATIONS

In M2 macrophages, none of the group displayed the blockage of the acidification of the phagolysosomes and between 25% (H37Rv, H37Ra) and 50% (more virulent/modern) of macrophages showed acidification.

- Acidification of phagolysosomes observed
- Acidification of phagolysosomes not observed (blocked)
- Acidification trend observed, stastically not significant

**Grouping: Basic**

**M2 – 6 h p.i.**

c) Effective MOI

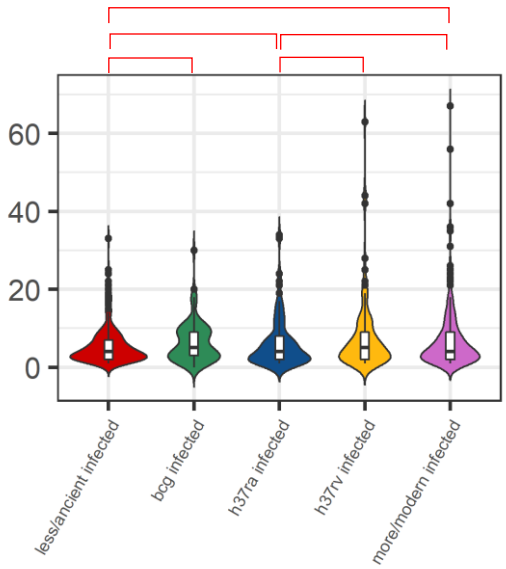


| Par | Value | Std.Error | p.value |
|---|---|---|---|
| (Intercept) | 1.4775 | 0.134 | 0 |
| groupbcg infected | 0.4793 | 0.1543 | 0.0029 |
| grouph37ra infected | 0.6163 | 0.1567 | 2e-04 |
| grouph37rv infected | 0.0909 | 0.1604 | 0.5728 |
| groupmore/modern infected | 0.2335 | 0.0988 | 0.0214 |

| Contrast | estimate | SE | p.value |
|---|---|---|---|
| less/ancient infected - bcg infected | -0.4793 | 0.1543 | 0.0096 |
| less/ancient infected - h37ra infected | -0.6163 | 0.1567 | 0.0014 |
| less/ancient infected - h37rv infected | -0.0909 | 0.1604 | 0.5728 |
| less/ancient infected - more/modern infected | -0.2335 | 0.0988 | 0.0428 |
| bcg infected - h37ra infected | -0.137 | 0.2153 | 0.5728 |
| bcg infected - h37rv infected | 0.3884 | 0.2177 | 0.1325 |
| bcg infected - more/modern infected | 0.2458 | 0.1797 | 0.2521 |
| h37ra infected - h37rv infected | 0.5254 | 0.1358 | 0.0014 |
| h37ra infected - more/modern infected | 0.3828 | 0.143 | 0.0239 |
| h37rv infected - more/modern infected | -0.1426 | 0.142 | 0.3992 |

d) Colocalization Index

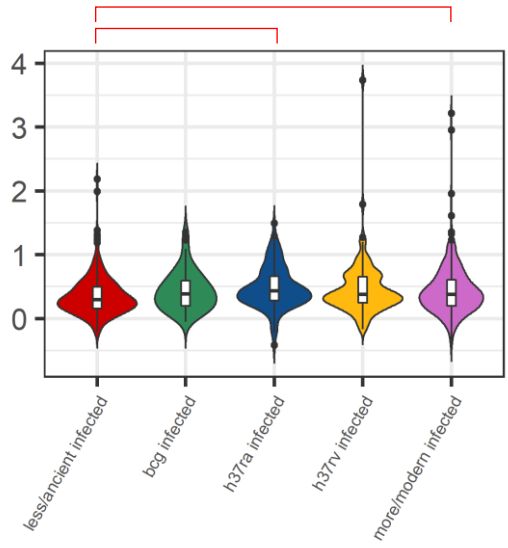


| Par | Value | Std.Error | p.value |
|---|---|---|---|
| (Intercept) | -0.2909 | 0.0544 | 0 |
| groupbcg infected | 0.2359 | 0.1063 | 0.0303 |
| grouph37ra infected | 0.4195 | 0.0929 | 0 |
| grouph37rv infected | 0.2242 | 0.0962 | 0.0232 |
| groupmore/modern infected | 0.2158 | 0.0678 | 0.0023 |

| Contrast | estimate | SE | p.value |
|---|---|---|---|
| less/ancient infected - bcg infected | -0.2359 | 0.1063 | 0.0606 |
| less/ancient infected - h37ra infected | -0.4195 | 0.0929 | 3e-04 |
| less/ancient infected - h37rv infected | -0.2242 | 0.0962 | 0.0606 |
| less/ancient infected - more/modern infected | -0.2158 | 0.0678 | 0.0116 |
| bcg infected - h37ra infected | -0.1836 | 0.1265 | 0.2172 |
| bcg infected - h37rv infected | 0.0117 | 0.1281 | 0.9273 |
| bcg infected - more/modern infected | 0.0201 | 0.1106 | 0.9273 |
| h37ra infected - h37rv infected | 0.1953 | 0.106 | 0.1173 |
| h37ra infected - more/modern infected | 0.2037 | 0.0888 | 0.0606 |
| h37rv infected - more/modern infected | 0.0084 | 0.0909 | 0.9273 |

OBSERVATIONS

Less virulent ancient strains showed lower MOI at 6 h p.i. compared to the other groups. Colocalization with acidified compartments was similar among all the groups.

**Grouping: Basic**

**M2 – 24 h p.i.**

a) Phagolysosomal acidification

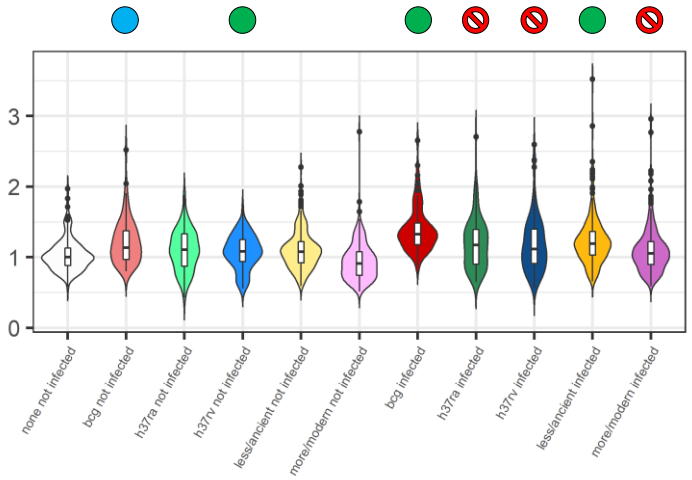


b) Percentage of cells showing acidified phagolysosomes

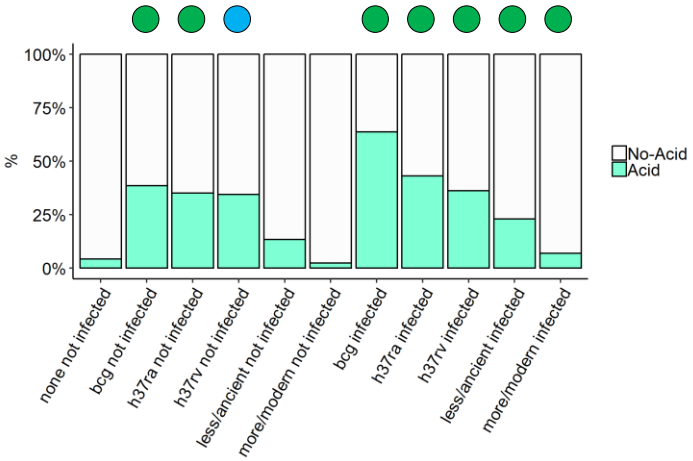


| Par | Value | Std.Error | p.value |
|---|---|---|---|
| (Intercept) | 0.0131 | 0.0546 | 0.8106 |
| groupbcg not infected | 0.0701 | 0.0522 | 0.1795 |
| grouph37ra not infected | -0.0471 | 0.0442 | 0.2871 |
| grouph37rv not infected | -0.1166 | 0.0449 | 0.0095 |
| groupless/ancient not infected | 0.0251 | 0.0314 | 0.4241 |
| groupmore/modern not infected | -0.0696 | 0.0316 | 0.0277 |
| groupbcg infected | 0.221 | 0.0516 | 0 |
| grouph37ra infected | 0.0611 | 0.0429 | 0.1542 |
| grouph37rv infected | -0.0506 | 0.0438 | 0.2482 |
| groupless/ancient infected | 0.1256 | 0.0314 | 1e-04 |
| groupmore/modern infected | 0.0386 | 0.0312 | 0.2161 |

| Par | Estimate | se | OR | pvalue |
|---|---|---|---|---|
| (Intercept) | -3.5118 | 0.6157 | 0.0298 | 0 |
| groupbcg not infected | 1.7216 | 0.5477 | 5.5932 | 0.0017 |
| grouph37ra not infected | 1.4539 | 0.585 | 4.2798 | 0.0129 |
| grouph37rv not infected | 1.2307 | 0.5873 | 3.4235 | 0.0361 |
| groupless/ancient not infected | 1.2008 | 0.5041 | 3.3227 | 0.0172 |
| groupmore/modern not infected | 0.4251 | 0.6559 | 1.5297 | 0.5169 |
| groupbcg infected | 2.7484 | 0.5419 | 15.6178 | 0 |
| grouph37ra infected | 2.3708 | 0.5715 | 10.7059 | 0 |
| grouph37rv infected | 1.7556 | 0.5749 | 5.7871 | 0.0023 |
| groupless/ancient infected | 1.9427 | 0.4906 | 6.9778 | 1e-04 |
| groupmore/modern infected | 1.4646 | 0.5336 | 4.3258 | 0.0061 |

| Contrast | estimate | SE | p.value |
|---|---|---|---|
| none not infected-bcg not infected | -0.0701 | 0.0522 | 0.2327 |
| none not infected-h37ra not infected | 0.0471 | 0.0442 | 0.3349 |
| none not infected-h37rv not infected | 0.1166 | 0.0449 | 0.0237 |
| none not infected-less/ancient not infected | -0.0251 | 0.0314 | 0.4498 |
| none not infected-more/modern not infected | 0.0696 | 0.0316 | 0.0511 |
| none not infected-bcg infected | -0.221 | 0.0516 | 2e-04 |
| none not infected-h37ra infected | -0.0611 | 0.0429 | 0.2159 |
| none not infected-h37rv infected | 0.0506 | 0.0438 | 0.2996 |
| none not infected-less/ancient infected | -0.1256 | 0.0314 | 3e-04 |
| none not infected-more/modern infected | -0.0386 | 0.0312 | 0.2701 |
| bcg not infected-h37ra not infected | 0.1172 | 0.0642 | 0.1086 |
| bcg not infected-h37rv not infected | 0.1867 | 0.0652 | 0.012 |
| bcg not infected-less/ancient not infected | 0.045 | 0.0486 | 0.3879 |
| bcg not infected-more/modern not infected | 0.1397 | 0.0544 | 0.024 |
| h37ra not infected-h37rv not infected | 0.0695 | 0.0479 | 0.2137 |
| h37ra not infected-less/ancient not infected | -0.0722 | 0.0471 | 0.1914 |
| h37ra not infected-more/modern not infected | 0.0225 | 0.0451 | 0.6186 |
| h37rv not infected-less/ancient not infected | -0.1417 | 0.0488 | 0.0119 |
| h37rv not infected-more/modern not infected | -0.0471 | 0.046 | 0.3455 |
| less/ancient not infected-more/modern not infected | 0.0947 | 0.0309 | 0.0078 |
| bcg infected-h37ra infected | 0.1599 | 0.0629 | 0.0242 |
| bcg infected-h37rv infected | 0.2716 | 0.064 | 2e-04 |
| bcg infected-less/ancient infected | 0.0954 | 0.0479 | 0.0779 |
| bcg infected-more/modern infected | 0.1824 | 0.0535 | 0.0026 |
| h37ra infected-h37rv infected | 0.1117 | 0.0457 | 0.0286 |
| h37ra infected-less/ancient infected | -0.0645 | 0.046 | 0.2167 |
| h37ra infected-more/modern infected | 0.0225 | 0.0437 | 0.6186 |
| h37rv infected-less/ancient infected | -0.1762 | 0.0478 | 0.001 |
| h37rv infected-more/modern infected | -0.0892 | 0.0444 | 0.0779 |
| less/ancient infected-more/modern infected | 0.087 | 0.0306 | 0.012 |
| bcg not infected-bcg infected | -0.1509 | 0.0295 | 0 |
| h37ra not infected-h37ra infected | -0.1082 | 0.0259 | 2e-04 |
| h37rv not infected-h37rv infected | -0.066 | 0.0263 | 0.0249 |
| less/ancient not infected-less/ancient infected | -0.1005 | 0.0158 | 0 |
| more/modern not infected-more/modern infected | -0.1081 | 0.0176 | 0 |

| Contrast | estimate | SE | p.value |
|---|---|---|---|
| none not infected-bcg not infected | -1.7216 | 0.5477 | 0.013 |
| none not infected-h37ra not infected | -1.4539 | 0.585 | 0.0412 |
| none not infected-h37rv not infected | -1.2307 | 0.5873 | 0.0843 |
| none not infected-less/ancient not infected | -1.2008 | 0.5041 | 0.0464 |
| none not infected-more/modern not infected | -0.4251 | 0.6559 | 0.6238 |
| none not infected-bcg infected | -2.7484 | 0.5419 | 0 |
| none not infected-h37ra infected | -2.3708 | 0.5715 | 6e-04 |
| none not infected-h37rv infected | -1.7556 | 0.5749 | 0.013 |
| none not infected-less/ancient infected | -1.9427 | 0.4906 | 9e-04 |
| none not infected-more/modern infected | -1.4646 | 0.5336 | 0.0236 |
| bcg not infected-h37ra not infected | 0.2676 | 0.594 | 0.6918 |
| bcg not infected-h37rv not infected | 0.4909 | 0.5992 | 0.5349 |
| bcg not infected-less/ancient not infected | 0.5208 | 0.3434 | 0.2157 |
| bcg not infected-more/modern not infected | 1.2965 | 0.5924 | 0.0716 |
| h37ra not infected-h37rv not infected | 0.2233 | 0.3902 | 0.6404 |
| h37ra not infected-less/ancient not infected | 0.2531 | 0.5402 | 0.6918 |
| h37ra not infected-more/modern not infected | 1.0288 | 0.6494 | 0.2021 |
| h37rv not infected-less/ancient not infected | 0.0299 | 0.5461 | 0.9564 |
| h37rv not infected-more/modern not infected | 0.8056 | 0.6525 | 0.3037 |
| less/ancient not infected-more/modern not infected | 0.7757 | 0.5309 | 0.2191 |
| bcg infected-h37ra infected | 0.3776 | 0.5684 | 0.6238 |
| bcg infected-h37rv infected | 0.9928 | 0.5778 | 0.1667 |
| bcg infected-less/ancient infected | 0.8057 | 0.3235 | 0.0412 |
| bcg infected-more/modern infected | 1.2838 | 0.4482 | 0.0183 |
| h37ra infected-h37rv infected | 0.6152 | 0.3908 | 0.2021 |
| h37ra infected-less/ancient infected | 0.4281 | 0.5 | 0.5276 |
| h37ra infected-more/modern infected | 0.9062 | 0.4999 | 0.1438 |
| h37rv infected-less/ancient infected | -0.1871 | 0.5115 | 0.7355 |
| h37rv infected-more/modern infected | 0.291 | 0.5021 | 0.6404 |
| less/ancient infected-more/modern infected | 0.4781 | 0.3476 | 0.2463 |
| bcg not infected-bcg infected | -1.0269 | 0.3387 | 0.013 |
| h37ra not infected-h37ra infected | -0.9169 | 0.3755 | 0.0426 |
| h37rv not infected-h37rv infected | -0.525 | 0.3581 | 0.2191 |
| less/ancient not infected-less/ancient infected | -0.7419 | 0.2464 | 0.013 |
| more/modern not infected-more/modern infected | -1.0395 | 0.5248 | 0.1042 |

OBSERVATIONS

At 24 h p.i. only H37Rv, H37Ra and more virulent/modern strains displayed a blockade of the acidification of the phagolysosomes; however, whereas the percentage of acidified cells remained high for BCG (60%), H37Rv and H37Ra (40%), it dropped for less virulent and ancient strains (25%) and for more virulent and modern strains (<10%).

- Acidification of phagolysosomes observed
- Acidification of phagolysosomes not observed (blocked)
- Acidification trend observed, stastically not significant

**Grouping: Basic**

**M2 – 24 h p.i.**

c) Effective MOI

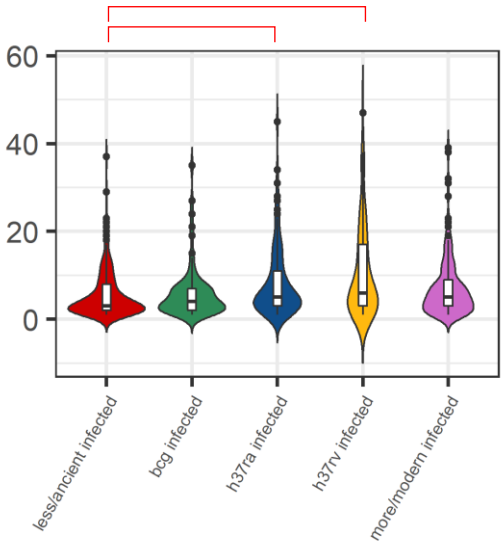


| Par | Value | Std.Error | p.value |
|---|---|---|---|
| (Intercept) | 1.3419 | 0.1293 | 0 |
| groupbcg infected | 0.1459 | 0.1918 | 0.4498 |
| grouph37ra infected | 0.5265 | 0.1857 | 0.0062 |
| grouph37rv infected | 0.5935 | 0.1938 | 0.0033 |
| groupmore/modern infected | 0.1622 | 0.1228 | 0.1913 |

| Contrast | estimate | SE | p.value |
|---|---|---|---|
| less/ancient infected - bcg infected | -0.1459 | 0.1918 | 0.5622 |
| less/ancient infected - h37ra infected | -0.5265 | 0.1857 | 0.0312 |
| less/ancient infected - h37rv infected | -0.5935 | 0.1938 | 0.0312 |
| less/ancient infected - more/modern infected | -0.1622 | 0.1228 | 0.2733 |
| bcg infected - h37ra infected | -0.3806 | 0.2569 | 0.2396 |
| bcg infected - h37rv infected | -0.4476 | 0.2621 | 0.1856 |
| bcg infected - more/modern infected | -0.0163 | 0.2196 | 0.9411 |
| h37ra infected - h37rv infected | -0.067 | 0.1794 | 0.7891 |
| h37ra infected - more/modern infected | 0.3643 | 0.1749 | 0.1037 |
| h37rv infected - more/modern infected | 0.4313 | 0.178 | 0.0615 |

d) Colocalization Index

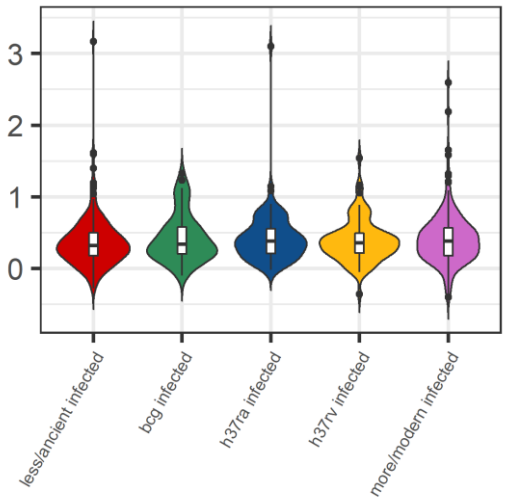


| Par | Value | Std.Error | p.value |
|---|---|---|---|
| (Intercept) | -0.1921 | 0.0656 | 0.0035 |
| groupbcg infected | 0.2212 | 0.1216 | 0.074 |
| grouph37ra infected | 0.1895 | 0.1101 | 0.0904 |
| grouph37rv infected | 0.069 | 0.1169 | 0.5571 |
| groupmore/modern infected | 0.1861 | 0.0832 | 0.0291 |

| Contrast | estimate | SE | p.value |
|---|---|---|---|
| less/ancient infected - bcg infected | -0.2212 | 0.1216 | 0.3014 |
| less/ancient infected - h37ra infected | -0.1895 | 0.1101 | 0.3014 |
| less/ancient infected - h37rv infected | -0.069 | 0.1169 | 0.7958 |
| less/ancient infected - more/modern infected | -0.1861 | 0.0832 | 0.2909 |
| bcg infected - h37ra infected | 0.0317 | 0.1507 | 0.9267 |
| bcg infected - h37rv infected | 0.1522 | 0.155 | 0.5503 |
| bcg infected - more/modern infected | 0.0351 | 0.1348 | 0.9267 |
| h37ra infected - h37rv infected | 0.1205 | 0.1193 | 0.5503 |
| h37ra infected - more/modern infected | 0.0033 | 0.1089 | 0.9756 |
| h37rv infected - more/modern infected | -0.1171 | 0.1143 | 0.5503 |

OBSERVATIONS

Less virulent ancient strains showed lower MOI compared to H37Ra and H37Rv only. Colocalization with acidified compartments was similar among all the groups.

**Grouping: Disease**

**M1 – 6 h p.i.**

a) Phagolysosomal acidification

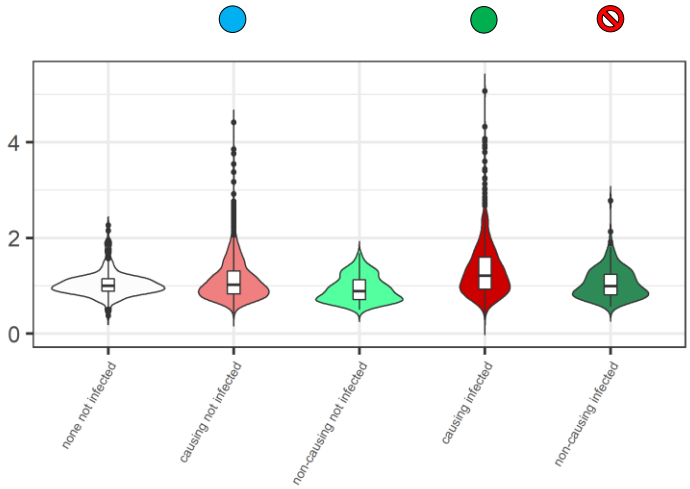


| Par | Value | Std.Error | p.value |
|---|---|---|---|
| (Intercept) | 0.0033 | 0.0806 | 0.9677 |
| groupcausing not infected | 0.0601 | 0.0468 | 0.1988 |
| groupnon-causing not infected | -0.1065 | 0.0655 | 0.1044 |
| groupcausing infected | 0.1912 | 0.0468 | 0 |
| groupnon-causing infected | -0.0322 | 0.0657 | 0.624 |

| Contrast | estimate | SE | p.value |
|---|---|---|---|
| none not infected-causing not infected | -0.0601 | 0.0468 | 0.2272 |
| none not infected-non-causing not infected | 0.1065 | 0.0655 | 0.1392 |
| none not infected-causing infected | -0.1912 | 0.0468 | 1e-04 |
| none not infected-non-causing infected | 0.0322 | 0.0657 | 0.624 |
| causing not infected-non-causing not infected | 0.1666 | 0.0602 | 0.0091 |
| causing infected-non-causing infected | 0.2234 | 0.0604 | 4e-04 |
| causing not infected-causing infected | -0.1311 | 0.0091 | 0 |
| non-causing not infected-non-causing infected | -0.0743 | 0.0176 | 1e-04 |

b) Percentage of cells showing acidified phagolysosomes

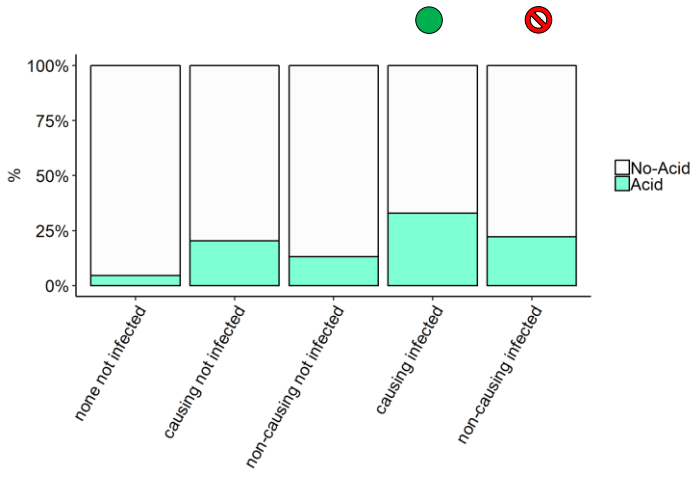


| Par | Estimate | se | OR | pvalue |
|---|---|---|---|---|
| (Intercept) | -3.6546 | 0.8901 | 0.0259 | 0 |
| groupcausing not infected | 1.0725 | 0.5749 | 2.9227 | 0.0621 |
| groupnon-causing not infected | 0.2613 | 0.7424 | 1.2986 | 0.7249 |
| groupcausing infected | 2.3925 | 0.572 | 10.9406 | 0 |
| groupnon-causing infected | 0.933 | 0.729 | 2.5422 | 0.2006 |

| Contrast | estimate | SE | p.value |
|---|---|---|---|
| none not infected-causing not infected | -1.0725 | 0.5749 | 0.0993 |
| none not infected-non-causing not infected | -0.2613 | 0.7424 | 0.7249 |
| none not infected-causing infected | -2.3925 | 0.572 | 1e-04 |
| none not infected-non-causing infected | -0.933 | 0.729 | 0.2293 |
| causing not infected-non-causing not infected | 0.8112 | 0.6205 | 0.2293 |
| causing infected-non-causing infected | 1.4595 | 0.602 | 0.0409 |
| causing not infected-causing infected | -1.32 | 0.1771 | 0 |
| non-causing not infected-non-causing infected | -0.6717 | 0.3259 | 0.0785 |

OBSERVATIONS

In M1 macrophages, non-causing disease strains are blocking the phagolysosomal acidification at 6 h p.i., but the percentage of acidified cells remains low (30%) also in the category disease causing.

- Acidification of phagolysosomes observed
- Acidification of phagolysosomes not observed (blocked)
- Acidification trend observed, stastically not significant

**Grouping: Disease**

**M1 – 6 h p.i.**

c) Effective MOI

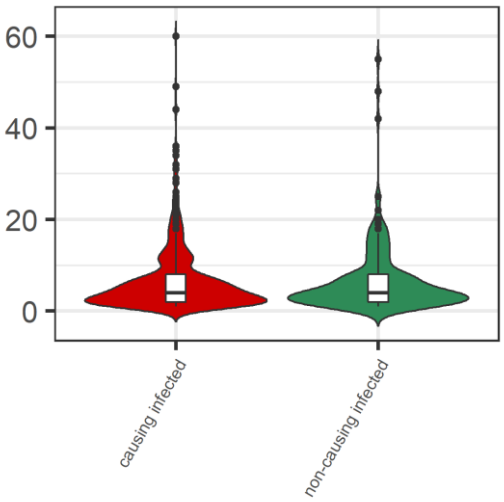


| Par | Value | Std.Error | p.value |
|---|---|---|---|
| (Intercept) | 1.4382 | 0.0858 | 0 |
| groupnon-causing infected | 0.0226 | 0.1292 | 0.8619 |

| Contrast | estimate | SE | p.value |
|---|---|---|---|
| causing infected - non-causing infected | -0.0226 | 0.1292 | 0.8619 |

d) Colocalization Index

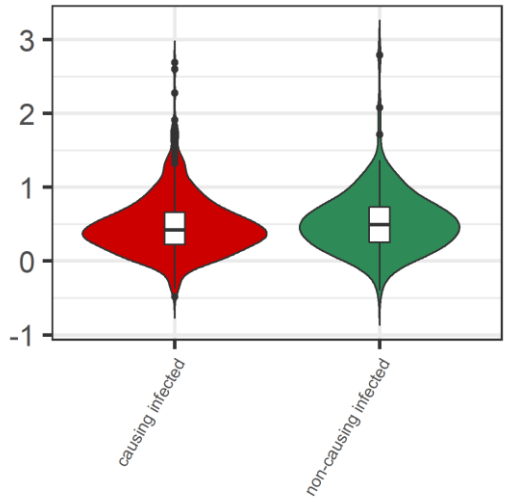


| Par | Value | Std.Error | p.value |
|---|---|---|---|
| (Intercept) | 0.0046 | 0.0699 | 0.9479 |
| groupnon-causing infected | 0.1905 | 0.1097 | 0.0874 |

| Contrast | estimate | SE | p.value |
|---|---|---|---|
| causing infected - non-causing infected | -0.1905 | 0.1097 | 0.0874 |

OBSERVATIONS

Non-causing disease strains showed higher MOI values. Colocalization with acidified compartments was similar among all the groups.

**Grouping: Disease**

**M1 – 24 h p.i.**

a) Phagolysosomal acidification

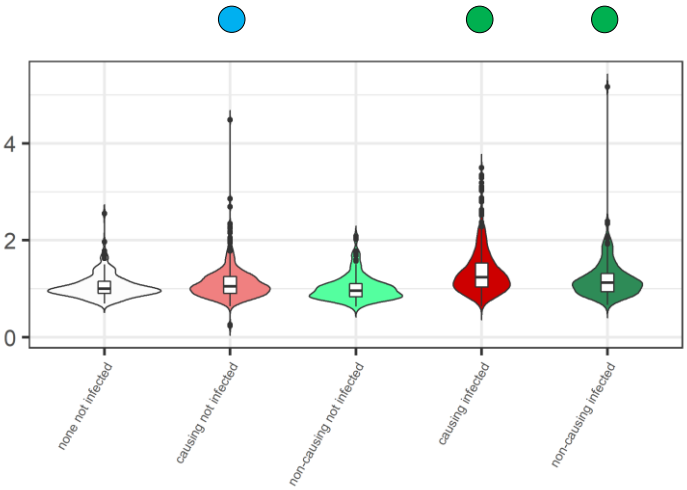


| Par | Value | Std.Error | p.value |
|---|---|---|---|
| (Intercept) | 0.0097 | 0.0408 | 0.8124 |
| groupcausing not infected | 0.0341 | 0.0281 | 0.225 |
| groupnon-causing not infected | -0.0209 | 0.0389 | 0.5903 |
| groupcausing infected | 0.1785 | 0.0279 | 0 |
| groupnon-causing infected | 0.1265 | 0.0376 | 8e-04 |

| Contrast | estimate | SE | p.value |
|---|---|---|---|
| none not infected-causing not infected | -0.0341 | 0.0281 | 0.2572 |
| none not infected-non-causing not infected | 0.0209 | 0.0389 | 0.5903 |
| none not infected-causing infected | -0.1785 | 0.0279 | 0 |
| none not infected-non-causing infected | -0.1265 | 0.0376 | 0.0015 |
| causing not infected-non-causing not infected | 0.055 | 0.0342 | 0.1492 |
| causing infected-non-causing infected | 0.052 | 0.0327 | 0.1492 |
| causing not infected-causing infected | -0.1444 | 0.0122 | 0 |
| non-causing not infected-non-causing infected | -0.1475 | 0.0236 | 0 |

b) Percentage of cells showing acidified phagolysosomes

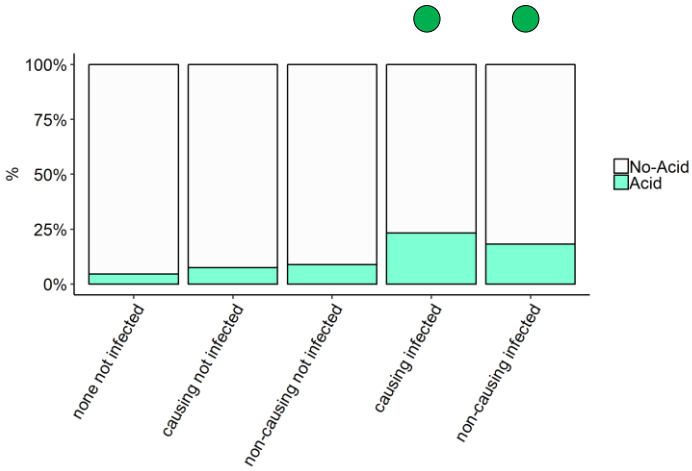


| Par | Estimate | se | OR | pvalue |
|---|---|---|---|---|
| (Intercept) | -3.186 | 0.456 | 0.0413 | 0 |
| groupcausing not infected | 0.4347 | 0.4456 | 1.5446 | 0.3292 |
| groupnon-causing not infected | 0.9095 | 0.5479 | 2.4832 | 0.0969 |
| groupcausing infected | 1.8308 | 0.4246 | 6.2387 | 0 |
| groupnon-causing infected | 1.7686 | 0.4844 | 5.8628 | 3e-04 |

| Contrast | estimate | SE | p.value |
|---|---|---|---|
| none not infected-causing not infected | -0.4347 | 0.4456 | 0.3763 |
| none not infected-non-causing not infected | -0.9095 | 0.5479 | 0.155 |
| none not infected-causing infected | -1.8308 | 0.4246 | 1e-04 |
| none not infected-non-causing infected | -1.7686 | 0.4844 | 7e-04 |
| causing not infected-non-causing not infected | -0.4748 | 0.4191 | 0.343 |
| causing infected-non-causing infected | 0.0621 | 0.3017 | 0.8368 |
| causing not infected-causing infected | -1.396 | 0.1963 | 0 |
| non-causing not infected-non-causing infected | -0.8591 | 0.3752 | 0.0441 |

OBSERVATIONS

At 24 h p.i. none of the category is blocking the acidification of the phagolysosomes. However, despite an increase in the acidification of the phagolysosomes was observed, the number of macrophages displaying such acidification was found generally low (<25%).

- Acidification of phagolysosomes observed
- Acidification of phagolysosomes not observed (blocked)
- Acidification trend observed, stastically not significant

**Grouping: Disease**

**M1 – 24 h p.i.**

c) Effective MOI

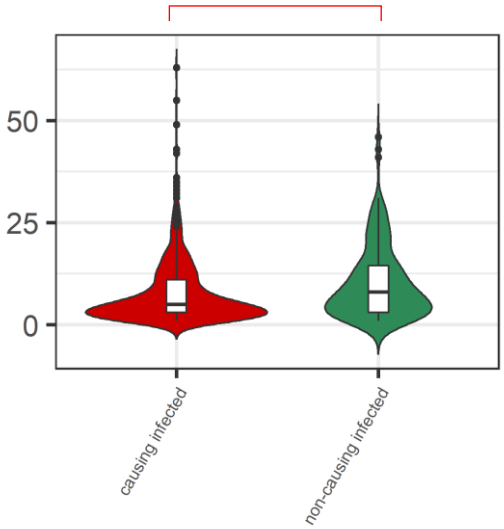


| Par | Value | Std.Error | p.value |
|---|---|---|---|
| (Intercept) | 1.5863 | 0.1249 | 0 |
| groupnon-causing infected | 0.4806 | 0.0974 | 0 |

| Contrast | estimate | SE | p.value |
|---|---|---|---|
| causing infected - non-causing infected | -0.4806 | 0.0974 | 0 |

d) Colocalization Index

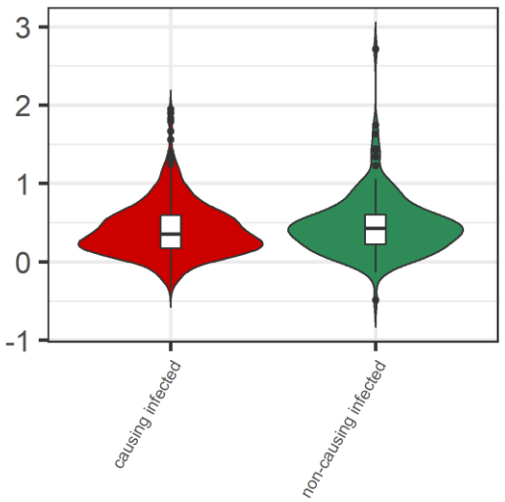


| Par | Value | Std.Error | p.value |
|---|---|---|---|
| (Intercept) | -0.0421 | 0.0717 | 0.5571 |
| groupnon-causing infected | 0.1552 | 0.1161 | 0.1859 |

| Contrast | estimate | SE | p.value |
|---|---|---|---|
| causing infected - non-causing infected | -0.1552 | 0.1161 | 0.1859 |

OBSERVATIONS

Non-causing disease strains showed higher MOI values. Colocalization with acidified compartments was similar among all the groups.

**Grouping: Disease**

**M2 – 6 h p.i.**

a) Phagolysosomal acidification

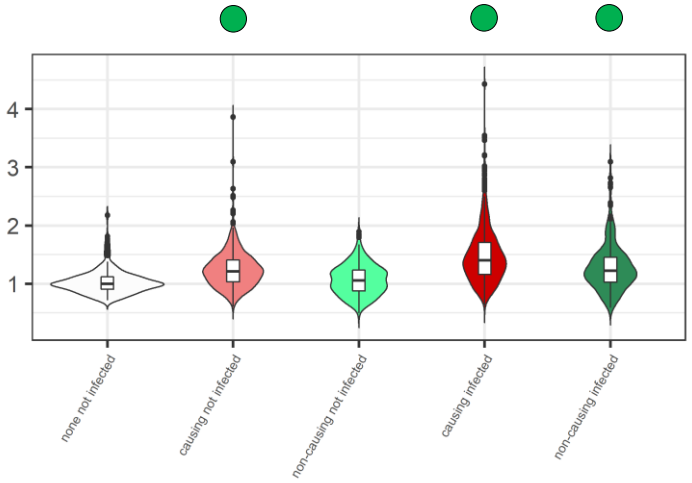


| Par | Value | Std.Error | p.value |
|---|---|---|---|
| (Intercept) | -0.0092 | 0.0487 | 0.8495 |
| groupcausing not infected | 0.1646 | 0.0377 | 0 |
| groupnon-causing not infected | 0.0662 | 0.0521 | 0.2044 |
| groupcausing infected | 0.2905 | 0.0377 | 0 |
| groupnon-causing infected | 0.2055 | 0.0523 | 1e-04 |

| Contrast | estimate | SE | p.value |
|---|---|---|---|
| none not infected-causing not infected | -0.1646 | 0.0377 | 0 |
| none not infected-non-causing not infected | -0.0662 | 0.0521 | 0.2044 |
| none not infected-causing infected | -0.2905 | 0.0377 | 0 |
| none not infected-non-causing infected | -0.2055 | 0.0523 | 1e-04 |
| causing not infected-non-causing not infected | 0.0984 | 0.0479 | 0.0536 |
| causing infected-non-causing infected | 0.085 | 0.0481 | 0.0883 |
| causing not infected-causing infected | -0.1259 | 0.0088 | 0 |
| non-causing not infected-non-causing infected | -0.1393 | 0.0168 | 0 |

b) Percentage of cells showing acidified phagolysosomes

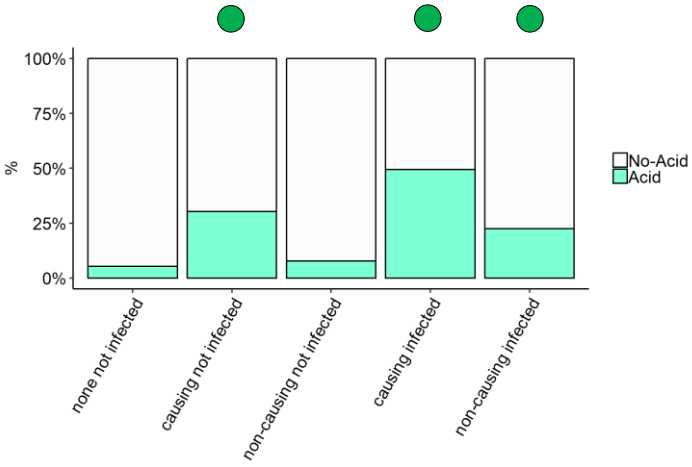


| Par | Estimate | se | OR | pvalue |
|---|---|---|---|---|
| (Intercept) | -3.197 | 0.6331 | 0.0409 | 0 |
| groupcausing not infected | 1.7001 | 0.5059 | 5.4745 | 8e-04 |
| groupnon-causing not infected | 1.179 | 0.6744 | 3.2511 | 0.0804 |
| groupcausing infected | 2.9537 | 0.5039 | 19.1775 | 0 |
| groupnon-causing infected | 2.5538 | 0.6396 | 12.8565 | 1e-04 |

| Contrast | estimate | SE | p.value |
|---|---|---|---|
| none not infected-causing not infected | -1.7001 | 0.5059 | 0.0012 |
| none not infected-non-causing not infected | -1.179 | 0.6744 | 0.1072 |
| none not infected-causing infected | -2.9537 | 0.5039 | 0 |
| none not infected-non-causing infected | -2.5538 | 0.6396 | 1e-04 |
| causing not infected-non-causing not infected | 0.5211 | 0.5464 | 0.3889 |
| causing infected-non-causing infected | 0.3999 | 0.4973 | 0.4214 |
| causing not infected-causing infected | -1.2536 | 0.1449 | 0 |
| non-causing not infected-non-causing infected | -1.3749 | 0.3264 | 1e-04 |

OBSERVATIONS

In M2 macrophages, none of the category is blocking the acidification of the phagolysosomes at 6 h p.i.. Whereas the category causing disease displayed acidification in 50% of cells, non-causing disease strains showed acidification in less than 25% of macrophages.

Acidification of phagolysosomes observed

Acidification of phagolysosomes not observed (blocked)

Acidification trend observed, stastically not significant

**Grouping: Disease**

**M2 – 6 h p.i.**

c) Effective MOI

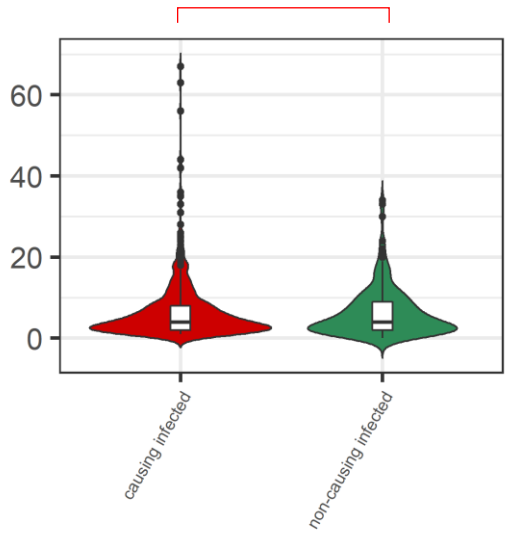


| Par | Value | Std.Error | p.value |
|---|---|---|---|
| (Intercept) | 1.5863 | 0.1249 | 0 |
| groupnon-causing infected | 0.4806 | 0.0974 | 0 |

| Contrast | estimate | SE | p.value |
|---|---|---|---|
| causing infected - non-causing infected | -0.4806 | 0.0974 | 0 |

d) Colocalization Index

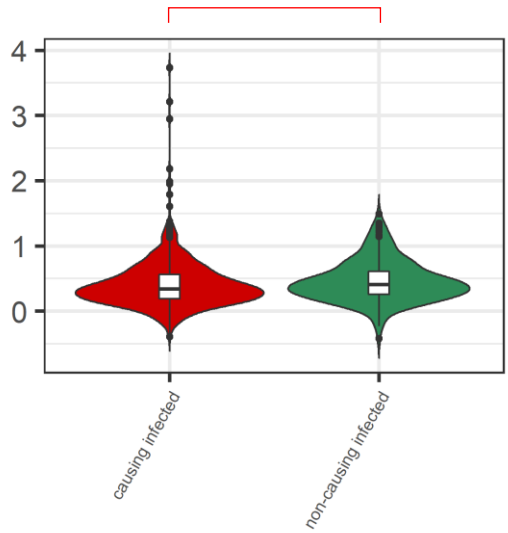


| Par | Value | Std.Error | p.value |
|---|---|---|---|
| (Intercept) | -0.1642 | 0.0535 | 0.0022 |
| groupnon-causing infected | 0.2582 | 0.0714 | 6e-04 |

| Contrast | estimate | SE | p.value |
|---|---|---|---|
| causing infected - non-causing infected | -0.2582 | 0.0714 | 6e-04 |

OBSERVATIONS

Non-causing disease strains showed also higher MOI values. Colocalization with acidified compartments was found lower for disease causing strains.

**Grouping: Disease**

**M2 – 24 h p.i.**

a) Phagolysosomal acidification

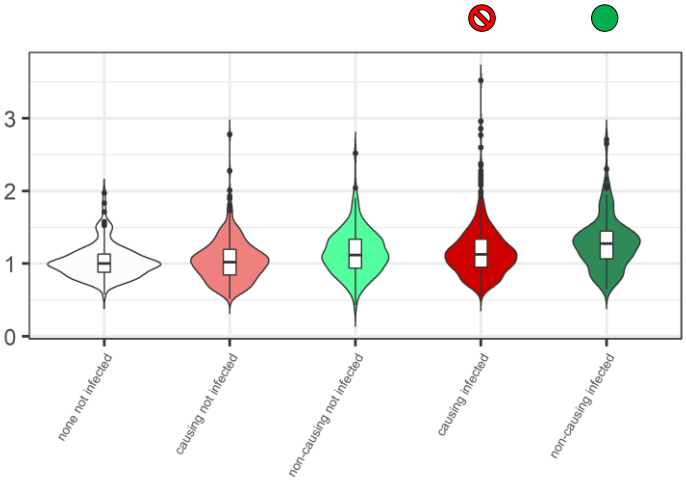


| Par | Value | Std.Error | p.value |
|---|---|---|---|
| (Intercept) | 0.0118 | 0.057 | 0.8355 |
| groupcausing not infected | -0.0395 | 0.0277 | 0.1538 |
| groupnon-causing not infected | -0.0037 | 0.0378 | 0.9227 |
| groupcausing infected | 0.0537 | 0.0276 | 0.052 |
| groupnon-causing infected | 0.121 | 0.0371 | 0.0011 |

| Contrast | estimate | SE | p.value |
|---|---|---|---|
| none not infected-causing not infected | 0.0395 | 0.0277 | 0.2051 |
| none not infected-non-causing not infected | 0.0037 | 0.0378 | 0.9227 |
| none not infected-causing infected | -0.0537 | 0.0276 | 0.0833 |
| none not infected-non-causing infected | -0.121 | 0.0371 | 0.003 |
| causing not infected-non-causing not infected | -0.0358 | 0.0334 | 0.3235 |
| causing infected-non-causing infected | -0.0674 | 0.0325 | 0.0772 |
| causing not infected-causing infected | -0.0932 | 0.0107 | 0 |
| non-causing not infected-non-causing infected | -0.1247 | 0.0194 | 0 |

b) Percentage of cells showing acidified phagolysosomes

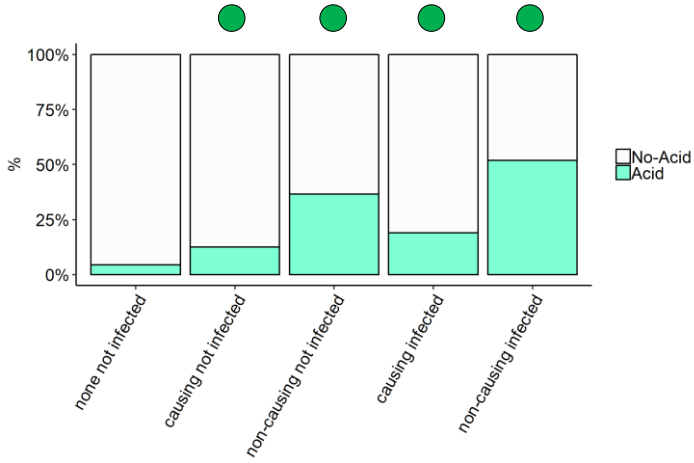


| Par | Estimate | se | OR | pvalue |
|---|---|---|---|---|
| (Intercept) | -3.6245 | 0.6384 | 0.0267 | 0 |
| groupcausing not infected | 1.1272 | 0.4645 | 3.087 | 0.0152 |
| groupnon-causing not infected | 1.5586 | 0.4802 | 4.7521 | 0.0012 |
| groupcausing infected | 1.8374 | 0.4592 | 6.2804 | 1e-04 |
| groupnon-causing infected | 2.5484 | 0.4778 | 12.7873 | 0 |

| Contrast | estimate | SE | p.value |
|---|---|---|---|
| none not infected-causing not infected | -1.1272 | 0.4645 | 0.0174 |
| none not infected-non-causing not infected | -1.5586 | 0.4802 | 0.0019 |
| none not infected-causing infected | -1.8374 | 0.4592 | 2e-04 |
| none not infected-non-causing infected | -2.5484 | 0.4778 | 0 |
| causing not infected-non-causing not infected | -0.4314 | 0.2499 | 0.0843 |
| causing infected-non-causing infected | -0.711 | 0.2394 | 0.004 |
| causing not infected-causing infected | -0.7102 | 0.1873 | 3e-04 |
| non-causing not infected-non-causing infected | -0.9899 | 0.2525 | 2e-04 |

OBSERVATIONS

As the infection progresses, disease causing strains are blocking the acidification of the phagolysosomes. In this case, the percentage of macrophages displaying acidification was higher for non-causing disease strains (50%) compared to causing disease strains (<25%).

- Acidification of phagolysosomes observed
- Acidification of phagolysosomes not observed (blocked)
- Acidification trend observed, stastically not significant

**Grouping: Disease**

**M2 – 24 h p.i.**

c) Effective MOI

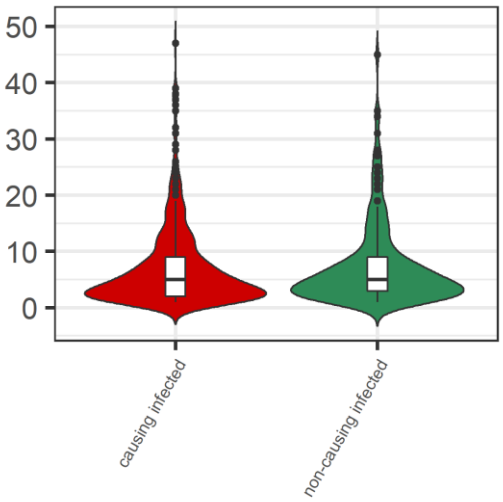


| Par | Value | Std.Error | p.value |
|---|---|---|---|
| (Intercept) | 1.5343 | 0.1207 | 0 |
| groupnon-causing infected | 0.1865 | 0.1183 | 0.1198 |

| Contrast | estimate | SE | p.value |
|---|---|---|---|
| causing infected - non-causing infected | -0.1865 | 0.1183 | 0.1198 |

d) Colocalization Index

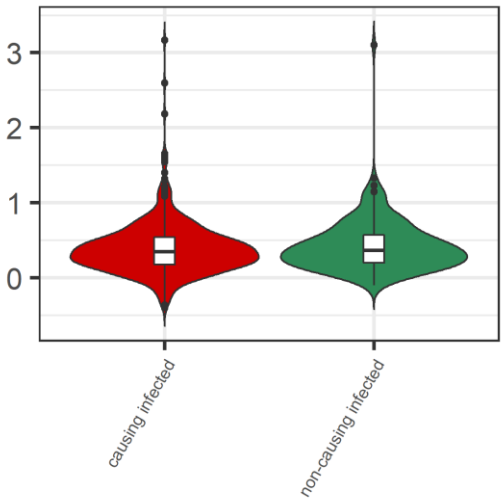


| Par | Value | Std.Error | p.value |
|---|---|---|---|
| (Intercept) | -0.1051 | 0.047 | 0.0258 |
| groupnon-causing infected | 0.1232 | 0.0796 | 0.1267 |

| Contrast | estimate | SE | p.value |
|---|---|---|---|
| causing infected - non-causing infected | -0.1232 | 0.0796 | 0.1267 |

OBSERVATIONS

Colocalization with acidified compartments was similar among all the groups.

**Grouping: Lab adaptation**

**M1 – 6 h p.i.**

a) Phagolysosomal acidification

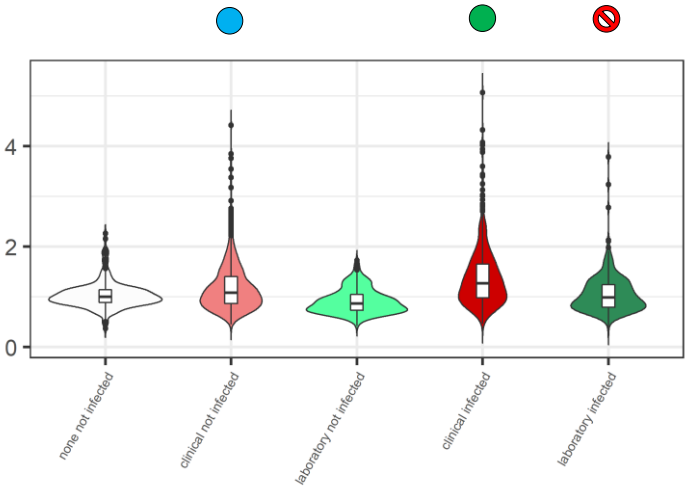


| Par | Value | Std.Error | p.value |
|---|---|---|---|
| (Intercept) | 0.0048 | 0.0752 | 0.9496 |
| groupclinical not infected | 0.0872 | 0.0495 | 0.0782 |
| grouplaboratory not infected | -0.0864 | 0.0584 | 0.139 |
| groupclinical infected | 0.2227 | 0.0495 | 0 |
| grouplaboratory infected | 3e-04 | 0.0585 | 0.9957 |

| Contrast | estimate | SE | p.value |
|---|---|---|---|
| none not infected-clinical not infected | -0.0872 | 0.0495 | 0.1043 |
| none not infected-laboratory not infected | 0.0864 | 0.0584 | 0.1589 |
| none not infected-clinical infected | -0.2227 | 0.0495 | 0 |
| none not infected-laboratory infected | -3e-04 | 0.0585 | 0.9957 |
| clinical not infected-laboratory not infected | 0.1735 | 0.0575 | 0.0041 |
| clinical infected-laboratory infected | 0.2223 | 0.0576 | 2e-04 |
| clinical not infected-clinical infected | -0.1355 | 0.0099 | 0 |
| laboratory not infected-laboratory infected | -0.0867 | 0.014 | 0 |

b) Percentage of cells showing acidified phagolysosomes

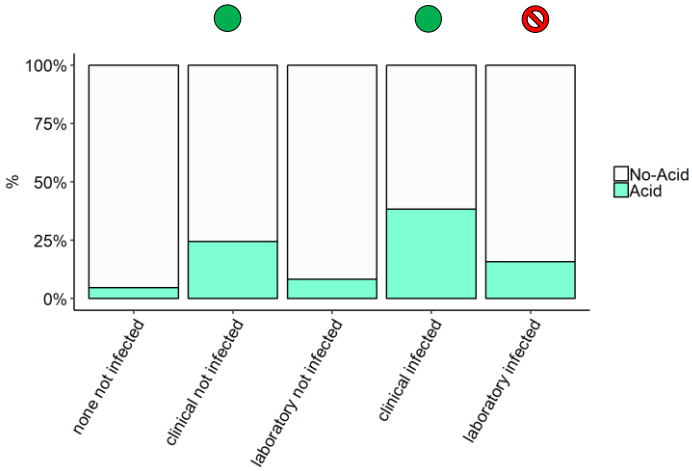


| Par | Estimate | se | OR | pvalue |
|---|---|---|---|---|
| (Intercept) | -3.6022 | 0.8358 | 0.0273 | 0 |
| groupclinical not infected | 1.379 | 0.5906 | 3.9711 | 0.0195 |
| grouplaboratory not infected | 0.043 | 0.6915 | 1.0439 | 0.9504 |
| groupclinical infected | 2.6821 | 0.5897 | 14.6163 | 0 |
| grouplaboratory infected | 0.8566 | 0.6756 | 2.3551 | 0.2049 |

| Contrast | estimate | SE | p.value |
|---|---|---|---|
| none not infected-clinical not infected | -1.379 | 0.5906 | 0.0313 |
| none not infected-laboratory not infected | -0.043 | 0.6915 | 0.9504 |
| none not infected-clinical infected | -2.6821 | 0.5897 | 0 |
| none not infected-laboratory infected | -0.8566 | 0.6756 | 0.2341 |
| clinical not infected-laboratory not infected | 1.336 | 0.6205 | 0.0417 |
| clinical infected-laboratory infected | 1.8256 | 0.6025 | 0.0065 |
| clinical not infected-clinical infected | -1.3031 | 0.1806 | 0 |
| laboratory not infected-laboratory infected | -0.8136 | 0.3045 | 0.0151 |

OBSERVATIONS

In M1 macrophages, laboratory strains are blocking the phagolysosomal acidification at 6 h p.i. but the percentage of acidified cells remains low (30%) also in the category of clinical strains.

- Acidification of phagolysosomes observed
- Acidification of phagolysosomes not observed (blocked)
- Acidification trend observed, stastically not significant

**Grouping: Lab adaptation**

**M1 – 6 h p.i.**

c) Effective MOI

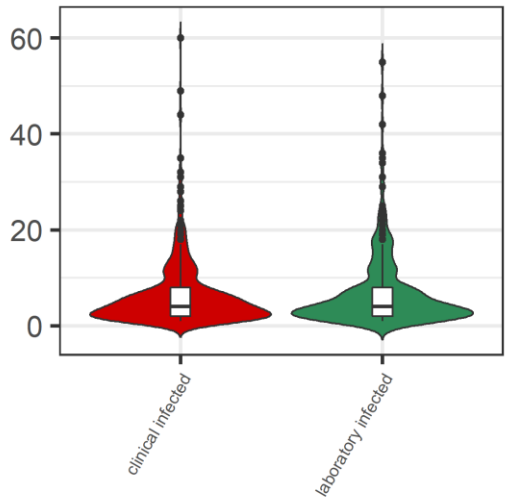


| Par | Value | Std.Error | p.value |
|---|---|---|---|
| (Intercept) | 1.4239 | 0.0933 | 0 |
| grouplaboratory infected | 0.0521 | 0.1209 | 0.6679 |

| Contrast | estimate | SE | p.value |
|---|---|---|---|
| clinical infected - laboratory infected | -0.0521 | 0.1209 | 0.6679 |

d) Colocalization Index

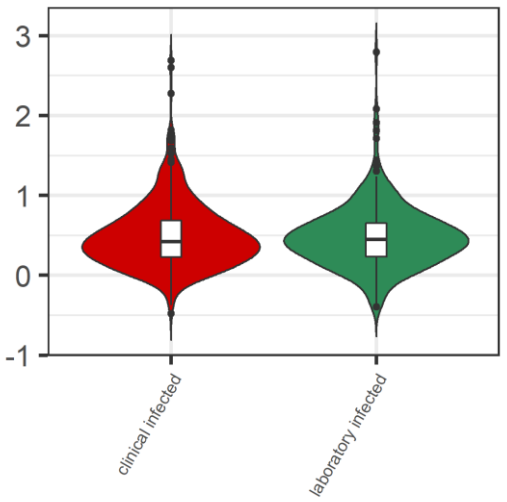


| Par | Value | Std.Error | p.value |
|---|---|---|---|
| (Intercept) | 0.0535 | 0.08 | 0.5039 |
| grouplaboratory infected | -0.034 | 0.103 | 0.7425 |

| Contrast | estimate | SE | p.value |
|---|---|---|---|
| clinical infected - laboratory infected | 0.034 | 0.103 | 0.7425 |

OBSERVATIONS

Colocalization with acidified compartments was similar among all the groups. Laboratory strains showed higher MOI values.

**Grouping: Lab adaptation**

**M1 – 24 h p.i.**

a) Phagolysosomal acidification

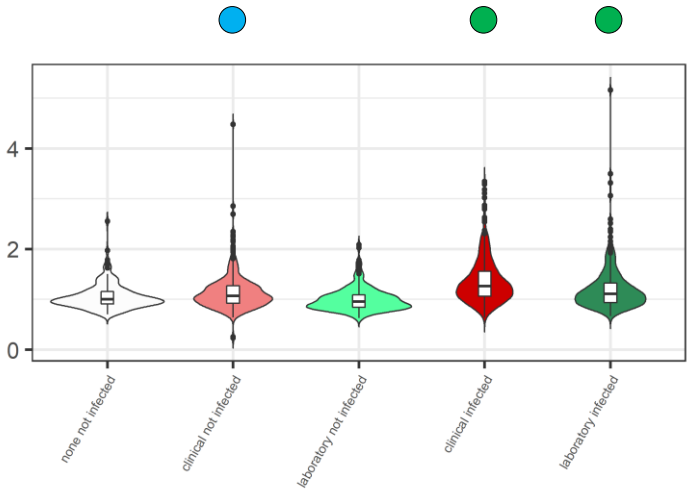


| Par | Value | Std.Error | p.value |
|---|---|---|---|
| (Intercept) | 0.0141 | 0.0388 | 0.7169 |
| groupclinical not infected | 0.0404 | 0.0293 | 0.1686 |
| grouplaboratory not infected | -0.0191 | 0.0352 | 0.5874 |
| groupclinical infected | 0.1864 | 0.0292 | 0 |
| grouplaboratory infected | 0.1256 | 0.0344 | 3e-04 |

| Contrast | estimate | SE | p.value |
|---|---|---|---|
| none not infected-clinical not infected | -0.0404 | 0.0293 | 0.1927 |
| none not infected-laboratory not infected | 0.0191 | 0.0352 | 0.5874 |
| none not infected-clinical infected | -0.1864 | 0.0292 | 0 |
| none not infected-laboratory infected | -0.1256 | 0.0344 | 5e-04 |
| clinical not infected-laboratory not infected | 0.0595 | 0.0325 | 0.0902 |
| clinical infected-laboratory infected | 0.0608 | 0.0316 | 0.0875 |
| clinical not infected-clinical infected | -0.1459 | 0.0134 | 0 |
| laboratory not infected-laboratory infected | -0.1447 | 0.0186 | 0 |

b) Percentage of cells showing acidified phagolysosomes

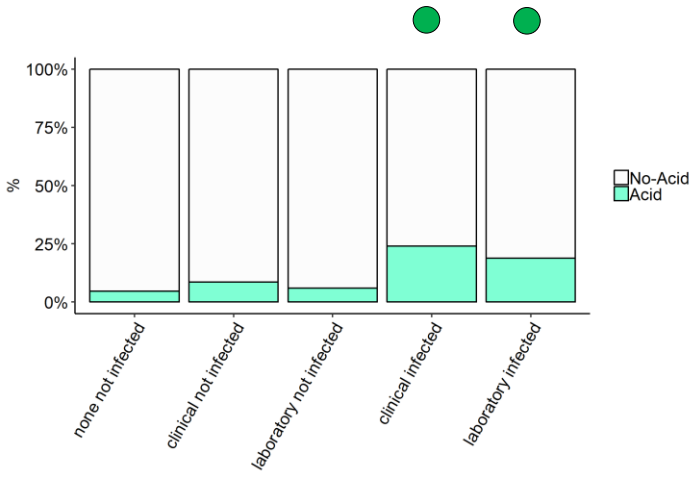


| Contrast | estimate | SE | p.value |
|---|---|---|---|
| none not infected-clinical not infected | -0.5354 | 0.4509 | 0.3761 |
| none not infected-laboratory not infected | -0.485 | 0.5275 | 0.4771 |
| none not infected-clinical infected | -1.8155 | 0.4306 | 1e-04 |
| none not infected-laboratory infected | -1.8084 | 0.4605 | 2e-04 |
| clinical not infected-laboratory not infected | 0.0504 | 0.4028 | 0.9796 |
| clinical infected-laboratory infected | 0.0071 | 0.2774 | 0.9796 |
| clinical not infected-clinical infected | -1.2801 | 0.2035 | 0 |
| laboratory not infected-laboratory infected | -1.3234 | 0.3381 | 2e-04 |

OBSERVATIONS

At 24 h p.i. none of the category is blocking the acidification of the phagolysosomes. However, despite an increase in the acidification of the phagolysosomes was observed, the number of macrophages displaying such acidification was found generally low (<25%).

Acidification of phagolysosomes observed

Acidification of phagolysosomes not observed (blocked)

Acidification trend observed, stastically not significant

**Grouping: Lab adaptation**

**M1 – 24 h p.i.**

c) Effective MOI

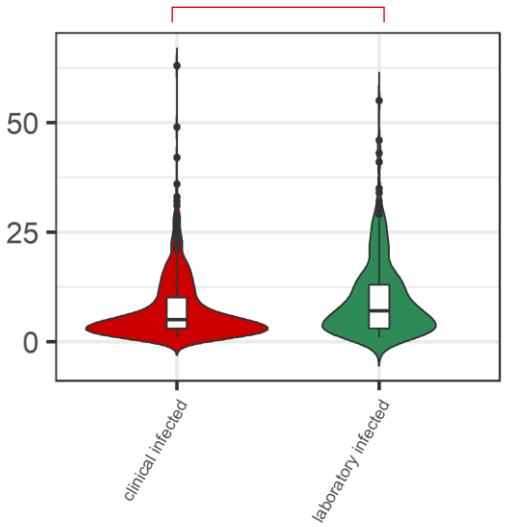


| Par | Value | Std.Error | p.value |
|---|---|---|---|
| (Intercept) | 1.5888 | 0.1164 | 0 |
| grouplaboratory infected | 0.2835 | 0.1099 | 0.0122 |

| Contrast | estimate | SE | p.value |
|---|---|---|---|
| clinical infected - laboratory infected | -0.2835 | 0.1099 | 0.0122 |

d) Colocalization Index

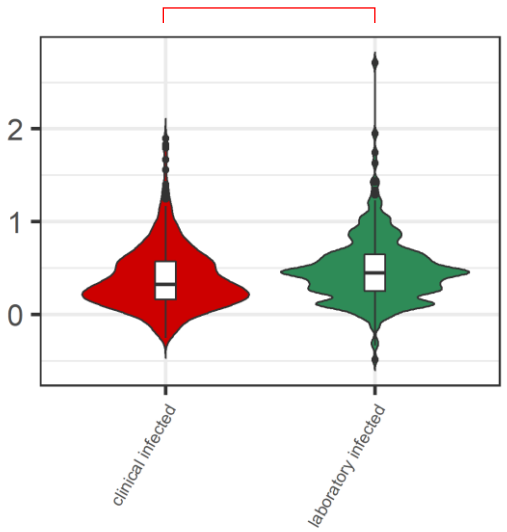


| Par | Value | Std.Error | p.value |
|---|---|---|---|
| (Intercept) | -0.1587 | 0.08 | 0.0478 |
| grouplaboratory infected | 0.4017 | 0.1017 | 2e-04 |

| Contrast | estimate | SE | p.value |
|---|---|---|---|
| clinical infected - laboratory infected | -0.4017 | 0.1017 | 2e-04 |

OBSERVATIONS

Laboratory strains showed higher MOI values. Colocalization with acidified compartments was higher for laboratory strains.

**Grouping: Lab adaptation**

**M2 – 6 h p.i.**

a) Phagolysosomal acidification

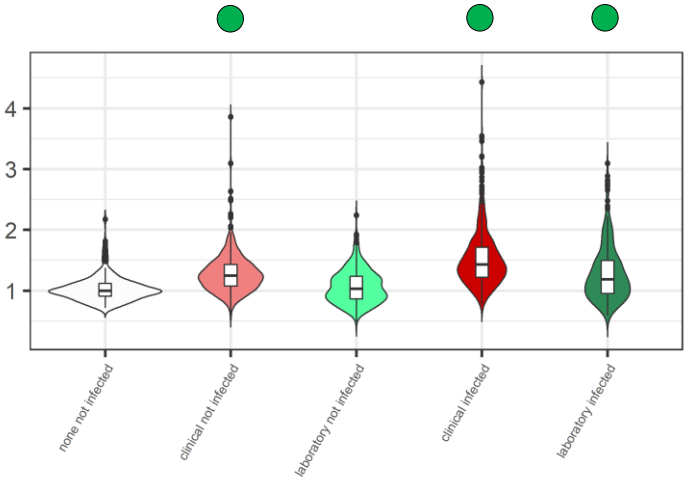


| Par | Value | Std.Error | p.value |
|---|---|---|---|
| (Intercept) | -0.0099 | 0.0439 | 0.8208 |
| groupclinical not infected | 0.1958 | 0.039 | 0 |
| grouplaboratory not infected | 0.0543 | 0.045 | 0.2276 |
| groupclinical infected | 0.3222 | 0.039 | 0 |
| grouplaboratory infected | 0.1888 | 0.0451 | 0 |

| Contrast | estimate | SE | p.value |
|---|---|---|---|
| none not infected-clinical not infected | -0.1958 | 0.039 | 0 |
| none not infected-laboratory not infected | -0.0543 | 0.045 | 0.2276 |
| none not infected-clinical infected | -0.3222 | 0.039 | 0 |
| none not infected-laboratory infected | -0.1888 | 0.0451 | 0 |
| clinical not infected-laboratory not infected | 0.1414 | 0.0437 | 0.0016 |
| clinical infected-laboratory infected | 0.1334 | 0.0438 | 0.0027 |
| clinical not infected-clinical infected | -0.1265 | 0.0095 | 0 |
| laboratory not infected-laboratory infected | -0.1345 | 0.0134 | 0 |

b) Percentage of cells showing acidified phagolysosomes

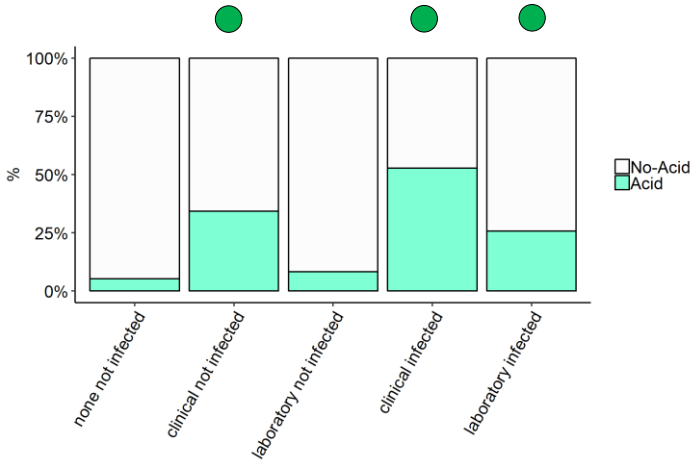


| Par | Estimate | se | OR | pvalue |
|---|---|---|---|---|
| (Intercept) | -3.1627 | 0.5886 | 0.0423 | 0 |
| groupclinical not infected | 1.9879 | 0.5178 | 7.3005 | 1e-04 |
| grouplaboratory not infected | 0.6482 | 0.608 | 1.912 | 0.2864 |
| groupclinical infected | 3.1213 | 0.5166 | 22.6749 | 0 |
| grouplaboratory infected | 2.3513 | 0.5791 | 10.4992 | 0 |

| Contrast | estimate | SE | p.value |
|---|---|---|---|
| none not infected-clinical not infected | -1.9879 | 0.5178 | 2e-04 |
| none not infected-laboratory not infected | -0.6482 | 0.608 | 0.2864 |
| none not infected-clinical infected | -3.1213 | 0.5166 | 0 |
| none not infected-laboratory infected | -2.3513 | 0.5791 | 1e-04 |
| clinical not infected-laboratory not infected | 1.3398 | 0.5031 | 0.0103 |
| clinical infected-laboratory infected | 0.77 | 0.4652 | 0.1119 |
| clinical not infected-clinical infected | -1.1333 | 0.1521 | 0 |
| laboratory not infected-laboratory infected | -1.7031 | 0.2761 | 0 |

OBSERVATIONS

In M2 macrophages, none of the category is blocking the acidification of the phagolysosomes at 6 h p.i.. Whereas the category of clinical strains displayed acidification in 50% of cells, laboratory strains showed acidification in approx. 25% of macrophages.

Acidification of phagolysosomes observed

Acidification of phagolysosomes not observed (blocked)

Acidification trend observed, stastically not significant

**Grouping: Lab adaptation**

**M2 – 6 h p.i.**

c) Effective MOI

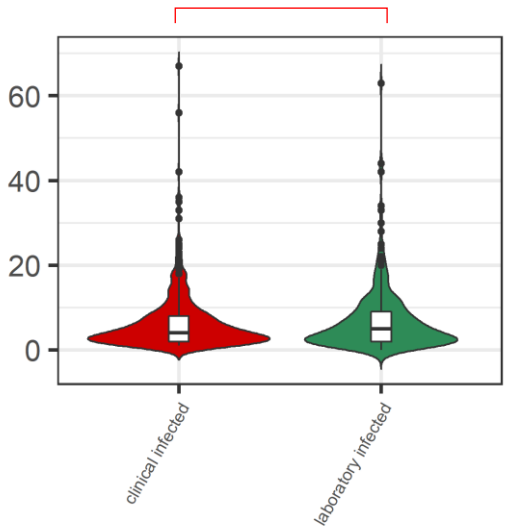


| Par | Value | Std.Error | p.value |
|---|---|---|---|
| (Intercept) | 1.5888 | 0.1164 | 0 |
| grouplaboratory infected | 0.2835 | 0.1099 | 0.0122 |

| Contrast | estimate | SE | p.value |
|---|---|---|---|
| clinical infected - laboratory infected | -0.2835 | 0.1099 | 0.0122 |

d) Colocalization Index

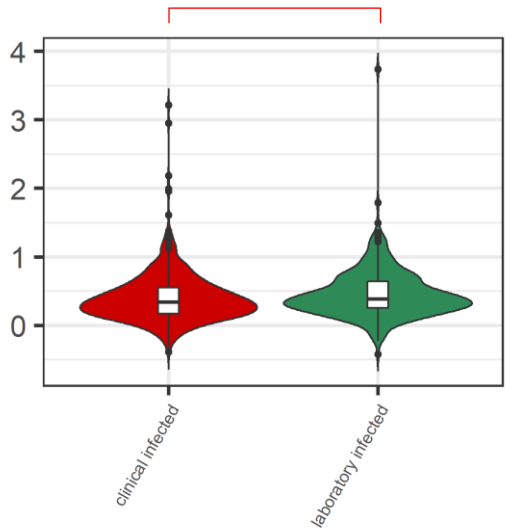


| Par | Value | Std.Error | p.value |
|---|---|---|---|
| (Intercept) | -0.1716 | 0.0503 | 7e-04 |
| grouplaboratory infected | 0.1868 | 0.0671 | 0.0071 |

| Contrast | estimate | SE | p.value |
|---|---|---|---|
| clinical infected - laboratory infected | -0.1868 | 0.0671 | 0.0071 |

OBSERVATIONS

Colocalization with acidified compartments was higher for laboratory strains. Laboratory strains showed higher MOI values.

**Grouping: Lab adaptation**

**M2 – 24 h p.i.**

a) Phagolysosomal acidification

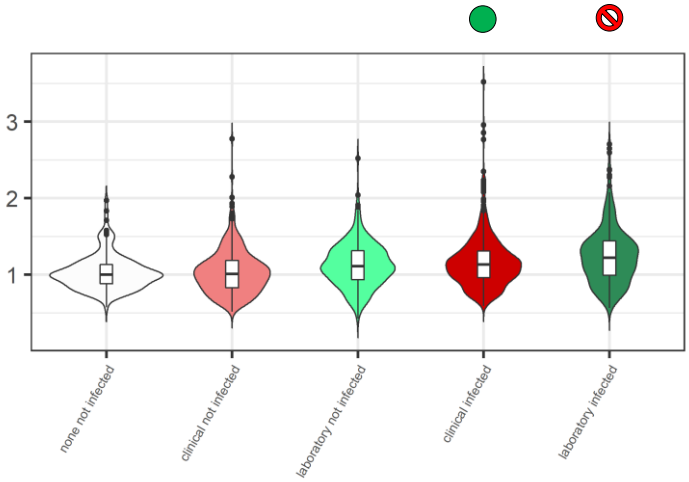


| Par | Value | Std.Error | p.value |
|---|---|---|---|
| (Intercept) | 0.0083 | 0.0569 | 0.8839 |
| groupclinical not infected | -0.0263 | 0.0293 | 0.3689 |
| grouplaboratory not infected | -0.0328 | 0.0349 | 0.348 |
| groupclinical infected | 0.0732 | 0.0292 | 0.0123 |
| grouplaboratory infected | 0.0694 | 0.0344 | 0.0436 |

| Contrast | estimate | SE | p.value |
|---|---|---|---|
| none not infected-clinical not infected | 0.0263 | 0.0293 | 0.4918 |
| none not infected-laboratory not infected | 0.0328 | 0.0349 | 0.4918 |
| none not infected-clinical infected | -0.0732 | 0.0292 | 0.0329 |
| none not infected-laboratory infected | -0.0694 | 0.0344 | 0.0872 |
| clinical not infected-laboratory not infected | 0.0064 | 0.0329 | 0.908 |
| clinical infected-laboratory infected | 0.0037 | 0.0323 | 0.908 |
| clinical not infected-clinical infected | -0.0995 | 0.0117 | 0 |
| laboratory not infected-laboratory infected | -0.1022 | 0.0156 | 0 |

b) Percentage of cells showing acidified phagolysosomes

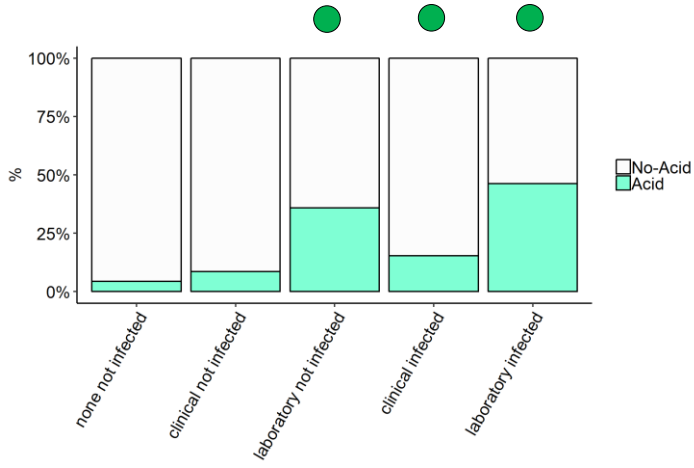


| Par | Estimate | se | OR | pvalue |
|---|---|---|---|---|
| (Intercept) | -3.5886 | 0.6313 | 0.0276 | 0 |
| groupclinical not infected | 0.9306 | 0.4839 | 2.536 | 0.0545 |
| grouplaboratory not infected | 1.5423 | 0.4771 | 4.6754 | 0.0012 |
| groupclinical infected | 1.7192 | 0.4723 | 5.5801 | 3e-04 |
| grouplaboratory infected | 2.3722 | 0.4727 | 10.7213 | 0 |

| Contrast | estimate | SE | p.value |
|---|---|---|---|
| none not infected-clinical not infected | -0.9306 | 0.4839 | 0.0545 |
| none not infected-laboratory not infected | -1.5423 | 0.4771 | 0.002 |
| none not infected-clinical infected | -1.7192 | 0.4723 | 7e-04 |
| none not infected-laboratory infected | -2.3722 | 0.4727 | 0 |
| clinical not infected-laboratory not infected | -0.6117 | 0.295 | 0.0436 |
| clinical infected-laboratory infected | -0.653 | 0.2656 | 0.0186 |
| clinical not infected-clinical infected | -0.7886 | 0.2217 | 8e-04 |
| laboratory not infected-laboratory infected | -0.8299 | 0.2063 | 2e-04 |

OBSERVATIONS

As the infection progresses, laboratory strains are blocking the acidification of the phagolysosomes. In this case, the percentage of macrophages displaying acidification was higher for laboratory strains (40%) compared to causing disease strains (<10%).

- Acidification of phagolysosomes observed
- Acidification of phagolysosomes not observed (blocked)
- Acidification trend observed, stastically not significant

**Grouping: Lab adaptation**

**M2 – 24 h p.i.**

c) Effective MOI

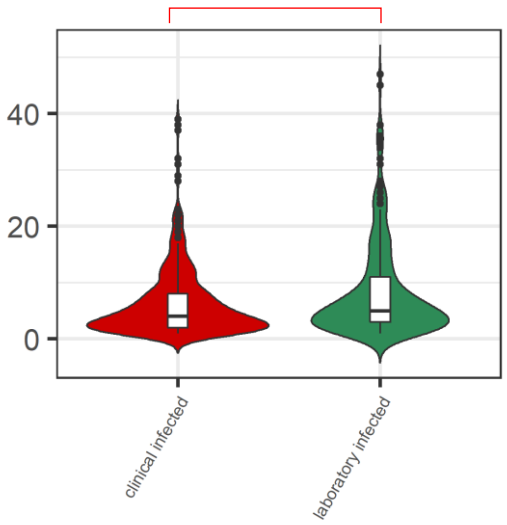


| Par | Value | Std.Error | p.value |
|---|---|---|---|
| (Intercept) | 1.4563 | 0.1233 | 0 |
| grouplaboratory infected | 0.3249 | 0.1199 | 0.0086 |

| Contrast | estimate | SE | p.value |
|---|---|---|---|
| clinical infected - laboratory infected | -0.3249 | 0.1199 | 0.0086 |

d) Colocalization Index

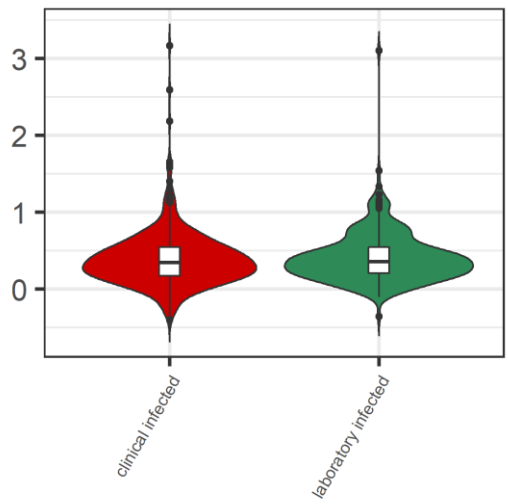


| Par | Value | Std.Error | p.value |
|---|---|---|---|
| (Intercept) | -0.1052 | 0.0513 | 0.0405 |
| grouplaboratory infected | 0.0934 | 0.0761 | 0.2246 |

| Contrast | estimate | SE | p.value |
|---|---|---|---|
| clinical infected - laboratory infected | -0.0934 | 0.0761 | 0.2246 |

OBSERVATIONS

Laboratory strains showed higher MOI values. Colocalization with acidified compartments was similar among all the groups.

**Grouping: Phylogeny**

**M1 – 6 h p.i.**

a) Phagolysosomal acidification

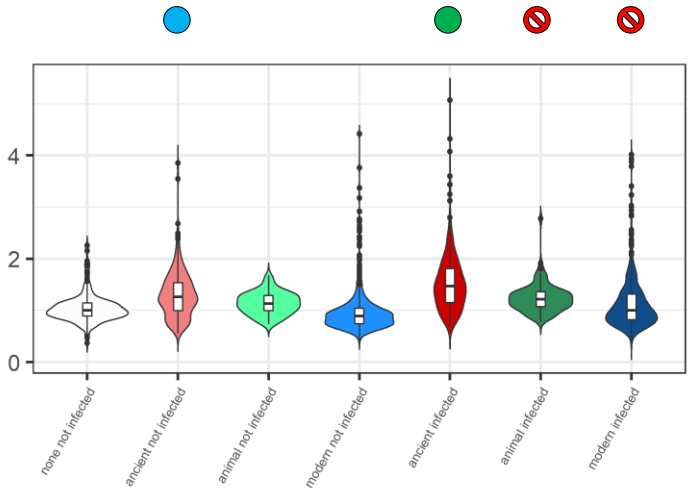


| Par | Value | Std.Error | p.value |
|---|---|---|---|
| (Intercept) | 0.0032 | 0.0766 | 0.9672 |
| groupancient not infected | 0.1108 | 0.059 | 0.0606 |
| groupanimal not infected | -0.0011 | 0.1047 | 0.9914 |
| groupmodern not infected | -0.0159 | 0.0513 | 0.7564 |
| groupancient infected | 0.261 | 0.0591 | 0 |
| groupanimal infected | 0.0641 | 0.1046 | 0.54 |
| groupmodern infected | 0.0963 | 0.0514 | 0.0612 |

| Contrast | estimate | SE | p.value |
|---|---|---|---|
| none not infected-ancient not infected | -0.1108 | 0.059 | 0.102 |
| none not infected-animal not infected | 0.0011 | 0.1047 | 0.9914 |
| none not infected-modern not infected | 0.0159 | 0.0513 | 0.8824 |
| none not infected-ancient infected | -0.261 | 0.0591 | 1e-04 |
| none not infected-animal infected | -0.0641 | 0.1046 | 0.7363 |
| none not infected-modern infected | -0.0963 | 0.0514 | 0.102 |
| ancient not infected-animal not infected | 0.1119 | 0.0996 | 0.3921 |
| ancient not infected-modern not infected | 0.1267 | 0.0576 | 0.0696 |
| animal not infected-modern not infected | 0.0148 | 0.1075 | 0.9542 |
| ancient infected-animal infected | 0.1969 | 0.0996 | 0.102 |
| ancient infected-modern infected | 0.1647 | 0.0577 | 0.0165 |
| animal infected-modern infected | -0.0322 | 0.1074 | 0.8824 |
| ancient not infected-ancient infected | -0.1502 | 0.0143 | 0 |
| animal not infected-animal infected | -0.0653 | 0.0266 | 0.043 |
| modern not infected-modern infected | -0.1122 | 0.0106 | 0 |

b) Percentage of cells showing acidified phagolysosomes

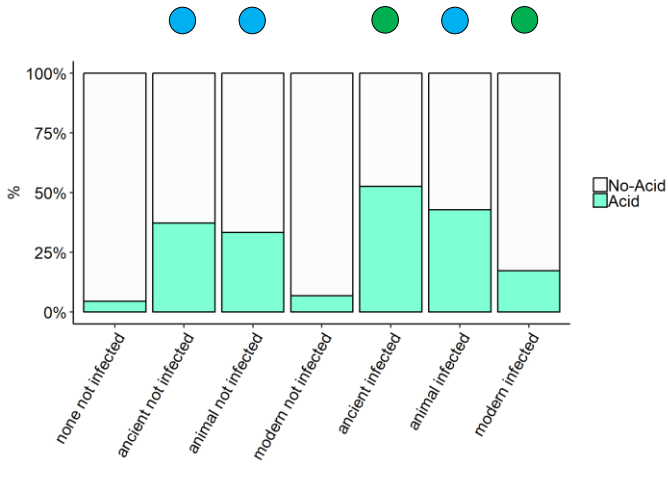


| Par | Estimate | se | OR | pvalue |
|---|---|---|---|---|
| (Intercept) | -3.5696 | 0.8413 | 0.0282 | 0 |
| groupancient not infected | 1.4974 | 0.64 | 4.4702 | 0.0193 |
| groupanimal not infected | 0.6781 | 0.9758 | 1.9702 | 0.4871 |
| groupmodern not infected | 0.176 | 0.6525 | 1.1924 | 0.7874 |
| groupancient infected | 2.6522 | 0.6409 | 14.1849 | 0 |
| groupanimal infected | 1.0873 | 0.9706 | 2.9661 | 0.2626 |
| groupmodern infected | 1.87 | 0.6288 | 6.4882 | 0.0029 |

| Contrast | estimate | SE | p.value |
|---|---|---|---|
| none not infected-ancient not infected | -1.4974 | 0.64 | 0.055 |
| none not infected-animal not infected | -0.6781 | 0.9758 | 0.562 |
| none not infected-modern not infected | -0.176 | 0.6525 | 0.7874 |
| none not infected-ancient infected | -2.6522 | 0.6409 | 2e-04 |
| none not infected-animal infected | -1.0873 | 0.9706 | 0.3939 |
| none not infected-modern infected | -1.87 | 0.6288 | 0.011 |
| ancient not infected-animal not infected | 0.8193 | 0.8766 | 0.4773 |
| ancient not infected-modern not infected | 1.3215 | 0.5769 | 0.055 |
| animal not infected-modern not infected | 0.5022 | 0.9926 | 0.6567 |
| ancient infected-animal infected | 1.5649 | 0.8776 | 0.1598 |
| ancient infected-modern infected | 0.7822 | 0.5522 | 0.2937 |
| animal infected-modern infected | -0.7827 | 0.9736 | 0.5267 |
| ancient not infected-ancient infected | -1.1548 | 0.2261 | 0 |
| animal not infected-animal infected | -0.4091 | 0.3478 | 0.3939 |
| modern not infected-modern infected | -1.694 | 0.286 | 0 |

OBSERVATIONS

In M1 macrophages, animal and modern lineages are blocking the acidification of phagolysosomes at 6 h p.i. Ancient strains also induced acidification in a higher percentage (50%) of cells compared to the other groups.

- Acidification of phagolysosomes observed
- Acidification of phagolysosomes not observed (blocked)
- Acidification trend observed, stastically not significant

**Grouping: Phylogeny**

**M1 – 6 h p.i.**

c) Effective MOI

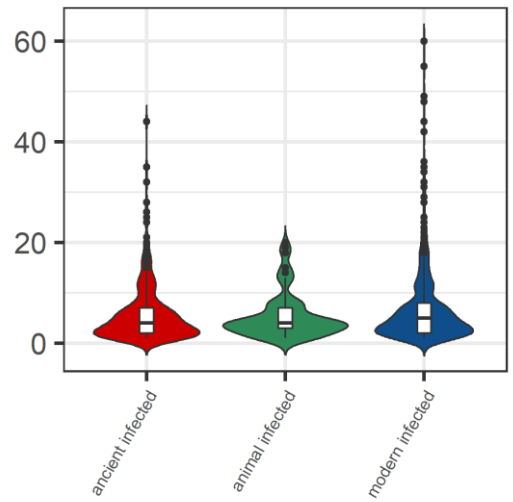


| Par | Value | Std.Error | p.value |
|---|---|---|---|
| (Intercept) | 1.4071 | 0.1117 | 0 |
| groupanimal infected | -0.0237 | 0.2083 | 0.9097 |
| groupmodern infected | 0.0615 | 0.1206 | 0.6117 |

| Contrast | estimate | SE | p.value |
|---|---|---|---|
| ancient infected - animal infected | 0.0237 | 0.2083 | 0.9097 |
| ancient infected - modern infected | -0.0615 | 0.1206 | 0.9097 |
| animal infected - modern infected | -0.0853 | 0.222 | 0.9097 |

d) Colocalization Index

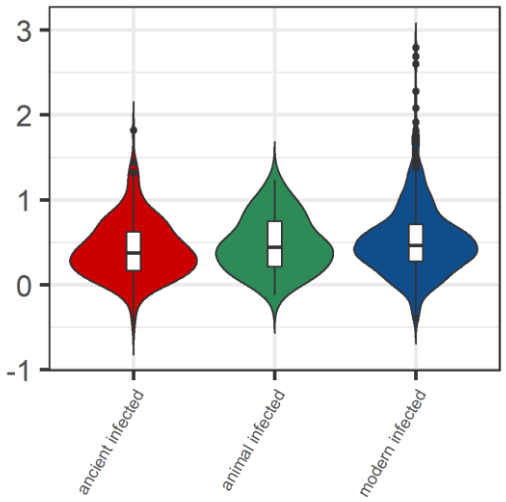


| Par | Value | Std.Error | p.value |
|---|---|---|---|
| (Intercept) | -0.0986 | 0.0866 | 0.2548 |
| groupanimal infected | 0.1444 | 0.1671 | 0.3907 |
| groupmodern infected | 0.2167 | 0.0979 | 0.0306 |

| Contrast | estimate | SE | p.value |
|---|---|---|---|
| ancient infected - animal infected | -0.1444 | 0.1671 | 0.5861 |
| ancient infected - modern infected | -0.2167 | 0.0979 | 0.0917 |
| animal infected - modern infected | -0.0723 | 0.1745 | 0.6801 |

OBSERVATIONS

Colocalization with acidified compartments was similar among all the groups.

**Grouping: Phylogeny**

**M1 – 24 h p.i.**

a) Phagolysosomal acidification

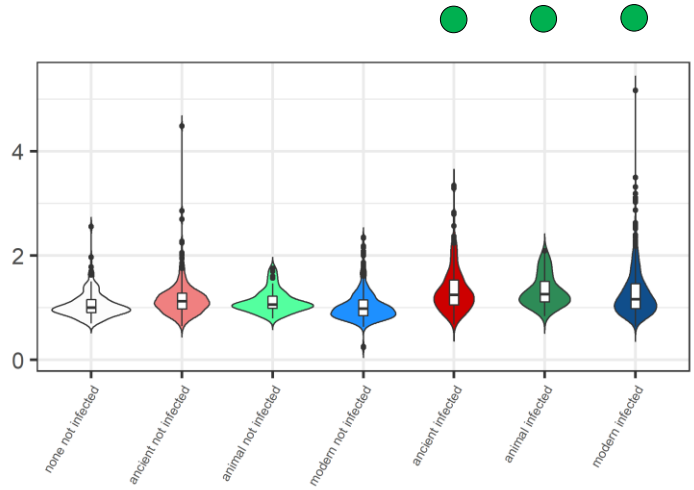


| Par | Value | Std.Error | p.value |
|---|---|---|---|
| (Intercept) | 0.0087 | 0.0431 | 0.8401 |
| groupancient not infected | 0.0315 | 0.0331 | 0.3422 |
| groupanimal not infected | 0.0434 | 0.0571 | 0.4478 |
| groupmodern not infected | 0.0117 | 0.0303 | 0.6992 |
| groupancient infected | 0.142 | 0.0332 | 0 |
| groupanimal infected | 0.2007 | 0.0548 | 3e-04 |
| groupmodern infected | 0.1799 | 0.0299 | 0 |

| Contrast | estimate | SE | p.value |
|---|---|---|---|
| none not infected-ancient not infected | -0.0315 | 0.0331 | 0.5703 |
| none not infected-animal not infected | -0.0434 | 0.0571 | 0.6718 |
| none not infected-modern not infected | -0.0117 | 0.0303 | 0.76 |
| none not infected-ancient infected | -0.142 | 0.0332 | 1e-04 |
| none not infected-animal infected | -0.2007 | 0.0548 | 6e-04 |
| none not infected-modern infected | -0.1799 | 0.0299 | 0 |
| ancient not infected-animal not infected | -0.0119 | 0.0538 | 0.8247 |
| ancient not infected-modern not infected | 0.0198 | 0.0313 | 0.7202 |
| animal not infected-modern not infected | 0.0317 | 0.0582 | 0.7328 |
| ancient infected-animal infected | -0.0587 | 0.0515 | 0.4769 |
| ancient infected-modern infected | -0.0379 | 0.031 | 0.4755 |
| animal infected-modern infected | 0.0208 | 0.0557 | 0.76 |
| ancient not infected-ancient infected | -0.1105 | 0.0181 | 0 |
| animal not infected-animal infected | -0.1573 | 0.036 | 0 |
| modern not infected-modern infected | -0.1682 | 0.0146 | 0 |

b) Percentage of cells showing acidified phagolysosomes

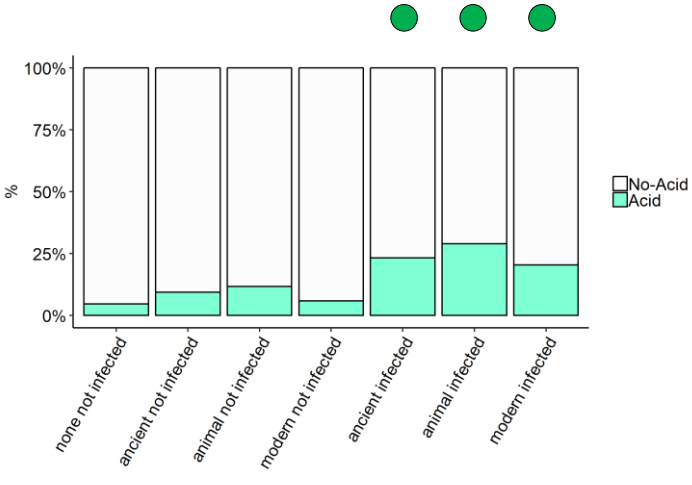


| Par | Estimate | se | OR | pvalue |
|---|---|---|---|---|
| (Intercept) | -3.1891 | 0.4578 | 0.0412 | 0 |
| groupancient not infected | 0.5115 | 0.4775 | 1.6678 | 0.284 |
| groupanimal not infected | 0.8163 | 0.6713 | 2.2622 | 0.224 |
| groupmodern not infected | 0.4505 | 0.4799 | 1.569 | 0.3479 |
| groupancient infected | 1.6627 | 0.4509 | 5.2737 | 2e-04 |
| groupanimal infected | 1.9547 | 0.569 | 7.0621 | 6e-04 |
| groupmodern infected | 1.8919 | 0.4403 | 6.6322 | 0 |

| Contrast | estimate | SE | p.value |
|---|---|---|---|
| none not infected-ancient not infected | -0.5115 | 0.4775 | 0.5325 |
| none not infected-animal not infected | -0.8163 | 0.6713 | 0.4799 |
| none not infected-modern not infected | -0.4505 | 0.4799 | 0.5798 |
| none not infected-ancient infected | -1.6627 | 0.4509 | 8e-04 |
| none not infected-animal infected | -1.9547 | 0.569 | 0.0018 |
| none not infected-modern infected | -1.8919 | 0.4403 | 1e-04 |
| ancient not infected-animal not infected | -0.3048 | 0.5788 | 0.6905 |
| ancient not infected-modern not infected | 0.0611 | 0.3735 | 0.8945 |
| animal not infected-modern not infected | 0.3659 | 0.6218 | 0.6905 |
| ancient infected-animal infected | -0.292 | 0.4286 | 0.676 |
| ancient infected-modern infected | -0.2292 | 0.2814 | 0.6231 |
| animal infected-modern infected | 0.0628 | 0.4737 | 0.8945 |
| ancient not infected-ancient infected | -1.1512 | 0.2683 | 1e-04 |
| animal not infected-animal infected | -1.1384 | 0.5062 | 0.0613 |
| modern not infected-modern infected | -1.4415 | 0.2592 | 0 |

OBSERVATIONS

At 24 h p.i. none of the category is blocking the acidification of the phagolysosomes. However, despite an increase in the acidification of the phagolysosomes was observed, the number of macrophages displaying such acidification was found generally low (25%).

Acidification of phagolysosomes observed

Acidification of phagolysosomes not observed (blocked)

Acidification trend observed, stastically not significant

**Grouping: Phylogeny**

**M1 – 24 h p.i.**

c) Effective MOI

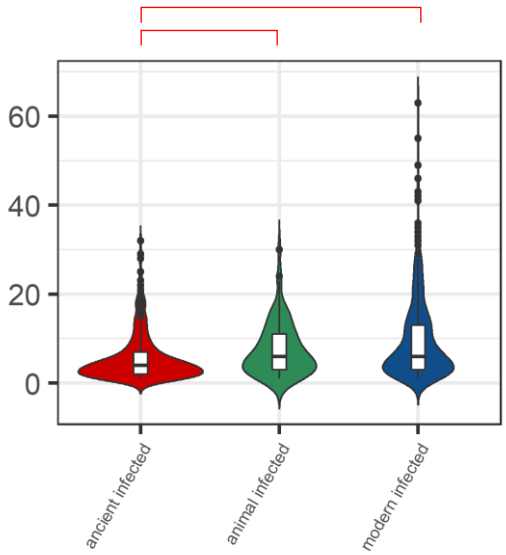


| Par | Value | Std.Error | p.value |
|---|---|---|---|
| (Intercept) | 1.4813 | 0.1278 | 0 |
| groupanimal infected | 0.4699 | 0.1713 | 0.008 |
| groupmodern infected | 0.2946 | 0.1056 | 0.007 |

| Contrast | estimate | SE | p.value |
|---|---|---|---|
| ancient infected - animal infected | -0.4699 | 0.1713 | 0.012 |
| ancient infected - modern infected | -0.2946 | 0.1056 | 0.012 |
| animal infected - modern infected | 0.1752 | 0.1954 | 0.3733 |

d) Colocalization Index

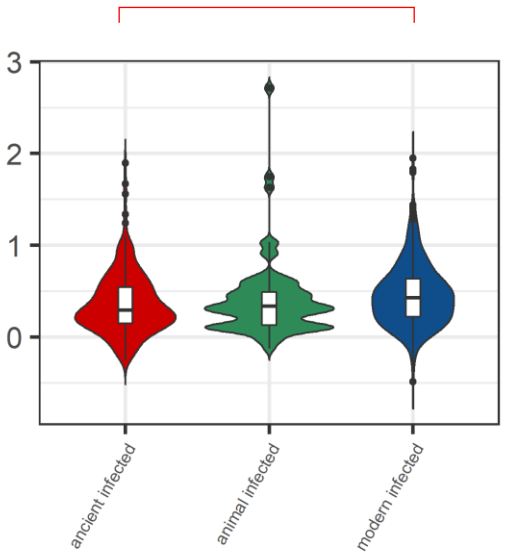


| Par | Value | Std.Error | p.value |
|---|---|---|---|
| (Intercept) | -0.1795 | 0.0799 | 0.0251 |
| groupanimal infected | 0.0118 | 0.1634 | 0.9427 |
| groupmodern infected | 0.2982 | 0.0973 | 0.0032 |

| Contrast | estimate | SE | p.value |
|---|---|---|---|
| ancient infected - animal infected | -0.0118 | 0.1634 | 0.9427 |
| ancient infected - modern infected | -0.2982 | 0.0973 | 0.0097 |
| animal infected - modern infected | -0.2864 | 0.1623 | 0.124 |

OBSERVATIONS

Colocalization with acidified compartments was found higher for modern lineages strains. Also, ancient lineages showed lower MOI compared to the other categories.

**Grouping: Phylogeny**

**M2 – 6 h p.i.**

a) Phagolysosomal acidification

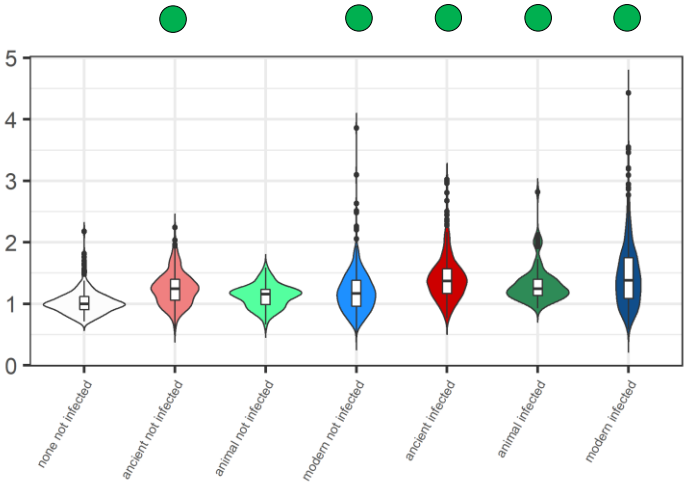


| Par | Value | Std.Error | p.value |
|---|---|---|---|
| (Intercept) | -0.0101 | 0.0525 | 0.8478 |
| groupancient not infected | 0.1614 | 0.0472 | 6e-04 |
| groupanimal not infected | 0.1094 | 0.0831 | 0.1883 |
| groupmodern not infected | 0.1363 | 0.0405 | 8e-04 |
| groupancient infected | 0.2705 | 0.0473 | 0 |
| groupanimal infected | 0.216 | 0.083 | 0.0093 |
| groupmodern infected | 0.2824 | 0.0405 | 0 |

| Contrast | estimate | SE | p.value |
|---|---|---|---|
| none not infected-ancient not infected | -0.1614 | 0.0472 | 0.0016 |
| none not infected-animal not infected | -0.1094 | 0.0831 | 0.3138 |
| none not infected-modern not infected | -0.1363 | 0.0405 | 0.0017 |
| none not infected-ancient infected | -0.2705 | 0.0473 | 0 |
| none not infected-animal infected | -0.216 | 0.083 | 0.0174 |
| none not infected-modern infected | -0.2824 | 0.0405 | 0 |
| ancient not infected-animal not infected | 0.052 | 0.0792 | 0.6389 |
| ancient not infected-modern not infected | 0.0252 | 0.0455 | 0.6697 |
| animal not infected-modern not infected | -0.0269 | 0.0848 | 0.794 |
| ancient infected-animal infected | 0.0544 | 0.079 | 0.6389 |
| ancient infected-modern infected | -0.0119 | 0.0456 | 0.794 |
| animal infected-modern infected | -0.0663 | 0.0846 | 0.6389 |
| ancient not infected-ancient infected | -0.109 | 0.0139 | 0 |
| animal not infected-animal infected | -0.1066 | 0.0264 | 2e-04 |
| modern not infected-modern infected | -0.1461 | 0.01 | 0 |

b) Percentage of cells showing acidified phagolysosomes

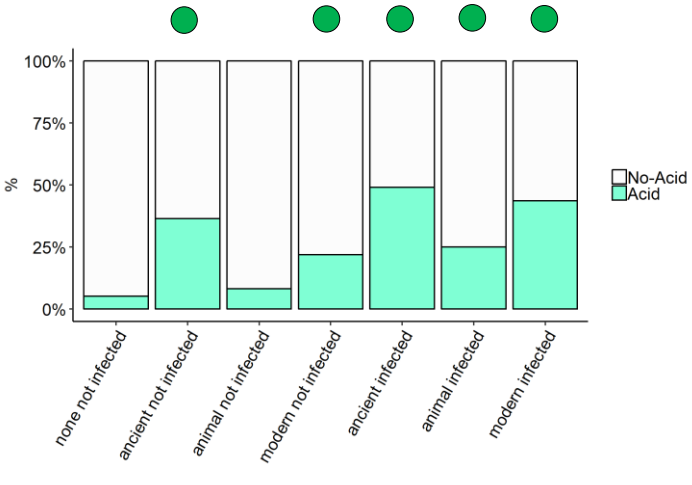


| Par | Estimate | se | OR | pvalue |
|---|---|---|---|---|
| (Intercept) | -3.208 | 0.6462 | 0.0404 | 0 |
| groupancient not infected | 1.9331 | 0.572 | 6.9106 | 7e-04 |
| groupanimal not infected | 0.6619 | 0.9518 | 1.9385 | 0.4868 |
| groupmodern not infected | 1.5069 | 0.5249 | 4.5128 | 0.0041 |
| groupancient infected | 2.816 | 0.572 | 16.7104 | 0 |
| groupanimal infected | 2.0926 | 0.882 | 8.1062 | 0.0177 |
| groupmodern infected | 2.978 | 0.5202 | 19.6488 | 0 |

| Contrast | estimate | SE | p.value |
|---|---|---|---|
| none not infected-ancient not infected | -1.9331 | 0.572 | 0.0022 |
| none not infected-animal not infected | -0.6619 | 0.9518 | 0.5216 |
| none not infected-modern not infected | -1.5069 | 0.5249 | 0.0102 |
| none not infected-ancient infected | -2.816 | 0.572 | 0 |
| none not infected-animal infected | -2.0926 | 0.882 | 0.0331 |
| none not infected-modern infected | -2.978 | 0.5202 | 0 |
| ancient not infected-animal not infected | 1.2712 | 0.8495 | 0.2243 |
| ancient not infected-modern not infected | 0.4261 | 0.4678 | 0.4181 |
| animal not infected-modern not infected | -0.845 | 0.9196 | 0.4181 |
| ancient infected-animal infected | 0.7234 | 0.7688 | 0.4181 |
| ancient infected-modern infected | -0.162 | 0.4623 | 0.7261 |
| animal infected-modern infected | -0.8854 | 0.8444 | 0.4181 |
| ancient not infected-ancient infected | -0.883 | 0.2261 | 4e-04 |
| animal not infected-animal infected | -1.4307 | 0.5082 | 0.0104 |
| modern not infected-modern infected | -1.4711 | 0.173 | 0 |

OBSERVATIONS

In M2 macrophages, none of the category is blocking the acidification of the phagolysosomes at 6 h p.i. and between 25% (animal) and 50% (ancient, modern) of macrophages showed acidification.

Acidification of phagolysosomes observed

Acidification of phagolysosomes not observed (blocked)

Acidification trend observed, stastically not significant

**Grouping: Phylogeny**

**M2 – 6 h p.i.**

c) Effective MOI

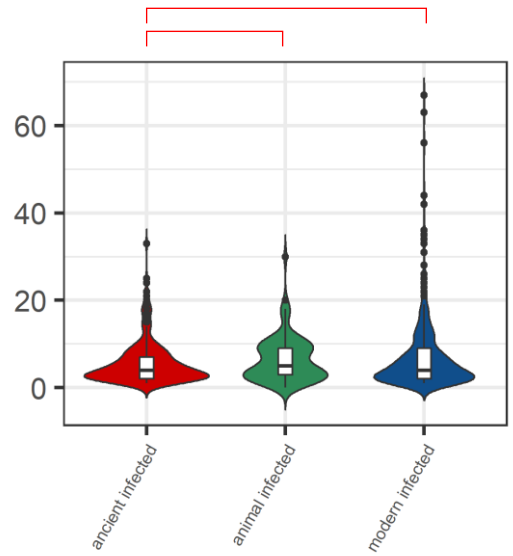


| Par | Value | Std.Error | p.value |
|---|---|---|---|
| (Intercept) | 1.4813 | 0.1278 | 0 |
| groupanimal infected | 0.4699 | 0.1713 | 0.008 |
| groupmodern infected | 0.2946 | 0.1056 | 0.007 |

| Contrast | estimate | SE | p.value |
|---|---|---|---|
| ancient infected - animal infected | -0.4699 | 0.1713 | 0.012 |
| ancient infected - modern infected | -0.2946 | 0.1056 | 0.012 |
| animal infected - modern infected | 0.1752 | 0.1954 | 0.3733 |

d) Colocalization Index

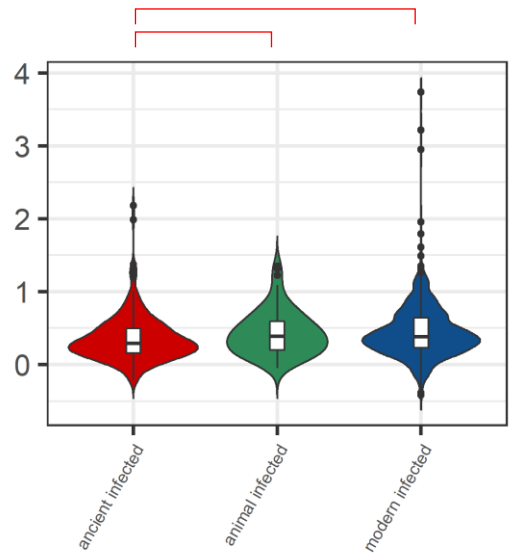


| Par | Value | Std.Error | p.value |
|---|---|---|---|
| (Intercept) | -0.2813 | 0.0575 | 0 |
| groupanimal infected | 0.2535 | 0.1085 | 0.0227 |
| groupmodern infected | 0.2415 | 0.0643 | 4e-04 |

| Contrast | estimate | SE | p.value |
|---|---|---|---|
| ancient infected - animal infected | -0.2535 | 0.1085 | 0.0341 |
| ancient infected - modern infected | -0.2415 | 0.0643 | 0.0012 |
| animal infected - modern infected | 0.0119 | 0.1124 | 0.9156 |

OBSERVATIONS

Ancient lineages showed lower MOI compared to the other categories. Colocalization with acidified compartments was found lower for ancient lineages strains.

**Grouping: Phylogeny**

**M2 – 24 h p.i.**

a) Phagolysosomal acidification

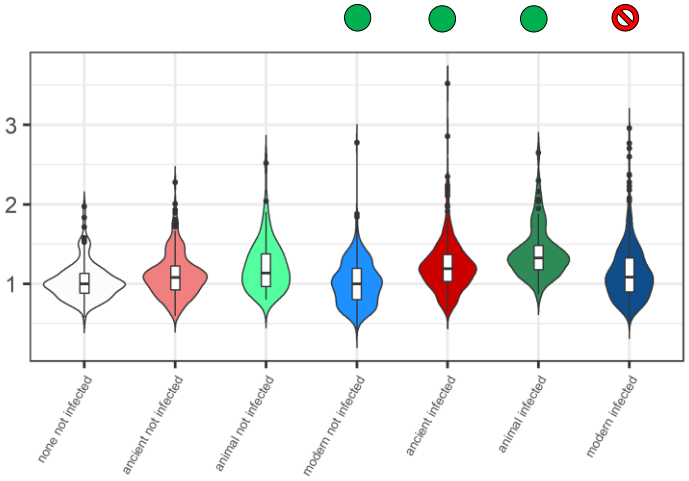


| Par | Value | Std.Error | p.value |
|---|---|---|---|
| (Intercept) | 0.0119 | 0.053 | 0.8229 |
| groupancient not infected | 0.0204 | 0.0317 | 0.519 |
| groupanimal not infected | 0.0679 | 0.0534 | 0.2033 |
| groupmodern not infected | -0.0721 | 0.0289 | 0.0126 |
| groupancient infected | 0.121 | 0.0317 | 1e-04 |
| groupanimal infected | 0.2187 | 0.0528 | 0 |
| groupmodern infected | 0.0273 | 0.0285 | 0.3386 |

| Contrast | estimate | SE | p.value |
|---|---|---|---|
| none not infected-ancient not infected | -0.0204 | 0.0317 | 0.519 |
| none not infected-animal not infected | -0.0679 | 0.0534 | 0.2542 |
| none not infected-modern not infected | 0.0721 | 0.0289 | 0.0189 |
| none not infected-ancient infected | -0.121 | 0.0317 | 4e-04 |
| none not infected-animal infected | -0.2187 | 0.0528 | 1e-04 |
| none not infected-modern infected | -0.0273 | 0.0285 | 0.3651 |
| ancient not infected-animal not infected | -0.0475 | 0.0499 | 0.3651 |
| ancient not infected-modern not infected | 0.0925 | 0.0299 | 0.0038 |
| animal not infected-modern not infected | 0.14 | 0.0545 | 0.0172 |
| ancient infected-animal infected | -0.0977 | 0.0492 | 0.0645 |
| ancient infected-modern infected | 0.0937 | 0.0297 | 0.0035 |
| animal infected-modern infected | 0.1914 | 0.0538 | 0.001 |
| ancient not infected-ancient infected | -0.1006 | 0.0157 | 0 |
| animal not infected-animal infected | -0.1508 | 0.0293 | 0 |
| modern not infected-modern infected | -0.0994 | 0.0127 | 0 |

b) Percentage of cells showing acidified phagolysosomes

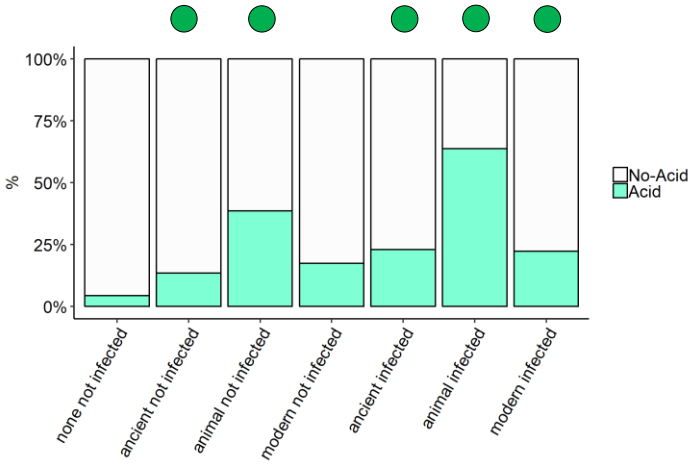


| Par | Estimate | se | OR | pvalue |
|---|---|---|---|---|
| (Intercept) | -3.5319 | 0.6429 | 0.0292 | 0 |
| groupancient not infected | 1.3448 | 0.5089 | 3.8376 | 0.0082 |
| groupanimal not infected | 1.8666 | 0.5611 | 6.4663 | 9e-04 |
| groupmodern not infected | 0.9158 | 0.5047 | 2.4987 | 0.0696 |
| groupancient infected | 2.0863 | 0.495 | 8.0549 | 0 |
| groupanimal infected | 2.8936 | 0.5554 | 18.0578 | 0 |
| groupmodern infected | 1.6916 | 0.4911 | 5.4284 | 6e-04 |

| Contrast | estimate | SE | p.value |
|---|---|---|---|
| none not infected-ancient not infected | -1.3448 | 0.5089 | 0.0137 |
| none not infected-animal not infected | -1.8666 | 0.5611 | 0.0026 |
| none not infected-modern not infected | -0.9158 | 0.5047 | 0.087 |
| none not infected-ancient infected | -2.0863 | 0.495 | 2e-04 |
| none not infected-animal infected | -2.8936 | 0.5554 | 0 |
| none not infected-modern infected | -1.6916 | 0.4911 | 0.0026 |
| ancient not infected-animal not infected | -0.5218 | 0.3587 | 0.1682 |
| ancient not infected-modern not infected | 0.4291 | 0.3725 | 0.2494 |
| animal not infected-modern not infected | 0.9508 | 0.4641 | 0.0552 |
| ancient infected-animal infected | -0.8073 | 0.3397 | 0.0262 |
| ancient infected-modern infected | 0.3946 | 0.3171 | 0.2285 |
| animal infected-modern infected | 1.2019 | 0.4349 | 0.0107 |
| ancient not infected-ancient infected | -0.7414 | 0.247 | 0.0058 |
| animal not infected-animal infected | -1.027 | 0.3393 | 0.0058 |
| modern not infected-modern infected | -0.7759 | 0.2306 | 0.0026 |

OBSERVATIONS

As the infection progresses, modern strains are blocking the acidification of the phagolysosomes. The percentage of acidified cells for these categories dropped below 25%, whereas animal strains induced acidification of phagolysosomes in more than 60% of macrophages.

- Acidification of phagolysosomes observed
- Acidification of phagolysosomes not observed (blocked)
- Acidification trend observed, stastically not significant

**Grouping: Phylogeny**

**M2 – 24 h p.i.**

c) Effective MOI

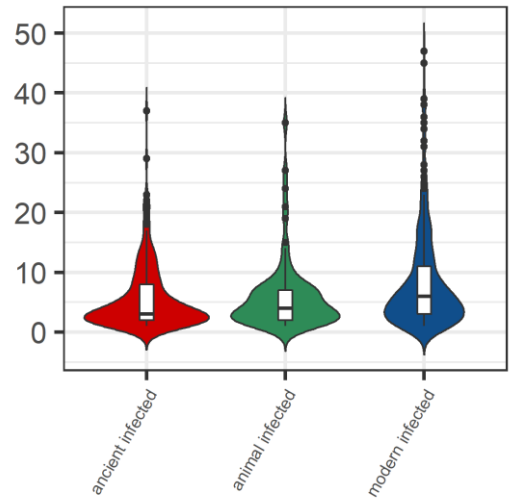


| Par | Value | Std.Error | p.value |
|---|---|---|---|
| (Intercept) | 1.4013 | 0.1241 | 0 |
| groupanimal infected | 0.1285 | 0.1929 | 0.508 |
| groupmodern infected | 0.2535 | 0.1182 | 0.0359 |

| Contrast | estimate | SE | p.value |
|---|---|---|---|
| ancient infected - animal infected | -0.1285 | 0.1929 | 0.5652 |
| ancient infected - modern infected | -0.2535 | 0.1182 | 0.1076 |
| animal infected - modern infected | -0.1251 | 0.2163 | 0.5652 |

d) Colocalization Index

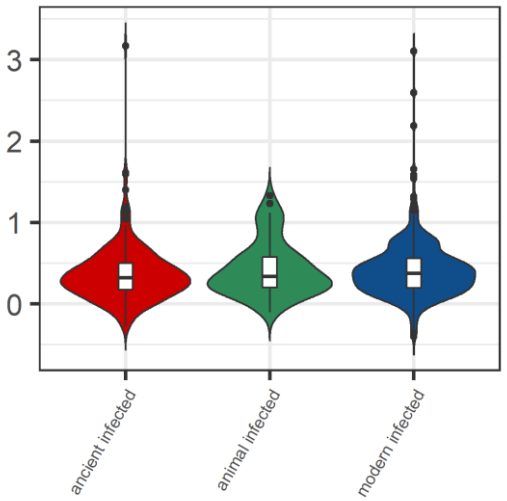


| Par | Value | Std.Error | p.value |
|---|---|---|---|
| (Intercept) | -0.1895 | 0.061 | 0.002 |
| groupanimal infected | 0.2084 | 0.1193 | 0.0857 |
| groupmodern infected | 0.1631 | 0.0733 | 0.0298 |

| Contrast | estimate | SE | p.value |
|---|---|---|---|
| ancient infected - animal infected | -0.2084 | 0.1193 | 0.1285 |
| ancient infected - modern infected | -0.1631 | 0.0733 | 0.0895 |
| animal infected - modern infected | 0.0453 | 0.1231 | 0.7143 |

OBSERVATIONS

Differences in the MOI were cleared, even though modern strains showed higher MOI distribution. Colocalization with acidified compartments was similar among all the groups.

## Grouping: Sample

## M1 – 6 h p.i.

a) Phagolysosomal acidification

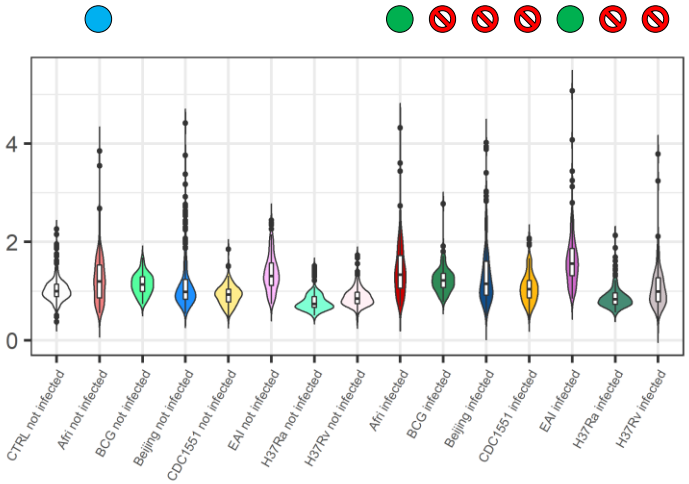


b) Percentage of cells showing acidified phagolysosomes

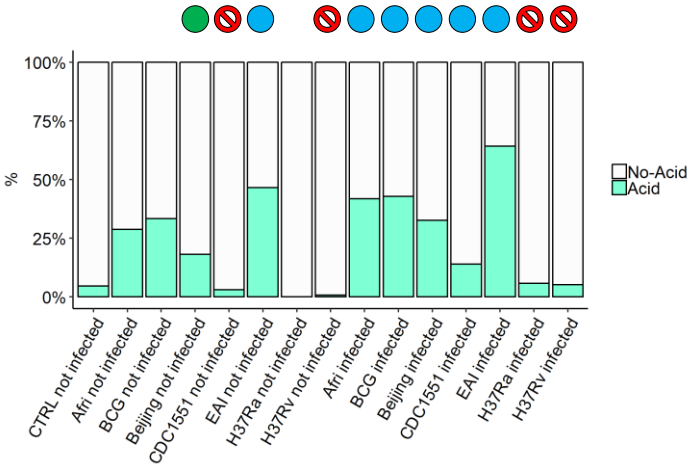


| Par | Value | Std.Error | p.value |
|---|---|---|---|
| (Intercept) | 0.0058 | 0.0668 | 0.9308 |
| groupAfri not infected | 0.1237 | 0.0695 | 0.0754 |
| groupBCG not infected | 0.0317 | 0.1052 | 0.7631 |
| groupBeijing not infected | 0.0952 | 0.0641 | 0.1379 |
| groupCDC1551 not infected | -0.0414 | 0.0774 | 0.5923 |
| groupEAI not infected | 0.1613 | 0.075 | 0.0315 |
| groupH37Ra not infected | -0.1934 | 0.0796 | 0.0152 |
| groupH37Rv not infected | -0.0723 | 0.0801 | 0.3668 |
| groupAfri infected | 0.2767 | 0.0697 | 1e-04 |
| groupBCG infected | 0.097 | 0.1051 | 0.3562 |
| groupBeijing infected | 0.2043 | 0.064 | 0.0014 |
| groupCDC1551 infected | 0.1113 | 0.0776 | 0.1516 |
| groupEAI infected | 0.3083 | 0.0752 | 0 |
| groupH37Ra infected | -0.112 | 0.08 | 0.1614 |
| groupH37Rv infected | 0.0413 | 0.0806 | 0.6083 |

| Par | Estimate | se | OR | pvalue |
|---|---|---|---|---|
| (Intercept) | -3.505 | 0.7631 | 0.03 | 0 |
| groupAfri not infected | 1.8572 | 0.7306 | 6.4057 | 0.011 |
| groupBCG not infected | 0.8416 | 0.9631 | 2.32 | 0.3822 |
| groupBeijing not infected | 1.1595 | 0.7357 | 3.1882 | 0.115 |
| groupCDC1551 not infected | 0.1986 | 0.9662 | 1.2197 | 0.8371 |
| groupEAI not infected | 1.7238 | 0.7466 | 5.6058 | 0.021 |
| groupH37Ra not infected | -14.8469 | 583.2223 | 0 | 0.9797 |
| groupH37Rv not infected | -1.2751 | 1.3749 | 0.2794 | 0.3537 |
| groupAfri infected | 2.998 | 0.7254 | 20.046 | 0 |
| groupBCG infected | 1.25 | 0.9578 | 3.4903 | 0.1919 |
| groupBeijing infected | 2.6757 | 0.7166 | 14.5219 | 2e-04 |
| groupCDC1551 infected | 1.9659 | 0.8611 | 7.1411 | 0.0224 |
| groupEAI infected | 2.8677 | 0.7499 | 17.5963 | 1e-04 |
| groupH37Ra infected | 0.8593 | 0.9051 | 2.3614 | 0.3424 |
| groupH37Rv infected | 0.723 | 1.0227 | 2.0606 | 0.4796 |

| Contrast | estimate | SE | p.value |
|---|---|---|---|
| none not infected-Afri not infected | -0.1295 | 0.079 | 0.2473 |
| none not infected-BCG not infected | -0.0375 | 0.1119 | 0.7622 |
| none not infected-Beijing not infected | -0.101 | 0.0743 | 0.3244 |
| none not infected-CDC1551 not infected | 0.0356 | 0.086 | 0.7407 |
| none not infected-EAI not infected | -0.1671 | 0.084 | 0.1734 |
| none not infected-H37Ra not infected | 0.1876 | 0.0873 | 0.1516 |
| none not infected-H37Rv not infected | 0.0665 | 0.0877 | 0.5734 |
| none not infected-Afri infected | -0.2825 | 0.0791 | 0.0403 |
| none not infected-BCG infected | -0.1028 | 0.1118 | 0.5209 |
| none not infected-Beijing infected | -0.2101 | 0.0742 | 0.0799 |
| none not infected-CDC1551 infected | -0.1171 | 0.0862 | 0.3244 |
| none not infected-EAI infected | -0.3141 | 0.0842 | 0.0356 |
| none not infected-H37Ra infected | 0.1062 | 0.0877 | 0.3793 |
| none not infected-H37Rv infected | -0.0471 | 0.0882 | 0.6986 |
| Afri not infected-BCG not infected | 0.092 | 0.1167 | 0.5427 |
| Afri not infected-Beijing not infected | 0.0285 | 0.0724 | 0.7407 |
| Afri not infected-CDC1551 not infected | 0.1651 | 0.0858 | 0.1334 |
| Afri not infected-EAI not infected | -0.0376 | 0.0853 | 0.7315 |
| Afri not infected-H37Ra not infected | 0.317 | 0.0932 | 0.0039 |
| Afri not infected-H37Rv not infected | 0.196 | 0.096 | 0.1135 |
| BCG not infected-Beijing not infected | -0.0635 | 0.1143 | 0.6752 |
| BCG not infected-CDC1551 not infected | 0.0732 | 0.1243 | 0.6612 |
| BCG not infected-EAI not infected | -0.1296 | 0.0989 | 0.3074 |
| BCG not infected-H37Ra not infected | 0.2251 | 0.1265 | 0.1585 |
| BCG not infected-H37Rv not infected | 0.104 | 0.127 | 0.5422 |
| Beijing not infected-CDC1551 not infected | 0.1366 | 0.0802 | 0.1734 |
| Beijing not infected-EAI not infected | -0.0662 | 0.0827 | 0.5427 |
| Beijing not infected-H37Ra not infected | 0.2885 | 0.0891 | 0.0064 |
| Beijing not infected-H37Rv not infected | 0.1674 | 0.0895 | 0.1436 |
| CDC1551 not infected-EAI not infected | -0.2028 | 0.098 | 0.1106 |
| CDC1551 not infected-H37Ra not infected | 0.1519 | 0.0968 | 0.2102 |
| CDC1551 not infected-H37Rv not infected | 0.0308 | 0.0968 | 0.7622 |
| EAI not infected-H37Ra not infected | 0.3547 | 0.1017 | 0.0035 |
| EAI not infected-H37Rv not infected | 0.2336 | 0.1025 | 0.0754 |
| H37Ra not infected-H37Rv not infected | -0.1211 | 0.0898 | 0.2947 |
| Afri infected-BCG infected | 0.1798 | 0.1167 | 0.2162 |
| Afri infected-Beijing infected | 0.0725 | 0.0725 | 0.4445 |
| Afri infected-CDC1551 infected | 0.1654 | 0.0862 | 0.1334 |
| Afri infected-EAI infected | -0.0316 | 0.0856 | 0.7478 |
| Afri infected-H37Ra infected | 0.3888 | 0.0936 | 4e-04 |
| Afri infected-H37Rv infected | 0.2354 | 0.0966 | 0.0551 |
| BCG infected-Beijing infected | -0.1073 | 0.1141 | 0.4756 |
| BCG infected-CDC1551 infected | -0.0143 | 0.1244 | 0.9083 |
| BCG infected-EAI infected | -0.2113 | 0.099 | 0.0987 |
| BCG infected-H37Ra infected | 0.209 | 0.1267 | 0.1837 |
| BCG infected-H37Rv infected | 0.0557 | 0.1273 | 0.7315 |
| Beijing infected-CDC1551 infected | 0.093 | 0.0803 | 0.3621 |
| Beijing infected-EAI infected | -0.1041 | 0.0827 | 0.3244 |

| Contrast | estimate | SE | p.value |
|---|---|---|---|
| none not infected-Afri not infected | 1.6478 | 0.7801 | 0.1456 |
| none not infected-BCG not infected | 2.6634 | 1.0411 | 0.0663 |
| none not infected-Beijing not infected | 2.3455 | 0.777 | 0.0239 |
| none not infected-CDC1551 not infected | 3.3063 | 0.9888 | 0.0104 |
| none not infected-EAI not infected | 1.7812 | 0.8266 | 0.1403 |
| none not infected-H37Ra not infected | 18.3519 | 583.2224 | 0.9814 |
| none not infected-H37Rv not infected | 4.7801 | 1.3959 | 0.0097 |
| none not infected-Afri infected | 0.5069 | 0.7747 | 0.718 |
| none not infected-BCG infected | 2.255 | 1.0362 | 0.1403 |
| none not infected-Beijing infected | 0.8293 | 0.7559 | 0.5029 |
| none not infected-CDC1551 infected | 1.5391 | 0.8854 | 0.2071 |
| none not infected-EAI infected | 0.6373 | 0.828 | 0.6468 |
| none not infected-H37Ra infected | 2.6457 | 0.9386 | 0.038 |
| none not infected-H37Rv infected | 2.782 | 1.0503 | 0.0566 |
| Afri not infected-BCG not infected | 1.0156 | 1.035 | 0.5274 |
| Afri not infected-Beijing not infected | 0.6977 | 0.6778 | 0.5029 |
| Afri not infected-CDC1551 not infected | 1.6586 | 0.9211 | 0.1917 |
| Afri not infected-EAI not infected | 0.1334 | 0.7717 | 0.9814 |
| Afri not infected-H37Ra not infected | 16.7041 | 583.2224 | 0.9814 |
| Afri not infected-H37Rv not infected | 3.1323 | 1.4441 | 0.1403 |
| BCG not infected-Beijing not infected | -0.3179 | 1.0413 | 0.939 |
| BCG not infected-CDC1551 not infected | 0.6429 | 1.2377 | 0.8089 |
| BCG not infected-EAI not infected | -0.8822 | 0.837 | 0.5029 |
| BCG not infected-H37Ra not infected | 15.6885 | 583.2229 | 0.9814 |
| BCG not infected-H37Rv not infected | 2.1167 | 1.6078 | 0.3948 |
| Beijing not infected-CDC1551 not infected | 0.9608 | 0.9201 | 0.5029 |
| Beijing not infected-EAI not infected | -0.5643 | 0.7826 | 0.6742 |
| Beijing not infected-H37Ra not infected | 16.0064 | 583.2224 | 0.9814 |
| Beijing not infected-H37Rv not infected | 2.4346 | 1.4383 | 0.2112 |
| CDC1551 not infected-EAI not infected | -1.5252 | 1.043 | 0.3232 |
| CDC1551 not infected-H37Ra not infected | 15.0455 | 583.2227 | 0.9814 |
| CDC1551 not infected-H37Rv not infected | 1.4737 | 1.5552 | 0.5275 |
| EAI not infected-H37Ra not infected | 16.5707 | 583.2225 | 0.9814 |
| EAI not infected-H37Rv not infected | 2.9989 | 1.4773 | 0.157 |
| H37Ra not infected-H37Rv not infected | -13.5718 | 583.2232 | 0.9814 |
| Afri infected-BCG infected | 1.748 | 1.0262 | 0.2112 |
| Afri infected-Beijing infected | 0.3224 | 0.6516 | 0.8147 |
| Afri infected-CDC1551 infected | 1.0322 | 0.8074 | 0.4087 |
| Afri infected-EAI infected | 0.1303 | 0.7644 | 0.9814 |
| Afri infected-H37Ra infected | 2.1388 | 0.9561 | 0.1403 |
| Afri infected-H37Rv infected | 2.275 | 1.109 | 0.157 |
| BCG infected-Beijing infected | -1.4257 | 1.0247 | 0.3566 |
| BCG infected-CDC1551 infected | -0.7159 | 1.1531 | 0.7323 |
| BCG infected-EAI infected | -1.6177 | 0.8452 | 0.1752 |
| BCG infected-H37Ra infected | 0.3907 | 1.2151 | 0.939 |
| BCG infected-H37Rv infected | 0.527 | 1.3151 | 0.8854 |
| Beijing infected-CDC1551 infected | 0.7098 | 0.7852 | 0.549 |
| Beijing infected-EAI infected | -0.192 | 0.767 | 0.972 |

Acidification of phagolysosomes observed

Acidification of phagolysosomes not observed (blocked)

Acidification trend observed, stastically not significant

## Grouping: Sample

### M1 – 6 h p.i.

c) Effective MOI

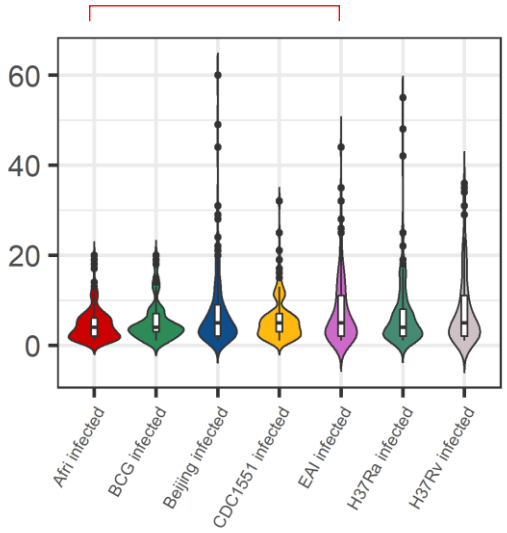


| Par | Value | Std.Error | p.value |
|---|---|---|---|
| (Intercept) | 1.1618 | 0.1532 | 0 |
| groupBCG infected | 0.5123 | 0.2551 | 0.0493 |
| groupBeijing infected | 0.2666 | 0.146 | 0.0729 |
| groupCDC1551 infected | 0.0771 | 0.1751 | 0.6612 |
| groupEAI infected | 0.6082 | 0.183 | 0.0015 |
| groupH37Ra infected | 0.3031 | 0.1976 | 0.1306 |
| groupH37Rv infected | 0.2976 | 0.2059 | 0.1539 |

| Contrast | estimate | SE | p.value |
|---|---|---|---|
| Afri infected - BCG infected | -0.5123 | 0.2551 | 0.3061 |
| Afri infected - Beijing infected | -0.2666 | 0.146 | 0.3061 |
| Afri infected - CDC1551 infected | -0.0771 | 0.1751 | 0.7713 |
| Afri infected - EAI infected | -0.6082 | 0.183 | 0.0324 |
| Afri infected - H37Ra infected | -0.3031 | 0.1976 | 0.3867 |
| Afri infected - H37Rv infected | -0.2976 | 0.2059 | 0.3867 |
| BCG infected - Beijing infected | 0.2457 | 0.2511 | 0.498 |
| BCG infected - CDC1551 infected | 0.4352 | 0.2743 | 0.3867 |
| BCG infected - EAI infected | -0.0959 | 0.2033 | 0.7713 |
| BCG infected - H37Ra infected | 0.2092 | 0.2835 | 0.6083 |
| BCG infected - H37Rv infected | 0.2148 | 0.2855 | 0.6083 |
| Beijing infected - CDC1551 infected | 0.1895 | 0.1614 | 0.4502 |
| Beijing infected - EAI infected | -0.3416 | 0.1787 | 0.3061 |
| Beijing infected - H37Ra infected | -0.0364 | 0.1881 | 0.9146 |
| Beijing infected - H37Rv infected | -0.0309 | 0.1897 | 0.9146 |
| CDC1551 infected - EAI infected | -0.5311 | 0.2133 | 0.1645 |
| CDC1551 infected - H37Ra infected | -0.226 | 0.2009 | 0.4502 |
| CDC1551 infected - H37Rv infected | -0.2204 | 0.2016 | 0.4502 |
| EAI infected - H37Ra infected | 0.3051 | 0.227 | 0.3867 |
| EAI infected - H37Rv infected | 0.3107 | 0.2299 | 0.3867 |
| H37Ra infected - H37Rv infected | 0.0055 | 0.1847 | 0.9763 |

d) Colocalization Index

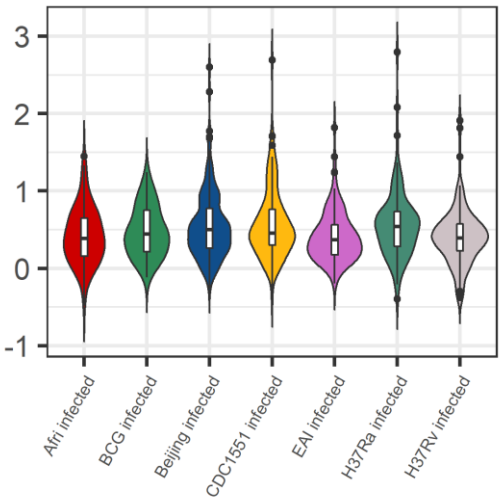


| Par | Value | Std.Error | p.value |
|---|---|---|---|
| (Intercept) | -0.009 | 0.1222 | 0.9412 |
| groupBCG infected | 0.0397 | 0.2109 | 0.8513 |
| groupBeijing infected | 0.2322 | 0.1282 | 0.0752 |
| groupCDC1551 infected | 0.1699 | 0.1498 | 0.2613 |
| groupEAI infected | -0.0855 | 0.1555 | 0.5845 |
| groupH37Ra infected | 0.2281 | 0.1663 | 0.1756 |
| groupH37Rv infected | -0.2072 | 0.1721 | 0.2335 |

| Contrast | estimate | SE | p.value |
|---|---|---|---|
| Afri infected - BCG infected | -0.0397 | 0.2109 | 0.8939 |
| Afri infected - Beijing infected | -0.2322 | 0.1282 | 0.3157 |
| Afri infected - CDC1551 infected | -0.1699 | 0.1498 | 0.5486 |
| Afri infected - EAI infected | 0.0855 | 0.1555 | 0.722 |
| Afri infected - H37Ra infected | -0.2281 | 0.1663 | 0.4609 |
| Afri infected - H37Rv infected | 0.2072 | 0.1721 | 0.5449 |
| BCG infected - Beijing infected | -0.1925 | 0.2068 | 0.6223 |
| BCG infected - CDC1551 infected | -0.1302 | 0.2242 | 0.722 |
| BCG infected - EAI infected | 0.1252 | 0.173 | 0.7081 |
| BCG infected - H37Ra infected | -0.1883 | 0.231 | 0.6756 |
| BCG infected - H37Rv infected | 0.2469 | 0.2313 | 0.5539 |
| Beijing infected - CDC1551 infected | 0.0623 | 0.1381 | 0.7623 |
| Beijing infected - EAI infected | 0.3177 | 0.151 | 0.2084 |
| Beijing infected - H37Ra infected | 0.0042 | 0.1592 | 0.9791 |
| Beijing infected - H37Rv infected | 0.4395 | 0.1583 | 0.0962 |
| CDC1551 infected - EAI infected | 0.2554 | 0.1773 | 0.4609 |
| CDC1551 infected - H37Ra infected | -0.0581 | 0.1698 | 0.8106 |
| CDC1551 infected - H37Rv infected | 0.3771 | 0.1691 | 0.2076 |
| EAI infected - H37Ra infected | -0.3135 | 0.1874 | 0.349 |
| EAI infected - H37Rv infected | 0.1217 | 0.1882 | 0.722 |
| H37Ra infected - H37Rv infected | 0.4353 | 0.1614 | 0.0962 |

## Grouping: Sample

### M1 – 24 h p.i.

a) Phagolysosomal acidification

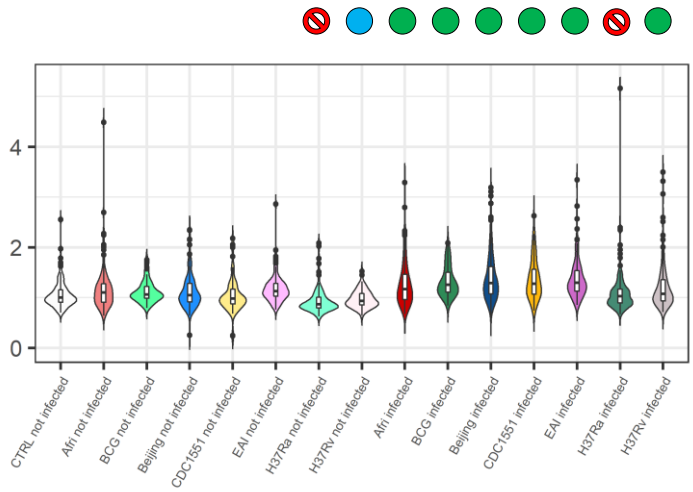


b) Percentage of cells showing acidified phagolysosomes

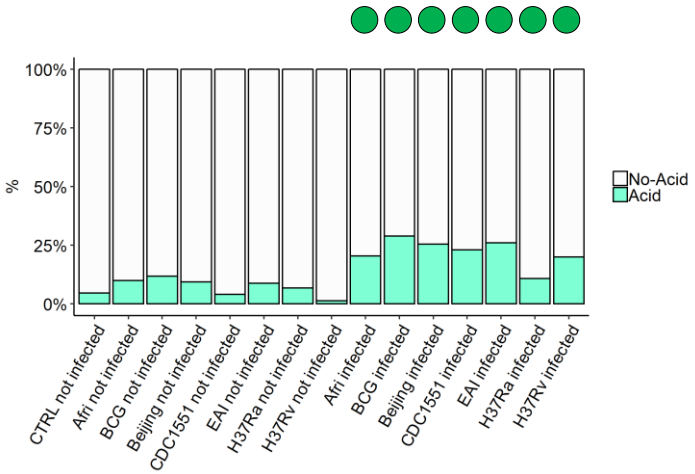


| Par | Value | Std.Error | p.value |
|---|---|---|---|
| (Intercept) | 0.0184 | 0.0353 | 0.6021 |
| groupAfri not infected | 0.0221 | 0.0389 | 0.5709 |
| groupBCG not infected | 0.0757 | 0.0572 | 0.1858 |
| groupBeijing not infected | 0.0485 | 0.0368 | 0.1871 |
| groupCDC1551 not infected | 0.0033 | 0.0444 | 0.9402 |
| groupEAI not infected | 0.0742 | 0.0406 | 0.0675 |
| groupH37Ra not infected | -0.0957 | 0.0466 | 0.0403 |
| groupH37Rv not infected | -0.0249 | 0.0462 | 0.5902 |
| groupAfri infected | 0.1127 | 0.0389 | 0.0038 |
| groupBCG infected | 0.2329 | 0.0548 | 0 |
| groupBeijing infected | 0.2026 | 0.0358 | 0 |
| groupCDC1551 infected | 0.2551 | 0.0435 | 0 |
| groupEAI infected | 0.1992 | 0.0408 | 0 |
| groupH37Ra infected | 0.0394 | 0.0448 | 0.3793 |
| groupH37Rv infected | 0.1119 | 0.045 | 0.0129 |

| Par | Estimate | se | OR | pvalue |
|---|---|---|---|---|
| (Intercept) | -3.1573 | 0.4472 | 0.0425 | 0 |
| groupAfri not infected | 0.6976 | 0.5452 | 2.0088 | 0.2007 |
| groupBCG not infected | 0.8584 | 0.683 | 2.3594 | 0.2088 |
| groupBeijing not infected | 0.6945 | 0.5348 | 2.0028 | 0.1941 |
| groupCDC1551 not infected | 0.0581 | 0.7516 | 1.0598 | 0.9384 |
| groupEAI not infected | 0.4412 | 0.5449 | 1.5546 | 0.4181 |
| groupH37Ra not infected | 0.9405 | 0.6736 | 2.5612 | 0.1626 |
| groupH37Rv not infected | -1.0996 | 1.115 | 0.333 | 0.324 |
| groupAfri infected | 1.6261 | 0.5024 | 5.0838 | 0.0012 |
| groupBCG infected | 1.9978 | 0.5825 | 7.3727 | 6e-04 |
| groupBeijing infected | 1.9321 | 0.4719 | 6.9042 | 0 |
| groupCDC1551 infected | 1.9848 | 0.5336 | 7.2773 | 2e-04 |
| groupEAI infected | 1.7757 | 0.496 | 5.9046 | 3e-04 |
| groupH37Ra infected | 1.422 | 0.5799 | 4.1452 | 0.0142 |
| groupH37Rv infected | 1.855 | 0.5356 | 6.3916 | 5e-04 |

| Contrast | estimate | SE | p.value |
|---|---|---|---|
| none not infected-Afri not infected | -0.0405 | 0.0408 | 0.4642 |
| none not infected-BCG not infected | -0.0941 | 0.0591 | 0.2506 |
| none not infected-Beijing not infected | -0.067 | 0.0387 | 0.2413 |
| none not infected-CDC1551 not infected | -0.0218 | 0.0459 | 0.7302 |
| none not infected-EAI not infected | -0.0927 | 0.0429 | 0.1486 |
| none not infected-H37Ra not infected | 0.0773 | 0.047 | 0.2436 |
| none not infected-H37Rv not infected | 0.0065 | 0.0467 | 0.9384 |
| none not infected-Afri infected | -0.1312 | 0.0407 | 0.0438 |
| none not infected-BCG infected | -0.2514 | 0.0568 | 0.0128 |
| none not infected-Beijing infected | -0.2211 | 0.0378 | 0.0039 |
| none not infected-CDC1551 infected | -0.2735 | 0.045 | 0.0039 |
| none not infected-EAI infected | -0.2176 | 0.0431 | 0.0077 |
| none not infected-H37Ra infected | -0.0578 | 0.0452 | 0.354 |
| none not infected-H37Rv infected | -0.1303 | 0.0454 | 0.0631 |
| Afri not infected-BCG not infected | -0.0536 | 0.0626 | 0.4942 |
| Afri not infected-Beijing not infected | -0.0265 | 0.0399 | 0.6188 |
| Afri not infected-CDC1551 not infected | 0.0187 | 0.0479 | 0.7557 |
| Afri not infected-EAI not infected | -0.0522 | 0.0453 | 0.3578 |
| Afri not infected-H37Ra not infected | 0.1178 | 0.052 | 0.0631 |
| Afri not infected-H37Rv not infected | 0.047 | 0.0529 | 0.4823 |
| BCG not infected-Beijing not infected | 0.0271 | 0.0618 | 0.7302 |
| BCG not infected-CDC1551 not infected | 0.0723 | 0.0677 | 0.3947 |
| BCG not infected-EAI not infected | 0.0014 | 0.0535 | 0.9868 |
| BCG not infected-H37Ra not infected | 0.1714 | 0.0694 | 0.0431 |
| BCG not infected-H37Rv not infected | 0.1006 | 0.0693 | 0.2436 |
| Beijing not infected-CDC1551 not infected | 0.0452 | 0.0453 | 0.4275 |
| Beijing not infected-EAI not infected | -0.0257 | 0.0445 | 0.6703 |
| Beijing not infected-H37Ra not infected | 0.1443 | 0.0502 | 0.0144 |
| Beijing not infected-H37Rv not infected | 0.0734 | 0.0501 | 0.2436 |
| CDC1551 not infected-EAI not infected | -0.0709 | 0.0532 | 0.2814 |
| CDC1551 not infected-H37Ra not infected | 0.099 | 0.0548 | 0.1486 |
| CDC1551 not infected-H37Rv not infected | 0.0282 | 0.0544 | 0.6959 |
| EAI not infected-H37Ra not infected | 0.17 | 0.0558 | 0.0114 |
| EAI not infected-H37Rv not infected | 0.0991 | 0.0557 | 0.1535 |
| H37Ra not infected-H37Rv not infected | -0.0708 | 0.0509 | 0.2588 |
| Afri infected-BCG infected | -0.1202 | 0.0605 | 0.1186 |
| Afri infected-Beijing infected | -0.0899 | 0.0392 | 0.0625 |
| Afri infected-CDC1551 infected | -0.1424 | 0.0471 | 0.0115 |
| Afri infected-EAI infected | -0.0864 | 0.0455 | 0.1375 |
| Afri infected-H37Ra infected | 0.0733 | 0.0504 | 0.2436 |
| Afri infected-H37Rv infected | 9e-04 | 0.0518 | 0.9868 |
| BCG infected-Beijing infected | 0.0303 | 0.059 | 0.6959 |
| BCG infected-CDC1551 infected | -0.0222 | 0.0651 | 0.7835 |
| BCG infected-EAI infected | 0.0338 | 0.0513 | 0.6188 |
| BCG infected-H37Ra infected | 0.1935 | 0.0663 | 0.0132 |
| BCG infected-H37Rv infected | 0.1211 | 0.0665 | 0.1486 |
| Beijing infected-CDC1551 infected | -0.0525 | 0.0438 | 0.3465 |
| Beijing infected-EAI infected | 0.0035 | 0.0438 | 0.9676 |

| Contrast | estimate | SE | p.value |
|---|---|---|---|
| none not infected-Afri not infected | 2.4597 | 0.4095 | 0 |
| none not infected-BCG not infected | 2.2988 | 0.5951 | 6e-04 |
| none not infected-Beijing not infected | 2.4627 | 0.3939 | 0 |
| none not infected-CDC1551 not infected | 3.0991 | 0.6548 | 0 |
| none not infected-EAI not infected | 2.716 | 0.4226 | 0 |
| none not infected-H37Ra not infected | 2.2168 | 0.5547 | 5e-04 |
| none not infected-H37Rv not infected | 4.2569 | 1.0504 | 5e-04 |
| none not infected-Afri infected | 1.5312 | 0.349 | 1e-04 |
| none not infected-BCG infected | 1.1595 | 0.4765 | 0.0524 |
| none not infected-Beijing infected | 1.2251 | 0.3016 | 5e-04 |
| none not infected-CDC1551 infected | 1.1725 | 0.3853 | 0.0098 |
| none not infected-EAI infected | 1.3815 | 0.3567 | 6e-04 |
| none not infected-H37Ra infected | 1.7353 | 0.4357 | 5e-04 |
| none not infected-H37Rv infected | 1.3023 | 0.3821 | 0.003 |
| Afri not infected-BCG not infected | -0.1609 | 0.6796 | 0.9145 |
| Afri not infected-Beijing not infected | 0.003 | 0.4857 | 0.995 |
| Afri not infected-CDC1551 not infected | 0.6394 | 0.7259 | 0.6934 |
| Afri not infected-EAI not infected | 0.2563 | 0.5149 | 0.8655 |
| Afri not infected-H37Ra not infected | -0.2429 | 0.6584 | 0.8697 |
| Afri not infected-H37Rv not infected | 1.7972 | 1.1098 | 0.2766 |
| BCG not infected-Beijing not infected | 0.1639 | 0.6755 | 0.9145 |
| BCG not infected-CDC1551 not infected | 0.8003 | 0.8647 | 0.6934 |
| BCG not infected-EAI not infected | 0.4172 | 0.6115 | 0.7797 |
| BCG not infected-H37Ra not infected | -0.082 | 0.7989 | 0.9483 |
| BCG not infected-H37Rv not infected | 1.958 | 1.1967 | 0.2766 |
| Beijing not infected-CDC1551 not infected | 0.6364 | 0.71 | 0.6934 |
| Beijing not infected-EAI not infected | 0.2533 | 0.5127 | 0.8655 |
| Beijing not infected-H37Ra not infected | -0.2459 | 0.6453 | 0.8697 |
| Beijing not infected-H37Rv not infected | 1.7942 | 1.0982 | 0.2766 |
| CDC1551 not infected-EAI not infected | -0.3831 | 0.7501 | 0.8655 |
| CDC1551 not infected-H37Ra not infected | -0.8823 | 0.8231 | 0.6585 |
| CDC1551 not infected-H37Rv not infected | 1.1577 | 1.2072 | 0.6934 |
| EAI not infected-H37Ra not infected | -0.4992 | 0.6765 | 0.7635 |
| EAI not infected-H37Rv not infected | 1.5408 | 1.1186 | 0.4243 |
| H37Ra not infected-H37Rv not infected | 2.0401 | 1.1464 | 0.2255 |
| Afri infected-BCG infected | -0.3717 | 0.5393 | 0.7797 |
| Afri infected-Beijing infected | -0.3061 | 0.3608 | 0.6934 |
| Afri infected-CDC1551 infected | -0.3587 | 0.4494 | 0.7232 |
| Afri infected-EAI infected | -0.1497 | 0.4142 | 0.8697 |
| Afri infected-H37Ra infected | 0.2041 | 0.5203 | 0.8697 |
| Afri infected-H37Rv infected | -0.2289 | 0.478 | 0.8655 |
| BCG infected-Beijing infected | 0.0657 | 0.5166 | 0.9438 |
| BCG infected-CDC1551 infected | 0.013 | 0.5839 | 0.995 |
| BCG infected-EAI infected | 0.2221 | 0.4403 | 0.8655 |
| BCG infected-H37Ra infected | 0.5758 | 0.6279 | 0.6934 |
| BCG infected-H37Rv infected | 0.1428 | 0.59 | 0.9145 |
| Beijing infected-CDC1551 infected | -0.0526 | 0.397 | 0.9438 |
| Beijing infected-EAI infected | 0.1564 | 0.3882 | 0.8697 |

Acidification of phagolysosomes observed

Acidification of phagolysosomes not observed (blocked)

Acidification trend observed, stastically not significant

## Grouping: Sample

### M1 – 24 h p.i.

c) Effective MOI

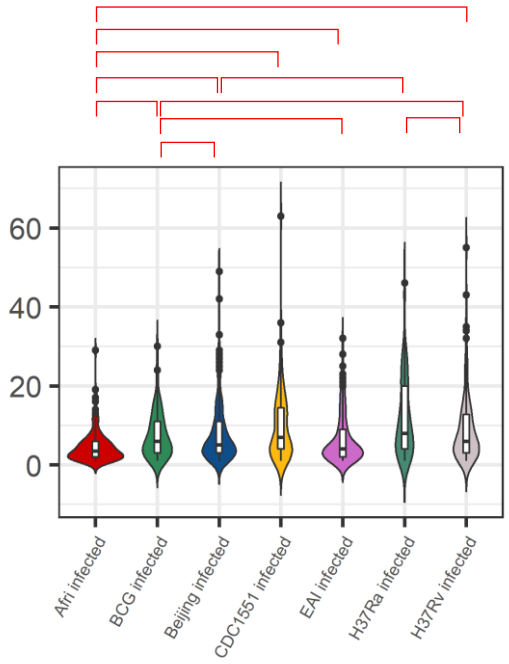


| Par | Value | Std.Error | p.value |
|---|---|---|---|
| (Intercept) | 1.3459 | 0.1565 | 0 |
| groupBCG infected | 0.8519 | 0.2039 | 1e-04 |
| groupBeijing infected | 0.3098 | 0.1109 | 0.0071 |
| groupCDC1551 infected | 0.367 | 0.1412 | 0.0119 |
| groupEAI infected | 0.3906 | 0.1448 | 0.0091 |
| groupH37Ra infected | 0.7005 | 0.162 | 1e-04 |
| groupH37Rv infected | 0.1793 | 0.1664 | 0.2859 |

| Contrast | estimate | SE | p.value |
|---|---|---|---|
| Afri infected - BCG infected | -0.8519 | 0.2039 | 0.0011 |
| Afri infected - Beijing infected | -0.3098 | 0.1109 | 0.0247 |
| Afri infected - CDC1551 infected | -0.367 | 0.1412 | 0.0256 |
| Afri infected - EAI infected | -0.3906 | 0.1448 | 0.0249 |
| Afri infected - H37Ra infected | -0.7005 | 0.162 | 0.0011 |
| Afri infected - H37Rv infected | -0.1793 | 0.1664 | 0.3753 |
| BCG infected - Beijing infected | 0.5421 | 0.202 | 0.0249 |
| BCG infected - CDC1551 infected | 0.4849 | 0.2259 | 0.0688 |
| BCG infected - EAI infected | 0.4613 | 0.1516 | 0.0185 |
| BCG infected - H37Ra infected | 0.1514 | 0.2369 | 0.6128 |
| BCG infected - H37Rv infected | 0.6726 | 0.2381 | 0.0247 |
| Beijing infected - CDC1551 infected | -0.0572 | 0.1262 | 0.6847 |
| Beijing infected - EAI infected | -0.0808 | 0.1427 | 0.6337 |
| Beijing infected - H37Ra infected | -0.3907 | 0.151 | 0.0256 |
| Beijing infected - H37Rv infected | 0.1305 | 0.1506 | 0.4812 |
| CDC1551 infected - EAI infected | -0.0236 | 0.1761 | 0.8938 |
| CDC1551 infected - H37Ra infected | -0.3335 | 0.1598 | 0.0723 |
| CDC1551 infected - H37Rv infected | 0.1877 | 0.1579 | 0.3591 |
| EAI infected - H37Ra infected | -0.3099 | 0.1911 | 0.1781 |
| EAI infected - H37Rv infected | 0.2113 | 0.1926 | 0.3753 |
| H37Ra infected - H37Rv infected | 0.5212 | 0.1322 | 0.0015 |

d) Colocalization Index

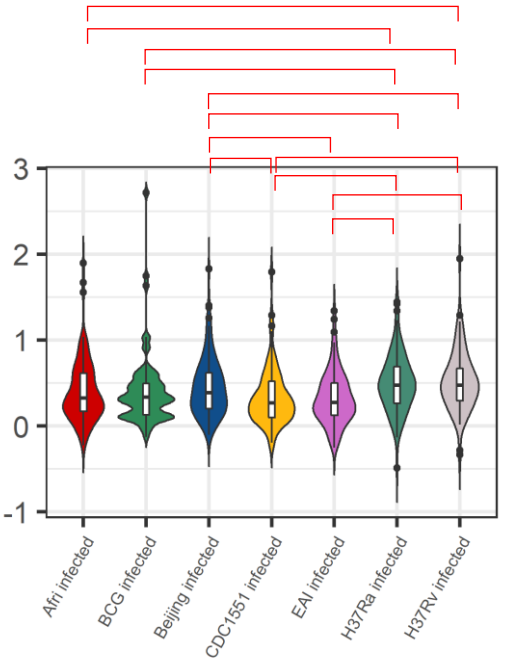


| Par | Value | Std.Error | p.value |
|---|---|---|---|
| (Intercept) | -0.1611 | 0.1235 | 0.1926 |
| groupBCG infected | -0.1594 | 0.1916 | 0.409 |
| groupBeijing infected | 0.131 | 0.1114 | 0.2443 |
| groupCDC1551 infected | -0.1753 | 0.1453 | 0.2326 |
| groupEAI infected | -0.2812 | 0.1399 | 0.0492 |
| groupH37Ra infected | 0.629 | 0.1562 | 2e-04 |
| groupH37Rv infected | 0.6642 | 0.1575 | 1e-04 |

| Contrast | estimate | SE | p.value |
|---|---|---|---|
| Afri infected - BCG infected | 0.1594 | 0.1916 | 0.482 |
| Afri infected - Beijing infected | -0.131 | 0.1114 | 0.3206 |
| Afri infected - CDC1551 infected | 0.1753 | 0.1453 | 0.3206 |
| Afri infected - EAI infected | 0.2812 | 0.1399 | 0.0795 |
| Afri infected - H37Ra infected | -0.629 | 0.1562 | 6e-04 |
| Afri infected - H37Rv infected | -0.6642 | 0.1575 | 4e-04 |
| BCG infected - Beijing infected | -0.2904 | 0.1889 | 0.1944 |
| BCG infected - CDC1551 infected | 0.0159 | 0.2133 | 0.9408 |
| BCG infected - EAI infected | 0.1218 | 0.1478 | 0.482 |
| BCG infected - H37Ra infected | -0.7884 | 0.2173 | 0.0014 |
| BCG infected - H37Rv infected | -0.8236 | 0.2164 | 0.001 |
| Beijing infected - CDC1551 infected | 0.3063 | 0.1345 | 0.0463 |
| Beijing infected - EAI infected | 0.4123 | 0.1368 | 0.0073 |
| Beijing infected - H37Ra infected | -0.498 | 0.1486 | 0.003 |
| Beijing infected - H37Rv infected | -0.5332 | 0.1463 | 0.0014 |
| CDC1551 infected - EAI infected | 0.1059 | 0.1717 | 0.5967 |
| CDC1551 infected - H37Ra infected | -0.8043 | 0.1586 | 0 |
| CDC1551 infected - H37Rv infected | -0.8395 | 0.1494 | 0 |
| EAI infected - H37Ra infected | -0.9102 | 0.1782 | 0 |
| EAI infected - H37Rv infected | -0.9454 | 0.1772 | 0 |
| H37Ra infected - H37Rv infected | -0.0352 | 0.1294 | 0.8259 |

## Grouping: Sample

## M2 – 6 h p.i.

a) Phagolysosomal acidification

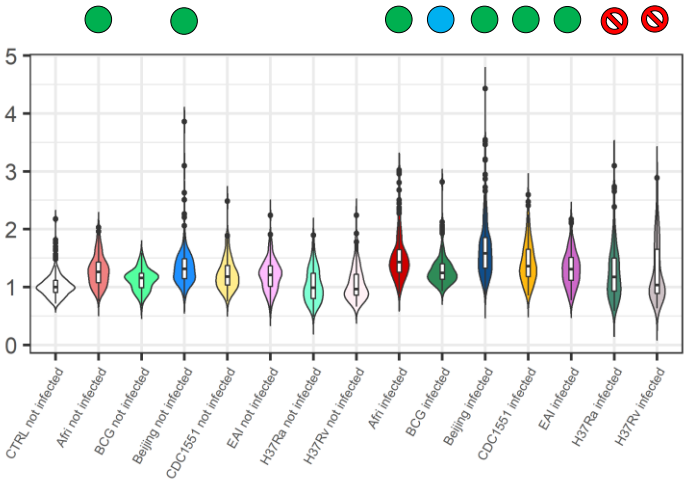


b) Percentage of cells showing acidified phagolysosomes

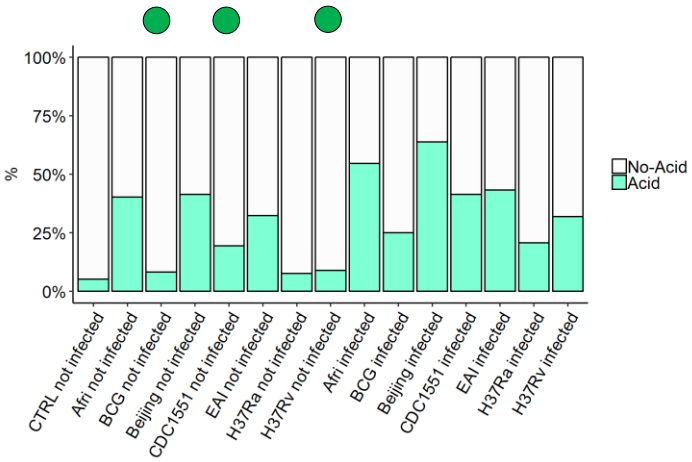


| Par | Value | Std.Error | p.value |
|---|---|---|---|
| (Intercept) | -0.0102 | 0.0427 | 0.8114 |
| groupAfri not infected | 0.2373 | 0.0532 | 0 |
| groupBCG not infected | 0.0963 | 0.0789 | 0.2224 |
| groupBeijing not infected | 0.2672 | 0.0491 | 0 |
| groupCDC1551 not infected | 0.1257 | 0.0587 | 0.0325 |
| groupEAI not infected | 0.1354 | 0.0569 | 0.0174 |
| groupH37Ra not infected | 0.0167 | 0.0593 | 0.7779 |
| groupH37Rv not infected | 0.0451 | 0.0599 | 0.4519 |
| groupAfri infected | 0.3544 | 0.0535 | 0 |
| groupBCG infected | 0.1968 | 0.0788 | 0.0125 |
| groupBeijing infected | 0.4182 | 0.0489 | 0 |
| groupCDC1551 infected | 0.2551 | 0.059 | 0 |
| groupEAI infected | 0.242 | 0.0569 | 0 |
| groupH37Ra infected | 0.178 | 0.0597 | 0.0029 |
| groupH37Rv infected | 0.1709 | 0.06 | 0.0045 |

| Par | Estimate | se | OR | pvalue |
|---|---|---|---|---|
| (Intercept) | -3.1634 | 0.5967 | 0.0423 | 0 |
| groupAfri not infected | 2.4272 | 0.639 | 11.3268 | 1e-04 |
| groupBCG not infected | 0.4143 | 0.9521 | 1.5133 | 0.6634 |
| groupBeijing not infected | 2.3782 | 0.5865 | 10.7859 | 1e-04 |
| groupCDC1551 not infected | 1.0524 | 0.6893 | 2.8645 | 0.1268 |
| groupEAI not infected | 1.6846 | 0.6812 | 5.3902 | 0.0134 |
| groupH37Ra not infected | 1.351 | 0.7642 | 3.8612 | 0.0771 |
| groupH37Rv not infected | -0.0155 | 0.7984 | 0.9846 | 0.9845 |
| groupAfri infected | 3.4862 | 0.6419 | 32.6619 | 0 |
| groupBCG infected | 1.8422 | 0.8825 | 6.3104 | 0.0369 |
| groupBeijing infected | 3.6119 | 0.5845 | 37.0353 | 0 |
| groupCDC1551 infected | 2.579 | 0.6714 | 13.1845 | 1e-04 |
| groupEAI infected | 2.3989 | 0.6793 | 11.0112 | 4e-04 |
| groupH37Ra infected | 2.6859 | 0.7168 | 14.6711 | 2e-04 |
| groupH37Rv infected | 2.3284 | 0.7232 | 10.2615 | 0.0013 |

| Contrast | estimate | SE | p.value |
|---|---|---|---|
| none not infected-Afri not infected | -0.2271 | 0.0533 | 0.0147 |
| none not infected-BCG not infected | -0.0861 | 0.079 | 0.4273 |
| none not infected-Beijing not infected | -0.257 | 0.0493 | 0.0055 |
| none not infected-CDC1551 not infected | -0.1155 | 0.059 | 0.1639 |
| none not infected-EAI not infected | -0.1252 | 0.0569 | 0.1297 |
| none not infected-H37Ra not infected | -0.0065 | 0.0597 | 0.9175 |
| none not infected-H37Rv not infected | -0.0349 | 0.0603 | 0.6881 |
| none not infected-Afri infected | -0.3442 | 0.0536 | 0.0019 |
| none not infected-BCG infected | -0.1866 | 0.0789 | 0.1048 |
| none not infected-Beijing infected | -0.408 | 0.049 | 6e-04 |
| none not infected-CDC1551 infected | -0.245 | 0.0592 | 0.0158 |
| none not infected-EAI infected | -0.2319 | 0.057 | 0.0158 |
| none not infected-H37Ra infected | -0.1679 | 0.0601 | 0.0651 |
| none not infected-H37Rv infected | -0.1607 | 0.0605 | 0.076 |
| Afri not infected-BCG not infected | 0.141 | 0.0873 | 0.1867 |
| Afri not infected-Beijing not infected | -0.0299 | 0.0555 | 0.6881 |
| Afri not infected-CDC1551 not infected | 0.1116 | 0.0653 | 0.1621 |
| Afri not infected-EAI not infected | 0.1019 | 0.0646 | 0.1906 |
| Afri not infected-H37Ra not infected | 0.2205 | 0.0696 | 0.0066 |
| Afri not infected-H37Rv not infected | 0.1922 | 0.0719 | 0.0232 |
| BCG not infected-Beijing not infected | -0.1709 | 0.0854 | 0.0988 |
| BCG not infected-CDC1551 not infected | -0.0294 | 0.0926 | 0.8301 |
| BCG not infected-EAI not infected | -0.0391 | 0.0754 | 0.6919 |
| BCG not infected-H37Ra not infected | 0.0796 | 0.0936 | 0.5107 |
| BCG not infected-H37Rv not infected | 0.0512 | 0.0941 | 0.6881 |
| Beijing not infected-CDC1551 not infected | 0.1415 | 0.0611 | 0.0522 |
| Beijing not infected-EAI not infected | 0.1318 | 0.0624 | 0.0784 |
| Beijing not infected-H37Ra not infected | 0.2504 | 0.0666 | 0.0012 |
| Beijing not infected-H37Rv not infected | 0.2221 | 0.0672 | 0.0047 |
| CDC1551 not infected-EAI not infected | -0.0097 | 0.0734 | 0.9175 |
| CDC1551 not infected-H37Ra not infected | 0.109 | 0.0726 | 0.2106 |
| CDC1551 not infected-H37Rv not infected | 0.0806 | 0.0729 | 0.3846 |
| EAI not infected-H37Ra not infected | 0.1187 | 0.0752 | 0.1906 |
| EAI not infected-H37Rv not infected | 0.0903 | 0.076 | 0.3606 |
| H37Ra not infected-H37Rv not infected | -0.0283 | 0.0686 | 0.7647 |
| Afri infected-BCG infected | 0.1576 | 0.0874 | 0.1409 |
| Afri infected-Beijing infected | -0.0638 | 0.0556 | 0.369 |
| Afri infected-CDC1551 infected | 0.0993 | 0.0658 | 0.2106 |
| Afri infected-EAI infected | 0.1124 | 0.0649 | 0.1591 |
| Afri infected-H37Ra infected | 0.1764 | 0.0702 | 0.0317 |
| Afri infected-H37Rv infected | 0.1835 | 0.0722 | 0.0305 |
| BCG infected-Beijing infected | -0.2214 | 0.0851 | 0.0268 |
| BCG infected-CDC1551 infected | -0.0583 | 0.0926 | 0.6667 |
| BCG infected-EAI infected | -0.0452 | 0.0753 | 0.6773 |
| BCG infected-H37Ra infected | 0.0188 | 0.0937 | 0.8981 |
| BCG infected-H37Rv infected | 0.0259 | 0.094 | 0.8501 |
| Beijing infected-CDC1551 infected | 0.1631 | 0.0612 | 0.0232 |
| Beijing infected-EAI infected | 0.1762 | 0.0623 | 0.0158 |

| Contrast | estimate | SE | p.value |
|---|---|---|---|
| none not infected-Afri not infected | 0.7362 | 0.6118 | 0.3897 |
| none not infected-BCG not infected | 2.749 | 0.9388 | 0.0239 |
| none not infected-Beijing not infected | 0.7851 | 0.5609 | 0.3384 |
| none not infected-CDC1551 not infected | 2.1109 | 0.6688 | 0.0153 |
| none not infected-EAI not infected | 1.4788 | 0.6612 | 0.114 |
| none not infected-H37Ra not infected | 1.8124 | 0.7267 | 0.0663 |
| none not infected-H37Rv not infected | 3.1789 | 0.7727 | 6e-04 |
| none not infected-Afri infected | -0.3229 | 0.6143 | 0.7402 |
| none not infected-BCG infected | 1.3212 | 0.8681 | 0.2881 |
| none not infected-Beijing infected | -0.4485 | 0.5584 | 0.5844 |
| none not infected-CDC1551 infected | 0.5843 | 0.6499 | 0.553 |
| none not infected-EAI infected | 0.7644 | 0.6589 | 0.4078 |
| none not infected-H37Ra infected | 0.4775 | 0.6767 | 0.6177 |
| none not infected-H37Rv infected | 0.835 | 0.6913 | 0.3897 |
| Afri not infected-BCG not infected | 2.0129 | 0.9882 | 0.1544 |
| Afri not infected-Beijing not infected | 0.0489 | 0.5653 | 0.9334 |
| Afri not infected-CDC1551 not infected | 1.3748 | 0.6868 | 0.1581 |
| Afri not infected-EAI not infected | 0.7426 | 0.6922 | 0.4501 |
| Afri not infected-H37Ra not infected | 1.0762 | 0.7976 | 0.3384 |
| Afri not infected-H37Rv not infected | 2.4427 | 0.8509 | 0.0258 |
| BCG not infected-Beijing not infected | -1.9639 | 0.9638 | 0.1544 |
| BCG not infected-CDC1551 not infected | -0.6381 | 1.0514 | 0.6853 |
| BCG not infected-EAI not infected | -1.2703 | 0.8324 | 0.2881 |
| BCG not infected-H37Ra not infected | -0.9367 | 1.1066 | 0.5799 |
| BCG not infected-H37Rv not infected | 0.4298 | 1.1354 | 0.8059 |
| Beijing not infected-CDC1551 not infected | 1.3258 | 0.631 | 0.1496 |
| Beijing not infected-EAI not infected | 0.6936 | 0.6611 | 0.4519 |
| Beijing not infected-H37Ra not infected | 1.0273 | 0.7566 | 0.3384 |
| Beijing not infected-H37Rv not infected | 2.3937 | 0.7908 | 0.0195 |
| CDC1551 not infected-EAI not infected | -0.6322 | 0.7953 | 0.5844 |
| CDC1551 not infected-H37Ra not infected | -0.2986 | 0.8218 | 0.8059 |
| CDC1551 not infected-H37Rv not infected | 1.0679 | 0.8434 | 0.3698 |
| EAI not infected-H37Ra not infected | 0.3336 | 0.873 | 0.8059 |
| EAI not infected-H37Rv not infected | 1.7001 | 0.91 | 0.1944 |
| H37Ra not infected-H37Rv not infected | 1.3665 | 0.8538 | 0.276 |
| Afri infected-BCG infected | 1.644 | 0.9248 | 0.2067 |
| Afri infected-Beijing infected | -0.1257 | 0.5665 | 0.8657 |
| Afri infected-CDC1551 infected | 0.9072 | 0.6688 | 0.3384 |
| Afri infected-EAI infected | 1.0873 | 0.6953 | 0.2856 |
| Afri infected-H37Ra infected | 0.8003 | 0.7498 | 0.4501 |
| Afri infected-H37Rv infected | 1.1578 | 0.7825 | 0.302 |
| BCG infected-Beijing infected | -1.7697 | 0.8937 | 0.1581 |
| BCG infected-CDC1551 infected | -0.7368 | 0.9763 | 0.6004 |
| BCG infected-EAI infected | -0.5567 | 0.7492 | 0.6004 |
| BCG infected-H37Ra infected | -0.8437 | 1.0131 | 0.5799 |
| BCG infected-H37Rv infected | -0.4862 | 1.0232 | 0.7544 |
| Beijing infected-CDC1551 infected | 1.0328 | 0.6103 | 0.2377 |
| Beijing infected-EAI infected | 1.213 | 0.6569 | 0.1945 |

- Acidification of phagolysosomes observed
- Acidification of phagolysosomes not observed (blocked)
- Acidification trend observed, stastically not significant

## Grouping: Sample

### M2 – 6 h p.i.

c) Effective MOI

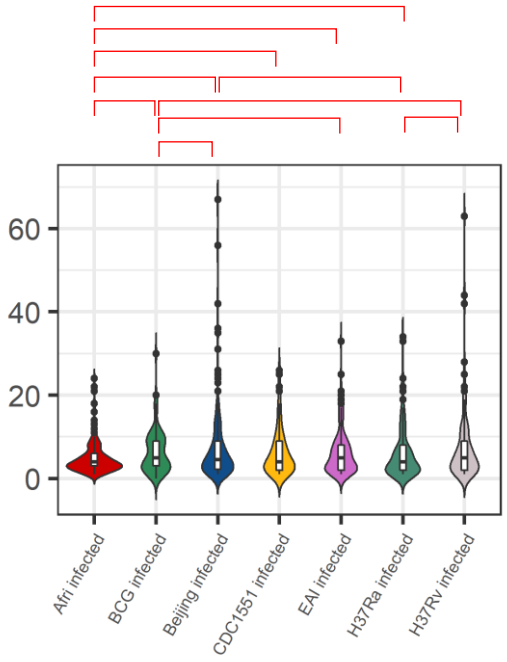


| Par | Value | Std.Error | p.value |
|---|---|---|---|
| (Intercept) | 1.3459 | 0.1565 | 0 |
| groupBCG infected | 0.8519 | 0.2039 | 1e-04 |
| groupBeijing infected | 0.3098 | 0.1109 | 0.0071 |
| groupCDC1551 infected | 0.367 | 0.1412 | 0.0119 |
| groupEAI infected | 0.3906 | 0.1448 | 0.0091 |
| groupH37Ra infected | 0.7005 | 0.162 | 1e-04 |
| groupH37Rv infected | 0.1793 | 0.1664 | 0.2859 |

| Contrast | estimate | SE | p.value |
|---|---|---|---|
| Afri infected - BCG infected | -0.8519 | 0.2039 | 0.0011 |
| Afri infected - Beijing infected | -0.3098 | 0.1109 | 0.0247 |
| Afri infected - CDC1551 infected | -0.367 | 0.1412 | 0.0256 |
| Afri infected - EAI infected | -0.3906 | 0.1448 | 0.0249 |
| Afri infected - H37Ra infected | -0.7005 | 0.162 | 0.0011 |
| Afri infected - H37Rv infected | -0.1793 | 0.1664 | 0.3753 |
| BCG infected - Beijing infected | 0.5421 | 0.202 | 0.0249 |
| BCG infected - CDC1551 infected | 0.4849 | 0.2259 | 0.0688 |
| BCG infected - EAI infected | 0.4613 | 0.1516 | 0.0185 |
| BCG infected - H37Ra infected | 0.1514 | 0.2369 | 0.6128 |
| BCG infected - H37Rv infected | 0.6726 | 0.2381 | 0.0247 |
| Beijing infected - CDC1551 infected | -0.0572 | 0.1262 | 0.6847 |
| Beijing infected - EAI infected | -0.0808 | 0.1427 | 0.6337 |
| Beijing infected - H37Ra infected | -0.3907 | 0.151 | 0.0256 |
| Beijing infected - H37Rv infected | 0.1305 | 0.1506 | 0.4812 |
| CDC1551 infected - EAI infected | -0.0236 | 0.1761 | 0.8938 |
| CDC1551 infected - H37Ra infected | -0.3335 | 0.1598 | 0.0723 |
| CDC1551 infected - H37Rv infected | 0.1877 | 0.1579 | 0.3591 |
| EAI infected - H37Ra infected | -0.3099 | 0.1911 | 0.1781 |
| EAI infected - H37Rv infected | 0.2113 | 0.1926 | 0.3753 |
| H37Ra infected - H37Rv infected | 0.5212 | 0.1322 | 0.0015 |

d) Colocalization Index

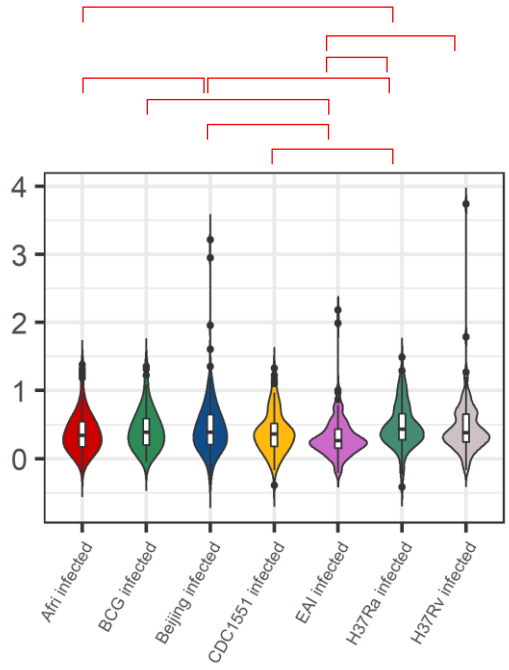


| Par | Value | Std.Error | p.value |
|---|---|---|---|
| (Intercept) | -0.2367 | 0.0657 | 3e-04 |
| groupBCG infected | 0.1292 | 0.1071 | 0.2323 |
| groupBeijing infected | 0.2211 | 0.084 | 0.0108 |
| groupCDC1551 infected | 0.054 | 0.0961 | 0.5762 |
| groupEAI infected | -0.1516 | 0.0943 | 0.1135 |
| groupH37Ra infected | 0.3735 | 0.0968 | 3e-04 |
| groupH37Rv infected | 0.1878 | 0.0981 | 0.0605 |

| Contrast | estimate | SE | p.value |
|---|---|---|---|
| Afri infected - BCG infected | -0.1292 | 0.1071 | 0.3049 |
| Afri infected - Beijing infected | -0.2211 | 0.084 | 0.036 |
| Afri infected - CDC1551 infected | -0.054 | 0.0961 | 0.6318 |
| Afri infected - EAI infected | 0.1516 | 0.0943 | 0.1702 |
| Afri infected - H37Ra infected | -0.3735 | 0.0968 | 0.002 |
| Afri infected - H37Rv infected | -0.1878 | 0.0981 | 0.1163 |
| BCG infected - Beijing infected | -0.0919 | 0.0994 | 0.4433 |
| BCG infected - CDC1551 infected | 0.0752 | 0.1098 | 0.5787 |
| BCG infected - EAI infected | 0.2808 | 0.1083 | 0.036 |
| BCG infected - H37Ra infected | -0.2443 | 0.1104 | 0.0811 |
| BCG infected - H37Rv infected | -0.0585 | 0.1116 | 0.6318 |
| Beijing infected - CDC1551 infected | 0.1671 | 0.0874 | 0.1163 |
| Beijing infected - EAI infected | 0.3727 | 0.0855 | 6e-04 |
| Beijing infected - H37Ra infected | -0.1524 | 0.0882 | 0.1445 |
| Beijing infected - H37Rv infected | 0.0334 | 0.0896 | 0.7111 |
| CDC1551 infected - EAI infected | 0.2056 | 0.0974 | 0.0913 |
| CDC1551 infected - H37Ra infected | -0.3195 | 0.0998 | 0.0093 |
| CDC1551 infected - H37Rv infected | -0.1338 | 0.1011 | 0.2673 |
| EAI infected - H37Ra infected | -0.5251 | 0.0981 | 0 |
| EAI infected - H37Rv infected | -0.3394 | 0.0994 | 0.0062 |
| H37Ra infected - H37Rv infected | 0.1858 | 0.1018 | 0.1278 |

## Grouping: Sample

## M2 – 24 h p.i.

a) Phagolysosomal acidification

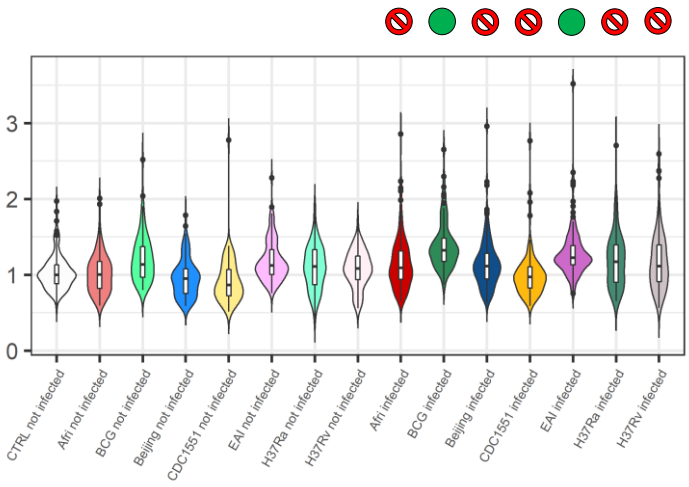


b) Percentage of cells showing acidified phagolysosomes

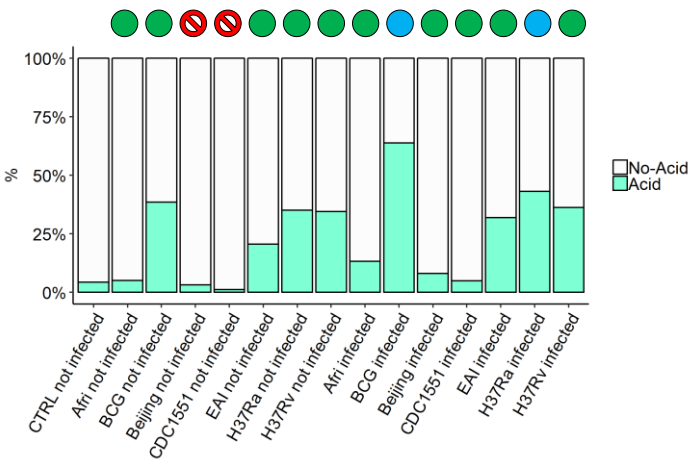


| Par | Value | Std.Error | p.value |
|---|---|---|---|
| (Intercept) | 0.0139 | 0.0526 | 0.7917 |
| groupAfri not infected | -0.0115 | 0.0369 | 0.7548 |
| groupBCG not infected | 0.0972 | 0.054 | 0.0724 |
| groupBeijing not infected | -0.0691 | 0.0351 | 0.0492 |
| groupCDC1551 not infected | -0.0907 | 0.0411 | 0.0275 |
| groupEAI not infected | 0.0767 | 0.0392 | 0.0506 |
| groupH37Ra not infected | -0.0554 | 0.044 | 0.2083 |
| groupH37Rv not infected | -0.1223 | 0.0446 | 0.0061 |
| groupAfri infected | 0.1065 | 0.0368 | 0.0039 |
| groupBCG infected | 0.2481 | 0.0534 | 0 |
| groupBeijing infected | 0.0653 | 0.034 | 0.055 |
| groupCDC1551 infected | -0.023 | 0.0416 | 0.5806 |
| groupEAI infected | 0.1561 | 0.0393 | 1e-04 |
| groupH37Ra infected | 0.0528 | 0.0426 | 0.2149 |
| groupH37Rv infected | -0.0563 | 0.0435 | 0.195 |

| Par | Estimate | se | OR | pvalue |
|---|---|---|---|---|
| (Intercept) | -3.484 | 0.6133 | 0.0307 | 0 |
| groupAfri not infected | 0.9109 | 0.6428 | 2.4866 | 0.1565 |
| groupBCG not infected | 1.7782 | 0.5663 | 5.9191 | 0.0017 |
| groupBeijing not infected | 0.5988 | 0.7014 | 1.82 | 0.3933 |
| groupCDC1551 not infected | -0.2013 | 1.1277 | 0.8176 | 0.8583 |
| groupEAI not infected | 1.3244 | 0.5316 | 3.7599 | 0.0127 |
| groupH37Ra not infected | 1.4107 | 0.5892 | 4.0989 | 0.0166 |
| groupH37Rv not infected | 1.1886 | 0.5907 | 3.2824 | 0.0442 |
| groupAfri infected | 1.9846 | 0.5506 | 7.2758 | 3e-04 |
| groupBCG infected | 2.805 | 0.5607 | 16.5272 | 0 |
| groupBeijing infected | 1.4598 | 0.5585 | 4.3052 | 0.009 |
| groupCDC1551 infected | 1.3262 | 0.7207 | 3.7668 | 0.0657 |
| groupEAI infected | 1.951 | 0.5188 | 7.0354 | 2e-04 |
| groupH37Ra infected | 2.3266 | 0.5764 | 10.243 | 1e-04 |
| groupH37Rv infected | 1.7108 | 0.5785 | 5.5335 | 0.0031 |

| Contrast | estimate | SE | p.value |
|---|---|---|---|
| none not infected-Afri not infected | -0.0024 | 0.056 | 0.9672 |
| none not infected-BCG not infected | -0.1111 | 0.0691 | 0.2339 |
| none not infected-Beijing not infected | 0.0552 | 0.0549 | 0.4292 |
| none not infected-CDC1551 not infected | 0.0768 | 0.0588 | 0.3256 |
| none not infected-EAI not infected | -0.0906 | 0.058 | 0.2376 |
| none not infected-H37Ra not infected | 0.0415 | 0.0602 | 0.5771 |
| none not infected-H37Rv not infected | 0.1084 | 0.0606 | 0.1932 |
| none not infected-Afri infected | -0.1203 | 0.056 | 0.1202 |
| none not infected-BCG infected | -0.262 | 0.0687 | 0.0207 |
| none not infected-Beijing infected | -0.0792 | 0.0541 | 0.2675 |
| none not infected-CDC1551 infected | 0.0091 | 0.0591 | 0.8966 |
| none not infected-EAI infected | -0.17 | 0.0581 | 0.0498 |
| none not infected-H37Ra infected | -0.0667 | 0.0592 | 0.3739 |
| none not infected-H37Rv infected | 0.0424 | 0.0598 | 0.5771 |
| Afri not infected-BCG not infected | -0.1087 | 0.0593 | 0.1202 |
| Afri not infected-Beijing not infected | 0.0576 | 0.0376 | 0.202 |
| Afri not infected-CDC1551 not infected | 0.0792 | 0.0441 | 0.1238 |
| Afri not infected-EAI not infected | -0.0882 | 0.0434 | 0.0835 |
| Afri not infected-H37Ra not infected | 0.0438 | 0.0495 | 0.4553 |
| Afri not infected-H37Rv not infected | 0.1108 | 0.0514 | 0.0664 |
| BCG not infected-Beijing not infected | 0.1663 | 0.0588 | 0.0158 |
| BCG not infected-CDC1551 not infected | 0.1879 | 0.064 | 0.0126 |
| BCG not infected-EAI not infected | 0.0205 | 0.049 | 0.7218 |
| BCG not infected-H37Ra not infected | 0.1525 | 0.0666 | 0.0498 |
| BCG not infected-H37Rv not infected | 0.2195 | 0.0672 | 0.0054 |
| Beijing not infected-CDC1551 not infected | 0.0216 | 0.0418 | 0.6575 |
| Beijing not infected-EAI not infected | -0.1458 | 0.043 | 0.0041 |
| Beijing not infected-H37Ra not infected | -0.0138 | 0.0478 | 0.8113 |
| Beijing not infected-H37Rv not infected | 0.0532 | 0.0488 | 0.3547 |
| CDC1551 not infected-EAI not infected | -0.1674 | 0.0507 | 0.0051 |
| CDC1551 not infected-H37Ra not infected | -0.0354 | 0.0509 | 0.5771 |
| CDC1551 not infected-H37Rv not infected | 0.0316 | 0.0515 | 0.5966 |
| EAI not infected-H37Ra not infected | 0.132 | 0.0542 | 0.0395 |
| EAI not infected-H37Rv not infected | 0.199 | 0.0551 | 0.0022 |
| H37Ra not infected-H37Rv not infected | 0.067 | 0.0474 | 0.2367 |
| Afri infected-BCG infected | -0.1417 | 0.0587 | 0.0395 |
| Afri infected-Beijing infected | 0.0411 | 0.0367 | 0.3514 |
| Afri infected-CDC1551 infected | 0.1294 | 0.0446 | 0.0131 |
| Afri infected-EAI infected | -0.0496 | 0.0434 | 0.3468 |
| Afri infected-H37Ra infected | 0.0536 | 0.0484 | 0.3514 |
| Afri infected-H37Rv infected | 0.1628 | 0.0504 | 0.0057 |
| BCG infected-Beijing infected | 0.1828 | 0.0576 | 0.0064 |
| BCG infected-CDC1551 infected | 0.2711 | 0.0638 | 3e-04 |
| BCG infected-EAI infected | 0.092 | 0.0484 | 0.1061 |
| BCG infected-H37Ra infected | 0.1953 | 0.0652 | 0.011 |
| BCG infected-H37Rv infected | 0.3045 | 0.066 | 1e-04 |
| Beijing infected-CDC1551 infected | 0.0883 | 0.0414 | 0.0674 |
| Beijing infected-EAI infected | -0.0908 | 0.0422 | 0.0664 |

| Contrast | estimate | SE | p.value |
|---|---|---|---|
| none not infected-Afri not infected | 2.5731 | 0.6172 | 0.001 |
| none not infected-BCG not infected | 1.7058 | 0.5856 | 0.0189 |
| none not infected-Beijing not infected | 2.8851 | 0.6739 | 0.001 |
| none not infected-CDC1551 not infected | 3.6853 | 1.1059 | 0.0077 |
| none not infected-EAI not infected | 2.1596 | 0.5412 | 0.0011 |
| none not infected-H37Ra not infected | 2.0732 | 0.5744 | 0.0032 |
| none not infected-H37Rv not infected | 2.2954 | 0.5766 | 0.0011 |
| none not infected-Afri infected | 1.4994 | 0.5203 | 0.0192 |
| none not infected-BCG infected | 0.6789 | 0.5802 | 0.3944 |
| none not infected-Beijing infected | 2.0241 | 0.5265 | 0.0015 |
| none not infected-CDC1551 infected | 2.1577 | 0.6859 | 0.0116 |
| none not infected-EAI infected | 1.533 | 0.5264 | 0.0189 |
| none not infected-H37Ra infected | 1.1574 | 0.5541 | 0.1178 |
| none not infected-H37Rv infected | 1.7731 | 0.56 | 0.0116 |
| Afri not infected-BCG not infected | -0.8673 | 0.5955 | 0.2996 |
| Afri not infected-Beijing not infected | 0.3121 | 0.6701 | 0.7089 |
| Afri not infected-CDC1551 not infected | 1.1122 | 1.1161 | 0.4785 |
| Afri not infected-EAI not infected | -0.4135 | 0.543 | 0.5859 |
| Afri not infected-H37Ra not infected | -0.4998 | 0.6498 | 0.5859 |
| Afri not infected-H37Rv not infected | -0.2777 | 0.6554 | 0.7174 |
| BCG not infected-Beijing not infected | 1.1794 | 0.6683 | 0.2131 |
| BCG not infected-CDC1551 not infected | 1.9795 | 1.1224 | 0.2131 |
| BCG not infected-EAI not infected | 0.4538 | 0.3524 | 0.3666 |
| BCG not infected-H37Ra not infected | 0.3675 | 0.6323 | 0.6653 |
| BCG not infected-H37Rv not infected | 0.5896 | 0.6358 | 0.5065 |
| Beijing not infected-CDC1551 not infected | 0.8001 | 1.1422 | 0.6218 |
| Beijing not infected-EAI not infected | -0.7256 | 0.6229 | 0.3944 |
| Beijing not infected-H37Ra not infected | -0.8119 | 0.6971 | 0.3944 |
| Beijing not infected-H37Rv not infected | -0.5898 | 0.701 | 0.5602 |
| CDC1551 not infected-EAI not infected | -1.5257 | 1.0974 | 0.3237 |
| CDC1551 not infected-H37Ra not infected | -1.6121 | 1.1087 | 0.2996 |
| CDC1551 not infected-H37Rv not infected | -1.3899 | 1.1093 | 0.3679 |
| EAI not infected-H37Ra not infected | -0.0863 | 0.5905 | 0.898 |
| EAI not infected-H37Rv not infected | 0.1358 | 0.5944 | 0.8569 |
| H37Ra not infected-H37Rv not infected | 0.2221 | 0.3913 | 0.6653 |
| Afri infected-BCG infected | -0.8205 | 0.4894 | 0.2459 |
| Afri infected-Beijing infected | 0.5247 | 0.4148 | 0.3679 |
| Afri infected-CDC1551 infected | 0.6583 | 0.6258 | 0.45 |
| Afri infected-EAI infected | 0.0336 | 0.4105 | 0.9348 |
| Afri infected-H37Ra infected | -0.342 | 0.5317 | 0.6424 |
| Afri infected-H37Rv infected | 0.2737 | 0.5451 | 0.7051 |
| BCG infected-Beijing infected | 1.3452 | 0.5093 | 0.0372 |
| BCG infected-CDC1551 infected | 1.4788 | 0.7104 | 0.1178 |
| BCG infected-EAI infected | 0.8541 | 0.3319 | 0.0423 |
| BCG infected-H37Ra infected | 0.4784 | 0.6097 | 0.5859 |
| BCG infected-H37Rv infected | 1.0942 | 0.6158 | 0.2131 |
| Beijing infected-CDC1551 infected | 0.1336 | 0.621 | 0.8569 |
| Beijing infected-EAI infected | -0.4911 | 0.4352 | 0.4082 |

Acidification of phagolysosomes observed

Acidification of phagolysosomes not observed (blocked)

Acidification trend observed, stastically not significant

## Grouping: Sample

### M2 – 24 h p.i.

c) Effective MOI

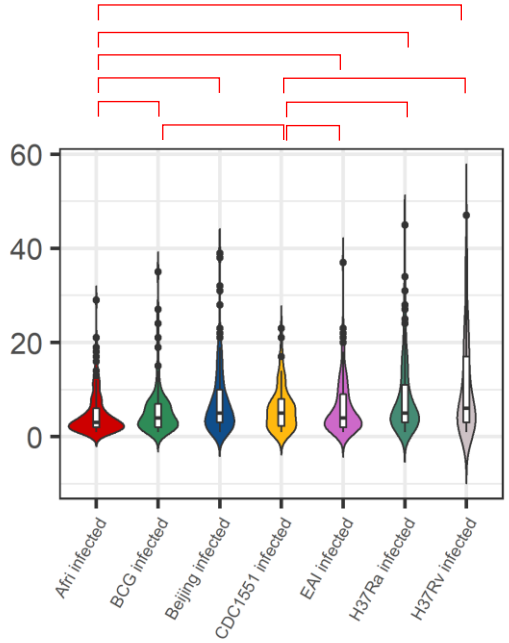


| Par | Value | Std.Error | p.value |
|---|---|---|---|
| (Intercept) | 1.126 | 0.1674 | 0 |
| groupBCG infected | 0.7435 | 0.235 | 0.0025 |
| groupBeijing infected | 0.3785 | 0.1311 | 0.0055 |
| groupCDC1551 infected | 0.1261 | 0.1629 | 0.4418 |
| groupEAI infected | 0.6265 | 0.1691 | 5e-04 |
| groupH37Ra infected | 0.6752 | 0.186 | 6e-04 |
| groupH37Rv infected | 0.7453 | 0.1955 | 3e-04 |

| Contrast | estimate | SE | p.value |
|---|---|---|---|
| Afri infected - BCG infected | -0.7435 | 0.235 | 0.0104 |
| Afri infected - Beijing infected | -0.3785 | 0.1311 | 0.0164 |
| Afri infected - CDC1551 infected | -0.1261 | 0.1629 | 0.6185 |
| Afri infected - EAI infected | -0.6265 | 0.1691 | 0.0042 |
| Afri infected - H37Ra infected | -0.6752 | 0.186 | 0.0042 |
| Afri infected - H37Rv infected | -0.7453 | 0.1955 | 0.0042 |
| BCG infected - Beijing infected | 0.365 | 0.2331 | 0.1984 |
| BCG infected - CDC1551 infected | 0.6174 | 0.2601 | 0.0488 |
| BCG infected - EAI infected | 0.117 | 0.1746 | 0.6634 |
| BCG infected - H37Ra infected | 0.0684 | 0.271 | 0.8669 |
| BCG infected - H37Rv infected | -0.0018 | 0.2748 | 0.9949 |
| Beijing infected - CDC1551 infected | 0.2524 | 0.1509 | 0.1744 |
| Beijing infected - EAI infected | -0.248 | 0.1672 | 0.215 |
| Beijing infected - H37Ra infected | -0.2966 | 0.1765 | 0.1744 |
| Beijing infected - H37Rv infected | -0.3667 | 0.18 | 0.0968 |
| CDC1551 infected - EAI infected | -0.5004 | 0.2047 | 0.0461 |
| CDC1551 infected - H37Ra infected | -0.549 | 0.1879 | 0.0164 |
| CDC1551 infected - H37Rv infected | -0.6192 | 0.1915 | 0.0104 |
| EAI infected - H37Ra infected | -0.0486 | 0.2197 | 0.8669 |
| EAI infected - H37Rv infected | -0.1187 | 0.2246 | 0.7399 |
| H37Ra infected - H37Rv infected | -0.0701 | 0.1606 | 0.7748 |

d) Colocalization Index

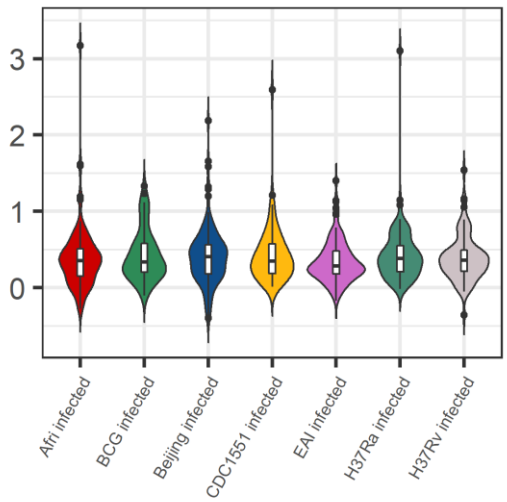


| Par | Value | Std.Error | p.value |
|---|---|---|---|
| (Intercept) | -0.1201 | 0.0896 | 0.1804 |
| groupBCG infected | 0.1305 | 0.1528 | 0.3968 |
| groupBeijing infected | 0.1024 | 0.1093 | 0.3527 |
| groupCDC1551 infected | 0.1207 | 0.1284 | 0.3511 |
| groupEAI infected | -0.1137 | 0.119 | 0.3433 |
| groupH37Ra infected | 0.121 | 0.1261 | 0.3414 |
| groupH37Rv infected | 0.0021 | 0.1336 | 0.9873 |

| Contrast | estimate | SE | p.value |
|---|---|---|---|
| Afri infected - BCG infected | -0.1305 | 0.1528 | 0.6543 |
| Afri infected - Beijing infected | -0.1024 | 0.1093 | 0.6543 |
| Afri infected - CDC1551 infected | -0.1207 | 0.1284 | 0.6543 |
| Afri infected - EAI infected | 0.1137 | 0.119 | 0.6543 |
| Afri infected - H37Ra infected | -0.121 | 0.1261 | 0.6543 |
| Afri infected - H37Rv infected | -0.0021 | 0.1336 | 0.9985 |
| BCG infected - Beijing infected | 0.0281 | 0.1498 | 0.9985 |
| BCG infected - CDC1551 infected | 0.0098 | 0.1651 | 0.9985 |
| BCG infected - EAI infected | 0.2442 | 0.1298 | 0.4907 |
| BCG infected - H37Ra infected | 0.0095 | 0.1599 | 0.9985 |
| BCG infected - H37Rv infected | 0.1283 | 0.1637 | 0.6543 |
| Beijing infected - CDC1551 infected | -0.0183 | 0.1235 | 0.9985 |
| Beijing infected - EAI infected | 0.2161 | 0.1154 | 0.4907 |
| Beijing infected - H37Ra infected | -0.0185 | 0.1226 | 0.9985 |
| Beijing infected - H37Rv infected | 0.1003 | 0.1274 | 0.6543 |
| CDC1551 infected - EAI infected | 0.2344 | 0.1374 | 0.4907 |
| CDC1551 infected - H37Ra infected | -3e-04 | 0.1352 | 0.9985 |
| CDC1551 infected - H37Rv infected | 0.1186 | 0.1404 | 0.6543 |
| EAI infected - H37Ra infected | -0.2346 | 0.1318 | 0.4907 |
| EAI infected - H37Rv infected | -0.1158 | 0.1365 | 0.6543 |
| H37Ra infected - H37Rv infected | 0.1188 | 0.1235 | 0.6543 |

**Grouping: Virulence (absolute)**

**M1 – 6 h p.i.**

a) Phagolysosomal acidification

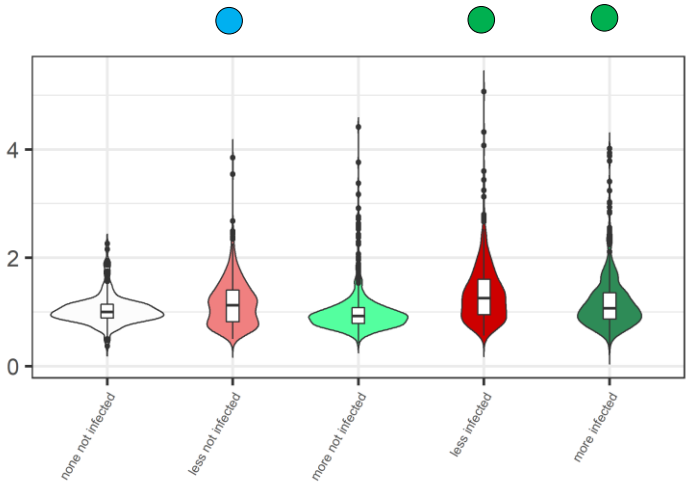


| Par | Value | Std.Error | p.value |
|---|---|---|---|
| (Intercept) | 0.002 | 0.0846 | 0.9808 |
| groupless not infected | 0.0275 | 0.0535 | 0.6078 |
| groupmore not infected | 0.0253 | 0.0549 | 0.6455 |
| groupless infected | 0.146 | 0.0536 | 0.0065 |
| groupmore infected | 0.1435 | 0.055 | 0.0091 |

| Contrast | estimate | SE | p.value |
|---|---|---|---|
| none not infected-less not infected | -0.0275 | 0.0535 | 0.8607 |
| none not infected-more not infected | -0.0253 | 0.0549 | 0.8607 |
| none not infected-less infected | -0.146 | 0.0536 | 0.0174 |
| none not infected-more infected | -0.1435 | 0.055 | 0.0183 |
| less not infected-more not infected | 0.0022 | 0.0526 | 0.9666 |
| less infected-more infected | 0.0024 | 0.0527 | 0.9666 |
| less not infected-less infected | -0.1185 | 0.0111 | 0 |
| more not infected-more infected | -0.1183 | 0.0119 | 0 |

b) Percentage of cells showing acidified phagolysosomes

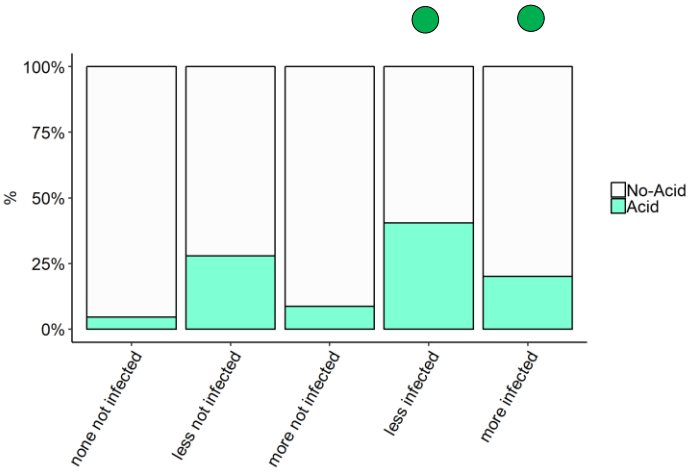


| Par | Estimate | se | OR | pvalue |
|---|---|---|---|---|
| (Intercept) | -3.6062 | 0.8803 | 0.0272 | 0 |
| groupless not infected | 1.0881 | 0.6079 | 2.9687 | 0.0735 |
| groupmore not infected | 0.3838 | 0.6742 | 1.4679 | 0.5692 |
| groupless infected | 2.0723 | 0.6054 | 7.9427 | 6e-04 |
| groupmore infected | 2.024 | 0.6518 | 7.5685 | 0.0019 |

| Contrast | estimate | SE | p.value |
|---|---|---|---|
| none not infected-less not infected | -1.0881 | 0.6079 | 0.1175 |
| none not infected-more not infected | -0.3838 | 0.6742 | 0.6505 |
| none not infected-less infected | -2.0723 | 0.6054 | 0.0017 |
| none not infected-more infected | -2.024 | 0.6518 | 0.0038 |
| less not infected-more not infected | 0.7043 | 0.5425 | 0.2589 |
| less infected-more infected | 0.0483 | 0.5109 | 0.9248 |
| less not infected-less infected | -0.9841 | 0.1835 | 0 |
| more not infected-more infected | -1.6402 | 0.2963 | 0 |

OBSERVATIONS

In M1 macrophages, none of the category is blocking the acidification of the phagolysosomes irrespective from the time point considered. The percentage of acidified macrophage was anyway found higher (40%) in the category less virulent at 6 h p.i.

- Acidification of phagolysosomes observed
- Acidification of phagolysosomes not observed (blocked)
- Acidification trend observed, stastically not significant

**Grouping: Virulence (absolute)**

**M1 – 6 h p.i.**

c) Effective MOI

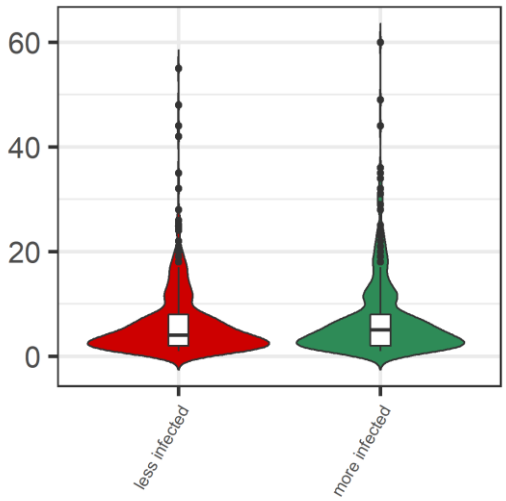


| Par | Value | Std.Error | p.value |
|---|---|---|---|
| (Intercept) | 1.4301 | 0.0942 | 0 |
| groupmore infected | 0.0276 | 0.1075 | 0.7984 |

| Contrast | estimate | SE | p.value |
|---|---|---|---|
| less infected - more infected | -0.0276 | 0.1075 | 0.7984 |

d) Colocalization Index

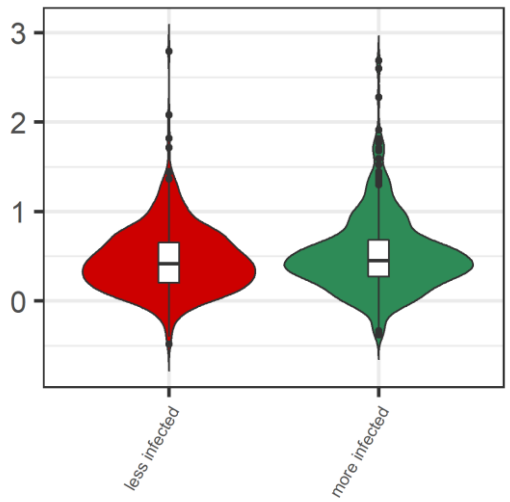


| Par | Value | Std.Error | p.value |
|---|---|---|---|
| (Intercept) | 0.0118 | 0.079 | 0.881 |
| groupmore infected | 0.0669 | 0.0917 | 0.4683 |

| Contrast | estimate | SE | p.value |
|---|---|---|---|
| less infected - more infected | -0.0669 | 0.0917 | 0.4683 |

OBSERVATIONS

No statistically relevant differences in effective MOI were observed among the categories in M1 macrophages, irrespectively from the time point considered. Colocalization with acidified compartments was similar among all the groups.

**Grouping: Virulence (absolute)**

**M1 – 24 h p.i.**

a) Phagolysosomal acidification

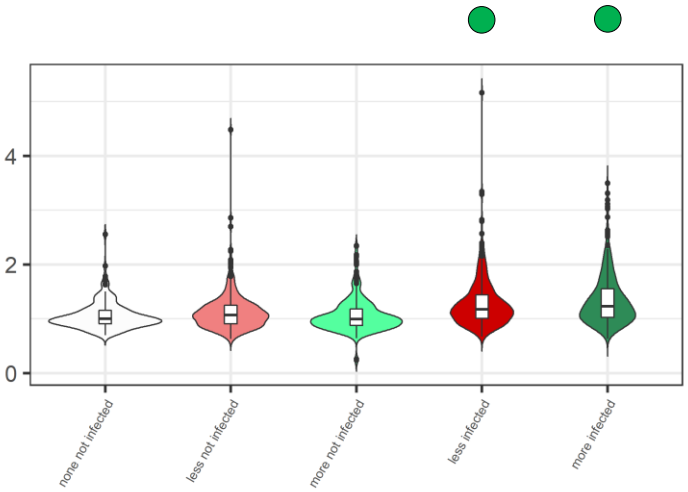


| Par | Value | Std.Error | p.value |
|---|---|---|---|
| (Intercept) | 0.0084 | 0.0437 | 0.848 |
| groupless not infected | 0.0103 | 0.0292 | 0.7237 |
| groupmore not infected | 0.0295 | 0.0303 | 0.3296 |
| groupless infected | 0.1331 | 0.029 | 0 |
| groupmore infected | 0.2074 | 0.0299 | 0 |

| Contrast | estimate | SE | p.value |
|---|---|---|---|
| none not infected-less not infected | -0.0103 | 0.0292 | 0.7237 |
| none not infected-more not infected | -0.0295 | 0.0303 | 0.4395 |
| none not infected-less infected | -0.1331 | 0.029 | 0 |
| none not infected-more infected | -0.2074 | 0.0299 | 0 |
| less not infected-more not infected | -0.0192 | 0.0272 | 0.5482 |
| less infected-more infected | -0.0743 | 0.0265 | 0.0082 |
| less not infected-less infected | -0.1228 | 0.0142 | 0 |
| more not infected-more infected | -0.1779 | 0.0165 | 0 |

b) Percentage of cells showing acidified phagolysosomes

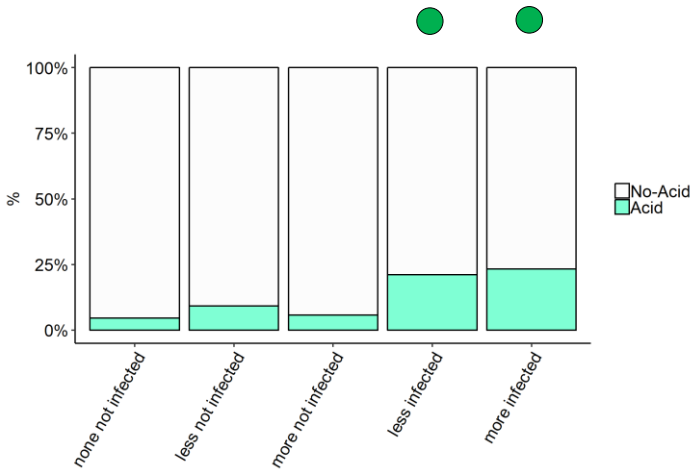


| Par | Estimate | se | OR | pvalue |
|---|---|---|---|---|
| (Intercept) | -3.1891 | 0.4561 | 0.0412 | 0 |
| groupless not infected | 0.6196 | 0.4567 | 1.8581 | 0.1749 |
| groupmore not infected | 0.3275 | 0.498 | 1.3875 | 0.5107 |
| groupless infected | 1.6859 | 0.436 | 5.3974 | 1e-04 |
| groupmore infected | 1.9742 | 0.4445 | 7.201 | 0 |

| Contrast | estimate | SE | p.value |
|---|---|---|---|
| none not infected-less not infected | -0.6196 | 0.4567 | 0.2799 |
| none not infected-more not infected | -0.3275 | 0.498 | 0.5107 |
| none not infected-less infected | -1.6859 | 0.436 | 2e-04 |
| none not infected-more infected | -1.9742 | 0.4445 | 0 |
| less not infected-more not infected | 0.292 | 0.3643 | 0.4831 |
| less infected-more infected | -0.2883 | 0.2523 | 0.3376 |
| less not infected-less infected | -1.0664 | 0.2188 | 0 |
| more not infected-more infected | -1.6467 | 0.2934 | 0 |

OBSERVATIONS

In M1 macrophages, none of the category is blocking the acidification of the phagolysosomes irrespective from the time point considered. The percentage of acidified macrophage decreased (25%) in the category less virulent and was found similar to the one observed for more virulent strains.

Acidification of phagolysosomes observed

Acidification of phagolysosomes not observed (blocked)

Acidification trend observed, stastically not significant

**Grouping: Virulence (absolute)**

**M1 – 24 h p.i.**

c) Effective MOI

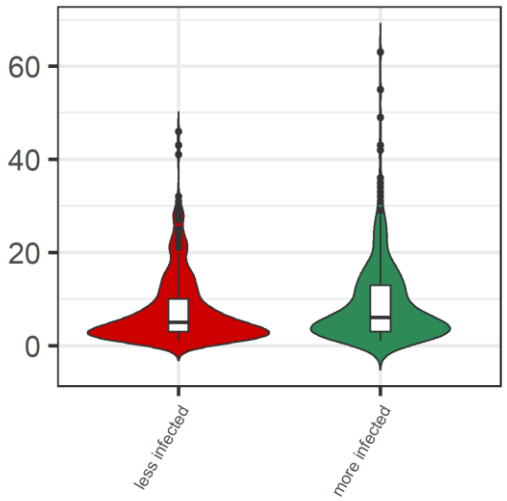


| Par | Value | Std.Error | p.value |
|---|---|---|---|
| (Intercept) | 1.7065 | 0.1352 | 0 |
| groupmore infected | -0.0243 | 0.0952 | 0.7994 |

| Contrast | estimate | SE | p.value |
|---|---|---|---|
| less infected - more infected | 0.0243 | 0.0952 | 0.7994 |

d) Colocalization Index

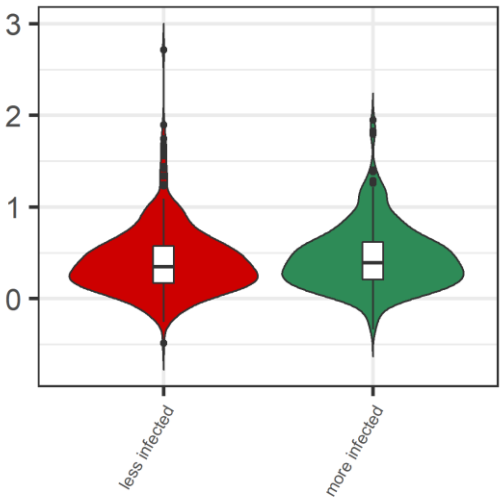


| Par | Value | Std.Error | p.value |
|---|---|---|---|
| (Intercept) | -0.0793 | 0.0691 | 0.2518 |
| groupmore infected | 0.146 | 0.0958 | 0.1326 |

| Contrast | estimate | SE | p.value |
|---|---|---|---|
| less infected - more infected | -0.146 | 0.0958 | 0.1326 |

OBSERVATIONS

No statistically relevant differences in effective MOI were observed among the categories in M1 macrophages, irrespectively from the time point considered. Colocalization with acidified compartments was similar among all the groups.

**Grouping: Virulence (absolute)**

**M2 – 6 h p.i.**

a) Phagolysosomal acidification

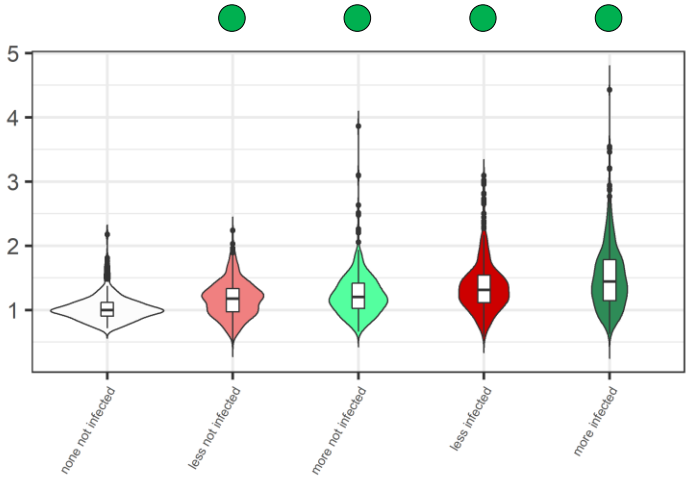


| Par | Value | Std.Error | p.value |
|---|---|---|---|
| (Intercept) | -0.0062 | 0.0521 | 0.9055 |
| groupless not infected | 0.1224 | 0.0411 | 0.003 |
| groupmore not infected | 0.1602 | 0.0421 | 1e-04 |
| groupless infected | 0.2403 | 0.0412 | 0 |
| groupmore infected | 0.2978 | 0.0421 | 0 |

| Contrast | estimate | SE | p.value |
|---|---|---|---|
| none not infected-less not infected | -0.1224 | 0.0411 | 0.0039 |
| none not infected-more not infected | -0.1602 | 0.0421 | 2e-04 |
| none not infected-less infected | -0.2403 | 0.0412 | 0 |
| none not infected-more infected | -0.2978 | 0.0421 | 0 |
| less not infected-more not infected | -0.0377 | 0.0402 | 0.3484 |
| less infected-more infected | -0.0576 | 0.0403 | 0.1752 |
| less not infected-less infected | -0.1178 | 0.0107 | 0 |
| more not infected-more infected | -0.1377 | 0.0113 | 0 |

b) Percentage of cells showing acidified phagolysosomes

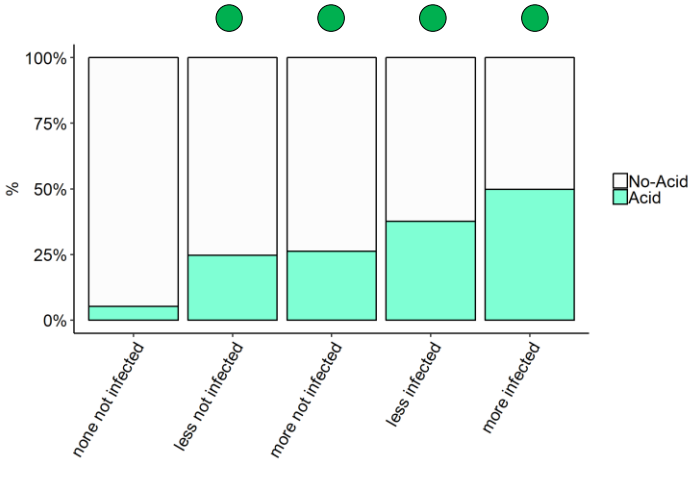


| Par | Estimate | se | OR | pvalue |
|---|---|---|---|---|
| (Intercept) | -3.2188 | 0.6551 | 0.04 | 0 |
| groupless not infected | 1.7554 | 0.5414 | 5.7858 | 0.0012 |
| groupmore not infected | 1.4685 | 0.5411 | 4.3427 | 0.0067 |
| groupless infected | 2.8003 | 0.5384 | 16.4504 | 0 |
| groupmore infected | 2.9692 | 0.5354 | 19.4768 | 0 |

| Contrast | estimate | SE | p.value |
|---|---|---|---|
| none not infected-less not infected | -1.7554 | 0.5414 | 0.0019 |
| none not infected-more not infected | -1.4685 | 0.5411 | 0.0089 |
| none not infected-less infected | -2.8003 | 0.5384 | 0 |
| none not infected-more infected | -2.9692 | 0.5354 | 0 |
| less not infected-more not infected | 0.2869 | 0.4268 | 0.5731 |
| less infected-more infected | -0.1689 | 0.4134 | 0.6829 |
| less not infected-less infected | -1.0449 | 0.1839 | 0 |
| more not infected-more infected | -1.5007 | 0.1895 | 0 |

OBSERVATIONS

In M2 macrophages, none of the category is blocking the acidification of the phagolysosomes at 6 h p.i. and between 30% (less virulent) and 50% (more virulent) of cells are showing acidification. A bystander effect in non-infected M2a macrophages was observed for both less and more virulent strains.

Acidification of phagolysosomes observed

Acidification of phagolysosomes not observed (blocked)

Acidification trend observed, stastically not significant

**Grouping: Virulence (absolute)**

**M2 – 6 h p.i.**

c) Effective MOI

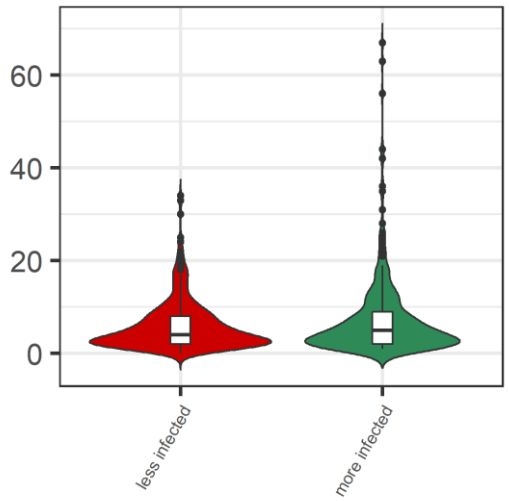


| Par | Value | Std.Error | p.value |
|---|---|---|---|
| (Intercept) | 1.7065 | 0.1352 | 0 |
| groupmore infected | -0.0243 | 0.0952 | 0.7994 |

| Contrast | estimate | SE | p.value |
|---|---|---|---|
| less infected - more infected | 0.0243 | 0.0952 | 0.7994 |

d) Colocalization Index

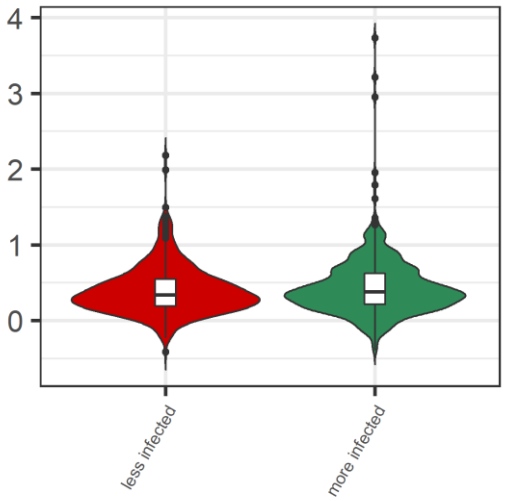


| Par | Value | Std.Error | p.value |
|---|---|---|---|
| (Intercept) | -0.1285 | 0.0572 | 0.0249 |
| groupmore infected | 0.04 | 0.0641 | 0.5354 |

| Contrast | estimate | SE | p.value |
|---|---|---|---|
| less infected - more infected | -0.04 | 0.0641 | 0.5354 |

OBSERVATIONS

No statistically relevant differences in effective MOI were observed among the categories in M2 macrophages, irrespectively from the time point considered. Colocalization with acidified compartments was similar among all the groups.

**Grouping: Virulence (absolute)**

**M2 – 24 h p.i.**

a) Phagolysosomal acidification

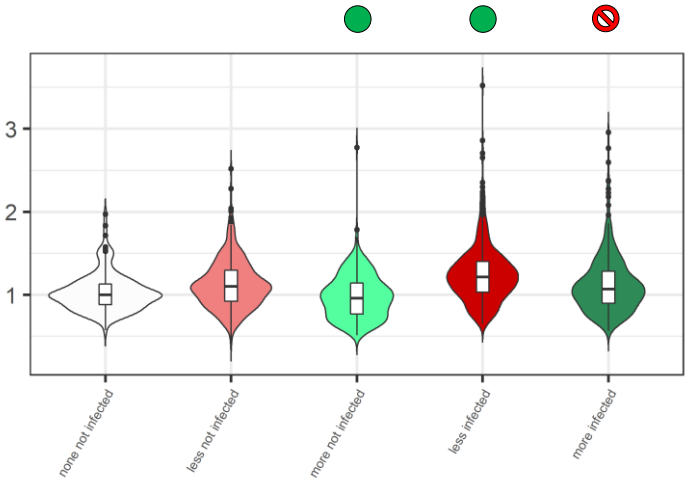


| Par | Value | Std.Error | p.value |
|---|---|---|---|
| (Intercept) | 0.0091 | 0.0541 | 0.8666 |
| groupless not infected | 0.0102 | 0.0281 | 0.7169 |
| groupmore not infected | -0.0721 | 0.0293 | 0.014 |
| groupless infected | 0.1174 | 0.028 | 0 |
| groupmore infected | 0.0238 | 0.029 | 0.4125 |

| Contrast | estimate | SE | p.value |
|---|---|---|---|
| none not infected-less not infected | -0.0102 | 0.0281 | 0.7169 |
| none not infected-more not infected | 0.0721 | 0.0293 | 0.0186 |
| none not infected-less infected | -0.1174 | 0.028 | 1e-04 |
| none not infected-more infected | -0.0238 | 0.029 | 0.4714 |
| less not infected-more not infected | 0.0823 | 0.0261 | 0.0027 |
| less infected-more infected | 0.0936 | 0.0257 | 6e-04 |
| less not infected-less infected | -0.1072 | 0.0123 | 0 |
| more not infected-more infected | -0.0958 | 0.0146 | 0 |

b) Percentage of cells showing acidified phagolysosomes

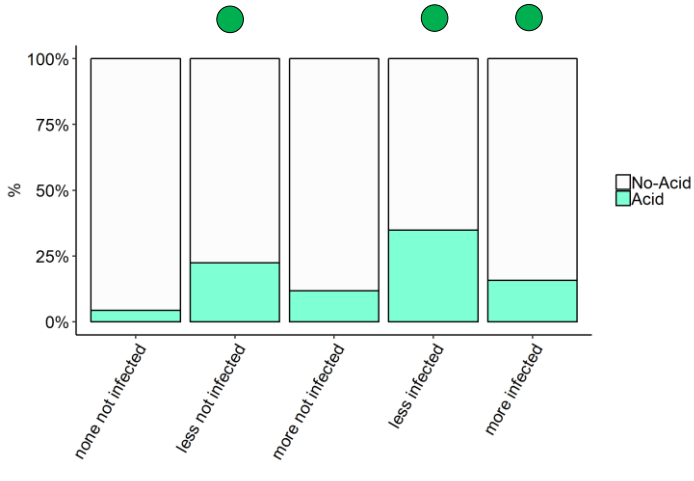


| Par | Estimate | se | OR | pvalue |
|---|---|---|---|---|
| (Intercept) | -3.585 | 0.6451 | 0.0277 | 0 |
| groupless not infected | 1.3491 | 0.4714 | 3.8539 | 0.0042 |
| groupmore not infected | 0.9519 | 0.5148 | 2.5906 | 0.0644 |
| groupless infected | 2.2141 | 0.4669 | 9.1531 | 0 |
| groupmore infected | 1.6312 | 0.4988 | 5.1099 | 0.0011 |

| Contrast | estimate | SE | p.value |
|---|---|---|---|
| none not infected-less not infected | -1.3491 | 0.4714 | 0.0084 |
| none not infected-more not infected | -0.9519 | 0.5148 | 0.0737 |
| none not infected-less infected | -2.2141 | 0.4669 | 0 |
| none not infected-more infected | -1.6312 | 0.4988 | 0.0029 |
| less not infected-more not infected | 0.3972 | 0.3048 | 0.1926 |
| less infected-more infected | 0.5829 | 0.2669 | 0.0386 |
| less not infected-less infected | -0.865 | 0.176 | 0 |
| more not infected-more infected | -0.6793 | 0.2867 | 0.0285 |

OBSERVATIONS

However, as the infection progresses, more virulent strains are blocking the acidification of the phagolysosomes. The percentage of acidified cells remained constant for less virulent strains, whereas it dropped below 25% for more virulent strains.

- Acidification of phagolysosomes observed
- Acidification of phagolysosomes not observed (blocked)
- Acidification trend observed, stastically not significant

**Grouping: Virulence (absolute)**

**M2 – 24 h p.i.**

c) Effective MOI

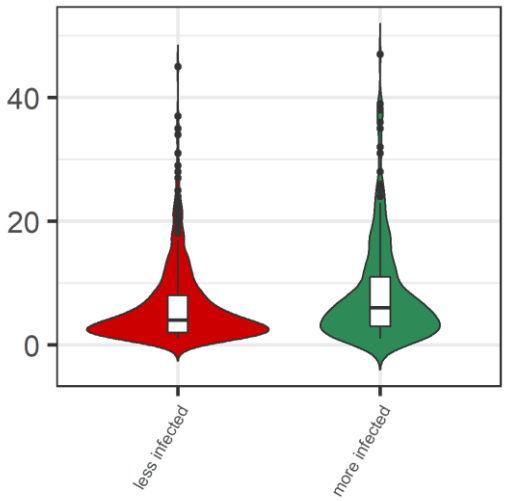


| Par | Value | Std.Error | p.value |
|---|---|---|---|
| (Intercept) | 1.5323 | 0.1172 | 0 |
| groupmore infected | 0.0789 | 0.1043 | 0.4523 |

| Contrast | estimate | SE | p.value |
|---|---|---|---|
| less infected - more infected | -0.0789 | 0.1043 | 0.4523 |

d) Colocalization Index

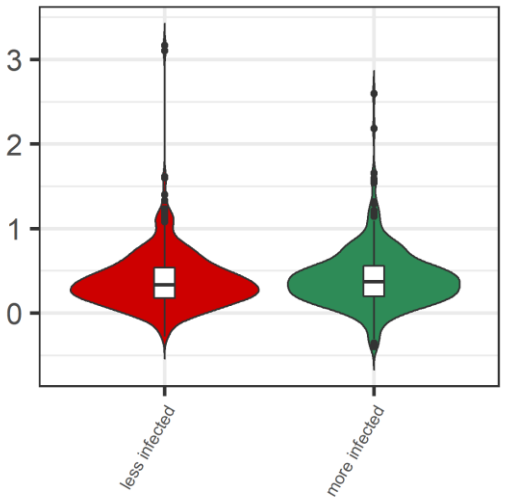


| Par | Value | Std.Error | p.value |
|---|---|---|---|
| (Intercept) | -0.1034 | 0.0503 | 0.0402 |
| groupmore infected | 0.0671 | 0.0705 | 0.3444 |

| Contrast | estimate | SE | p.value |
|---|---|---|---|
| less infected - more infected | -0.0671 | 0.0705 | 0.3444 |

OBSERVATIONS

No statistically relevant differences in effective MOI were observed among the categories in M2 macrophages, irrespectively from the time point considered. Colocalization with acidified compartments was similar among all the groups.

**Grouping: Virulence (relative)**

**M1 – 6 h p.i.**

a) Phagolysosomal acidification

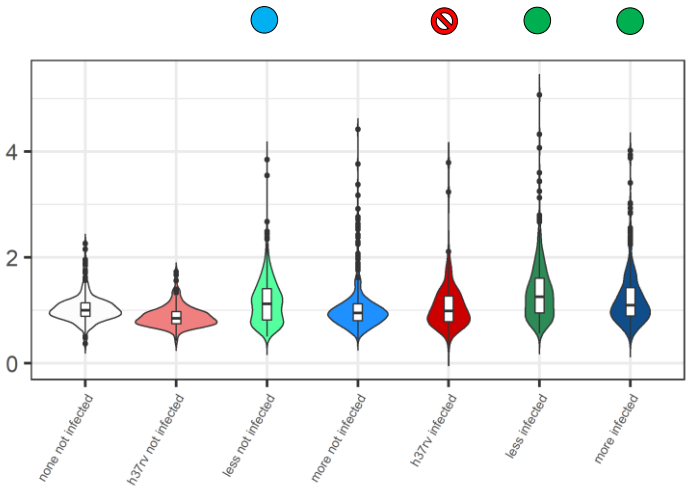


| Par | Value | Std.Error | p.value |
|---|---|---|---|
| (Intercept) | 0.0024 | 0.0838 | 0.9773 |
| grouph37rv not infected | 0.0038 | 0.0834 | 0.9633 |
| groupless not infected | 0.0285 | 0.0539 | 0.5975 |
| groupmore not infected | 0.0336 | 0.0605 | 0.5786 |
| grouph37rv infected | 0.1172 | 0.0839 | 0.1625 |
| groupless infected | 0.147 | 0.054 | 0.0065 |
| groupmore infected | 0.1569 | 0.0605 | 0.0096 |

| Contrast | estimate | SE | p.value |
|---|---|---|---|
| none not infected-h37rv not infected | -0.0038 | 0.0834 | 0.9633 |
| none not infected-less not infected | -0.0285 | 0.0539 | 0.9596 |
| none not infected-more not infected | -0.0336 | 0.0605 | 0.9596 |
| none not infected-h37rv infected | -0.1172 | 0.0839 | 0.4063 |
| none not infected-less infected | -0.147 | 0.054 | 0.0245 |
| none not infected-more infected | -0.1569 | 0.0605 | 0.0288 |
| h37rv not infected-less not infected | -0.0246 | 0.0834 | 0.9596 |
| h37rv not infected-more not infected | -0.0298 | 0.0871 | 0.9596 |
| less not infected-more not infected | -0.0052 | 0.0576 | 0.9633 |
| h37rv infected-less infected | -0.0298 | 0.0839 | 0.9596 |
| h37rv infected-more infected | -0.0397 | 0.0875 | 0.9596 |
| less infected-more infected | -0.0099 | 0.0576 | 0.9633 |
| h37rv not infected-h37rv infected | -0.1134 | 0.0232 | 0 |
| less not infected-less infected | -0.1185 | 0.0111 | 0 |
| more not infected-more infected | -0.1233 | 0.0139 | 0 |

b) Percentage of cells showing acidified phagolysosomes

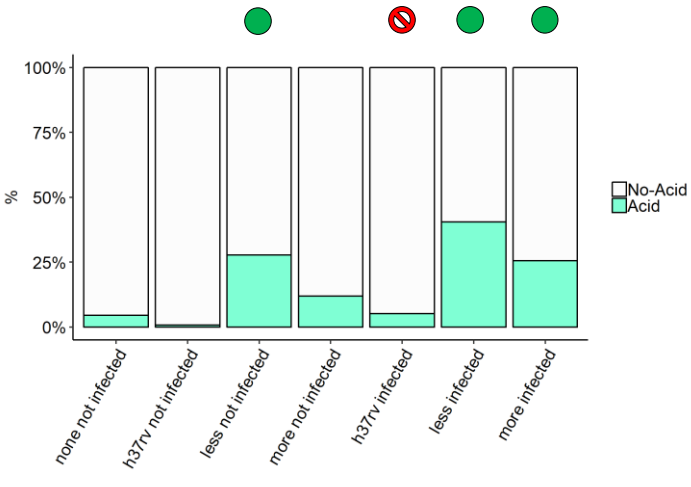


| Par | Estimate | se | OR | pvalue |
|---|---|---|---|---|
| (Intercept) | -3.5774 | 0.8537 | 0.0279 | 0 |
| grouph37rv not infected | -0.5903 | 1.3921 | 0.5542 | 0.6715 |
| groupless not infected | 1.115 | 0.6074 | 3.0497 | 0.0664 |
| groupmore not infected | 0.5864 | 0.7119 | 1.7976 | 0.4101 |
| grouph37rv infected | 1.4056 | 1.0433 | 4.078 | 0.1779 |
| groupless infected | 2.0973 | 0.6048 | 8.144 | 5e-04 |
| groupmore infected | 2.2031 | 0.6926 | 9.0534 | 0.0015 |

| Contrast | estimate | SE | p.value |
|---|---|---|---|
| none not infected-h37rv not infected | 0.5903 | 1.3921 | 0.7195 |
| none not infected-less not infected | -1.115 | 0.6074 | 0.177 |
| none not infected-more not infected | -0.5864 | 0.7119 | 0.5552 |
| none not infected-h37rv infected | -1.4056 | 1.0433 | 0.3812 |
| none not infected-less infected | -2.0973 | 0.6048 | 0.0026 |
| none not infected-more infected | -2.2031 | 0.6926 | 0.0055 |
| h37rv not infected-less not infected | -1.7053 | 1.3492 | 0.3867 |
| h37rv not infected-more not infected | -1.1767 | 1.4085 | 0.5552 |
| less not infected-more not infected | 0.5286 | 0.5785 | 0.5552 |
| h37rv infected-less infected | -0.6917 | 0.9818 | 0.5552 |
| h37rv infected-more infected | -0.7975 | 1.0485 | 0.5552 |
| less infected-more infected | -0.1059 | 0.5515 | 0.8478 |
| h37rv not infected-h37rv infected | -1.9959 | 1.1047 | 0.177 |
| less not infected-less infected | -0.9823 | 0.1833 | 0 |
| more not infected-more infected | -1.6167 | 0.3103 | 0 |

OBSERVATIONS

In M1 macrophages, H37Rv is blocking the phagolysosomal acidification at 6 h p.i. The percentage of acidified macrophase was anyway found higher (40%) in the category less virulent at 6 h p.i.

- Acidification of phagolysosomes observed
- Acidification of phagolysosomes not observed (blocked)
- Acidification trend observed, stastically not significant

**Grouping: Virulence (relative)**

**M1 – 6 h p.i.**

c) Effective MOI

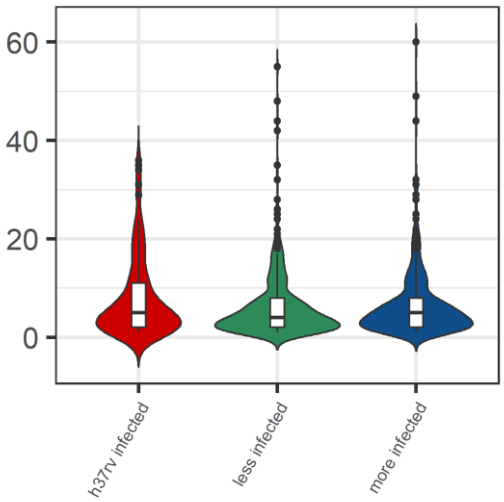


| Par | Value | Std.Error | p.value |
|---|---|---|---|
| (Intercept) | 1.4927 | 0.1598 | 0 |
| groupless infected | -0.0639 | 0.1702 | 0.7087 |
| groupmore infected | -0.0496 | 0.1761 | 0.7793 |

| Contrast | estimate | SE | p.value |
|---|---|---|---|
| h37rv infected - less infected | 0.0639 | 0.1702 | 0.9031 |
| h37rv infected - more infected | 0.0496 | 0.1761 | 0.9031 |
| less infected - more infected | -0.0143 | 0.1171 | 0.9031 |

d) Colocalization Index

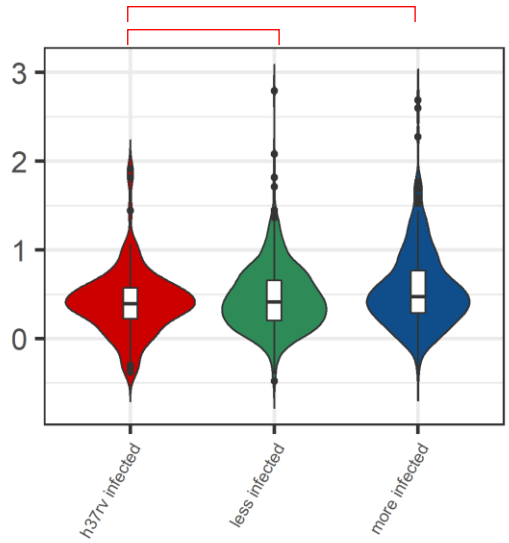


| Par | Value | Std.Error | p.value |
|---|---|---|---|
| (Intercept) | -0.274 | 0.1405 | 0.0516 |
| groupless infected | 0.3106 | 0.1384 | 0.0283 |
| groupmore infected | 0.4833 | 0.1413 | 0.0011 |

| Contrast | estimate | SE | p.value |
|---|---|---|---|
| h37rv infected - less infected | -0.3106 | 0.1384 | 0.0425 |
| h37rv infected - more infected | -0.4833 | 0.1413 | 0.0033 |
| less infected - more infected | -0.1727 | 0.0945 | 0.0724 |

OBSERVATIONS

Colocalization with acidified compartments was found higher for more virulent strains at 6 h p.i.

**Grouping: Virulence (relative)**

**M1 – 24 h p.i.**

a) Phagolysosomal acidification

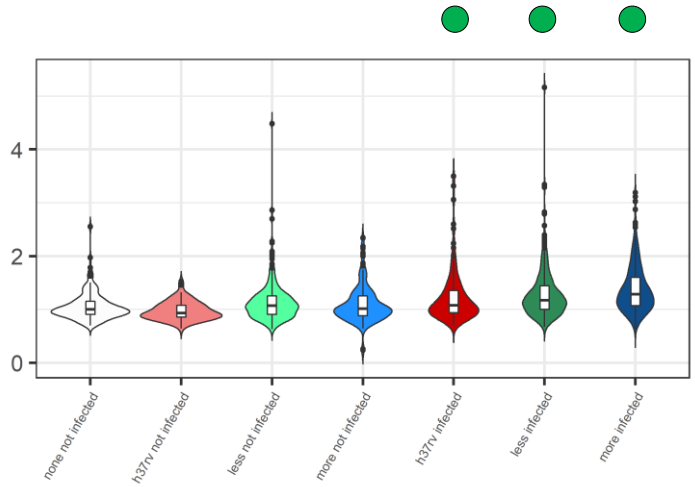


| Par | Value | Std.Error | p.value |
|---|---|---|---|
| (Intercept) | 0.0095 | 0.0424 | 0.8227 |
| grouph37rv not infected | 0.0183 | 0.0448 | 0.6826 |
| groupless not infected | 0.0111 | 0.0292 | 0.7038 |
| groupmore not infected | 0.0323 | 0.0328 | 0.3242 |
| grouph37rv infected | 0.155 | 0.0436 | 4e-04 |
| groupless infected | 0.1336 | 0.029 | 0 |
| groupmore infected | 0.2277 | 0.0321 | 0 |

| Contrast | estimate | SE | p.value |
|---|---|---|---|
| none not infected-h37rv not infected | -0.0183 | 0.0448 | 0.812 |
| none not infected-less not infected | -0.0111 | 0.0292 | 0.812 |
| none not infected-more not infected | -0.0323 | 0.0328 | 0.5404 |
| none not infected-h37rv infected | -0.155 | 0.0436 | 0.001 |
| none not infected-less infected | -0.1336 | 0.029 | 0 |
| none not infected-more infected | -0.2277 | 0.0321 | 0 |
| h37rv not infected-less not infected | 0.0072 | 0.0432 | 0.8672 |
| h37rv not infected-more not infected | -0.014 | 0.0456 | 0.8131 |
| less not infected-more not infected | -0.0212 | 0.0297 | 0.712 |
| h37rv infected-less infected | 0.0213 | 0.0416 | 0.812 |
| h37rv infected-more infected | -0.0728 | 0.0436 | 0.1791 |
| less infected-more infected | -0.0941 | 0.0289 | 0.0024 |
| h37rv not infected-h37rv infected | -0.1367 | 0.03 | 0 |
| less not infected-less infected | -0.1225 | 0.0142 | 0 |
| more not infected-more infected | -0.1954 | 0.0197 | 0 |

b) Percentage of cells showing acidified phagolysosomes

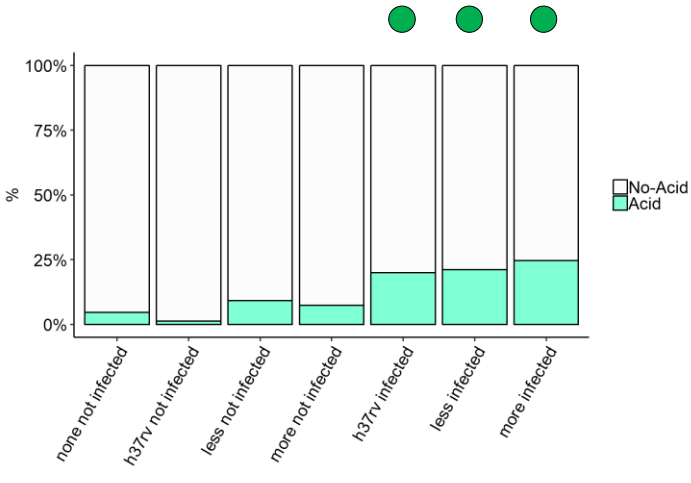


| Par | Estimate | se | OR | pvalue |
|---|---|---|---|---|
| (Intercept) | -3.183 | 0.4538 | 0.0415 | 0 |
| grouph37rv not infected | -1.0349 | 1.1117 | 0.3552 | 0.3519 |
| groupless not infected | 0.6288 | 0.457 | 1.8753 | 0.1689 |
| groupmore not infected | 0.5519 | 0.5093 | 1.7366 | 0.2785 |
| grouph37rv infected | 1.9228 | 0.5288 | 6.84 | 3e-04 |
| groupless infected | 1.6912 | 0.4361 | 5.426 | 1e-04 |
| groupmore infected | 1.9824 | 0.4561 | 7.2598 | 0 |

| Contrast | estimate | SE | p.value |
|---|---|---|---|
| none not infected-h37rv not infected | 1.0349 | 1.1117 | 0.4398 |
| none not infected-less not infected | -0.6288 | 0.457 | 0.2815 |
| none not infected-more not infected | -0.5519 | 0.5093 | 0.3836 |
| none not infected-h37rv infected | -1.9228 | 0.5288 | 8e-04 |
| none not infected-less infected | -1.6912 | 0.4361 | 4e-04 |
| none not infected-more infected | -1.9824 | 0.4561 | 1e-04 |
| h37rv not infected-less not infected | -1.6637 | 1.0623 | 0.2514 |
| h37rv not infected-more not infected | -1.5869 | 1.0787 | 0.2649 |
| less not infected-more not infected | 0.0768 | 0.3765 | 0.8784 |
| h37rv infected-less infected | 0.2316 | 0.3862 | 0.6331 |
| h37rv infected-more infected | -0.0596 | 0.3893 | 0.8784 |
| less infected-more infected | -0.2911 | 0.2702 | 0.3836 |
| h37rv not infected-h37rv infected | -2.9577 | 1.0388 | 0.011 |
| less not infected-less infected | -1.0625 | 0.2188 | 0 |
| more not infected-more infected | -1.4304 | 0.3144 | 0 |

OBSERVATIONS

At 24 h p.i. none of the category is blocking the acidification of the phagolysosomes. The percentage of acidified macrophase was found below 25%.

- Acidification of phagolysosomes observed
- Acidification of phagolysosomes not observed (blocked)
- Acidification trend observed, stastically not significant

**Grouping: Virulence (relative)**

**M1 – 24 h p.i.**

c) Effective MOI

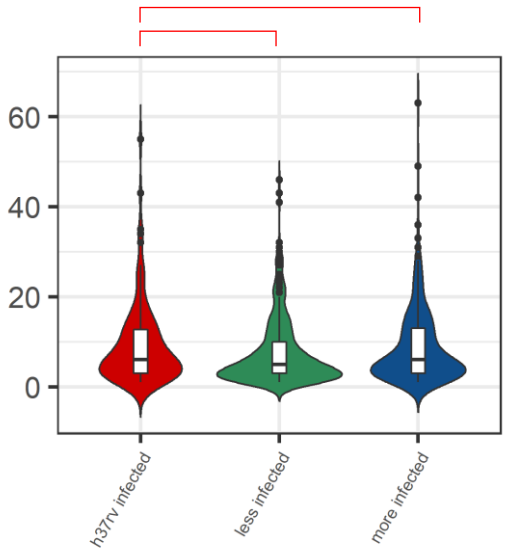


| Par | Value | Std.Error | p.value |
|---|---|---|---|
| (Intercept) | 1.4019 | 0.1849 | 0 |
| groupless infected | 0.3265 | 0.1363 | 0.0197 |
| groupmore infected | 0.3724 | 0.1425 | 0.0113 |

| Contrast | estimate | SE | p.value |
|---|---|---|---|
| h37rv infected - less infected | -0.3265 | 0.1363 | 0.0295 |
| h37rv infected - more infected | -0.3724 | 0.1425 | 0.0295 |
| less infected - more infected | -0.0459 | 0.0961 | 0.6351 |

d) Colocalization Index

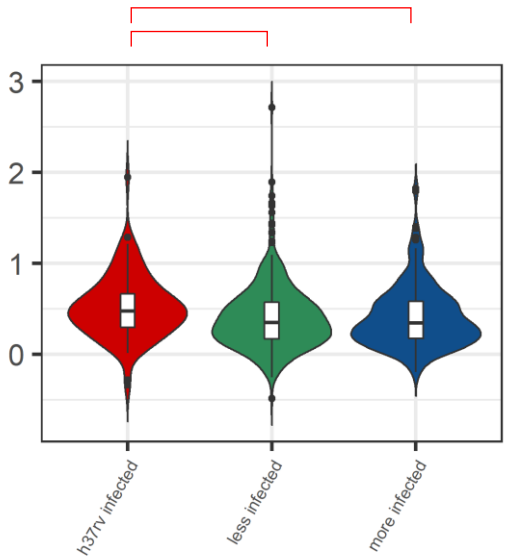


| Par | Value | Std.Error | p.value |
|---|---|---|---|
| (Intercept) | 0.3599 | 0.1222 | 0.0033 |
| groupless infected | -0.4429 | 0.1358 | 0.0018 |
| groupmore infected | -0.4322 | 0.1442 | 0.0039 |

| Contrast | estimate | SE | p.value |
|---|---|---|---|
| h37rv infected - less infected | 0.4429 | 0.1358 | 0.0054 |
| h37rv infected - more infected | 0.4322 | 0.1442 | 0.0059 |
| less infected - more infected | -0.0107 | 0.0999 | 0.9152 |

OBSERVATIONS

Colocalization was found higher for H37Rv at 24 h p.i. H37Rv showed higher MOI at 24 h p.i.

**Grouping: Virulence (relative)**

**M2 – 6 h p.i.**

a) Phagolysosomal acidification

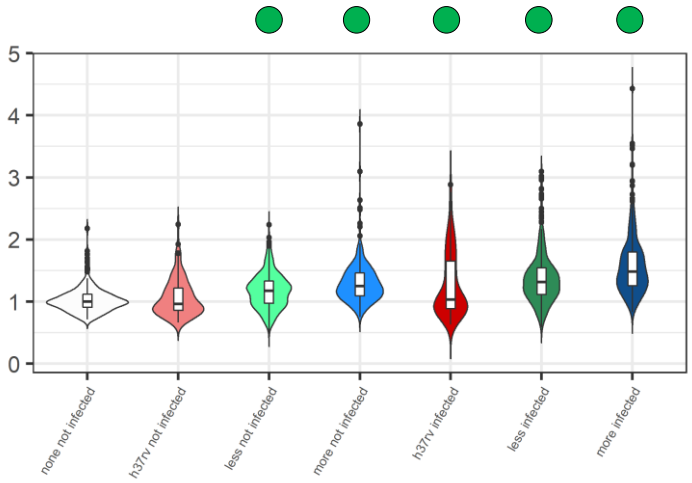


b) Percentage of cells showing acidified phagolysosomes

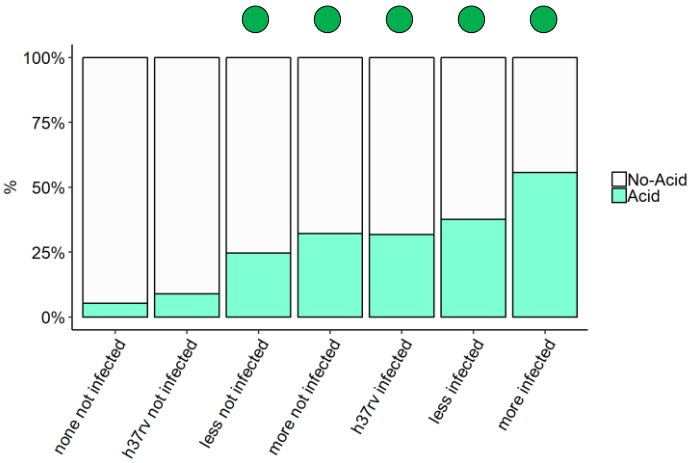


| Par | Value | Std.Error | p.value |
|---|---|---|---|
| (Intercept) | -0.0092 | 0.0468 | 0.8444 |
| grouph37rv not infected | 0.0701 | 0.062 | 0.2582 |
| groupless not infected | 0.1306 | 0.0407 | 0.0013 |
| groupmore not infected | 0.2014 | 0.0457 | 0 |
| grouph37rv infected | 0.196 | 0.0622 | 0.0016 |
| groupless infected | 0.249 | 0.0408 | 0 |
| groupmore infected | 0.3473 | 0.0456 | 0 |

| Par | Estimate | se | OR | pvalue |
|---|---|---|---|---|
| (Intercept) | -3.1983 | 0.6306 | 0.0408 | 0 |
| grouph37rv not infected | 0.0529 | 0.8209 | 1.0543 | 0.9486 |
| groupless not infected | 1.7791 | 0.5405 | 5.9247 | 0.001 |
| groupmore not infected | 1.806 | 0.5651 | 6.0859 | 0.0014 |
| grouph37rv infected | 2.4272 | 0.7421 | 11.3272 | 0.0011 |
| groupless infected | 2.8201 | 0.5373 | 16.7779 | 0 |
| groupmore infected | 3.1457 | 0.5618 | 23.2369 | 0 |

| Contrast | estimate | SE | p.value |
|---|---|---|---|
| none not infected-h37rv not infected | -0.0701 | 0.062 | 0.298 |
| none not infected-less not infected | -0.1306 | 0.0407 | 0.0029 |
| none not infected-more not infected | -0.2014 | 0.0457 | 0 |
| none not infected-h37rv infected | -0.196 | 0.0622 | 0.0031 |
| none not infected-less infected | -0.249 | 0.0408 | 0 |
| none not infected-more infected | -0.3473 | 0.0456 | 0 |
| h37rv not infected-less not infected | -0.0605 | 0.0621 | 0.3534 |
| h37rv not infected-more not infected | -0.1313 | 0.0648 | 0.0584 |
| less not infected-more not infected | -0.0708 | 0.043 | 0.1247 |
| h37rv infected-less infected | -0.053 | 0.0623 | 0.3947 |
| h37rv infected-more infected | -0.1512 | 0.0648 | 0.033 |
| less infected-more infected | -0.0982 | 0.043 | 0.0338 |
| h37rv not infected-h37rv infected | -0.1259 | 0.0224 | 0 |
| less not infected-less infected | -0.1184 | 0.0108 | 0 |
| more not infected-more infected | -0.1459 | 0.0132 | 0 |

| Contrast | estimate | SE | p.value |
|---|---|---|---|
| none not infected-h37rv not infected | -0.0529 | 0.8209 | 0.9526 |
| none not infected-less not infected | -1.7791 | 0.5405 | 0.0023 |
| none not infected-more not infected | -1.806 | 0.5651 | 0.0026 |
| none not infected-h37rv infected | -2.4272 | 0.7421 | 0.0023 |
| none not infected-less infected | -2.8201 | 0.5373 | 0 |
| none not infected-more infected | -3.1457 | 0.5618 | 0 |
| h37rv not infected-less not infected | -1.7262 | 0.7637 | 0.0357 |
| h37rv not infected-more not infected | -1.7531 | 0.77 | 0.0357 |
| less not infected-more not infected | -0.0268 | 0.4515 | 0.9526 |
| h37rv infected-less infected | -0.3929 | 0.6699 | 0.6433 |
| h37rv infected-more infected | -0.7185 | 0.6881 | 0.4041 |
| less infected-more infected | -0.3257 | 0.4428 | 0.5775 |
| h37rv not infected-h37rv infected | -2.3743 | 0.5099 | 0 |
| less not infected-less infected | -1.0409 | 0.1835 | 0 |
| more not infected-more infected | -1.3398 | 0.2066 | 0 |

OBSERVATIONS

In M2 macrophages, none of the category is blocking the acidification of the phagolysosomes at 6 h p.i. and between 30% (less virulent and H37Rv) and 50% (more virulent) of cells are showing acidification. A bystander effect in non-infected M2a macrophages was consistently observed for less virulent strains.

- Acidification of phagolysosomes observed
- Acidification of phagolysosomes not observed (blocked)
- Acidification trend observed, stastically not significant

**Grouping: Virulence (relative)**

**M2 – 6 h p.i.**

c) Effective MOI

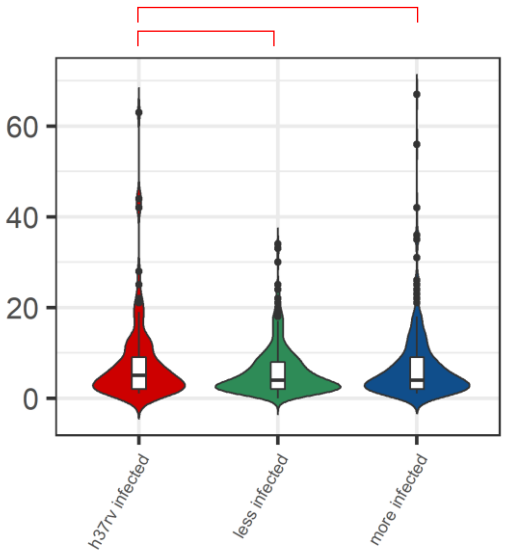


| Par | Value | Std.Error | p.value |
|---|---|---|---|
| (Intercept) | 1.4019 | 0.1849 | 0 |
| groupless infected | 0.3265 | 0.1363 | 0.0197 |
| groupmore infected | 0.3724 | 0.1425 | 0.0113 |

| Contrast | estimate | SE | p.value |
|---|---|---|---|
| h37rv infected - less infected | -0.3265 | 0.1363 | 0.0295 |
| h37rv infected - more infected | -0.3724 | 0.1425 | 0.0295 |
| less infected - more infected | -0.0459 | 0.0961 | 0.6351 |

d) Colocalization Index

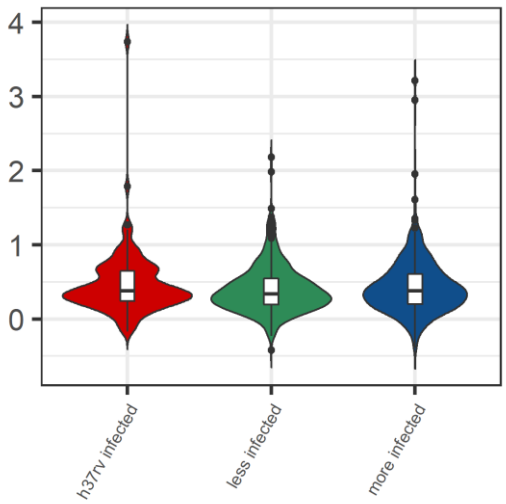


| Par | Value | Std.Error | p.value |
|---|---|---|---|
| (Intercept) | -0.1544 | 0.0986 | 0.1178 |
| groupless infected | 0.035 | 0.1015 | 0.7316 |
| groupmore infected | 0.0949 | 0.1037 | 0.3634 |

| Contrast | estimate | SE | p.value |
|---|---|---|---|
| h37rv infected - less infected | -0.035 | 0.1015 | 0.7316 |
| h37rv infected - more infected | -0.0949 | 0.1037 | 0.5812 |
| less infected - more infected | -0.06 | 0.0689 | 0.5812 |

OBSERVATIONS

H37Rv showed higher MOI. Colocalization with acidified compartments was similar among all the groups.

**Grouping: Virulence (relative)**

**M2 – 24 h p.i.**

a) Phagolysosomal acidification

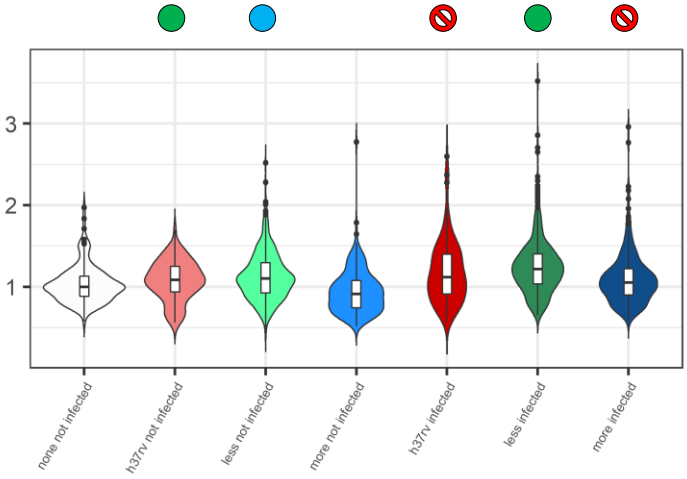


| Par | Value | Std.Error | p.value |
|---|---|---|---|
| (Intercept) | 0.0101 | 0.0549 | 0.8537 |
| grouph37rv not infected | -0.0953 | 0.0434 | 0.0281 |
| groupless not infected | 0.0111 | 0.028 | 0.6931 |
| groupmore not infected | -0.0639 | 0.0316 | 0.0429 |
| grouph37rv infected | -0.0298 | 0.0423 | 0.4809 |
| groupless infected | 0.1181 | 0.0279 | 0 |
| groupmore infected | 0.0422 | 0.0311 | 0.1752 |

| Contrast | estimate | SE | p.value |
|---|---|---|---|
| none not infected-h37rv not infected | 0.0953 | 0.0434 | 0.0469 |
| none not infected-less not infected | -0.0111 | 0.028 | 0.6931 |
| none not infected-more not infected | 0.0639 | 0.0316 | 0.0644 |
| none not infected-h37rv infected | 0.0298 | 0.0423 | 0.5153 |
| none not infected-less infected | -0.1181 | 0.0279 | 1e-04 |
| none not infected-more infected | -0.0422 | 0.0311 | 0.219 |
| h37rv not infected-less not infected | -0.1064 | 0.0418 | 0.0238 |
| h37rv not infected-more not infected | -0.0313 | 0.0441 | 0.5153 |
| less not infected-more not infected | 0.075 | 0.0284 | 0.0207 |
| h37rv infected-less infected | -0.1479 | 0.0406 | 0.001 |
| h37rv infected-more infected | -0.0721 | 0.0426 | 0.1238 |
| less infected-more infected | 0.0759 | 0.0278 | 0.0196 |
| h37rv not infected-h37rv infected | -0.0655 | 0.0264 | 0.0248 |
| less not infected-less infected | -0.107 | 0.0123 | 0 |
| more not infected-more infected | -0.1062 | 0.0176 | 0 |

b) Percentage of cells showing acidified phagolysosomes

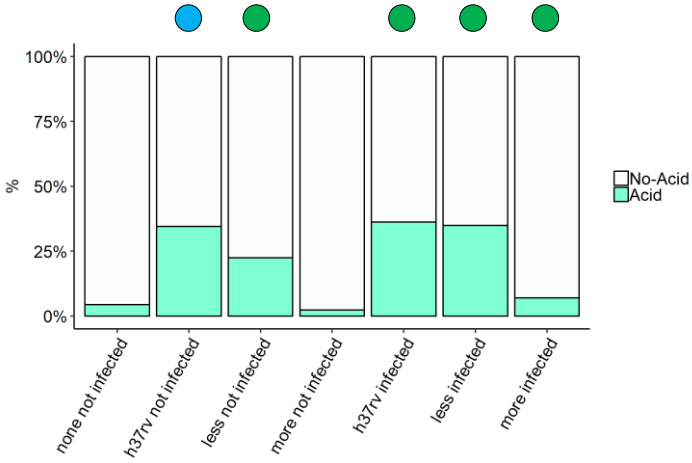


| Par | Estimate | se | OR | pvalue |
|---|---|---|---|---|
| (Intercept) | -3.5499 | 0.636 | 0.0287 | 0 |
| grouph37rv not infected | 1.1603 | 0.5574 | 3.1908 | 0.0374 |
| groupless not infected | 1.3347 | 0.4707 | 3.7989 | 0.0046 |
| groupmore not infected | 0.5412 | 0.6621 | 1.718 | 0.4137 |
| grouph37rv infected | 1.6871 | 0.5497 | 5.4039 | 0.0021 |
| groupless infected | 2.1921 | 0.4664 | 8.9544 | 0 |
| groupmore infected | 1.5756 | 0.5424 | 4.8338 | 0.0037 |

| Contrast | estimate | SE | p.value |
|---|---|---|---|
| none not infected-h37rv not infected | -1.1603 | 0.5574 | 0.0934 |
| none not infected-less not infected | -1.3347 | 0.4707 | 0.0137 |
| none not infected-more not infected | -0.5412 | 0.6621 | 0.4773 |
| none not infected-h37rv infected | -1.6871 | 0.5497 | 0.0107 |
| none not infected-less infected | -2.1921 | 0.4664 | 0 |
| none not infected-more infected | -1.5756 | 0.5424 | 0.0137 |
| h37rv not infected-less not infected | -0.1744 | 0.3789 | 0.6913 |
| h37rv not infected-more not infected | 0.6191 | 0.6029 | 0.3806 |
| less not infected-more not infected | 0.7935 | 0.513 | 0.2032 |
| h37rv infected-less infected | -0.505 | 0.3672 | 0.2305 |
| h37rv infected-more infected | 0.1115 | 0.4481 | 0.8036 |
| less infected-more infected | 0.6165 | 0.3323 | 0.1192 |
| h37rv not infected-h37rv infected | -0.5268 | 0.36 | 0.2151 |
| less not infected-less infected | -0.8574 | 0.1754 | 0 |
| more not infected-more infected | -1.0345 | 0.525 | 0.1045 |

OBSERVATIONS

As the infection progresses, H37Rv and more virulent strains are blocking the acidification of the phagolysosomes. The percentage of acidified cells remained constant for less virulent strains and H37Rv, whereas it dropped below 10% for more virulent strains. A bystander effect in non-infected M2a macrophages was consistently observed for less virulent strains.

- Acidification of phagolysosomes observed
- Acidification of phagolysosomes not observed (blocked)
- Acidification trend observed, stastically not significant

**Grouping: Virulence (relative)**

**M2 – 24 h p.i.**

c) Effective MOI

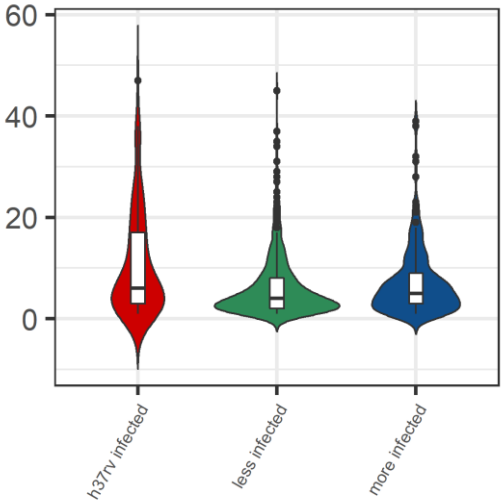


| Par | Value | Std.Error | p.value |
|---|---|---|---|
| (Intercept) | 1.8249 | 0.1664 | 0 |
| groupless infected | -0.3148 | 0.1656 | 0.062 |
| groupmore infected | -0.2826 | 0.1734 | 0.1082 |

| Contrast | estimate | SE | p.value |
|---|---|---|---|
| h37rv infected - less infected | 0.3148 | 0.1656 | 0.1623 |
| h37rv infected - more infected | 0.2826 | 0.1734 | 0.1623 |
| less infected - more infected | -0.0322 | 0.1146 | 0.7798 |

d) Colocalization Index

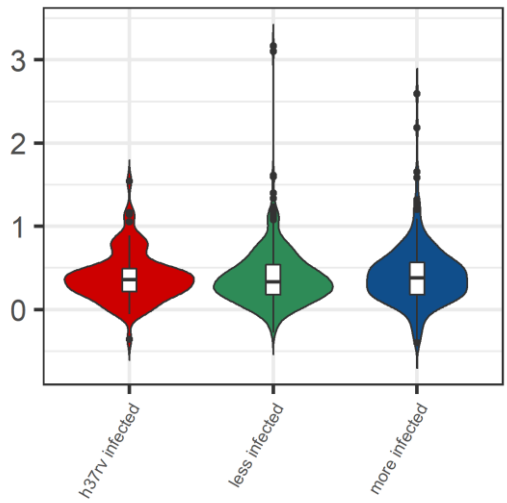


| Par | Value | Std.Error | p.value |
|---|---|---|---|
| (Intercept) | -0.1339 | 0.1023 | 0.1911 |
| groupless infected | 0.0343 | 0.1102 | 0.7563 |
| groupmore infected | 0.1336 | 0.1187 | 0.2646 |

| Contrast | estimate | SE | p.value |
|---|---|---|---|
| h37rv infected - less infected | -0.0343 | 0.1102 | 0.7563 |
| h37rv infected - more infected | -0.1336 | 0.1187 | 0.397 |
| less infected - more infected | -0.0993 | 0.0797 | 0.397 |

OBSERVATIONS

H37Rv showed higher MOI. Colocalization with acidified compartments was similar among all the groups.

# Autophagy

| | CYTO-ID |
|---|---|
| **Wells/sample** | 2+2 |
| **Acquisition positions/well** | 2 |
| **Channels** | Hoeschest, CYTO-ID, dsRed |
| **Z-stacks** | 1.48 µm x4 |

| | | NOT infected | | Infected | | TOT | |
|---|---|---|---|---|---|---|---|
| | | N of cells | Replicates | N of cells | Replicates | Not inf | Inf |
| | CTRL | 121 | 5 | *na* | *na* | | |
| | RapaChlo | 95 | 5 | *na* | *na* | | |
| | DMSO | 67 | 5 | *na* | *na* | | |
| | H37Rv | 48 | 3 | 80 | 3 | | |
| M1 | H37Ra | 49 | 2 | 51 | 2 | *609* | *403* |
| | CDC1551 | | | | | | |
| | Beijing | 114 | 5 | 141 | 5 | | |
| | EAI | | | | | | |
| | Afri | 115 | 5 | 131 | 5 | | |
| | CTRL | 108 | 5 | *na* | *na* | | |
| | RapaChlo | 87 | 5 | *na* | *na* | | |
| | DMSO | 66 | 5 | *na* | *na* | | |
| | H37Rv | 64 | 3 | 70 | 3 | | |
| M2 | H37Ra | 46 | 2 | 55 | 2 | *572* | *376* |
| | CDC1551 | | | | | | |
| | Beijing | 85 | 5 | 133 | 5 | | |
| | EAI | | | | | | |
| | Afri | 116 | 5 | 118 | 5 | | |
| | *TOT* | *1181* | | *779* | | | |
| | | 1960 | | | | | |

*Acquisition:*

obj. **63x, oil NA 1.40**
**z-stacks: 1.48 µm x 4 stacks**
Res. **16-bit** format: **1024x1024**
Laser 405 (for Hoechst) = **40%**; gain: 935, offset: 0%
Laser 488 (for CYTO-ID) = **20% (Argon power: 30%); gain: 780**, offset: 0%
Laser 453 (for dsRed) = **18%; gain:** 905, offset: 0%
Confocal: AP **22** FD **6 O** INT **0** FIM **100%**

**Hoechst (Ex/Em 350/461)**
**CYTO-ID (Ex/Em 499/548)**
**dsRed (Ex/Em 584-557)**

*Analysis:*

24 h p.i.; N of autophagosomes, size of autophagosomes

**CYTO-ID (Ex/Em 499/548)**

**threshold (Default, Red; no flags on Dark background and Stack histogram) = 160**
**size = 5-infinity pixel units circularity = 0-1 (Show: nothing; Flags on Add to Manager, Display results)**

**Grouping: Geo-host adaptation**

**M1 – 24 h p.i.**

a) Number of autophagosomes

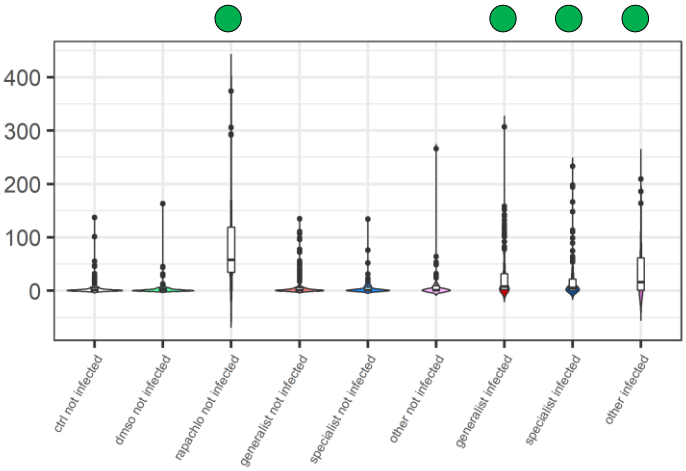


b) Area of autophagosomes

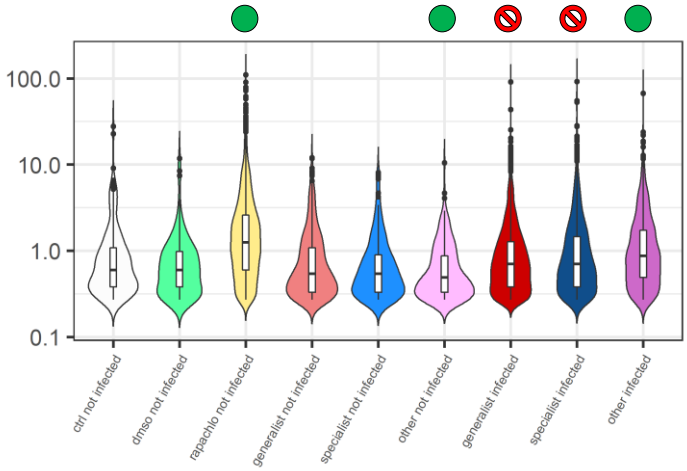


| Conditional model | Estimate | SE | p-value |
|---|---|---|---|
| (Intercept) | 1.7344 | 0.3377 | 0 |
| groupdmso not infected | -0.0036 | 0.4416 | 0.9935 |
| grouprapachlo not infected | 2.4301 | 0.3888 | 0 |
| groupgeneralist not infected | 0.5395 | 0.3541 | 0.1276 |
| groupspecialist not infected | 0.0695 | 0.3828 | 0.8559 |
| groupother not infected | 0.461 | 0.5017 | 0.3581 |
| groupgeneralist infected | 1.4475 | 0.3533 | 0 |
| groupspecialist infected | 1.1038 | 0.3813 | 0.0038 |
| groupother infected | 1.4338 | 0.5005 | 0.0042 |

| Zero-inflation model | Estimate | SE | p-value |
|---|---|---|---|
| (Intercept) | -0.7759 | 0.379 | 0.0406 |
| groupdmso not infected | 0.1688 | 0.5801 | 0.7711 |
| grouprapachlo not infected | -2.4906 | 0.6896 | 3e-04 |
| groupgeneralist not infected | 0.2177 | 0.4579 | 0.6345 |
| groupspecialist not infected | 0.3014 | 0.4855 | 0.5348 |
| groupother not infected | 0.2938 | 0.6353 | 0.6438 |
| groupgeneralist infected | -1.2833 | 0.468 | 0.0061 |
| groupspecialist infected | -0.8256 | 0.4963 | 0.0962 |
| groupother infected | -0.7705 | 0.6669 | 0.2479 |

| Contrast | estimate | SE | p.value |
|---|---|---|---|
| ctrl not infected-dmso not infected | 0.0036 | 0.4416 | 0.9935 |
| ctrl not infected-rapachlo not infected | -2.4301 | 0.3888 | 0 |
| ctrl not infected-generalist not infected | -0.5395 | 0.3541 | 0.2133 |
| ctrl not infected-specialist not infected | -0.0695 | 0.3828 | 0.9305 |
| ctrl not infected-other not infected | -0.461 | 0.5017 | 0.4886 |
| ctrl not infected-generalist infected | -1.4475 | 0.3533 | 2e-04 |
| ctrl not infected-specialist infected | -1.1038 | 0.3813 | 0.0089 |
| ctrl not infected-other infected | -1.4338 | 0.5005 | 0.0091 |
| dmso not infected-rapachlo not infected | -2.4337 | 0.4259 | 0 |
| dmso not infected-generalist not infected | -0.5431 | 0.3959 | 0.2557 |
| dmso not infected-specialist not infected | -0.0731 | 0.4208 | 0.9305 |
| dmso not infected-other not infected | -0.4646 | 0.5279 | 0.4944 |
| dmso not infected-generalist infected | -1.4511 | 0.3952 | 7e-04 |
| dmso not infected-specialist infected | -1.1074 | 0.4194 | 0.0158 |
| dmso not infected-other infected | -1.4374 | 0.5268 | 0.0129 |
| rapachlo not infected-generalist not infected | 1.8905 | 0.3318 | 0 |
| rapachlo not infected-specialist not infected | 2.3605 | 0.3632 | 0 |
| rapachlo not infected-other not infected | 1.969 | 0.4894 | 2e-04 |
| rapachlo not infected-generalist infected | 0.9825 | 0.3309 | 0.0076 |
| rapachlo not infected-specialist infected | 1.3262 | 0.3616 | 7e-04 |
| rapachlo not infected-other infected | 0.9962 | 0.4882 | 0.0734 |
| generalist not infected-specialist not infected | 0.47 | 0.3216 | 0.2277 |
| generalist not infected-other not infected | 0.0785 | 0.4738 | 0.9305 |
| specialist not infected-other not infected | -0.3915 | 0.4875 | 0.5276 |
| generalist infected-specialist infected | 0.3437 | 0.3188 | 0.4018 |
| generalist infected-other infected | 0.0137 | 0.4719 | 0.9935 |
| specialist infected-other infected | -0.33 | 0.485 | 0.5957 |
| generalist not infected-generalist infected | -0.908 | 0.0295 | 0 |
| specialist not infected-specialist infected | -1.0343 | 0.0429 | 0 |
| other not infected-other infected | -0.9728 | 0.0457 | 0 |

| Par | Value | Std.Error | p.value |
|---|---|---|---|
| (Intercept) | -0.2579 | 0.1042 | 0.0133 |
| groupdmso not infected | -0.0571 | 0.1545 | 0.7136 |
| grouprapachlo not infected | 0.497 | 0.1119 | 1e-04 |
| groupgeneralist not infected | -0.0992 | 0.1161 | 0.3931 |
| groupspecialist not infected | -0.2413 | 0.1295 | 0.0625 |
| groupother not infected | -0.3661 | 0.1437 | 0.0108 |
| groupgeneralist infected | 0.0123 | 0.1082 | 0.9097 |
| groupspecialist infected | 0.0023 | 0.1169 | 0.9846 |
| groupother infected | 0.3443 | 0.1269 | 0.0067 |

| Contrast | estimate | SE | p.value |
|---|---|---|---|
| ctrl not infected-dmso not infected | 0.0571 | 0.1545 | 0.8234 |
| ctrl not infected-rapachlo not infected | -0.497 | 0.1119 | 2e-04 |
| ctrl not infected-generalist not infected | 0.0992 | 0.1161 | 0.5127 |
| ctrl not infected-specialist not infected | 0.2413 | 0.1295 | 0.1041 |
| ctrl not infected-other not infected | 0.3661 | 0.1437 | 0.0232 |
| ctrl not infected-generalist infected | -0.0123 | 0.1082 | 0.9411 |
| ctrl not infected-specialist infected | -0.0023 | 0.1169 | 0.9846 |
| ctrl not infected-other infected | -0.3443 | 0.1269 | 0.0166 |
| dmso not infected-rapachlo not infected | -0.5541 | 0.1356 | 6e-04 |
| dmso not infected-generalist not infected | 0.0421 | 0.1386 | 0.8474 |
| dmso not infected-specialist not infected | 0.1842 | 0.1501 | 0.3227 |
| dmso not infected-other not infected | 0.309 | 0.1616 | 0.1041 |
| dmso not infected-generalist infected | -0.0693 | 0.132 | 0.7524 |
| dmso not infected-specialist infected | -0.0593 | 0.1394 | 0.8069 |
| dmso not infected-other infected | -0.4013 | 0.147 | 0.0206 |
| rapachlo not infected-generalist not infected | 0.5962 | 0.0864 | 0 |
| rapachlo not infected-specialist not infected | 0.7383 | 0.1038 | 0 |
| rapachlo not infected-other not infected | 0.8631 | 0.1226 | 0 |
| rapachlo not infected-generalist infected | 0.4848 | 0.0755 | 0 |
| rapachlo not infected-specialist infected | 0.4948 | 0.0873 | 0 |
| rapachlo not infected-other infected | 0.1527 | 0.1022 | 0.2241 |
| generalist not infected-specialist not infected | 0.1421 | 0.108 | 0.2823 |
| generalist not infected-other not infected | 0.2669 | 0.1199 | 0.0487 |
| specialist not infected-other not infected | 0.1248 | 0.1384 | 0.501 |
| generalist infected-specialist infected | 0.01 | 0.0822 | 0.9411 |
| generalist infected-other infected | -0.332 | 0.0872 | 5e-04 |
| specialist infected-other infected | -0.342 | 0.107 | 0.0038 |
| generalist not infected-generalist infected | -0.1114 | 0.0487 | 0.0441 |
| specialist not infected-specialist infected | -0.2435 | 0.0704 | 0.0016 |
| other not infected-other infected | -0.7104 | 0.0768 | 0 |

OBSERVATIONS

In M1 macrophages, only the group "other" showed some degree of autophagy; indeed, whereas also generalist and specialist groups are showing an increase in the number of autophagosomes, their size does not show statistically increased size, thus suggesting poor maturation and progression in the autophagic flux.

Autophagosomes observed

Autophagosomes not observed (blocked)

**Grouping: Geo-host adaptation**

**M2 – 24 h p.i.**

a) Number of autophagosomes

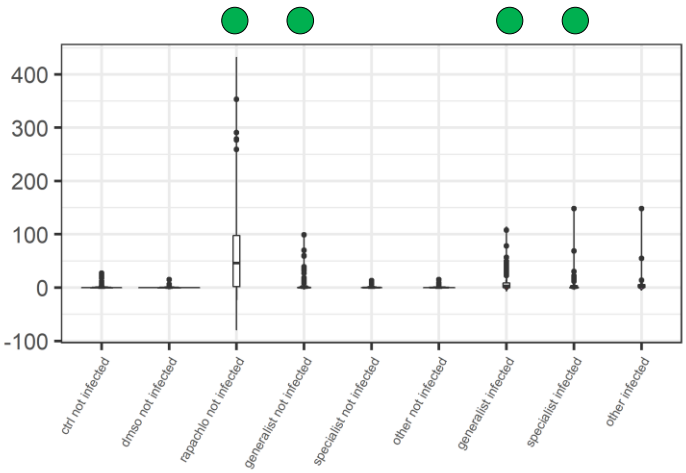


b) Area of autophagosomes

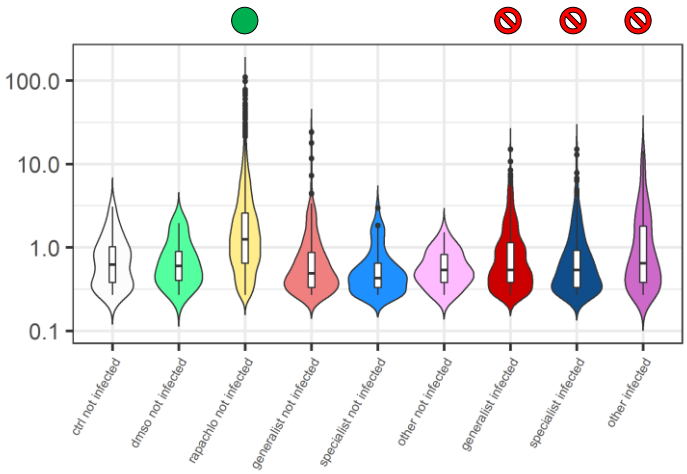


| Conditional model | Estimate | SE | p-value |
|---|---|---|---|
| (Intercept) | 0.903 | 0.345 | 0.0089 |
| groupdmso not infected | -0.4088 | 0.4775 | 0.3919 |
| grouprapachlo not infected | 2.9446 | 0.389 | 0 |
| groupgeneralist not infected | 0.9518 | 0.3649 | 0.0091 |
| groupspecialist not infected | -0.2611 | 0.3975 | 0.5114 |
| groupother not infected | -0.4535 | 0.5153 | 0.3788 |
| groupgeneralist infected | 1.3009 | 0.3636 | 3e-04 |
| groupspecialist infected | 0.8508 | 0.3901 | 0.0292 |
| groupother infected | 0.638 | 0.5016 | 0.2034 |

| Zero-inflation model | Estimate | SE | p-value |
|---|---|---|---|
| (Intercept) | 0.0905 | 0.3961 | 0.8193 |
| groupdmso not infected | 0.6714 | 0.5867 | 0.2524 |
| grouprapachlo not infected | -2.111 | 0.5777 | 3e-04 |
| groupgeneralist not infected | -0.1886 | 0.4582 | 0.6806 |
| groupspecialist not infected | -0.1775 | 0.4964 | 0.7207 |
| groupother not infected | -0.3559 | 0.6681 | 0.5942 |
| groupgeneralist infected | -1.4032 | 0.4586 | 0.0022 |
| groupspecialist infected | -0.663 | 0.4796 | 0.1669 |
| groupother infected | -1.3147 | 0.6501 | 0.0431 |

| Contrast | estimate | SE | p.value |
|---|---|---|---|
| ctrl not infected-dmso not infected | 0.4088 | 0.4775 | 0.4705 |
| ctrl not infected-rapachlo not infected | -2.9446 | 0.389 | 0 |
| ctrl not infected-generalist not infected | -0.9518 | 0.3649 | 0.0154 |
| ctrl not infected-specialist not infected | 0.2611 | 0.3975 | 0.5902 |
| ctrl not infected-other not infected | 0.4535 | 0.5153 | 0.4705 |
| ctrl not infected-generalist infected | -1.3009 | 0.3636 | 8e-04 |
| ctrl not infected-specialist infected | -0.8508 | 0.3901 | 0.0465 |
| ctrl not infected-other infected | -0.638 | 0.5016 | 0.2658 |
| dmso not infected-rapachlo not infected | -3.3534 | 0.4289 | 0 |
| dmso not infected-generalist not infected | -1.3606 | 0.4288 | 0.0031 |
| dmso not infected-specialist not infected | -0.1478 | 0.4584 | 0.7731 |
| dmso not infected-other not infected | 0.0447 | 0.5682 | 0.9373 |
| dmso not infected-generalist infected | -1.7097 | 0.4277 | 2e-04 |
| dmso not infected-specialist infected | -1.2596 | 0.452 | 0.0096 |
| dmso not infected-other infected | -1.0468 | 0.5558 | 0.09 |
| rapachlo not infected-generalist not infected | 1.9928 | 0.3227 | 0 |
| rapachlo not infected-specialist not infected | 3.2057 | 0.3617 | 0 |
| rapachlo not infected-other not infected | 3.3981 | 0.4938 | 0 |
| rapachlo not infected-generalist infected | 1.6437 | 0.3211 | 0 |
| rapachlo not infected-specialist infected | 2.0938 | 0.3533 | 0 |
| rapachlo not infected-other infected | 2.3067 | 0.4796 | 0 |
| generalist not infected-specialist not infected | 1.2129 | 0.3292 | 6e-04 |
| generalist not infected-other not infected | 1.4053 | 0.484 | 0.0071 |
| specialist not infected-other not infected | 0.1925 | 0.5027 | 0.752 |
| generalist infected-specialist infected | 0.4501 | 0.3182 | 0.2149 |
| generalist infected-other infected | 0.6629 | 0.4685 | 0.2149 |
| specialist infected-other infected | 0.2128 | 0.4827 | 0.7326 |
| generalist not infected-generalist infected | -0.3491 | 0.046 | 0 |
| specialist not infected-specialist infected | -1.1118 | 0.0942 | 0 |
| other not infected-other infected | -1.0915 | 0.1381 | 0 |

| Par | Value | Std.Error | p.value |
|---|---|---|---|
| (Intercept) | -0.5251 | 0.1368 | 1e-04 |
| groupdmso not infected | -0.0041 | 0.2487 | 0.987 |
| grouprapachlo not infected | 0.7515 | 0.1483 | 0 |
| groupgeneralist not infected | -0.0939 | 0.1564 | 0.5485 |
| groupspecialist not infected | -0.3087 | 0.1945 | 0.1125 |
| groupother not infected | -0.2501 | 0.2381 | 0.2936 |
| groupgeneralist infected | 0.0301 | 0.1472 | 0.8381 |
| groupspecialist infected | -0.1507 | 0.162 | 0.3522 |
| groupother infected | 0.1919 | 0.1829 | 0.2941 |

| Contrast | estimate | SE | p.value |
|---|---|---|---|
| ctrl not infected-dmso not infected | 0.0041 | 0.2487 | 0.987 |
| ctrl not infected-rapachlo not infected | -0.7515 | 0.1483 | 0 |
| ctrl not infected-generalist not infected | 0.0939 | 0.1564 | 0.6582 |
| ctrl not infected-specialist not infected | 0.3087 | 0.1945 | 0.2597 |
| ctrl not infected-other not infected | 0.2501 | 0.2381 | 0.4644 |
| ctrl not infected-generalist infected | -0.0301 | 0.1472 | 0.8979 |
| ctrl not infected-specialist infected | 0.1507 | 0.162 | 0.5283 |
| ctrl not infected-other infected | -0.1919 | 0.1829 | 0.4644 |
| dmso not infected-rapachlo not infected | -0.7555 | 0.2157 | 0.0017 |
| dmso not infected-generalist not infected | 0.0898 | 0.222 | 0.7913 |
| dmso not infected-specialist not infected | 0.3046 | 0.2501 | 0.4292 |
| dmso not infected-other not infected | 0.246 | 0.2852 | 0.5548 |
| dmso not infected-generalist infected | -0.0341 | 0.2155 | 0.9043 |
| dmso not infected-specialist infected | 0.1467 | 0.2257 | 0.6448 |
| dmso not infected-other infected | -0.1959 | 0.241 | 0.5675 |
| rapachlo not infected-generalist not infected | 0.8453 | 0.0968 | 0 |
| rapachlo not infected-specialist not infected | 1.0602 | 0.1506 | 0 |
| rapachlo not infected-other not infected | 1.0015 | 0.2039 | 0 |
| rapachlo not infected-generalist infected | 0.7214 | 0.0809 | 0 |
| rapachlo not infected-specialist infected | 0.9022 | 0.1052 | 0 |
| rapachlo not infected-other infected | 0.5596 | 0.1353 | 2e-04 |
| generalist not infected-specialist not infected | 0.2148 | 0.1589 | 0.3778 |
| generalist not infected-other not infected | 0.1562 | 0.2101 | 0.5964 |
| specialist not infected-other not infected | -0.0586 | 0.2396 | 0.8964 |
| generalist infected-specialist infected | 0.1808 | 0.1039 | 0.223 |
| generalist infected-other infected | -0.1618 | 0.1345 | 0.4292 |
| specialist infected-other infected | -0.3426 | 0.1501 | 0.0676 |
| generalist not infected-generalist infected | -0.1239 | 0.0739 | 0.2344 |
| specialist not infected-specialist infected | -0.158 | 0.1441 | 0.4644 |
| other not infected-other infected | -0.442 | 0.193 | 0.0676 |

OBSERVATIONS

In M2 macrophages, despite a certain increase in the number of autophagosomes, their size does not show statistically increased size, thus suggesting poor maturation and progression in the autophagic flux. None of the group is inducing autophagy.

Autophagosomes observed

Autophagosomes not observed (blocked)

## Grouping: Basic

## M1 – 24 h p.i.

a) Number of autophagosomes

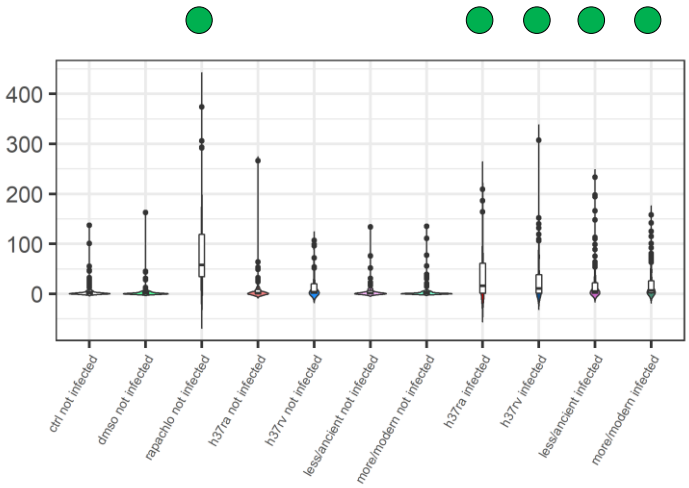


b) Area of autophagosomes

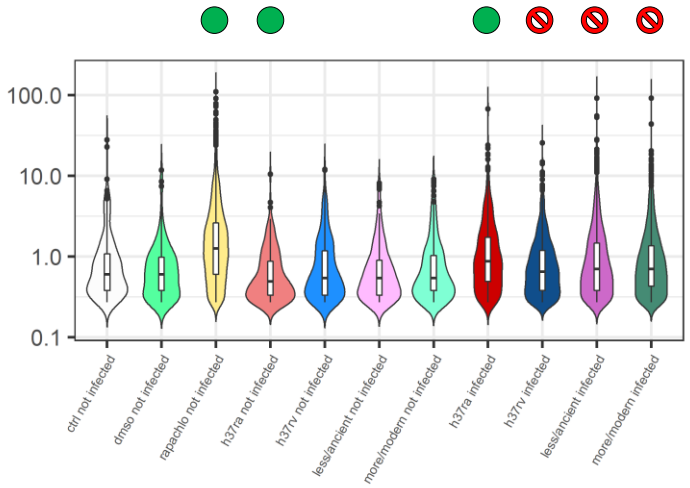


| Conditional model | Estimate | SE | p-value |
|---|---|---|---|
| (Intercept) | 1.7318 | 0.3391 | 0 |
| groupdmso not infected | -0.0094 | 0.4321 | 0.9826 |
| grouprapachlo not infected | 2.4283 | 0.3804 | 0 |
| grouph37ra not infected | 0.4201 | 0.492 | 0.3931 |
| grouph37rv not infected | 0.8728 | 0.4393 | 0.047 |
| groupless/ancient not infected | 0.072 | 0.3747 | 0.8476 |
| groupmore/modern not infected | 0.3621 | 0.3744 | 0.3336 |
| grouph37ra infected | 1.393 | 0.4908 | 0.0045 |
| grouph37rv infected | 1.7815 | 0.438 | 0 |
| groupless/ancient infected | 1.1064 | 0.3731 | 0.003 |
| groupmore/modern infected | 1.2688 | 0.3729 | 7e-04 |

| Par | Value | Std.Error | p.value |
|---|---|---|---|
| (Intercept) | -0.2574 | 0.1046 | 0.0138 |
| groupdmso not infected | -0.0567 | 0.1556 | 0.717 |
| grouprapachlo not infected | 0.4966 | 0.1129 | 1e-04 |
| grouph37ra not infected | -0.3725 | 0.1464 | 0.011 |
| grouph37rv not infected | -0.0446 | 0.1376 | 0.7462 |
| groupless/ancient not infected | -0.2415 | 0.1305 | 0.0642 |
| groupmore/modern not infected | -0.172 | 0.1312 | 0.1898 |
| grouph37ra infected | 0.3378 | 0.1302 | 0.0095 |
| grouph37rv infected | -0.006 | 0.1246 | 0.9618 |
| groupless/ancient infected | 0.0021 | 0.1179 | 0.986 |
| groupmore/modern infected | 0.0308 | 0.1161 | 0.7908 |

| Zero-inflation model | Estimate | SE | p-value |
|---|---|---|---|
| (Intercept) | -0.7554 | 0.3686 | 0.0404 |
| groupdmso not infected | 0.1755 | 0.5553 | 0.752 |
| grouprapachlo not infected | -2.4925 | 0.6732 | 2e-04 |
| grouph37ra not infected | 0.323 | 0.6114 | 0.5973 |
| grouph37rv not infected | -0.459 | 0.6239 | 0.462 |
| groupless/ancient not infected | 0.2864 | 0.4651 | 0.5381 |
| groupmore/modern not infected | 0.4171 | 0.4636 | 0.3683 |
| grouph37ra infected | -0.7319 | 0.6441 | 0.2558 |
| grouph37rv infected | -1.1875 | 0.5809 | 0.0409 |
| groupless/ancient infected | -0.8359 | 0.4764 | 0.0794 |
| groupmore/modern infected | -1.3416 | 0.4919 | 0.0064 |

| Contrast | estimate | SE | p.value |
|---|---|---|---|
| ctrl not infected-dmso not infected | 0.0094 | 0.4321 | 0.9826 |
| ctrl not infected-rapachlo not infected | -2.4283 | 0.3804 | 0 |
| ctrl not infected-h37ra not infected | -0.4201 | 0.492 | 0.5211 |
| ctrl not infected-h37rv not infected | -0.8728 | 0.4393 | 0.0923 |
| ctrl not infected-less/ancient not infected | -0.072 | 0.3747 | 0.889 |
| ctrl not infected-more/modern not infected | -0.3621 | 0.3744 | 0.4949 |
| ctrl not infected-h37ra infected | -1.393 | 0.4908 | 0.0111 |
| ctrl not infected-h37rv infected | -1.7815 | 0.438 | 2e-04 |
| ctrl not infected-less/ancient infected | -1.1064 | 0.3731 | 0.0078 |
| ctrl not infected-more/modern infected | -1.2688 | 0.3729 | 0.0021 |
| dmso not infected-rapachlo not infected | -2.4377 | 0.4167 | 0 |
| dmso not infected-h37ra not infected | -0.4296 | 0.5176 | 0.5211 |
| dmso not infected-h37rv not infected | -0.8822 | 0.4736 | 0.1125 |
| dmso not infected-less/ancient not infected | -0.0815 | 0.4118 | 0.889 |
| dmso not infected-more/modern not infected | -0.3715 | 0.4115 | 0.5211 |
| dmso not infected-h37ra infected | -1.4024 | 0.5165 | 0.0145 |
| dmso not infected-h37rv infected | -1.7909 | 0.4723 | 6e-04 |
| dmso not infected-less/ancient infected | -1.1158 | 0.4104 | 0.0145 |
| dmso not infected-more/modern infected | -1.2783 | 0.4101 | 0.0051 |
| rapachlo not infected-h37ra not infected | 2.0082 | 0.4803 | 2e-04 |
| rapachlo not infected-h37rv not infected | 1.5555 | 0.4204 | 8e-04 |
| rapachlo not infected-less/ancient not infected | 2.3563 | 0.3553 | 0 |
| rapachlo not infected-more/modern not infected | 2.0663 | 0.3548 | 0 |
| rapachlo not infected-h37ra infected | 1.0353 | 0.4791 | 0.0633 |
| rapachlo not infected-h37rv infected | 0.6468 | 0.419 | 0.2035 |
| rapachlo not infected-less/ancient infected | 1.3219 | 0.3536 | 7e-04 |
| rapachlo not infected-more/modern infected | 1.1595 | 0.3532 | 0.003 |
| h37ra not infected-h37rv not infected | -0.4526 | 0.5515 | 0.5211 |
| h37ra not infected-less/ancient not infected | 0.3481 | 0.4787 | 0.5729 |
| h37ra not infected-more/modern not infected | 0.0581 | 0.4785 | 0.9249 |
| h37rv not infected-less/ancient not infected | 0.8007 | 0.4108 | 0.0964 |
| h37rv not infected-more/modern not infected | 0.5107 | 0.4104 | 0.328 |
| less/ancient not infected-more/modern not infected | -0.29 | 0.3471 | 0.5211 |
| h37ra infected-h37rv infected | -0.3885 | 0.5494 | 0.5729 |
| h37ra infected-less/ancient infected | 0.2866 | 0.4763 | 0.6362 |
| h37ra infected-more/modern infected | 0.1242 | 0.476 | 0.8757 |
| h37rv infected-less/ancient infected | 0.6751 | 0.4079 | 0.1689 |
| h37rv infected-more/modern infected | 0.5127 | 0.4075 | 0.328 |
| less/ancient infected-more/modern infected | -0.1625 | 0.3437 | 0.7203 |

| Contrast | estimate | SE | p.value |
|---|---|---|---|
| ctrl not infected-dmso not infected | 0.0567 | 0.1556 | 0.855 |
| ctrl not infected-rapachlo not infected | -0.4966 | 0.1129 | 3e-04 |
| ctrl not infected-h37ra not infected | 0.3725 | 0.1464 | 0.0276 |
| ctrl not infected-h37rv not infected | 0.0446 | 0.1376 | 0.855 |
| ctrl not infected-less/ancient not infected | 0.2415 | 0.1305 | 0.1315 |
| ctrl not infected-more/modern not infected | 0.172 | 0.1312 | 0.3265 |
| ctrl not infected-h37ra infected | -0.3378 | 0.1302 | 0.0255 |
| ctrl not infected-h37rv infected | 0.006 | 0.1246 | 0.9847 |
| ctrl not infected-less/ancient infected | -0.0021 | 0.1179 | 0.986 |
| ctrl not infected-more/modern infected | -0.0308 | 0.1161 | 0.872 |
| dmso not infected-rapachlo not infected | -0.5533 | 0.1366 | 8e-04 |
| dmso not infected-h37ra not infected | 0.3157 | 0.1642 | 0.1305 |
| dmso not infected-h37rv not infected | -0.0122 | 0.1571 | 0.9843 |
| dmso not infected-less/ancient not infected | 0.1847 | 0.151 | 0.3764 |
| dmso not infected-more/modern not infected | 0.1153 | 0.1516 | 0.6688 |
| dmso not infected-h37ra infected | -0.3945 | 0.15 | 0.0276 |
| dmso not infected-h37rv infected | -0.0508 | 0.1458 | 0.855 |
| dmso not infected-less/ancient infected | -0.0588 | 0.1404 | 0.855 |
| dmso not infected-more/modern infected | -0.0875 | 0.1387 | 0.7612 |
| rapachlo not infected-h37ra not infected | 0.8691 | 0.1255 | 0 |
| rapachlo not infected-h37rv not infected | 0.5411 | 0.1133 | 1e-04 |
| rapachlo not infected-less/ancient not infected | 0.738 | 0.1046 | 0 |
| rapachlo not infected-more/modern not infected | 0.6686 | 0.1056 | 0 |
| rapachlo not infected-h37ra infected | 0.1588 | 0.1059 | 0.2629 |
| rapachlo not infected-h37rv infected | 0.5026 | 0.0971 | 0 |
| rapachlo not infected-less/ancient infected | 0.4945 | 0.0884 | 0 |
| rapachlo not infected-more/modern infected | 0.4658 | 0.0861 | 0 |
| h37ra not infected-h37rv not infected | -0.3279 | 0.1325 | 0.0302 |
| h37ra not infected-less/ancient not infected | -0.131 | 0.1409 | 0.5416 |
| h37ra not infected-more/modern not infected | -0.2005 | 0.1417 | 0.2813 |
| h37rv not infected-less/ancient not infected | 0.1969 | 0.1303 | 0.2558 |
| h37rv not infected-more/modern not infected | 0.1274 | 0.1301 | 0.5214 |
| less/ancient not infected-more/modern not infected | -0.0695 | 0.124 | 0.7732 |
| h37ra infected-h37rv infected | 0.3438 | 0.0947 | 0.0011 |
| h37ra infected-less/ancient infected | 0.3357 | 0.1106 | 0.0079 |
| h37ra infected-more/modern infected | 0.307 | 0.1083 | 0.0141 |
| h37rv infected-less/ancient infected | -0.008 | 0.1023 | 0.9843 |
| h37rv infected-more/modern infected | -0.0368 | 0.0994 | 0.855 |
| less/ancient infected-more/modern infected | -0.0287 | 0.0923 | 0.855 |
| h37ra not infected-h37ra infected | -0.7103 | 0.0768 | 0 |
| h37rv not infected-h37rv infected | -0.0386 | 0.0653 | 0.7693 |
| less/ancient not infected-less/ancient infected | -0.2435 | 0.0704 | 0.002 |
| more/modern not infected-more/modern infected | -0.2028 | 0.0729 | 0.0155 |

Autophagosomes observed

Autophagosomes not observed (blocked)

## Grouping: Basic

## M2 – 24 h p.i.

a) Number of autophagosomes

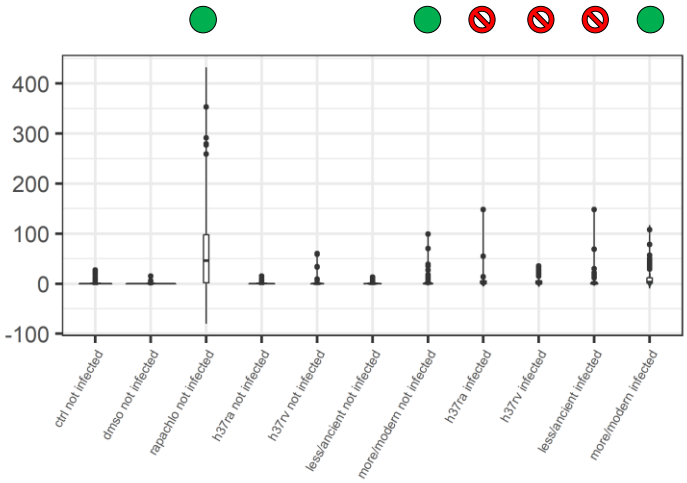


b) Area of autophagosomes

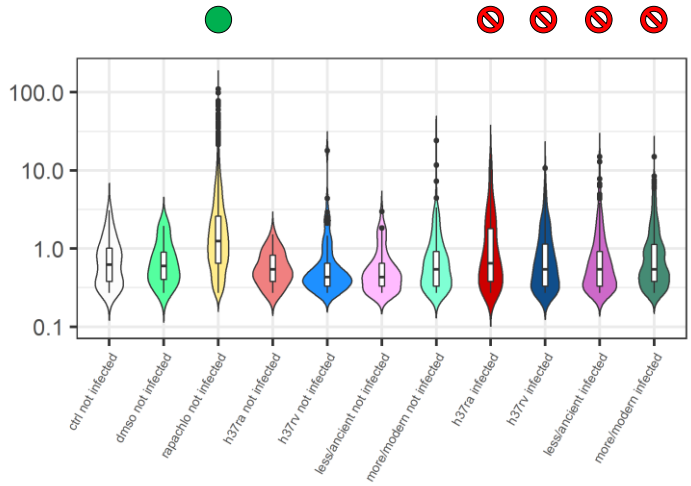


| Conditional model | Estimate | SE | p-value |
|---|---|---|---|
| (Intercept) | 0.9132 | 0.3393 | 0.0071 |
| groupdmso not infected | -0.4106 | 0.4739 | 0.3863 |
| grouprapachlo not infected | 2.9377 | 0.3858 | 0 |
| grouph37ra not infected | -0.4356 | 0.5111 | 0.394 |
| grouph37rv not infected | 0.8393 | 0.4565 | 0.066 |
| groupless/ancient not infected | -0.2701 | 0.3944 | 0.4934 |
| groupmore/modern not infected | 1.0085 | 0.3868 | 0.0091 |
| grouph37ra infected | 0.6558 | 0.4973 | 0.1873 |
| grouph37rv infected | 0.9766 | 0.4541 | 0.0315 |
| groupless/ancient infected | 0.8416 | 0.3869 | 0.0296 |
| groupmore/modern infected | 1.4501 | 0.3847 | 2e-04 |

| Zero-inflation model | Estimate | SE | p-value |
|---|---|---|---|
| (Intercept) | 0.092 | 0.3961 | 0.8163 |
| groupdmso not infected | 0.674 | 0.5865 | 0.2505 |
| grouprapachlo not infected | -2.1108 | 0.5782 | 3e-04 |
| grouph37ra not infected | -0.3638 | 0.6681 | 0.5861 |
| grouph37rv not infected | -0.0641 | 0.5851 | 0.9127 |
| groupless/ancient not infected | -0.1785 | 0.4967 | 0.7193 |
| groupmore/modern not infected | -0.2535 | 0.4915 | 0.606 |
| grouph37ra infected | -1.3229 | 0.6502 | 0.0419 |
| grouph37rv infected | -1.3892 | 0.5963 | 0.0198 |
| groupless/ancient infected | -0.6637 | 0.4802 | 0.1669 |
| groupmore/modern infected | -1.4196 | 0.4873 | 0.0036 |

| Contrast | estimate | SE | p.value |
|---|---|---|---|
| ctrl not infected-dmso not infected | 0.4106 | 0.4739 | 0.4843 |
| ctrl not infected-rapachlo not infected | -2.9377 | 0.3858 | 0 |
| ctrl not infected-h37ra not infected | 0.4356 | 0.5111 | 0.4843 |
| ctrl not infected-h37rv not infected | -0.8393 | 0.4565 | 0.1019 |
| ctrl not infected-less/ancient not infected | 0.2701 | 0.3944 | 0.5895 |
| ctrl not infected-more/modern not infected | -1.0085 | 0.3868 | 0.0181 |
| ctrl not infected-h37ra infected | -0.6558 | 0.4973 | 0.2521 |
| ctrl not infected-h37rv infected | -0.9766 | 0.4541 | 0.0525 |
| ctrl not infected-less/ancient infected | -0.8416 | 0.3869 | 0.0514 |
| ctrl not infected-more/modern infected | -1.4501 | 0.3847 | 5e-04 |
| dmso not infected-rapachlo not infected | -3.3484 | 0.4261 | 0 |
| dmso not infected-h37ra not infected | 0.025 | 0.5638 | 0.9647 |
| dmso not infected-h37rv not infected | -1.2499 | 0.5062 | 0.0256 |
| dmso not infected-less/ancient not infected | -0.1405 | 0.4552 | 0.7757 |
| dmso not infected-more/modern not infected | -1.4192 | 0.4487 | 0.0041 |
| dmso not infected-h37ra infected | -1.0664 | 0.5514 | 0.0851 |
| dmso not infected-h37rv infected | -1.3873 | 0.504 | 0.013 |
| dmso not infected-less/ancient infected | -1.2522 | 0.4487 | 0.0121 |
| dmso not infected-more/modern infected | -1.8607 | 0.4468 | 1e-04 |
| rapachlo not infected-h37ra not infected | 3.3734 | 0.4897 | 0 |
| rapachlo not infected-h37rv not infected | 2.0985 | 0.4209 | 0 |
| rapachlo not infected-less/ancient not infected | 3.2079 | 0.3588 | 0 |
| rapachlo not infected-more/modern not infected | 1.9292 | 0.3498 | 0 |
| rapachlo not infected-h37ra infected | 2.282 | 0.4754 | 0 |
| rapachlo not infected-h37rv infected | 1.9611 | 0.4181 | 0 |
| rapachlo not infected-less/ancient infected | 2.0962 | 0.3503 | 0 |
| rapachlo not infected-more/modern infected | 1.4877 | 0.3474 | 1e-04 |
| h37ra not infected-h37rv not infected | -1.2749 | 0.5642 | 0.0431 |
| h37ra not infected-less/ancient not infected | -0.1655 | 0.4986 | 0.7757 |
| h37ra not infected-more/modern not infected | -1.4441 | 0.4925 | 0.0082 |
| h37rv not infected-less/ancient not infected | 1.1094 | 0.4239 | 0.0181 |
| h37rv not infected-more/modern not infected | -0.1693 | 0.4156 | 0.7694 |
| less/ancient not infected-more/modern not infected | -1.2786 | 0.3573 | 0.001 |
| h37ra infected-h37rv infected | -0.3208 | 0.5498 | 0.6504 |
| h37ra infected-less/ancient infected | -0.1858 | 0.4784 | 0.7694 |
| h37ra infected-more/modern infected | -0.7943 | 0.4766 | 0.1332 |
| h37rv infected-less/ancient infected | 0.135 | 0.4137 | 0.7757 |
| h37rv infected-more/modern infected | -0.4734 | 0.4106 | 0.3247 |
| less/ancient infected-more/modern infected | -0.6085 | 0.3463 | 0.1174 |

| Par | Value | Std.Error | p.value |
|---|---|---|---|
| (Intercept) | -0.525 | 0.138 | 1e-04 |
| groupdmso not infected | -0.0035 | 0.251 | 0.989 |
| grouprapachlo not infected | 0.7501 | 0.151 | 0 |
| grouph37ra not infected | -0.2585 | 0.2404 | 0.2823 |
| grouph37rv not infected | -0.2842 | 0.1956 | 0.1464 |
| groupless/ancient not infected | -0.3039 | 0.1967 | 0.1224 |
| groupmore/modern not infected | -0.0075 | 0.1677 | 0.9645 |
| grouph37ra infected | 0.1817 | 0.1861 | 0.3288 |
| grouph37rv infected | 0.0488 | 0.1728 | 0.7775 |
| groupless/ancient infected | -0.1504 | 0.1645 | 0.3606 |
| groupmore/modern infected | 0.0289 | 0.1543 | 0.8513 |

| Contrast | estimate | SE | p.value |
|---|---|---|---|
| ctrl not infected-dmso not infected | 0.0035 | 0.251 | 0.989 |
| ctrl not infected-rapachlo not infected | -0.7501 | 0.151 | 0 |
| ctrl not infected-h37ra not infected | 0.2585 | 0.2404 | 0.4951 |
| ctrl not infected-h37rv not infected | 0.2842 | 0.1956 | 0.3325 |
| ctrl not infected-less/ancient not infected | 0.3039 | 0.1967 | 0.3096 |
| ctrl not infected-more/modern not infected | 0.0075 | 0.1677 | 0.989 |
| ctrl not infected-h37ra infected | -0.1817 | 0.1861 | 0.5437 |
| ctrl not infected-h37rv infected | -0.0488 | 0.1728 | 0.989 |
| ctrl not infected-less/ancient infected | 0.1504 | 0.1645 | 0.5743 |
| ctrl not infected-more/modern infected | -0.0289 | 0.1543 | 0.989 |
| dmso not infected-rapachlo not infected | -0.7535 | 0.2179 | 0.0024 |
| dmso not infected-h37ra not infected | 0.255 | 0.2877 | 0.5764 |
| dmso not infected-h37rv not infected | 0.2807 | 0.2514 | 0.4951 |
| dmso not infected-less/ancient not infected | 0.3004 | 0.2523 | 0.4951 |
| dmso not infected-more/modern not infected | 0.004 | 0.2304 | 0.989 |
| dmso not infected-h37ra infected | -0.1852 | 0.2441 | 0.6421 |
| dmso not infected-h37rv infected | -0.0523 | 0.2341 | 0.989 |
| dmso not infected-less/ancient infected | 0.1469 | 0.228 | 0.7206 |
| dmso not infected-more/modern infected | -0.0324 | 0.2208 | 0.989 |
| rapachlo not infected-h37ra not infected | 1.0086 | 0.2063 | 0 |
| rapachlo not infected-h37rv not infected | 1.0342 | 0.1517 | 0 |
| rapachlo not infected-less/ancient not infected | 1.054 | 0.153 | 0 |
| rapachlo not infected-more/modern not infected | 0.7575 | 0.1134 | 0 |
| rapachlo not infected-h37ra infected | 0.5683 | 0.1391 | 2e-04 |
| rapachlo not infected-h37rv infected | 0.7012 | 0.1208 | 0 |
| rapachlo not infected-less/ancient infected | 0.9004 | 0.1085 | 0 |
| rapachlo not infected-more/modern infected | 0.7211 | 0.0925 | 0 |
| h37ra not infected-h37rv not infected | 0.0257 | 0.2409 | 0.989 |
| h37ra not infected-less/ancient not infected | 0.0454 | 0.2417 | 0.989 |
| h37ra not infected-more/modern not infected | -0.251 | 0.2188 | 0.4951 |
| h37rv not infected-less/ancient not infected | 0.0197 | 0.1972 | 0.989 |
| h37rv not infected-more/modern not infected | -0.2767 | 0.1684 | 0.2876 |
| less/ancient not infected-more/modern not infected | -0.2964 | 0.1696 | 0.2474 |
| h37ra infected-h37rv infected | 0.1329 | 0.1626 | 0.6135 |
| h37ra infected-less/ancient infected | 0.3321 | 0.1536 | 0.1015 |
| h37ra infected-more/modern infected | 0.1528 | 0.1428 | 0.4951 |
| h37rv infected-less/ancient infected | 0.1992 | 0.1373 | 0.3325 |
| h37rv infected-more/modern infected | 0.0199 | 0.125 | 0.989 |
| less/ancient infected-more/modern infected | -0.1793 | 0.1132 | 0.3041 |
| h37ra not infected-h37ra infected | -0.4402 | 0.1931 | 0.0813 |
| h37rv not infected-h37rv infected | -0.333 | 0.1384 | 0.0631 |
| less/ancient not infected-less/ancient infected | -0.1535 | 0.1444 | 0.4951 |
| more/modern not infected-more/modern infected | -0.0364 | 0.088 | 0.9124 |

Autophagosomes observed

Autophagosomes not observed (blocked)

## Grouping: Disease

## M1 – 24 h p.i.

a) Number of autophagosomes

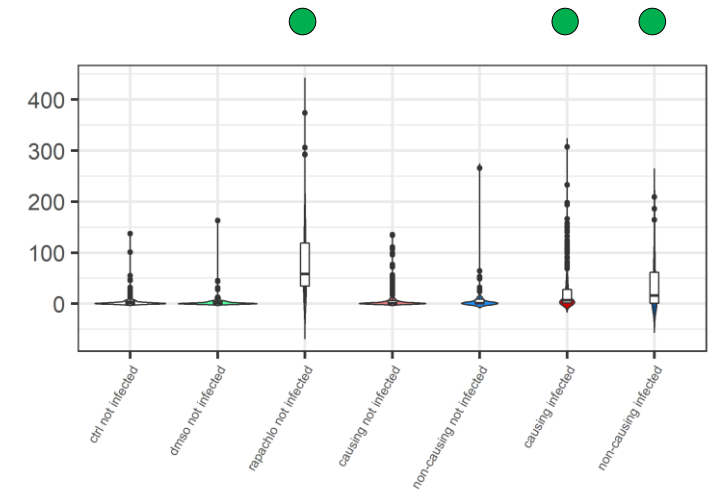


b) Area of autophagosomes

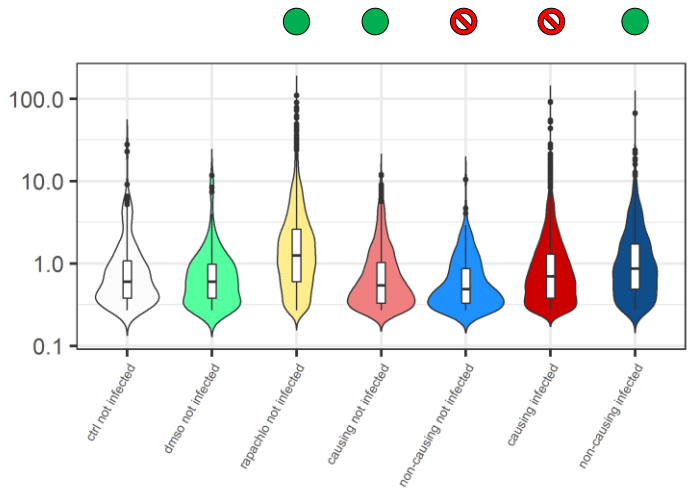


| Conditional model | Estimate | SE | p-value |
|---|---|---|---|
| (Intercept) | 1.7349 | 0.3388 | 0 |
| groupdmso not infected | -0.0012 | 0.4486 | 0.9978 |
| grouprapachlo not infected | 2.4316 | 0.3951 | 0 |
| groupcausing not infected | 0.3608 | 0.3353 | 0.282 |
| groupnon-causing not infected | 0.4802 | 0.5093 | 0.3458 |
| groupcausing infected | 1.3104 | 0.3347 | 1e-04 |
| groupnon-causing infected | 1.453 | 0.5081 | 0.0042 |

| Zero-inflation model | Estimate | SE | p-value |
|---|---|---|---|
| (Intercept) | -0.7823 | 0.3792 | 0.0391 |
| groupdmso not infected | 0.1665 | 0.5845 | 0.7757 |
| grouprapachlo not infected | -2.4847 | 0.6921 | 3e-04 |
| groupcausing not infected | 0.2565 | 0.4255 | 0.5466 |
| groupnon-causing not infected | 0.2787 | 0.6387 | 0.6625 |
| groupcausing infected | -1.0903 | 0.4317 | 0.0116 |
| groupnon-causing infected | -0.7849 | 0.6697 | 0.2412 |

| Contrast | estimate | SE | p.value |
|---|---|---|---|
| ctrl not infected-dmso not infected | 0.0012 | 0.4486 | 0.9978 |
| ctrl not infected-rapachlo not infected | -2.4316 | 0.3951 | 0 |
| ctrl not infected-causing not infected | -0.3608 | 0.3353 | 0.4125 |
| ctrl not infected-non-causing not infected | -0.4802 | 0.5093 | 0.4383 |
| ctrl not infected-causing infected | -1.3104 | 0.3347 | 3e-04 |
| ctrl not infected-non-causing infected | -1.453 | 0.5081 | 0.0082 |
| dmso not infected-rapachlo not infected | -2.4329 | 0.4327 | 0 |
| dmso not infected-causing not infected | -0.362 | 0.3801 | 0.4383 |
| dmso not infected-non-causing not infected | -0.4814 | 0.536 | 0.4386 |
| dmso not infected-causing infected | -1.3116 | 0.3796 | 0.0012 |
| dmso not infected-non-causing infected | -1.4542 | 0.5349 | 0.0115 |
| rapachlo not infected-causing not infected | 2.0709 | 0.3116 | 0 |
| rapachlo not infected-non-causing not infected | 1.9515 | 0.4969 | 3e-04 |
| rapachlo not infected-causing infected | 1.1213 | 0.311 | 8e-04 |
| rapachlo not infected-non-causing infected | 0.9786 | 0.4957 | 0.077 |
| causing not infected-non-causing not infected | -0.1194 | 0.4592 | 0.8391 |
| causing infected-non-causing infected | -0.1426 | 0.4575 | 0.8391 |
| causing not infected-causing infected | -0.9496 | 0.0243 | 0 |
| non-causing not infected-non-causing infected | -0.9728 | 0.0457 | 0 |

| Par | Value | Std.Error | p.value |
|---|---|---|---|
| (Intercept) | -0.2578 | 0.1037 | 0.0129 |
| groupdmso not infected | -0.0574 | 0.154 | 0.7111 |
| grouprapachlo not infected | 0.4975 | 0.1114 | 1e-04 |
| groupcausing not infected | -0.148 | 0.1091 | 0.1748 |
| groupnon-causing not infected | -0.3676 | 0.1429 | 0.0101 |
| groupcausing infected | 0.0067 | 0.1038 | 0.9488 |
| groupnon-causing infected | 0.3425 | 0.1259 | 0.0065 |

| Contrast | estimate | SE | p.value |
|---|---|---|---|
| ctrl not infected-dmso not infected | 0.0574 | 0.154 | 0.7507 |
| ctrl not infected-rapachlo not infected | -0.4975 | 0.1114 | 2e-04 |
| ctrl not infected-causing not infected | 0.148 | 0.1091 | 0.2214 |
| ctrl not infected-non-causing not infected | 0.3676 | 0.1429 | 0.0174 |
| ctrl not infected-causing infected | -0.0067 | 0.1038 | 0.9488 |
| ctrl not infected-non-causing infected | -0.3425 | 0.1259 | 0.0138 |
| dmso not infected-rapachlo not infected | -0.5549 | 0.1351 | 4e-04 |
| dmso not infected-causing not infected | 0.0906 | 0.1327 | 0.5916 |
| dmso not infected-non-causing not infected | 0.3103 | 0.1609 | 0.0877 |
| dmso not infected-causing infected | -0.0641 | 0.1284 | 0.6932 |
| dmso not infected-non-causing infected | -0.3999 | 0.1462 | 0.0167 |
| rapachlo not infected-causing not infected | 0.6455 | 0.0769 | 0 |
| rapachlo not infected-non-causing not infected | 0.8651 | 0.1218 | 0 |
| rapachlo not infected-causing infected | 0.4908 | 0.0692 | 0 |
| rapachlo not infected-non-causing infected | 0.155 | 0.1012 | 0.1796 |
| causing not infected-non-causing not infected | 0.2196 | 0.1152 | 0.0877 |
| causing infected-non-causing infected | -0.3358 | 0.0852 | 3e-04 |
| causing not infected-causing infected | -0.1547 | 0.04 | 3e-04 |
| non-causing not infected-non-causing infected | -0.7101 | 0.0768 | 0 |

Autophagosomes observed

Autophagosomes not observed (blocked)

## Grouping: Disease

## M2 – 24 h p.i.

a) Number of autophagosomes

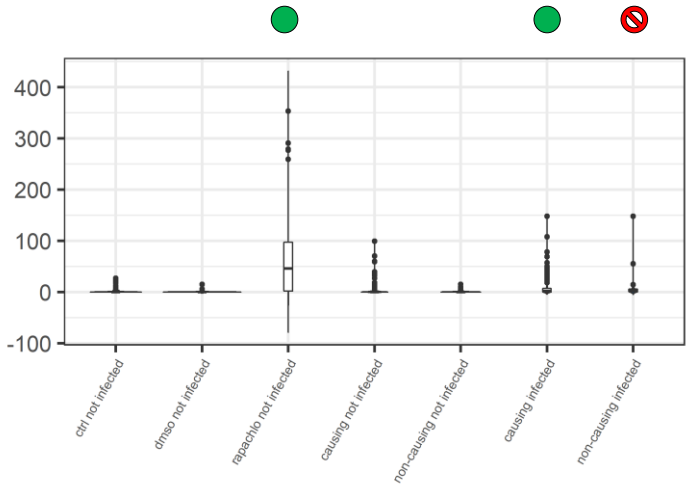


b) Area of autophagosomes

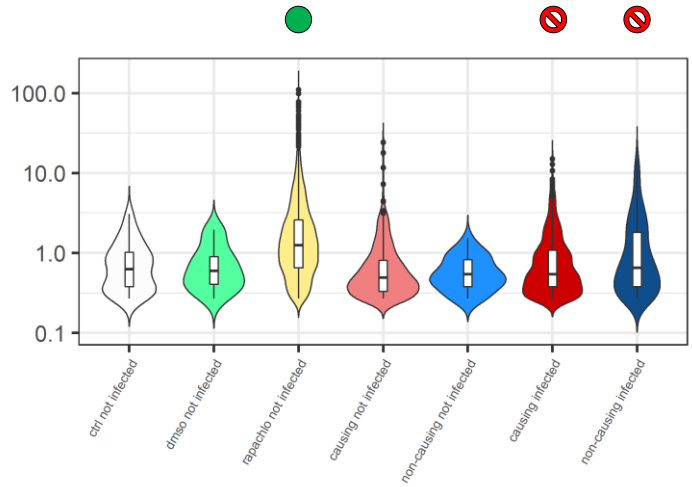


| Conditional model | Estimate | SE | p-value |
|---|---|---|---|
| (Intercept) | 0.9022 | 0.3512 | 0.0102 |
| groupdmso not infected | -0.4225 | 0.4959 | 0.3942 |
| grouprapachlo not infected | 2.9525 | 0.4065 | 0 |
| groupcausing not infected | 0.5802 | 0.3565 | 0.1036 |
| groupnon-causing not infected | -0.4175 | 0.5371 | 0.437 |
| groupcausing infected | 1.1025 | 0.3554 | 0.0019 |
| groupnon-causing infected | 0.6735 | 0.524 | 0.1988 |

| Zero-inflation model | Estimate | SE | p-value |
|---|---|---|---|
| (Intercept) | 0.0662 | 0.4045 | 0.8701 |
| groupdmso not infected | 0.6852 | 0.6036 | 0.2563 |
| grouprapachlo not infected | -2.1235 | 0.5937 | 3e-04 |
| groupcausing not infected | -0.0818 | 0.4352 | 0.8509 |
| groupnon-causing not infected | -0.3562 | 0.6839 | 0.6025 |
| groupcausing infected | -1.0945 | 0.4354 | 0.012 |
| groupnon-causing infected | -1.3206 | 0.6667 | 0.0476 |

| Contrast | estimate | SE | p.value |
|---|---|---|---|
| ctrl not infected-dmso not infected | 0.4225 | 0.4959 | 0.4408 |
| ctrl not infected-rapachlo not infected | -2.9525 | 0.4065 | 0 |
| ctrl not infected-causing not infected | -0.5802 | 0.3565 | 0.141 |
| ctrl not infected-non-causing not infected | 0.4175 | 0.5371 | 0.4615 |
| ctrl not infected-causing infected | -1.1025 | 0.3554 | 0.0038 |
| ctrl not infected-non-causing infected | -0.6735 | 0.524 | 0.2522 |
| dmso not infected-rapachlo not infected | -3.375 | 0.4437 | 0 |
| dmso not infected-causing not infected | -1.0027 | 0.4246 | 0.0318 |
| dmso not infected-non-causing not infected | -0.005 | 0.5899 | 0.9933 |
| dmso not infected-causing infected | -1.525 | 0.4236 | 7e-04 |
| dmso not infected-non-causing infected | -1.096 | 0.5781 | 0.0852 |
| rapachlo not infected-causing not infected | 2.3723 | 0.3112 | 0 |
| rapachlo not infected-non-causing not infected | 3.37 | 0.5146 | 0 |
| rapachlo not infected-causing infected | 1.85 | 0.3099 | 0 |
| rapachlo not infected-non-causing infected | 2.2791 | 0.501 | 0 |
| causing not infected-non-causing not infected | 0.9977 | 0.4825 | 0.0616 |
| causing infected-non-causing infected | 0.429 | 0.4672 | 0.4259 |
| causing not infected-causing infected | -0.5222 | 0.041 | 0 |
| non-causing not infected-non-causing infected | -1.091 | 0.1381 | 0 |

| Par | Value | Std.Error | p.value |
|---|---|---|---|
| (Intercept) | -0.5249 | 0.1379 | 1e-04 |
| groupdmso not infected | -0.0036 | 0.251 | 0.9885 |
| grouprapachlo not infected | 0.7501 | 0.1509 | 0 |
| groupcausing not infected | -0.1532 | 0.1538 | 0.3192 |
| groupnon-causing not infected | -0.2587 | 0.2404 | 0.2819 |
| groupcausing infected | -0.0253 | 0.1461 | 0.8624 |
| groupnon-causing infected | 0.1814 | 0.1859 | 0.3292 |

| Contrast | estimate | SE | p.value |
|---|---|---|---|
| ctrl not infected-dmso not infected | 0.0036 | 0.251 | 0.9885 |
| ctrl not infected-rapachlo not infected | -0.7501 | 0.1509 | 0 |
| ctrl not infected-causing not infected | 0.1532 | 0.1538 | 0.5212 |
| ctrl not infected-non-causing not infected | 0.2587 | 0.2404 | 0.5212 |
| ctrl not infected-causing infected | 0.0253 | 0.1461 | 0.9639 |
| ctrl not infected-non-causing infected | -0.1814 | 0.1859 | 0.5212 |
| dmso not infected-rapachlo not infected | -0.7537 | 0.2179 | 0.0017 |
| dmso not infected-causing not infected | 0.1496 | 0.2205 | 0.6301 |
| dmso not infected-non-causing not infected | 0.2551 | 0.2877 | 0.5485 |
| dmso not infected-causing infected | 0.0217 | 0.2152 | 0.9707 |
| dmso not infected-non-causing infected | -0.1851 | 0.244 | 0.6083 |
| rapachlo not infected-causing not infected | 0.9034 | 0.0916 | 0 |
| rapachlo not infected-non-causing not infected | 1.0088 | 0.2062 | 0 |
| rapachlo not infected-causing infected | 0.7755 | 0.078 | 0 |
| rapachlo not infected-non-causing infected | 0.5687 | 0.1389 | 2e-04 |
| causing not infected-non-causing not infected | 0.1054 | 0.2083 | 0.7278 |
| causing infected-non-causing infected | -0.2068 | 0.1337 | 0.2579 |
| causing not infected-causing infected | -0.1279 | 0.066 | 0.125 |
| non-causing not infected-non-causing infected | -0.4401 | 0.1932 | 0.0618 |

Autophagosomes observed

Autophagosomes not observed (blocked)

## Grouping: Laboratory adaptation

### M1 – 24 h p.i.

a) Number of autophagosomes

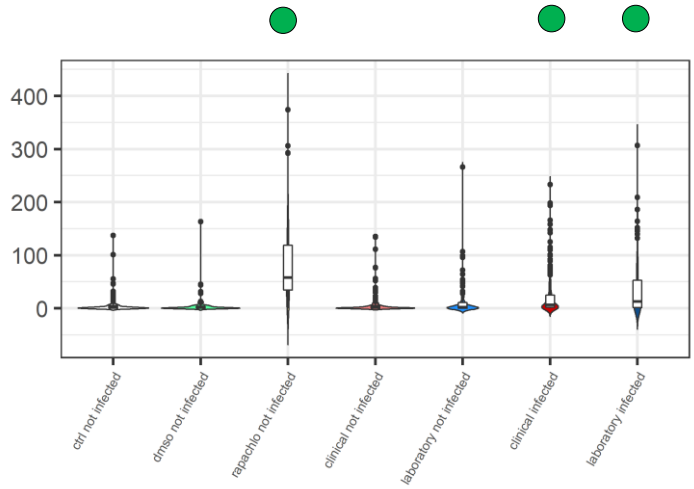


b) Area of autophagosomes

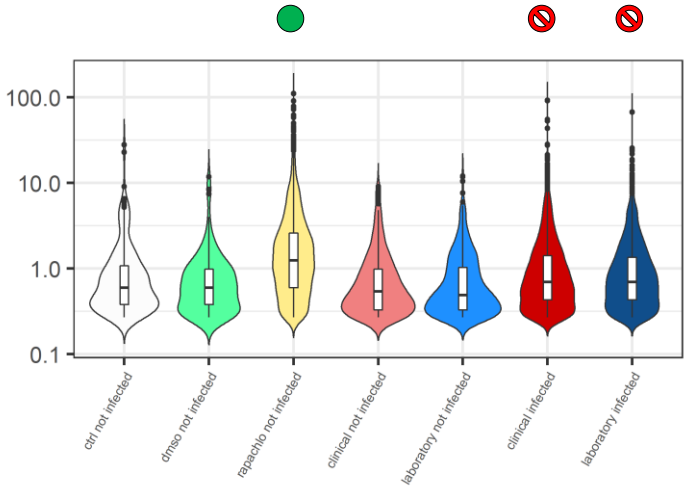


| Conditional model | Estimate | SE | p-value |
|---|---|---|---|
| (Intercept) | 1.7348 | 0.3358 | 0 |
| groupdmso not infected | -0.0045 | 0.4386 | 0.9918 |
| grouprapachlo not infected | 2.4297 | 0.386 | 0 |
| groupclinical not infected | 0.2143 | 0.3366 | 0.5243 |
| grouplaboratory not infected | 0.6847 | 0.379 | 0.0708 |
| groupclinical infected | 1.1845 | 0.3357 | 4e-04 |
| grouplaboratory infected | 1.6229 | 0.3782 | 0 |

| Zero-inflation model | Estimate | SE | p-value |
|---|---|---|---|
| (Intercept) | -0.7799 | 0.3708 | 0.0354 |
| groupdmso not infected | 0.1674 | 0.5769 | 0.7717 |
| grouprapachlo not infected | -2.4772 | 0.6863 | 3e-04 |
| groupclinical not infected | 0.3778 | 0.427 | 0.3763 |
| grouplaboratory not infected | -0.0615 | 0.5003 | 0.9021 |
| groupclinical infected | -1.0595 | 0.4375 | 0.0154 |
| grouplaboratory infected | -0.9966 | 0.5011 | 0.0467 |

| Contrast | estimate | SE | p.value |
|---|---|---|---|
| ctrl not infected-dmso not infected | 0.0045 | 0.4386 | 0.9918 |
| ctrl not infected-rapachlo not infected | -2.4297 | 0.386 | 0 |
| ctrl not infected-clinical not infected | -0.2143 | 0.3366 | 0.5861 |
| ctrl not infected-laboratory not infected | -0.6847 | 0.379 | 0.1039 |
| ctrl not infected-clinical infected | -1.1845 | 0.3357 | 8e-04 |
| ctrl not infected-laboratory infected | -1.6229 | 0.3782 | 1e-04 |
| dmso not infected-rapachlo not infected | -2.4342 | 0.4228 | 0 |
| dmso not infected-clinical not infected | -0.2188 | 0.3785 | 0.5946 |
| dmso not infected-laboratory not infected | -0.6893 | 0.4166 | 0.1335 |
| dmso not infected-clinical infected | -1.1891 | 0.3778 | 0.0029 |
| dmso not infected-laboratory infected | -1.6274 | 0.4159 | 2e-04 |
| rapachlo not infected-clinical not infected | 2.2154 | 0.3143 | 0 |
| rapachlo not infected-laboratory not infected | 1.7449 | 0.3593 | 0 |
| rapachlo not infected-clinical infected | 1.2452 | 0.3134 | 2e-04 |
| rapachlo not infected-laboratory infected | 0.8068 | 0.3585 | 0.039 |
| clinical not infected-laboratory not infected | -0.4704 | 0.3039 | 0.1544 |
| clinical infected-laboratory infected | -0.4383 | 0.3019 | 0.1744 |
| clinical not infected-clinical infected | -0.9702 | 0.0299 | 0 |
| laboratory not infected-laboratory infected | -0.9381 | 0.0308 | 0 |

| Par | Value | Std.Error | p.value |
|---|---|---|---|
| (Intercept) | -0.2652 | 0.1037 | 0.0105 |
| groupdmso not infected | -0.0596 | 0.1533 | 0.6991 |
| grouprapachlo not infected | 0.503 | 0.1106 | 0 |
| groupclinical not infected | -0.199 | 0.1133 | 0.0791 |
| grouplaboratory not infected | -0.1809 | 0.1231 | 0.1416 |
| groupclinical infected | 0.0245 | 0.1055 | 0.8161 |
| grouplaboratory infected | 0.1363 | 0.1156 | 0.2384 |

| Contrast | estimate | SE | p.value |
|---|---|---|---|
| ctrl not infected-dmso not infected | 0.0596 | 0.1533 | 0.7814 |
| ctrl not infected-rapachlo not infected | -0.503 | 0.1106 | 1e-04 |
| ctrl not infected-clinical not infected | 0.199 | 0.1133 | 0.167 |
| ctrl not infected-laboratory not infected | 0.1809 | 0.1231 | 0.2556 |
| ctrl not infected-clinical infected | -0.0245 | 0.1055 | 0.8545 |
| ctrl not infected-laboratory infected | -0.1363 | 0.1156 | 0.3484 |
| dmso not infected-rapachlo not infected | -0.5626 | 0.1344 | 3e-04 |
| dmso not infected-clinical not infected | 0.1394 | 0.1362 | 0.4228 |
| dmso not infected-laboratory not infected | 0.1213 | 0.1439 | 0.5116 |
| dmso not infected-clinical infected | -0.0842 | 0.1298 | 0.6173 |
| dmso not infected-laboratory infected | -0.1959 | 0.1377 | 0.2556 |
| rapachlo not infected-clinical not infected | 0.702 | 0.0831 | 0 |
| rapachlo not infected-laboratory not infected | 0.6839 | 0.0967 | 0 |
| rapachlo not infected-clinical infected | 0.4784 | 0.072 | 0 |
| rapachlo not infected-laboratory infected | 0.3667 | 0.0869 | 3e-04 |
| clinical not infected-laboratory not infected | -0.0181 | 0.0987 | 0.8545 |
| clinical infected-laboratory infected | -0.1118 | 0.0791 | 0.2556 |
| clinical not infected-clinical infected | -0.2235 | 0.0508 | 0 |
| laboratory not infected-laboratory infected | -0.3172 | 0.0499 | 0 |

Autophagosomes observed

Autophagosomes not observed (blocked)

## Grouping: Laboratory adaptation

### M2 – 24 h p.i.

a) Number of autophagosomes

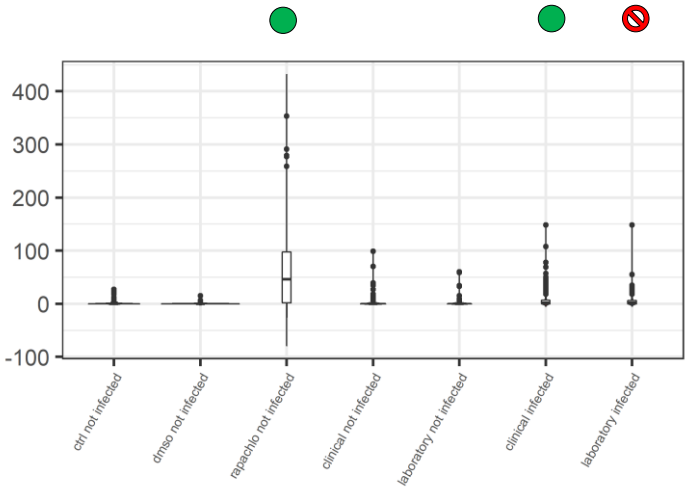


b) Area of autophagosomes

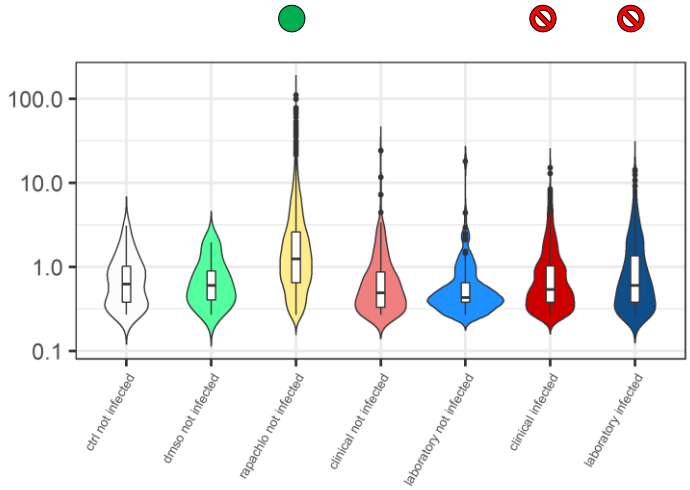


| Conditional model | Estimate | SE | p-value |
|---|---|---|---|
| (Intercept) | 0.914 | 0.3485 | 0.0087 |
| groupdmso not infected | -0.4316 | 0.5008 | 0.3889 |
| grouprapachlo not infected | 2.9482 | 0.4113 | 0 |
| groupclinical not infected | 0.4813 | 0.3687 | 0.1918 |
| grouplaboratory not infected | 0.4107 | 0.4155 | 0.323 |
| groupclinical infected | 1.1228 | 0.3671 | 0.0022 |
| grouplaboratory infected | 0.8507 | 0.4128 | 0.0393 |

| Par | Value | Std.Error | p.value |
|---|---|---|---|
| (Intercept) | -0.5257 | 0.1401 | 2e-04 |
| groupdmso not infected | -0.0016 | 0.2538 | 0.9948 |
| grouprapachlo not infected | 0.7482 | 0.1542 | 0 |
| groupclinical not infected | -0.1113 | 0.1612 | 0.4898 |
| grouplaboratory not infected | -0.273 | 0.1815 | 0.1325 |
| groupclinical infected | -0.0453 | 0.151 | 0.7641 |
| grouplaboratory infected | 0.1032 | 0.1626 | 0.5253 |

| Zero-inflation model | Estimate | SE | p-value |
|---|---|---|---|
| (Intercept) | 0.068 | 0.4064 | 0.8671 |
| groupdmso not infected | 0.6889 | 0.6069 | 0.2563 |
| grouprapachlo not infected | -2.1348 | 0.5971 | 3e-04 |
| groupclinical not infected | -0.1002 | 0.4465 | 0.8224 |
| grouplaboratory not infected | -0.0604 | 0.5069 | 0.9052 |
| groupclinical infected | -1.0259 | 0.4446 | 0.021 |
| grouplaboratory infected | -1.3583 | 0.5156 | 0.0084 |

| Contrast | estimate | SE | p.value |
|---|---|---|---|
| ctrl not infected-dmso not infected | 0.4316 | 0.5008 | 0.421 |
| ctrl not infected-rapachlo not infected | -2.9482 | 0.4113 | 0 |
| ctrl not infected-clinical not infected | -0.4813 | 0.3687 | 0.2434 |
| ctrl not infected-laboratory not infected | -0.4107 | 0.4155 | 0.3839 |
| ctrl not infected-clinical infected | -1.1228 | 0.3671 | 0.0043 |
| ctrl not infected-laboratory infected | -0.8507 | 0.4128 | 0.0579 |
| dmso not infected-rapachlo not infected | -3.3798 | 0.4478 | 0 |
| dmso not infected-clinical not infected | -0.9129 | 0.4366 | 0.0579 |
| dmso not infected-laboratory not infected | -0.8422 | 0.4766 | 0.1052 |
| dmso not infected-clinical infected | -1.5543 | 0.4352 | 8e-04 |
| dmso not infected-laboratory infected | -1.2822 | 0.4742 | 0.0121 |
| rapachlo not infected-clinical not infected | 2.4669 | 0.3263 | 0 |
| rapachlo not infected-laboratory not infected | 2.5376 | 0.3781 | 0 |
| rapachlo not infected-clinical infected | 1.8255 | 0.3243 | 0 |
| rapachlo not infected-laboratory infected | 2.0976 | 0.3749 | 0 |
| clinical not infected-laboratory not infected | 0.0706 | 0.328 | 0.8296 |
| clinical infected-laboratory infected | 0.2721 | 0.3224 | 0.421 |
| clinical not infected-clinical infected | -0.6415 | 0.0478 | 0 |
| laboratory not infected-laboratory infected | -0.44 | 0.0682 | 0 |

| Contrast | estimate | SE | p.value |
|---|---|---|---|
| ctrl not infected-dmso not infected | 0.0016 | 0.2538 | 0.9948 |
| ctrl not infected-rapachlo not infected | -0.7482 | 0.1542 | 0 |
| ctrl not infected-clinical not infected | 0.1113 | 0.1612 | 0.713 |
| ctrl not infected-laboratory not infected | 0.273 | 0.1815 | 0.2894 |
| ctrl not infected-clinical infected | 0.0453 | 0.151 | 0.854 |
| ctrl not infected-laboratory infected | -0.1032 | 0.1626 | 0.713 |
| dmso not infected-rapachlo not infected | -0.7499 | 0.2206 | 0.0022 |
| dmso not infected-clinical not infected | 0.1097 | 0.2262 | 0.765 |
| dmso not infected-laboratory not infected | 0.2714 | 0.241 | 0.4496 |
| dmso not infected-clinical infected | 0.0437 | 0.2191 | 0.8887 |
| dmso not infected-laboratory infected | -0.1049 | 0.2271 | 0.765 |
| rapachlo not infected-clinical not infected | 0.8595 | 0.1025 | 0 |
| rapachlo not infected-laboratory not infected | 1.0212 | 0.1321 | 0 |
| rapachlo not infected-clinical infected | 0.7935 | 0.0856 | 0 |
| rapachlo not infected-laboratory infected | 0.645 | 0.1046 | 0 |
| clinical not infected-laboratory not infected | 0.1617 | 0.1402 | 0.4496 |
| clinical infected-laboratory infected | -0.1486 | 0.0999 | 0.2894 |
| clinical not infected-clinical infected | -0.066 | 0.0754 | 0.6035 |
| laboratory not infected-laboratory infected | -0.3763 | 0.1126 | 0.0023 |

Autophagosomes observed

Autophagosomes not observed (blocked)

## Grouping: Phylogeny

### M1 – 24 h p.i.

a) Number of autophagosomes

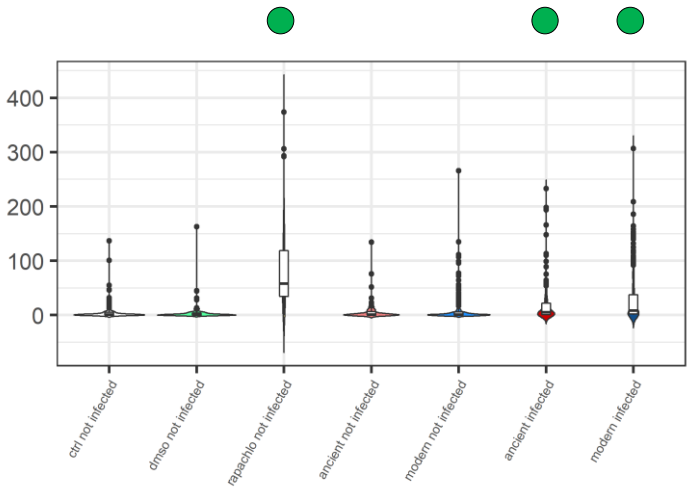


| Conditional model | Estimate | SE | p-value |
|---|---|---|---|
| (Intercept) | 1.7337 | 0.3375 | 0 |
| groupdmso not infected | -0.0032 | 0.4421 | 0.9943 |
| grouprapachlo not infected | 2.431 | 0.3892 | 0 |
| groupancient not infected | 0.0702 | 0.3831 | 0.8547 |
| groupmodern not infected | 0.5187 | 0.339 | 0.1259 |
| groupancient infected | 1.1045 | 0.3816 | 0.0038 |
| groupmodern infected | 1.4461 | 0.3384 | 0 |

| Zero-inflation model | Estimate | SE | p-value |
|---|---|---|---|
| (Intercept) | -0.7825 | 0.3777 | 0.0383 |
| groupdmso not infected | 0.1651 | 0.585 | 0.7778 |
| grouprapachlo not infected | -2.4843 | 0.6922 | 3e-04 |
| groupancient not infected | 0.3061 | 0.4891 | 0.5315 |
| groupmodern not infected | 0.233 | 0.4371 | 0.594 |
| groupancient infected | -0.8203 | 0.4998 | 0.1007 |
| groupmodern infected | -1.1715 | 0.4466 | 0.0087 |

| Contrast | estimate | SE | p.value |
|---|---|---|---|
| ctrl not infected-dmso not infected | 0.0032 | 0.4421 | 0.9943 |
| ctrl not infected-rapachlo not infected | -2.431 | 0.3892 | 0 |
| ctrl not infected-ancient not infected | -0.0702 | 0.3831 | 0.9097 |
| ctrl not infected-modern not infected | -0.5187 | 0.339 | 0.1845 |
| ctrl not infected-ancient infected | -1.1045 | 0.3816 | 0.0067 |
| ctrl not infected-modern infected | -1.4461 | 0.3384 | 1e-04 |
| dmso not infected-rapachlo not infected | -2.4341 | 0.4263 | 0 |
| dmso not infected-ancient not infected | -0.0733 | 0.4211 | 0.9097 |
| dmso not infected-modern not infected | -0.5219 | 0.3813 | 0.2171 |
| dmso not infected-ancient infected | -1.1076 | 0.4197 | 0.0134 |
| dmso not infected-modern infected | -1.4492 | 0.3808 | 4e-04 |
| rapachlo not infected-ancient not infected | 2.3608 | 0.3636 | 0 |
| rapachlo not infected-modern not infected | 1.9122 | 0.3166 | 0 |
| rapachlo not infected-ancient infected | 1.3265 | 0.3619 | 5e-04 |
| rapachlo not infected-modern infected | 0.9849 | 0.3159 | 0.0036 |
| ancient not infected-modern not infected | -0.4486 | 0.3074 | 0.1966 |
| ancient infected-modern infected | -0.3416 | 0.3048 | 0.312 |
| ancient not infected-ancient infected | -1.0343 | 0.0429 | 0 |
| modern not infected-modern infected | -0.9273 | 0.0248 | 0 |

b) Area of autophagosomes

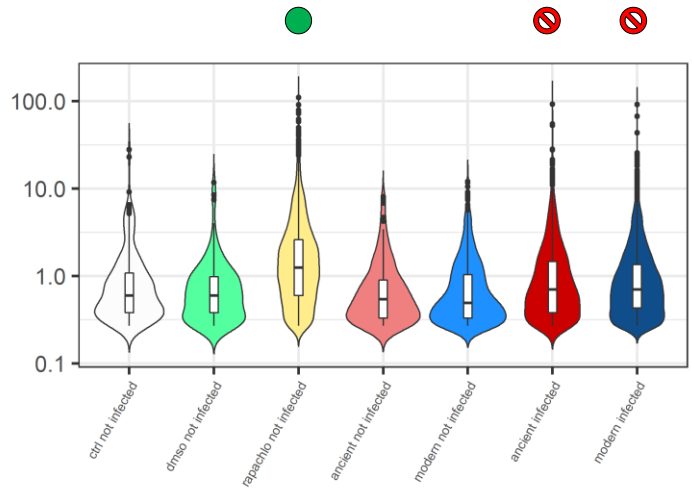


| Par | Value | Std.Error | p.value |
|---|---|---|---|
| (Intercept) | -0.2654 | 0.1031 | 0.0101 |
| groupdmso not infected | -0.0604 | 0.1533 | 0.6955 |
| grouprapachlo not infected | 0.5039 | 0.1106 | 0 |
| groupancient not infected | -0.2355 | 0.1285 | 0.0669 |
| groupmodern not infected | -0.192 | 0.1111 | 0.0839 |
| groupancient infected | 0.0086 | 0.1156 | 0.9405 |
| groupmodern infected | 0.0885 | 0.1055 | 0.4016 |

| Contrast | estimate | SE | p.value |
|---|---|---|---|
| ctrl not infected-dmso not infected | 0.0604 | 0.1533 | 0.7342 |
| ctrl not infected-rapachlo not infected | -0.5039 | 0.1106 | 1e-04 |
| ctrl not infected-ancient not infected | 0.2355 | 0.1285 | 0.1412 |
| ctrl not infected-modern not infected | 0.192 | 0.1111 | 0.1594 |
| ctrl not infected-ancient infected | -0.0086 | 0.1156 | 0.9405 |
| ctrl not infected-modern infected | -0.0885 | 0.1055 | 0.5086 |
| dmso not infected-rapachlo not infected | -0.5643 | 0.1344 | 3e-04 |
| dmso not infected-ancient not infected | 0.1751 | 0.1491 | 0.4057 |
| dmso not infected-modern not infected | 0.1316 | 0.1341 | 0.4498 |
| dmso not infected-ancient infected | -0.069 | 0.1382 | 0.7342 |
| dmso not infected-modern infected | -0.1489 | 0.1295 | 0.4057 |
| rapachlo not infected-ancient not infected | 0.7394 | 0.1028 | 0 |
| rapachlo not infected-modern not infected | 0.6959 | 0.0805 | 0 |
| rapachlo not infected-ancient infected | 0.4953 | 0.0861 | 0 |
| rapachlo not infected-modern infected | 0.4154 | 0.0726 | 0 |
| ancient not infected-modern not infected | -0.0435 | 0.1033 | 0.7342 |
| ancient infected-modern infected | -0.0799 | 0.0794 | 0.4498 |
| ancient not infected-ancient infected | -0.2441 | 0.0706 | 0.0013 |
| modern not infected-modern infected | -0.2805 | 0.0412 | 0 |

Autophagosomes observed

Autophagosomes not observed (blocked)

## Grouping: Phylogeny

## M2 – 24 h p.i.

a) Number of autophagosomes

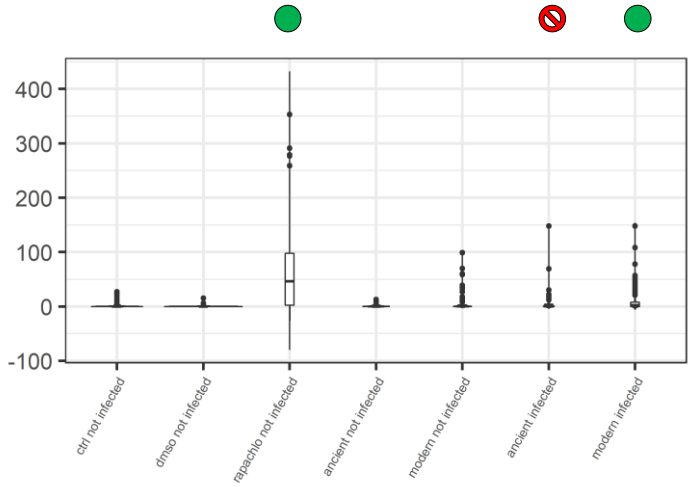


b) Area of autophagosomes

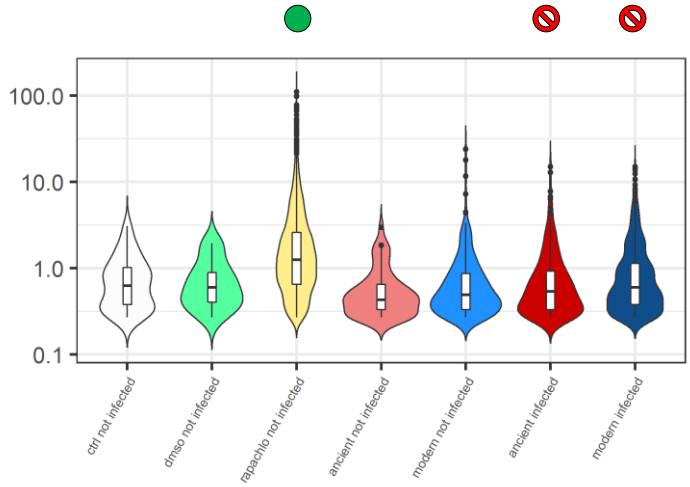


| Conditional model | Estimate | SE | p-value |
|---|---|---|---|
| (Intercept) | 0.9155 | 0.3453 | 0.008 |
| groupdmso not infected | -0.4274 | 0.4938 | 0.3868 |
| grouprapachlo not infected | 2.9445 | 0.4047 | 0 |
| groupancient not infected | -0.2741 | 0.4129 | 0.5069 |
| groupmodern not infected | 0.7098 | 0.3628 | 0.0504 |
| groupancient infected | 0.8379 | 0.4057 | 0.0389 |
| groupmodern infected | 1.1514 | 0.3615 | 0.0014 |

| Zero-inflation model | Estimate | SE | p-value |
|---|---|---|---|
| (Intercept) | 0.0742 | 0.3978 | 0.852 |
| groupdmso not infected | 0.6855 | 0.5952 | 0.2495 |
| grouprapachlo not infected | -2.1116 | 0.5851 | 3e-04 |
| groupancient not infected | -0.1643 | 0.5037 | 0.7443 |
| groupmodern not infected | -0.1464 | 0.4402 | 0.7395 |
| groupancient infected | -0.6477 | 0.4867 | 0.1833 |
| groupmodern infected | -1.3785 | 0.4416 | 0.0018 |

| Contrast | estimate | SE | p.value |
|---|---|---|---|
| ctrl not infected-dmso not infected | 0.4274 | 0.4938 | 0.4326 |
| ctrl not infected-rapachlo not infected | -2.9445 | 0.4047 | 0 |
| ctrl not infected-ancient not infected | 0.2741 | 0.4129 | 0.5352 |
| ctrl not infected-modern not infected | -0.7098 | 0.3628 | 0.0642 |
| ctrl not infected-ancient infected | -0.8379 | 0.4057 | 0.0532 |
| ctrl not infected-modern infected | -1.1514 | 0.3615 | 0.0028 |
| dmso not infected-rapachlo not infected | -3.3719 | 0.4423 | 0 |
| dmso not infected-ancient not infected | -0.1533 | 0.4738 | 0.7464 |
| dmso not infected-modern not infected | -1.1372 | 0.4306 | 0.0123 |
| dmso not infected-ancient infected | -1.2652 | 0.4675 | 0.011 |
| dmso not infected-modern infected | -1.5787 | 0.4296 | 5e-04 |
| rapachlo not infected-ancient not infected | 3.2186 | 0.3768 | 0 |
| rapachlo not infected-modern not infected | 2.2347 | 0.3204 | 0 |
| rapachlo not infected-ancient infected | 2.1066 | 0.3687 | 0 |
| rapachlo not infected-modern infected | 1.7931 | 0.3189 | 0 |
| ancient not infected-modern not infected | -0.9839 | 0.3283 | 0.0048 |
| ancient infected-modern infected | -0.3135 | 0.3174 | 0.3842 |
| ancient not infected-ancient infected | -1.112 | 0.0942 | 0 |
| modern not infected-modern infected | -0.4416 | 0.0432 | 0 |

| Par | Value | Std.Error | p.value |
|---|---|---|---|
| (Intercept) | -0.5245 | 0.1368 | 1e-04 |
| groupdmso not infected | -0.0046 | 0.2495 | 0.9852 |
| grouprapachlo not infected | 0.7512 | 0.1492 | 0 |
| groupancient not infected | -0.305 | 0.1952 | 0.1183 |
| groupmodern not infected | -0.1101 | 0.1546 | 0.4762 |
| groupancient infected | -0.1494 | 0.1627 | 0.3586 |
| groupmodern infected | 0.0554 | 0.1461 | 0.7044 |

| Contrast | estimate | SE | p.value |
|---|---|---|---|
| ctrl not infected-dmso not infected | 0.0046 | 0.2495 | 0.9852 |
| ctrl not infected-rapachlo not infected | -0.7512 | 0.1492 | 0 |
| ctrl not infected-ancient not infected | 0.305 | 0.1952 | 0.2498 |
| ctrl not infected-modern not infected | 0.1101 | 0.1546 | 0.6463 |
| ctrl not infected-ancient infected | 0.1494 | 0.1627 | 0.5241 |
| ctrl not infected-modern infected | -0.0554 | 0.1461 | 0.7872 |
| dmso not infected-rapachlo not infected | -0.7558 | 0.2165 | 0.0015 |
| dmso not infected-ancient not infected | 0.3003 | 0.2509 | 0.3997 |
| dmso not infected-modern not infected | 0.1055 | 0.2208 | 0.7514 |
| dmso not infected-ancient infected | 0.1448 | 0.2266 | 0.6622 |
| dmso not infected-modern infected | -0.06 | 0.2149 | 0.8233 |
| rapachlo not infected-ancient not infected | 1.0561 | 0.1515 | 0 |
| rapachlo not infected-modern not infected | 0.8613 | 0.0935 | 0 |
| rapachlo not infected-ancient infected | 0.9006 | 0.1064 | 0 |
| rapachlo not infected-modern infected | 0.6958 | 0.0786 | 0 |
| ancient not infected-modern not infected | -0.1948 | 0.1568 | 0.3997 |
| ancient infected-modern infected | -0.2048 | 0.102 | 0.106 |
| ancient not infected-ancient infected | -0.1555 | 0.1442 | 0.4447 |
| modern not infected-modern infected | -0.1655 | 0.0691 | 0.0451 |

Autophagosomes observed

Autophagosomes not observed (blocked)

## Grouping: Sample

### M1 – 24 h p.i.

a) Number of autophagosomes

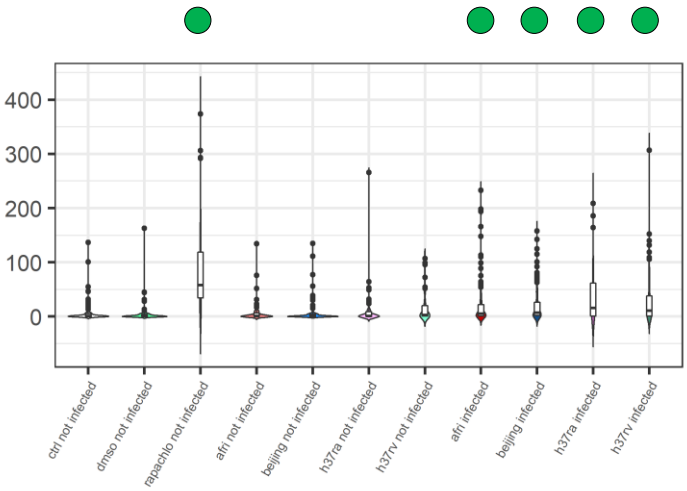


b) Area of autophagosomes

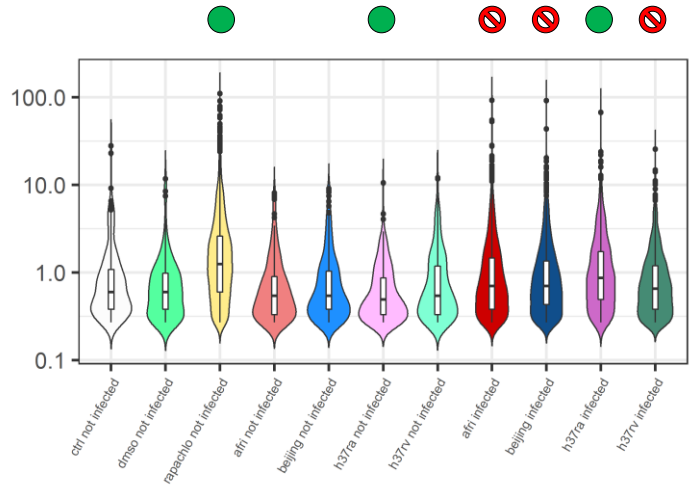


| Conditional model | Estimate | SE | p-value |
|---|---|---|---|
| (Intercept) | 1.7318 | 0.3391 | 0 |
| groupdmso not infected | -0.0094 | 0.4321 | 0.9826 |
| grouprapachlo not infected | 2.4283 | 0.3804 | 0 |
| groupafri not infected | 0.072 | 0.3747 | 0.8476 |
| groupbeijing not infected | 0.3621 | 0.3744 | 0.3336 |
| grouph37ra not infected | 0.4201 | 0.492 | 0.3931 |
| grouph37rv not infected | 0.8728 | 0.4393 | 0.047 |
| groupafri infected | 1.1064 | 0.3731 | 0.003 |
| groupbeijing infected | 1.2688 | 0.3729 | 7e-04 |
| grouph37ra infected | 1.393 | 0.4908 | 0.0045 |
| grouph37rv infected | 1.7815 | 0.438 | 0 |

| Zero-inflation model | Estimate | SE | p-value |
|---|---|---|---|
| (Intercept) | -0.7554 | 0.3686 | 0.0404 |
| groupdmso not infected | 0.1755 | 0.5553 | 0.752 |
| grouprapachlo not infected | -2.4925 | 0.6732 | 2e-04 |
| groupafri not infected | 0.2864 | 0.4651 | 0.5381 |
| groupbeijing not infected | 0.4171 | 0.4636 | 0.3683 |
| grouph37ra not infected | 0.323 | 0.6114 | 0.5973 |
| grouph37rv not infected | -0.459 | 0.6239 | 0.462 |
| groupafri infected | -0.8359 | 0.4764 | 0.0794 |
| groupbeijing infected | -1.3416 | 0.4919 | 0.0064 |
| grouph37ra infected | -0.7319 | 0.6441 | 0.2558 |
| grouph37rv infected | -1.1875 | 0.5809 | 0.0409 |

| Contrast | estimate | SE | p.value |
|---|---|---|---|
| ctrl not infected-dmso not infected | 0.0094 | 0.4321 | 0.9826 |
| ctrl not infected-rapachlo not infected | -2.4283 | 0.3804 | 0 |
| ctrl not infected-afri not infected | -0.072 | 0.3747 | 0.889 |
| ctrl not infected-beijing not infected | -0.3621 | 0.3744 | 0.4949 |
| ctrl not infected-h37ra not infected | -0.4201 | 0.492 | 0.5211 |
| ctrl not infected-h37rv not infected | -0.8728 | 0.4393 | 0.0923 |
| ctrl not infected-afri infected | -1.1064 | 0.3731 | 0.0078 |
| ctrl not infected-beijing infected | -1.2688 | 0.3729 | 0.0021 |
| ctrl not infected-h37ra infected | -1.393 | 0.4908 | 0.0111 |
| ctrl not infected-h37rv infected | -1.7815 | 0.438 | 2e-04 |
| dmso not infected-rapachlo not infected | -2.4377 | 0.4167 | 0 |
| dmso not infected-afri not infected | -0.0815 | 0.4118 | 0.889 |
| dmso not infected-beijing not infected | -0.3715 | 0.4115 | 0.5211 |
| dmso not infected-h37ra not infected | -0.4296 | 0.5176 | 0.5211 |
| dmso not infected-h37rv not infected | -0.8822 | 0.4736 | 0.1125 |
| dmso not infected-afri infected | -1.1158 | 0.4104 | 0.0145 |
| dmso not infected-beijing infected | -1.2783 | 0.4101 | 0.0051 |
| dmso not infected-h37ra infected | -1.4024 | 0.5165 | 0.0145 |
| dmso not infected-h37rv infected | -1.7909 | 0.4723 | 6e-04 |
| rapachlo not infected-afri not infected | 2.3563 | 0.3553 | 0 |
| rapachlo not infected-beijing not infected | 2.0663 | 0.3548 | 0 |
| rapachlo not infected-h37ra not infected | 2.0082 | 0.4803 | 2e-04 |
| rapachlo not infected-h37rv not infected | 1.5555 | 0.4204 | 8e-04 |
| rapachlo not infected-afri infected | 1.3219 | 0.3536 | 7e-04 |
| rapachlo not infected-beijing infected | 1.1595 | 0.3532 | 0.003 |
| rapachlo not infected-h37ra infected | 1.0353 | 0.4791 | 0.0633 |
| rapachlo not infected-h37rv infected | 0.6468 | 0.419 | 0.2035 |
| afri not infected-beijing not infected | -0.29 | 0.3471 | 0.5211 |
| afri not infected-h37ra not infected | -0.3481 | 0.4787 | 0.5729 |
| afri not infected-h37rv not infected | -0.8007 | 0.4108 | 0.0964 |
| beijing not infected-h37ra not infected | -0.0581 | 0.4785 | 0.9249 |
| beijing not infected-h37rv not infected | -0.5107 | 0.4104 | 0.328 |
| h37ra not infected-h37rv not infected | -0.4526 | 0.5515 | 0.5211 |
| afri infected-beijing infected | -0.1625 | 0.3437 | 0.7203 |
| afri infected-h37ra infected | -0.2866 | 0.4763 | 0.6362 |
| afri infected-h37rv infected | -0.6751 | 0.4079 | 0.1689 |
| beijing infected-h37ra infected | -0.1242 | 0.476 | 0.8757 |
| beijing infected-h37rv infected | -0.5127 | 0.4075 | 0.328 |
| h37ra infected-h37rv infected | -0.3885 | 0.5494 | 0.5729 |

| Par | Value | Std.Error | p.value |
|---|---|---|---|
| (Intercept) | -0.2574 | 0.1046 | 0.0138 |
| groupdmso not infected | -0.0567 | 0.1556 | 0.717 |
| grouprapachlo not infected | 0.4966 | 0.1129 | 1e-04 |
| groupafri not infected | -0.2415 | 0.1305 | 0.0642 |
| groupbeijing not infected | -0.172 | 0.1312 | 0.1898 |
| grouph37ra not infected | -0.3725 | 0.1464 | 0.011 |
| grouph37rv not infected | -0.0446 | 0.1376 | 0.7462 |
| groupafri infected | 0.0021 | 0.1179 | 0.986 |
| groupbeijing infected | 0.0308 | 0.1161 | 0.7908 |
| grouph37ra infected | 0.3378 | 0.1302 | 0.0095 |
| grouph37rv infected | -0.006 | 0.1246 | 0.9618 |

| Contrast | estimate | SE | p.value |
|---|---|---|---|
| ctrl not infected-dmso not infected | 0.0567 | 0.1556 | 0.855 |
| ctrl not infected-rapachlo not infected | -0.4966 | 0.1129 | 3e-04 |
| ctrl not infected-afri not infected | 0.2415 | 0.1305 | 0.1315 |
| ctrl not infected-beijing not infected | 0.172 | 0.1312 | 0.3265 |
| ctrl not infected-h37ra not infected | 0.3725 | 0.1464 | 0.0276 |
| ctrl not infected-h37rv not infected | 0.0446 | 0.1376 | 0.855 |
| ctrl not infected-afri infected | -0.0021 | 0.1179 | 0.986 |
| ctrl not infected-beijing infected | -0.0308 | 0.1161 | 0.872 |
| ctrl not infected-h37ra infected | -0.3378 | 0.1302 | 0.0255 |
| ctrl not infected-h37rv infected | 0.006 | 0.1246 | 0.9847 |
| dmso not infected-rapachlo not infected | -0.5533 | 0.1366 | 8e-04 |
| dmso not infected-afri not infected | 0.1847 | 0.151 | 0.3764 |
| dmso not infected-beijing not infected | 0.1153 | 0.1516 | 0.6688 |
| dmso not infected-h37ra not infected | 0.3157 | 0.1642 | 0.1305 |
| dmso not infected-h37rv not infected | -0.0122 | 0.1571 | 0.9843 |
| dmso not infected-afri infected | -0.0588 | 0.1404 | 0.855 |
| dmso not infected-beijing infected | -0.0875 | 0.1387 | 0.7612 |
| dmso not infected-h37ra infected | -0.3945 | 0.15 | 0.0276 |
| dmso not infected-h37rv infected | -0.0508 | 0.1458 | 0.855 |
| rapachlo not infected-afri not infected | 0.738 | 0.1046 | 0 |
| rapachlo not infected-beijing not infected | 0.6686 | 0.1056 | 0 |
| rapachlo not infected-h37ra not infected | 0.8691 | 0.1255 | 0 |
| rapachlo not infected-h37rv not infected | 0.5411 | 0.1133 | 1e-04 |
| rapachlo not infected-afri infected | 0.4945 | 0.0884 | 0 |
| rapachlo not infected-beijing infected | 0.4658 | 0.0861 | 0 |
| rapachlo not infected-h37ra infected | 0.1588 | 0.1059 | 0.2629 |
| rapachlo not infected-h37rv infected | 0.5026 | 0.0971 | 0 |
| afri not infected-beijing not infected | -0.0695 | 0.124 | 0.7732 |
| afri not infected-h37ra not infected | 0.131 | 0.1409 | 0.5416 |
| afri not infected-h37rv not infected | -0.1969 | 0.1303 | 0.2558 |
| beijing not infected-h37ra not infected | 0.2005 | 0.1417 | 0.2813 |
| beijing not infected-h37rv not infected | -0.1274 | 0.1301 | 0.5214 |
| h37ra not infected-h37rv not infected | -0.3279 | 0.1325 | 0.0302 |
| afri infected-beijing infected | -0.0287 | 0.0923 | 0.855 |
| afri infected-h37ra infected | -0.3357 | 0.1106 | 0.0079 |
| afri infected-h37rv infected | 0.008 | 0.1023 | 0.9843 |
| beijing infected-h37ra infected | -0.307 | 0.1083 | 0.0141 |
| beijing infected-h37rv infected | 0.0368 | 0.0994 | 0.855 |
| h37ra infected-h37rv infected | 0.3438 | 0.0947 | 0.0011 |
| afri not infected-afri infected | -0.2435 | 0.0704 | 0.002 |
| beijing not infected-beijing infected | -0.2028 | 0.0729 | 0.0155 |
| h37ra not infected-h37ra infected | -0.7103 | 0.0768 | 0 |
| h37rv not infected-h37rv infected | -0.0386 | 0.0653 | 0.7693 |

🟢 Autophagosomes observed

🚫 Autophagosomes not observed (blocked)

## Grouping: Sample

## M2 – 24 h p.i.

a) Number of autophagosomes

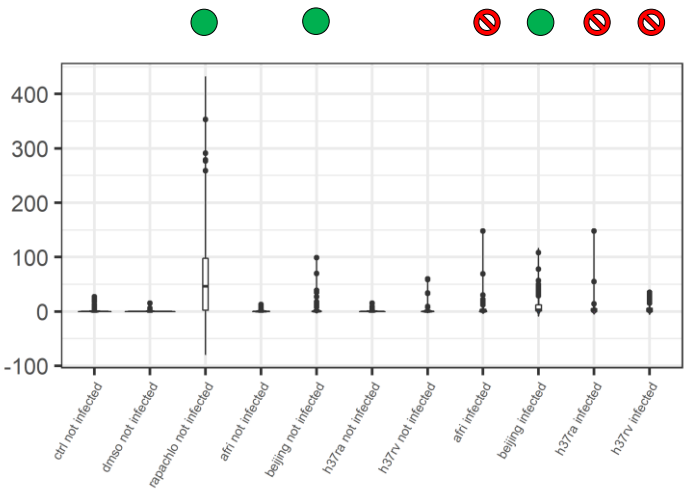


b) Area of autophagosomes

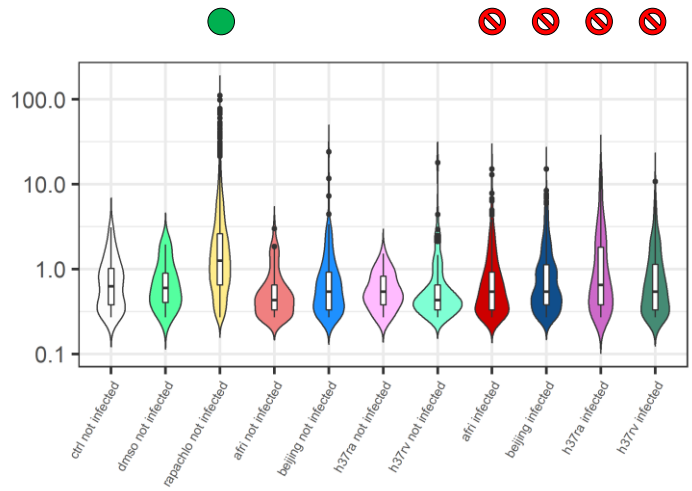


| Conditional model | Estimate | SE | p-value |
|---|---|---|---|
| (Intercept) | 0.9132 | 0.3393 | 0.0071 |
| groupdmso not infected | -0.4106 | 0.4739 | 0.3863 |
| grouprapachlo not infected | 2.9377 | 0.3858 | 0 |
| groupafri not infected | -0.2701 | 0.3944 | 0.4934 |
| groupbeijing not infected | 1.0085 | 0.3868 | 0.0091 |
| grouph37ra not infected | -0.4356 | 0.5111 | 0.394 |
| grouph37rv not infected | 0.8393 | 0.4565 | 0.066 |
| groupafri infected | 0.8416 | 0.3869 | 0.0296 |
| groupbeijing infected | 1.4501 | 0.3847 | 2e-04 |
| grouph37ra infected | 0.6558 | 0.4973 | 0.1873 |
| grouph37rv infected | 0.9766 | 0.4541 | 0.0315 |

| Zero-inflation model | Estimate | SE | p-value |
|---|---|---|---|
| (Intercept) | 0.092 | 0.3961 | 0.8163 |
| groupdmso not infected | 0.674 | 0.5865 | 0.2505 |
| grouprapachlo not infected | -2.1108 | 0.5782 | 3e-04 |
| groupafri not infected | -0.1785 | 0.4967 | 0.7193 |
| groupbeijing not infected | -0.2535 | 0.4915 | 0.606 |
| grouph37ra not infected | -0.3638 | 0.6681 | 0.5861 |
| grouph37rv not infected | -0.0641 | 0.5851 | 0.9127 |
| groupafri infected | -0.6637 | 0.4802 | 0.1669 |
| groupbeijing infected | -1.4196 | 0.4873 | 0.0036 |
| grouph37ra infected | -1.3229 | 0.6502 | 0.0419 |
| grouph37rv infected | -1.3892 | 0.5963 | 0.0198 |

| Contrast | estimate | SE | p.value |
|---|---|---|---|
| ctrl not infected-dmso not infected | 0.4106 | 0.4739 | 0.4843 |
| ctrl not infected-rapachlo not infected | -2.9377 | 0.3858 | 0 |
| ctrl not infected-afri not infected | 0.2701 | 0.3944 | 0.5895 |
| ctrl not infected-beijing not infected | -1.0085 | 0.3868 | 0.0181 |
| ctrl not infected-h37ra not infected | 0.4356 | 0.5111 | 0.4843 |
| ctrl not infected-h37rv not infected | -0.8393 | 0.4565 | 0.1019 |
| ctrl not infected-afri infected | -0.8416 | 0.3869 | 0.0514 |
| ctrl not infected-beijing infected | -1.4501 | 0.3847 | 5e-04 |
| ctrl not infected-h37ra infected | -0.6558 | 0.4973 | 0.2521 |
| ctrl not infected-h37rv infected | -0.9766 | 0.4541 | 0.0525 |
| dmso not infected-rapachlo not infected | -3.3484 | 0.4261 | 0 |
| dmso not infected-afri not infected | -0.1405 | 0.4552 | 0.7757 |
| dmso not infected-beijing not infected | -1.4192 | 0.4487 | 0.0041 |
| dmso not infected-h37ra not infected | 0.025 | 0.5638 | 0.9647 |
| dmso not infected-h37rv not infected | -1.2499 | 0.5062 | 0.0256 |
| dmso not infected-afri infected | -1.2522 | 0.4487 | 0.0121 |
| dmso not infected-beijing infected | -1.8607 | 0.4468 | 1e-04 |
| dmso not infected-h37ra infected | -1.0664 | 0.5514 | 0.0851 |
| dmso not infected-h37rv infected | -1.3873 | 0.504 | 0.013 |
| rapachlo not infected-afri not infected | 3.2079 | 0.3588 | 0 |
| rapachlo not infected-beijing not infected | 1.9292 | 0.3498 | 0 |
| rapachlo not infected-h37ra not infected | 3.3734 | 0.4897 | 0 |
| rapachlo not infected-h37rv not infected | 2.0985 | 0.4209 | 0 |
| rapachlo not infected-afri infected | 2.0962 | 0.3503 | 0 |
| rapachlo not infected-beijing infected | 1.4877 | 0.3474 | 1e-04 |
| rapachlo not infected-h37ra infected | 2.282 | 0.4754 | 0 |
| rapachlo not infected-h37rv infected | 1.9611 | 0.4181 | 0 |
| afri not infected-beijing not infected | -1.2786 | 0.3573 | 0.001 |
| afri not infected-h37ra not infected | 0.1655 | 0.4986 | 0.7757 |
| afri not infected-h37rv not infected | -1.1094 | 0.4239 | 0.0181 |
| beijing not infected-h37ra not infected | 1.4441 | 0.4925 | 0.0082 |
| beijing not infected-h37rv not infected | 0.1693 | 0.4156 | 0.7694 |
| h37ra not infected-h37rv not infected | -1.2749 | 0.5642 | 0.0431 |
| afri infected-beijing infected | -0.6085 | 0.3463 | 0.1174 |
| afri infected-h37ra infected | 0.1858 | 0.4784 | 0.7694 |
| afri infected-h37rv infected | -0.135 | 0.4137 | 0.7757 |
| beijing infected-h37ra infected | 0.7943 | 0.4766 | 0.1332 |
| beijing infected-h37rv infected | 0.4734 | 0.4106 | 0.3247 |
| h37ra infected-h37rv infected | -0.3208 | 0.5498 | 0.6504 |

| Par | Value | Std.Error | p.value |
|---|---|---|---|
| (Intercept) | -0.525 | 0.138 | 1e-04 |
| groupdmso not infected | -0.0035 | 0.251 | 0.989 |
| grouprapachlo not infected | 0.7501 | 0.151 | 0 |
| groupafri not infected | -0.3039 | 0.1967 | 0.1224 |
| groupbeijing not infected | -0.0075 | 0.1677 | 0.9645 |
| grouph37ra not infected | -0.2585 | 0.2404 | 0.2823 |
| grouph37rv not infected | -0.2842 | 0.1956 | 0.1464 |
| groupafri infected | -0.1504 | 0.1645 | 0.3606 |
| groupbeijing infected | 0.0289 | 0.1543 | 0.8513 |
| grouph37ra infected | 0.1817 | 0.1861 | 0.3288 |
| grouph37rv infected | 0.0488 | 0.1728 | 0.7775 |

| Contrast | estimate | SE | p.value |
|---|---|---|---|
| ctrl not infected-dmso not infected | 0.0035 | 0.251 | 0.989 |
| ctrl not infected-rapachlo not infected | -0.7501 | 0.151 | 0 |
| ctrl not infected-afri not infected | 0.3039 | 0.1967 | 0.3096 |
| ctrl not infected-beijing not infected | 0.0075 | 0.1677 | 0.989 |
| ctrl not infected-h37ra not infected | 0.2585 | 0.2404 | 0.4951 |
| ctrl not infected-h37rv not infected | 0.2842 | 0.1956 | 0.3325 |
| ctrl not infected-afri infected | 0.1504 | 0.1645 | 0.5743 |
| ctrl not infected-beijing infected | -0.0289 | 0.1543 | 0.989 |
| ctrl not infected-h37ra infected | -0.1817 | 0.1861 | 0.5437 |
| ctrl not infected-h37rv infected | -0.0488 | 0.1728 | 0.989 |
| dmso not infected-rapachlo not infected | -0.7535 | 0.2179 | 0.0024 |
| dmso not infected-afri not infected | 0.3004 | 0.2523 | 0.4951 |
| dmso not infected-beijing not infected | 0.004 | 0.2304 | 0.989 |
| dmso not infected-h37ra not infected | 0.255 | 0.2877 | 0.5764 |
| dmso not infected-h37rv not infected | 0.2807 | 0.2514 | 0.4951 |
| dmso not infected-afri infected | 0.1469 | 0.228 | 0.7206 |
| dmso not infected-beijing infected | -0.0324 | 0.2208 | 0.989 |
| dmso not infected-h37ra infected | -0.1852 | 0.2441 | 0.6421 |
| dmso not infected-h37rv infected | -0.0523 | 0.2341 | 0.989 |
| rapachlo not infected-afri not infected | 1.054 | 0.153 | 0 |
| rapachlo not infected-beijing not infected | 0.7575 | 0.1134 | 0 |
| rapachlo not infected-h37ra not infected | 1.0086 | 0.2063 | 0 |
| rapachlo not infected-h37rv not infected | 1.0342 | 0.1517 | 0 |
| rapachlo not infected-afri infected | 0.9004 | 0.1085 | 0 |
| rapachlo not infected-beijing infected | 0.7211 | 0.0925 | 0 |
| rapachlo not infected-h37ra infected | 0.5683 | 0.1391 | 2e-04 |
| rapachlo not infected-h37rv infected | 0.7012 | 0.1208 | 0 |
| afri not infected-beijing not infected | -0.2964 | 0.1696 | 0.2474 |
| afri not infected-h37ra not infected | -0.0454 | 0.2417 | 0.989 |
| afri not infected-h37rv not infected | -0.0197 | 0.1972 | 0.989 |
| beijing not infected-h37ra not infected | 0.251 | 0.2188 | 0.4951 |
| beijing not infected-h37rv not infected | 0.2767 | 0.1684 | 0.2876 |
| h37ra not infected-h37rv not infected | 0.0257 | 0.2409 | 0.989 |
| afri infected-beijing infected | -0.1793 | 0.1132 | 0.3041 |
| afri infected-h37ra infected | -0.3321 | 0.1536 | 0.1015 |
| afri infected-h37rv infected | -0.1992 | 0.1373 | 0.3325 |
| beijing infected-h37ra infected | -0.1528 | 0.1428 | 0.4951 |
| beijing infected-h37rv infected | -0.0199 | 0.125 | 0.989 |
| h37ra infected-h37rv infected | 0.1329 | 0.1626 | 0.6135 |
| afri not infected-afri infected | -0.1535 | 0.1444 | 0.4951 |
| beijing not infected-beijing infected | -0.0364 | 0.088 | 0.9124 |
| h37ra not infected-h37ra infected | -0.4402 | 0.1931 | 0.0813 |
| h37rv not infected-h37rv infected | -0.333 | 0.1384 | 0.0631 |

Autophagosomes observed

Autophagosomes not observed (blocked)

## Grouping: Virulence (absolute)

### M1 – 24 h p.i.

a) Number of autophagosomes

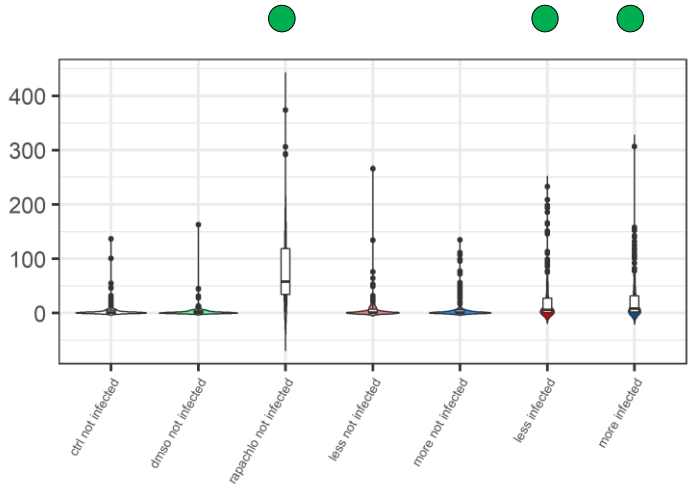


b) Area of autophagosomes

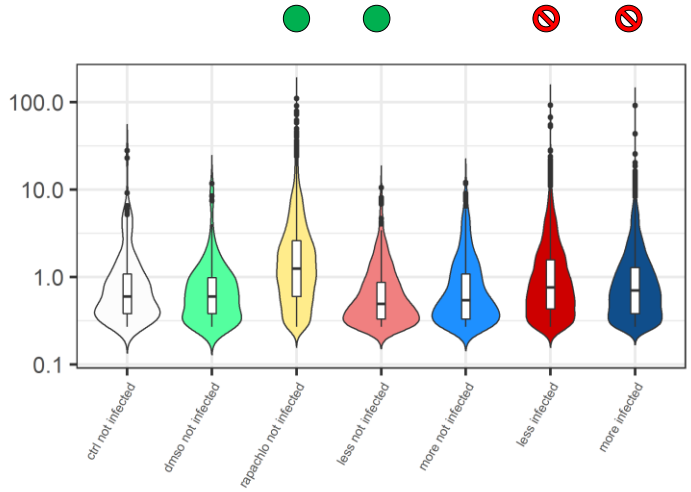


| Conditional model | Estimate | SE | p-value |
|---|---|---|---|
| (Intercept) | 1.7288 | 0.3423 | 0 |
| groupdmso not infected | -0.0058 | 0.4427 | 0.9896 |
| grouprapachlo not infected | 2.4329 | 0.3898 | 0 |
| groupless not infected | 0.1886 | 0.3587 | 0.599 |
| groupmore not infected | 0.5518 | 0.3548 | 0.1199 |
| groupless infected | 1.1944 | 0.3578 | 8e-04 |
| groupmore infected | 1.4598 | 0.354 | 0 |

| Zero-inflation model | Estimate | SE | p-value |
|---|---|---|---|
| (Intercept) | -0.7778 | 0.3791 | 0.0402 |
| groupdmso not infected | 0.1669 | 0.5813 | 0.774 |
| grouprapachlo not infected | -2.4891 | 0.6899 | 3e-04 |
| groupless not infected | 0.303 | 0.4541 | 0.5046 |
| groupmore not infected | 0.22 | 0.4574 | 0.6305 |
| groupless infected | -0.8096 | 0.4637 | 0.0808 |
| groupmore infected | -1.2812 | 0.4676 | 0.0061 |

| Contrast | estimate | SE | p.value |
|---|---|---|---|
| ctrl not infected-dmso not infected | 0.0058 | 0.4427 | 0.9896 |
| ctrl not infected-rapachlo not infected | -2.4329 | 0.3898 | 0 |
| ctrl not infected-less not infected | -0.1886 | 0.3587 | 0.6601 |
| ctrl not infected-more not infected | -0.5518 | 0.3548 | 0.1758 |
| ctrl not infected-less infected | -1.1944 | 0.3578 | 0.0017 |
| ctrl not infected-more infected | -1.4598 | 0.354 | 1e-04 |
| dmso not infected-rapachlo not infected | -2.4387 | 0.427 | 0 |
| dmso not infected-less not infected | -0.1944 | 0.3979 | 0.6601 |
| dmso not infected-more not infected | -0.5575 | 0.3965 | 0.2172 |
| dmso not infected-less infected | -1.2001 | 0.3972 | 0.0045 |
| dmso not infected-more infected | -1.4655 | 0.3958 | 5e-04 |
| rapachlo not infected-less not infected | 2.2443 | 0.3386 | 0 |
| rapachlo not infected-more not infected | 1.8811 | 0.3325 | 0 |
| rapachlo not infected-less infected | 1.2385 | 0.3377 | 5e-04 |
| rapachlo not infected-more infected | 0.9731 | 0.3316 | 0.0054 |
| less not infected-more not infected | -0.3632 | 0.2993 | 0.2854 |
| less infected-more infected | -0.2654 | 0.2973 | 0.442 |
| less not infected-less infected | -1.0058 | 0.0313 | 0 |
| more not infected-more infected | -0.908 | 0.0295 | 0 |

| Par | Value | Std.Error | p.value |
|---|---|---|---|
| (Intercept) | -0.2615 | 0.1042 | 0.0121 |
| groupdmso not infected | -0.0602 | 0.1576 | 0.7041 |
| grouprapachlo not infected | 0.5016 | 0.1147 | 1e-04 |
| groupless not infected | -0.3127 | 0.1195 | 0.0089 |
| groupmore not infected | -0.1227 | 0.1182 | 0.2992 |
| groupless infected | 0.1492 | 0.1115 | 0.1809 |
| groupmore infected | -0.0145 | 0.1104 | 0.8952 |

| Contrast | estimate | SE | p.value |
|---|---|---|---|
| ctrl not infected-dmso not infected | 0.0602 | 0.1576 | 0.776 |
| ctrl not infected-rapachlo not infected | -0.5016 | 0.1147 | 2e-04 |
| ctrl not infected-less not infected | 0.3127 | 0.1195 | 0.0211 |
| ctrl not infected-more not infected | 0.1227 | 0.1182 | 0.379 |
| ctrl not infected-less infected | -0.1492 | 0.1115 | 0.2455 |
| ctrl not infected-more infected | 0.0145 | 0.1104 | 0.8952 |
| dmso not infected-rapachlo not infected | -0.5618 | 0.1382 | 5e-04 |
| dmso not infected-less not infected | 0.2524 | 0.1416 | 0.1286 |
| dmso not infected-more not infected | 0.0625 | 0.1408 | 0.776 |
| dmso not infected-less infected | -0.2094 | 0.135 | 0.1865 |
| dmso not infected-more infected | -0.0457 | 0.1342 | 0.776 |
| rapachlo not infected-less not infected | 0.8143 | 0.0907 | 0 |
| rapachlo not infected-more not infected | 0.6243 | 0.0881 | 0 |
| rapachlo not infected-less infected | 0.3524 | 0.0798 | 2e-04 |
| rapachlo not infected-more infected | 0.5161 | 0.0772 | 0 |
| less not infected-more not infected | -0.1899 | 0.0912 | 0.0645 |
| less infected-more infected | 0.1638 | 0.0669 | 0.0303 |
| less not infected-less infected | -0.4619 | 0.0519 | 0 |
| more not infected-more infected | -0.1082 | 0.0487 | 0.0501 |

Autophagosomes observed

Autophagosomes not observed (blocked)

## Grouping: Virulence (absolute)

### M2 – 24 h p.i.

a) Number of autophagosomes

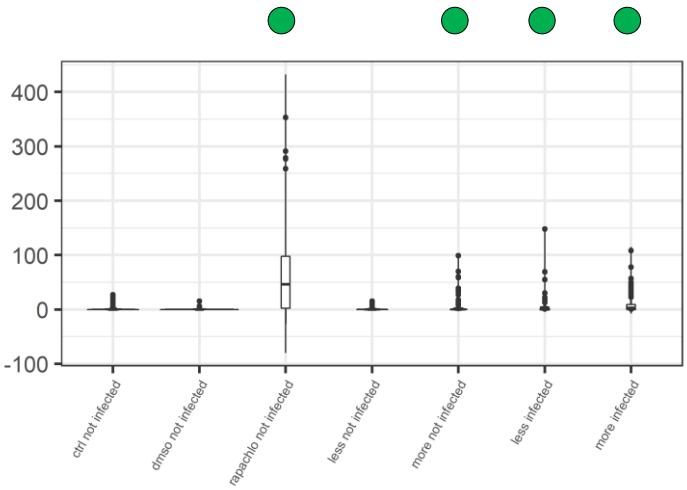


b) Area of autophagosomes

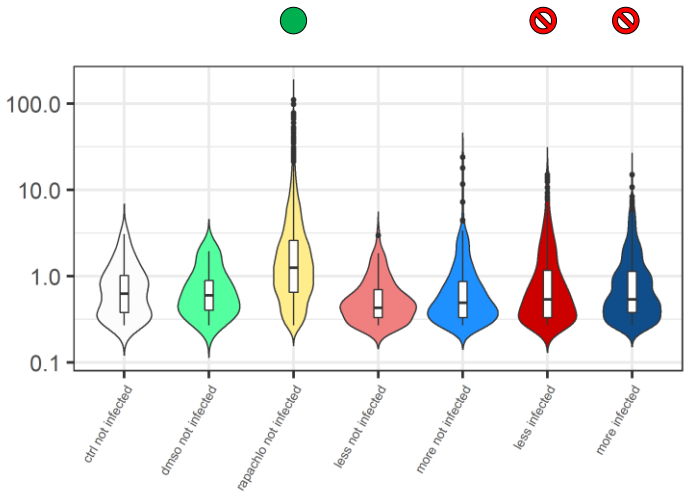


| Conditional model | Estimate | SE | p-value |
|---|---|---|---|
| (Intercept) | 0.9112 | 0.3425 | 0.0078 |
| groupdmso not infected | -0.4118 | 0.4779 | 0.3889 |
| grouprapachlo not infected | 2.9391 | 0.3895 | 0 |
| groupless not infected | -0.3171 | 0.3708 | 0.3924 |
| groupmore not infected | 0.9399 | 0.3647 | 0.01 |
| groupless infected | 0.7887 | 0.3652 | 0.0308 |
| groupmore infected | 1.2889 | 0.3634 | 4e-04 |

| Zero-inflation model | Estimate | SE | p-value |
|---|---|---|---|
| (Intercept) | 0.1093 | 0.4008 | 0.7851 |
| groupdmso not infected | 0.663 | 0.5865 | 0.2583 |
| grouprapachlo not infected | -2.1417 | 0.579 | 2e-04 |
| groupless not infected | -0.2317 | 0.4615 | 0.6157 |
| groupmore not infected | -0.2147 | 0.457 | 0.6385 |
| groupless infected | -0.8417 | 0.4466 | 0.0595 |
| groupmore infected | -1.4343 | 0.4574 | 0.0017 |

| Contrast | estimate | SE | p.value |
|---|---|---|---|
| ctrl not infected-dmso not infected | 0.4118 | 0.4779 | 0.4145 |
| ctrl not infected-rapachlo not infected | -2.9391 | 0.3895 | 0 |
| ctrl not infected-less not infected | 0.3171 | 0.3708 | 0.4145 |
| ctrl not infected-more not infected | -0.9399 | 0.3647 | 0.0137 |
| ctrl not infected-less infected | -0.7887 | 0.3652 | 0.0393 |
| ctrl not infected-more infected | -1.2889 | 0.3634 | 7e-04 |
| dmso not infected-rapachlo not infected | -3.3509 | 0.4292 | 0 |
| dmso not infected-less not infected | -0.0946 | 0.437 | 0.8286 |
| dmso not infected-more not infected | -1.3517 | 0.4287 | 0.0026 |
| dmso not infected-less infected | -1.2005 | 0.4322 | 0.0082 |
| dmso not infected-more infected | -1.7007 | 0.4276 | 1e-04 |
| rapachlo not infected-less not infected | 3.2562 | 0.3344 | 0 |
| rapachlo not infected-more not infected | 1.9992 | 0.3229 | 0 |
| rapachlo not infected-less infected | 2.1504 | 0.3281 | 0 |
| rapachlo not infected-more infected | 1.6502 | 0.3213 | 0 |
| less not infected-more not infected | -1.2571 | 0.3042 | 1e-04 |
| less infected-more infected | -0.5002 | 0.2954 | 0.1078 |
| less not infected-less infected | -1.1058 | 0.0778 | 0 |
| more not infected-more infected | -0.349 | 0.046 | 0 |

| Par | Value | Std.Error | p.value |
|---|---|---|---|
| (Intercept) | -0.5253 | 0.1391 | 2e-04 |
| groupdmso not infected | -0.0026 | 0.2525 | 0.9918 |
| grouprapachlo not infected | 0.7491 | 0.1526 | 0 |
| groupless not infected | -0.2982 | 0.1804 | 0.0983 |
| groupmore not infected | -0.0932 | 0.1602 | 0.5606 |
| groupless infected | -0.0376 | 0.1574 | 0.8113 |
| groupmore infected | 0.0296 | 0.1509 | 0.8447 |

| Contrast | estimate | SE | p.value |
|---|---|---|---|
| ctrl not infected-dmso not infected | 0.0026 | 0.2525 | 0.9918 |
| ctrl not infected-rapachlo not infected | -0.7491 | 0.1526 | 0 |
| ctrl not infected-less not infected | 0.2982 | 0.1804 | 0.2084 |
| ctrl not infected-more not infected | 0.0932 | 0.1602 | 0.8193 |
| ctrl not infected-less infected | 0.0376 | 0.1574 | 0.9322 |
| ctrl not infected-more infected | -0.0296 | 0.1509 | 0.9322 |
| dmso not infected-rapachlo not infected | -0.7517 | 0.2193 | 0.0019 |
| dmso not infected-less not infected | 0.2956 | 0.24 | 0.3769 |
| dmso not infected-more not infected | 0.0906 | 0.2252 | 0.9322 |
| dmso not infected-less infected | 0.035 | 0.2233 | 0.9322 |
| dmso not infected-more infected | -0.0322 | 0.2187 | 0.9322 |
| rapachlo not infected-less not infected | 1.0473 | 0.1309 | 0 |
| rapachlo not infected-more not infected | 0.8424 | 0.1013 | 0 |
| rapachlo not infected-less infected | 0.7867 | 0.0969 | 0 |
| rapachlo not infected-more infected | 0.7196 | 0.0859 | 0 |
| less not infected-more not infected | -0.205 | 0.1397 | 0.2703 |
| less infected-more infected | -0.0671 | 0.0942 | 0.7538 |
| less not infected-less infected | -0.2606 | 0.1158 | 0.0664 |
| more not infected-more infected | -0.1228 | 0.0743 | 0.2084 |

Autophagosomes observed

Autophagosomes not observed (blocked)

## Grouping: Virulence (relative)

### M1 – 24 h p.i.

a) Number of autophagosomes

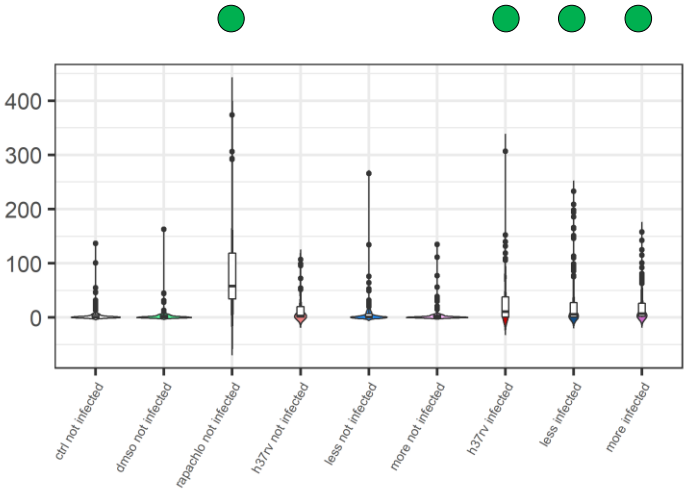


b) Area of autophagosomes

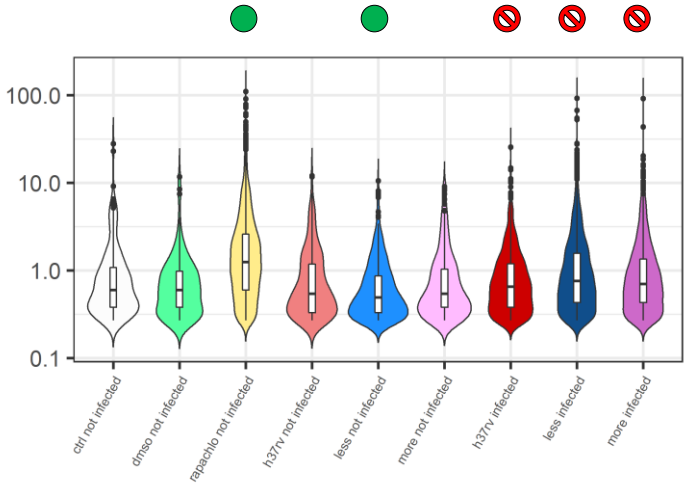


| Conditional model | Estimate | SE | p-value |
|---|---|---|---|
| (Intercept) | 1.7265 | 0.3436 | 0 |
| groupdmso not infected | -0.0113 | 0.4328 | 0.9791 |
| grouprapachlo not infected | 2.431 | 0.381 | 0 |
| grouph37rv not infected | 0.8953 | 0.4389 | 0.0414 |
| groupless not infected | 0.1788 | 0.3507 | 0.6101 |
| groupmore not infected | 0.3672 | 0.375 | 0.3275 |
| grouph37rv infected | 1.8041 | 0.4376 | 0 |
| groupless infected | 1.1846 | 0.3498 | 7e-04 |
| groupmore infected | 1.274 | 0.3735 | 6e-04 |

| Zero-inflation model | Estimate | SE | p-value |
|---|---|---|---|
| (Intercept) | -0.7583 | 0.3682 | 0.0394 |
| groupdmso not infected | 0.1736 | 0.5571 | 0.7554 |
| grouprapachlo not infected | -2.49 | 0.6738 | 2e-04 |
| grouph37rv not infected | -0.4497 | 0.6209 | 0.4689 |
| groupless not infected | 0.2999 | 0.4349 | 0.4905 |
| groupmore not infected | 0.4204 | 0.4643 | 0.3652 |
| grouph37rv infected | -1.1795 | 0.5786 | 0.0415 |
| groupless infected | -0.807 | 0.4448 | 0.0696 |
| groupmore infected | -1.3388 | 0.4926 | 0.0066 |

| Contrast | estimate | SE | p.value |
|---|---|---|---|
| ctrl not infected-dmso not infected | 0.0113 | 0.4328 | 0.9791 |
| ctrl not infected-rapachlo not infected | -2.431 | 0.381 | 0 |
| ctrl not infected-h37rv not infected | -0.8953 | 0.4389 | 0.0735 |
| ctrl not infected-less not infected | -0.1788 | 0.3507 | 0.6698 |
| ctrl not infected-more not infected | -0.3672 | 0.375 | 0.4097 |
| ctrl not infected-h37rv infected | -1.8041 | 0.4376 | 2e-04 |
| ctrl not infected-less infected | -1.1846 | 0.3498 | 0.0017 |
| ctrl not infected-more infected | -1.274 | 0.3735 | 0.0017 |
| dmso not infected-rapachlo not infected | -2.4423 | 0.4173 | 0 |
| dmso not infected-h37rv not infected | -0.9066 | 0.473 | 0.0926 |
| dmso not infected-less not infected | -0.1901 | 0.389 | 0.6698 |
| dmso not infected-more not infected | -0.3785 | 0.412 | 0.4302 |
| dmso not infected-h37rv infected | -1.8154 | 0.4718 | 4e-04 |
| dmso not infected-less infected | -1.196 | 0.3882 | 0.004 |
| dmso not infected-more infected | -1.2853 | 0.4106 | 0.0036 |
| rapachlo not infected-h37rv not infected | 1.5357 | 0.4201 | 7e-04 |
| rapachlo not infected-less not infected | 2.2522 | 0.331 | 0 |
| rapachlo not infected-more not infected | 2.0638 | 0.3554 | 0 |
| rapachlo not infected-h37rv infected | 0.6269 | 0.4187 | 0.1924 |
| rapachlo not infected-less infected | 1.2463 | 0.33 | 5e-04 |
| rapachlo not infected-more infected | 1.157 | 0.3538 | 0.0024 |
| h37rv not infected-less not infected | 0.7165 | 0.3998 | 0.116 |
| h37rv not infected-more not infected | 0.5281 | 0.4103 | 0.2587 |
| less not infected-more not infected | -0.1884 | 0.3238 | 0.6472 |
| h37rv infected-less infected | 0.6194 | 0.3976 | 0.1793 |
| h37rv infected-more infected | 0.5301 | 0.4074 | 0.2587 |
| less infected-more infected | -0.0893 | 0.3211 | 0.8078 |
| h37rv not infected-h37rv infected | -0.9087 | 0.0416 | 0 |
| less not infected-less infected | -1.0058 | 0.0313 | 0 |
| more not infected-more infected | -0.9068 | 0.0419 | 0 |

| Par | Value | Std.Error | p.value |
|---|---|---|---|
| (Intercept) | -0.2603 | 0.1046 | 0.0129 |
| groupdmso not infected | -0.06 | 0.159 | 0.7074 |
| grouprapachlo not infected | 0.5009 | 0.116 | 1e-04 |
| grouph37rv not infected | -0.1042 | 0.1389 | 0.453 |
| groupless not infected | -0.3207 | 0.1209 | 0.008 |
| groupmore not infected | -0.1729 | 0.134 | 0.1968 |
| grouph37rv infected | -0.0696 | 0.1256 | 0.5794 |
| groupless infected | 0.1404 | 0.1131 | 0.2147 |
| groupmore infected | 0.0302 | 0.1192 | 0.7997 |

| Contrast | estimate | SE | p.value |
|---|---|---|---|
| ctrl not infected-dmso not infected | 0.06 | 0.159 | 0.786 |
| ctrl not infected-rapachlo not infected | -0.5009 | 0.116 | 3e-04 |
| ctrl not infected-h37rv not infected | 0.1042 | 0.1389 | 0.6387 |
| ctrl not infected-less not infected | 0.3207 | 0.1209 | 0.0218 |
| ctrl not infected-more not infected | 0.1729 | 0.134 | 0.3293 |
| ctrl not infected-h37rv infected | 0.0696 | 0.1256 | 0.6919 |
| ctrl not infected-less infected | -0.1404 | 0.1131 | 0.339 |
| ctrl not infected-more infected | -0.0302 | 0.1192 | 0.8272 |
| dmso not infected-rapachlo not infected | -0.5609 | 0.1394 | 7e-04 |
| dmso not infected-h37rv not infected | 0.0442 | 0.1587 | 0.8272 |
| dmso not infected-less not infected | 0.2607 | 0.143 | 0.1603 |
| dmso not infected-more not infected | 0.1129 | 0.1544 | 0.6387 |
| dmso not infected-h37rv infected | 0.0096 | 0.1472 | 0.9484 |
| dmso not infected-less infected | -0.2004 | 0.1365 | 0.2977 |
| dmso not infected-more infected | -0.0903 | 0.1417 | 0.6876 |
| rapachlo not infected-h37rv not infected | 0.6051 | 0.1137 | 0 |
| rapachlo not infected-less not infected | 0.8216 | 0.0921 | 0 |
| rapachlo not infected-more not infected | 0.6738 | 0.1081 | 0 |
| rapachlo not infected-h37rv infected | 0.5705 | 0.097 | 0 |
| rapachlo not infected-less infected | 0.3605 | 0.0814 | 2e-04 |
| rapachlo not infected-more infected | 0.4706 | 0.0892 | 0 |
| h37rv not infected-less not infected | 0.2165 | 0.1117 | 0.1215 |
| h37rv not infected-more not infected | 0.0687 | 0.1309 | 0.6919 |
| less not infected-more not infected | -0.1478 | 0.1136 | 0.3293 |
| h37rv infected-less infected | -0.21 | 0.0825 | 0.0273 |
| h37rv infected-more infected | -0.0999 | 0.0999 | 0.4763 |
| less infected-more infected | 0.1101 | 0.0855 | 0.3293 |
| h37rv not infected-h37rv infected | -0.0346 | 0.0654 | 0.6919 |
| less not infected-less infected | -0.4611 | 0.0519 | 0 |
| more not infected-more infected | -0.2032 | 0.073 | 0.0163 |

Autophagosomes observed

Autophagosomes not observed (blocked)

## Grouping: Virulence (relative)

### M2 – 24 h p.i.

a) Number of autophagosomes

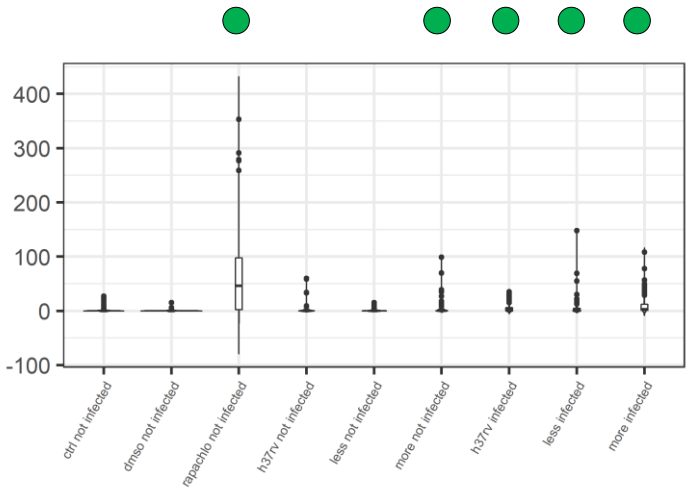


b) Area of autophagosomes

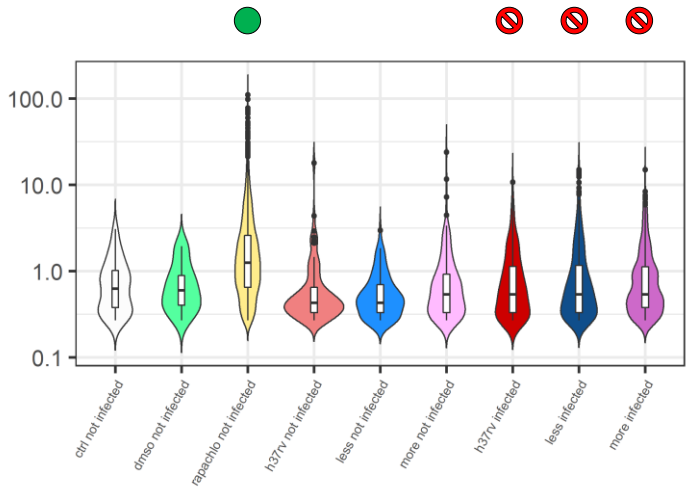


| Conditional model | Estimate | SE | p-value |
|---|---|---|---|
| (Intercept) | 0.9214 | 0.3369 | 0.0062 |
| groupdmso not infected | -0.4132 | 0.474 | 0.3833 |
| grouprapachlo not infected | 2.9321 | 0.386 | 0 |
| grouph37rv not infected | 0.8209 | 0.4548 | 0.0711 |
| groupless not infected | -0.3188 | 0.3676 | 0.3857 |
| groupmore not infected | 1.0011 | 0.3869 | 0.0097 |
| grouph37rv infected | 0.9582 | 0.4523 | 0.0342 |
| groupless infected | 0.7869 | 0.3619 | 0.0297 |
| groupmore infected | 1.4426 | 0.3847 | 2e-04 |

| Zero-inflation model | Estimate | SE | p-value |
|---|---|---|---|
| (Intercept) | 0.1127 | 0.4009 | 0.7786 |
| groupdmso not infected | 0.6644 | 0.586 | 0.2569 |
| grouprapachlo not infected | -2.1435 | 0.5792 | 2e-04 |
| grouph37rv not infected | -0.1159 | 0.5828 | 0.8423 |
| groupless not infected | -0.2352 | 0.4612 | 0.61 |
| groupmore not infected | -0.2675 | 0.4911 | 0.586 |
| grouph37rv infected | -1.4435 | 0.5945 | 0.0152 |
| groupless infected | -0.8454 | 0.4464 | 0.0582 |
| groupmore infected | -1.4417 | 0.4866 | 0.003 |

| Contrast | estimate | SE | p.value |
|---|---|---|---|
| ctrl not infected-dmso not infected | 0.4132 | 0.474 | 0.4289 |
| ctrl not infected-rapachlo not infected | -2.9321 | 0.386 | 0 |
| ctrl not infected-h37rv not infected | -0.8209 | 0.4548 | 0.0931 |
| ctrl not infected-less not infected | 0.3188 | 0.3676 | 0.4289 |
| ctrl not infected-more not infected | -1.0011 | 0.3869 | 0.0163 |
| ctrl not infected-h37rv infected | -0.9582 | 0.4523 | 0.0492 |
| ctrl not infected-less infected | -0.7869 | 0.3619 | 0.0449 |
| ctrl not infected-more infected | -1.4426 | 0.3847 | 4e-04 |
| dmso not infected-rapachlo not infected | -3.3453 | 0.4261 | 0 |
| dmso not infected-h37rv not infected | -1.2341 | 0.5049 | 0.0232 |
| dmso not infected-less not infected | -0.0944 | 0.4336 | 0.8277 |
| dmso not infected-more not infected | -1.4144 | 0.4486 | 0.0036 |
| dmso not infected-h37rv infected | -1.3714 | 0.5027 | 0.0114 |
| dmso not infected-less infected | -1.2001 | 0.4288 | 0.0101 |
| dmso not infected-more infected | -1.8559 | 0.4468 | 1e-04 |
| rapachlo not infected-h37rv not infected | 2.1112 | 0.4199 | 0 |
| rapachlo not infected-less not infected | 3.2509 | 0.3314 | 0 |
| rapachlo not infected-more not infected | 1.9309 | 0.3501 | 0 |
| rapachlo not infected-h37rv infected | 1.9739 | 0.4171 | 0 |
| rapachlo not infected-less infected | 2.1452 | 0.325 | 0 |
| rapachlo not infected-more infected | 1.4894 | 0.3477 | 1e-04 |
| h37rv not infected-less not infected | 1.1397 | 0.4087 | 0.0101 |
| h37rv not infected-more not infected | -0.1802 | 0.4148 | 0.6922 |
| less not infected-more not infected | -1.32 | 0.3313 | 2e-04 |
| h37rv infected-less infected | 0.1713 | 0.4006 | 0.6922 |
| h37rv infected-more infected | -0.4845 | 0.4099 | 0.285 |
| less infected-more infected | -0.6557 | 0.3223 | 0.0575 |
| h37rv not infected-h37rv infected | -0.1373 | 0.0824 | 0.1203 |
| less not infected-less infected | -1.1057 | 0.0778 | 0 |
| more not infected-more infected | -0.4415 | 0.0559 | 0 |

| Par | Value | Std.Error | p.value |
|---|---|---|---|
| (Intercept) | -0.5258 | 0.1404 | 2e-04 |
| groupdmso not infected | -0.0014 | 0.2542 | 0.9956 |
| grouprapachlo not infected | 0.748 | 0.1546 | 0 |
| grouph37rv not infected | -0.2846 | 0.1997 | 0.1543 |
| groupless not infected | -0.2985 | 0.1819 | 0.1009 |
| groupmore not infected | -0.0061 | 0.1712 | 0.9716 |
| grouph37rv infected | 0.0521 | 0.1769 | 0.7686 |
| groupless infected | -0.0394 | 0.1592 | 0.8048 |
| groupmore infected | 0.0283 | 0.1579 | 0.8578 |

| Contrast | estimate | SE | p.value |
|---|---|---|---|
| ctrl not infected-dmso not infected | 0.0014 | 0.2542 | 0.9956 |
| ctrl not infected-rapachlo not infected | -0.748 | 0.1546 | 0 |
| ctrl not infected-h37rv not infected | 0.2846 | 0.1997 | 0.3307 |
| ctrl not infected-less not infected | 0.2985 | 0.1819 | 0.2459 |
| ctrl not infected-more not infected | 0.0061 | 0.1712 | 0.9956 |
| ctrl not infected-h37rv infected | -0.0521 | 0.1769 | 0.9956 |
| ctrl not infected-less infected | 0.0394 | 0.1592 | 0.9956 |
| ctrl not infected-more infected | -0.0283 | 0.1579 | 0.9956 |
| dmso not infected-rapachlo not infected | -0.7494 | 0.221 | 0.0026 |
| dmso not infected-h37rv not infected | 0.2832 | 0.2552 | 0.5009 |
| dmso not infected-less not infected | 0.2971 | 0.2415 | 0.4371 |
| dmso not infected-more not infected | 0.0047 | 0.2335 | 0.9956 |
| dmso not infected-h37rv infected | -0.0535 | 0.2377 | 0.9956 |
| dmso not infected-less infected | 0.038 | 0.2249 | 0.9956 |
| dmso not infected-more infected | -0.0297 | 0.2239 | 0.9956 |
| rapachlo not infected-h37rv not infected | 1.0325 | 0.1561 | 0 |
| rapachlo not infected-less not infected | 1.0465 | 0.1326 | 0 |
| rapachlo not infected-more not infected | 0.7541 | 0.1174 | 0 |
| rapachlo not infected-h37rv infected | 0.6959 | 0.1256 | 0 |
| rapachlo not infected-less infected | 0.7873 | 0.0992 | 0 |
| rapachlo not infected-more infected | 0.7197 | 0.0971 | 0 |
| h37rv not infected-less not infected | 0.014 | 0.1832 | 0.9956 |
| h37rv not infected-more not infected | -0.2785 | 0.1725 | 0.2459 |
| less not infected-more not infected | -0.2924 | 0.1516 | 0.1465 |
| h37rv infected-less infected | 0.0914 | 0.1312 | 0.8579 |
| h37rv infected-more infected | 0.0238 | 0.1296 | 0.9956 |
| less infected-more infected | -0.0677 | 0.1042 | 0.8604 |
| h37rv not infected-h37rv infected | -0.3366 | 0.1391 | 0.0519 |
| less not infected-less infected | -0.2592 | 0.116 | 0.0764 |
| more not infected-more infected | -0.0344 | 0.0883 | 0.9956 |

Autophagosomes observed

Autophagosomes not observed (blocked)

# Apoptosis

| Apoptosis/necrosis kit | |
|---|---|
| **Wells/sample** | 2 |
| **Acquisition positions/well** | 2 |
| **Channels** | Cytocalcein, dsRed/7-AAD, apopxin |
| **Z-stacks** | 1.48 µm x 4 |

| | | NOT infected N of cells | Infected N of cells | TOT NOT inf | TOT Inf | TOT |
|---|---|---|---|---|---|---|
| M1 | Afri | 205 | 136 | | | |
| | Bei | 164 | 163 | | | |
| | H37Ra | 94 | 82 | 689 | 451 | 1140 |
| | H37Rv | 88 | 70 | | | |
| | CTRL | 138 | *na* | | | |
| M2 | Afri | 180 | 133 | | | |
| | Bei | 188 | 179 | | | |
| | H37Ra | 107 | 81 | 725 | 475 | 1200 |
| | H37Rv | 86 | 82 | | | |
| | CTRL | 164 | *na* | | | |
| | TOT | 1414 | 926 | | | |
| | | 2340 | | | | |

*Acquisition:* obj. **63x, oil NA 1.40**
**z-stacks: 1.48 µm x 4 stacks**
Res. **16-bit** format: **1024x1024**
Laser 405 (for CytoCalcein Violet) = **6%**; gain: **625**, offset: 0% **pinhole: 95.60**
Laser 488 (for Apopxin) = **10% (Argon power: 20%); gain: 670**, offset: 0% **pinhole: 330**
Laser 561 (for dsRed and 7-AAD) = **8%; gain: 700**, offset: 0% **pinhole: 95.60; Emission window: 570-662**
Confocal: AP **24** FD **6 O** INT **0** FIM **100%**

**CytoCalcein (Ex/Em 405/450)**
**Apopxin (Ex/Em 490/525)**
**dsRed (Ex/Em 584-557)**
**7-AAD (Ex/Em 546/657)**

*Analysis:* 24 h p.i.; percentages of apoptotic/necrotic/live cells

## **Automated gating** of apopxin-positive (apoptosis) and cytocalcein-positive (live) cells using **flowClust**[1]

Rule for identifying outliers: 83% quantile
Number of outliers: 232 (9.39%)

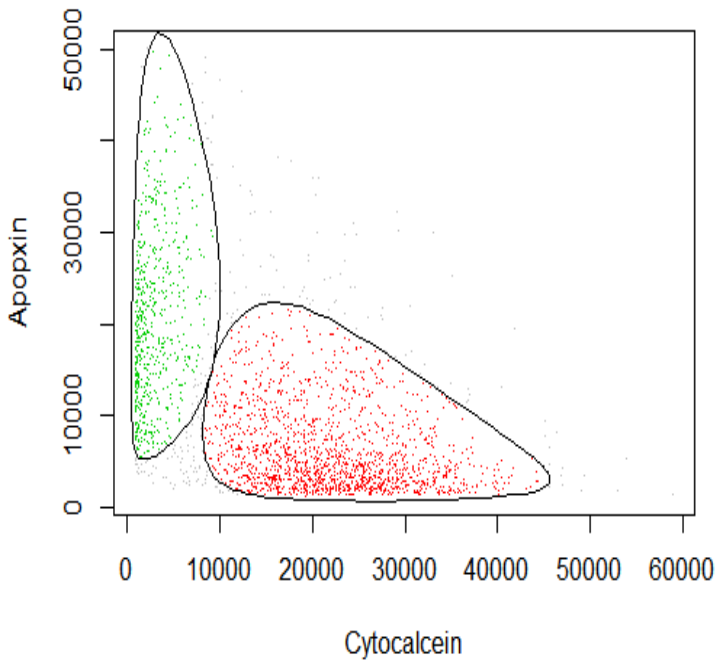


[1] Lo K, Hahne F, Brinkman RR, Gottardo R. flowClust: a Bioconductor package for automated gating of flow cytometry data. BMC Bioinformatics. 2009 May 14;10:145. doi: 10.1186/1471-2105-10-145. PMID: 19442304; PMCID: PMC2701419.

**Grouping: Geo-host adaptation**

**M1 – 24 h p.i.**

a) Percentage of live/apoptotic cells

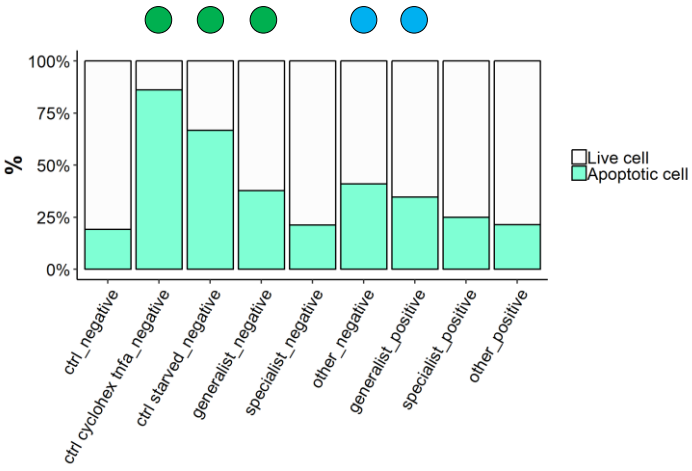


b) Percentage of live/apoptotic cells per mycobacterial burden

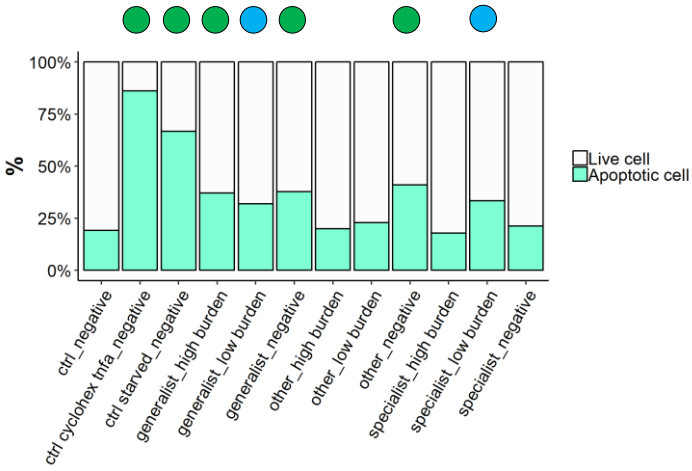


| Par | Estimate | se | OR | pvalue |
|---|---|---|---|---|
| (Intercept) | -1.2682 | 0.3791 | 0.2813 | 8e-04 |
| group_Mycctrl cyclohex tnfa_negative | 2.8044 | 0.6405 | 16.5175 | 0 |
| group_Mycctrl starved_negative | 1.6833 | 0.5879 | 5.3834 | 0.0042 |
| group_Mycgeneralist_negative | 0.9441 | 0.3532 | 2.5704 | 0.0075 |
| group_Mycspecialist_negative | 0.0385 | 0.3808 | 1.0392 | 0.9195 |
| group_Mycother_negative | 0.9317 | 0.4243 | 2.5387 | 0.0281 |
| group_Mycgeneralist_positive | 0.6259 | 0.3592 | 1.8698 | 0.0814 |
| group_Mycspecialist_positive | 0.1463 | 0.3962 | 1.1576 | 0.7119 |
| group_Mycother_positive | -0.0624 | 0.4652 | 0.9395 | 0.8933 |

| Contrast | estimate | SE | p.value |
|---|---|---|---|
| ctrl_negative-ctrl cyclohex tnfa_negative | -2.8044 | 0.6405 | 1e-04 |
| ctrl_negative-ctrl starved_negative | -1.6833 | 0.5879 | 0.0117 |
| ctrl_negative-generalist_negative | -0.9441 | 0.3532 | 0.0174 |
| ctrl_negative-specialist_negative | -0.0385 | 0.3808 | 0.9513 |
| ctrl_negative-other_negative | -0.9317 | 0.4243 | 0.0527 |
| ctrl_negative-generalist_positive | -0.6259 | 0.3592 | 0.1357 |
| ctrl_negative-specialist_positive | -0.1463 | 0.3962 | 0.791 |
| ctrl_negative-other_positive | 0.0624 | 0.4652 | 0.9513 |
| ctrl cyclohex tnfa_negative-ctrl starved_negative | 1.1211 | 0.74 | 0.1883 |
| ctrl cyclohex tnfa_negative-generalist_negative | 1.8604 | 0.5942 | 0.0086 |
| ctrl cyclohex tnfa_negative-specialist_negative | 2.766 | 0.6083 | 1e-04 |
| ctrl cyclohex tnfa_negative-other_negative | 1.8727 | 0.6364 | 0.0108 |
| ctrl cyclohex tnfa_negative-generalist_positive | 2.1786 | 0.5921 | 0.0014 |
| ctrl cyclohex tnfa_negative-specialist_positive | 2.6581 | 0.616 | 1e-04 |
| ctrl cyclohex tnfa_negative-other_positive | 2.8668 | 0.6622 | 1e-04 |
| ctrl starved_negative-generalist_negative | 0.7393 | 0.5371 | 0.2201 |
| ctrl starved_negative-specialist_negative | 1.6449 | 0.5527 | 0.0108 |
| ctrl starved_negative-other_negative | 0.7516 | 0.5835 | 0.2471 |
| ctrl starved_negative-generalist_positive | 1.0575 | 0.5348 | 0.0847 |
| ctrl starved_negative-specialist_positive | 1.537 | 0.5612 | 0.0154 |
| ctrl starved_negative-other_positive | 1.7457 | 0.6115 | 0.0117 |
| generalist_negative-specialist_negative | 0.9056 | 0.293 | 0.0086 |
| generalist_negative-other_negative | 0.0124 | 0.3476 | 0.9716 |
| specialist_negative-other_negative | -0.8932 | 0.3754 | 0.0347 |
| generalist_positive-specialist_positive | 0.4795 | 0.3182 | 0.1883 |
| generalist_positive-other_positive | 0.6883 | 0.4008 | 0.1357 |
| specialist_positive-other_positive | 0.2087 | 0.4345 | 0.7571 |
| generalist_negative-generalist_positive | 0.3182 | 0.2155 | 0.1906 |
| specialist_negative-specialist_positive | -0.1079 | 0.2834 | 0.791 |
| other_negative-other_positive | 0.9941 | 0.3758 | 0.0175 |

| Par | Estimate | se | OR | pvalue |
|---|---|---|---|---|
| (Intercept) | -1.2669 | 0.3822 | 0.2817 | 9e-04 |
| group_Myc3ctrl cyclohex tnfa_negative | 2.8078 | 0.6485 | 16.5731 | 0 |
| group_Myc3ctrl starved_negative | 1.6874 | 0.5967 | 5.4052 | 0.0047 |
| group_Myc3generalist_high burden | 0.7716 | 0.3911 | 2.1632 | 0.0485 |
| group_Myc3generalist_low burden | 0.4496 | 0.4057 | 1.5676 | 0.2679 |
| group_Myc3generalist_negative | 0.946 | 0.3596 | 2.5755 | 0.0085 |
| group_Myc3other_high burden | -0.1119 | 0.5629 | 0.8941 | 0.8424 |
| group_Myc3other_low burden | -0.0179 | 0.5552 | 0.9823 | 0.9743 |
| group_Myc3other_negative | 0.9275 | 0.4321 | 2.5282 | 0.0318 |
| group_Myc3specialist_high burden | -0.3219 | 0.4755 | 0.7248 | 0.4984 |
| group_Myc3specialist_low burden | 0.5749 | 0.4474 | 1.777 | 0.1988 |
| group_Myc3specialist_negative | 0.029 | 0.3876 | 1.0294 | 0.9403 |

OBSERVATIONS

In M1 macrophages, bystander non-infected cells of generalist and other strains showed increased apoptosis (40%). Despite not statistically significant, also macrophages infected with generalist strains showed a similar increase in the percentage of apoptosis. Stratification of the data by mycobacterial burden showed higher apoptotic levels in bystander non-infected cells or in cells infected with lower mycobacterial load. In M2 macrophages, only bystander non-infected cells of other strains showed a slight, statistically not significant increase in apoptosis (30%).

Apoptosis > not infected control

Increased apoptosis observed, not statistically significant

**Grouping: Geo-host adaptation**

**M2 – 24 h p.i.**

a) Percentage of live/apoptotic cells

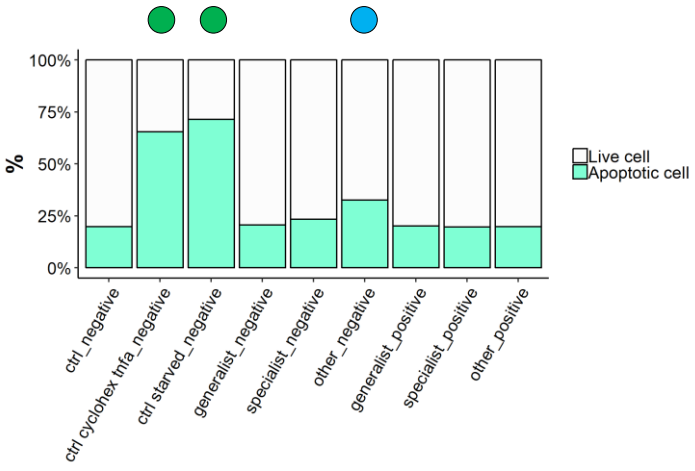


b) Percentage of live/apoptotic cells per mycobacterial burden

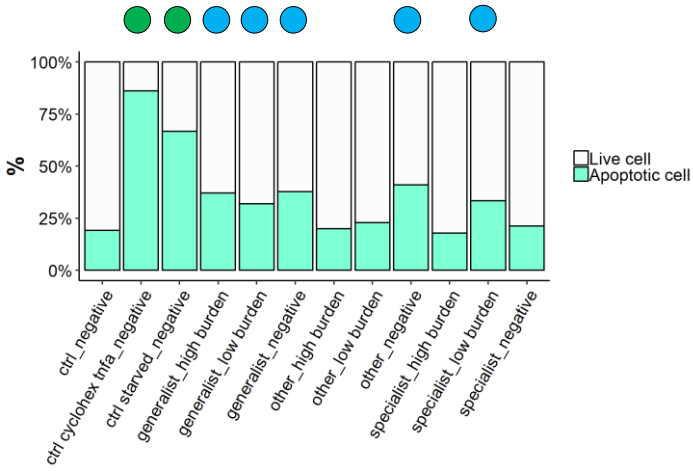


| Par | Estimate | se | OR | pvalue |
|---|---|---|---|---|
| (Intercept) | -1.4453 | 0.4587 | 0.2357 | 0.0016 |
| group_Mycctrl cyclohex tnfa_negative | 1.6424 | 0.6211 | 5.1677 | 0.0082 |
| group_Mycctrl starved_negative | 1.9314 | 0.6735 | 6.8991 | 0.0041 |
| group_Mycgeneralist_negative | 0.1847 | 0.376 | 1.2029 | 0.6233 |
| group_Mycspecialist_negative | 0.3807 | 0.403 | 1.4634 | 0.3448 |
| group_Mycother_negative | 0.7893 | 0.4487 | 2.2018 | 0.0786 |
| group_Mycgeneralist_positive | 0.0858 | 0.38 | 1.0896 | 0.8213 |
| group_Mycspecialist_positive | -0.0294 | 0.4383 | 0.971 | 0.9465 |
| group_Mycother_positive | 0.077 | 0.4908 | 1.08 | 0.8754 |

| Contrast | estimate | SE | p.value |
|---|---|---|---|
| ctrl_negative-ctrl cyclohex tnfa_negative | -1.6424 | 0.6211 | 0.0314 |
| ctrl_negative-ctrl starved_negative | -1.9314 | 0.6735 | 0.0314 |
| ctrl_negative-generalist_negative | -0.1847 | 0.376 | 0.8499 |
| ctrl_negative-specialist_negative | -0.3807 | 0.403 | 0.5172 |
| ctrl_negative-other_negative | -0.7893 | 0.4487 | 0.1684 |
| ctrl_negative-generalist_positive | -0.0858 | 0.38 | 0.9177 |
| ctrl_negative-specialist_positive | 0.0294 | 0.4383 | 0.9792 |
| ctrl_negative-other_positive | -0.077 | 0.4908 | 0.9379 |
| ctrl cyclohex tnfa_negative-ctrl starved_negative | -0.289 | 0.7839 | 0.8905 |
| ctrl cyclohex tnfa_negative-generalist_negative | 1.4577 | 0.5727 | 0.0364 |
| ctrl cyclohex tnfa_negative-specialist_negative | 1.2617 | 0.5907 | 0.0817 |
| ctrl cyclohex tnfa_negative-other_negative | 0.8531 | 0.6223 | 0.3007 |
| ctrl cyclohex tnfa_negative-generalist_positive | 1.5566 | 0.5753 | 0.0314 |
| ctrl cyclohex tnfa_negative-specialist_positive | 1.6718 | 0.6127 | 0.0314 |
| ctrl cyclohex tnfa_negative-other_positive | 1.5654 | 0.6533 | 0.0452 |
| ctrl starved_negative-generalist_negative | 1.7467 | 0.6291 | 0.0314 |
| ctrl starved_negative-specialist_negative | 1.5507 | 0.6455 | 0.0452 |
| ctrl starved_negative-other_negative | 1.1421 | 0.6746 | 0.1809 |
| ctrl starved_negative-generalist_positive | 1.8456 | 0.6314 | 0.0314 |
| ctrl starved_negative-specialist_positive | 1.9608 | 0.6657 | 0.0314 |
| ctrl starved_negative-other_positive | 1.8544 | 0.7032 | 0.0314 |
| generalist_negative-specialist_negative | -0.196 | 0.3238 | 0.7784 |
| generalist_negative-other_negative | -0.6046 | 0.3792 | 0.2078 |
| specialist_negative-other_negative | -0.4086 | 0.4059 | 0.4961 |
| generalist_positive-specialist_positive | 0.1152 | 0.3707 | 0.9071 |
| generalist_positive-other_positive | 0.0089 | 0.4316 | 0.9836 |
| specialist_positive-other_positive | -0.1064 | 0.4836 | 0.9177 |
| generalist_negative-generalist_positive | 0.0989 | 0.2299 | 0.8702 |
| specialist_negative-specialist_positive | 0.4101 | 0.322 | 0.338 |
| other_negative-other_positive | 0.7123 | 0.3748 | 0.1325 |

| Par | Estimate | se | OR | pvalue |
|---|---|---|---|---|
| (Intercept) | -1.4519 | 0.4671 | 0.2341 | 0.0019 |
| group_Myc3ctrl cyclohex tnfa_negative | 1.6437 | 0.6321 | 5.1741 | 0.0093 |
| group_Myc3ctrl starved_negative | 1.9332 | 0.6838 | 6.9113 | 0.0047 |
| group_Myc3generalist_high burden | 0.2176 | 0.4263 | 1.2431 | 0.6097 |
| group_Myc3generalist_low burden | -0.0153 | 0.4183 | 0.9849 | 0.9709 |
| group_Myc3generalist_negative | 0.1931 | 0.384 | 1.213 | 0.6152 |
| group_Myc3other_high burden | -0.0368 | 0.6144 | 0.9639 | 0.9523 |
| group_Myc3other_low burden | 0.17 | 0.5606 | 1.1853 | 0.7617 |
| group_Myc3other_negative | 0.7962 | 0.4586 | 2.2171 | 0.0825 |
| group_Myc3specialist_high burden | -0.5125 | 0.5468 | 0.599 | 0.3487 |
| group_Myc3specialist_low burden | 0.3892 | 0.4961 | 1.4757 | 0.4328 |
| group_Myc3specialist_negative | 0.389 | 0.4118 | 1.4755 | 0.3448 |

OBSERVATIONS

In M2 macrophages, only bystander non-infected cells of other strains showed a slight, statistically not significant increase in apoptosis (30%).

Apoptosis > not infected control

Increased apoptosis observed, not statistically significant

**Grouping: Basic**

**M1 – 24 h p.i.**

a) Percentage of live/apoptotic cells

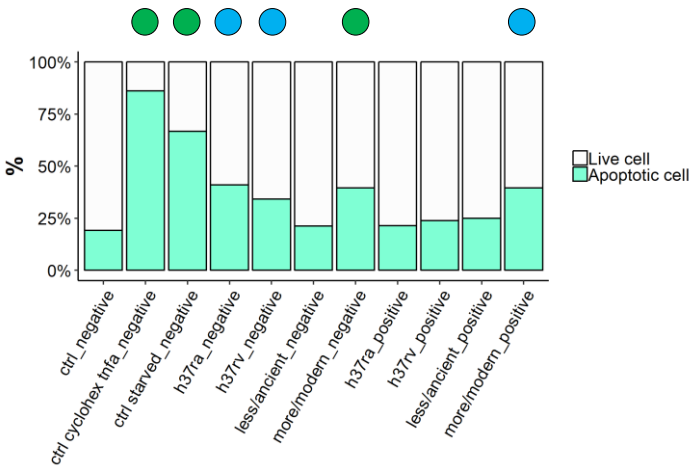


b) Percentage of live/apoptotic cells per mycobacterial burden

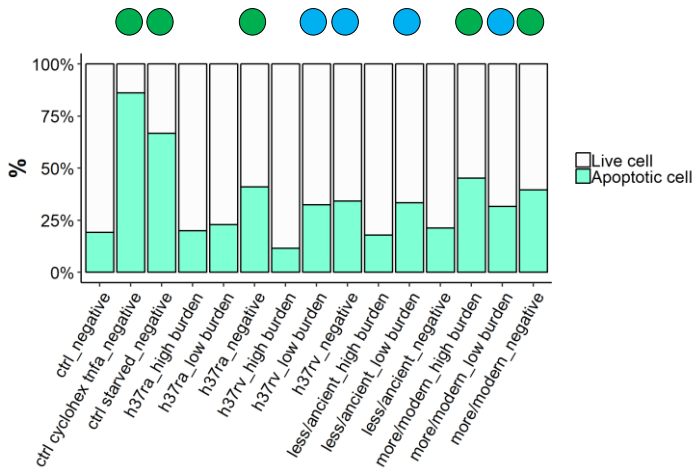


| Par | Estimate | se | OR | pvalue |
|---|---|---|---|---|
| (Intercept) | -1.2726 | 0.3691 | 0.2801 | 6e-04 |
| group_Mycctrl cyclohex tnfa_negative | 2.8169 | 0.6296 | 16.7247 | 0 |
| group_Mycctrl starved_negative | 1.6948 | 0.576 | 5.4457 | 0.0033 |
| group_Mych37ra_negative | 0.9373 | 0.4135 | 2.553 | 0.0234 |
| group_Mych37rv_negative | 0.7326 | 0.4232 | 2.0805 | 0.0834 |
| group_Mycless/ancient_negative | 0.0445 | 0.3715 | 1.0455 | 0.9047 |
| group_Mycmore/modern_negative | 1.0439 | 0.367 | 2.8402 | 0.0045 |
| group_Mych37ra_positive | -0.0568 | 0.4554 | 0.9448 | 0.9008 |
| group_Mych37rv_positive | 0.1894 | 0.4636 | 1.2086 | 0.6828 |
| group_Mycless/ancient_positive | 0.1552 | 0.3872 | 1.1679 | 0.6886 |
| group_Mycmore/modern_positive | 0.8104 | 0.3706 | 2.2489 | 0.0288 |

| Contrast | estimate | SE | p.value |
|---|---|---|---|
| ctrl_negative-ctrl cyclohex tnfa_negative | -2.8169 | 0.6296 | 1e-04 |
| ctrl_negative-ctrl starved_negative | -1.6948 | 0.576 | 0.0116 |
| ctrl_negative-h37ra_negative | -0.9373 | 0.4135 | 0.053 |
| ctrl_negative-h37rv_negative | -0.7326 | 0.4232 | 0.1494 |
| ctrl_negative-less/ancient_negative | -0.0445 | 0.3715 | 0.9263 |
| ctrl_negative-more/modern_negative | -1.0439 | 0.367 | 0.0137 |
| ctrl_negative-h37ra_positive | 0.0568 | 0.4554 | 0.9263 |
| ctrl_negative-h37rv_positive | -0.1894 | 0.4636 | 0.7666 |
| ctrl_negative-less/ancient_positive | -0.1552 | 0.3872 | 0.7666 |
| ctrl_negative-more/modern_positive | -0.8104 | 0.3706 | 0.0618 |
| ctrl cyclohex tnfa_negative-ctrl starved_negative | 1.1221 | 0.7278 | 0.1961 |
| ctrl cyclohex tnfa_negative-h37ra_negative | 1.8796 | 0.6255 | 0.0114 |
| ctrl cyclohex tnfa_negative-h37rv_negative | 2.0843 | 0.634 | 0.0062 |
| ctrl cyclohex tnfa_negative-less/ancient_negative | 2.7724 | 0.5987 | 1e-04 |
| ctrl cyclohex tnfa_negative-more/modern_negative | 1.773 | 0.599 | 0.0116 |
| ctrl cyclohex tnfa_negative-h37ra_positive | 2.8737 | 0.6516 | 1e-04 |
| ctrl cyclohex tnfa_negative-h37rv_positive | 2.6274 | 0.6601 | 6e-04 |
| ctrl cyclohex tnfa_negative-less/ancient_positive | 2.6617 | 0.6064 | 1e-04 |
| ctrl cyclohex tnfa_negative-more/modern_positive | 2.0064 | 0.5936 | 0.0052 |
| ctrl starved_negative-h37ra_negative | 0.7575 | 0.5714 | 0.2651 |
| ctrl starved_negative-h37rv_negative | 0.9622 | 0.5807 | 0.164 |
| ctrl starved_negative-less/ancient_negative | 1.6504 | 0.5419 | 0.0111 |
| ctrl starved_negative-more/modern_negative | 0.6509 | 0.5423 | 0.3191 |
| ctrl starved_negative-h37ra_positive | 1.7516 | 0.5999 | 0.0116 |
| ctrl starved_negative-h37rv_positive | 1.5054 | 0.6091 | 0.034 |
| ctrl starved_negative-less/ancient_positive | 1.5396 | 0.5505 | 0.0148 |
| ctrl starved_negative-more/modern_positive | 0.8844 | 0.5364 | 0.164 |
| h37ra_negative-h37rv_negative | 0.2047 | 0.4185 | 0.7463 |
| h37ra_negative-less/ancient_negative | 0.8928 | 0.3661 | 0.0352 |
| h37ra_negative-more/modern_negative | -0.1066 | 0.3618 | 0.8259 |
| h37rv_negative-less/ancient_negative | 0.6881 | 0.3771 | 0.1272 |
| h37rv_negative-more/modern_negative | -0.3113 | 0.3724 | 0.5254 |
| less/ancient_negative-more/modern_negative | -0.9994 | 0.3129 | 0.0075 |
| h37ra_positive-h37rv_positive | -0.2462 | 0.4972 | 0.7463 |
| h37ra_positive-less/ancient_positive | -0.212 | 0.4263 | 0.7463 |
| h37ra_positive-more/modern_positive | -0.8672 | 0.4106 | 0.071 |
| h37rv_positive-less/ancient_positive | 0.0343 | 0.4356 | 0.9373 |
| h37rv_positive-more/modern_positive | -0.621 | 0.4208 | 0.215 |
| less/ancient_positive-more/modern_positive | -0.6553 | 0.3337 | 0.0969 |
| h37ra_negative-h37ra_positive | 0.9941 | 0.3754 | 0.0217 |
| h37rv_negative-h37rv_positive | 0.5432 | 0.3864 | 0.2369 |
| less/ancient_negative-less/ancient_positive | -0.1107 | 0.2827 | 0.7666 |
| more/modern_negative-more/modern_positive | 0.2334 | 0.2607 | 0.4981 |

| Par | Estimate | se | OR | pvalue |
|---|---|---|---|---|
| (Intercept) | -1.2712 | 0.3719 | 0.2805 | 6e-04 |
| group_Myc3ctrl cyclohex tnfa_negative | 2.8327 | 0.6446 | 16.9909 | 0 |
| group_Myc3ctrl starved_negative | 1.7119 | 0.5924 | 5.5396 | 0.0039 |
| group_Myc3h37ra_high burden | -0.1092 | 0.56 | 0.8965 | 0.8454 |
| group_Myc3h37ra_low burden | -0.0101 | 0.5521 | 0.9899 | 0.9854 |
| group_Myc3h37ra_negative | 0.9303 | 0.4284 | 2.5352 | 0.0299 |
| group_Myc3h37rv_high burden | -0.5856 | 0.7226 | 0.5568 | 0.4178 |
| group_Myc3h37rv_low burden | 0.5727 | 0.5218 | 1.7731 | 0.2723 |
| group_Myc3h37rv_negative | 0.7139 | 0.438 | 2.0419 | 0.1032 |
| group_Myc3less/ancient_high burden | -0.315 | 0.4725 | 0.7298 | 0.505 |
| group_Myc3less/ancient_low burden | 0.5803 | 0.4445 | 1.7867 | 0.1917 |
| group_Myc3less/ancient_negative | 0.032 | 0.3843 | 1.0326 | 0.9336 |
| group_Myc3more/modern_high burden | 1.0956 | 0.409 | 2.991 | 0.0074 |
| group_Myc3more/modern_low burden | 0.3759 | 0.4518 | 1.4563 | 0.4054 |
| group_Myc3more/modern_negative | 1.051 | 0.3801 | 2.8606 | 0.0057 |

OBSERVATIONS

In M1 macrophages, bystander non-infected cells of more/modern strains showed increased apoptosis (40%). Despite not statistically significant, also bystander non-infected cells of H37Ra and H37Rv and macrophages infected with more/modern strains showed a similar increase in the percentage of apoptosis. Stratification of the data by mycobacterial burden showed higher apoptotic levels in bystander non-infected cells or in cells infected with lower mycobacterial load.

Apoptosis > not infected control

Increased apoptosis observed, not statistically significant

**Grouping: Basic**

**M2 – 24 h p.i.**

a) Percentage of live/apoptotic cells

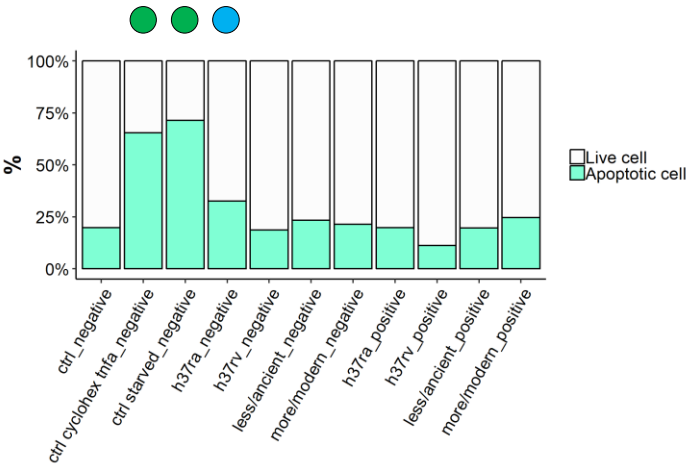


b) Percentage of live/apoptotic cells per mycobacterial burden

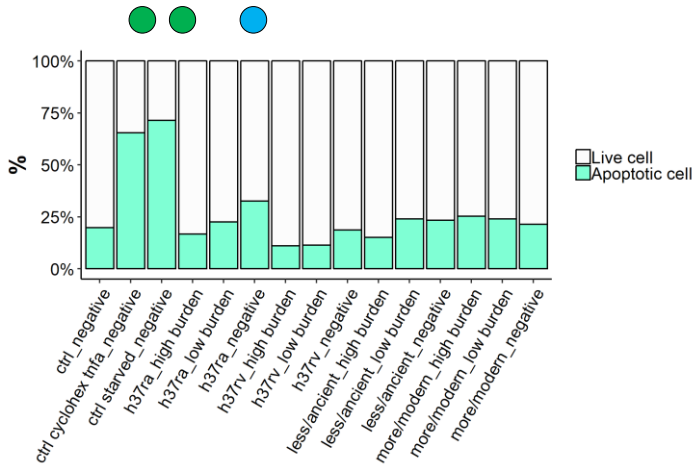


| Par | Estimate | se | OR | pvalue |
|---|---|---|---|---|
| (Intercept) | -1.4301 | 0.4477 | 0.2393 | 0.0014 |
| group_Mycctrl cyclohex tnfa_negative | 1.626 | 0.5984 | 5.0835 | 0.0066 |
| group_Mycctrl starved_negative | 1.9138 | 0.6521 | 6.7791 | 0.0033 |
| group_Mych37ra_negative | 0.7735 | 0.428 | 2.1674 | 0.0707 |
| group_Mych37rv_negative | -0.0049 | 0.4601 | 0.9951 | 0.9915 |
| group_Mycless/ancient_negative | 0.3668 | 0.3852 | 1.4432 | 0.341 |
| group_Mycmore/modern_negative | 0.2543 | 0.3839 | 1.2896 | 0.5077 |
| group_Mych37ra_positive | 0.0671 | 0.4716 | 1.0694 | 0.8869 |
| group_Mych37rv_positive | -0.5298 | 0.5107 | 0.5887 | 0.2995 |
| group_Mycless/ancient_positive | -0.0332 | 0.4215 | 0.9674 | 0.9373 |
| group_Mycmore/modern_positive | 0.31 | 0.3841 | 1.3634 | 0.4197 |

| Contrast | estimate | SE | p.value |
|---|---|---|---|
| ctrl_negative-ctrl cyclohex tnfa_negative | -1.626 | 0.5984 | 0.0369 |
| ctrl_negative-ctrl starved_negative | -1.9138 | 0.6521 | 0.0358 |
| ctrl_negative-h37ra_negative | -0.7735 | 0.428 | 0.1689 |
| ctrl_negative-h37rv_negative | 0.0049 | 0.4601 | 0.9915 |
| ctrl_negative-less/ancient_negative | -0.3668 | 0.3852 | 0.4887 |
| ctrl_negative-more/modern_negative | -0.2543 | 0.3839 | 0.642 |
| ctrl_negative-h37ra_positive | -0.0671 | 0.4716 | 0.9302 |
| ctrl_negative-h37rv_positive | 0.5298 | 0.5107 | 0.46 |
| ctrl_negative-less/ancient_positive | 0.0332 | 0.4215 | 0.9596 |
| ctrl_negative-more/modern_positive | -0.31 | 0.3841 | 0.5468 |
| ctrl cyclohex tnfa_negative-ctrl starved_negative | -0.2879 | 0.7613 | 0.8197 |
| ctrl cyclohex tnfa_negative-h37ra_negative | 0.8524 | 0.6003 | 0.3042 |
| ctrl cyclohex tnfa_negative-h37rv_negative | 1.6309 | 0.6232 | 0.0381 |
| ctrl cyclohex tnfa_negative-less/ancient_negative | 1.2592 | 0.5712 | 0.0739 |
| ctrl cyclohex tnfa_negative-more/modern_negative | 1.3716 | 0.5708 | 0.0499 |
| ctrl cyclohex tnfa_negative-h37ra_positive | 1.5589 | 0.6322 | 0.0452 |
| ctrl cyclohex tnfa_negative-h37rv_positive | 2.1558 | 0.6634 | 0.0248 |
| ctrl cyclohex tnfa_negative-less/ancient_positive | 1.6592 | 0.5936 | 0.0369 |
| ctrl cyclohex tnfa_negative-more/modern_positive | 1.316 | 0.57 | 0.0601 |
| ctrl starved_negative-h37ra_negative | 1.1403 | 0.6539 | 0.1745 |
| ctrl starved_negative-h37rv_negative | 1.9187 | 0.6749 | 0.0369 |
| ctrl starved_negative-less/ancient_negative | 1.547 | 0.6272 | 0.0452 |
| ctrl starved_negative-more/modern_negative | 1.6595 | 0.6268 | 0.0381 |
| ctrl starved_negative-h37ra_positive | 1.8468 | 0.6832 | 0.0369 |
| ctrl starved_negative-h37rv_positive | 2.4436 | 0.7122 | 0.0248 |
| ctrl starved_negative-less/ancient_positive | 1.947 | 0.6477 | 0.0358 |
| ctrl starved_negative-more/modern_positive | 1.6039 | 0.6261 | 0.0407 |
| h37ra_negative-h37rv_negative | 0.7784 | 0.4633 | 0.1903 |
| h37ra_negative-less/ancient_negative | 0.4067 | 0.3892 | 0.46 |
| h37ra_negative-more/modern_negative | 0.5192 | 0.3879 | 0.3379 |
| h37rv_negative-less/ancient_negative | -0.3717 | 0.4242 | 0.5117 |
| h37rv_negative-more/modern_negative | -0.2592 | 0.423 | 0.6634 |
| less/ancient_negative-more/modern_negative | 0.1125 | 0.3401 | 0.8383 |
| h37ra_positive-h37rv_positive | 0.5969 | 0.5506 | 0.46 |
| h37ra_positive-less/ancient_positive | 0.1002 | 0.4689 | 0.8994 |
| h37ra_positive-more/modern_positive | -0.2429 | 0.4357 | 0.6894 |
| h37rv_positive-less/ancient_positive | -0.4966 | 0.5084 | 0.4873 |
| h37rv_positive-more/modern_positive | -0.8398 | 0.4778 | 0.1745 |
| less/ancient_positive-more/modern_positive | -0.3432 | 0.3808 | 0.5097 |
| h37ra_negative-h37ra_positive | 0.7065 | 0.374 | 0.1489 |
| h37rv_negative-h37rv_positive | 0.5249 | 0.4546 | 0.4269 |
| less/ancient_negative-less/ancient_positive | 0.4 | 0.3207 | 0.3803 |
| more/modern_negative-more/modern_positive | -0.0556 | 0.2698 | 0.8994 |

| Par | Estimate | se | OR | pvalue |
|---|---|---|---|---|
| (Intercept) | -1.4382 | 0.456 | 0.2373 | 0.0016 |
| group_Myc3ctrl cyclohex tnfa_negative | 1.6302 | 0.6108 | 5.1051 | 0.0076 |
| group_Myc3ctrl starved_negative | 1.9187 | 0.6637 | 6.8121 | 0.0038 |
| group_Myc3h37ra_high burden | -0.0443 | 0.5994 | 0.9567 | 0.9411 |
| group_Myc3h37ra_low burden | 0.1597 | 0.5445 | 1.1731 | 0.7693 |
| group_Myc3h37ra_negative | 0.782 | 0.4392 | 2.1859 | 0.075 |
| group_Myc3h37rv_high burden | -0.4505 | 0.7279 | 0.6373 | 0.536 |
| group_Myc3h37rv_low burden | -0.5554 | 0.577 | 0.5738 | 0.3358 |
| group_Myc3h37rv_negative | 0.004 | 0.4704 | 1.004 | 0.9932 |
| group_Myc3less/ancient_high burden | -0.5063 | 0.5331 | 0.6027 | 0.3422 |
| group_Myc3less/ancient_low burden | 0.3776 | 0.4817 | 1.4588 | 0.4332 |
| group_Myc3less/ancient_negative | 0.3765 | 0.3951 | 1.4571 | 0.3407 |
| group_Myc3more/modern_high burden | 0.4025 | 0.4347 | 1.4956 | 0.3545 |
| group_Myc3more/modern_low burden | 0.2268 | 0.4393 | 1.2546 | 0.6056 |
| group_Myc3more/modern_negative | 0.2645 | 0.3935 | 1.3028 | 0.5014 |

OBSERVATIONS

In contrast to what observed for M1, none of the category induced apoptosis in M2a macrophages at the time point considered.

Apoptosis > not infected control

Increased apoptosis observed, not statistically significant

**Grouping: Disease**

**M1 – 24 h p.i.**

a) Percentage of live/apoptotic cells

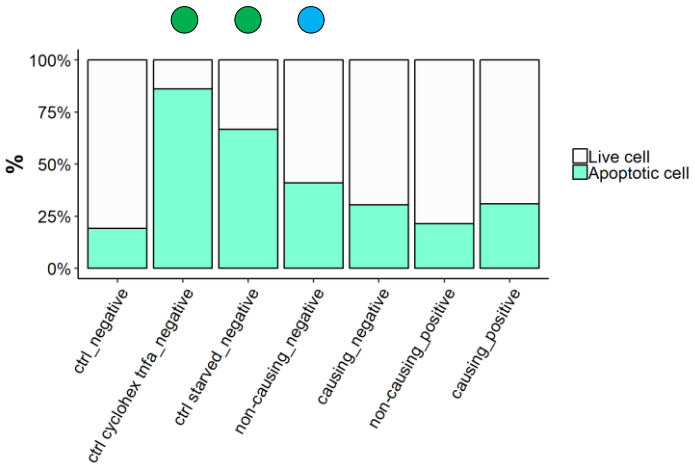


b) Percentage of live/apoptotic cells per mycobacterial burden

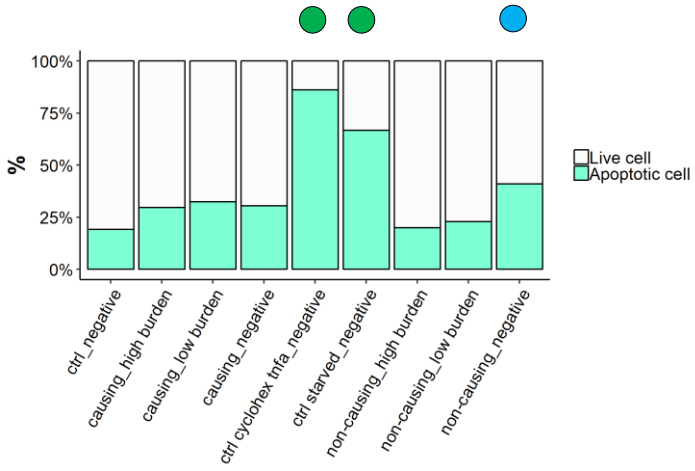


| Par | Estimate | se | OR | pvalue |
|---|---|---|---|---|
| (Intercept) | -1.2627 | 0.3961 | 0.2829 | 0.0014 |
| group_Mycctrl cyclohex tnfa_negative | 2.832 | 0.6877 | 16.9798 | 0 |
| group_Mycctrl starved_negative | 1.7147 | 0.6395 | 5.555 | 0.0073 |
| group_Mycnon-causing_negative | 0.9165 | 0.4703 | 2.5005 | 0.0513 |
| group_Myccausing_negative | 0.5746 | 0.37 | 1.7764 | 0.1204 |
| group_Mycnon-causing_positive | -0.071 | 0.5076 | 0.9315 | 0.8888 |
| group_Myccausing_positive | 0.4299 | 0.375 | 1.5372 | 0.2516 |

| Contrast | estimate | SE | p.value |
|---|---|---|---|
| ctrl_negative-ctrl cyclohex tnfa_negative | -2.832 | 0.6877 | 4e-04 |
| ctrl_negative-ctrl starved_negative | -1.7147 | 0.6395 | 0.0199 |
| ctrl_negative-non-causing_negative | -0.9165 | 0.4703 | 0.0887 |
| ctrl_negative-causing_negative | -0.5746 | 0.37 | 0.1906 |
| ctrl_negative-non-causing_positive | 0.071 | 0.5076 | 0.8888 |
| ctrl_negative-causing_positive | -0.4299 | 0.375 | 0.2987 |
| ctrl cyclohex tnfa_negative-ctrl starved_negative | 1.1173 | 0.7935 | 0.2325 |
| ctrl cyclohex tnfa_negative-non-causing_negative | 1.9155 | 0.6838 | 0.0193 |
| ctrl cyclohex tnfa_negative-causing_negative | 2.2575 | 0.6205 | 0.0013 |
| ctrl cyclohex tnfa_negative-non-causing_positive | 2.903 | 0.7083 | 4e-04 |
| ctrl cyclohex tnfa_negative-causing_positive | 2.4021 | 0.6199 | 7e-04 |
| ctrl starved_negative-non-causing_negative | 0.7982 | 0.6353 | 0.2836 |
| ctrl starved_negative-causing_negative | 1.1401 | 0.5666 | 0.084 |
| ctrl starved_negative-non-causing_positive | 1.7856 | 0.6615 | 0.0199 |
| ctrl starved_negative-causing_positive | 1.2847 | 0.5659 | 0.0489 |
| non-causing_negative-causing_negative | 0.3419 | 0.3643 | 0.3889 |
| non-causing_positive-causing_positive | -0.5009 | 0.4151 | 0.2883 |
| non-causing_negative-non-causing_positive | 0.9875 | 0.377 | 0.0209 |
| causing_negative-causing_positive | 0.1446 | 0.1722 | 0.4232 |

| Par | Estimate | se | OR | pvalue |
|---|---|---|---|---|
| (Intercept) | -1.2631 | 0.3952 | 0.2828 | 0.0014 |
| group_Myc3causing_high burden | 0.3793 | 0.3949 | 1.4613 | 0.3368 |
| group_Myc3causing_low burden | 0.4877 | 0.3996 | 1.6286 | 0.2222 |
| group_Myc3causing_negative | 0.5731 | 0.3712 | 1.7738 | 0.1226 |
| group_Myc3ctrl cyclohex tnfa_negative | 2.8381 | 0.6893 | 17.0825 | 0 |
| group_Myc3ctrl starved_negative | 1.7208 | 0.6412 | 5.5892 | 0.0073 |
| group_Myc3non-causing_high burden | -0.1357 | 0.5944 | 0.8731 | 0.8194 |
| group_Myc3non-causing_low burden | -0.0066 | 0.5873 | 0.9935 | 0.9911 |
| group_Myc3non-causing_negative | 0.9146 | 0.4719 | 2.4957 | 0.0526 |

OBSERVATIONS

Despite not statistically significant, in M1 macrophages bystander non-infected cells of non-causing disease strains showed increased apoptosis (40%). Also macrophages infected with non-causing disease strains showed an increase in the percentage of apoptosis. Stratification of the data by mycobacterial burden showed higher apoptotic levels in bystander non-infected cells.

Apoptosis > not infected control

Increased apoptosis observed, not statistically significant

**Grouping: Disease**

**M2 – 24 h p.i.**

a) Percentage of live/apoptotic cells

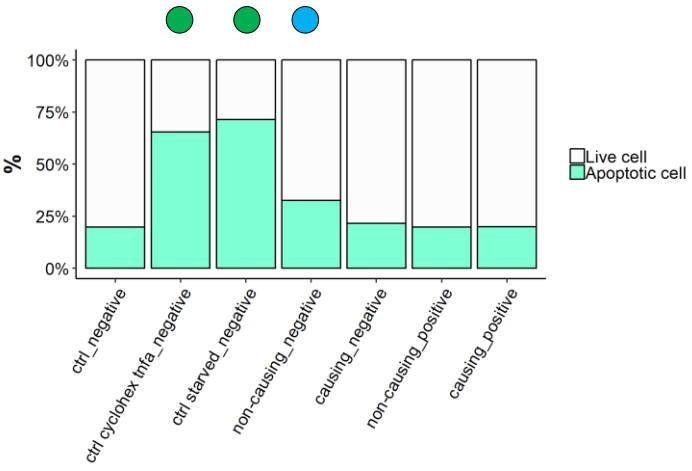


b) Percentage of live/apoptotic cells per mycobacterial burden

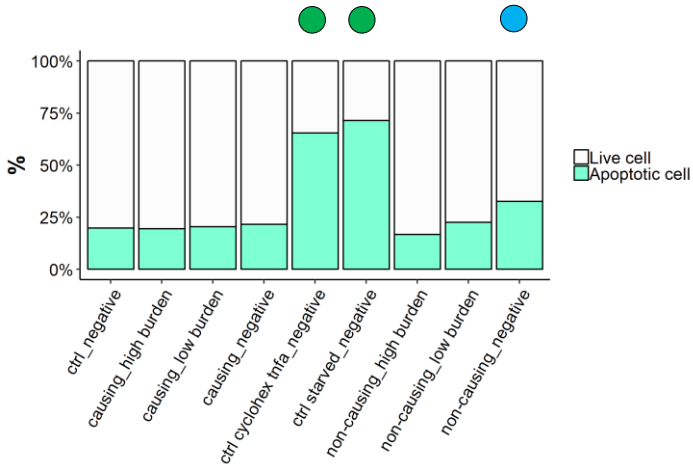


| Par | Estimate | se | OR | pvalue |
|---|---|---|---|---|
| (Intercept) | -1.4453 | 0.4574 | 0.2357 | 0.0016 |
| group_Mycctrl cyclohex tnfa_negative | 1.6451 | 0.621 | 5.1815 | 0.0081 |
| group_Mycctrl starved_negative | 1.9341 | 0.6734 | 6.9175 | 0.0041 |
| group_Mycnon-causing_negative | 0.7893 | 0.4487 | 2.2019 | 0.0785 |
| group_Myccausing_negative | 0.262 | 0.353 | 1.2995 | 0.4579 |
| group_Mycnon-causing_positive | 0.077 | 0.4907 | 1.0801 | 0.8752 |
| group_Myccausing_positive | 0.0543 | 0.3599 | 1.0558 | 0.88 |

| Contrast | estimate | SE | p.value |
|---|---|---|---|
| ctrl_negative-ctrl cyclohex tnfa_negative | -1.6451 | 0.621 | 0.0262 |
| ctrl_negative-ctrl starved_negative | -1.9341 | 0.6734 | 0.0262 |
| ctrl_negative-non-causing_negative | -0.7893 | 0.4487 | 0.1492 |
| ctrl_negative-causing_negative | -0.262 | 0.353 | 0.5801 |
| ctrl_negative-non-causing_positive | -0.077 | 0.4907 | 0.9289 |
| ctrl_negative-causing_positive | -0.0543 | 0.3599 | 0.9289 |
| ctrl cyclohex tnfa_negative-ctrl starved_negative | -0.289 | 0.7838 | 0.8459 |
| ctrl cyclohex tnfa_negative-non-causing_negative | 0.8557 | 0.6222 | 0.247 |
| ctrl cyclohex tnfa_negative-causing_negative | 1.3831 | 0.5577 | 0.0356 |
| ctrl cyclohex tnfa_negative-non-causing_positive | 1.568 | 0.6532 | 0.0389 |
| ctrl cyclohex tnfa_negative-causing_positive | 1.5908 | 0.5613 | 0.0262 |
| ctrl starved_negative-non-causing_negative | 1.1447 | 0.6745 | 0.1549 |
| ctrl starved_negative-causing_negative | 1.6721 | 0.6154 | 0.0262 |
| ctrl starved_negative-non-causing_positive | 1.857 | 0.7032 | 0.0262 |
| ctrl starved_negative-causing_positive | 1.8797 | 0.6187 | 0.0262 |
| non-causing_negative-causing_negative | 0.5274 | 0.3563 | 0.2198 |
| non-causing_positive-causing_positive | 0.0227 | 0.414 | 0.9562 |
| non-causing_negative-non-causing_positive | 0.7123 | 0.3748 | 0.1211 |
| causing_negative-causing_positive | 0.2077 | 0.1861 | 0.359 |

| Par | Estimate | se | OR | pvalue |
|---|---|---|---|---|
| (Intercept) | -1.4466 | 0.4572 | 0.2354 | 0.0016 |
| group_Myc3causing_high burden | -0.002 | 0.3928 | 0.9981 | 0.996 |
| group_Myc3causing_low burden | 0.1032 | 0.3827 | 1.1087 | 0.7875 |
| group_Myc3causing_negative | 0.2629 | 0.3543 | 1.3007 | 0.458 |
| group_Myc3ctrl cyclohex tnfa_negative | 1.6485 | 0.6229 | 5.1994 | 0.0081 |
| group_Myc3ctrl starved_negative | 1.9376 | 0.6751 | 6.9421 | 0.0041 |
| group_Myc3non-causing_high burden | -0.0406 | 0.6078 | 0.9602 | 0.9467 |
| group_Myc3non-causing_low burden | 0.1668 | 0.5536 | 1.1815 | 0.7632 |
| group_Myc3non-causing_negative | 0.7906 | 0.4502 | 2.2047 | 0.0791 |

OBSERVATIONS

Despite not statistically significant, in M2a macrophages bystander non-infected cells of non-causing disease strains showed increased apoptosis (30%). Stratification of the data by mycobacterial burden showed higher apoptotic levels in bystander non-infected cells.

Apoptosis > not infected control

Increased apoptosis observed, not statistically significant

**Grouping: Lab adaptation**

**M1 – 24 h p.i.**

a) Percentage of live/apoptotic cells

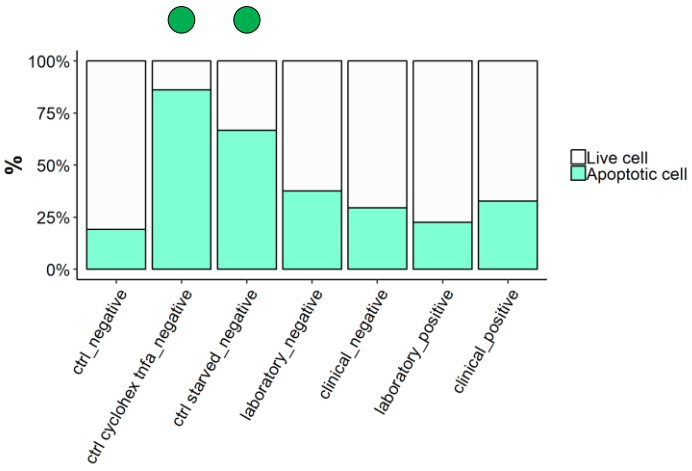


b) Percentage of live/apoptotic cells per mycobacterial burden

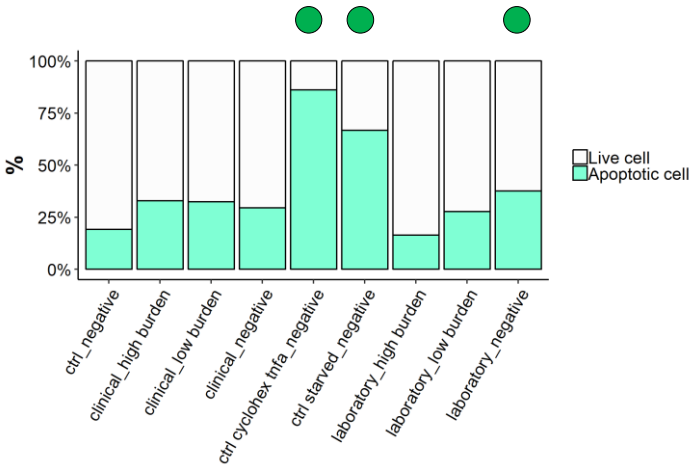


| Par | Estimate | se | OR | pvalue |
|---|---|---|---|---|
| (Intercept) | -1.2641 | 0.392 | 0.2825 | 0.0013 |
| group_Mycctrl cyclohex tnfa_negative | 2.8407 | 0.6851 | 17.1286 | 0 |
| group_Mycctrl starved_negative | 1.7232 | 0.6367 | 5.6026 | 0.0068 |
| group_Myclaboratory_negative | 0.8194 | 0.4091 | 2.2692 | 0.0452 |
| group_Mycclinical_negative | 0.5345 | 0.3765 | 1.7065 | 0.1557 |
| group_Myclaboratory_positive | 0.0477 | 0.431 | 1.0488 | 0.9119 |
| group_Mycclinical_positive | 0.4889 | 0.3813 | 1.6305 | 0.1998 |

| Contrast | estimate | SE | p.value |
|---|---|---|---|
| ctrl_negative-ctrl cyclohex tnfa_negative | -2.8407 | 0.6851 | 3e-04 |
| ctrl_negative-ctrl starved_negative | -1.7232 | 0.6367 | 0.0161 |
| ctrl_negative-laboratory_negative | -0.8194 | 0.4091 | 0.078 |
| ctrl_negative-clinical_negative | -0.5345 | 0.3765 | 0.2138 |
| ctrl_negative-laboratory_positive | -0.0477 | 0.431 | 0.9119 |
| ctrl_negative-clinical_positive | -0.4889 | 0.3813 | 0.2373 |
| ctrl cyclohex tnfa_negative-ctrl starved_negative | 1.1175 | 0.7906 | 0.2138 |
| ctrl cyclohex tnfa_negative-laboratory_negative | 2.0213 | 0.6431 | 0.0064 |
| ctrl cyclohex tnfa_negative-clinical_negative | 2.3063 | 0.6232 | 0.001 |
| ctrl cyclohex tnfa_negative-laboratory_positive | 2.7931 | 0.6557 | 3e-04 |
| ctrl cyclohex tnfa_negative-clinical_positive | 2.3518 | 0.622 | 0.001 |
| ctrl starved_negative-laboratory_negative | 0.9038 | 0.5912 | 0.2001 |
| ctrl starved_negative-clinical_negative | 1.1888 | 0.5695 | 0.07 |
| ctrl starved_negative-laboratory_positive | 1.6756 | 0.6048 | 0.0152 |
| ctrl starved_negative-clinical_positive | 1.2343 | 0.5682 | 0.063 |
| laboratory_negative-clinical_negative | 0.285 | 0.2932 | 0.37 |
| laboratory_positive-clinical_positive | -0.4412 | 0.3281 | 0.2264 |
| laboratory_negative-laboratory_positive | 0.7718 | 0.2703 | 0.0136 |
| clinical_negative-clinical_positive | 0.0455 | 0.1922 | 0.8578 |

| Par | Estimate | se | OR | pvalue |
|---|---|---|---|---|
| (Intercept) | -1.2656 | 0.3889 | 0.2821 | 0.0011 |
| group_Myc3clinical_high burden | 0.5064 | 0.4029 | 1.6592 | 0.2088 |
| group_Myc3clinical_low burden | 0.4703 | 0.416 | 1.6004 | 0.2583 |
| group_Myc3clinical_negative | 0.5338 | 0.3795 | 1.7054 | 0.1595 |
| group_Myc3ctrl cyclohex tnfa_negative | 2.8591 | 0.689 | 17.445 | 0 |
| group_Myc3ctrl starved_negative | 1.7418 | 0.6408 | 5.7077 | 0.0066 |
| group_Myc3laboratory_high burden | -0.3025 | 0.5165 | 0.739 | 0.5581 |
| group_Myc3laboratory_low burden | 0.303 | 0.4688 | 1.354 | 0.518 |
| group_Myc3laboratory_negative | 0.8105 | 0.4125 | 2.2491 | 0.0494 |

OBSERVATIONS

Despite not statistically significant, in M1 macrophages bystander non-infected cells of laboratory strains and macrophages infected with clinical isolates showed increased apoptosis (35-40%). Stratification of the data by mycobacterial burden showed higher apoptotic levels in bystander non-infected cells or in cells infected with lower mycobacterial load for laboratory strains.

Apoptosis > not infected control

Increased apoptosis observed, not statistically significant

**Grouping: Lab adaptation**

**M2 – 24 h p.i.**

a) Percentage of live/apoptotic cells

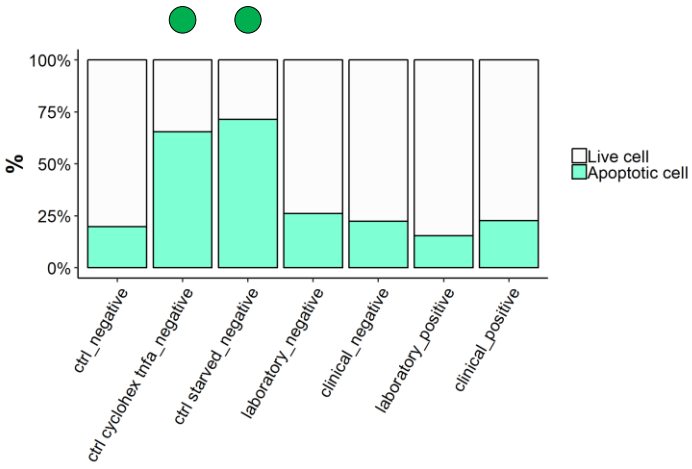


b) Percentage of live/apoptotic cells per mycobacterial burden

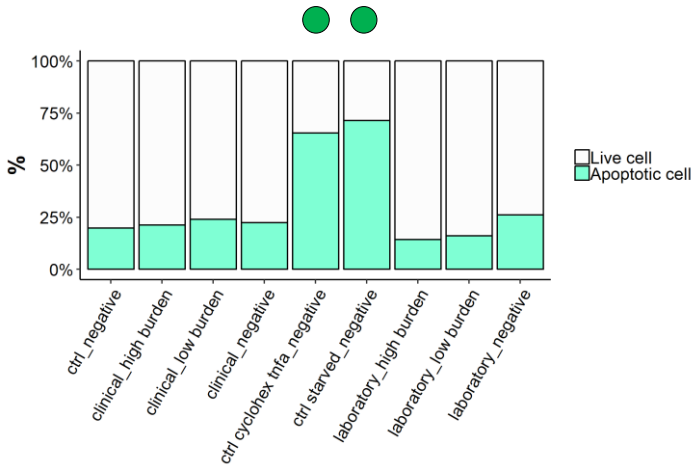


| Par | Estimate | se | OR | pvalue |
|---|---|---|---|---|
| (Intercept) | -1.4503 | 0.4578 | 0.2345 | 0.0015 |
| group_Mycctrl cyclohex tnfa_negative | 1.6569 | 0.6283 | 5.243 | 0.0084 |
| group_Mycctrl starved_negative | 1.9462 | 0.6802 | 7.0022 | 0.0042 |
| group_Myclaboratory_negative | 0.4384 | 0.4 | 1.5502 | 0.2731 |
| group_Mycclinical_negative | 0.3283 | 0.3666 | 1.3886 | 0.3705 |
| group_Myclaboratory_positive | -0.2024 | 0.4269 | 0.8168 | 0.6355 |
| group_Mycclinical_positive | 0.1872 | 0.3741 | 1.2059 | 0.6168 |

| Contrast | estimate | SE | p.value |
|---|---|---|---|
| ctrl_negative-ctrl cyclohex tnfa_negative | -1.6569 | 0.6283 | 0.0278 |
| ctrl_negative-ctrl starved_negative | -1.9462 | 0.6802 | 0.0246 |
| ctrl_negative-laboratory_negative | -0.4384 | 0.4 | 0.3991 |
| ctrl_negative-clinical_negative | -0.3283 | 0.3666 | 0.5029 |
| ctrl_negative-laboratory_positive | 0.2024 | 0.4269 | 0.7103 |
| ctrl_negative-clinical_positive | -0.1872 | 0.3741 | 0.7103 |
| ctrl cyclohex tnfa_negative-ctrl starved_negative | -0.2893 | 0.791 | 0.7146 |
| ctrl cyclohex tnfa_negative-laboratory_negative | 1.2185 | 0.5903 | 0.0673 |
| ctrl cyclohex tnfa_negative-clinical_negative | 1.3286 | 0.5691 | 0.0413 |
| ctrl cyclohex tnfa_negative-laboratory_positive | 1.8593 | 0.6098 | 0.0218 |
| ctrl cyclohex tnfa_negative-clinical_positive | 1.4697 | 0.5725 | 0.0278 |
| ctrl starved_negative-laboratory_negative | 1.5078 | 0.6453 | 0.0413 |
| ctrl starved_negative-clinical_negative | 1.6179 | 0.626 | 0.0278 |
| ctrl starved_negative-laboratory_positive | 2.1486 | 0.6632 | 0.0218 |
| ctrl starved_negative-clinical_positive | 1.759 | 0.6291 | 0.0246 |
| laboratory_negative-clinical_negative | 0.1101 | 0.2988 | 0.7146 |
| laboratory_positive-clinical_positive | -0.3896 | 0.3422 | 0.3991 |
| laboratory_negative-laboratory_positive | 0.6407 | 0.2872 | 0.0488 |
| clinical_negative-clinical_positive | 0.1411 | 0.2053 | 0.6233 |

| Par | Estimate | se | OR | pvalue |
|---|---|---|---|---|
| (Intercept) | -1.4512 | 0.4583 | 0.2343 | 0.0015 |
| group_Myc3clinical_high burden | 0.0859 | 0.4078 | 1.0897 | 0.8331 |
| group_Myc3clinical_low burden | 0.2856 | 0.4027 | 1.3306 | 0.4782 |
| group_Myc3clinical_negative | 0.3286 | 0.3677 | 1.389 | 0.3715 |
| group_Myc3ctrl cyclohex tnfa_negative | 1.6585 | 0.6297 | 5.2512 | 0.0084 |
| group_Myc3ctrl starved_negative | 1.9478 | 0.6816 | 7.0136 | 0.0043 |
| group_Myc3laboratory_high burden | -0.2418 | 0.5206 | 0.7852 | 0.6423 |
| group_Myc3laboratory_low burden | -0.1774 | 0.463 | 0.8374 | 0.7016 |
| group_Myc3laboratory_negative | 0.4391 | 0.4011 | 1.5513 | 0.2736 |

OBSERVATIONS

In contrast, clinical isolates showed similar apoptotic levels irrespective of the mycobacterial load. In contrast, none of the category induced apoptosis in M2a macrophages at the time point considered.

Apoptosis > not infected control

Increased apoptosis observed, not statistically significant

**Grouping: Phylogeny**

**M1 – 24 h p.i.**

a) Percentage of live/apoptotic cells

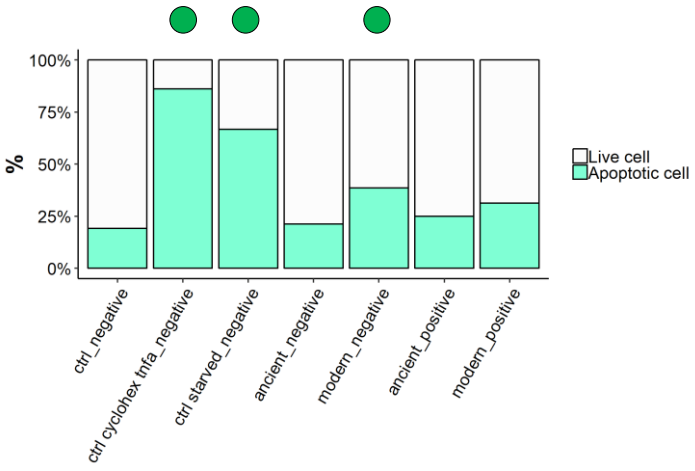


b) Percentage of live/apoptotic cells per mycobacterial burden

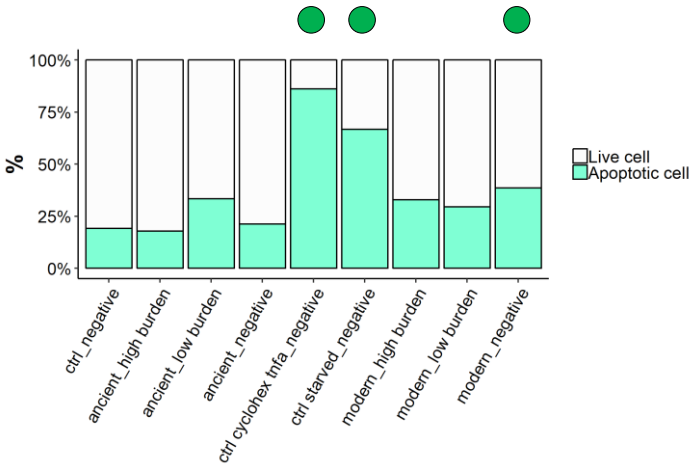


| Par | Estimate | se | OR | pvalue |
|---|---|---|---|---|
| (Intercept) | -1.2657 | 0.3852 | 0.282 | 0.001 |
| group_Mycctrl cyclohex tnfa_negative | 2.7973 | 0.6474 | 16.4006 | 0 |
| group_Mycctrl starved_negative | 1.6768 | 0.5955 | 5.3484 | 0.0049 |
| group_Mycancient_negative | 0.0349 | 0.3866 | 1.0355 | 0.928 |
| group_Mycmodern_negative | 0.9448 | 0.3457 | 2.5722 | 0.0063 |
| group_Mycancient_positive | 0.1412 | 0.4018 | 1.1516 | 0.7253 |
| group_Mycmodern_positive | 0.4561 | 0.3521 | 1.5779 | 0.1952 |

| Contrast | estimate | SE | p.value |
|---|---|---|---|
| ctrl_negative-ctrl cyclohex tnfa_negative | -2.7973 | 0.6474 | 1e-04 |
| ctrl_negative-ctrl starved_negative | -1.6768 | 0.5955 | 0.0116 |
| ctrl_negative-ancient_negative | -0.0349 | 0.3866 | 0.928 |
| ctrl_negative-modern_negative | -0.9448 | 0.3457 | 0.013 |
| ctrl_negative-ancient_positive | -0.1412 | 0.4018 | 0.7656 |
| ctrl_negative-modern_positive | -0.4561 | 0.3521 | 0.2472 |
| ctrl cyclohex tnfa_negative-ctrl starved_negative | 1.1205 | 0.7477 | 0.1958 |
| ctrl cyclohex tnfa_negative-ancient_negative | 2.7624 | 0.6145 | 1e-04 |
| ctrl cyclohex tnfa_negative-modern_negative | 1.8526 | 0.5917 | 0.0055 |
| ctrl cyclohex tnfa_negative-ancient_positive | 2.6561 | 0.6222 | 1e-04 |
| ctrl cyclohex tnfa_negative-modern_positive | 2.3412 | 0.5905 | 3e-04 |
| ctrl starved_negative-ancient_negative | 1.6419 | 0.5595 | 0.0091 |
| ctrl starved_negative-modern_negative | 0.732 | 0.5344 | 0.2317 |
| ctrl starved_negative-ancient_positive | 1.5356 | 0.568 | 0.013 |
| ctrl starved_negative-modern_positive | 1.2207 | 0.5331 | 0.0349 |
| ancient_negative-modern_negative | -0.9098 | 0.2814 | 0.0047 |
| ancient_positive-modern_positive | -0.3149 | 0.3081 | 0.3642 |
| ancient_negative-ancient_positive | -0.1063 | 0.2838 | 0.7656 |
| modern_negative-modern_positive | 0.4886 | 0.1865 | 0.0152 |

| Par | Estimate | se | OR | pvalue |
|---|---|---|---|---|
| (Intercept) | -1.2645 | 0.3886 | 0.2824 | 0.0011 |
| group_Myc3ancient_high burden | -0.3279 | 0.4789 | 0.7204 | 0.4935 |
| group_Myc3ancient_low burden | 0.5719 | 0.4509 | 1.7717 | 0.2047 |
| group_Myc3ancient_negative | 0.0262 | 0.3914 | 1.0266 | 0.9466 |
| group_Myc3ctrl cyclohex tnfa_negative | 2.7964 | 0.6531 | 16.386 | 0 |
| group_Myc3ctrl starved_negative | 1.6764 | 0.6018 | 5.3462 | 0.0053 |
| group_Myc3modern_high burden | 0.5664 | 0.3775 | 1.7619 | 0.1335 |
| group_Myc3modern_low burden | 0.3257 | 0.3876 | 1.385 | 0.4007 |
| group_Myc3modern_negative | 0.9465 | 0.3501 | 2.5767 | 0.0069 |

OBSERVATIONS

In M1 macrophages, bystander non-infected cells of modern strains showed increased apoptosis (40%). Despite not statistically significant and to a lesser extent, also macrophages infected with modern strains showed a similar increase in the percentage of apoptosis. Stratification of the data by mycobacterial burden showed similar apoptotic levels irrespective of the mycobacterial load in modern strains. Despite not statistically significant, also bystander non-infected cells of ancient strains with lower mycobacterial load showed a similar increase in the percentage of apoptosis.

Apoptosis > not infected control

Increased apoptosis observed, not statistically significant

**Grouping: Phylogeny**

**M2 – 24 h p.i.**

a) Percentage of live/apoptotic cells

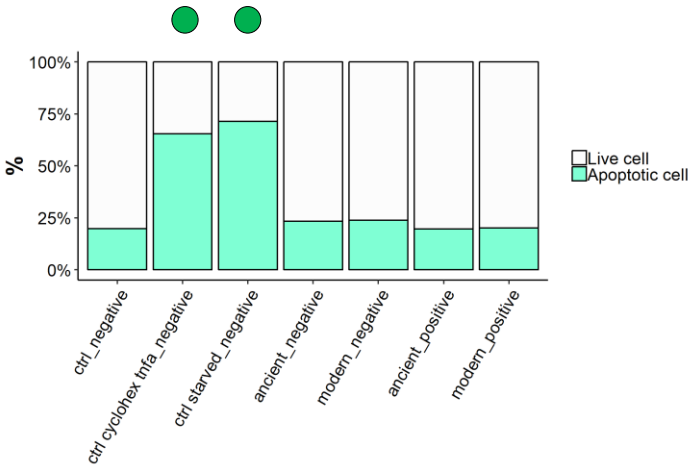


b) Percentage of live/apoptotic cells per mycobacterial burden

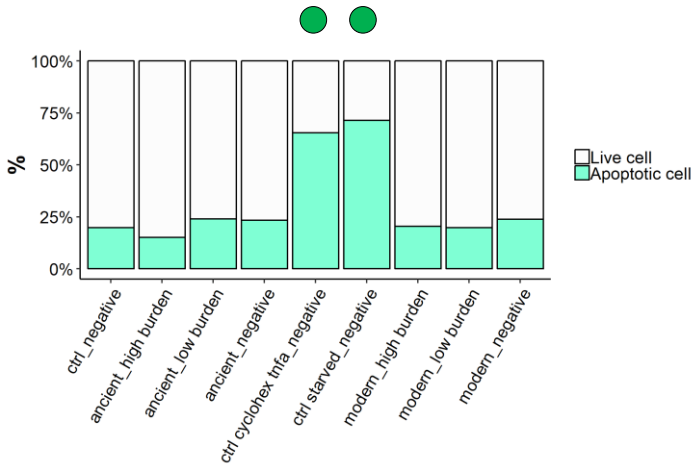


| Par | Estimate | se | OR | pvalue |
|---|---|---|---|---|
| (Intercept) | -1.4534 | 0.4649 | 0.2338 | 0.0018 |
| group_Mycctrl cyclohex tnfa_negative | 1.6515 | 0.6339 | 5.215 | 0.0092 |
| group_Mycctrl starved_negative | 1.9411 | 0.6855 | 6.9665 | 0.0046 |
| group_Mycancient_negative | 0.3881 | 0.4129 | 1.4741 | 0.3473 |
| group_Mycmodern_negative | 0.3686 | 0.3681 | 1.4458 | 0.3166 |
| group_Mycancient_positive | -0.0272 | 0.4476 | 0.9732 | 0.9516 |
| group_Mycmodern_positive | 0.0892 | 0.3746 | 1.0933 | 0.8118 |

| Contrast | estimate | SE | p.value |
|---|---|---|---|
| ctrl_negative-ctrl cyclohex tnfa_negative | -1.6515 | 0.6339 | 0.029 |
| ctrl_negative-ctrl starved_negative | -1.9411 | 0.6855 | 0.0269 |
| ctrl_negative-ancient_negative | -0.3881 | 0.4129 | 0.4714 |
| ctrl_negative-modern_negative | -0.3686 | 0.3681 | 0.4628 |
| ctrl_negative-ancient_positive | 0.0272 | 0.4476 | 0.9516 |
| ctrl_negative-modern_positive | -0.0892 | 0.3746 | 0.9073 |
| ctrl cyclohex tnfa_negative-ctrl starved_negative | -0.2896 | 0.7965 | 0.8877 |
| ctrl cyclohex tnfa_negative-ancient_negative | 1.2635 | 0.6016 | 0.0678 |
| ctrl cyclohex tnfa_negative-modern_negative | 1.2829 | 0.5717 | 0.0524 |
| ctrl cyclohex tnfa_negative-ancient_positive | 1.6787 | 0.6233 | 0.0269 |
| ctrl cyclohex tnfa_negative-modern_positive | 1.5623 | 0.576 | 0.0269 |
| ctrl starved_negative-ancient_negative | 1.5531 | 0.6557 | 0.0424 |
| ctrl starved_negative-modern_negative | 1.5725 | 0.6284 | 0.0335 |
| ctrl starved_negative-ancient_positive | 1.9683 | 0.6758 | 0.0269 |
| ctrl starved_negative-modern_positive | 1.8519 | 0.6323 | 0.0269 |
| ancient_negative-modern_negative | 0.0194 | 0.31 | 0.9516 |
| ancient_positive-modern_positive | -0.1164 | 0.3616 | 0.8877 |
| ancient_negative-ancient_positive | 0.4152 | 0.3227 | 0.3138 |
| modern_negative-modern_positive | 0.2795 | 0.1948 | 0.2616 |

| Par | Estimate | se | OR | pvalue |
|---|---|---|---|---|
| (Intercept) | -1.4594 | 0.4738 | 0.2324 | 0.0021 |
| group_Myc3ancient_high burden | -0.5157 | 0.5546 | 0.5971 | 0.3524 |
| group_Myc3ancient_low burden | 0.3953 | 0.5042 | 1.4849 | 0.433 |
| group_Myc3ancient_negative | 0.3957 | 0.4211 | 1.4855 | 0.3474 |
| group_Myc3ctrl cyclohex tnfa_negative | 1.6502 | 0.6441 | 5.2079 | 0.0104 |
| group_Myc3ctrl starved_negative | 1.9402 | 0.6952 | 6.9604 | 0.0053 |
| group_Myc3modern_high burden | 0.1666 | 0.4136 | 1.1813 | 0.6871 |
| group_Myc3modern_low burden | 0.034 | 0.4046 | 1.0346 | 0.933 |
| group_Myc3modern_negative | 0.3751 | 0.3755 | 1.4552 | 0.3178 |

OBSERVATIONS

In contrast, none of the category induced apoptosis in M2a macrophages at the time point considered.

Apoptosis > not infected control

Increased apoptosis observed, not statistically significant

## Grouping: Sample

### M1 – 24 h p.i.

a) Percentage of live/apoptotic cells

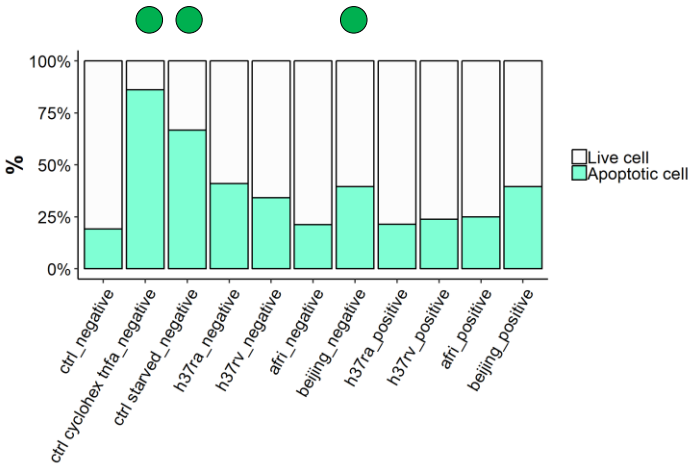


b) Percentage of live/apoptotic cells per mycobacterial burden

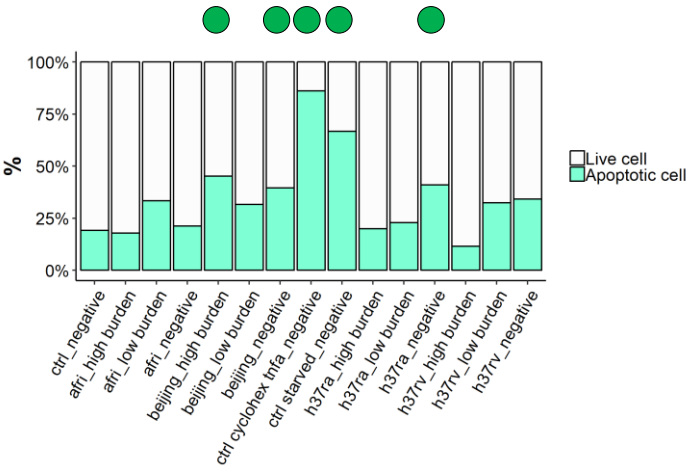


| Par | Estimate | se | OR | pvalue |
|---|---|---|---|---|
| (Intercept) | -1.2726 | 0.3691 | 0.2801 | 6e-04 |
| group_Mycctrl cyclohex tnfa_negative | 2.8169 | 0.6296 | 16.7247 | 0 |
| group_Mycctrl starved_negative | 1.6948 | 0.576 | 5.4457 | 0.0033 |
| group_Mych37ra_negative | 0.9373 | 0.4135 | 2.553 | 0.0234 |
| group_Mych37rv_negative | 0.7326 | 0.4232 | 2.0805 | 0.0834 |
| group_Mycafri_negative | 0.0445 | 0.3715 | 1.0455 | 0.9047 |
| group_Mycbeijing_negative | 1.0439 | 0.367 | 2.8402 | 0.0045 |
| group_Mych37ra_positive | -0.0568 | 0.4554 | 0.9448 | 0.9008 |
| group_Mych37rv_positive | 0.1894 | 0.4636 | 1.2086 | 0.6828 |
| group_Mycafri_positive | 0.1552 | 0.3872 | 1.1679 | 0.6886 |
| group_Mycbeijing_positive | 0.8104 | 0.3706 | 2.2489 | 0.0288 |

| Contrast | estimate | SE | p.value |
|---|---|---|---|
| ctrl_negative-ctrl cyclohex tnfa_negative | -2.8169 | 0.6296 | 1e-04 |
| ctrl_negative-ctrl starved_negative | -1.6948 | 0.576 | 0.0116 |
| ctrl_negative-h37ra_negative | -0.9373 | 0.4135 | 0.053 |
| ctrl_negative-h37rv_negative | -0.7326 | 0.4232 | 0.1494 |
| ctrl_negative-afri_negative | -0.0445 | 0.3715 | 0.9263 |
| ctrl_negative-beijing_negative | -1.0439 | 0.367 | 0.0137 |
| ctrl_negative-h37ra_positive | 0.0568 | 0.4554 | 0.9263 |
| ctrl_negative-h37rv_positive | -0.1894 | 0.4636 | 0.7666 |
| ctrl_negative-afri_positive | -0.1552 | 0.3872 | 0.7666 |
| ctrl_negative-beijing_positive | -0.8104 | 0.3706 | 0.0618 |
| ctrl cyclohex tnfa_negative-ctrl starved_negative | 1.1221 | 0.7278 | 0.1961 |
| ctrl cyclohex tnfa_negative-h37ra_negative | 1.8796 | 0.6255 | 0.0114 |
| ctrl cyclohex tnfa_negative-h37rv_negative | 2.0843 | 0.634 | 0.0062 |
| ctrl cyclohex tnfa_negative-afri_negative | 2.7724 | 0.5987 | 1e-04 |
| ctrl cyclohex tnfa_negative-beijing_negative | 1.773 | 0.599 | 0.0116 |
| ctrl cyclohex tnfa_negative-h37ra_positive | 2.8737 | 0.6516 | 1e-04 |
| ctrl cyclohex tnfa_negative-h37rv_positive | 2.6274 | 0.6601 | 6e-04 |
| ctrl cyclohex tnfa_negative-afri_positive | 2.6617 | 0.6064 | 1e-04 |
| ctrl cyclohex tnfa_negative-beijing_positive | 2.0064 | 0.5936 | 0.0052 |
| ctrl starved_negative-h37ra_negative | 0.7575 | 0.5714 | 0.2651 |
| ctrl starved_negative-h37rv_negative | 0.9622 | 0.5807 | 0.164 |
| ctrl starved_negative-afri_negative | 1.6504 | 0.5419 | 0.0111 |
| ctrl starved_negative-beijing_negative | 0.6509 | 0.5423 | 0.3191 |
| ctrl starved_negative-h37ra_positive | 1.7516 | 0.5999 | 0.0116 |
| ctrl starved_negative-h37rv_positive | 1.5054 | 0.6091 | 0.034 |
| ctrl starved_negative-afri_positive | 1.5396 | 0.5505 | 0.0148 |
| ctrl starved_negative-beijing_positive | 0.8844 | 0.5364 | 0.164 |
| h37ra_negative-h37rv_negative | 0.2047 | 0.4185 | 0.7463 |
| h37ra_negative-afri_negative | 0.8928 | 0.3661 | 0.0352 |
| h37ra_negative-beijing_negative | -0.1066 | 0.3618 | 0.8259 |
| h37rv_negative-afri_negative | 0.6881 | 0.3771 | 0.1272 |
| h37rv_negative-beijing_negative | -0.3113 | 0.3724 | 0.5254 |
| afri_negative-beijing_negative | -0.9994 | 0.3129 | 0.0075 |
| h37ra_positive-h37rv_positive | -0.2462 | 0.4972 | 0.7463 |
| h37ra_positive-afri_positive | -0.212 | 0.4263 | 0.7463 |
| h37ra_positive-beijing_positive | -0.8672 | 0.4106 | 0.071 |
| h37rv_positive-afri_positive | 0.0343 | 0.4356 | 0.9373 |
| h37rv_positive-beijing_positive | -0.621 | 0.4208 | 0.215 |
| afri_positive-beijing_positive | -0.6553 | 0.3337 | 0.0969 |
| h37ra_negative-h37ra_positive | 0.9941 | 0.3754 | 0.0217 |
| h37rv_negative-h37rv_positive | 0.5432 | 0.3864 | 0.2369 |
| afri_negative-afri_positive | -0.1107 | 0.2827 | 0.7666 |
| beijing_negative-beijing_positive | 0.2334 | 0.2607 | 0.4981 |

| Par | Estimate | se | OR | pvalue |
|---|---|---|---|---|
| (Intercept) | -1.2712 | 0.3719 | 0.2805 | 6e-04 |
| group_Myc3afri_high burden | -0.315 | 0.4725 | 0.7298 | 0.505 |
| group_Myc3afri_low burden | 0.5803 | 0.4445 | 1.7867 | 0.1917 |
| group_Myc3afri_negative | 0.032 | 0.3843 | 1.0326 | 0.9336 |
| group_Myc3beijing_high burden | 1.0956 | 0.409 | 2.991 | 0.0074 |
| group_Myc3beijing_low burden | 0.3759 | 0.4518 | 1.4563 | 0.4054 |
| group_Myc3beijing_negative | 1.051 | 0.3801 | 2.8606 | 0.0057 |
| group_Myc3ctrl cyclohex tnfa_negative | 2.8327 | 0.6446 | 16.9909 | 0 |
| group_Myc3ctrl starved_negative | 1.7119 | 0.5924 | 5.5396 | 0.0039 |
| group_Myc3h37ra_high burden | -0.1092 | 0.56 | 0.8965 | 0.8454 |
| group_Myc3h37ra_low burden | -0.0101 | 0.5521 | 0.9899 | 0.9854 |
| group_Myc3h37ra_negative | 0.9303 | 0.4284 | 2.5352 | 0.0299 |
| group_Myc3h37rv_high burden | -0.5856 | 0.7226 | 0.5568 | 0.4178 |
| group_Myc3h37rv_low burden | 0.5727 | 0.5218 | 1.7731 | 0.2723 |
| group_Myc3h37rv_negative | 0.7139 | 0.438 | 2.0419 | 0.1032 |

Apoptosis > not infected control

Increased apoptosis observed, not statistically significant

## Grouping: Sample

## M2 – 24 h p.i.

a) Percentage of live/apoptotic cells

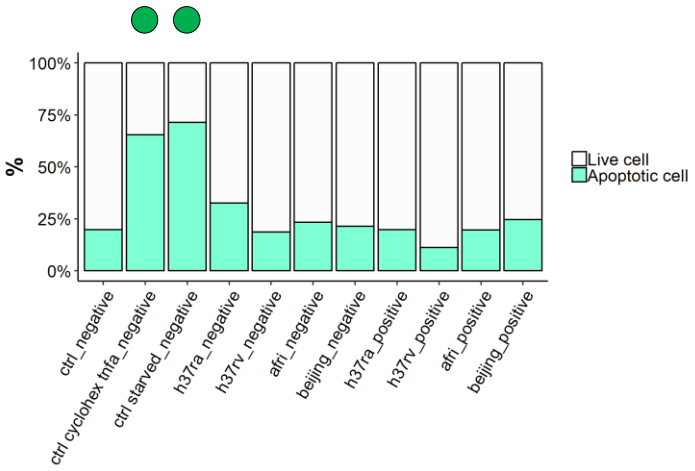


b) Percentage of live/apoptotic cells per mycobacterial burden

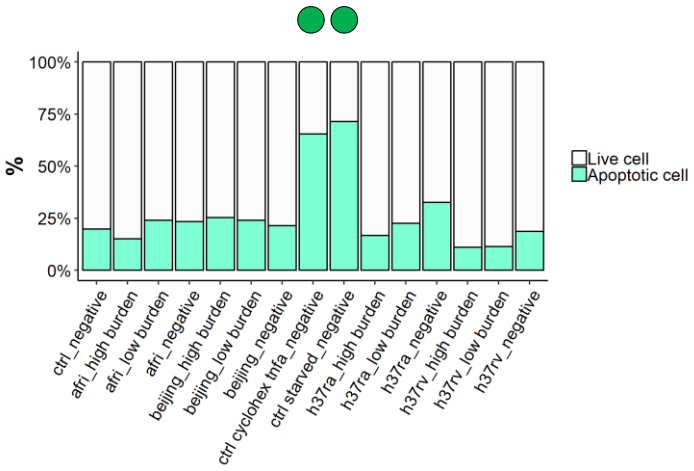


| Par | Estimate | se | OR | pvalue |
|---|---|---|---|---|
| (Intercept) | -1.4301 | 0.4477 | 0.2393 | 0.0014 |
| group_Mycctrl cyclohex tnfa_negative | 1.626 | 0.5984 | 5.0835 | 0.0066 |
| group_Mycctrl starved_negative | 1.9138 | 0.6521 | 6.7791 | 0.0033 |
| group_Mych37ra_negative | 0.7735 | 0.428 | 2.1674 | 0.0707 |
| group_Mych37rv_negative | -0.0049 | 0.4601 | 0.9951 | 0.9915 |
| group_Mycafri_negative | 0.3668 | 0.3852 | 1.4432 | 0.341 |
| group_Mycbeijing_negative | 0.2543 | 0.3839 | 1.2896 | 0.5077 |
| group_Mych37ra_positive | 0.0671 | 0.4716 | 1.0694 | 0.8869 |
| group_Mych37rv_positive | -0.5298 | 0.5107 | 0.5887 | 0.2995 |
| group_Mycafri_positive | -0.0332 | 0.4215 | 0.9674 | 0.9373 |
| group_Mycbeijing_positive | 0.31 | 0.3841 | 1.3634 | 0.4197 |

| Contrast | estimate | SE | p.value |
|---|---|---|---|
| ctrl_negative-ctrl cyclohex tnfa_negative | -1.626 | 0.5984 | 0.0369 |
| ctrl_negative-ctrl starved_negative | -1.9138 | 0.6521 | 0.0358 |
| ctrl_negative-h37ra_negative | -0.7735 | 0.428 | 0.1689 |
| ctrl_negative-h37rv_negative | 0.0049 | 0.4601 | 0.9915 |
| ctrl_negative-afri_negative | -0.3668 | 0.3852 | 0.4887 |
| ctrl_negative-beijing_negative | -0.2543 | 0.3839 | 0.642 |
| ctrl_negative-h37ra_positive | -0.0671 | 0.4716 | 0.9302 |
| ctrl_negative-h37rv_positive | 0.5298 | 0.5107 | 0.46 |
| ctrl_negative-afri_positive | 0.0332 | 0.4215 | 0.9596 |
| ctrl_negative-beijing_positive | -0.31 | 0.3841 | 0.5468 |
| ctrl cyclohex tnfa_negative-ctrl starved_negative | -0.2879 | 0.7613 | 0.8197 |
| ctrl cyclohex tnfa_negative-h37ra_negative | 0.8524 | 0.6003 | 0.3042 |
| ctrl cyclohex tnfa_negative-h37rv_negative | 1.6309 | 0.6232 | 0.0381 |
| ctrl cyclohex tnfa_negative-afri_negative | 1.2592 | 0.5712 | 0.0739 |
| ctrl cyclohex tnfa_negative-beijing_negative | 1.3716 | 0.5708 | 0.0499 |
| ctrl cyclohex tnfa_negative-h37ra_positive | 1.5589 | 0.6322 | 0.0452 |
| ctrl cyclohex tnfa_negative-h37rv_positive | 2.1558 | 0.6634 | 0.0248 |
| ctrl cyclohex tnfa_negative-afri_positive | 1.6592 | 0.5936 | 0.0369 |
| ctrl cyclohex tnfa_negative-beijing_positive | 1.316 | 0.57 | 0.0601 |
| ctrl starved_negative-h37ra_negative | 1.1403 | 0.6539 | 0.1745 |
| ctrl starved_negative-h37rv_negative | 1.9187 | 0.6749 | 0.0369 |
| ctrl starved_negative-afri_negative | 1.547 | 0.6272 | 0.0452 |
| ctrl starved_negative-beijing_negative | 1.6595 | 0.6268 | 0.0381 |
| ctrl starved_negative-h37ra_positive | 1.8468 | 0.6832 | 0.0369 |
| ctrl starved_negative-h37rv_positive | 2.4436 | 0.7122 | 0.0248 |
| ctrl starved_negative-afri_positive | 1.947 | 0.6477 | 0.0358 |
| ctrl starved_negative-beijing_positive | 1.6039 | 0.6261 | 0.0407 |
| h37ra_negative-h37rv_negative | 0.7784 | 0.4633 | 0.1903 |
| h37ra_negative-afri_negative | 0.4067 | 0.3892 | 0.46 |
| h37ra_negative-beijing_negative | 0.5192 | 0.3879 | 0.3379 |
| h37rv_negative-afri_negative | -0.3717 | 0.4242 | 0.5117 |
| h37rv_negative-beijing_negative | -0.2592 | 0.423 | 0.6634 |
| afri_negative-beijing_negative | 0.1125 | 0.3401 | 0.8383 |
| h37ra_positive-h37rv_positive | 0.5969 | 0.5506 | 0.46 |
| h37ra_positive-afri_positive | 0.1002 | 0.4689 | 0.8994 |
| h37ra_positive-beijing_positive | -0.2429 | 0.4357 | 0.6894 |
| h37rv_positive-afri_positive | -0.4966 | 0.5084 | 0.4873 |
| h37rv_positive-beijing_positive | -0.8398 | 0.4778 | 0.1745 |
| afri_positive-beijing_positive | -0.3432 | 0.3808 | 0.5097 |
| h37ra_negative-h37ra_positive | 0.7065 | 0.374 | 0.1489 |
| h37rv_negative-h37rv_positive | 0.5249 | 0.4546 | 0.4269 |
| afri_negative-afri_positive | 0.4 | 0.3207 | 0.3803 |
| beijing_negative-beijing_positive | -0.0556 | 0.2698 | 0.8994 |

| Par | Estimate | se | OR | pvalue |
|---|---|---|---|---|
| (Intercept) | -1.4382 | 0.456 | 0.2373 | 0.0016 |
| group_Myc3afri_high burden | -0.5063 | 0.5331 | 0.6027 | 0.3422 |
| group_Myc3afri_low burden | 0.3776 | 0.4817 | 1.4588 | 0.4332 |
| group_Myc3afri_negative | 0.3765 | 0.3951 | 1.4571 | 0.3407 |
| group_Myc3beijing_high burden | 0.4025 | 0.4347 | 1.4956 | 0.3545 |
| group_Myc3beijing_low burden | 0.2268 | 0.4393 | 1.2546 | 0.6056 |
| group_Myc3beijing_negative | 0.2645 | 0.3935 | 1.3028 | 0.5014 |
| group_Myc3ctrl cyclohex tnfa_negative | 1.6302 | 0.6108 | 5.1051 | 0.0076 |
| group_Myc3ctrl starved_negative | 1.9187 | 0.6637 | 6.8121 | 0.0038 |
| group_Myc3h37ra_high burden | -0.0443 | 0.5994 | 0.9567 | 0.9411 |
| group_Myc3h37ra_low burden | 0.1597 | 0.5445 | 1.1731 | 0.7693 |
| group_Myc3h37ra_negative | 0.782 | 0.4392 | 2.1859 | 0.075 |
| group_Myc3h37rv_high burden | -0.4505 | 0.7279 | 0.6373 | 0.536 |
| group_Myc3h37rv_low burden | -0.5554 | 0.577 | 0.5738 | 0.3358 |
| group_Myc3h37rv_negative | 0.004 | 0.4704 | 1.004 | 0.9932 |

Apoptosis > not infected control

Increased apoptosis observed, not statistically significant

**Grouping: Virulence (absolute)**

**M1 – 24 h p.i.**

a) Percentage of live/apoptotic cells

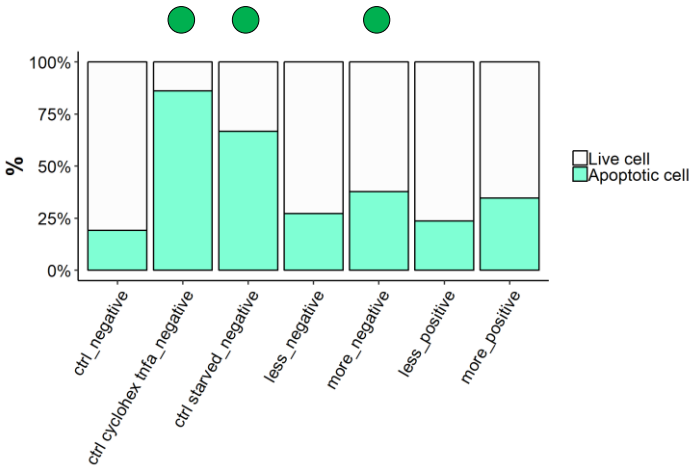


b) Percentage of live/apoptotic cells per mycobacterial burden

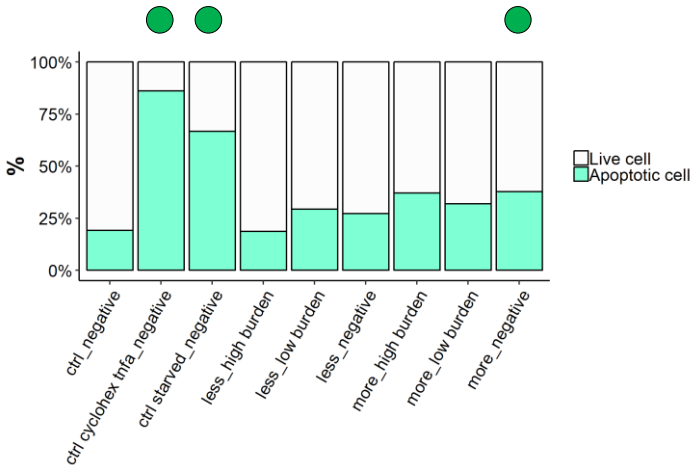


| Par | Estimate | se | OR | pvalue |
|---|---|---|---|---|
| (Intercept) | -1.2651 | 0.3868 | 0.2822 | 0.0011 |
| group_Mycctrl cyclohex tnfa_negative | 2.8053 | 0.6554 | 16.5318 | 0 |
| group_Mycctrl starved_negative | 1.6854 | 0.6042 | 5.3948 | 0.0053 |
| group_Mycless_negative | 0.3578 | 0.3645 | 1.4302 | 0.3262 |
| group_Mycmore_negative | 0.942 | 0.3651 | 2.5651 | 0.0099 |
| group_Mycless_positive | 0.0559 | 0.3786 | 1.0575 | 0.8827 |
| group_Mycmore_positive | 0.6232 | 0.3709 | 1.8648 | 0.0929 |

| Contrast | estimate | SE | p.value |
|---|---|---|---|
| ctrl_negative-ctrl cyclohex tnfa_negative | -2.8053 | 0.6554 | 2e-04 |
| ctrl_negative-ctrl starved_negative | -1.6854 | 0.6042 | 0.0143 |
| ctrl_negative-less_negative | -0.3578 | 0.3645 | 0.3443 |
| ctrl_negative-more_negative | -0.942 | 0.3651 | 0.0235 |
| ctrl_negative-less_positive | -0.0559 | 0.3786 | 0.8827 |
| ctrl_negative-more_positive | -0.6232 | 0.3709 | 0.1358 |
| ctrl cyclohex tnfa_negative-ctrl starved_negative | 1.1198 | 0.7567 | 0.178 |
| ctrl cyclohex tnfa_negative-less_negative | 2.4475 | 0.6039 | 3e-04 |
| ctrl cyclohex tnfa_negative-more_negative | 1.8633 | 0.6068 | 0.0081 |
| ctrl cyclohex tnfa_negative-less_positive | 2.7494 | 0.6102 | 1e-04 |
| ctrl cyclohex tnfa_negative-more_positive | 2.1821 | 0.6048 | 0.0015 |
| ctrl starved_negative-less_negative | 1.3276 | 0.5479 | 0.0325 |
| ctrl starved_negative-more_negative | 0.7435 | 0.5512 | 0.2013 |
| ctrl starved_negative-less_positive | 1.6296 | 0.5549 | 0.0105 |
| ctrl starved_negative-more_positive | 1.0623 | 0.549 | 0.0839 |
| less_negative-more_negative | -0.5842 | 0.2638 | 0.0509 |
| less_positive-more_positive | -0.5673 | 0.289 | 0.0839 |
| less_negative-less_positive | 0.3019 | 0.2253 | 0.2013 |
| more_negative-more_positive | 0.3188 | 0.2163 | 0.178 |

| Par | Estimate | se | OR | pvalue |
|---|---|---|---|---|
| (Intercept) | -1.2649 | 0.3877 | 0.2823 | 0.0011 |
| group_Myc3ctrl cyclohex tnfa_negative | 2.8168 | 0.6641 | 16.7232 | 0 |
| group_Myc3ctrl starved_negative | 1.6977 | 0.6138 | 5.4611 | 0.0057 |
| group_Myc3less_high burden | -0.267 | 0.4323 | 0.7657 | 0.5368 |
| group_Myc3less_low burden | 0.3554 | 0.418 | 1.4267 | 0.3952 |
| group_Myc3less_negative | 0.3494 | 0.3714 | 1.4182 | 0.3468 |
| group_Myc3more_high burden | 0.7701 | 0.4028 | 2.16 | 0.0559 |
| group_Myc3more_low burden | 0.448 | 0.4171 | 1.5652 | 0.2828 |
| group_Myc3more_negative | 0.9438 | 0.3721 | 2.5697 | 0.0112 |

OBSERVATIONS

In M1 macrophages, bystander non-infected cells of more virulent strains showed increased apoptosis (40%). Despite not statistically significant, also macrophages infected with more virulent strains showed a similar increase in the percentage of apoptosis. Stratification of the data by mycobacterial burden showed similar apoptotic levels irrespective of the mycobacterial load in more virulent strains, whereas for H37Rv higher level of apoptosis were induced in bystander non-infected cells or in cells infected with lower mycobacterial load.

Apoptosis > not infected control

Increased apoptosis observed, not statistically significant

**Grouping: Virulence (absolute)**

**M2 – 24 h p.i.**

a) Percentage of live/apoptotic cells

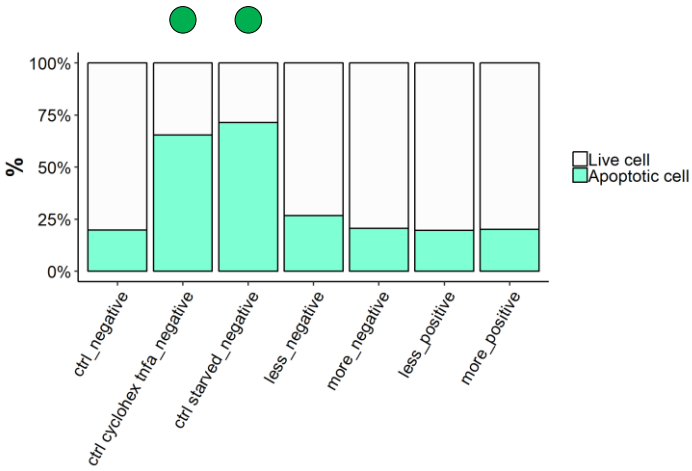


b) Percentage of live/apoptotic cells per mycobacterial burden

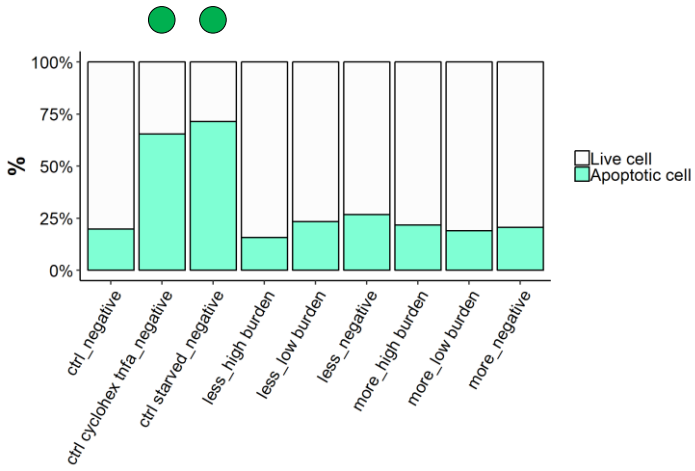


| Par | Estimate | se | OR | pvalue |
|---|---|---|---|---|
| (Intercept) | -1.4496 | 0.4623 | 0.2347 | 0.0017 |
| group_Mycctrl cyclohex tnfa_negative | 1.6467 | 0.628 | 5.1897 | 0.0087 |
| group_Mycctrl starved_negative | 1.936 | 0.6799 | 6.9308 | 0.0044 |
| group_Mycless_negative | 0.54 | 0.3768 | 1.716 | 0.1518 |
| group_Mycmore_negative | 0.1892 | 0.3811 | 1.2083 | 0.6196 |
| group_Mycless_positive | 0.0013 | 0.3991 | 1.0013 | 0.9974 |
| group_Mycmore_positive | 0.0888 | 0.385 | 1.0929 | 0.8176 |

| Contrast | estimate | SE | p.value |
|---|---|---|---|
| ctrl_negative-ctrl cyclohex tnfa_negative | -1.6467 | 0.628 | 0.0237 |
| ctrl_negative-ctrl starved_negative | -1.936 | 0.6799 | 0.0224 |
| ctrl_negative-less_negative | -0.54 | 0.3768 | 0.2404 |
| ctrl_negative-more_negative | -0.1892 | 0.3811 | 0.8392 |
| ctrl_negative-less_positive | -0.0013 | 0.3991 | 0.9974 |
| ctrl_negative-more_positive | -0.0888 | 0.385 | 0.863 |
| ctrl cyclohex tnfa_negative-ctrl starved_negative | -0.2893 | 0.7907 | 0.8484 |
| ctrl cyclohex tnfa_negative-less_negative | 1.1067 | 0.5752 | 0.0939 |
| ctrl cyclohex tnfa_negative-more_negative | 1.4575 | 0.5783 | 0.0279 |
| ctrl cyclohex tnfa_negative-less_positive | 1.6454 | 0.5885 | 0.0224 |
| ctrl cyclohex tnfa_negative-more_positive | 1.5579 | 0.5809 | 0.0232 |
| ctrl starved_negative-less_negative | 1.396 | 0.6315 | 0.0523 |
| ctrl starved_negative-more_negative | 1.7468 | 0.6344 | 0.0224 |
| ctrl starved_negative-less_positive | 1.9347 | 0.6436 | 0.0224 |
| ctrl starved_negative-more_positive | 1.8472 | 0.6367 | 0.0224 |
| less_negative-more_negative | 0.3508 | 0.2869 | 0.3237 |
| less_positive-more_positive | -0.0875 | 0.3203 | 0.863 |
| less_negative-less_positive | 0.5387 | 0.2444 | 0.0523 |
| more_negative-more_positive | 0.1004 | 0.23 | 0.8392 |

| Par | Estimate | se | OR | pvalue |
|---|---|---|---|---|
| (Intercept) | -1.4542 | 0.4666 | 0.2336 | 0.0018 |
| group_Myc3ctrl cyclohex tnfa_negative | 1.6503 | 0.6353 | 5.2083 | 0.0094 |
| group_Myc3ctrl starved_negative | 1.9399 | 0.6868 | 6.958 | 0.0047 |
| group_Myc3less_high burden | -0.3293 | 0.4683 | 0.7195 | 0.482 |
| group_Myc3less_low burden | 0.2742 | 0.4368 | 1.3154 | 0.5302 |
| group_Myc3less_negative | 0.546 | 0.3823 | 1.7263 | 0.1532 |
| group_Myc3more_high burden | 0.2189 | 0.4285 | 1.2447 | 0.6094 |
| group_Myc3more_low burden | -0.0136 | 0.4205 | 0.9864 | 0.9741 |
| group_Myc3more_negative | 0.1952 | 0.3864 | 1.2156 | 0.6134 |

OBSERVATIONS

In contrast, none of the category induced apoptosis in M2a macrophages at the time point considered.

Apoptosis > not infected control

Increased apoptosis observed, not statistically significant

**Grouping: Virulence (relative)**

**M1 – 24 h p.i.**

a) Percentage of live/apoptotic cells

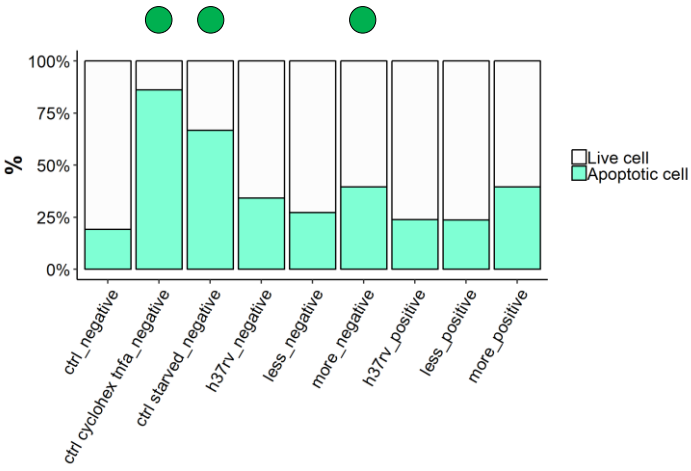


b) Percentage of live/apoptotic cells per mycobacterial burden

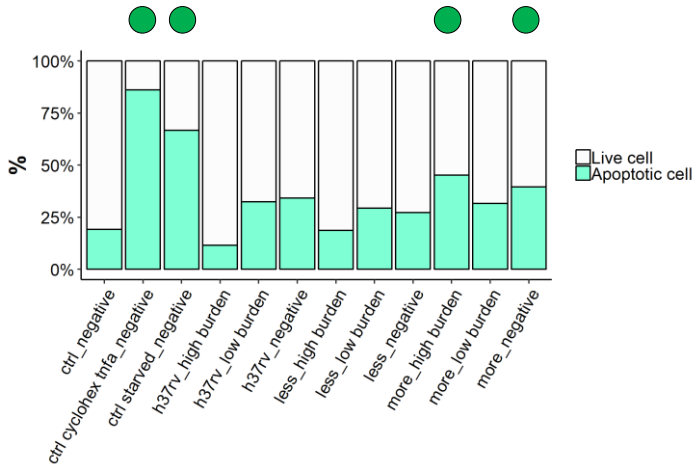


| Par | Estimate | se | OR | pvalue |
|---|---|---|---|---|
| (Intercept) | -1.269 | 0.377 | 0.2811 | 8e-04 |
| group_Mycctrl cyclohex tnfa_negative | 2.8168 | 0.6446 | 16.7231 | 0 |
| group_Mycctrl starved_negative | 1.696 | 0.5924 | 5.4523 | 0.0042 |
| group_Mych37rv_negative | 0.7271 | 0.438 | 2.0691 | 0.0969 |
| group_Mycless_negative | 0.3627 | 0.3559 | 1.4372 | 0.3082 |
| group_Mycmore_negative | 1.0425 | 0.38 | 2.8362 | 0.0061 |
| group_Mych37rv_positive | 0.1862 | 0.4775 | 1.2047 | 0.6965 |
| group_Mycless_positive | 0.0636 | 0.3703 | 1.0657 | 0.8636 |
| group_Mycmore_positive | 0.8085 | 0.3832 | 2.2445 | 0.0349 |

| Contrast | estimate | SE | p.value |
|---|---|---|---|
| ctrl_negative-ctrl cyclohex tnfa_negative | -2.8168 | 0.6446 | 2e-04 |
| ctrl_negative-ctrl starved_negative | -1.696 | 0.5924 | 0.014 |
| ctrl_negative-h37rv_negative | -0.7271 | 0.438 | 0.1791 |
| ctrl_negative-less_negative | -0.3627 | 0.3559 | 0.377 |
| ctrl_negative-more_negative | -1.0425 | 0.38 | 0.0182 |
| ctrl_negative-h37rv_positive | -0.1862 | 0.4775 | 0.7463 |
| ctrl_negative-less_positive | -0.0636 | 0.3703 | 0.8636 |
| ctrl_negative-more_positive | -0.8085 | 0.3832 | 0.0697 |
| ctrl cyclohex tnfa_negative-ctrl starved_negative | 1.1208 | 0.7446 | 0.2088 |
| ctrl cyclohex tnfa_negative-h37rv_negative | 2.0897 | 0.649 | 0.0064 |
| ctrl cyclohex tnfa_negative-less_negative | 2.4541 | 0.5946 | 4e-04 |
| ctrl cyclohex tnfa_negative-more_negative | 1.7743 | 0.6123 | 0.014 |
| ctrl cyclohex tnfa_negative-h37rv_positive | 2.6306 | 0.6748 | 7e-04 |
| ctrl cyclohex tnfa_negative-less_positive | 2.7532 | 0.601 | 1e-04 |
| ctrl cyclohex tnfa_negative-more_positive | 2.0083 | 0.607 | 0.0056 |
| ctrl starved_negative-h37rv_negative | 0.9689 | 0.5972 | 0.1791 |
| ctrl starved_negative-less_negative | 1.3334 | 0.5376 | 0.0358 |
| ctrl starved_negative-more_negative | 0.6536 | 0.5571 | 0.314 |
| ctrl starved_negative-h37rv_positive | 1.5098 | 0.6252 | 0.0368 |
| ctrl starved_negative-less_positive | 1.6324 | 0.5447 | 0.0117 |
| ctrl starved_negative-more_positive | 0.8875 | 0.5513 | 0.1791 |
| h37rv_negative-less_negative | 0.3644 | 0.3621 | 0.377 |
| h37rv_negative-more_negative | -0.3154 | 0.3855 | 0.4593 |
| less_negative-more_negative | -0.6798 | 0.2892 | 0.0402 |
| h37rv_positive-less_positive | 0.1226 | 0.4214 | 0.7977 |
| h37rv_positive-more_positive | -0.6223 | 0.4327 | 0.2256 |
| less_positive-more_positive | -0.7449 | 0.309 | 0.0368 |
| h37rv_negative-h37rv_positive | 0.5409 | 0.3871 | 0.2318 |
| less_negative-less_positive | 0.299 | 0.2248 | 0.2502 |
| more_negative-more_positive | 0.234 | 0.2621 | 0.4293 |

| Par | Estimate | se | OR | pvalue |
|---|---|---|---|---|
| (Intercept) | -1.2688 | 0.3779 | 0.2812 | 8e-04 |
| group_Myc3ctrl cyclohex tnfa_negative | 2.8409 | 0.6602 | 17.1315 | 0 |
| group_Myc3ctrl starved_negative | 1.7215 | 0.6095 | 5.5928 | 0.0047 |
| group_Myc3h37rv_high burden | -0.5929 | 0.7325 | 0.5527 | 0.4182 |
| group_Myc3h37rv_low burden | 0.5753 | 0.5357 | 1.7776 | 0.2829 |
| group_Myc3h37rv_negative | 0.7079 | 0.4535 | 2.0298 | 0.1185 |
| group_Myc3less_high burden | -0.2621 | 0.4296 | 0.7694 | 0.5418 |
| group_Myc3less_low burden | 0.3617 | 0.4152 | 1.4357 | 0.3838 |
| group_Myc3less_negative | 0.3518 | 0.3685 | 1.4217 | 0.3396 |
| group_Myc3more_high burden | 1.0983 | 0.4214 | 2.999 | 0.0092 |
| group_Myc3more_low burden | 0.3705 | 0.4635 | 1.4485 | 0.424 |
| group_Myc3more_negative | 1.0504 | 0.3935 | 2.8588 | 0.0076 |

OBSERVATIONS

In M1 macrophages, bystander non-infected cells of more virulent strains showed increased apoptosis (40%). Despite not statistically significant, also macrophages infected with more virulent strains showed a similar increase in the percentage of apoptosis. To a lesser extent, also H37Rv induced increased apoptosis of bystander non-infected cells (35%), but this was not found to be statistically significant. Stratification of the data by mycobacterial burden showed similar apoptotic levels irrespective of the mycobacterial load in more virulent strains.

Apoptosis > not infected control

Increased apoptosis observed, not statistically significant

## Grouping: Virulence (relative)

## M2 – 24 h p.i.

a) Percentage of live/apoptotic cells

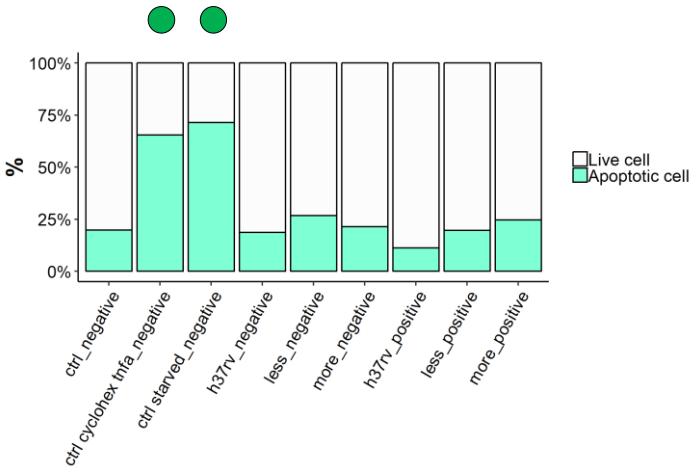


b) Percentage of live/apoptotic cells per mycobacterial burden

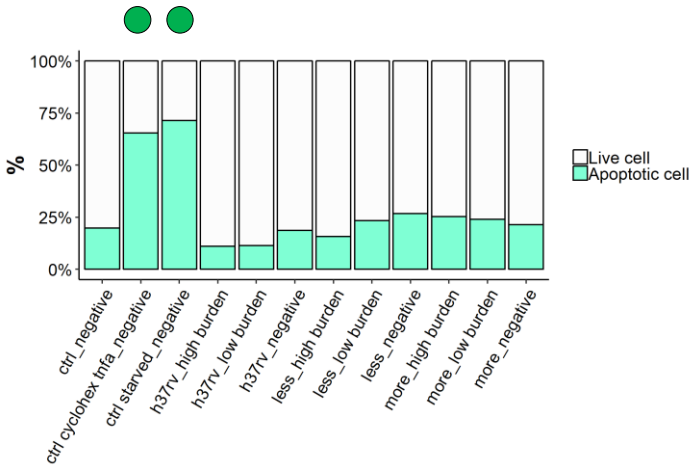


| Par | Estimate | se | OR | pvalue |
|---|---|---|---|---|
| (Intercept) | -1.435 | 0.4514 | 0.2381 | 0.0015 |
| group_Mycctrl cyclohex tnfa_negative | 1.6307 | 0.6055 | 5.1077 | 0.0071 |
| group_Mycctrl starved_negative | 1.919 | 0.6588 | 6.8139 | 0.0036 |
| group_Mych37rv_negative | 5e-04 | 0.4661 | 1.0005 | 0.9992 |
| group_Mycless_negative | 0.5266 | 0.3599 | 1.6931 | 0.1434 |
| group_Mycmore_negative | 0.2595 | 0.3895 | 1.2962 | 0.5053 |
| group_Mych37rv_positive | -0.5252 | 0.5162 | 0.5914 | 0.3089 |
| group_Mycless_positive | -0.0036 | 0.3829 | 0.9964 | 0.9924 |
| group_Mycmore_positive | 0.3132 | 0.3897 | 1.3678 | 0.4216 |

| Contrast | estimate | SE | p.value |
|---|---|---|---|
| ctrl_negative-ctrl cyclohex tnfa_negative | -1.6307 | 0.6055 | 0.0303 |
| ctrl_negative-ctrl starved_negative | -1.919 | 0.6588 | 0.0243 |
| ctrl_negative-h37rv_negative | -5e-04 | 0.4661 | 0.9992 |
| ctrl_negative-less_negative | -0.5266 | 0.3599 | 0.2531 |
| ctrl_negative-more_negative | -0.2595 | 0.3895 | 0.6064 |
| ctrl_negative-h37rv_positive | 0.5252 | 0.5162 | 0.4413 |
| ctrl_negative-less_positive | 0.0036 | 0.3829 | 0.9992 |
| ctrl_negative-more_positive | -0.3132 | 0.3897 | 0.527 |
| ctrl cyclohex tnfa_negative-ctrl starved_negative | -0.2882 | 0.7684 | 0.7862 |
| ctrl cyclohex tnfa_negative-h37rv_negative | 1.6303 | 0.6298 | 0.0321 |
| ctrl cyclohex tnfa_negative-less_negative | 1.1042 | 0.5566 | 0.0946 |
| ctrl cyclohex tnfa_negative-more_negative | 1.3713 | 0.5769 | 0.0476 |
| ctrl cyclohex tnfa_negative-h37rv_positive | 2.1559 | 0.6697 | 0.0193 |
| ctrl cyclohex tnfa_negative-less_positive | 1.6344 | 0.5702 | 0.0243 |
| ctrl cyclohex tnfa_negative-more_positive | 1.3176 | 0.5761 | 0.054 |
| ctrl starved_negative-h37rv_negative | 1.9185 | 0.6812 | 0.0243 |
| ctrl starved_negative-less_negative | 1.3924 | 0.6142 | 0.054 |
| ctrl starved_negative-more_negative | 1.6595 | 0.6326 | 0.0321 |
| ctrl starved_negative-h37rv_positive | 2.4442 | 0.7182 | 0.0193 |
| ctrl starved_negative-less_positive | 1.9226 | 0.6265 | 0.0215 |
| ctrl starved_negative-more_positive | 1.6058 | 0.6319 | 0.0331 |
| h37rv_negative-less_negative | -0.5261 | 0.4009 | 0.3158 |
| h37rv_negative-more_negative | -0.259 | 0.4277 | 0.6287 |
| less_negative-more_negative | 0.2671 | 0.3086 | 0.5045 |
| h37rv_positive-less_positive | -0.5216 | 0.4767 | 0.4108 |
| h37rv_positive-more_positive | -0.8384 | 0.482 | 0.1537 |
| less_positive-more_positive | -0.3168 | 0.3353 | 0.4702 |
| h37rv_negative-h37rv_positive | 0.5257 | 0.4546 | 0.3908 |
| less_negative-less_positive | 0.5302 | 0.2436 | 0.0633 |
| more_negative-more_positive | -0.0537 | 0.27 | 0.9025 |

| Par | Estimate | se | OR | pvalue |
|---|---|---|---|---|
| (Intercept) | -1.4407 | 0.4557 | 0.2368 | 0.0016 |
| group_Myc3ctrl cyclohex tnfa_negative | 1.6369 | 0.6143 | 5.1395 | 0.0077 |
| group_Myc3ctrl starved_negative | 1.9256 | 0.667 | 6.8592 | 0.0039 |
| group_Myc3h37rv_high burden | -0.4493 | 0.73 | 0.6381 | 0.5382 |
| group_Myc3h37rv_low burden | -0.5531 | 0.5795 | 0.5752 | 0.3398 |
| group_Myc3h37rv_negative | 0.0068 | 0.4734 | 1.0068 | 0.9885 |
| group_Myc3less_high burden | -0.3285 | 0.4548 | 0.72 | 0.4702 |
| group_Myc3less_low burden | 0.2653 | 0.4227 | 1.3038 | 0.5303 |
| group_Myc3less_negative | 0.5336 | 0.3665 | 1.7051 | 0.1454 |
| group_Myc3more_high burden | 0.4044 | 0.4372 | 1.4983 | 0.355 |
| group_Myc3more_low burden | 0.2283 | 0.4418 | 1.2565 | 0.6053 |
| group_Myc3more_negative | 0.267 | 0.3962 | 1.306 | 0.5005 |

OBSERVATIONS

In contrast, none of the category induced apoptosis in M2a macrophages at the time point considered.

Apoptosis > not infected control

Increased apoptosis observed, not statistically significant

# Immunofluorescence

The levels of IFNγ and TNFα cytokines were evaluated in fixed samples at the same positions acquired in live imaging for measuring the acidification of the phagolysosomes by the use of LysoSensor Green. We considered THP-1 M1 and M2a macrophages infected with H37Rv, H37Ra, L6, and L2 at 24 h p.i. A total of 818 single cells (405 macrophages for LysoSensor + IFNγ; 413 macrophages for LysoSensor + TNFα ) were considered for the analysis. Data were normalized on THP-1 macrophages not infected control.

The levels of MIP-1β and MCP-1 cytokines were evaluated in fixed samples. We considered THP-1 M1 and M2a macrophages infected with H37Rv, H37Ra, L6, and L2 at 24 h p.i. A total of 1268 single cells (652 macrophages for MIP-1β; 616 macrophages for MCP-1) were considered for the analysis. Data were normalized on THP-1 macrophages not infected control.

# Grouping: Geo-host adaptation

## M1 – IFNγ

a) BioPlex (bulk)

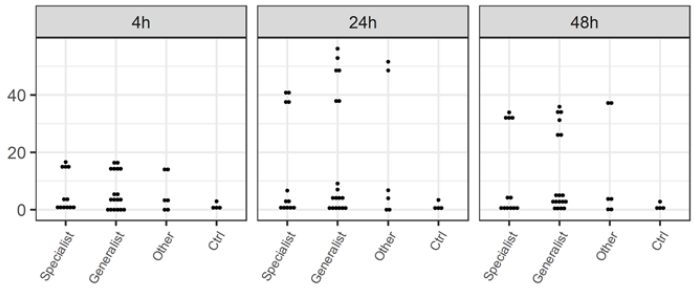


b) Immunofluorescence (single-cell) – 24 h p.i.

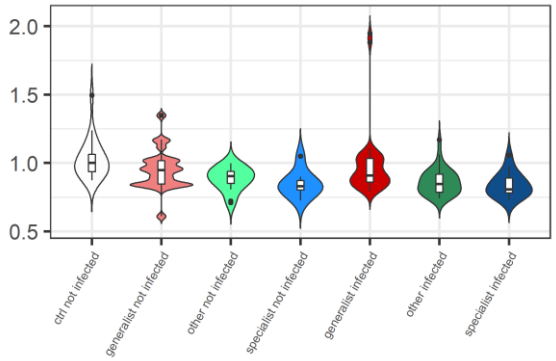


| Parameter | Estimate | Std.Error | p-value |
|---|---|---|---|
| (Intercept) | -0.218 | 0.4333 | 0.617 |
| Time24h | 0.2724 | 0.1579 | 0.0905 |
| Time48h | 0.0968 | 0.1579 | 0.5426 |
| Geo_host_adaptationGeneralist | 0.0992 | 0.1441 | 0.4944 |
| Time24h:Geo_host_adaptationGeneralist | 0.161 | 0.2038 | 0.4331 |
| Time48h:Geo_host_adaptationGeneralist | 0.1051 | 0.2038 | 0.6083 |

| contrast | Time | estimate | SE | p.value |
|---|---|---|---|---|
| Specialist - Generalist | 4h | -0.0992 | 0.1441 | 0.4944 |
| Specialist - Generalist | 24h | -0.2602 | 0.1441 | 0.0769 |
| Specialist - Generalist | 48h | -0.2043 | 0.1441 | 0.1624 |

**Linear mixed-effects model (orderNorm transformation)**

| Par | Value | Std.Error | p.value |
|---|---|---|---|
| (Intercept) | 0.5686 | 0.4369 | 0.195 |
| groupgeneralist not infected | -0.6214 | 0.2356 | 0.0092 |
| groupother not infected | -0.9222 | 0.2623 | 6e-04 |
| groupspecialist not infected | -0.7686 | 0.3654 | 0.037 |
| groupgeneralist infected | -0.5032 | 0.2162 | 0.0212 |
| groupother infected | -1.0982 | 0.2227 | 0 |
| groupspecialist infected | -0.8599 | 0.2966 | 0.0043 |

| Contrast | estimate | SE | p.value |
|---|---|---|---|
| ctrl not infected-generalist not infected | 0.6214 | 0.2356 | 0.0276 |
| ctrl not infected-other not infected | 0.9222 | 0.2623 | 0.0043 |
| ctrl not infected-specialist not infected | 0.7686 | 0.3654 | 0.0793 |
| ctrl not infected-generalist infected | 0.5032 | 0.2162 | 0.053 |
| ctrl not infected-other infected | 1.0982 | 0.2227 | 0 |
| ctrl not infected-specialist infected | 0.8599 | 0.2966 | 0.016 |
| generalist not infected-other not infected | 0.3008 | 0.255 | 0.3998 |
| generalist not infected-specialist not infected | 0.1471 | 0.3631 | 0.7349 |
| other not infected-specialist not infected | -0.1537 | 0.3684 | 0.7349 |
| generalist infected-other infected | 0.595 | 0.1903 | 0.0105 |
| generalist infected-specialist infected | 0.3567 | 0.2719 | 0.3591 |
| other infected-specialist infected | -0.2383 | 0.2593 | 0.5392 |
| generalist not infected-generalist infected | -0.1183 | 0.2061 | 0.7086 |
| other not infected-other infected | 0.1759 | 0.2378 | 0.6279 |
| specialist not infected-specialist infected | 0.0913 | 0.3557 | 0.7977 |

## M2 – IFNγ

a) BioPlex (bulk)

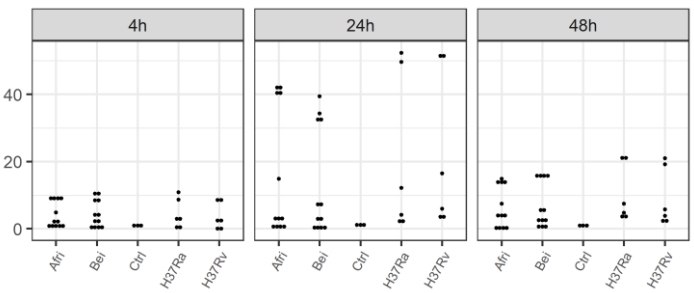


b) Immunofluorescence (single-cell) – 24 h p.i.

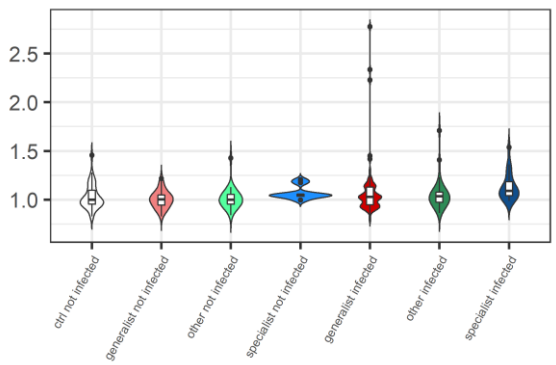


| Parameter | Estimate | Std.Error | p-value |
|---|---|---|---|
| (Intercept) | -0.2695 | 0.4404 | 0.5441 |
| Time24h | 0.626 | 0.1658 | 5e-04 |
| Time48h | 0.2761 | 0.1658 | 0.1037 |
| TypeBei | 0.0625 | 0.1658 | 0.7083 |
| Time24h:TypeBei | -0.3011 | 0.2344 | 0.2066 |
| Time48h:TypeBei | 0.0456 | 0.2344 | 0.8467 |

| contrast | Time | estimate | SE | p.value |
|---|---|---|---|---|
| Afri - Bei | 4h | -0.0625 | 0.1658 | 0.7083 |
| Afri - Bei | 24h | 0.2386 | 0.1658 | 0.158 |
| Afri - Bei | 48h | -0.1081 | 0.1658 | 0.5181 |

**Linear mixed-effects model (orderNorm transformation)**

| Par | Value | Std.Error | p.value |
|---|---|---|---|
| (Intercept) | -0.0978 | 0.3076 | 0.7508 |
| groupgeneralist not infected | -0.0621 | 0.23 | 0.7875 |
| groupother not infected | -0.1138 | 0.2514 | 0.6513 |
| groupspecialist not infected | 0.2591 | 0.3738 | 0.4889 |
| groupgeneralist infected | 0.2711 | 0.2111 | 0.2005 |
| groupother infected | 0.1776 | 0.2419 | 0.4637 |
| groupspecialist infected | 0.5534 | 0.2919 | 0.0593 |

| Contrast | estimate | SE | p.value |
|---|---|---|---|
| ctrl not infected-generalist not infected | 0.0621 | 0.23 | 0.832 |
| ctrl not infected-other not infected | 0.1138 | 0.2514 | 0.7646 |
| ctrl not infected-specialist not infected | -0.2591 | 0.3738 | 0.6667 |
| ctrl not infected-generalist infected | -0.2711 | 0.2111 | 0.6667 |
| ctrl not infected-other infected | -0.1776 | 0.2419 | 0.6667 |
| ctrl not infected-specialist infected | -0.5534 | 0.2919 | 0.5979 |
| generalist not infected-other not infected | 0.0517 | 0.2436 | 0.832 |
| generalist not infected-specialist not infected | -0.3212 | 0.376 | 0.6667 |
| other not infected-specialist not infected | -0.3729 | 0.382 | 0.6667 |
| generalist infected-other infected | 0.0936 | 0.2141 | 0.7646 |
| generalist infected-specialist infected | -0.2822 | 0.2781 | 0.6667 |
| other infected-specialist infected | -0.3758 | 0.2968 | 0.6667 |
| generalist not infected-generalist infected | -0.3332 | 0.1892 | 0.5979 |
| other not infected-other infected | -0.2914 | 0.243 | 0.6667 |
| specialist not infected-specialist infected | -0.2942 | 0.3792 | 0.6667 |

# Grouping: Geo-host adaptation

## M1 – TNFα

a) BioPlex (bulk)

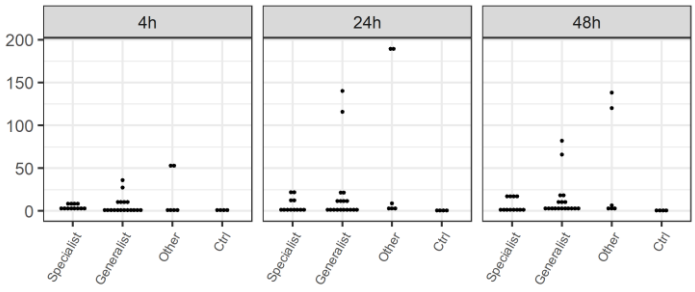


| Parameter | Estimate | Std.Error | p-value |
|---|---|---|---|
| (Intercept) | -0.2225 | 0.4461 | 0.62 |
| Time24h | 0.1489 | 0.2033 | 0.4672 |
| Time48h | 0.076 | 0.2033 | 0.71 |
| Geo_host_adaptationGeneralist | 0.1279 | 0.1856 | 0.4938 |
| Time24h:Geo_host_adaptationGeneralist | 0.1954 | 0.2625 | 0.46 |
| Time48h:Geo_host_adaptationGeneralist | 0.1498 | 0.2625 | 0.5706 |

| contrast | Time | estimate | SE | p.value |
|---|---|---|---|---|
| Specialist - Generalist | 4h | -0.1279 | 0.1856 | 0.4938 |
| Specialist - Generalist | 24h | -0.3233 | 0.1856 | 0.0875 |
| Specialist - Generalist | 48h | -0.2778 | 0.1856 | 0.1407 |

b) Immunofluorescence (single-cell) – 24 h p.i.

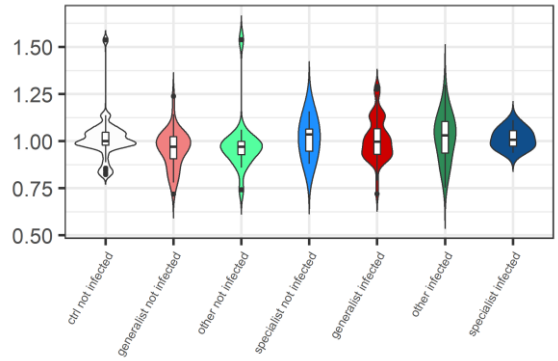


Linear mixed-effects model (orderNorm transformation)

| Par | Value | Std.Error | p.value |
|---|---|---|---|
| (Intercept) | 0.0802 | 0.201 | 0.6904 |
| groupgeneralist not infected | -0.5285 | 0.2284 | 0.0218 |
| groupother not infected | -0.3688 | 0.2884 | 0.2028 |
| groupspecialist not infected | 0.239 | 0.4778 | 0.6175 |
| groupgeneralist infected | -0.0776 | 0.2232 | 0.7284 |
| groupother infected | 0.1729 | 0.2403 | 0.4729 |
| groupspecialist infected | 0.2155 | 0.3029 | 0.4776 |

| Contrast | estimate | SE | p.value |
|---|---|---|---|
| ctrl not infected-generalist not infected | 0.5285 | 0.2284 | 0.2631 |
| ctrl not infected-other not infected | 0.3688 | 0.2884 | 0.5795 |
| ctrl not infected-specialist not infected | -0.239 | 0.4778 | 0.7718 |
| ctrl not infected-generalist infected | 0.0776 | 0.2232 | 0.8405 |
| ctrl not infected-other infected | -0.1729 | 0.2403 | 0.7165 |
| ctrl not infected-specialist infected | -0.2155 | 0.3029 | 0.7165 |
| generalist not infected-other not infected | -0.1598 | 0.2907 | 0.7718 |
| generalist not infected-specialist not infected | -0.7676 | 0.4873 | 0.4387 |
| other not infected-specialist not infected | -0.6078 | 0.5066 | 0.5795 |
| generalist infected-other infected | -0.2505 | 0.2393 | 0.6355 |
| generalist infected-specialist infected | -0.2932 | 0.3132 | 0.6571 |
| other infected-specialist infected | -0.0427 | 0.3056 | 0.9526 |
| generalist not infected-generalist infected | -0.4509 | 0.2123 | 0.2631 |
| other not infected-other infected | -0.5416 | 0.2968 | 0.3486 |
| specialist not infected-specialist infected | 0.0235 | 0.5003 | 0.9626 |

## M2 – TNFα

a) BioPlex (bulk)

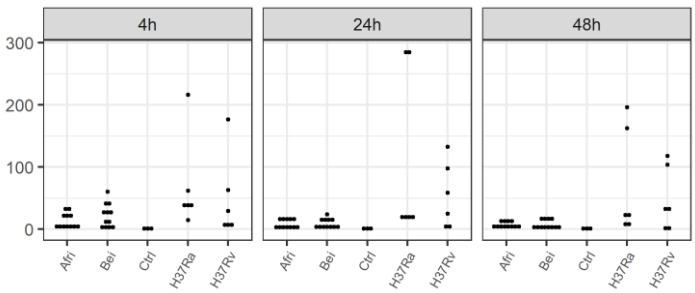


| Parameter | Estimate | Std.Error | p-value |
|---|---|---|---|
| (Intercept) | 0.1898 | 0.4231 | 0.6562 |
| Time24h | -0.4552 | 0.287 | 0.1208 |
| Time48h | -0.6237 | 0.287 | 0.0359 |
| TypeBei | 0.3431 | 0.287 | 0.2391 |
| Time24h:TypeBei | -0.2166 | 0.4059 | 0.5966 |
| Time48h:TypeBei | -0.1413 | 0.4059 | 0.7296 |

| contrast | Time | estimate | SE | p.value |
|---|---|---|---|---|
| Afri - Bei | 4h | -0.3431 | 0.287 | 0.2391 |
| Afri - Bei | 24h | -0.1265 | 0.287 | 0.6619 |
| Afri - Bei | 48h | -0.2018 | 0.287 | 0.4862 |

b) Immunofluorescence (single-cell) – 24 h p.i.

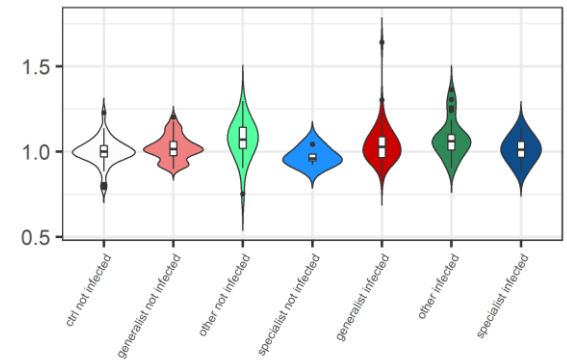


Linear mixed-effects model (orderNorm transformation)

| Par | Value | Std.Error | p.value |
|---|---|---|---|
| (Intercept) | -0.3527 | 0.2867 | 0.22 |
| groupgeneralist not infected | 0.1622 | 0.3621 | 0.6547 |
| groupother not infected | 0.6882 | 0.4296 | 0.1107 |
| groupspecialist not infected | -0.3673 | 0.6503 | 0.5728 |
| groupgeneralist infected | 0.4523 | 0.3577 | 0.2075 |
| groupother infected | 0.7937 | 0.4138 | 0.0565 |
| groupspecialist infected | 0.1405 | 0.516 | 0.7856 |

| Contrast | estimate | SE | p.value |
|---|---|---|---|
| ctrl not infected-generalist not infected | -0.1622 | 0.3621 | 0.7391 |
| ctrl not infected-other not infected | -0.6882 | 0.4296 | 0.4424 |
| ctrl not infected-specialist not infected | 0.3673 | 0.6503 | 0.716 |
| ctrl not infected-generalist infected | -0.4523 | 0.3577 | 0.4559 |
| ctrl not infected-other infected | -0.7937 | 0.4138 | 0.4424 |
| ctrl not infected-specialist infected | -0.1405 | 0.516 | 0.7856 |
| generalist not infected-other not infected | -0.5261 | 0.389 | 0.4559 |
| generalist not infected-specialist not infected | 0.5295 | 0.6242 | 0.5959 |
| other not infected-specialist not infected | 1.0555 | 0.6656 | 0.4424 |
| generalist infected-other infected | -0.3414 | 0.3671 | 0.589 |
| generalist infected-specialist infected | 0.3117 | 0.4794 | 0.7039 |
| other infected-specialist infected | 0.6532 | 0.5226 | 0.4559 |
| generalist not infected-generalist infected | -0.2901 | 0.1848 | 0.4424 |
| other not infected-other infected | -0.1055 | 0.2639 | 0.7391 |
| specialist not infected-specialist infected | -0.5078 | 0.5309 | 0.589 |

**Correlation between phagolysosomal acidification (LysoSensor) and IFNγ (immunofluorescence)**

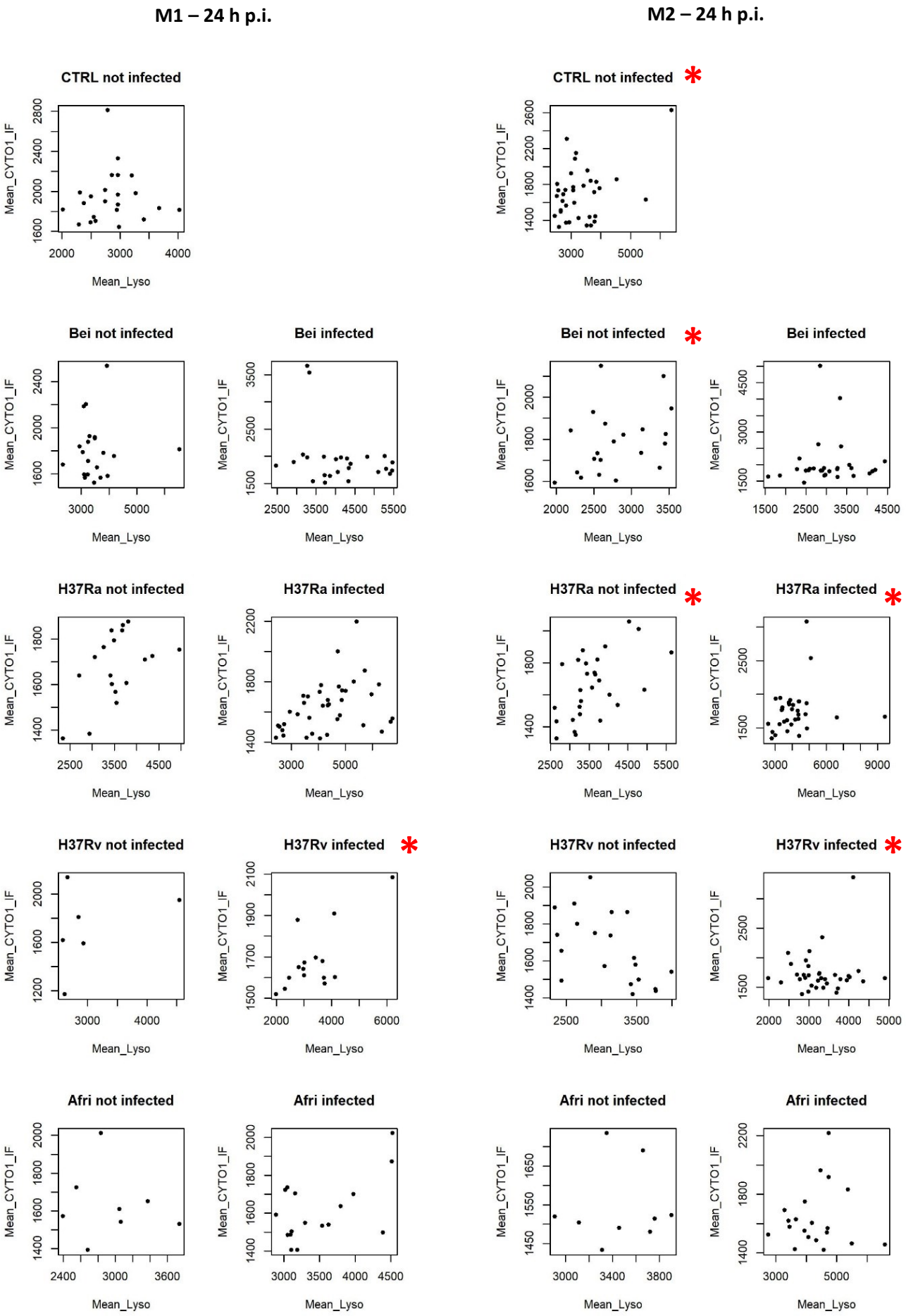


* Statistically significant correlation

**Correlation between phagolysosomal acidification (LysoSensor) and TNFα (immunofluorescence)**

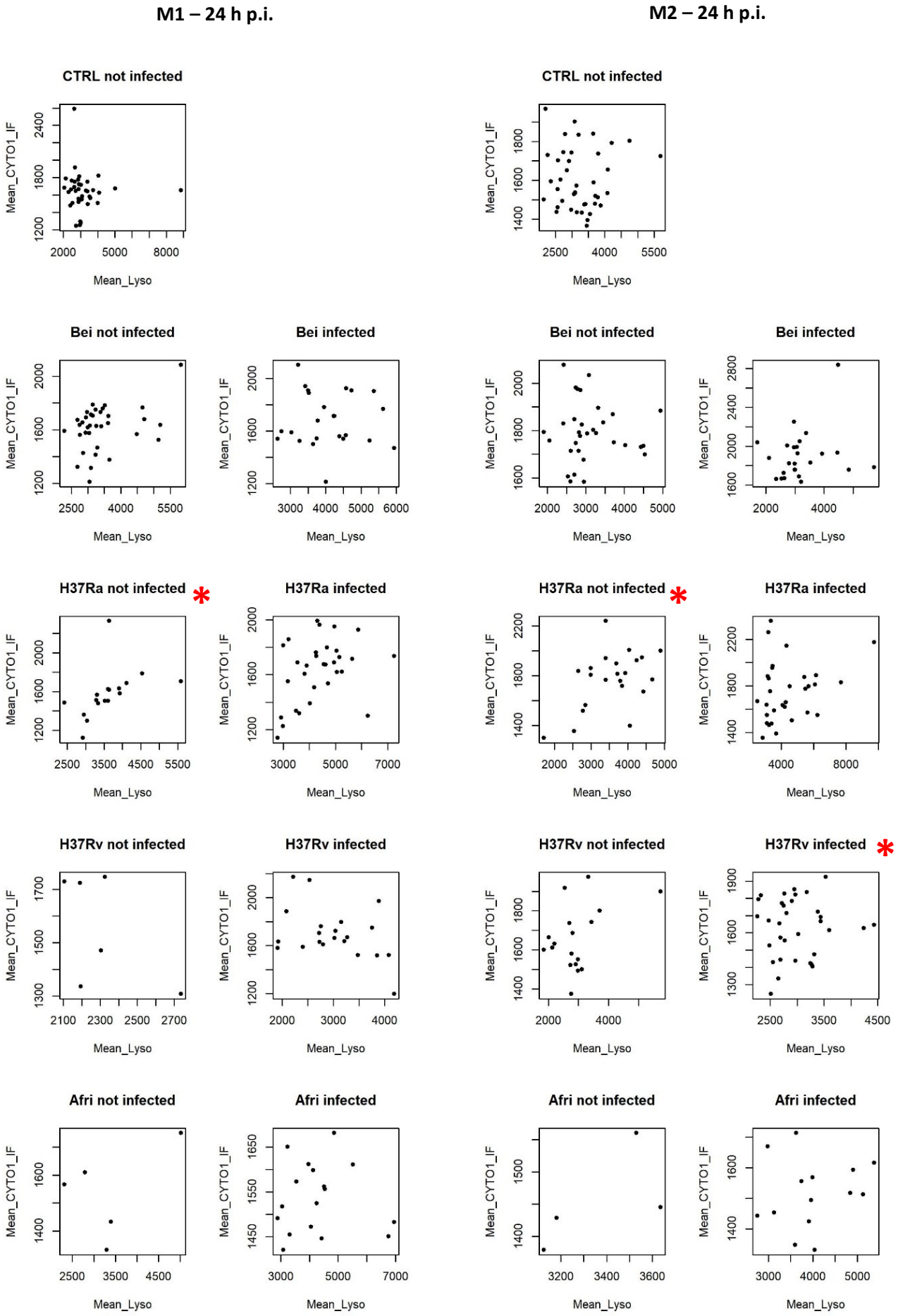


* Statistically significant correlation

# Grouping: Geo-host adaptation

## M1 – MIP-1β (CCL4)

a) BioPlex (bulk)

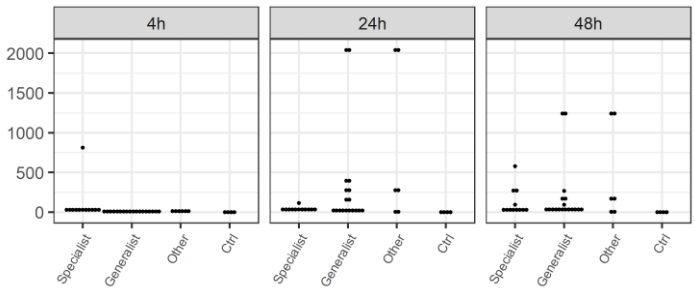


| Parameter | Estimate | Std.Error | p-value |
|---|---|---|---|
| (Intercept) | -0.8512 | 0.4674 | 0.0745 |
| Time24h | 0.5214 | 0.2749 | 0.0636 |
| Time48h | 0.6709 | 0.2749 | 0.0182 |
| Geo_host_adaptationGeneralist | 0.1332 | 0.251 | 0.5978 |
| Time24h:Geo_host_adaptationGeneralist | 0.5717 | 0.3549 | 0.1134 |
| Time48h:Geo_host_adaptationGeneralist | 0.0954 | 0.3549 | 0.7893 |

| contrast | Time | estimate | SE | p.value |
|---|---|---|---|---|
| Specialist - Generalist | 4h | -0.1332 | 0.251 | 0.5978 |
| Specialist - Generalist | 24h | -0.7049 | 0.251 | 0.007 |
| Specialist - Generalist | 48h | -0.2286 | 0.251 | 0.3667 |

b) Immunofluorescence (single-cell) – 24 h p.i.

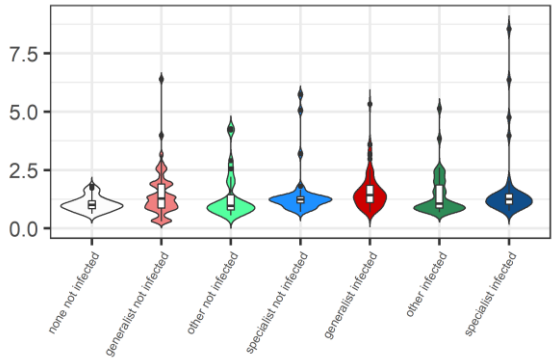


| Par | Value | Std.Error | p.value |
|---|---|---|---|
| (Intercept) | 0.0222 | 0.3033 | 0.9417 |
| groupgeneralist not infected | 0.4717 | 0.1851 | 0.0113 |
| groupother not infected | 0.3029 | 0.2097 | 0.1496 |
| groupspecialist not infected | -0.0756 | 0.222 | 0.7338 |
| groupgeneralist infected | 0.5263 | 0.1832 | 0.0044 |
| groupother infected | 0.2395 | 0.207 | 0.2483 |
| groupspecialist infected | -0.1113 | 0.2207 | 0.6145 |

| Contrast | estimate | SE | p.value |
|---|---|---|---|
| none not infected-generalist not infected | -0.4717 | 0.1851 | 0.0448 |
| none not infected-other not infected | -0.3029 | 0.2097 | 0.2805 |
| none not infected-specialist not infected | 0.0756 | 0.222 | 0.7338 |
| none not infected-generalist infected | -0.5263 | 0.1832 | 0.0329 |
| none not infected-other infected | -0.2395 | 0.207 | 0.4138 |
| none not infected-specialist infected | 0.1113 | 0.2207 | 0.6687 |
| generalist not infected-other not infected | 0.1688 | 0.189 | 0.4874 |
| generalist not infected-specialist not infected | 0.5473 | 0.2163 | 0.0448 |
| other not infected-specialist not infected | 0.3785 | 0.2258 | 0.2599 |
| generalist infected-other infected | 0.2868 | 0.1845 | 0.2599 |
| generalist infected-specialist infected | 0.6376 | 0.2136 | 0.0329 |
| other infected-specialist infected | 0.3508 | 0.2216 | 0.2599 |
| generalist not infected-generalist infected | -0.0546 | 0.0557 | 0.4874 |
| other not infected-other infected | 0.0634 | 0.0736 | 0.4874 |
| specialist not infected-specialist infected | 0.0357 | 0.0727 | 0.6687 |

## M2 – MIP-1β (CCL4)

a) BioPlex (bulk)

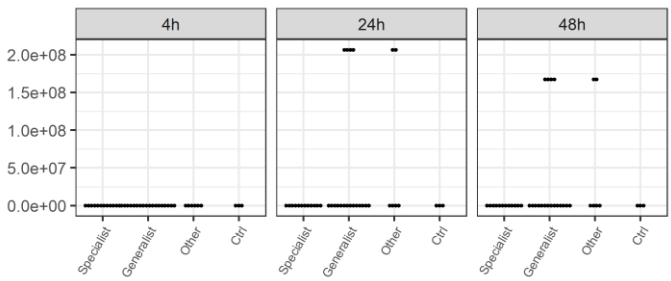


| Parameter | Estimate | Std.Error | p-value |
|---|---|---|---|
| (Intercept) | -1.0577 | 0.3966 | 0.0102 |
| Time24h | 1.2369 | 0.3517 | 9e-04 |
| Time48h | 0.83 | 0.3517 | 0.0221 |
| Geo_host_adaptationGeneralist | 0.5531 | 0.3211 | 0.091 |
| Time24h:Geo_host_adaptationGeneralist | -0.3937 | 0.4541 | 0.3899 |
| Time48h:Geo_host_adaptationGeneralist | -0.1473 | 0.4541 | 0.747 |

| contrast | Time | estimate | SE | p.value |
|---|---|---|---|---|
| Specialist - Generalist | 4h | -0.5531 | 0.3211 | 0.091 |
| Specialist - Generalist | 24h | -0.1594 | 0.3211 | 0.6217 |
| Specialist - Generalist | 48h | -0.4058 | 0.3211 | 0.212 |

b) Immunofluorescence (single-cell) – 24 h p.i.

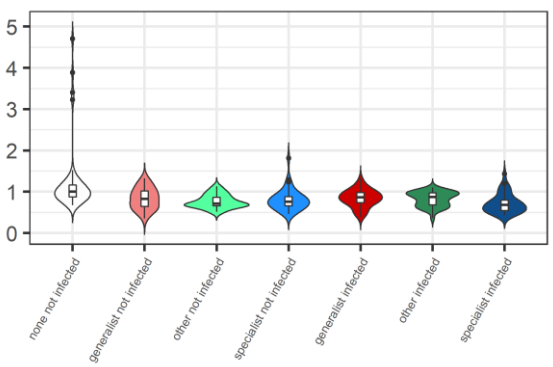


| Par | Value | Std.Error | p.value |
|---|---|---|---|
| (Intercept) | -0.0087 | 0.1779 | 0.9612 |
| groupgeneralist not infected | -0.2449 | 0.143 | 0.0877 |
| groupother not infected | -0.2794 | 0.1628 | 0.0871 |
| groupspecialist not infected | -0.105 | 0.1715 | 0.541 |
| groupgeneralist infected | -0.2823 | 0.1426 | 0.0487 |
| groupother infected | -0.2026 | 0.1619 | 0.2117 |
| groupspecialist infected | -0.2201 | 0.1716 | 0.2006 |

| Contrast | estimate | SE | p.value |
|---|---|---|---|
| none not infected-generalist not infected | 0.2449 | 0.143 | 0.3133 |
| none not infected-other not infected | 0.2794 | 0.1628 | 0.3133 |
| none not infected-specialist not infected | 0.105 | 0.1715 | 0.7216 |
| none not infected-generalist infected | 0.2823 | 0.1426 | 0.3133 |
| none not infected-other infected | 0.2026 | 0.1619 | 0.4536 |
| none not infected-specialist infected | 0.2201 | 0.1716 | 0.4536 |
| generalist not infected-other not infected | 0.0344 | 0.1442 | 0.8695 |
| generalist not infected-specialist not infected | -0.14 | 0.1631 | 0.5873 |
| other not infected-specialist not infected | -0.1744 | 0.1719 | 0.5189 |
| generalist infected-other infected | -0.0797 | 0.1428 | 0.7216 |
| generalist infected-specialist infected | -0.0622 | 0.163 | 0.8111 |
| other infected-specialist infected | 0.0174 | 0.1712 | 0.9189 |
| generalist not infected-generalist infected | 0.0373 | 0.033 | 0.4844 |
| other not infected-other infected | -0.0767 | 0.0471 | 0.3133 |
| specialist not infected-specialist infected | 0.1151 | 0.0444 | 0.1494 |

# Grouping: Geo-host adaptation

## M1 – MCP-1

a) BioPlex (bulk)

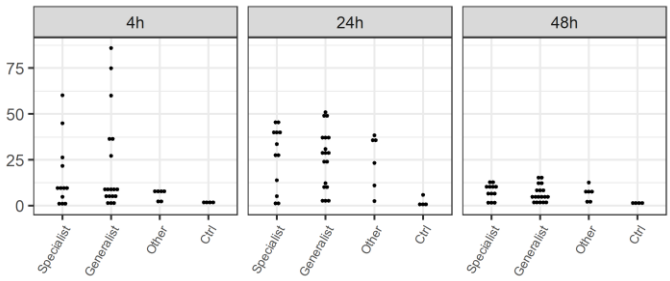


| Parameter | Estimate | Std.Error | p-value |
|---|---|---|---|
| (Intercept) | 1.3888 | 0.6863 | 0.0483 |
| Time24h | 0.9816 | 0.371 | 0.0108 |
| Time48h | -0.06 | 0.371 | 0.8721 |
| Geo_host_adaptationGeneralist | 0.5813 | 0.3387 | 0.0922 |
| Time24h:Geo_host_adaptationGeneralist | -0.3471 | 0.4789 | 0.4719 |
| Time48h:Geo_host_adaptationGeneralist | -0.5931 | 0.4789 | 0.2213 |

| contrast | Time | ratio | SE | p.value |
|---|---|---|---|---|
| Specialist / Generalist | 4h | 0.5592 | 0.1894 | 0.0922 |
| Specialist / Generalist | 24h | 0.7912 | 0.268 | 0.4924 |
| Specialist / Generalist | 48h | 1.0119 | 0.3427 | 0.9724 |

b) Immunofluorescence (single-cell) – 24 h p.i.

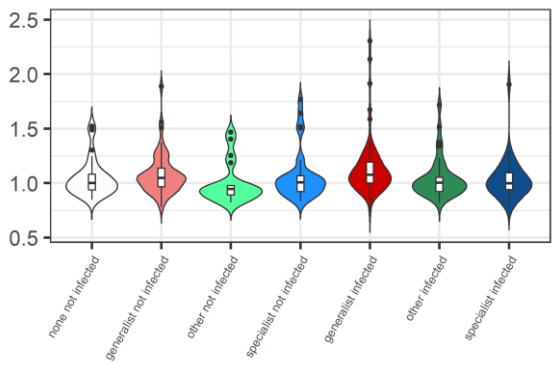


| Par | Value | Std.Error | p.value |
|---|---|---|---|
| (Intercept) | 0.003 | 0.047 | 0.9498 |
| groupgeneralist not infected | 0.0471 | 0.0579 | 0.4169 |
| groupother not infected | -0.0679 | 0.0691 | 0.3266 |
| groupspecialist not infected | -0.0236 | 0.0674 | 0.726 |
| groupgeneralist infected | 0.0709 | 0.0575 | 0.2184 |
| groupother infected | 0.0038 | 0.0665 | 0.9541 |
| groupspecialist infected | 0.0037 | 0.0664 | 0.955 |

| Contrast | estimate | SE | p.value |
|---|---|---|---|
| none not infected-generalist not infected | -0.0471 | 0.0579 | 0.6254 |
| none not infected-other not infected | 0.0679 | 0.0691 | 0.5443 |
| none not infected-specialist not infected | 0.0236 | 0.0674 | 0.9075 |
| none not infected-generalist infected | -0.0709 | 0.0575 | 0.5245 |
| none not infected-other infected | -0.0038 | 0.0665 | 0.999 |
| none not infected-specialist infected | -0.0037 | 0.0664 | 0.999 |
| generalist not infected-other not infected | 0.115 | 0.0609 | 0.4497 |
| generalist not infected-specialist not infected | 0.0707 | 0.0589 | 0.5245 |
| other not infected-specialist not infected | -0.0442 | 0.0699 | 0.7194 |
| generalist infected-other infected | 0.0671 | 0.0576 | 0.5245 |
| generalist infected-specialist infected | 0.0672 | 0.0573 | 0.5245 |
| other infected-specialist infected | 1e-04 | 0.0664 | 0.999 |
| generalist not infected-generalist infected | -0.0239 | 0.0185 | 0.5245 |
| other not infected-other infected | -0.0717 | 0.0314 | 0.3465 |
| specialist not infected-specialist infected | -0.0274 | 0.0271 | 0.5443 |

## M2 – MCP-1

a) BioPlex (bulk)

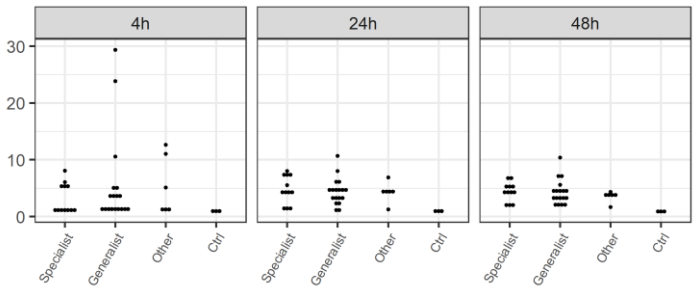


| Parameter | Estimate | Std.Error | p-value |
|---|---|---|---|
| (Intercept) | 0.7511 | 0.3205 | 0.023 |
| Time24h | 0.4851 | 0.3106 | 0.1246 |
| Time48h | 0.5348 | 0.3106 | 0.0912 |
| Geo_host_adaptationGeneralist | 0.2181 | 0.2836 | 0.4454 |
| Time24h:Geo_host_adaptationGeneralist | -0.2826 | 0.401 | 0.4842 |
| Time48h:Geo_host_adaptationGeneralist | -0.2724 | 0.401 | 0.5 |

| contrast | Time | ratio | SE | p.value |
|---|---|---|---|---|
| Specialist / Generalist | 4h | 0.8041 | 0.228 | 0.4454 |
| Specialist / Generalist | 24h | 1.0667 | 0.3025 | 0.8209 |
| Specialist / Generalist | 48h | 1.0559 | 0.2994 | 0.8487 |

b) Immunofluorescence (single-cell) – 24 h p.i.

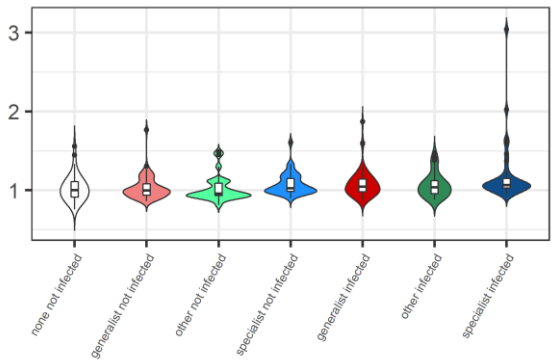


| Par | Value | Std.Error | p.value |
|---|---|---|---|
| (Intercept) | 0.0013 | 0.0304 | 0.9664 |
| groupgeneralist not infected | 0.0228 | 0.0249 | 0.3589 |
| groupother not infected | -0.0248 | 0.0299 | 0.4072 |
| groupspecialist not infected | 0.0361 | 0.0295 | 0.2223 |
| groupgeneralist infected | 0.0597 | 0.0245 | 0.0156 |
| groupother infected | 0.0603 | 0.0276 | 0.0298 |
| groupspecialist infected | 0.054 | 0.0305 | 0.0779 |

| Contrast | estimate | SE | p.value |
|---|---|---|---|
| none not infected-generalist not infected | -0.0228 | 0.0249 | 0.5981 |
| none not infected-other not infected | 0.0248 | 0.0299 | 0.6107 |
| none not infected-specialist not infected | -0.0361 | 0.0295 | 0.4168 |
| none not infected-generalist infected | -0.0597 | 0.0245 | 0.1173 |
| none not infected-other infected | -0.0603 | 0.0276 | 0.1488 |
| none not infected-specialist infected | -0.054 | 0.0305 | 0.1845 |
| generalist not infected-other not infected | 0.0477 | 0.0277 | 0.1845 |
| generalist not infected-specialist not infected | -0.0132 | 0.0279 | 0.7942 |
| other not infected-specialist not infected | -0.0609 | 0.031 | 0.1599 |
| generalist infected-other infected | -7e-04 | 0.0248 | 0.979 |
| generalist infected-specialist infected | 0.0057 | 0.0293 | 0.9073 |
| other infected-specialist infected | 0.0063 | 0.0303 | 0.9073 |
| generalist not infected-generalist infected | -0.0369 | 0.019 | 0.1599 |
| other not infected-other infected | -0.0852 | 0.0269 | 0.0262 |
| specialist not infected-specialist infected | -0.018 | 0.026 | 0.6679 |

# Cytokines

# IL-1β (logarithmic transformation)

## M1

### Geo_host_adaptation

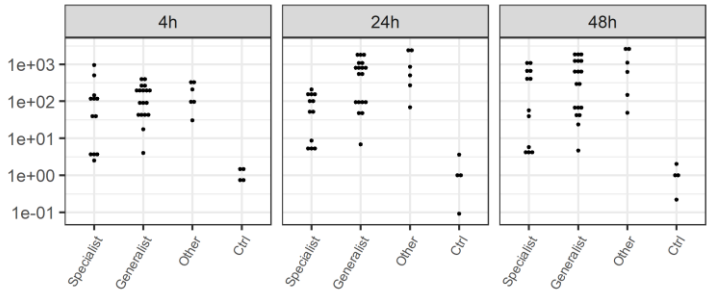


| Parameter | Estimate | Std.Error | p-value |
|---|---|---|---|
| (Intercept) | 3.1332 | 0.898 | 0.001 |
| Time24h | 0.126 | 0.5026 | 0.803 |
| Time48h | 0.6053 | 0.5026 | 0.234 |
| Geo_host_adaptationGeneralist | 1.0797 | 0.4588 | 0.0225 |
| Time24h:Geo_host_adaptationGeneralist | 1.0129 | 0.6488 | 0.1247 |
| Time48h:Geo_host_adaptationGeneralist | 0.2476 | 0.6488 | 0.7043 |

| contrast | Time | ratio | SE | p.value |
|---|---|---|---|---|
| Specialist / Generalist | 4h | 0.3397 | 0.1558 | 0.0225 |
| Specialist / Generalist | 24h | 0.1234 | 0.0566 | <0.0001 |
| Specialist / Generalist | 48h | 0.2652 | 0.1217 | 0.0056 |

### Lab_adaptation

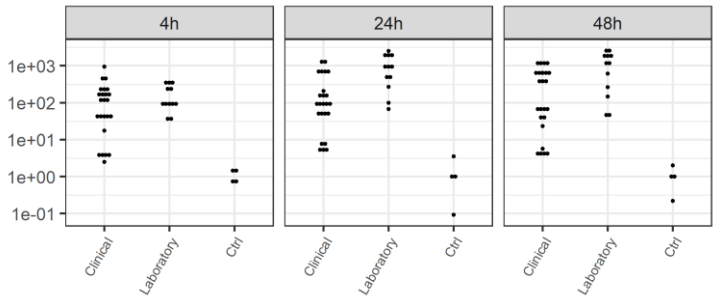


| Parameter | Estimate | Std.Error | p-value |
|---|---|---|---|
| (Intercept) | 3.5932 | 0.8327 | 1e-04 |
| Time24h | 0.4926 | 0.3461 | 0.1595 |
| Time48h | 0.5607 | 0.3461 | 0.1102 |
| Lab_adaptationLaboratory | 1.0004 | 0.4238 | 0.0214 |
| Time24h:Lab_adaptationLaboratory | 1.0395 | 0.5994 | 0.0877 |
| Time48h:Lab_adaptationLaboratory | 0.8204 | 0.5994 | 0.176 |

| contrast | Time | ratio | SE | p.value |
|---|---|---|---|---|
| Clinical / Laboratory | 4h | 0.3677 | 0.1559 | 0.0214 |
| Clinical / Laboratory | 24h | 0.13 | 0.0551 | <0.0001 |
| Clinical / Laboratory | 48h | 0.1619 | 0.0686 | 1e-04 |

## M2

### Geo_host_adaptation

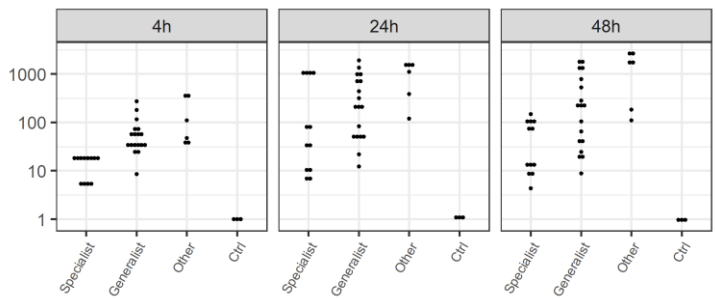


| Parameter | Estimate | Std.Error | p-value |
|---|---|---|---|
| (Intercept) | 2.2805 | 0.6836 | 0.0016 |
| Time24h | 1.5483 | 0.4843 | 0.0024 |
| Time48h | 0.8123 | 0.4843 | 0.0996 |
| Geo_host_adaptationGeneralist | 1.4036 | 0.4421 | 0.0025 |
| Time24h:Geo_host_adaptationGeneralist | -0.2928 | 0.6252 | 0.6415 |
| Time48h:Geo_host_adaptationGeneralist | 0.1804 | 0.6252 | 0.7741 |

| contrast | Time | ratio | SE | p.value |
|---|---|---|---|---|
| Specialist / Generalist | 4h | 0.2457 | 0.1086 | 0.0025 |
| Specialist / Generalist | 24h | 0.3293 | 0.1456 | 0.0152 |
| Specialist / Generalist | 48h | 0.2051 | 0.0907 | 8e-04 |

### Lab_adaptation

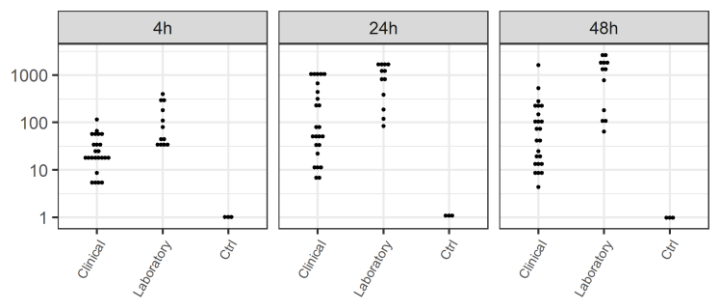


| Parameter | Estimate | Std.Error | p-value |
|---|---|---|---|
| (Intercept) | 2.8781 | 0.6266 | <0.0001 |
| Time24h | 1.2575 | 0.3153 | 2e-04 |
| Time48h | 0.7271 | 0.3153 | 0.0244 |
| Lab_adaptationLaboratory | 1.347 | 0.3862 | 9e-04 |
| Time24h:Lab_adaptationLaboratory | 0.6441 | 0.5462 | 0.2427 |
| Time48h:Lab_adaptationLaboratory | 1.111 | 0.5462 | 0.0462 |

| contrast | Time | ratio | SE | p.value |
|---|---|---|---|---|
| Clinical / Laboratory | 4h | 0.26 | 0.1004 | 9e-04 |
| Clinical / Laboratory | 24h | 0.1365 | 0.0527 | <0.0001 |
| Clinical / Laboratory | 48h | 0.0856 | 0.0331 | <0.0001 |

# IL-1ra (logarithmic transformation)

## M1

### Geo_host_adaptation

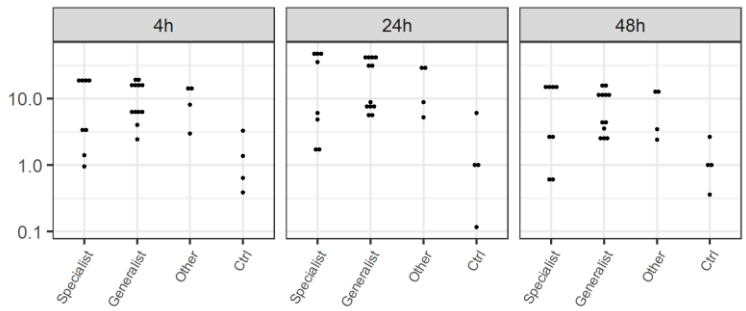


| Parameter | Estimate | Std.Error | p-value |
|---|---|---|---|
| (Intercept) | 1.4289 | 0.6462 | 0.0333 |
| Time24h | 0.5749 | 0.2723 | 0.0416 |
| Time48h | -0.3663 | 0.2723 | 0.1868 |
| Geo_host_adaptationGeneralist | 0.5735 | 0.2486 | 0.0268 |
| Time24h:Geo_host_adaptationGeneralist | -0.068 | 0.3516 | 0.8476 |
| Time48h:Geo_host_adaptationGeneralist | -0.0159 | 0.3516 | 0.9641 |

| contrast | Time | ratio | SE | p.value |
|---|---|---|---|---|
| Specialist / Generalist | 4h | 0.5636 | 0.1401 | 0.0268 |
| Specialist / Generalist | 24h | 0.6032 | 0.15 | 0.0493 |
| Specialist / Generalist | 48h | 0.5726 | 0.1424 | 0.031 |

### Lab_adaptation

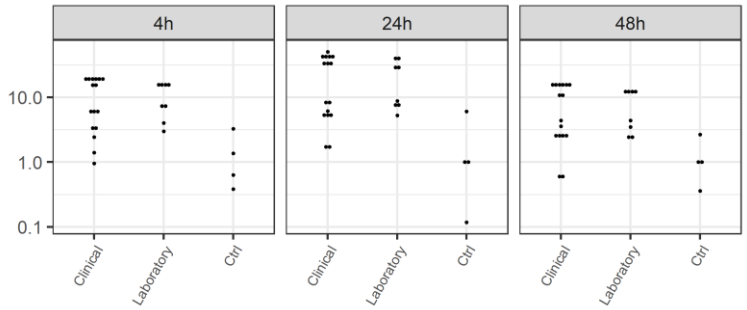


| Parameter | Estimate | Std.Error | p-value |
|---|---|---|---|
| (Intercept) | 1.7107 | 0.6045 | 0.0069 |
| Time24h | 0.529 | 0.2101 | 0.0154 |
| Time48h | -0.3688 | 0.2101 | 0.0859 |
| Lab_adaptationLaboratory | 0.2718 | 0.2574 | 0.2964 |
| Time24h:Lab_adaptationLaboratory | -0.0253 | 0.364 | 0.9449 |
| Time48h:Lab_adaptationLaboratory | -0.0273 | 0.364 | 0.9405 |

| contrast | Time | ratio | SE | p.value |
|---|---|---|---|---|
| Clinical / Laboratory | 4h | 0.762 | 0.1961 | 0.2964 |
| Clinical / Laboratory | 24h | 0.7815 | 0.2011 | 0.3431 |
| Clinical / Laboratory | 48h | 0.7831 | 0.2015 | 0.347 |

## M2

### Geo_host_adaptation

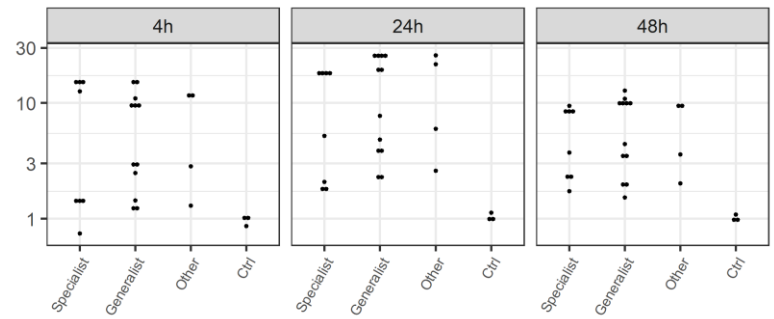


| Parameter | Estimate | Std.Error | p-value |
|---|---|---|---|
| (Intercept) | -0.8433 | 0.563 | 0.1427 |
| Time24h | 0.747 | 0.2766 | 0.0104 |
| Time48h | 0.46 | 0.2766 | 0.1047 |
| Geo_host_adaptationGeneralist | 0.3013 | 0.2525 | 0.2404 |
| Time24h:Geo_host_adaptationGeneralist | 0.1747 | 0.3571 | 0.6276 |
| Time48h:Geo_host_adaptationGeneralist | -0.1963 | 0.3571 | 0.5859 |

| contrast | Time | estimate | SE | p.value |
|---|---|---|---|---|
| Specialist - Generalist | 4h | -0.3013 | 0.2525 | 0.2404 |
| Specialist - Generalist | 24h | -0.476 | 0.2525 | 0.0673 |
| Specialist - Generalist | 48h | -0.105 | 0.2525 | 0.6799 |

### Lab_adaptation

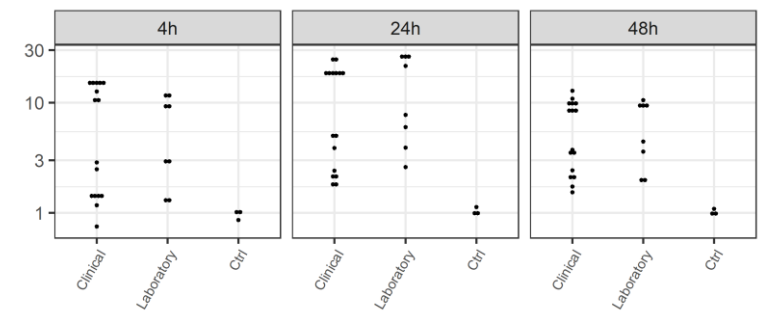


| Parameter | Estimate | Std.Error | p-value |
|---|---|---|---|
| (Intercept) | -0.6735 | 0.5481 | 0.2254 |
| Time24h | 0.7071 | 0.1945 | 7e-04 |
| Time48h | 0.312 | 0.1945 | 0.1154 |
| Lab_adaptationLaboratory | 0.0765 | 0.2382 | 0.7494 |
| Time24h:Lab_adaptationLaboratory | 0.4138 | 0.3368 | 0.2254 |
| Time48h:Lab_adaptationLaboratory | -0.0204 | 0.3368 | 0.952 |

| contrast | Time | estimate | SE | p.value |
|---|---|---|---|---|
| Clinical - Laboratory | 4h | -0.0765 | 0.2382 | 0.7494 |
| Clinical - Laboratory | 24h | -0.4904 | 0.2382 | 0.0452 |
| Clinical - Laboratory | 48h | -0.0562 | 0.2382 | 0.8146 |

# IL-6 (logarithmic transformation)

## M1

### Geo_host_adaptation

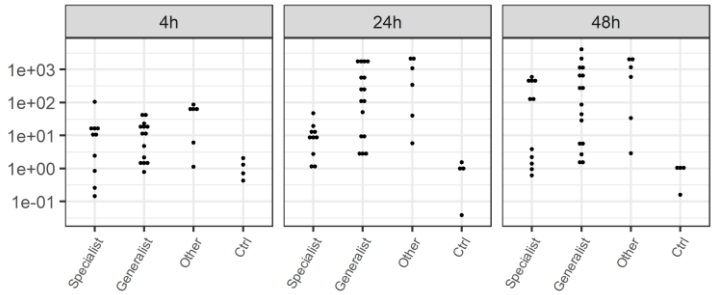


| Parameter | Estimate | Std.Error | p-value |
|---|---|---|---|
| (Intercept) | -0.4217 | 0.3601 | 0.247 |
| Time24h | 0.1159 | 0.3681 | 0.7541 |
| Time48h | 0.5162 | 0.3681 | 0.1669 |
| Geo_host_adaptationGeneralist | 0.0083 | 0.336 | 0.9805 |
| Time24h:Geo_host_adaptationGeneralist | 0.6241 | 0.4752 | 0.1949 |
| Time48h:Geo_host_adaptationGeneralist | 0.174 | 0.4752 | 0.7158 |

| contrast | Time | estimate | SE | p.value |
|---|---|---|---|---|
| Specialist - Generalist | 4h | -0.0083 | 0.336 | 0.9805 |
| Specialist - Generalist | 24h | -0.6324 | 0.336 | 0.0655 |
| Specialist - Generalist | 48h | -0.1823 | 0.336 | 0.5899 |

### Lab_adaptation

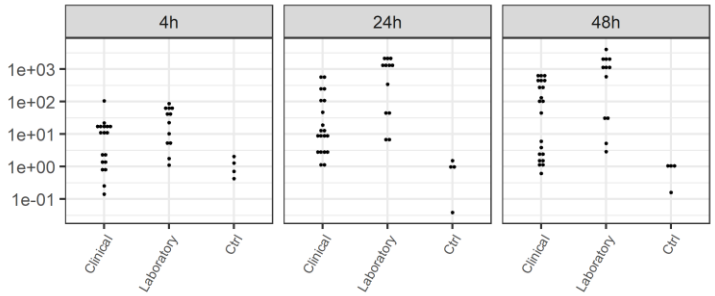


| Parameter | Estimate | Std.Error | p-value |
|---|---|---|---|
| (Intercept) | -0.7019 | 0.2885 | 0.0178 |
| Time24h | 0.4316 | 0.231 | 0.0664 |
| Time48h | 0.6115 | 0.231 | 0.0102 |
| Lab_adaptationLaboratory | 0.7652 | 0.2829 | 0.0088 |
| Time24h:Lab_adaptationLaboratory | 0.2533 | 0.4001 | 0.529 |
| Time48h:Lab_adaptationLaboratory | 0.0454 | 0.4001 | 0.9101 |

| contrast | Time | estimate | SE | p.value |
|---|---|---|---|---|
| Clinical - Laboratory | 4h | -0.7652 | 0.2829 | 0.0088 |
| Clinical - Laboratory | 24h | -1.0185 | 0.2829 | 6e-04 |
| Clinical - Laboratory | 48h | -0.8106 | 0.2829 | 0.0057 |

## M2

### Geo_host_adaptation

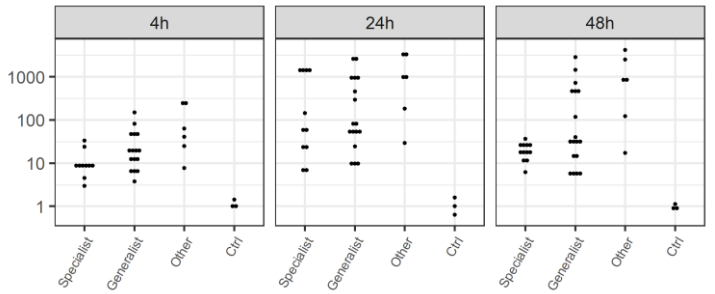


| Parameter | Estimate | Std.Error | p-value |
|---|---|---|---|
| (Intercept) | -0.95 | 0.3338 | 0.0064 |
| Time24h | 1.2182 | 0.3444 | 9e-04 |
| Time48h | 0.6859 | 0.3444 | 0.0518 |
| Geo_host_adaptationGeneralist | 0.467 | 0.3144 | 0.1436 |
| Time24h:Geo_host_adaptationGeneralist | -0.311 | 0.4446 | 0.4874 |
| Time48h:Geo_host_adaptationGeneralist | -0.0452 | 0.4446 | 0.9194 |

| contrast | Time | estimate | SE | p.value |
|---|---|---|---|---|
| Specialist - Generalist | 4h | -0.467 | 0.3144 | 0.1436 |
| Specialist - Generalist | 24h | -0.156 | 0.3144 | 0.6219 |
| Specialist - Generalist | 48h | -0.4218 | 0.3144 | 0.1856 |

### Lab_adaptation

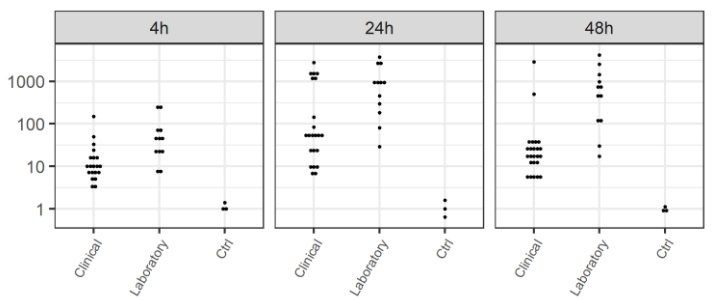


| Parameter | Estimate | Std.Error | p-value |
|---|---|---|---|
| (Intercept) | -0.9666 | 0.277 | 9e-04 |
| Time24h | 0.9737 | 0.2007 | <0.0001 |
| Time48h | 0.5709 | 0.2007 | 0.006 |
| Lab_adaptationLaboratory | 0.9 | 0.2459 | 5e-04 |
| Time24h:Lab_adaptationLaboratory | 0.0265 | 0.3477 | 0.9394 |
| Time48h:Lab_adaptationLaboratory | 0.2729 | 0.3477 | 0.4355 |

| contrast | Time | estimate | SE | p.value |
|---|---|---|---|---|
| Clinical - Laboratory | 4h | -0.9 | 0.2459 | 5e-04 |
| Clinical - Laboratory | 24h | -0.9265 | 0.2459 | 4e-04 |
| Clinical - Laboratory | 48h | -1.1729 | 0.2459 | <0.0001 |

# IL-8 (logarithmic transformation)

## M1

### Geo_host_adaptation

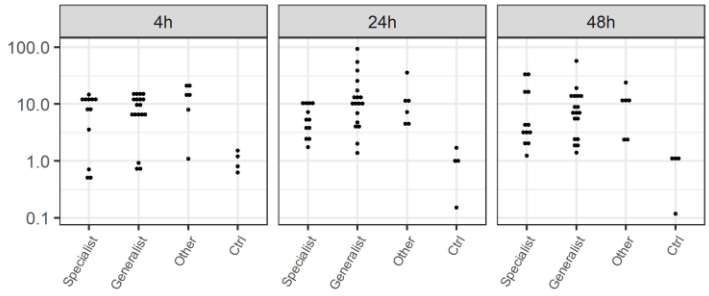


| Parameter | Estimate | Std.Error | p-value |
|---|---|---|---|
| (Intercept) | 1.1811 | 0.4599 | 0.0132 |
| Time24h | 0.3432 | 0.5055 | 0.5003 |
| Time48h | 0.354 | 0.5055 | 0.487 |
| Geo_host_adaptationGeneralist | 0.4805 | 0.4615 | 0.3027 |
| Time24h:Geo_host_adaptationGeneralist | 0.3484 | 0.6526 | 0.5958 |
| Time48h:Geo_host_adaptationGeneralist | -0.0511 | 0.6526 | 0.9378 |

| contrast | Time | ratio | SE | p.value |
|---|---|---|---|---|
| Specialist / Generalist | 4h | 0.6185 | 0.2854 | 0.3027 |
| Specialist / Generalist | 24h | 0.4365 | 0.2015 | 0.0784 |
| Specialist / Generalist | 48h | 0.6509 | 0.3004 | 0.3565 |

### Lab_adaptation

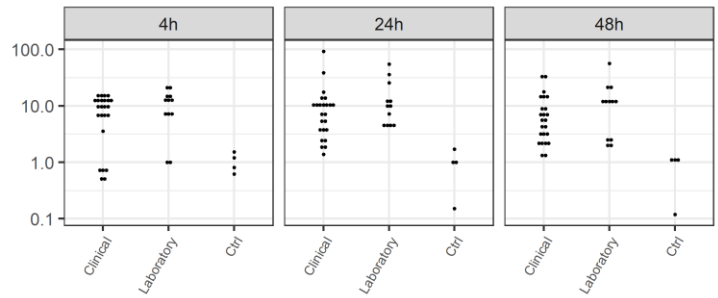


| Parameter | Estimate | Std.Error | p-value |
|---|---|---|---|
| (Intercept) | 1.3995 | 0.3552 | 2e-04 |
| Time24h | 0.4703 | 0.3583 | 0.1941 |
| Time48h | 0.207 | 0.3583 | 0.5655 |
| Lab_adaptationLaboratory | 0.4661 | 0.4388 | 0.2922 |
| Time24h:Lab_adaptationLaboratory | 0.1835 | 0.6206 | 0.7684 |
| Time48h:Lab_adaptationLaboratory | 0.299 | 0.6206 | 0.6316 |

| contrast | Time | ratio | SE | p.value |
|---|---|---|---|---|
| Clinical / Laboratory | 4h | 0.6274 | 0.2753 | 0.2922 |
| Clinical / Laboratory | 24h | 0.5222 | 0.2292 | 0.1437 |
| Clinical / Laboratory | 48h | 0.4653 | 0.2042 | 0.0861 |

## M2

### Geo_host_adaptation

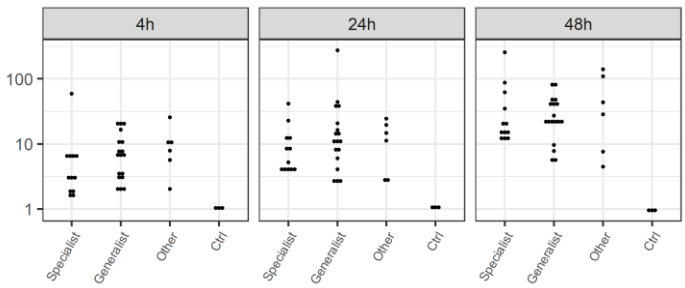


| Parameter | Estimate | Std.Error | p-value |
|---|---|---|---|
| (Intercept) | -0.8703 | 0.3132 | 0.0076 |
| Time24h | 0.6888 | 0.3625 | 0.0631 |
| Time48h | 1.7044 | 0.3625 | <0.0001 |
| Geo_host_adaptationGeneralist | 0.4926 | 0.3309 | 0.1427 |
| Time24h:Geo_host_adaptationGeneralist | -0.1275 | 0.4679 | 0.7863 |
| Time48h:Geo_host_adaptationGeneralist | -0.4968 | 0.4679 | 0.2934 |

| contrast | Time | estimate | SE | p.value |
|---|---|---|---|---|
| Specialist - Generalist | 4h | -0.4926 | 0.3309 | 0.1427 |
| Specialist - Generalist | 24h | -0.3651 | 0.3309 | 0.2751 |
| Specialist - Generalist | 48h | 0.0042 | 0.3309 | 0.9899 |

### Lab_adaptation

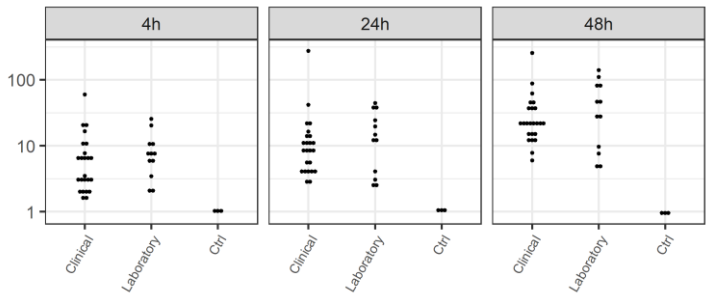


| Parameter | Estimate | Std.Error | p-value |
|---|---|---|---|
| (Intercept) | -0.6421 | 0.2705 | 0.0207 |
| Time24h | 0.583 | 0.2577 | 0.0271 |
| Time48h | 1.4078 | 0.2577 | <0.0001 |
| Lab_adaptationLaboratory | 0.3615 | 0.3156 | 0.2565 |
| Time24h:Lab_adaptationLaboratory | -0.1414 | 0.4464 | 0.7525 |
| Time48h:Lab_adaptationLaboratory | -0.1382 | 0.4464 | 0.7578 |

| contrast | Time | estimate | SE | p.value |
|---|---|---|---|---|
| Clinical - Laboratory | 4h | -0.3615 | 0.3156 | 0.2565 |
| Clinical - Laboratory | 24h | -0.2201 | 0.3156 | 0.4882 |
| Clinical - Laboratory | 48h | -0.2232 | 0.3156 | 0.482 |

# IL-10 (logarithmic transformation)

## M1

### Geo_host_adaptation

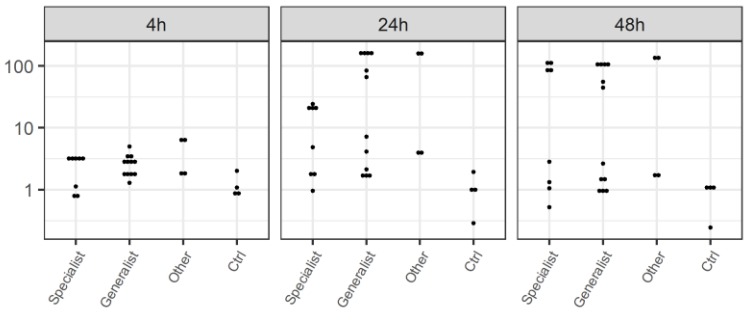


| Parameter | Estimate | Std.Error | p-value |
|---|---|---|---|
| (Intercept) | -0.7685 | 0.5475 | 0.1687 |
| Time24h | 0.5941 | 0.3544 | 0.1021 |
| Time48h | 0.3549 | 0.3544 | 0.3231 |
| Geo_host_adaptationGeneralist | 0.4255 | 0.3235 | 0.1965 |
| Time24h:Geo_host_adaptationGeneralist | 0.104 | 0.4576 | 0.8214 |
| Time48h:Geo_host_adaptationGeneralist | -0.3401 | 0.4576 | 0.4619 |

| contrast | Time | estimate | SE | p.value |
|---|---|---|---|---|
| Specialist - Generalist | 4h | -0.4255 | 0.3235 | 0.1965 |
| Specialist - Generalist | 24h | -0.5296 | 0.3235 | 0.1102 |
| Specialist - Generalist | 48h | -0.0854 | 0.3235 | 0.7933 |

### Lab_adaptation

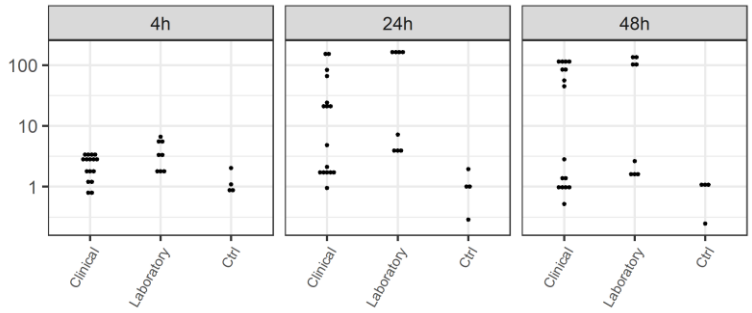


| Parameter | Estimate | Std.Error | p-value |
|---|---|---|---|
| (Intercept) | -0.6924 | 0.51 | 0.1811 |
| Time24h | 0.5825 | 0.2147 | 0.0093 |
| Time48h | 0.1375 | 0.2147 | 0.5252 |
| Lab_adaptationLaboratory | 0.465 | 0.263 | 0.0837 |
| Time24h:Lab_adaptationLaboratory | 0.4544 | 0.3719 | 0.228 |
| Time48h:Lab_adaptationLaboratory | 0.0271 | 0.3719 | 0.9423 |

| contrast | Time | estimate | SE | p.value |
|---|---|---|---|---|
| Clinical - Laboratory | 4h | -0.465 | 0.263 | 0.0837 |
| Clinical - Laboratory | 24h | -0.9194 | 0.263 | 0.0011 |
| Clinical - Laboratory | 48h | -0.492 | 0.263 | 0.0677 |

## M2

### Geo_host_adaptation

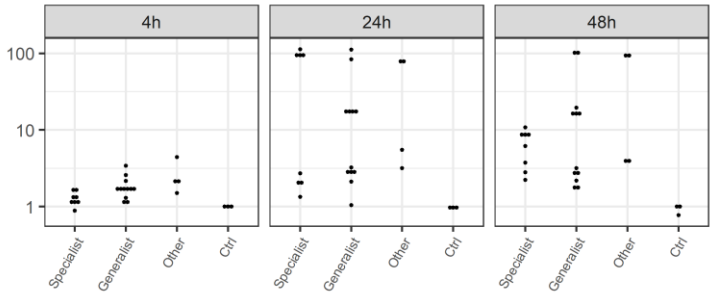


| Parameter | Estimate | Std.Error | p-value |
|---|---|---|---|
| (Intercept) | -1.3338 | 0.3722 | 0.001 |
| Time24h | 1.6934 | 0.3488 | <0.0001 |
| Time48h | 1.5947 | 0.3488 | 1e-04 |
| Geo_host_adaptationGeneralist | 0.6186 | 0.3184 | 0.0597 |
| Time24h:Geo_host_adaptationGeneralist | -0.7651 | 0.4503 | 0.0977 |
| Time48h:Geo_host_adaptationGeneralist | -0.5838 | 0.4503 | 0.2028 |

| contrast | Time | estimate | SE | p.value |
|---|---|---|---|---|
| Specialist - Generalist | 4h | -0.6186 | 0.3184 | 0.0597 |
| Specialist - Generalist | 24h | 0.1465 | 0.3184 | 0.6481 |
| Specialist - Generalist | 48h | -0.0348 | 0.3184 | 0.9136 |

### Lab_adaptation

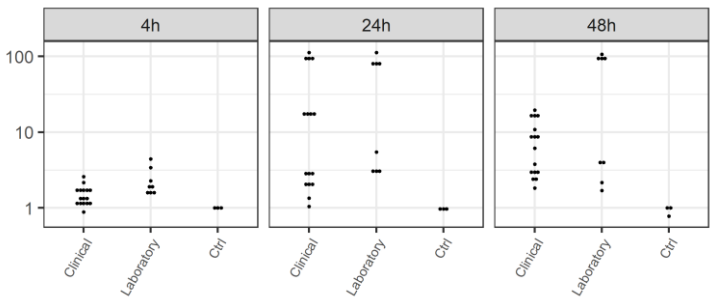


| Parameter | Estimate | Std.Error | p-value |
|---|---|---|---|
| (Intercept) | -1.1752 | 0.3293 | 9e-04 |
| Time24h | 1.2767 | 0.2369 | <0.0001 |
| Time48h | 1.3542 | 0.2369 | <0.0001 |
| Lab_adaptationLaboratory | 0.653 | 0.2902 | 0.0293 |
| Time24h:Lab_adaptationLaboratory | -0.1926 | 0.4104 | 0.6411 |
| Time48h:Lab_adaptationLaboratory | -0.3247 | 0.4104 | 0.4329 |

| contrast | Time | estimate | SE | p.value |
|---|---|---|---|---|
| Clinical - Laboratory | 4h | -0.653 | 0.2902 | 0.0293 |
| Clinical - Laboratory | 24h | -0.4604 | 0.2902 | 0.1195 |
| Clinical - Laboratory | 48h | -0.3283 | 0.2902 | 0.2638 |

# IL-15 (logarithmic transformation)

## M1

### Geo_host_adaptation

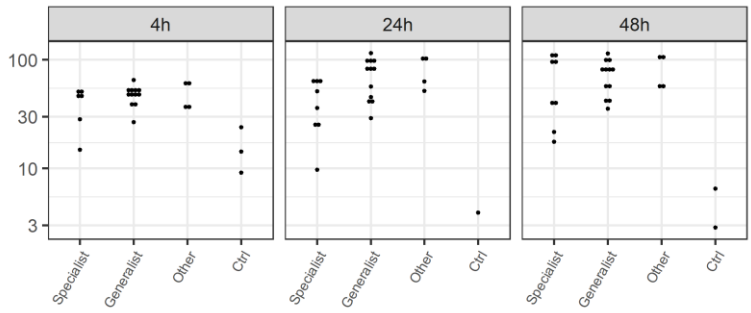


| Parameter | Estimate | Std.Error | p-value |
|---|---|---|---|
| (Intercept) | -1.1803 | 0.5086 | 0.0259 |
| Time24h | 0.4752 | 0.2854 | 0.1043 |
| Time48h | 1.0331 | 0.2854 | 9e-04 |
| Geo_host_adaptationGeneralist | 0.8558 | 0.2605 | 0.0022 |
| Time24h:Geo_host_adaptationGeneralist | 0.1315 | 0.3684 | 0.7232 |
| Time48h:Geo_host_adaptationGeneralist | -0.4369 | 0.3684 | 0.2432 |

| contrast | Time | estimate | SE | p.value |
|---|---|---|---|---|
| Specialist - Generalist | 4h | -0.8558 | 0.2605 | 0.0022 |
| Specialist - Generalist | 24h | -0.9873 | 0.2605 | 5e-04 |
| Specialist - Generalist | 48h | -0.4189 | 0.2605 | 0.1163 |

### Lab_adaptation

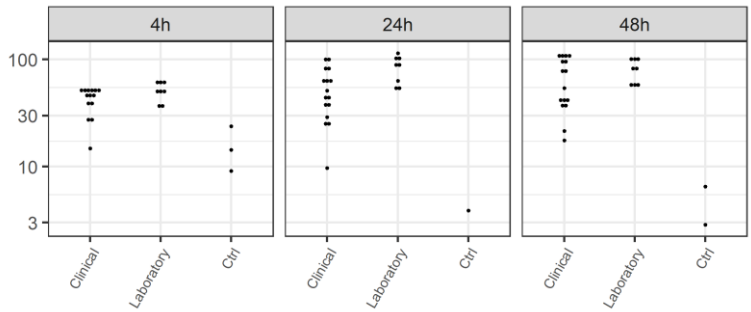


| Parameter | Estimate | Std.Error | p-value |
|---|---|---|---|
| (Intercept) | -0.9407 | 0.4765 | 0.0544 |
| Time24h | 0.4927 | 0.1892 | 0.0123 |
| Time48h | 0.8665 | 0.1892 | <0.0001 |
| Lab_adaptationLaboratory | 0.6391 | 0.2317 | 0.0083 |
| Time24h:Lab_adaptationLaboratory | 0.4892 | 0.3276 | 0.1422 |
| Time48h:Lab_adaptationLaboratory | -0.0112 | 0.3276 | 0.9728 |

| contrast | Time | estimate | SE | p.value |
|---|---|---|---|---|
| Clinical - Laboratory | 4h | -0.6391 | 0.2317 | 0.0083 |
| Clinical - Laboratory | 24h | -1.1283 | 0.2317 | <0.0001 |
| Clinical - Laboratory | 48h | -0.6278 | 0.2317 | 0.0094 |

## M2

### Geo_host_adaptation

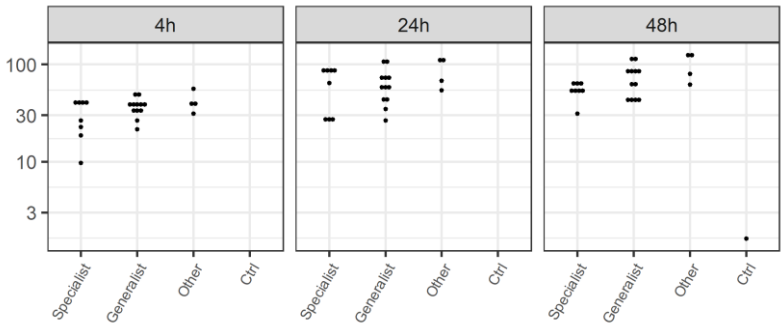


| Parameter | Estimate | Std.Error | p-value |
|---|---|---|---|
| (Intercept) | 3.2263 | 0.2128 | <0.0001 |
| Time24h | 0.6077 | 0.1759 | 0.0014 |
| Time48h | 0.706 | 0.1759 | 3e-04 |
| Geo_host_adaptationGeneralist | 0.3118 | 0.1606 | 0.0598 |
| Time24h:Geo_host_adaptationGeneralist | -0.1739 | 0.2271 | 0.4486 |
| Time48h:Geo_host_adaptationGeneralist | -0.1281 | 0.2271 | 0.5762 |

| contrast | Time | ratio | SE | p.value |
|---|---|---|---|---|
| Specialist / Generalist | 4h | 0.7321 | 0.1175 | 0.0598 |
| Specialist / Generalist | 24h | 0.8711 | 0.1399 | 0.3958 |
| Specialist / Generalist | 48h | 0.8321 | 0.1336 | 0.2597 |

### Lab_adaptation

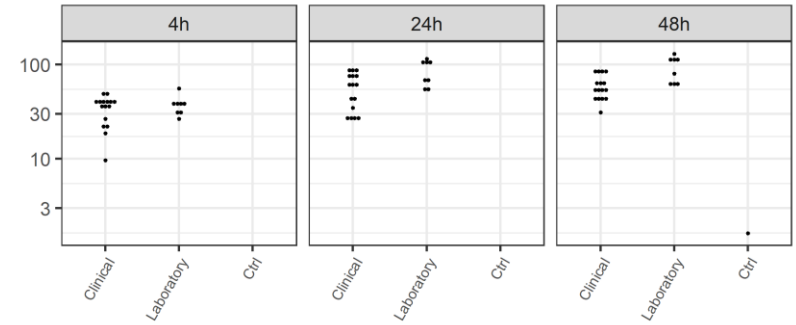


| Parameter | Estimate | Std.Error | p-value |
|---|---|---|---|
| (Intercept) | 3.3962 | 0.1865 | <0.0001 |
| Time24h | 0.424 | 0.1092 | 3e-04 |
| Time48h | 0.5719 | 0.1092 | <0.0001 |
| Lab_adaptationLaboratory | 0.1606 | 0.1338 | 0.2359 |
| Time24h:Lab_adaptationLaboratory | 0.3305 | 0.1892 | 0.0873 |
| Time48h:Lab_adaptationLaboratory | 0.2642 | 0.1892 | 0.1693 |

| contrast | Time | ratio | SE | p.value |
|---|---|---|---|---|
| Clinical / Laboratory | 4h | 0.8516 | 0.1139 | 0.2359 |
| Clinical / Laboratory | 24h | 0.6119 | 0.0818 | 6e-04 |
| Clinical / Laboratory | 48h | 0.6539 | 0.0875 | 0.0027 |

# FGF basic(logarithmic transformation)

## M1

### Geo_host_adaptation

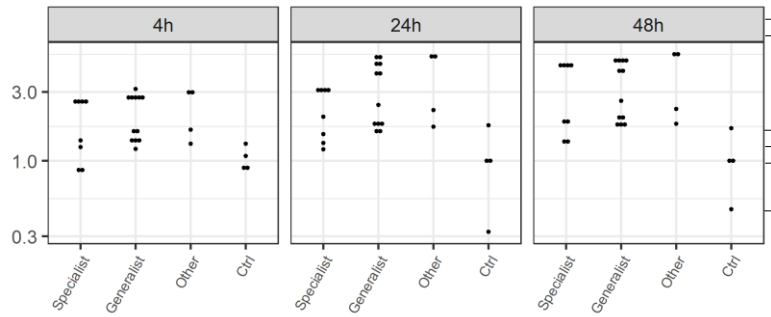


| Parameter | Estimate | Std.Error | p-value |
|---|---|---|---|
| (Intercept) | 0.3589 | 0.2914 | 0.2259 |
| Time24h | 0.2868 | 0.0874 | 0.0023 |
| Time48h | 0.4621 | 0.0874 | <0.0001 |
| Geo_host_adaptationGeneralist | 0.2224 | 0.0798 | 0.0084 |
| Time24h:Geo_host_adaptationGeneralist | 0.0455 | 0.1129 | 0.6893 |
| Time48h:Geo_host_adaptationGeneralist | -0.0766 | 0.1129 | 0.5016 |

| contrast | Time | ratio | SE | p.value |
|---|---|---|---|---|
| Specialist / Generalist | 4h | 0.8006 | 0.0639 | 0.0084 |
| Specialist / Generalist | 24h | 0.765 | 0.0611 | 0.0018 |
| Specialist / Generalist | 48h | 0.8643 | 0.069 | 0.0759 |

### Lab_adaptation

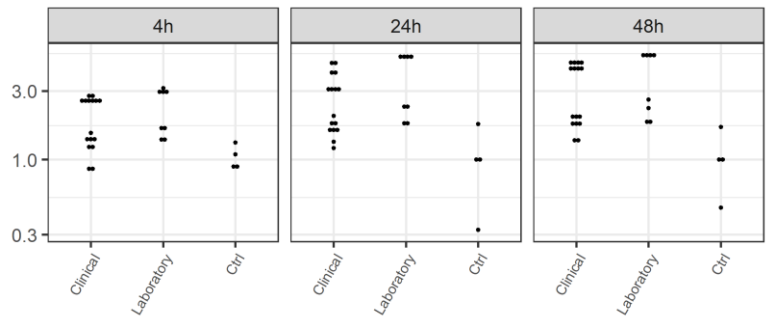


| Parameter | Estimate | Std.Error | p-value |
|---|---|---|---|
| (Intercept) | 0.4512 | 0.2905 | 0.1272 |
| Time24h | 0.2929 | 0.0617 | <0.0001 |
| Time48h | 0.4168 | 0.0617 | <0.0001 |
| Lab_adaptationLaboratory | 0.1875 | 0.0756 | 0.0168 |
| Time24h:Lab_adaptationLaboratory | 0.0984 | 0.1069 | 0.3618 |
| Time48h:Lab_adaptationLaboratory | -4e-04 | 0.1069 | 0.9971 |

| contrast | Time | ratio | SE | p.value |
|---|---|---|---|---|
| Clinical / Laboratory | 4h | 0.829 | 0.0627 | 0.0168 |
| Clinical / Laboratory | 24h | 0.7513 | 0.0568 | 4e-04 |
| Clinical / Laboratory | 48h | 0.8293 | 0.0627 | 0.017 |

## M2

### Geo_host_adaptation

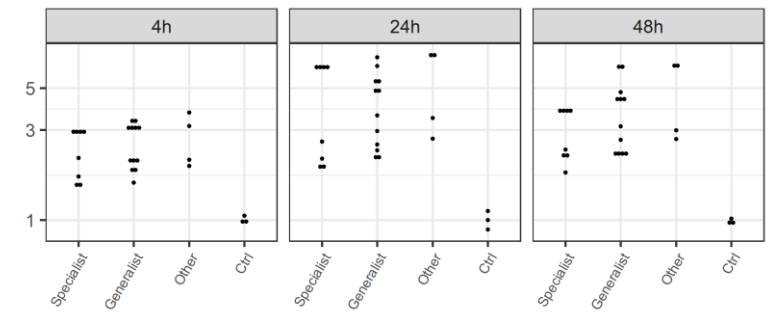


| Parameter | Estimate | Std.Error | p-value |
|---|---|---|---|
| (Intercept) | 0.7161 | 0.2443 | 0.0058 |
| Time24h | 0.4077 | 0.098 | 2e-04 |
| Time48h | 0.2303 | 0.098 | 0.0242 |
| Geo_host_adaptationGeneralist | 0.0969 | 0.0894 | 0.2858 |
| Time24h:Geo_host_adaptationGeneralist | -0.0125 | 0.1265 | 0.9219 |
| Time48h:Geo_host_adaptationGeneralist | 0.0875 | 0.1265 | 0.4931 |

| contrast | Time | ratio | SE | p.value |
|---|---|---|---|---|
| Specialist / Generalist | 4h | 0.9077 | 0.0812 | 0.2858 |
| Specialist / Generalist | 24h | 0.9191 | 0.0822 | 0.3516 |
| Specialist / Generalist | 48h | 0.8316 | 0.0744 | 0.0463 |

### Lab_adaptation

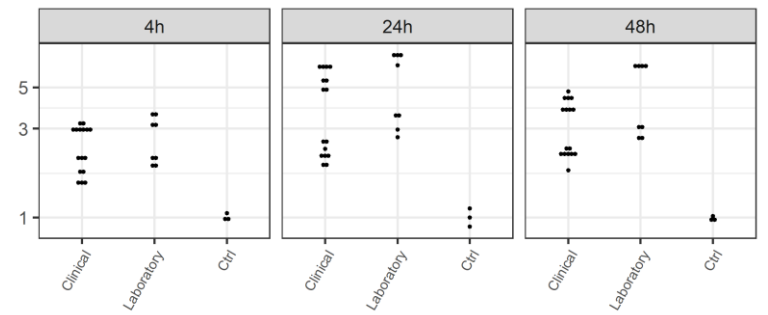


| Parameter | Estimate | Std.Error | p-value |
|---|---|---|---|
| (Intercept) | 0.7533 | 0.2404 | 0.003 |
| Time24h | 0.3584 | 0.054 | <0.0001 |
| Time48h | 0.2344 | 0.054 | 1e-04 |
| Lab_adaptationLaboratory | 0.1082 | 0.0661 | 0.1084 |
| Time24h:Lab_adaptationLaboratory | 0.2054 | 0.0935 | 0.033 |
| Time48h:Lab_adaptationLaboratory | 0.2325 | 0.0935 | 0.0166 |

| contrast | Time | ratio | SE | p.value |
|---|---|---|---|---|
| Clinical / Laboratory | 4h | 0.8974 | 0.0593 | 0.1084 |
| Clinical / Laboratory | 24h | 0.7308 | 0.0483 | <0.0001 |
| Clinical / Laboratory | 48h | 0.7113 | 0.047 | <0.0001 |

# G-CSF (logarithmic transformation)

## M1

### Geo_host_adaptation

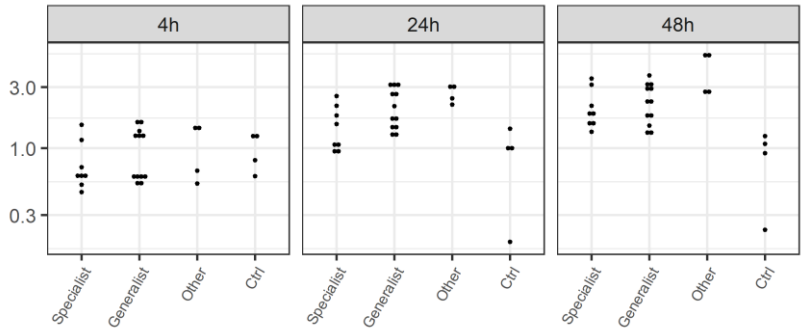


| Parameter | Estimate | Std.Error | p-value |
|---|---|---|---|
| (Intercept) | -0.2671 | 0.2404 | 0.2738 |
| Time24h | 0.7224 | 0.0987 | <0.0001 |
| Time48h | 1.0556 | 0.0987 | <0.0001 |
| Geo_host_adaptationGeneralist | 0.2886 | 0.0901 | 0.0028 |
| Time24h:Geo_host_adaptationGeneralist | 0.064 | 0.1274 | 0.6181 |
| Time48h:Geo_host_adaptationGeneralist | -0.1739 | 0.1274 | 0.1805 |

| contrast | Time | ratio | SE | p.value |
|---|---|---|---|---|
| Specialist / Generalist | 4h | 0.7493 | 0.0675 | 0.0028 |
| Specialist / Generalist | 24h | 0.7028 | 0.0633 | 4e-04 |
| Specialist / Generalist | 48h | 0.8916 | 0.0803 | 0.2107 |

### Lab_adaptation

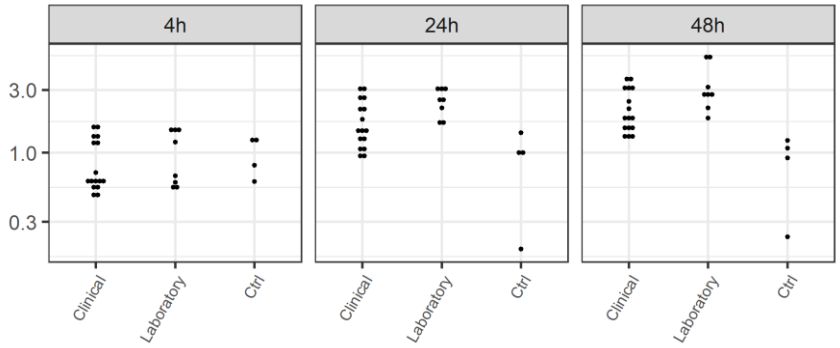


| Parameter | Estimate | Std.Error | p-value |
|---|---|---|---|
| (Intercept) | -0.1257 | 0.2112 | 0.5547 |
| Time24h | 0.736 | 0.1067 | <0.0001 |
| Time48h | 0.9548 | 0.1067 | <0.0001 |
| Lab_adaptationLaboratory | 0.1719 | 0.1307 | 0.195 |
| Time24h:Lab_adaptationLaboratory | 0.1599 | 0.1849 | 0.3915 |
| Time48h:Lab_adaptationLaboratory | 0.105 | 0.1849 | 0.5728 |

| contrast | Time | ratio | SE | p.value |
|---|---|---|---|---|
| Clinical / Laboratory | 4h | 0.8421 | 0.1101 | 0.195 |
| Clinical / Laboratory | 24h | 0.7176 | 0.0938 | 0.0146 |
| Clinical / Laboratory | 48h | 0.7581 | 0.0991 | 0.0396 |

## M2

### Geo_host_adaptation

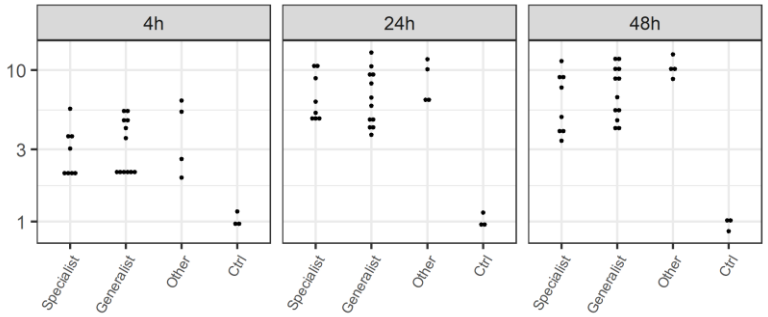


| Parameter | Estimate | Std.Error | p-value |
|---|---|---|---|
| (Intercept) | -0.9208 | 0.4711 | 0.0582 |
| Time24h | 1.5376 | 0.1944 | <0.0001 |
| Time48h | 1.362 | 0.1944 | <0.0001 |
| Geo_host_adaptationGeneralist | 0.3551 | 0.1774 | 0.0527 |
| Time24h:Geo_host_adaptationGeneralist | -0.3234 | 0.2509 | 0.2055 |
| Time48h:Geo_host_adaptationGeneralist | 0.017 | 0.2509 | 0.9462 |

| contrast | Time | estimate | SE | p.value |
|---|---|---|---|---|
| Specialist - Generalist | 4h | -0.3551 | 0.1774 | 0.0527 |
| Specialist - Generalist | 24h | -0.0317 | 0.1774 | 0.859 |
| Specialist - Generalist | 48h | -0.3721 | 0.1774 | 0.0428 |

### Lab_adaptatıon

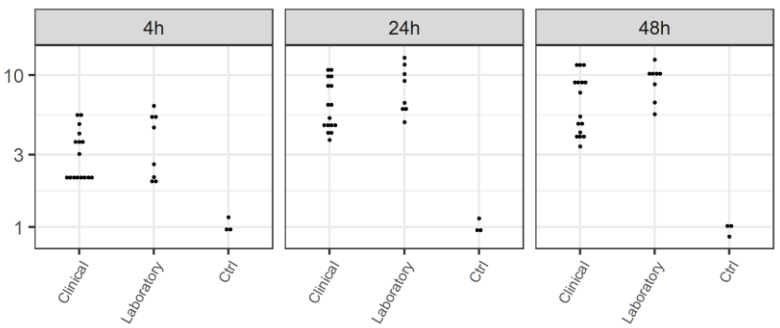


| Parameter | Estimate | Std.Error | p-value |
|---|---|---|---|
| (Intercept) | -0.7541 | 0.4436 | 0.0959 |
| Time24h | 1.1527 | 0.136 | <0.0001 |
| Time48h | 1.2307 | 0.136 | <0.0001 |
| Lab_adaptationLaboratory | 0.1201 | 0.1666 | 0.4747 |
| Time24h:Lab_adaptationLaboratory | 0.4738 | 0.2355 | 0.0501 |
| Time48h:Lab_adaptationLaboratory | 0.4992 | 0.2355 | 0.0395 |

| contrast | Time | estimate | SE | p.value |
|---|---|---|---|---|
| Clinical - Laboratory | 4h | -0.1201 | 0.1666 | 0.4747 |
| Clinical - Laboratory | 24h | -0.5939 | 0.1666 | 9e-04 |
| Clinical - Laboratory | 48h | -0.6192 | 0.1666 | 5e-04 |

# IFNγ (logarithmic transformation)

## M1

### Geo_host_adaptation

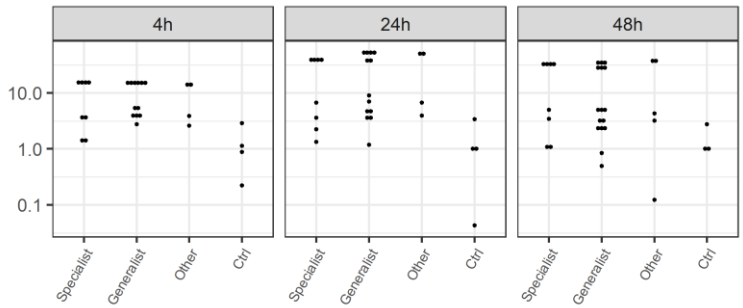


| Parameter | Estimate | Std.Error | p-value |
|---|---|---|---|
| (Intercept) | -0.218 | 0.4333 | 0.617 |
| Time24h | 0.2724 | 0.1579 | 0.0905 |
| Time48h | 0.0968 | 0.1579 | 0.5426 |
| Geo_host_adaptationGeneralist | 0.0992 | 0.1441 | 0.4944 |
| Time24h:Geo_host_adaptationGeneralist | 0.161 | 0.2038 | 0.4331 |
| Time48h:Geo_host_adaptationGeneralist | 0.1051 | 0.2038 | 0.6083 |

| contrast | Time | estimate | SE | p.value |
|---|---|---|---|---|
| Specialist - Generalist | 4h | -0.0992 | 0.1441 | 0.4944 |
| Specialist - Generalist | 24h | -0.2602 | 0.1441 | 0.0769 |
| Specialist - Generalist | 48h | -0.2043 | 0.1441 | 0.1624 |

### Lab_adaptation

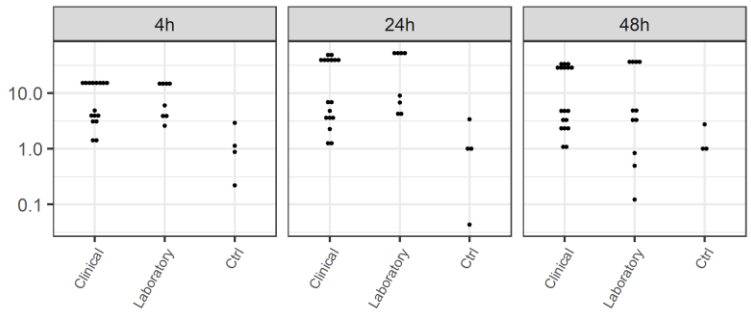


| Parameter | Estimate | Std.Error | p-value |
|---|---|---|---|
| (Intercept) | -0.1804 | 0.4267 | 0.6739 |
| Time24h | 0.3023 | 0.1088 | 0.0072 |
| Time48h | 0.1221 | 0.1088 | 0.2657 |
| Lab_adaptationLaboratory | 0.0454 | 0.1332 | 0.7344 |
| Time24h:Lab_adaptationLaboratory | 0.2353 | 0.1884 | 0.2163 |
| Time48h:Lab_adaptationLaboratory | 0.1518 | 0.1884 | 0.4232 |

| contrast | Time | estimate | SE | p.value |
|---|---|---|---|---|
| Clinical - Laboratory | 4h | -0.0454 | 0.1332 | 0.7344 |
| Clinical - Laboratory | 24h | -0.2807 | 0.1332 | 0.0391 |
| Clinical - Laboratory | 48h | -0.1972 | 0.1332 | 0.1436 |

## M2

### Geo_host_adaptation

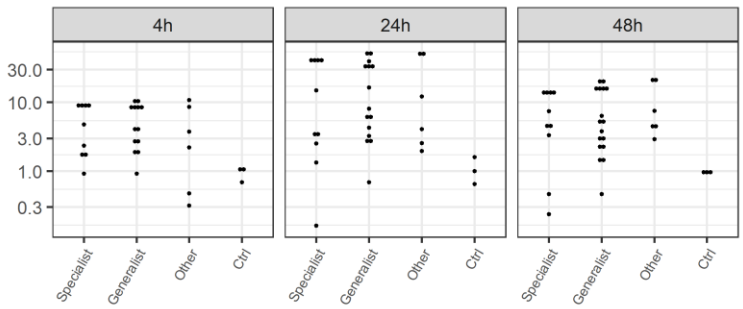


| Parameter | Estimate | Std.Error | p-value |
|---|---|---|---|
| (Intercept) | -0.3213 | 0.4337 | 0.4621 |
| Time24h | 0.5423 | 0.185 | 0.005 |
| Time48h | 0.2887 | 0.185 | 0.1248 |
| Geo_host_adaptationGeneralist | 0.0188 | 0.1689 | 0.9117 |
| Time24h:Geo_host_adaptationGeneralist | 0.1128 | 0.2388 | 0.6386 |
| Time48h:Geo_host_adaptationGeneralist | 0.1161 | 0.2388 | 0.629 |

| contrast | Time | estimate | SE | p.value |
|---|---|---|---|---|
| Specialist - Generalist | 4h | -0.0188 | 0.1689 | 0.9117 |
| Specialist - Generalist | 24h | -0.1317 | 0.1689 | 0.4393 |
| Specialist - Generalist | 48h | -0.1349 | 0.1689 | 0.4281 |

### Lab_adaptation

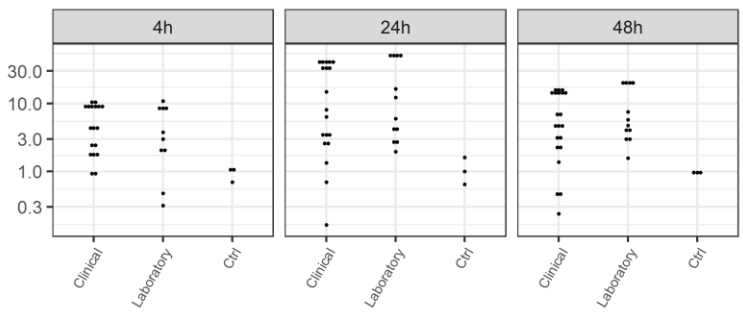


| Parameter | Estimate | Std.Error | p-value |
|---|---|---|---|
| (Intercept) | -0.3523 | 0.4187 | 0.4032 |
| Time24h | 0.4331 | 0.1186 | 5e-04 |
| Time48h | 0.3006 | 0.1186 | 0.0138 |
| Lab_adaptationLaboratory | 0.0092 | 0.1453 | 0.9497 |
| Time24h:Lab_adaptationLaboratory | 0.641 | 0.2055 | 0.0027 |
| Time48h:Lab_adaptationLaboratory | 0.321 | 0.2055 | 0.1232 |

| contrast | Time | estimate | SE | p.value |
|---|---|---|---|---|
| Clinical - Laboratory | 4h | -0.0092 | 0.1453 | 0.9497 |
| Clinical - Laboratory | 24h | -0.6502 | 0.1453 | <0.0001 |
| Clinical - Laboratory | 48h | -0.3302 | 0.1453 | 0.0264 |

# IP-10 (logarithmic transformation)

## M1

### Geo_host_adaptation

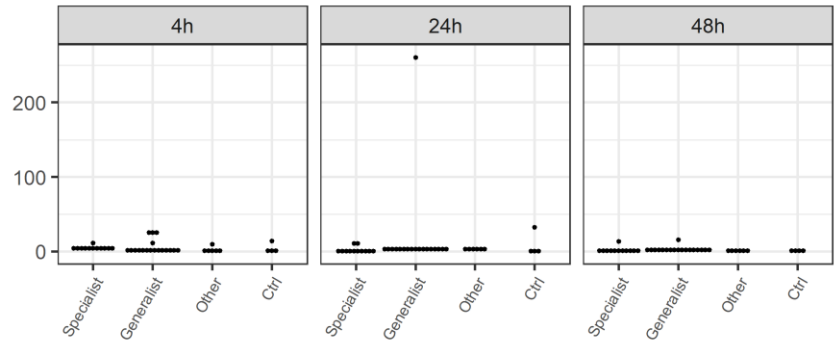


| Parameter | Estimate | Std.Error | p-value |
|---|---|---|---|
| (Intercept) | -0.8833 | 1.2153 | 0.4707 |
| Time24h | -0.1296 | 0.6331 | 0.8387 |
| Time48h | -0.4979 | 0.6331 | 0.4353 |
| Geo_host_adaptationGeneralist | 0.8554 | 0.578 | 0.145 |
| Time24h:Geo_host_adaptationGeneralist | 0.4414 | 0.8174 | 0.5916 |
| Time48h:Geo_host_adaptationGeneralist | -0.1404 | 0.8174 | 0.8643 |

| contrast | Time | ratio | SE | p.value |
|---|---|---|---|---|
| Specialist / Generalist | 4h | 0.4251 | 0.2457 | 0.145 |
| Specialist / Generalist | 24h | 0.2734 | 0.158 | 0.0292 |
| Specialist / Generalist | 48h | 0.4892 | 0.2827 | 0.2217 |

### Lab_adaptation

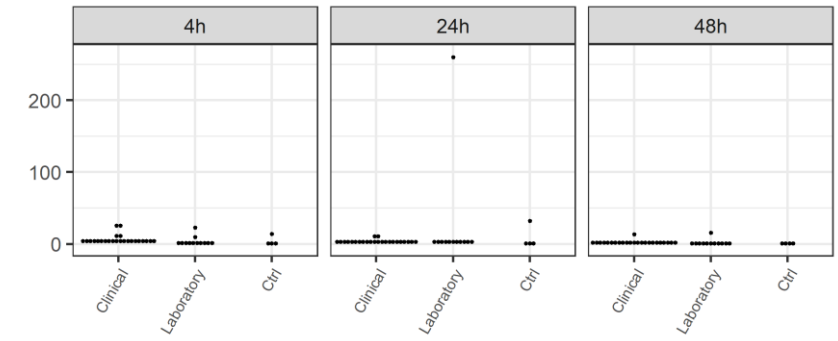


| Parameter | Estimate | Std.Error | p-value |
|---|---|---|---|
| (Intercept) | -0.3395 | 1.168 | 0.7723 |
| Time24h | -0.2199 | 0.4391 | 0.6182 |
| Time48h | -0.718 | 0.4391 | 0.107 |
| Lab_adaptationLaboratory | -0.2087 | 0.5378 | 0.6993 |
| Time24h:Lab_adaptationLaboratory | 1.258 | 0.7605 | 0.1031 |
| Time48h:Lab_adaptationLaboratory | 0.4712 | 0.7605 | 0.5377 |

| contrast | Time | ratio | SE | p.value |
|---|---|---|---|---|
| Clinical / Laboratory | 4h | 1.2321 | 0.6626 | 0.6993 |
| Clinical / Laboratory | 24h | 0.3502 | 0.1883 | 0.0555 |
| Clinical / Laboratory | 48h | 0.7691 | 0.4136 | 0.6271 |

## M2

### Geo_host_adaptation

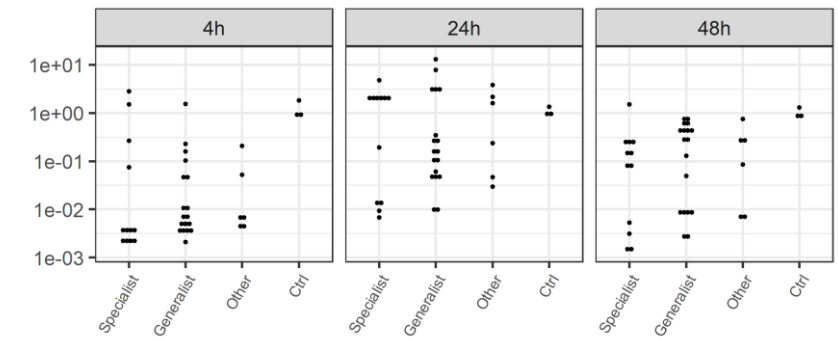


| Parameter | Estimate | Std.Error | p-value |
|---|---|---|---|
| (Intercept) | -3.2589 | 1.1109 | 0.005 |
| Time24h | 2.4912 | 0.7194 | 0.0011 |
| Time48h | 0.7057 | 0.7194 | 0.3313 |
| Geo_host_adaptationGeneralist | -0.323 | 0.6567 | 0.6249 |
| Time24h:Geo_host_adaptationGeneralist | 0.0789 | 0.9287 | 0.9326 |
| Time48h:Geo_host_adaptationGeneralist | 0.7564 | 0.9287 | 0.4192 |

| contrast | Time | ratio | SE | p.value |
|---|---|---|---|---|
| Specialist / Generalist | 4h | 1.3813 | 0.9071 | 0.6249 |
| Specialist / Generalist | 24h | 1.2764 | 0.8383 | 0.7117 |
| Specialist / Generalist | 48h | 0.6483 | 0.4258 | 0.5123 |

### Lab_adaptatıon

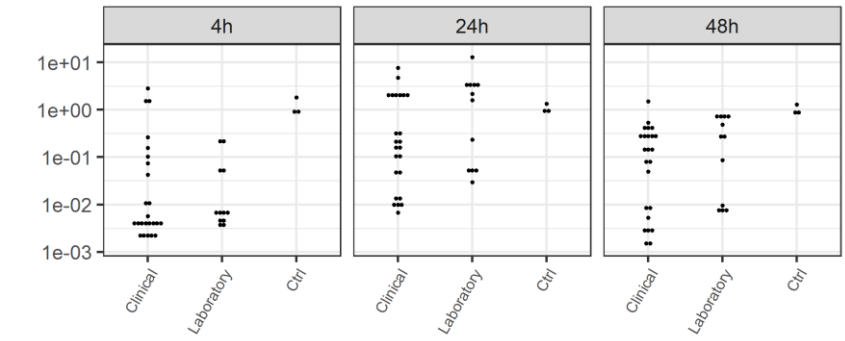


| Parameter | Estimate | Std.Error | p-value |
|---|---|---|---|
| (Intercept) | -3.3825 | 0.9938 | 0.0012 |
| Time24h | 2.1167 | 0.485 | <0.0001 |
| Time48h | 0.8923 | 0.485 | 0.0705 |
| Lab_adaptationLaboratory | -0.3566 | 0.594 | 0.5504 |
| Time24h:Lab_adaptationLaboratory | 1.4685 | 0.84 | 0.0853 |
| Time48h:Lab_adaptationLaboratory | 0.903 | 0.84 | 0.2865 |

| contrast | Time | ratio | SE | p.value |
|---|---|---|---|---|
| Clinical / Laboratory | 4h | 1.4284 | 0.8484 | 0.5504 |
| Clinical / Laboratory | 24h | 0.3289 | 0.1954 | 0.0659 |
| Clinical / Laboratory | 48h | 0.579 | 0.3439 | 0.3611 |

# MCP-1 (logarithmic transformation)

## M1

### Geo_host_adaptation

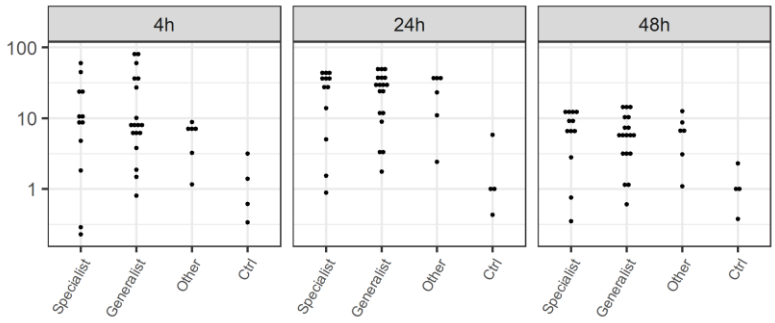


| Parameter | Estimate | Std.Error | p-value |
|---|---|---|---|
| (Intercept) | 1.3888 | 0.6863 | 0.0483 |
| Time24h | 0.9816 | 0.371 | 0.0108 |
| Time48h | -0.06 | 0.371 | 0.8721 |
| Geo_host_adaptationGeneralist | 0.5813 | 0.3387 | 0.0922 |
| Time24h:Geo_host_adaptationGeneralist | -0.3471 | 0.4789 | 0.4719 |
| Time48h:Geo_host_adaptationGeneralist | -0.5931 | 0.4789 | 0.2213 |

| contrast | Time | ratio | SE | p.value |
|---|---|---|---|---|
| Specialist / Generalist | 4h | 0.5592 | 0.1894 | 0.0922 |
| Specialist / Generalist | 24h | 0.7912 | 0.268 | 0.4924 |
| Specialist / Generalist | 48h | 1.0119 | 0.3427 | 0.9724 |

### Lab_adaptation

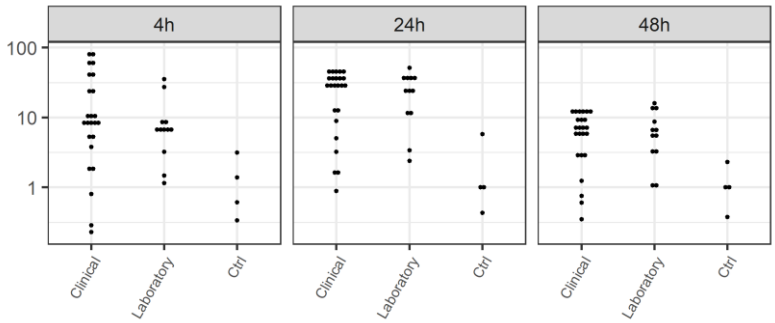


| Parameter | Estimate | Std.Error | p-value |
|---|---|---|---|
| (Intercept) | 1.6941 | 0.6324 | 0.0094 |
| Time24h | 0.7773 | 0.2573 | 0.0036 |
| Time48h | -0.3977 | 0.2573 | 0.1273 |
| Lab_adaptationLaboratory | -0.0707 | 0.3152 | 0.8232 |
| Time24h:Lab_adaptationLaboratory | 0.215 | 0.4457 | 0.6312 |
| Time48h:Lab_adaptationLaboratory | 0.1671 | 0.4457 | 0.709 |

| contrast | Time | ratio | SE | p.value |
|---|---|---|---|---|
| Clinical / Laboratory | 4h | 1.0733 | 0.3383 | 0.8232 |
| Clinical / Laboratory | 24h | 0.8656 | 0.2728 | 0.6487 |
| Clinical / Laboratory | 48h | 0.9081 | 0.2862 | 0.7608 |

## M2

### Geo_host_adaptation

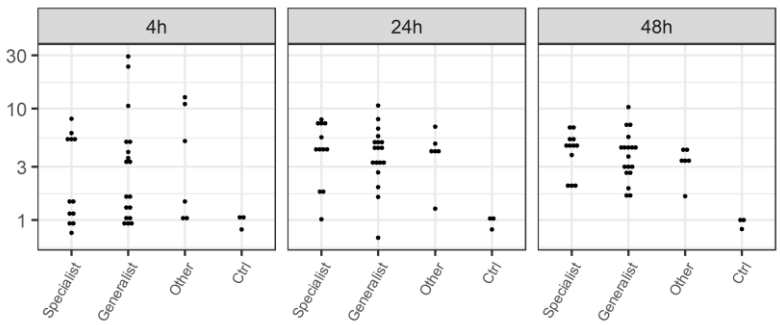


| Parameter | Estimate | Std.Error | p-value |
|---|---|---|---|
| (Intercept) | 0.7511 | 0.3205 | 0.023 |
| Time24h | 0.4851 | 0.3106 | 0.1246 |
| Time48h | 0.5348 | 0.3106 | 0.0912 |
| Geo_host_adaptationGeneralist | 0.2181 | 0.2836 | 0.4454 |
| Time24h:Geo_host_adaptationGeneralist | -0.2826 | 0.401 | 0.4842 |
| Time48h:Geo_host_adaptationGeneralist | -0.2724 | 0.401 | 0.5 |

| contrast | Time | ratio | SE | p.value |
|---|---|---|---|---|
| Specialist / Generalist | 4h | 0.8041 | 0.228 | 0.4454 |
| Specialist / Generalist | 24h | 1.0667 | 0.3025 | 0.8209 |
| Specialist / Generalist | 48h | 1.0559 | 0.2994 | 0.8487 |

### Lab_adaptation

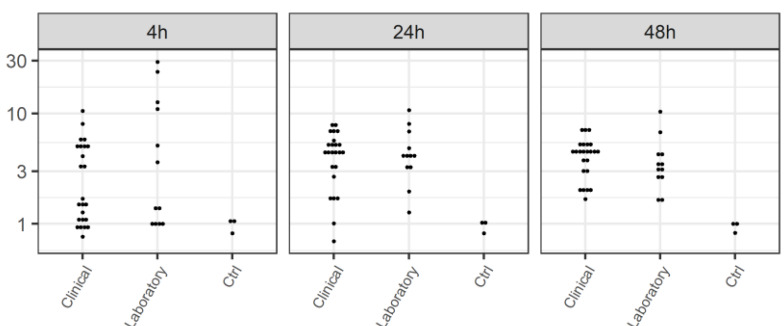


| Parameter | Estimate | Std.Error | p-value |
|---|---|---|---|
| (Intercept) | 0.809 | 0.2809 | 0.0054 |
| Time24h | 0.3495 | 0.2138 | 0.1071 |
| Time48h | 0.4657 | 0.2138 | 0.0332 |
| Lab_adaptationLaboratory | 0.3206 | 0.2619 | 0.2254 |
| Time24h:Lab_adaptationLaboratory | -0.1925 | 0.3704 | 0.6051 |
| Time48h:Lab_adaptationLaboratory | -0.4586 | 0.3704 | 0.2202 |

| contrast | Time | ratio | SE | p.value |
|---|---|---|---|---|
| Clinical / Laboratory | 4h | 0.7257 | 0.19 | 0.2254 |
| Clinical / Laboratory | 24h | 0.8797 | 0.2304 | 0.6263 |
| Clinical / Laboratory | 48h | 1.148 | 0.3006 | 0.6001 |

# MIP-1α (logarithmic transformation)

## M1

### Geo_host_adaptation

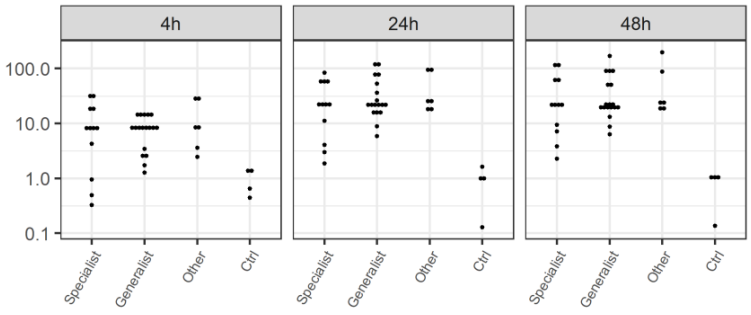


| Parameter | Estimate | Std.Error | p-value |
|---|---|---|---|
| (Intercept) | 1.3076 | 0.5729 | 0.0267 |
| Time24h | 1.2163 | 0.2701 | <0.0001 |
| Time48h | 1.3856 | 0.2701 | <0.0001 |
| Geo_host_adaptationGeneralist | 0.3435 | 0.2466 | 0.1697 |
| Time24h:Geo_host_adaptationGeneralist | 0.246 | 0.3487 | 0.4838 |
| Time48h:Geo_host_adaptationGeneralist | 0.1089 | 0.3487 | 0.7561 |

| contrast | Time | ratio | SE | p.value |
|---|---|---|---|---|
| Specialist / Generalist | 4h | 0.7093 | 0.1749 | 0.1697 |
| Specialist / Generalist | 24h | 0.5546 | 0.1368 | 0.0206 |
| Specialist / Generalist | 48h | 0.6361 | 0.1569 | 0.0724 |

### Lab_adaptation

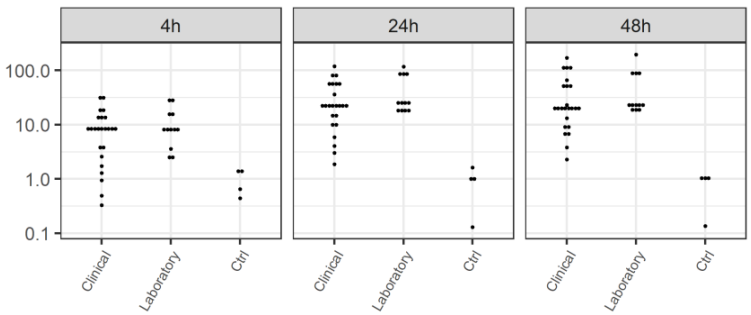


| Parameter | Estimate | Std.Error | p-value |
|---|---|---|---|
| (Intercept) | 1.4163 | 0.5382 | 0.0107 |
| Time24h | 1.3372 | 0.1814 | <0.0001 |
| Time48h | 1.4548 | 0.1814 | <0.0001 |
| Lab_adaptationLaboratory | 0.5009 | 0.2221 | 0.0276 |
| Time24h:Lab_adaptationLaboratory | 0.1245 | 0.3141 | 0.6933 |
| Time48h:Lab_adaptationLaboratory | 0.0332 | 0.3141 | 0.9161 |

| contrast | Time | ratio | SE | p.value |
|---|---|---|---|---|
| Clinical / Laboratory | 4h | 0.606 | 0.1346 | 0.0276 |
| Clinical / Laboratory | 24h | 0.535 | 0.1189 | 0.0065 |
| Clinical / Laboratory | 48h | 0.5862 | 0.1302 | 0.0191 |

## M2

### Geo_host_adaptation

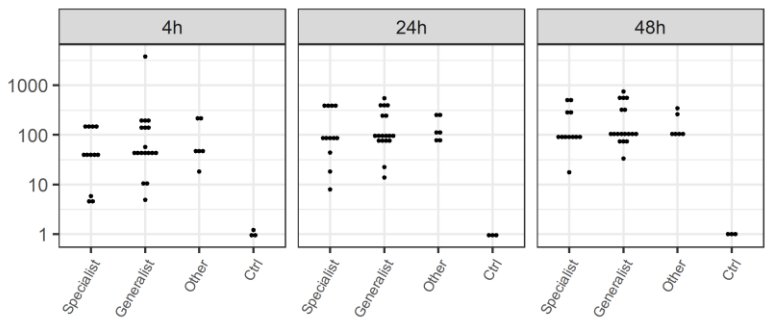


| Parameter | Estimate | Std.Error | p-value |
|---|---|---|---|
| (Intercept) | 3.2355 | 0.5833 | <0.0001 |
| Time24h | 1.0178 | 0.4495 | 0.0278 |
| Time48h | 1.4443 | 0.4495 | 0.0023 |
| Geo_host_adaptationGeneralist | 0.8325 | 0.4104 | 0.0477 |
| Time24h:Geo_host_adaptationGeneralist | -0.5476 | 0.5803 | 0.3499 |
| Time48h:Geo_host_adaptationGeneralist | -0.6548 | 0.5803 | 0.2645 |

| contrast | Time | ratio | SE | p.value |
|---|---|---|---|---|
| Specialist / Generalist | 4h | 0.435 | 0.1785 | 0.0477 |
| Specialist / Generalist | 24h | 0.7521 | 0.3086 | 0.4906 |
| Specialist / Generalist | 48h | 0.8371 | 0.3435 | 0.6667 |

### Lab_adaptation

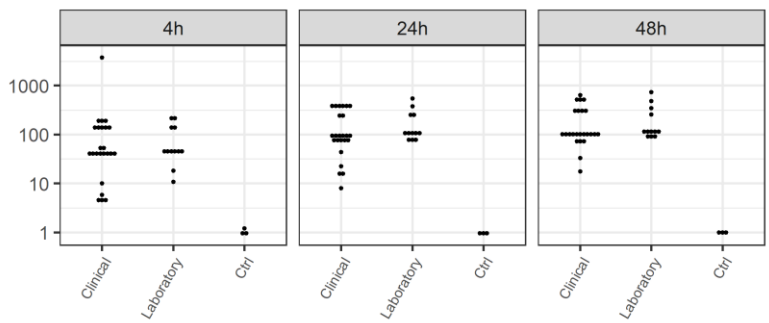


| Parameter | Estimate | Std.Error | p-value |
|---|---|---|---|
| (Intercept) | 3.7428 | 0.507 | <0.0001 |
| Time24h | 0.5634 | 0.3037 | 0.0683 |
| Time48h | 0.9728 | 0.3037 | 0.0021 |
| Lab_adaptationLaboratory | 0.0968 | 0.372 | 0.7955 |
| Time24h:Lab_adaptationLaboratory | 0.4144 | 0.5261 | 0.4339 |
| Time48h:Lab_adaptationLaboratory | 0.1681 | 0.5261 | 0.7504 |

| contrast | Time | ratio | SE | p.value |
|---|---|---|---|---|
| Clinical / Laboratory | 4h | 0.9077 | 0.3377 | 0.7955 |
| Clinical / Laboratory | 24h | 0.5998 | 0.2231 | 0.1743 |
| Clinical / Laboratory | 48h | 0.7673 | 0.2854 | 0.479 |

# PDGF-bb (logarithmic transformation)

## M1

### Geo_host_adaptation

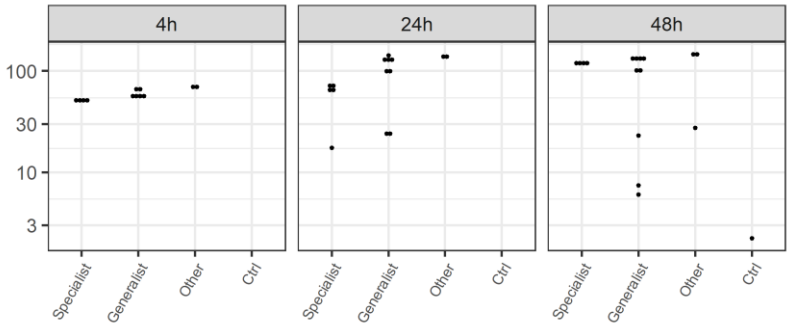


| Parameter | Estimate | Std.Error | p-value |
|---|---|---|---|
| (Intercept) | -0.558 | 0.5215 | 0.2916 |
| Time24h | 0.2519 | 0.1985 | 0.2123 |
| Time48h | 0.3579 | 0.1985 | 0.0795 |
| Geo_host_adaptationGeneralist | 0.0681 | 0.1812 | 0.7094 |
| Time24h:Geo_host_adaptationGeneralist | 0.3353 | 0.2562 | 0.1988 |
| Time48h:Geo_host_adaptationGeneralist | 0.235 | 0.2562 | 0.365 |

| contrast | Time | estimate | SE | p.value |
|---|---|---|---|---|
| Specialist - Generalist | 4h | -0.0681 | 0.1812 | 0.7094 |
| Specialist - Generalist | 24h | -0.4034 | 0.1812 | 0.0322 |
| Specialist - Generalist | 48h | -0.3031 | 0.1812 | 0.1028 |

### Lab_adaptation

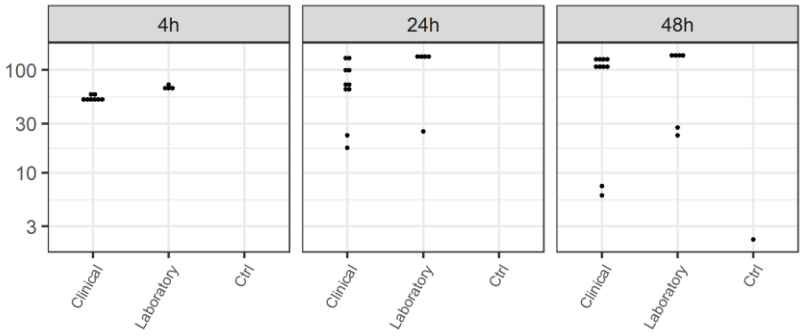


| Parameter | Estimate | Std.Error | p-value |
|---|---|---|---|
| (Intercept) | -0.5309 | 0.5114 | 0.3046 |
| Time24h | 0.3182 | 0.137 | 0.0246 |
| Time48h | 0.3875 | 0.137 | 0.0069 |
| Lab_adaptationLaboratory | 0.1071 | 0.1678 | 0.5265 |
| Time24h:Lab_adaptationLaboratory | 0.198 | 0.2372 | 0.4083 |
| Time48h:Lab_adaptationLaboratory | 0.3445 | 0.2372 | 0.1533 |

| contrast | Time | estimate | SE | p.value |
|---|---|---|---|---|
| Clinical - Laboratory | 4h | -0.1071 | 0.1678 | 0.5265 |
| Clinical - Laboratory | 24h | -0.305 | 0.1678 | 0.0755 |
| Clinical - Laboratory | 48h | -0.4516 | 0.1678 | 0.0099 |

## M2

### Geo_host_adaptation

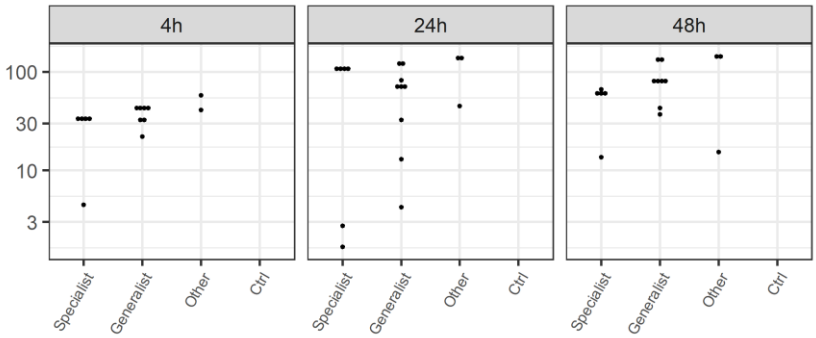


| Parameter | Estimate | Std.Error | p-value |
|---|---|---|---|
| (Intercept) | -0.5241 | 0.5273 | 0.3267 |
| Time24h | 0.515 | 0.2487 | 0.0454 |
| Time48h | 0.1805 | 0.2487 | 0.4724 |
| Geo_host_adaptationGeneralist | 0.0283 | 0.227 | 0.9015 |
| Time24h:Geo_host_adaptationGeneralist | -0.0309 | 0.321 | 0.9239 |
| Time48h:Geo_host_adaptationGeneralist | 0.3858 | 0.321 | 0.2371 |

| contrast | Time | estimate | SE | p.value |
|---|---|---|---|---|
| Specialist - Generalist | 4h | -0.0283 | 0.227 | 0.9015 |
| Specialist - Generalist | 24h | 0.0026 | 0.227 | 0.991 |
| Specialist - Generalist | 48h | -0.4141 | 0.227 | 0.0762 |

### Lab_adaptation

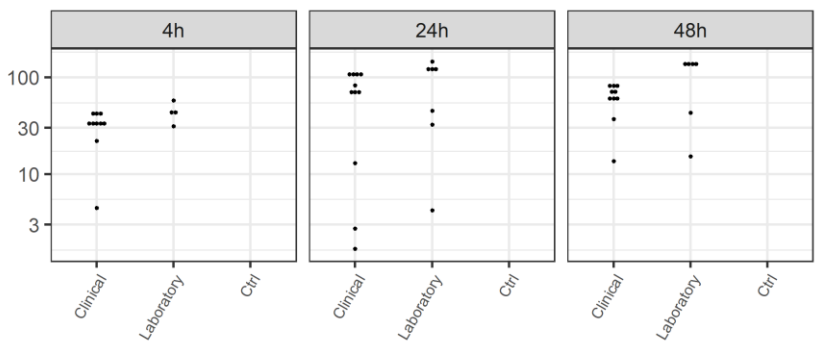


| Parameter | Estimate | Std.Error | p-value |
|---|---|---|---|
| (Intercept) | -0.5167 | 0.5097 | 0.316 |
| Time24h | 0.3338 | 0.1473 | 0.0282 |
| Time48h | 0.2434 | 0.1473 | 0.1053 |
| Lab_adaptationLaboratory | -0.059 | 0.1805 | 0.7451 |
| Time24h:Lab_adaptationLaboratory | 0.6088 | 0.2552 | 0.0212 |
| Time48h:Lab_adaptationLaboratory | 0.6619 | 0.2552 | 0.0127 |

| contrast | Time | estimate | SE | p.value |
|---|---|---|---|---|
| Clinical - Laboratory | 4h | 0.059 | 0.1805 | 0.7451 |
| Clinical - Laboratory | 24h | -0.5497 | 0.1805 | 0.0038 |
| Clinical - Laboratory | 48h | -0.6029 | 0.1805 | 0.0017 |

# MIP-1β (logarithmic transformation)

## M1

### Geo_host_adaptation

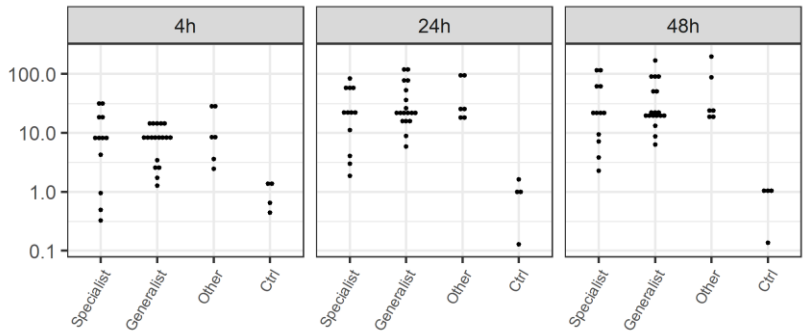


| Parameter | Estimate | Std.Error | p-value |
|---|---|---|---|
| (Intercept) | 1.3076 | 0.5729 | 0.0267 |
| Time24h | 1.2163 | 0.2701 | <0.0001 |
| Time48h | 1.3856 | 0.2701 | <0.0001 |
| Geo_host_adaptationGeneralist | 0.3435 | 0.2466 | 0.1697 |
| Time24h:Geo_host_adaptationGeneralist | 0.246 | 0.3487 | 0.4838 |
| Time48h:Geo_host_adaptationGeneralist | 0.1089 | 0.3487 | 0.7561 |

| contrast | Time | ratio | SE | p.value |
|---|---|---|---|---|
| Specialist / Generalist | 4h | 0.7093 | 0.1749 | 0.1697 |
| Specialist / Generalist | 24h | 0.5546 | 0.1368 | 0.0206 |
| Specialist / Generalist | 48h | 0.6361 | 0.1569 | 0.0724 |

### Lab_adaptation

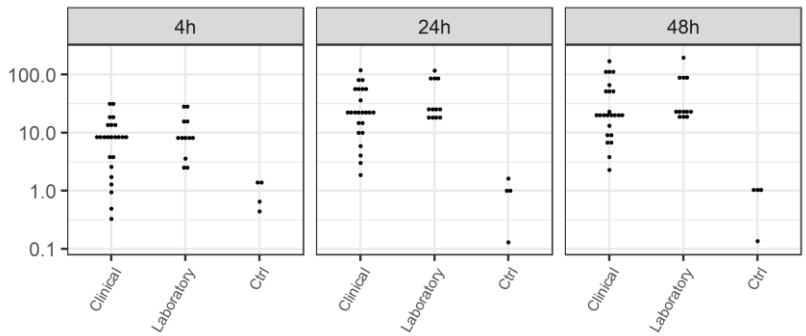


| Parameter | Estimate | Std.Error | p-value |
|---|---|---|---|
| (Intercept) | 1.4163 | 0.5382 | 0.0107 |
| Time24h | 1.3372 | 0.1814 | <0.0001 |
| Time48h | 1.4548 | 0.1814 | <0.0001 |
| Lab_adaptationLaboratory | 0.5009 | 0.2221 | 0.0276 |
| Time24h:Lab_adaptationLaboratory | 0.1245 | 0.3141 | 0.6933 |
| Time48h:Lab_adaptationLaboratory | 0.0332 | 0.3141 | 0.9161 |

| contrast | Time | ratio | SE | p.value |
|---|---|---|---|---|
| Clinical / Laboratory | 4h | 0.606 | 0.1346 | 0.0276 |
| Clinical / Laboratory | 24h | 0.535 | 0.1189 | 0.0065 |
| Clinical / Laboratory | 48h | 0.5862 | 0.1302 | 0.0191 |

## M2

### Geo_host_adaptation

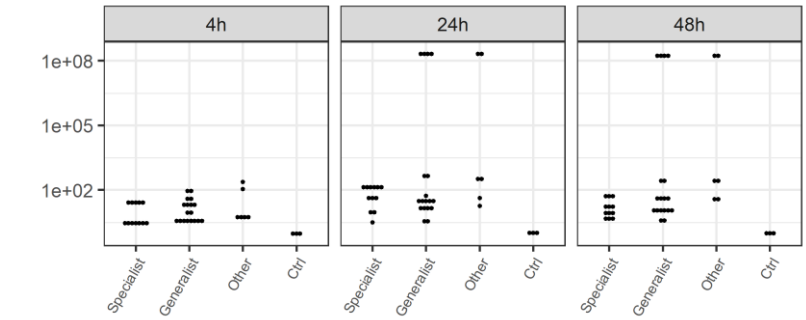


| Parameter | Estimate | Std.Error | p-value |
|---|---|---|---|
| (Intercept) | -1.0577 | 0.3966 | 0.0102 |
| Time24h | 1.2369 | 0.3517 | 9e-04 |
| Time48h | 0.83 | 0.3517 | 0.0221 |
| Geo_host_adaptationGeneralist | 0.5531 | 0.3211 | 0.091 |
| Time24h:Geo_host_adaptationGeneralist | -0.3937 | 0.4541 | 0.3899 |
| Time48h:Geo_host_adaptationGeneralist | -0.1473 | 0.4541 | 0.747 |

| contrast | Time | estimate | SE | p.value |
|---|---|---|---|---|
| Specialist - Generalist | 4h | -0.5531 | 0.3211 | 0.091 |
| Specialist - Generalist | 24h | -0.1594 | 0.3211 | 0.6217 |
| Specialist - Generalist | 48h | -0.4058 | 0.3211 | 0.212 |

### Lab_adaptation

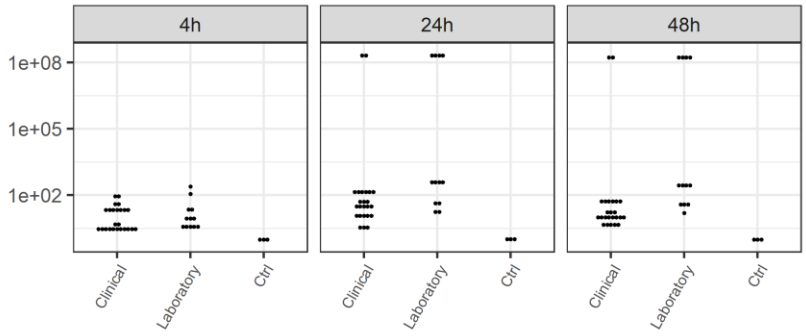


| Parameter | Estimate | Std.Error | p-value |
|---|---|---|---|
| (Intercept) | -0.8692 | 0.3472 | 0.0149 |
| Time24h | 0.8608 | 0.213 | 1e-04 |
| Time48h | 0.6255 | 0.213 | 0.0046 |
| Lab_adaptationLaboratory | 0.3031 | 0.2608 | 0.2496 |
| Time24h:Lab_adaptationLaboratory | 0.5193 | 0.3689 | 0.1641 |
| Time48h:Lab_adaptationLaboratory | 0.5802 | 0.3689 | 0.1207 |

| contrast | Time | estimate | SE | p.value |
|---|---|---|---|---|
| Clinical - Laboratory | 4h | -0.3031 | 0.2608 | 0.2496 |
| Clinical - Laboratory | 24h | -0.8224 | 0.2608 | 0.0025 |
| Clinical - Laboratory | 48h | -0.8833 | 0.2608 | 0.0012 |

# RANTES (logarithmic transformation)

## M1

### Geo_host_adaptation

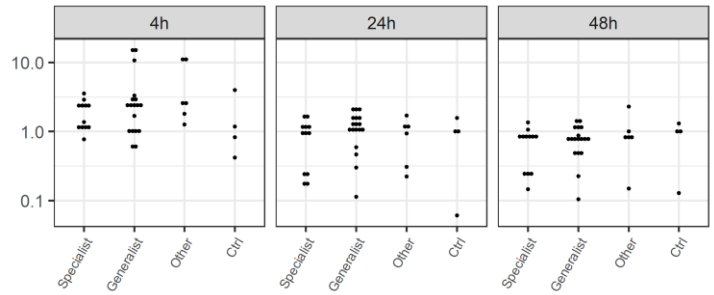


| Parameter | Estimate | Std.Error | p-value |
|---|---|---|---|
| (Intercept) | 0.6918 | 0.3923 | 0.0838 |
| Time24h | -0.9155 | 0.2712 | 0.0014 |
| Time48h | -1.2338 | 0.2712 | <0.0001 |
| Geo_host_adaptationGeneralist | 0.3405 | 0.2476 | 0.175 |
| Time24h:Geo_host_adaptationGeneralist | 0.0679 | 0.3502 | 0.8469 |
| Time48h:Geo_host_adaptationGeneralist | -0.1782 | 0.3502 | 0.6131 |

| contrast | Time | estimate | SE | p.value |
|---|---|---|---|---|
| Specialist - Generalist | 4h | -0.3405 | 0.2476 | 0.175 |
| Specialist - Generalist | 24h | -0.4085 | 0.2476 | 0.1051 |
| Specialist - Generalist | 48h | -0.1624 | 0.2476 | 0.5149 |

### Lab_adaptation

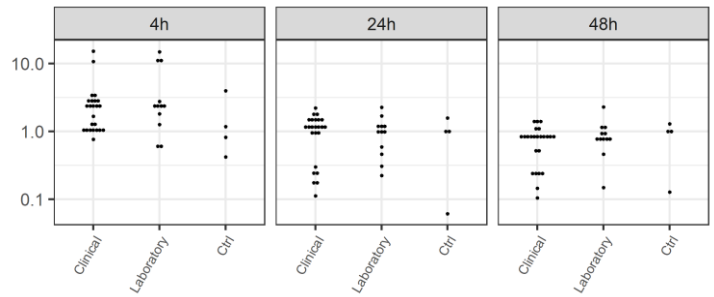


| Parameter | Estimate | Std.Error | p-value |
|---|---|---|---|
| (Intercept) | 0.8742 | 0.351 | 0.0154 |
| Time24h | -0.8917 | 0.195 | <0.0001 |
| Time48h | -1.3747 | 0.195 | <0.0001 |
| Lab_adaptationLaboratory | 0.1473 | 0.2388 | 0.5395 |
| Time24h:Lab_adaptationLaboratory | -0.198 | 0.3377 | 0.5598 |
| Time48h:Lab_adaptationLaboratory | 0.0408 | 0.3377 | 0.9042 |

| contrast | Time | estimate | SE | p.value |
|---|---|---|---|---|
| Clinical - Laboratory | 4h | -0.1473 | 0.2388 | 0.5395 |
| Clinical - Laboratory | 24h | 0.0507 | 0.2388 | 0.8326 |
| Clinical - Laboratory | 48h | -0.1881 | 0.2388 | 0.4338 |

## M2

### Geo_host_adaptation

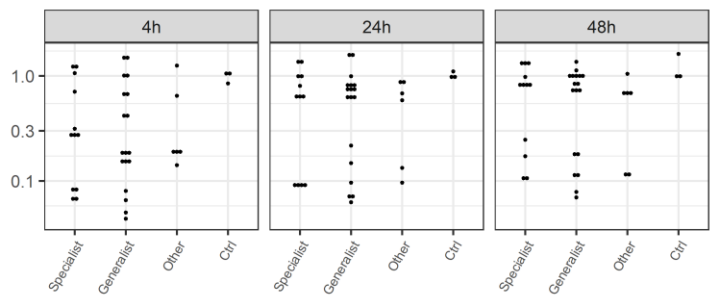


| Parameter | Estimate | Std.Error | p-value |
|---|---|---|---|
| (Intercept) | 0.0341 | 0.5314 | 0.9491 |
| Time24h | 0.3003 | 0.2471 | 0.2298 |
| Time48h | 0.5398 | 0.2471 | 0.0335 |
| Geo_host_adaptationGeneralist | -0.0249 | 0.2256 | 0.9127 |
| Time24h:Geo_host_adaptationGeneralist | -0.0387 | 0.319 | 0.9039 |
| Time48h:Geo_host_adaptationGeneralist | -0.1805 | 0.319 | 0.5739 |

| contrast | Time | estimate | SE | p.value |
|---|---|---|---|---|
| Specialist - Generalist | 4h | 0.0249 | 0.2256 | 0.9127 |
| Specialist - Generalist | 24h | 0.0636 | 0.2256 | 0.7792 |
| Specialist - Generalist | 48h | 0.2054 | 0.2256 | 0.3668 |

### Lab_adaptation

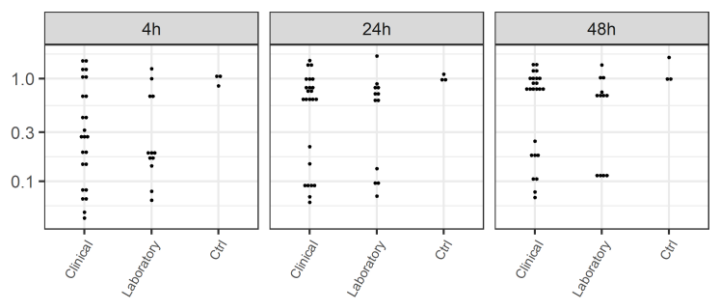


| Parameter | Estimate | Std.Error | p-value |
|---|---|---|---|
| (Intercept) | 0.1017 | 0.517 | 0.8447 |
| Time24h | 0.1852 | 0.1759 | 0.2964 |
| Time48h | 0.3968 | 0.1759 | 0.0276 |
| Lab_adaptationLaboratory | -0.1775 | 0.2154 | 0.413 |
| Time24h:Lab_adaptationLaboratory | 0.1739 | 0.3046 | 0.57 |
| Time48h:Lab_adaptationLaboratory | -0.0267 | 0.3046 | 0.9304 |

| contrast | Time | estimate | SE | p.value |
|---|---|---|---|---|
| Clinical - Laboratory | 4h | 0.1775 | 0.2154 | 0.413 |
| Clinical - Laboratory | 24h | 0.0036 | 0.2154 | 0.9868 |
| Clinical - Laboratory | 48h | 0.2042 | 0.2154 | 0.3467 |

# TNFα (logarithmic transformation)

## M1

### Geo_host_adaptation

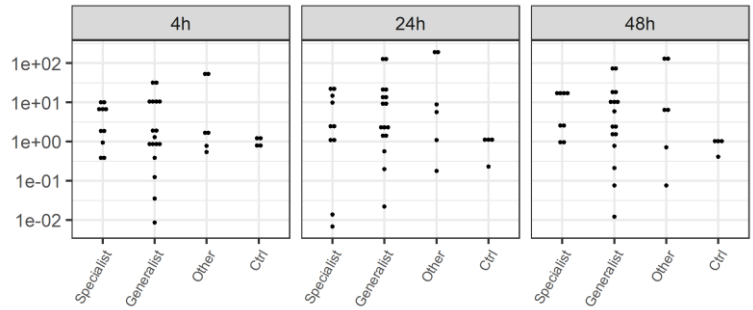


| Parameter | Estimate | Std.Error | p-value |
|---|---|---|---|
| (Intercept) | -0.2225 | 0.4461 | 0.62 |
| Time24h | 0.1489 | 0.2033 | 0.4672 |
| Time48h | 0.076 | 0.2033 | 0.71 |
| Geo_host_adaptationGeneralist | 0.1279 | 0.1856 | 0.4938 |
| Time24h:Geo_host_adaptationGeneralist | 0.1954 | 0.2625 | 0.46 |
| Time48h:Geo_host_adaptationGeneralist | 0.1498 | 0.2625 | 0.5706 |

| contrast | Time | estimate | SE | p.value |
|---|---|---|---|---|
| Specialist - Generalist | 4h | -0.1279 | 0.1856 | 0.4938 |
| Specialist - Generalist | 24h | -0.3233 | 0.1856 | 0.0875 |
| Specialist - Generalist | 48h | -0.2778 | 0.1856 | 0.1407 |

### Lab_adaptation

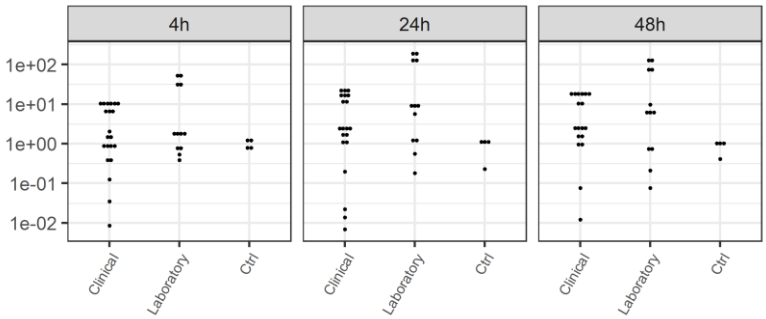


| Parameter | Estimate | Std.Error | p-value |
|---|---|---|---|
| (Intercept) | -0.2978 | 0.4328 | 0.4939 |
| Time24h | 0.176 | 0.1081 | 0.1083 |
| Time48h | 0.107 | 0.1081 | 0.326 |
| Lab_adaptationLaboratory | 0.4612 | 0.1323 | 9e-04 |
| Time24h:Lab_adaptationLaboratory | 0.2714 | 0.1872 | 0.152 |
| Time48h:Lab_adaptationLaboratory | 0.1501 | 0.1872 | 0.4254 |

| contrast | Time | estimate | SE | p.value |
|---|---|---|---|---|
| Clinical - Laboratory | 4h | -0.4612 | 0.1323 | 9e-04 |
| Clinical - Laboratory | 24h | -0.7326 | 0.1323 | <0.0001 |
| Clinical - Laboratory | 48h | -0.6113 | 0.1323 | <0.0001 |

## M2

### Geo_host_adaptation

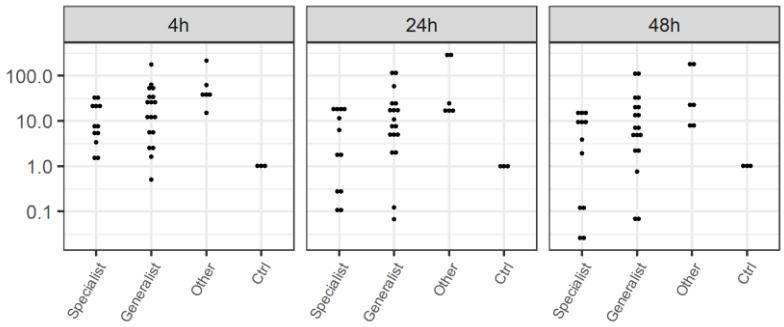


| Parameter | Estimate | Std.Error | p-value |
|---|---|---|---|
| (Intercept) | -0.0157 | 0.4183 | 0.9703 |
| Time24h | -0.397 | 0.3221 | 0.2233 |
| Time48h | -0.5288 | 0.3221 | 0.1068 |
| Geo_host_adaptationGeneralist | 0.3967 | 0.294 | 0.1832 |
| Time24h:Geo_host_adaptationGeneralist | 0.1372 | 0.4158 | 0.7428 |
| Time48h:Geo_host_adaptationGeneralist | 0.176 | 0.4158 | 0.6739 |

| contrast | Time | estimate | SE | p.value |
|---|---|---|---|---|
| Specialist - Generalist | 4h | -0.3967 | 0.294 | 0.1832 |
| Specialist - Generalist | 24h | -0.5339 | 0.294 | 0.0753 |
| Specialist - Generalist | 48h | -0.5727 | 0.294 | 0.0569 |

### Lab_adaptation

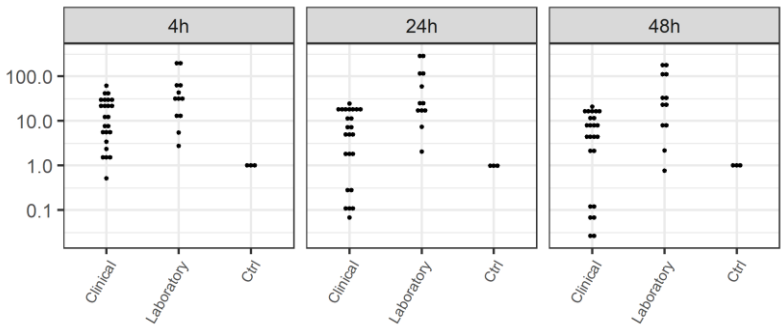


| Parameter | Estimate | Std.Error | p-value |
|---|---|---|---|
| (Intercept) | -0.0655 | 0.3515 | 0.8528 |
| Time24h | -0.4378 | 0.1778 | 0.0166 |
| Time48h | -0.5388 | 0.1778 | 0.0035 |
| Lab_adaptationLaboratory | 0.7376 | 0.2178 | 0.0012 |
| Time24h:Lab_adaptationLaboratory | 0.5497 | 0.308 | 0.0792 |
| Time48h:Lab_adaptationLaboratory | 0.4619 | 0.308 | 0.1387 |

| contrast | Time | estimate | SE | p.value |
|---|---|---|---|---|
| Clinical - Laboratory | 4h | -0.7376 | 0.2178 | 0.0012 |
| Clinical - Laboratory | 24h | -1.2873 | 0.2178 | <0.0001 |
| Clinical - Laboratory | 48h | -1.1995 | 0.2178 | <0.0001 |

# VEGF (logarithmic transformation)

## M1

### Geo_host_adaptation

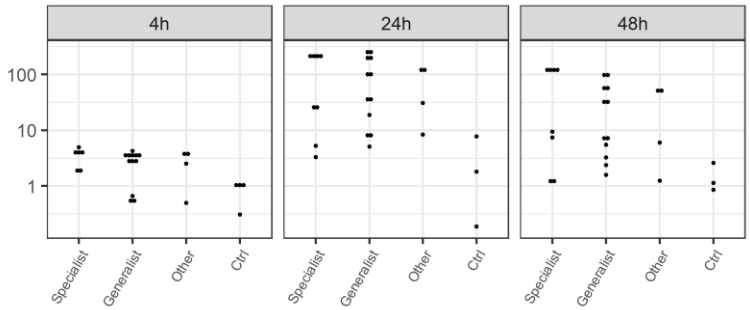


| Parameter | Estimate | Std.Error | p-value |
|---|---|---|---|
| (Intercept) | -1.1476 | 0.4705 | 0.0196 |
| Time24h | 1.6351 | 0.1782 | <0.0001 |
| Time48h | 1.0868 | 0.1782 | <0.0001 |
| Geo_host_adaptationGeneralist | 0.1966 | 0.1627 | 0.2346 |
| Time24h:Geo_host_adaptationGeneralist | -0.0845 | 0.2301 | 0.7154 |
| Time48h:Geo_host_adaptationGeneralist | -0.2596 | 0.2301 | 0.2665 |

| contrast | Time | estimate | SE | p.value |
|---|---|---|---|---|
| Specialist - Generalist | 4h | -0.1966 | 0.1627 | 0.2346 |
| Specialist - Generalist | 24h | -0.112 | 0.1627 | 0.4953 |
| Specialist - Generalist | 48h | 0.063 | 0.1627 | 0.7008 |

### Lab_adaptation

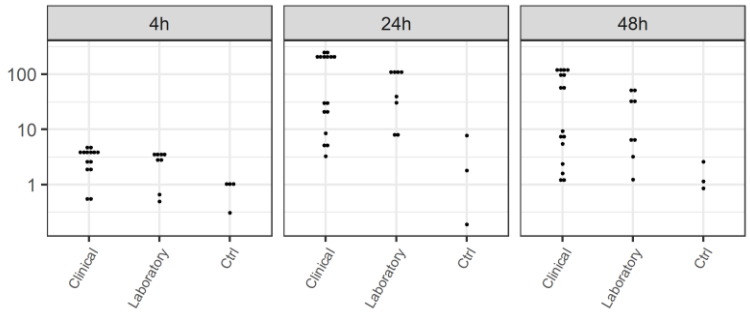


| Parameter | Estimate | Std.Error | p-value |
|---|---|---|---|
| (Intercept) | -1.059 | 0.4622 | 0.0266 |
| Time24h | 1.6708 | 0.1246 | <0.0001 |
| Time48h | 0.9798 | 0.1246 | <0.0001 |
| Lab_adaptationLaboratory | 0.0884 | 0.1526 | 0.5651 |
| Time24h:Lab_adaptationLaboratory | -0.2281 | 0.2159 | 0.2963 |
| Time48h:Lab_adaptationLaboratory | -0.1895 | 0.2159 | 0.3845 |

| contrast | Time | estimate | SE | p.value |
|---|---|---|---|---|
| Clinical - Laboratory | 4h | -0.0884 | 0.1526 | 0.5651 |
| Clinical - Laboratory | 24h | 0.1396 | 0.1526 | 0.3651 |
| Clinical - Laboratory | 48h | 0.1011 | 0.1526 | 0.5111 |

## M2

### Geo_host_adaptation

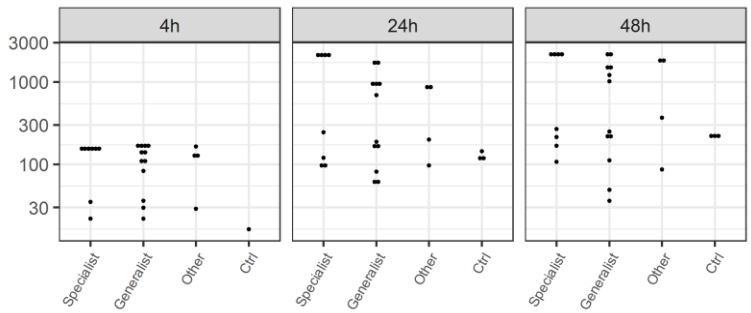


| Parameter | Estimate | Std.Error | p-value |
|---|---|---|---|
| (Intercept) | -0.8316 | 0.5494 | 0.1386 |
| Time24h | 1.0045 | 0.2026 | <0.0001 |
| Time48h | 1.3884 | 0.2026 | <0.0001 |
| Geo_host_adaptationGeneralist | -0.0697 | 0.1849 | 0.7082 |
| Time24h:Geo_host_adaptationGeneralist | -0.2576 | 0.2615 | 0.3311 |
| Time48h:Geo_host_adaptationGeneralist | -0.4135 | 0.2615 | 0.1223 |

| contrast | Time | estimate | SE | p.value |
|---|---|---|---|---|
| Specialist - Generalist | 4h | 0.0697 | 0.1849 | 0.7082 |
| Specialist - Generalist | 24h | 0.3273 | 0.1849 | 0.085 |
| Specialist - Generalist | 48h | 0.4833 | 0.1849 | 0.0129 |

### Lab_adaptation

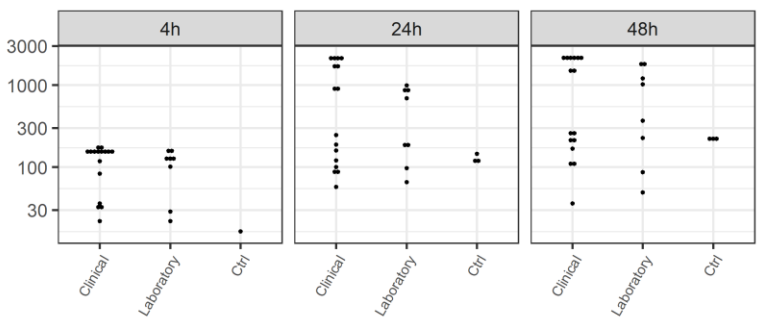


| Parameter | Estimate | Std.Error | p-value |
|---|---|---|---|
| (Intercept) | -0.8031 | 0.5438 | 0.1466 |
| Time24h | 0.8377 | 0.1492 | <0.0001 |
| Time48h | 1.1834 | 0.1492 | <0.0001 |
| Lab_adaptationLaboratory | -0.2022 | 0.1828 | 0.2744 |
| Time24h:Lab_adaptationLaboratory | 0.0332 | 0.2585 | 0.8985 |
| Time48h:Lab_adaptationLaboratory | -0.1473 | 0.2585 | 0.5716 |

| contrast | Time | estimate | SE | p.value |
|---|---|---|---|---|
| Clinical - Laboratory | 4h | 0.2022 | 0.1828 | 0.2744 |
| Clinical - Laboratory | 24h | 0.169 | 0.1828 | 0.36 |
| Clinical - Laboratory | 48h | 0.3494 | 0.1828 | 0.0621 |

# SDS-1α(logarithmic transformation)

## M1

### Geo_host_adaptation

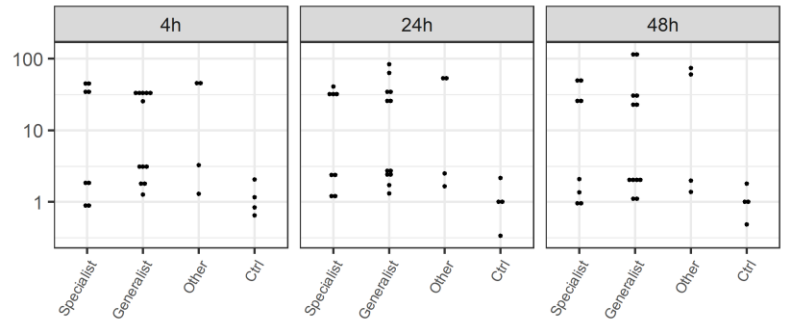


| Parameter | Estimate | Std.Error | p-value |
|---|---|---|---|
| (Intercept) | -0.6082 | 0.5798 | 0.301 |
| Time24h | 0.3134 | 0.343 | 0.3669 |
| Time48h | 0.0983 | 0.343 | 0.7761 |
| Geo_host_adaptationGeneralist | 0.478 | 0.3132 | 0.1354 |
| Time24h:Geo_host_adaptationGeneralist | -0.1994 | 0.4429 | 0.6552 |
| Time48h:Geo_host_adaptationGeneralist | -0.1983 | 0.4429 | 0.6569 |

| contrast | Time | estimate | SE | p.value |
|---|---|---|---|---|
| Specialist - Generalist | 4h | -0.478 | 0.3132 | 0.1354 |
| Specialist - Generalist | 24h | -0.2786 | 0.3132 | 0.3794 |
| Specialist - Generalist | 48h | -0.2797 | 0.3132 | 0.3776 |

### Lab_adaptation

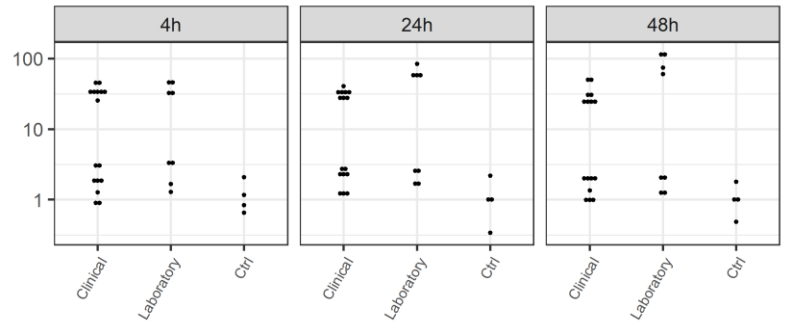


| Parameter | Estimate | Std.Error | p-value |
|---|---|---|---|
| (Intercept) | -0.4496 | 0.5522 | 0.4197 |
| Time24h | 0.1715 | 0.2307 | 0.461 |
| Time48h | -0.0914 | 0.2307 | 0.6936 |
| Lab_adaptationLaboratory | 0.3502 | 0.2825 | 0.2214 |
| Time24h:Lab_adaptationLaboratory | 0.0703 | 0.3995 | 0.8612 |
| Time48h:Lab_adaptationLaboratory | 0.306 | 0.3995 | 0.4477 |

| contrast | Time | estimate | SE | p.value |
|---|---|---|---|---|
| Clinical - Laboratory | 4h | -0.3502 | 0.2825 | 0.2214 |
| Clinical - Laboratory | 24h | -0.4205 | 0.2825 | 0.1435 |
| Clinical - Laboratory | 48h | -0.6562 | 0.2825 | 0.0247 |

## M2

### Geo_host_adaptation

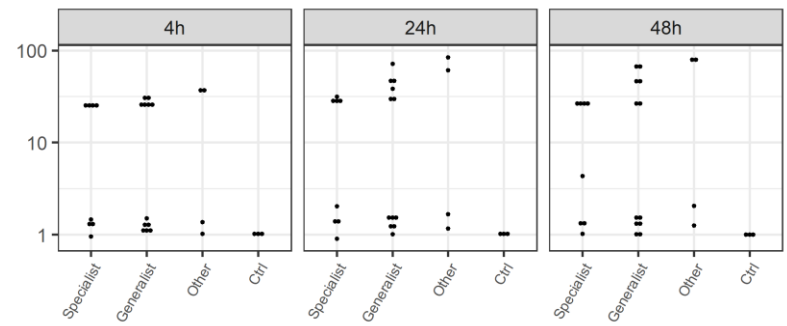


| Parameter | Estimate | Std.Error | p-value |
|---|---|---|---|
| (Intercept) | -0.5888 | 0.59 | 0.3249 |
| Time24h | 0.2506 | 0.3115 | 0.4262 |
| Time48h | 0.2537 | 0.3115 | 0.4206 |
| Geo_host_adaptationGeneralist | 0.1978 | 0.2843 | 0.4911 |
| Time24h:Geo_host_adaptationGeneralist | 0.1468 | 0.4021 | 0.7171 |
| Time48h:Geo_host_adaptationGeneralist | 0.0464 | 0.4021 | 0.9087 |

| contrast | Time | estimate | SE | p.value |
|---|---|---|---|---|
| Specialist - Generalist | 4h | -0.1978 | 0.2843 | 0.4911 |
| Specialist - Generalist | 24h | -0.3446 | 0.2843 | 0.2332 |
| Specialist - Generalist | 48h | -0.2442 | 0.2843 | 0.396 |

### Lab_adaptatıon

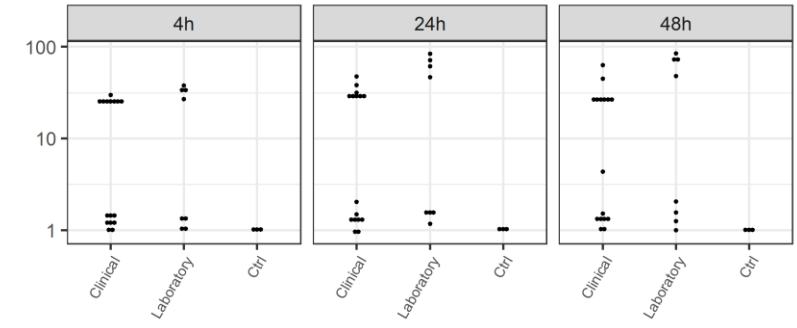


| Parameter | Estimate | Std.Error | p-value |
|---|---|---|---|
| (Intercept) | -0.524 | 0.5676 | 0.3607 |
| Time24h | 0.158 | 0.209 | 0.4534 |
| Time48h | 0.231 | 0.209 | 0.2747 |
| Lab_adaptationLaboratory | 0.1257 | 0.2559 | 0.6256 |
| Time24h:Lab_adaptationLaboratory | 0.4703 | 0.362 | 0.2003 |
| Time48h:Lab_adaptationLaboratory | 0.3237 | 0.362 | 0.3758 |

| contrast | Time | estimate | SE | p.value |
|---|---|---|---|---|
| Clinical - Laboratory | 4h | -0.1257 | 0.2559 | 0.6256 |
| Clinical - Laboratory | 24h | -0.5961 | 0.2559 | 0.0243 |
| Clinical - Laboratory | 48h | -0.4494 | 0.2559 | 0.0858 |

# IL-18 (logarithmic transformation)

## M1

### Geo_host_adaptation

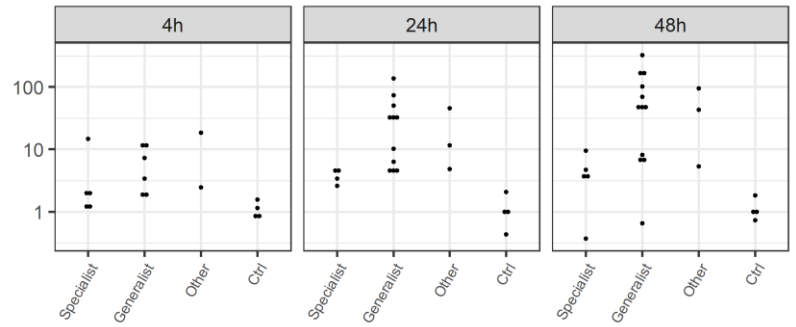


| Parameter | Estimate | Std.Error | p-value |
|---|---|---|---|
| (Intercept) | -0.4429 | 0.2657 | 0.1039 |
| Time24h | -0.053 | 0.3295 | 0.873 |
| Time48h | 0.0883 | 0.3295 | 0.7903 |
| Geo_host_adaptationGeneralist | 0.0281 | 0.3007 | 0.9261 |
| Time24h:Geo_host_adaptationGeneralist | 1.0793 | 0.4253 | 0.0155 |
| Time48h:Geo_host_adaptationGeneralist | 1.4113 | 0.4253 | 0.002 |

| contrast | Time | estimate | SE | p.value |
|---|---|---|---|---|
| Specialist - Generalist | 4h | -0.0281 | 0.3007 | 0.9261 |
| Specialist - Generalist | 24h | -1.1074 | 0.3007 | 7e-04 |
| Specialist - Generalist | 48h | -1.4394 | 0.3007 | <0.0001 |

### Lab_adaptation

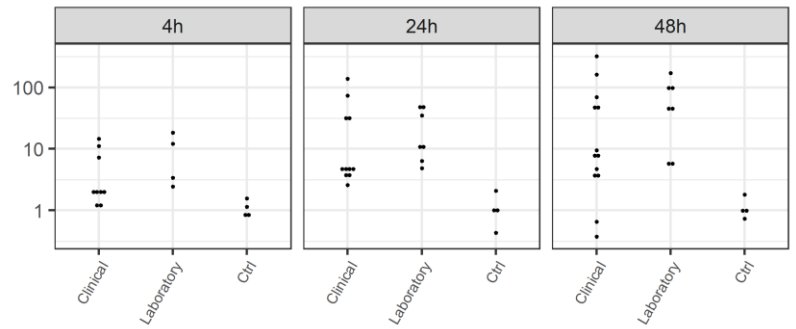


| Parameter | Estimate | Std.Error | p-value |
|---|---|---|---|
| (Intercept) | -0.4358 | 0.2491 | 0.0869 |
| Time24h | 0.4554 | 0.3 | 0.1359 |
| Time48h | 0.7678 | 0.3 | 0.0138 |
| Lab_adaptationLaboratory | 0.1101 | 0.3675 | 0.7658 |
| Time24h:Lab_adaptationLaboratory | 0.3462 | 0.5197 | 0.5086 |
| Time48h:Lab_adaptationLaboratory | 0.389 | 0.5197 | 0.4579 |

| contrast | Time | estimate | SE | p.value |
|---|---|---|---|---|
| Clinical - Laboratory | 4h | -0.1101 | 0.3675 | 0.7658 |
| Clinical - Laboratory | 24h | -0.4563 | 0.3675 | 0.2206 |
| Clinical - Laboratory | 48h | -0.4991 | 0.3675 | 0.181 |

## M2

### Geo_host_adaptation

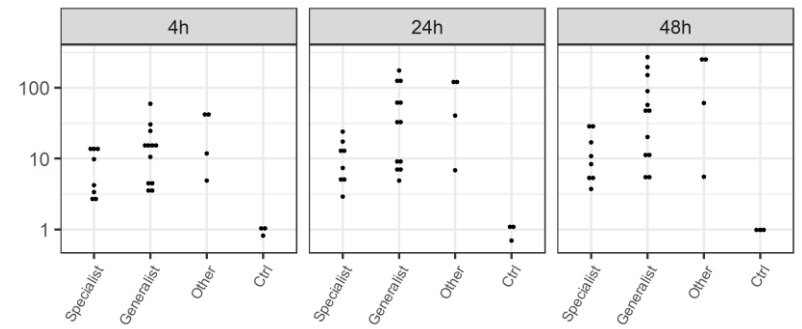


| Parameter | Estimate | Std.Error | p-value |
|---|---|---|---|
| (Intercept) | -1.1197 | 0.4162 | 0.0106 |
| Time24h | 0.567 | 0.4155 | 0.1806 |
| Time48h | 0.7678 | 0.4155 | 0.0726 |
| Geo_host_adaptationGeneralist | 0.8471 | 0.3793 | 0.0317 |
| Time24h:Geo_host_adaptationGeneralist | 0.0445 | 0.5364 | 0.9344 |
| Time48h:Geo_host_adaptationGeneralist | 0.0519 | 0.5364 | 0.9235 |

| contrast | Time | estimate | SE | p.value |
|---|---|---|---|---|
| Specialist - Generalist | 4h | -0.8471 | 0.3793 | 0.0317 |
| Specialist - Generalist | 24h | -0.8915 | 0.3793 | 0.0242 |
| Specialist - Generalist | 48h | -0.899 | 0.3793 | 0.0231 |

### Lab_adaptation

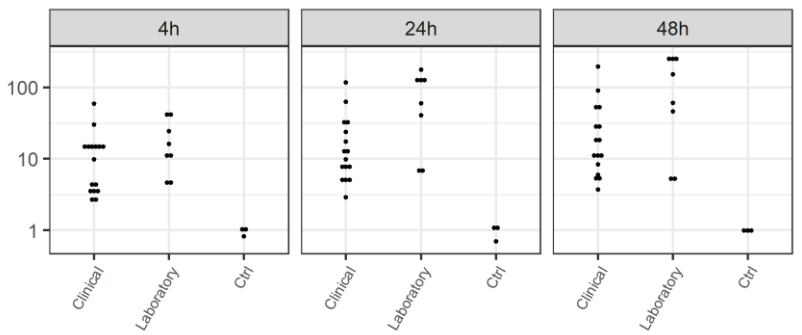


| Parameter | Estimate | Std.Error | p-value |
|---|---|---|---|
| (Intercept) | -0.8219 | 0.383 | 0.0372 |
| Time24h | 0.5042 | 0.2958 | 0.095 |
| Time48h | 0.7526 | 0.2958 | 0.0144 |
| Lab_adaptationLaboratory | 0.5731 | 0.3622 | 0.1204 |
| Time24h:Lab_adaptationLaboratory | 0.2571 | 0.5123 | 0.6181 |
| Time48h:Lab_adaptationLaboratory | 0.2004 | 0.5123 | 0.6975 |

| contrast | Time | estimate | SE | p.value |
|---|---|---|---|---|
| Clinical - Laboratory | 4h | -0.5731 | 0.3622 | 0.1204 |
| Clinical - Laboratory | 24h | -0.8303 | 0.3622 | 0.0265 |
| Clinical - Laboratory | 48h | -0.7735 | 0.3622 | 0.0381 |

# Gro- α (logarithmic transformation)

## M1

### Geo_host_adaptation

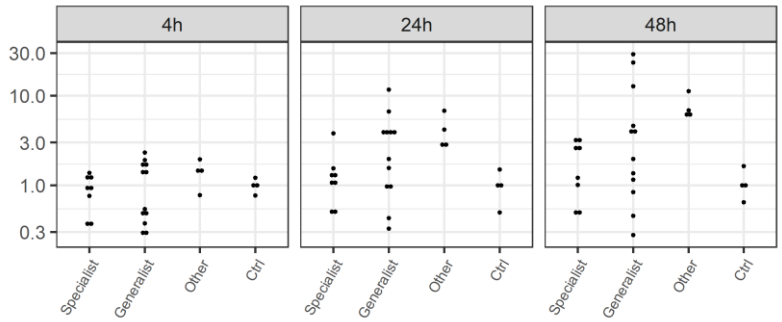


| Parameter | Estimate | Std.Error | p-value |
|---|---|---|---|
| (Intercept) | -0.1115 | 0.4353 | 0.7992 |
| Time24h | 0.3827 | 0.4786 | 0.4291 |
| Time48h | 0.5643 | 0.4786 | 0.246 |
| Geo_host_adaptationGeneralist | 0.142 | 0.4369 | 0.747 |
| Time24h:Geo_host_adaptationGeneralist | 0.4921 | 0.6179 | 0.4309 |
| Time48h:Geo_host_adaptationGeneralist | 0.5218 | 0.6179 | 0.4039 |

| contrast | Time | ratio | SE | p.value |
|---|---|---|---|---|
| Specialist / Generalist | 4h | 0.8676 | 0.3791 | 0.747 |
| Specialist / Generalist | 24h | 0.5304 | 0.2317 | 0.1551 |
| Specialist / Generalist | 48h | 0.5149 | 0.225 | 0.1372 |

### Lab_adaptation

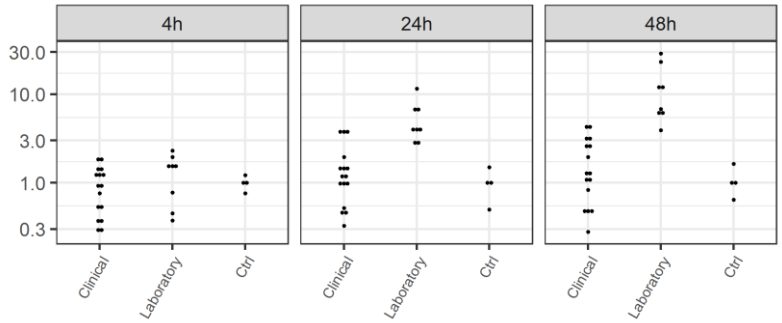


| Parameter | Estimate | Std.Error | p-value |
|---|---|---|---|
| (Intercept) | -0.0717 | 0.3046 | 0.815 |
| Time24h | 0.4123 | 0.2338 | 0.0845 |
| Time48h | 0.5163 | 0.2338 | 0.0323 |
| Lab_adaptationLaboratory | 0.3111 | 0.2864 | 0.283 |
| Time24h:Lab_adaptationLaboratory | 1.0089 | 0.405 | 0.0164 |
| Time48h:Lab_adaptationLaboratory | 1.5063 | 0.405 | 5e-04 |

| contrast | Time | ratio | SE | p.value |
|---|---|---|---|---|
| Clinical / Laboratory | 4h | 0.7326 | 0.2098 | 0.283 |
| Clinical / Laboratory | 24h | 0.2671 | 0.0765 | <0.0001 |
| Clinical / Laboratory | 48h | 0.1625 | 0.0465 | <0.0001 |

## M2

### Geo_host_adaptation

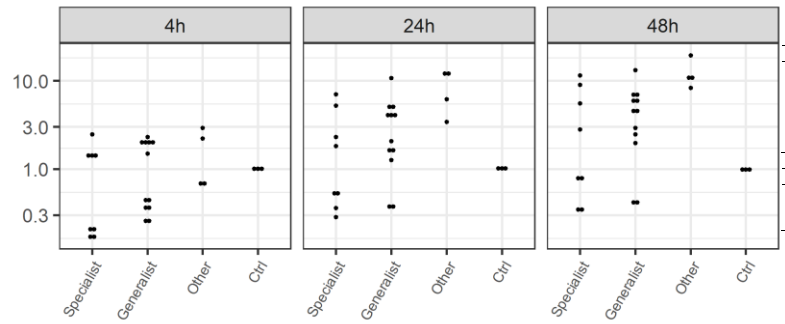


| Parameter | Estimate | Std.Error | p-value |
|---|---|---|---|
| (Intercept) | -0.702 | 0.4994 | 0.1682 |
| Time24h | 0.8553 | 0.2804 | 0.0042 |
| Time48h | 1.2686 | 0.2804 | 1e-04 |
| Geo_host_adaptationGeneralist | 0.4624 | 0.2559 | 0.0789 |
| Time24h:Geo_host_adaptationGeneralist | -0.1523 | 0.362 | 0.6764 |
| Time48h:Geo_host_adaptationGeneralist | -0.1506 | 0.362 | 0.6798 |

| contrast | Time | estimate | SE | p.value |
|---|---|---|---|---|
| Specialist - Generalist | 4h | -0.4624 | 0.2559 | 0.0789 |
| Specialist - Generalist | 24h | -0.3102 | 0.2559 | 0.2333 |
| Specialist - Generalist | 48h | -0.3118 | 0.2559 | 0.2308 |

### Lab_adaptation

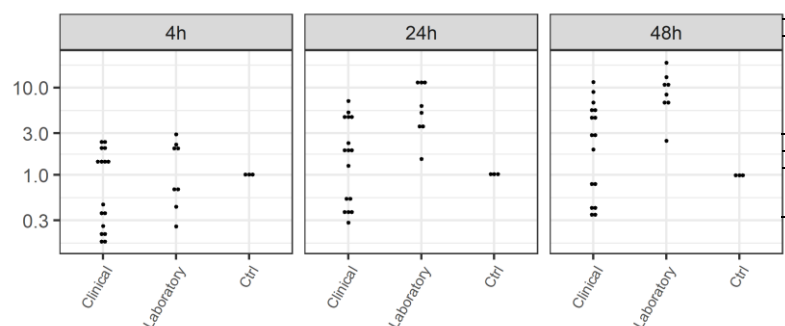


| Parameter | Estimate | Std.Error | p-value |
|---|---|---|---|
| (Intercept) | -0.6036 | 0.4145 | 0.1521 |
| Time24h | 0.6126 | 0.1738 | 0.001 |
| Time48h | 0.9337 | 0.1738 | <0.0001 |
| Lab_adaptationLaboratory | 0.3972 | 0.2129 | 0.0685 |
| Time24h:Lab_adaptationLaboratory | 0.6271 | 0.3011 | 0.0428 |
| Time48h:Lab_adaptationLaboratory | 0.7349 | 0.3011 | 0.0186 |

| contrast | Time | estimate | SE | p.value |
|---|---|---|---|---|
| Clinical - Laboratory | 4h | -0.3972 | 0.2129 | 0.0685 |
| Clinical - Laboratory | 24h | -1.0243 | 0.2129 | <0.0001 |
| Clinical - Laboratory | 48h | -1.132 | 0.2129 | <0.0001 |